



**HAL**  
open science

# Molecular mechanism of GluN3A containing NMDA receptors

Marco de Battista

► **To cite this version:**

Marco de Battista. Molecular mechanism of GluN3A containing NMDA receptors. Neuroscience. Université Paris sciences et lettres, 2022. English. NNT : 2022UPSLE061 . tel-04646744

**HAL Id: tel-04646744**

**<https://theses.hal.science/tel-04646744>**

Submitted on 12 Jul 2024

**HAL** is a multi-disciplinary open access archive for the deposit and dissemination of scientific research documents, whether they are published or not. The documents may come from teaching and research institutions in France or abroad, or from public or private research centers.

L'archive ouverte pluridisciplinaire **HAL**, est destinée au dépôt et à la diffusion de documents scientifiques de niveau recherche, publiés ou non, émanant des établissements d'enseignement et de recherche français ou étrangers, des laboratoires publics ou privés.

**THÈSE DE DOCTORAT**

**DE L'UNIVERSITÉ PSL**

Préparée à École Normale Supérieure

Mécanismes moléculaires des récepteurs NMDA non-  
conventionnels de type GluN3

-

Molecular mechanism of GluN3A containing NMDA  
receptors

Soutenue par

**Marco De Battista**

Le 12/12/2022

Ecole doctorale n° 158

**Cerveau, cognition,  
comportement (3C)**

Spécialité

**Neurosciences**

Composition du jury :

Dr. Philippe Rondard IGF Montpellier, FR	<i>Rapporteur</i>
Dr. Catherine Venien-Bryan UPMC-Sorbonne Université, FR	<i>Rapporteuse</i>
Dr. Martin Horak CAS Institute of Experimental Medicine, CZ	<i>Examineur</i>
Dr. Martin Picard IBPC-Sorbonne Université, FR	<i>Président du jury</i>
Dr. David Stroebel IBENS, PSL, FR	<i>Co-directeur de Thèse</i>
Dr. Pierre Paoletti IBENS, PSL, FR	<i>Co-directeur de Thèse</i>

PhD Thesis

Mécanismes moléculaires des récepteurs NMDA non-  
conventionnels de type GluN3

-

Molecular mechanism of GluN3A containing NMDA  
receptors

**Marco De Battista**

Institut de Biologie de l'ENS

CNRS UMR8197, INSERM U1024

École normale supérieure, Université PSL, 46 rue d'Ulm, 75005 Paris

Dr. Philippe Rondard Rapporteur

Dr. Venien-Bryan Catherine Rapportrice

Dr. Martin Horak Examineur

Dr. Martin Picard Examineur

Dr. David Stroebel Thesis co-director

Dr. Pierre Paoletti Thesis co-director





# Table of contents

Table of contents	3
Outline of Figures	6
Outline of Tables	7
English summary	8
Résumé en français	10
Acknowledgments	12
Preface	14

## **FIRST CHAPTER: INTRODUCTION** **15**

<b>1 INTRODUCTION: BRAIN TRANSMISSION, SYNAPTIC PLASTICITY AND LIGAND GATED ION CHANNELS</b>	<b>16</b>
1.1 Historical perspectives	18
1.2 Excitatory and inhibitory neurotransmission	19
1.2.1 Inhibitory transmission: GABA <sub>B</sub> , GABA <sub>A</sub> , Glycine receptors	22
1.2.2 Excitatory neurotransmission	24
1.2.2.1 mGluRs	24
1.2.2.2 iGluRs	26
1.2.2.2.1 Delta receptors	29
1.2.2.2.2 Kainate receptors	29
1.2.2.2.3 AMPARs	31
<b>2 INTRODUCTION TO NMDARs</b>	<b>34</b>
2.1 Developmental and regional expression	35
2.2 Function in physiology	39
2.3 NMDARs in pathology and drug development	41
2.4 Pharmacology of NMDARs	42
2.4.1 Orthosteric agonists	42
2.4.2 Orthosteric antagonists	44
2.4.3 Open channel blockers	44
2.4.4 Allosteric modulators	45
<b>3 RECEPTOR ARCHITECTURE: MODULAR DESIGN</b>	<b>50</b>
3.1 NMDARs crystal and Cryo-EM structures: a major advance in the field	52
3.2 Functional unit of the extracellular region: the bilobate clamshell-like domain	53
3.3 The Ligand Binding Domain (LBD)	56
3.3.1 LBD dimerization	57
3.3.2 Drugs targeting the LBD intradimer interface	62
3.4 The N-terminal Domain (NTD)	65
3.4.1 NTD dimerization and effect of allosteric modulators	67
3.5 The Transmembrane Domain (TMD)	69
3.6 The C-terminal domain (CTD)	72
<b>4 GATING MECHANISMS</b>	<b>75</b>
4.1 Macroscopic processes of activation and deactivation	75

4.2 Single channel properties and open probability _____	77
4.3 Kinetic scheme _____	79
4.4 Pore motions _____	82
4.5 Desensitization: AMPARs vs NMDARs _____	84
4.6 Allosteric modulation: focus on zinc, protons and ifenprodil _____	88
4.7 A unified model of NMDAR gating _____	90
<b>5 THE GLUN3 SUBUNITS _____</b>	<b>95</b>
5.1 Historical introduction _____	95
5.2 GluN3A expression: anatomical and developmental aspects, cell types specificity and subcellular localization _____	96
5.3 GluN3A modular architecture _____	100
5.4 GluN1/GluN3A unusual current phenotype: structural determinants _____	104
5.5 Pharmacology of GluN1/GluN3A receptors _____	107
5.5.1 Orthosteric agonists _____	107
5.5.2 Potentiators _____	108
5.5.3 Open channel blockers and inhibitors _____	109
5.6 GluN3A in plasticity, cognition and pathology. _____	111
5.7 GluN1/GluN3A diheteromers in the brain _____	115
5.8 Triheteromers containing GluN1/GluN2/GluN3A: fact or fiction? _____	118
5.9 GluN3B _____	122

---

**SECOND CHAPTER: RESULTS 123**

---

Question and objectives _____	124
Introduction: challenges and molecular perspectives of GluN1/GluN3A receptor study _____	125
<b>6: NEW MODULATORS, METHODOLOGIES AND TESTS TO STUDY GLUN1/GLUN3A RECEPTOR FUNCTIONS_</b>	<b>129</b>
6.1 Pore block: Magnesium _____	129
6.2 Pore block: Pentamidine _____	133
6.3 Echinatin modulation _____	135
6.4 Assessing channel open probability of GluN1/GluN3A receptors _____	136
6.4.1 Control experiments of MTSEA treatment on GluN1/GluN3A receptors _____	138
6.4.2 Behavior of MTSEA cross-linked receptors _____	139
6.5 State-dependency of D-serine action _____	145
6.6 Zinc modulation _____	146
<b>7: INVESTIGATING GLUN1/GLUN3A RECEPTOR MOLECULAR MECHANISMS: STABILIZING CONFORMATIONAL STATES _____</b>	<b>153</b>
7.1 Building a working 3D model of GluN1/GluN3A receptor _____	153
7.2 Investigating the role of domains and loops _____	154
7.3 Cysteine scanning of interfaces _____	157
7.3.1 Reducing agent treatment on cysteine mutants _____	160
7.3.2 Western blots on cysteine mutants _____	164
<b>8: THE LBD DIMER INTERFACE CONTROLS GLUN1/GLUN3A RECEPTOR ACTIVITY. _____</b>	<b>169</b>
8.1 Contact Maps of the LBD intradimer interface _____	169
8.2 Scanning approach to build a GluN3A LBD intradimer interface GluN2B-like chimera _____	177

<b>8.3 ARTICLE: THE LBD DIMER INTERFACE TUNES ACTIVATION OF GLYCINE-GATED GLUN1/GLUN3A RECEPTORS</b>	<b>181</b>
<hr/>	
<b>CONTINUATION OF THE SECOND CHAPTER: RESULTS</b>	<b>205</b>
8.4 Unnatural-Amino-Acid (UAA) crosslinking attempts at the LBD dimer interface	206
8.5 GluN1 agonist binding sites function in the GluN1/GluN3A context	216
8.6 Attempts to study the LBD-TMD transduction mechanism	217
8.7 Attempts to reveal triheteromeric GluN1/GluN2B/GluN3A receptor activity	219
<b>THIRD CHAPTER: DISCUSSION</b>	<b>223</b>
<hr/>	
<b>9 GENERAL DISCUSSION</b>	<b>224</b>
9.1 Methodological developments	225
9.2 GOF mutants	227
9.3 Molecular mechanisms of GluN3A containing receptors	228
9.4 Concluding remarks and future perspectives	232
<b>RESUME FRANÇAIS DE LA THESE</b>	<b>233</b>
<hr/>	
Introduction et discussion générale	234
Développements méthodologiques	235
Mutants GOF	237
Mécanismes moléculaires des récepteurs contenant GluN3A	239
Conclusions et perspectives futures	242
<b>BIBLIOGRAPHY</b>	<b>245</b>
<hr/>	

## Outline of Figures

FIGURE 1 SCHEMATIZATION OF THE SYNAPSE. _____	17
FIGURE 2 HISTORY OF RESEARCH ON BRAIN TRANSMISSION. _____	19
FIGURE 3 EXCITATORY AND INHIBITORY NEUROTRANSMISSIONS IN THE NEURON. _____	21
FIGURE 4 STRUCTURE AND DIVERSITY OF INHIBITORY METABOTROPIC AND LIGAND GATED ION CHANNELS. _____	23
FIGURE 5 IGLURs FUNCTIONAL CLASSES ORGANIZATION. _____	28
FIGURE 6 AMPARs AND NMDARs COMPARED IN THEIR KINETIC PROPERTIES. _____	32
FIGURE 7 NMDAR SUBUNIT DIVERSITY AND STRUCTURE. _____	35
FIGURE 8 NMDAR DEVELOPMENTAL AND REGIONAL EXPRESSION. _____	37
FIGURE 9 COMPARISON AMONG GRIN GENES EXPRESSION LEVELS IN THE RAT FOREBRAIN. _____	38
FIGURE 10 IGLUR SUBUNITS CO-AGONISM. _____	43
FIGURE 11 PHARMACOLOGY OF NMDARs. _____	47
FIGURE 12 SUBUNIT ARRANGEMENT IN IGLURs. _____	51
FIGURE 13 IGLUR AVAILABLE STRUCTURES AS A FUNCTION OF TIME. _____	53
FIGURE 14 EVOLUTION OF NMDAR DOMAINS. _____	55
FIGURE 15 CLAMSHELL CONFORMATIONS CHANGE DEPENDING ON LIGAND BINDING. _____	56
FIGURE 16 NMDAR LBD DIMERIZATION. _____	58
FIGURE 17 FUNCTION OF THE INTRADIMER INTERFACE IN NMDAR AND AMPARs. _____	61
FIGURE 18 GLUN2A-SELECTIVE PAM BINDING SITE LOCATED IN THE INTRADIMER INTERFACE. _____	63
FIGURE 19 IGLURs NTDs COMPARED WITHIN THE COMPLETE TETRAMERIC STRUCTURES FOR ALL 4 CLASSES OF IGLURs. _____	66
FIGURE 20 NTD INTRADIMER INTERFACE. _____	68
FIGURE 21 IGLUR AND NMDAR TRANSMEMBRANE DOMAIN. _____	71
FIGURE 22 SPLICE VARIANTS IN NMDAR SUBUNITS. _____	73
FIGURE 23 NMDAR SUBUNIT COMPOSITION DETERMINES RECEPTOR PROPERTIES. _____	77
FIGURE 24 NMDAR GLUN2A AND GLUN2B POS COMPARED. _____	79
FIGURE 25 KINETIC SCHEME OF NMDARs. _____	81
FIGURE 26: PORE MOTIONS IN IGLUR GATING. _____	83
FIGURE 27 AMPARs VS NMDAR DESENSITIZATION: _____	87
FIGURE 28 ALLOSTERIC MODULATION IN NMDARs: IFENPRODIL, PROTONS AND ZINC. _____	90
FIGURE 29 ACTIVATION SCHEME AND ALLOSTERIC ROUTES OF DIFFERENT TYPES OF IGLURs. _____	92
FIGURE 30 TEMPORAL EXPRESSION PATTERN OF GLUN3A IN THE BRAIN. _____	97
FIGURE 31 GLUN3A EXPRESSION IN THE MOUSE BRAIN. _____	99
FIGURE 32 COMPARISON OF LBDS OF DIFFERENT NMDAR SUBUNITS. _____	104
FIGURE 33 GLUN1/GLUN3A RECEPTOR GATING MECHANISM AND CURRENT PHENOTYPES. _____	106
FIGURE 34 CGP "AWAKENING" ON GLUN1/GLUN3A RECEPTORS. _____	109
FIGURE 35: PHARMACOLOGY OF GLUN1/GLUN3A NMDARs. _____	111
FIGURE 36 eGLYR CURRENTS IN THE ADULT MOUSE BRAIN. _____	117
FIGURE 37 GLYCINE DOSE RESPONSES OF GLUN1 BINDING SITE MUTANTS. _____	131
FIGURE 38 MAGNESIUM SENSITIVITY AND IV CURVE IN GLUN1 F484A/GLUN3A RECEPTORS. _____	132
FIGURE 39 PENTAMIDINE SENSITIVITY AND IV CURVES IN GLUN1/GLUN3A RECEPTORS. _____	134
FIGURE 40 KINETICS OF PENTAMIDINE INHIBITION. _____	135
FIGURE 41 ECHINATIN INHIBITION DOSE RESPONSES IN GLUN1/GLUN3A. _____	136
FIGURE 42 MTSEA ACTIVITY ON GLUN1 AND GLUN3A PORE MUTANTS. _____	138
FIGURE 43 CONTROL EXPERIMENTS FOR MTSEA TREATMENT. _____	140

FIGURE 44 CHARACTERIZATION OF GLUN1 WT/GLUN3A A765C.	142
FIGURE 45 SUMMARY OF MUTANTS TESTED WITH MTSEA.	144
FIGURE 46 D-SERINE STATE DEPENDENCY.	146
FIGURE 47 ZINC EFFECT ON GLUN1/GLUN3A RECEPTORS.	149
FIGURE 48 ZINC EFFECT IN MUTANTS.	150
FIGURE 49 MAJOR RECEPTOR DELETIONS AND MODIFICATIONS.	155
FIGURE 50 GLUN3A DELETIONS AND REORGANIZATIONS.	156
FIGURE 51 CYSTEINE BRIDGES INTERFACES.	159
FIGURE 52 REDUCING AGENT TREATMENT ON WT GLUN1/GLUN3A RECEPTORS AND CYSTEINE MUTANTS.	164
FIGURE 53 WESTERN BLOTS ON CYSTEINE MUTANTS.	167
FIGURE 54 CONTACT MAPS OF LBD INTERADIMER INTERFACE OF GLUN2s CONTAINING NMDARs.	172
FIGURE 55 ACTIVE CONFORMATIONS OF GLUN1/GLUN2s INTRADIMER INTERFACE.	174
FIGURE 56 INTRADIMER INTERFACES OF GLUN1/GLUN2B VS GLUN1/GLUN3A.	175
FIGURE 57 CHIMERIC MUTANTS IN THE INTRADIMER INTERFACE.	179
FIGURE 58 UNNATURAL AMINO ACID CROSSLINK IN NMDARs.	207
FIGURE 59 UAA MUTANTS IN GLUN1/GLUN3A INTRADIMER INTERFACE.	212
FIGURE 60 UAA PEAK CURRENTS AND DESENSITIZATION.	214
FIGURE 61 UV EFFECT ON DESENSITIZATION IN UAA MUTANTS.	214
FIGURE 62 GLUN1 P532 MUTANTS.	216
FIGURE 63 GLYCINE BINDING SITE MUTANT PO.	217
FIGURE 64 LBD-TMD LINKER MUTANTS.	219
FIGURE 65 TRIHETEROMER GLUN1/GLUN2B/GLUN3A EXPERIMENTS.	221

## Outline of Tables

TABLE 1. mGLUR SUMMARY TABLE.	25
TABLE 2 ZINC PROPERTIES AT GLUTAMATERGIC SYNAPSES.	48
TABLE 3 ALLOSTERIC MODULATORS BINDING THE LBD INTRADIMER INTERFACE OF GLUN1/GLUN2 RECEPTORS.	65
TABLE 4 GLUN3A MUTATIONS LINKED TO HUMAN PATHOLOGY.	115
TABLE 5 SUMMARY OF PAPERS AND MAIN FINDINGS ON TRIHETEROMERIC GLUN1/GLUN2/GLUN3A RECEPTORS.	120
TABLE 6 INTERPRETATION OF TRIHETEROMERIC VS DIHETEROMERIC GLUN1/GLUN2/GLUN3A DATASETS.	121
TABLE 7 MTSEA MUTANTS DESCRIPTIVE STATISTICS.	145
TABLE 8 SUMMARY OF NMDAR CONTACT MAPS.	176
TABLE 9 GLUN3A CHIMERIC APPROACH IN LBD INTRADIMER INTERFACE TO RECREATE FULL GLUN2B-LIKE CHARGES PROPERTIES.	177
TABLE 10 SUMMARY OF UAA TESTS IN GLUN1/GLUN3A.	208

## English summary

NMDA receptors (NMDARs) belong to the tetrameric ionotropic glutamate receptor (iGluRs) family. They exhibit a fundamental role in the excitatory glutamatergic neurotransmission, mediating key processes such as synaptic plasticity by long term potentiation (LTP) and depression (LTD), memory formation, and others. During my PhD project, we investigated the structural correlates of the gating mechanism of unconventional NMDAR containing the GluN3A subunit. This subunit assembles with GluN1 as functional excitatory glycine-gated receptors (eGlyRs) that are insensitive to glutamate. Recent data from our lab and others revealed that eGlyRs are widespread in the adult forebrain where they form a novel signaling modality whereby endogenous glycine controls neuronal excitability, circuit function and behavior. Our current knowledge of the structural determinants for GluN1/GluN3A receptors remain very limited however. When exposed to glycine, these receptors mediate small and quickly desensitizing currents, contributing to hinder their characterization for many years. Glycine binding these receptors causes a biphasic activation curve since glycine binding the GluN3A subunits activates the receptor, while glycine binding the GluN1 subunits inhibits it. By taking a structure-function methodological approach (site-directed mutagenesis and 2-electrode voltage clamp recordings in *xenopus* oocytes), we investigated the role of specific regions of GluN1/GluN3A receptors in the control of their gating mechanism. The results of our work can be divided in three main axes:

- 1) We developed a methodology to assess GluN1/GluN3A receptors open probability ( $P_o$ ) allowing evaluation of the effect of mutations on the receptor activity. We also characterized the effect of the open channel blocker pentamidine on GluN1/GluN3A receptor activity, alongside several other agents such as zinc, magnesium, echnatin, and D-serine.

- 2) We created a structural model of GluN1/GluN3A receptors and computed several subunit-subunit contact maps, to determine which sites to target to investigate GluN1/GluN3A function. We aimed at stabilizing specific conformational states by employing several different strategies. We thus attempted to crosslink several interfaces by disulphide bridge formation through cysteine scanning, by employing unnatural amino acids (UAAs) that crosslink upon UV light illumination, or by investigating the role of several domains and loops by performing genetic deletions of large functional portions of the receptors. Unfortunately, we obtained limited success with these approaches.

3) We investigated the role of the putative ligand binding domain (LBD) dimerization interface, that is of critical importance for the gating of all iGluRs but of unknown contribution to GluN1/GluN3A. Thanks to the discovery of large Gain-of-Function (GoF) mutants, we reveal that residues located at the LBD intra-dimer interface are key determinants of the gating behavior, in particular of the low  $P_o$  of GluN1/GluN3A receptors. Mutants that restore the GluN1/GluN2-like hydrophobicity profile, show greatly increased  $P_o$  and glycine affinity. Overall, our data suggest that the GluN3A LBD likely contact GluN1 LBD similarly to other NMDARs, albeit weaker.

Glycine-gated GluN1/GluN3A receptors are generating strong interest for their physiological role in brain signaling recently unveiled. Our understanding of their molecular mechanisms remained sparse however. In the present work, we demonstrated the functional importance of the GluN1-GluN3A LBD intra-dimer interface assembly for the gating of the receptor, highlighting similarities and differences with other iGluRs. We believe that the GoF mutants we characterized offer unique opportunities to further elucidate GluN1/GluN3A receptor gating mechanisms. The molecular tools we validated should be of interest for functional and pharmacological tests in the framework of the physiological and pathological roles of these receptors

## Résumé en français

Les récepteurs NMDA (NMDAR) appartiennent à la famille des récepteurs ionotropiques du glutamate (iGluR). Ils jouent un rôle fondamental dans la neurotransmission glutamatergique excitatrice et dans les processus clés de plasticité synaptique, eux-mêmes critiques pour la formation de la mémoire. Au cours de mon projet de doctorat, nous avons étudié les corrélats structurels du mécanisme de déclenchement du NMDAR non conventionnel contenant la sous-unité GluN3A. Cette sous-unité s'assemble avec GluN1 formant ainsi des récepteurs excitateurs dépendants de la glycine (eGlyR) et insensibles au glutamate. Des données récentes de notre laboratoire et d'autres ont révélé que les eGlyRs sont répandus dans le cerveau antérieur adulte où ils forment une nouvelle forme de signalisation par laquelle la glycine ambiante contrôle l'excitabilité neuronale et certains comportements. Les connaissances actuelles sur les déterminants structuraux des récepteurs GluN1/GluN3A restent cependant très limitées. En présence de glycine ces récepteurs génèrent des courants de faible amplitude et rapidement désensibilisants, ce qui a compliqué leur caractérisation. Les récepteurs GluN1/GluN3A présentent une courbe d'activation biphasique puisque la liaison de la glycine aux sous-unités GluN3A active le récepteur, tandis que la liaison de la glycine aux sous-unités GluN1 les inhibe. En adoptant une approche méthodologique structure-fonction (mutagenèse dirigée et TEVC dans les ovocytes de xénope), nous avons étudié le rôle fonctionnel de régions spécifiques des récepteurs GluN1/GluN3A dans le contrôle de leur mécanisme d'activation. Nous avons ainsi : 1) développé une méthodologie pour évaluer la probabilité d'ouverture ( $P_o$ ) des récepteurs GluN1/GluN3A-WT et mutants. Nous avons également caractérisé l'effet de plusieurs composés : pentamidine, zinc, magnésium, échinatine et D-sérine sur l'activité des récepteurs GluN1/GluN3A. 2) L'analyse de modèles structuraux des récepteurs GluN1/GluN3A a permis de déterminer d'identifier des sites potentiels pour stabiliser des états conformationnels spécifiques. Nous avons tenté de ponter plusieurs interfaces par ponts disulfures et utilisation d'acides aminés non naturels (UAA) photo-réactifs. Nous avons aussi tenté de retirer génétiquement de domaines et boucles du récepteur afin d'en étudier le rôle. Cependant, ces approches ont eu un succès limité. 3) Nous avons ensuite ciblé l'interface de dimérisation du domaine de liaison au ligand (LBD), région d'une importance critique pour l'activation de tous les iGluRs, mais de fonction inconnue chez les récepteurs GluN1/GluN3A. Grâce à la découverte d'un mutant Gain-de-Fonction (GoF), nous démontrons que les résidus situés à l'interface intra-dimère LBD sont des déterminants clés du comportement d'activation, en particulier de la faible  $P_o$  des récepteurs GluN1/GluN3A. Les mutants qui restaurent le profil d'hydrophobicité de type GluN1/GluN2 présentent une  $P_o$  et une affinité glycine considérablement



accrue (>10 fois). Dans l'ensemble, nos données suggèrent que l'interface de dimérisation des LBD chez GluN1/GluN3A joue un rôle clé dans les processus d'activation du récepteur.

Les récepteurs GluN1/GluN3A dépendants de la glycine suscitent un vif intérêt pour leur rôle physiologique dans la signalisation cérébrale qui a été récemment découvert. Dans ce présent travail, nous avons démontré l'importance fonctionnelle de l'assemblage de l'interface intra-dimère GluN1-GluN3A LBD pour l'activation du récepteur, en mettant en évidence des similitudes et des différences avec d'autres iGluRs. Nous pensons que les mutants GdF que nous avons caractérisés offrent des opportunités uniques pour élucider les mécanismes fonctionnels des récepteurs GluN1/GluN3A et leurs rôles physiologiques et pathologiques dans le cerveau. Les outils moléculaires que nous avons validés devraient présenter un intérêt pour de futurs développements pharmacologiques.

## Acknowledgments

This work has been possible thanks to the help I received from many individuals both in my professional and private life. Doing a PhD makes you experience some great moments when you discover new things and enriches you with the friends you make along the way. On the flip side it is difficult, and the support of friends and colleagues is invaluable when the experiments don't work or when you are living a stressful period of time. I would like to use these pages to make some acknowledgments.

First of all, I would like to thank the members of the jury who have accepted to read my manuscript, which is not trivial considering how busy the life of a scientist is. These are Dr. Philippe Rondard rapporteur, Dr. Venien-Bryan Catherine rapportrice, Dr. Martin Horak examinateur, Dr. Martin Picard examinateur, Dr. David Stroebel thesis co-director and Dr. Pierre Paoletti thesis co-director.

I will start by thanking David, who supervised me since the second year of my PhD and took me under his guidance. I simply would not have finished without him, as he was always there when I had a doubt on how to do something, alongside teaching me how to receive feedback and how to perform so many different tasks. He has helped me massively at many stages of the PhD, especially at the end while I was writing the thesis and the manuscript, when I was trying to put all of it together. David might be the most passionate person I have ever met, and I find it astounding how can a person love his job as much as he does. I think we should all take inspiration by him on how curiosity can bring so much wonder in our life.

I am very grateful to Pierre for having accepted me into the team and having believed in me when the experiments were not working very well during my first year of thesis. He is an exemplary scientist with the most rigorous morals, and he rivals David in its passion about science. Even if interacting less on the day-to-day basis, his comments on the work were always insightful and brilliant, showing how the increasingly time-consuming administrative tasks he performs have not tarnished at all his scientific acumen. During the team retreat at Porquerolles he has shown an informal side of his personality I really enjoyed to experience.

I specifically have to thank David, Pierre and Laetitia for taking turns in correcting my drafts of the thesis and digesting a refined product that seems to be readable

My colleagues have been maybe the best part of the PhD. In a scientific lab there is always a degree of turnover of the companions in the lab, and it is always sad to see dear friends depart. I loved working with Mélissa, who has been a true friend other than a great scientist that has helped me on so many

tasks. Allison too, who was very sweet and also helped me during the PhD with the creation of the mutants. Julie who was always in a good mood and willing to help you, Meilin with her absolute kindness. These people left the lab but their traces remain in the building.

My present colleagues: Lara has become a dear friend and has taught me that a scientist does not have to be a nerd, but the opposite. I hope we will remain friends for longtime. Antoine is also a good friend; he is the type of colleague everyone should have in a lab. Chloe has made me laugh uncountable times during the years, she is stronger than she thinks. Laura is a great person, I really liked working and debating with her. Laetitia has shown me how a good scientist is supposed to be, has helped me a lot, and revealed she is very funny at parties. Julia started recently, but I can easily tell she has a bright future ahead of her. I am very happy Cecile is part of the team, she always helps you when she can and is another example of an incredible kind person. I would also like to thank Mariano, Benjamin, Romain, Teddy and Simon. I wish I could talk about the other people in the building whom I really enjoyed working with, but then this text would start resembling too much to a requiem, so I will be brief and say thanks to all of you.

Completing this work would not have been possible without some people that have nothing to do with xenopus oocytes and protein interfaces. I would like to thanks my friends. I have very important friends in Italy which have always been there for me. Some of them traveled more than 1000 km to surprise me in Paris for my birthday when I was too stressed to travel down to Italy. Thanks Mario, Marghe, Alfre, Bianca, Cotti, Gabe, Ivan e Bubi. My climbing partners in Paris are slowly becoming an extended family, as I spend more time with them than I do with the majority of the other people in my life, I cherish you. I have made many friends along the way that I also take with me, both in Paris and in my previous experiences in Maastricht and Haifa.

Finally, thanks to the most important people. Thanks to my biggest fans, my parents who have always supported me throughout this process since the real day 0. Without your help coming in 1000 different forms this would not have been possible. I will be eternally grateful. Thanks to my grandma that has always cared so much for me. And finally thanks to Chiara, my significant other who I have met during my first year of PhD and that has become a fundamental part of my life. She has become my life and travel companion and has been there to listen whenever I needed. She listened willingly to my rehearsals of the presentations even though it must have bored her out of her mind. Thank you.

## **Preface**

The following manuscript details the work I undertook in 4 years of work at the Institut de Biologie de l'École Normale Supérieure, within l'École Normale Supérieure of Paris. I was a PhD candidate within the team "Glutamate Receptors and Excitatory Synapses" whose team leader is Pierre Paoletti. My project was under the jointed supervision of Pierre Paoletti and David Stroebel, who provided guidance for the directions of the work. I undertook a project aimed at studying the structure-function relationships of GluN1/GluN3A NMDARs, trying to uncover their molecular mechanisms controlling this gating. The thesis is divided in two main chapters, an introduction and a result section.

In the introduction, there are 5 main thematic sections. In the first section, I will give an overview on synaptic transmission to give a general overview of neuronal communication of the central nervous system and the main classes of ligand-gated ion channels. In the second section, I focus on the NMDAR family, giving an overview of their physiological role in the CNS, their molecular diversity and a brief excursus on their pharmacology. In the third section, I delve deeper within the NMDAR properties, with a focus on their structure, focusing on their modular architecture and on the inter and intra subunit interfaces that regulate receptor activity. In the fourth section, I try to dissect the current knowledge of the gating mechanisms and the several components that determine this process: receptor open probability, kinetic scheme, allosteric modulation, desensitization and others. Finally, in the last section I will focus on GluN3A containing NMDARs, trying to give an overview of what is currently known about these non-canonical NMDARs, explaining why these receptors show puzzling properties and why there is such a renewed enthusiasm for research surrounding these ion channels.

In the results section, I will talk about the different approaches we took to investigate the molecular mechanisms of GluN1/GluN3A receptors. I will talk about the two main directions undertaken within the project, which are 1) the development of new methodologies and pharmacological approaches to study GluN1/GluN3A receptors and 2) the investigation of the structural correlates of the molecular mechanisms of GluN1/GluN3A receptors. Finally, I will present the draft of a manuscript that we plan to submit for publication in the near future.

# First Chapter: Introduction

## 1 Introduction: Brain transmission, synaptic plasticity and ligand gated ion channels

In the central nervous system, cellular interconnectivity is a requirement necessary for the correct functioning of a complex organism. While employing different receptors, neurotransmitters, and signaling pathways, it is possible to trace common patterns of signal transmission among the various types of cells that populate the brain. It is possible to assign unique functions to distinct anatomical regions due to unique patterns of functional interconnections among different cells, and these interconnection types have proven to be extremely rich in diversity and properties (Kandel, 2001). Indeed, the origin of the signal processed by cells such as neurons of the central nervous system (CNS) is of varying nature, from chemical messengers, to mechanical force to temperature changes to modifications in membrane excitability. Often, neurons communicate with each other within specific cellular compartments which are called synapses (Figure 1 Panels A,D). Within these regions, the terminals of different neurons enter in close contact and can communicate through chemical and electrical inputs. Here, neurotransmitters are released as chemical messengers contained in presynaptic vesicles released by exocytosis (Figure 1 Panel B). These chemical messengers diffuse in the extracellular space and can bind and activate post-synaptic receptors. Various types of receptors can be found within synapses mediating this communication, by acting as sensors embedded in the lipid bilayer of the plasma membrane perceiving the surrounding environment, and communicating to the cell internal milieu (Figure 1 Panel C) (Alberts, 2010).

Within this large variety of receptors, we can distinguish between ligand gated ion channels (LGICs or ionotropic receptors) and metabotropic receptors. While metabotropic receptors have a slower modality of action activating cascades of secondary messengers upon activation, triggering transcription factors in the cell nucleus, LGICs are the key molecular machineries that control the excitability of neuronal cells. LGICs are transmembrane proteins which regulate the flow of ions through the membrane itself when they are activated by chemical messengers such as neurotransmitters. This component of neurotransmission is fast on the millisecond time scale. It is the mechanism allowing conversion of chemical energy into electrical energy and ensuring neuronal communication. For scale, more than  $10^8$  ions per second can pass through the hydrophilic pore of LGICs if these have been gated into an open state. (Alberts, 2010). These channels have been shown to mediate a long list of core brain processes, ranging from the neuronal excitability to complex functions such as learning and decision making (Kandel, n.d.). The correct functioning of LGICs is intrinsic to the brain requirements to sustain adaptation,

modulation of behavior and emotional responses. For these adaptations to be effective, synaptic plasticity has to take place. Activity dependent changes in synaptic function can lead to an increase (long term potentiation, LTP) or decrease (long term depression, LTD) of the synapses. Overall, two major classes of ionotropic receptors exist, one mediating excitatory neurotransmission and one mediating inhibitory neurotransmission. Both types of neurotransmission are fundamental for the fine tuning of synapses and the corrective homeostatic balance of excitation and inhibition in the brain (Kandel, n.d.)

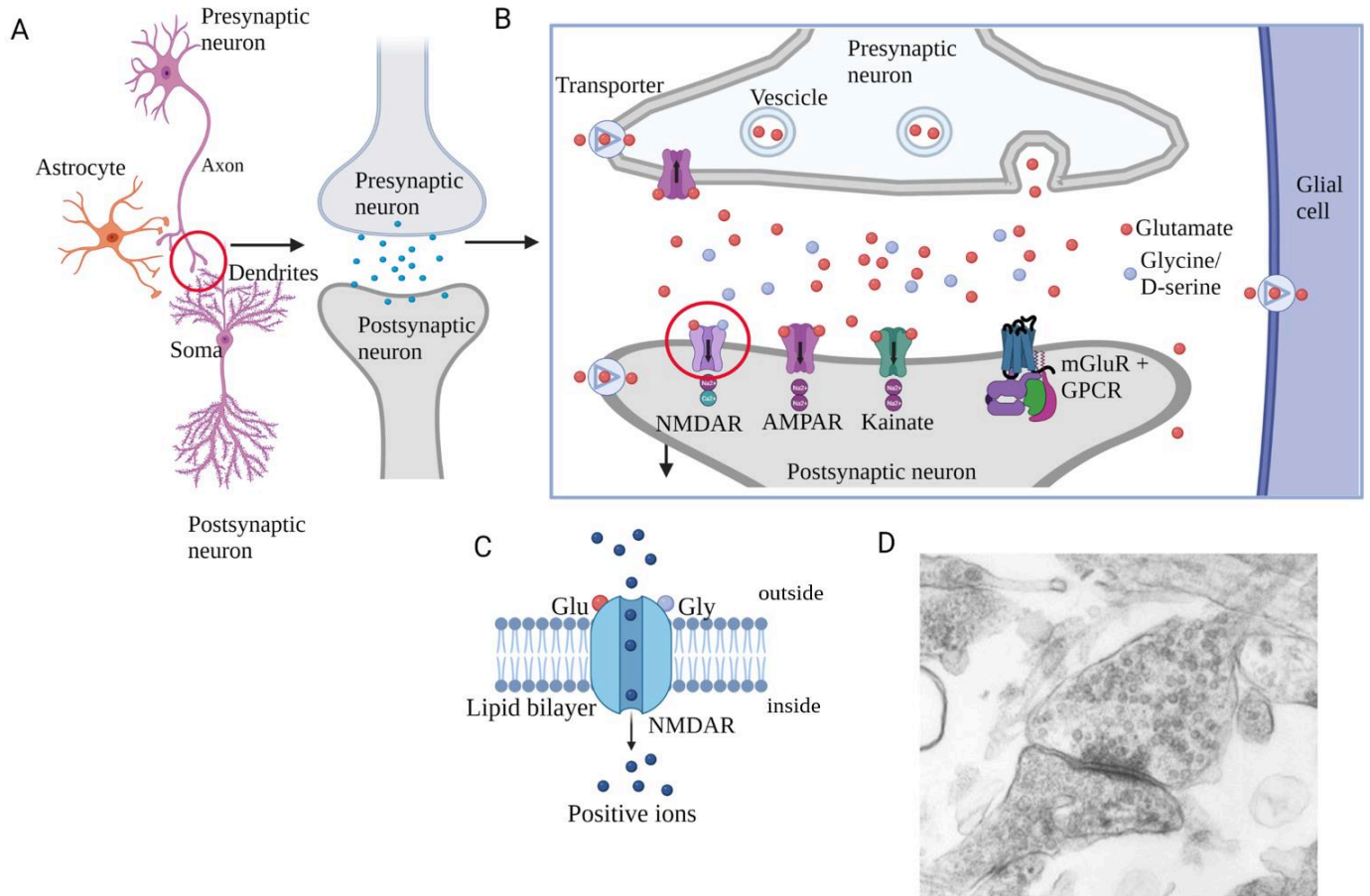


Figure 1 Schematization of the synapse.

Panel A, simplified schematic representation of the main synaptic actors: a pre synaptic neuron, a post synaptic neuron, and a glial cell. On the right, magnification of the area within the red circle where we can see a synapse where the pre and post synaptic neurons enter in close contact. Panel B, schematization of the excitatory synapse where we can see different types of ionotropic and metabotropic receptors being present both pre and post synaptically. Panel C, a schematization of an ion channel (NMDAR) embedded in the plasma membrane catalyzing the passage of positive ions in the cell. Panel D, inset taken from (Reingruber and Holcman, 2011) showing an electron microscopy picture of a synapse showing a synaptic cleft and the two pre and postsynaptic terminals. Created with BioRender.com.

## 1.1 Historical perspectives

It has been known for long time how the body depends on electrical energy to survive. However, the existence of cellular channels came into play much later in the 1840s when German biophysicists theorized that the existence of water pores that could explain the phenomenon of osmosis (Hille *et al.*, 1999). Although rudimental in its details, the idea of channels that could allow passage of small particles within the size of a pore diameter was correct. What was lacking at the time was the methodological tools to further investigate this innovative idea. In 1952, Hodgkin and Huxley published the first quantitative description of the action potential propagation (Hodgkin and Huxley, 1952), a research worthy of Nobel prize award which would pave the way for the exploration of the electrophysiological properties of the nervous system. Within their research, they performed voltage clamp in the squid giant axon, and they highlighted the role of Na<sup>+</sup> and K ions in the dynamics of membrane permeation, indicating how signal can be spread at high speed in the nerve cells (Figure 2 Panel A). Later, the work of Hille and Armstrong built on the idea that some molecular mechanisms of permeation need to exist in order to maintain membrane potentials, and pushed the idea of the existence of dedicated ion channels to the scientific community (Hille, 1978). By working on frog nodes of Ranvier, they characterized the activity of gated, and ion-selective pores that they would name Na<sup>+</sup> channels and K<sup>+</sup> channels (Hille, 1970, 2021). Further understanding of channel function would come thanks to the invention of the patch clamp methodology, allowing single-channel recordings (Hamill *et al.*, 1981). This invention fruited Neher and Sakmann a Nobel prize. With this technological advancement, they showed that opening of ion channel is an all or nothing event in which channel can suddenly shift from a structural state to another (Figure 2 Panel B). Understanding the molecular basis of behavior and brain signaling became successful when biologists started to employ a reductionist approach by employing simple animal models such as the *Aplysia* snail (Kandel, 2001). This allowed to firstly map the connectivity between different areas into a circuitry, and link those to behavior. Incredible advances followed in the upcoming years. Many methodologies that allowed to expand the field are protein cloning, fluorescent tagged proteins, genetic decoding, cell cultures, mutagenic techniques, crystallography, optogenetics, software imaging and bioinformatics and artificial intelligence in computational biology (Hille, 2021). From 1998, the first crystal structures of ion channels started to be available, starting from KcsA, a bacterial K<sup>+</sup> channel with no voltage sensitivity (Doyle *et al.*, 1998). This revolution in recording and imaging of protein structures has been one of the most important advancements for the characterization



of transmembrane channels, and the field still keeps evolving in new directions with the recent surge of cryo-EM microscopy (Figure 2 Panel C).

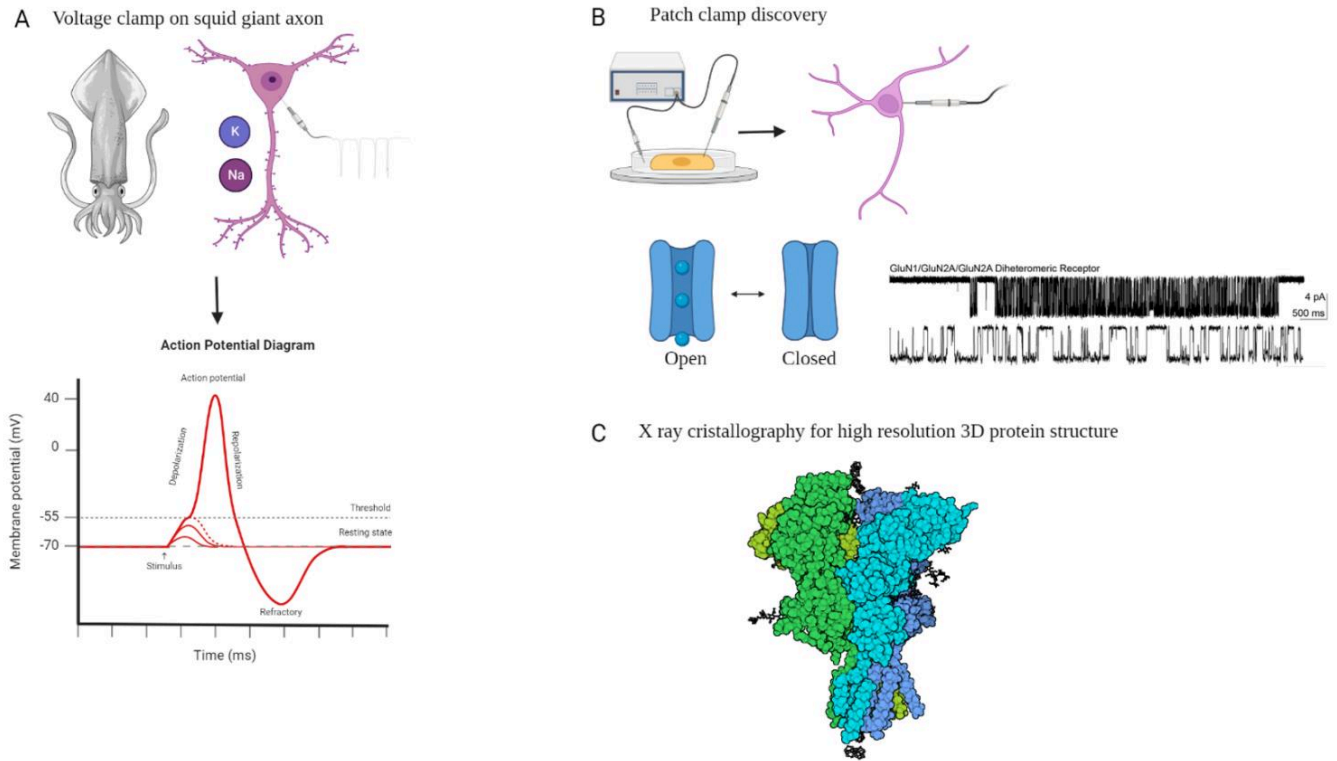


Figure 2 History of research on brain transmission.

Panel A, Hodgkin and Huxley's first quantitative description of the action potential propagation in a living organism: the squid giant axon. They obtained this process by employing a whole cell voltage clamp highlighting the role of sodium and potassium ions in the process. Panel B, Neher and Sakmann's invention of the patch clamp allowed for the first time to isolate and record activity from individual ionic channels. An example of a single channel trace obtained through patch clamp methodology is shown taken from (Bhattacharya et al., 2018), showing NMDAR currents following agonist application. This advancement led to the characterization of the cycling of ion channels through different states with distinct biophysical properties. Panel C, a NMDAR structure (PDB 4pe5) (Karakas and Furukawa, 2014) showing how with X-ray crystallography we are capable of obtaining complete high resolution 3D structures of the same channels that were once considered binary states. Created with BioRender.com

## 1.2 Excitatory and inhibitory neurotransmission

Brain activity rests on finely tuned mechanisms of activation and inhibition of neuronal activity. It is extremely important for this balance in the mammalian brain to be regulated from early stages in

development. For example, imbalances caused by genetic mutations in ion channels that alter their functioning can lead to macroscopic effects such as onset of severe neurodevelopmental disorders such as intellectual disabilities syndromes (see “2.3 NMDARs in pathology and drug development”) (Ghatak *et al.*, 2021). Within these diseases, in many cases the anatomy of the brain is not modified, but symptoms arise from the way in which the neurons communicate with each other, disturbing the overall neuronal network synchronicity (Kirischuk, 2022). This example highlights how a small change at the molecular level can have repercussions affecting the whole network level. There are some major differences between the excitatory and inhibitory components of neurotransmission in the CNS. Excitation and inhibition in the brain can be classified by the type of neurotransmitters employed, by different ion channel families mediating it, and by the type of ions flowing inside the cellular compartment. Usually, within neurons it is possible to find distinct inhibitory and excitatory synapses, where the components of excitatory and inhibitory transmission machinery cluster separately.

Cells usually maintain a certain hyperpolarized potential underlying a difference of voltage between the interior and the exterior of the cell, with the internal milieu resting at about -70 mV when compared to the extracellular space. This potential is never constant, but fluctuates depending if positive or negative ions enter in the cell through the ion channels pores. A key property of the ion channels is the ion selectivity, meaning that when channels enter the open conformation after being activated by a neurotransmitter, only certain types of ions can cross the transmembrane pore and flow inside the cell, while others are blocked outside the cell. The existence of a selectivity filter, which is a very narrow part in the pore of the ion channel, can determine if the type of ions that pass through the channel itself are cations or anions (Alberts, 2010), hence determining if the channel is excitatory or inhibitory in nature. The types of ion influxes mediated by the LGICs are excitatory postsynaptic potentials (EPSPs) or inhibitory postsynaptic potentials (IPSPs), shifting the membrane potential towards depolarization (more positive potential) or hyperpolarization (more negative potentials) (Figure 3). EPSPs are mediated by cations such as Sodium ( $\text{Na}^+$ ) and calcium ( $\text{Ca}^{2+}$ ), while IPSPs are often mediated by chlorine ( $\text{Cl}^-$ ) anions. If a certain threshold of depolarization is reached by the neuron by cationic influx, a chain reaction of rise and fall of membrane potentials called action potential is triggered, propagating spatially the electrical signal alongside the body of a neuron. This spatial and temporal communication constitutes the core of cell-to cell communication in excitable cells within the CNS (Kandel, n.d.).

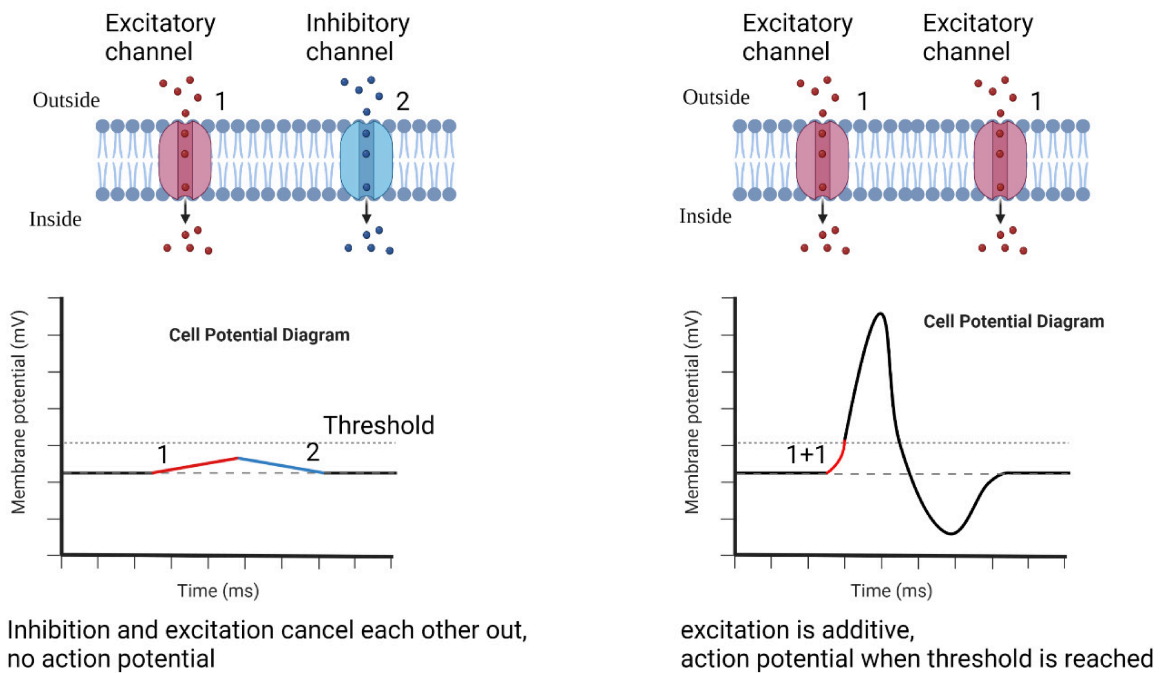


Figure 3 Excitatory and inhibitory neurotransmissions in the neuron.

Schematized comparison between two competing scenarios in which in 1) the excitatory and inhibitory components of EPSPs and IPSPs cancel each other out and the resting membrane potential in a neuron does not reach the action potential threshold, resting at -70 mV, 2) the excitatory components (EPSPs) cause sufficient membrane depolarization to reach the threshold and consequently trigger signal propagation by action potential.

An additional common denominator among excitation and inhibition is also the type of ligand gating the channel. When talking about excitatory transmission, the most important neurotransmitter is surely the molecule glutamate. Its role was highlighted in 1981 (Watkins and Evans, 1981), when the role for the action of this acidic amino-acid was firstly hypothesized, and later demonstrated. The molecules gamma aminobutyric acid (GABA) and glycine mediate the core of inhibitory transmission. In the cerebral cortex, approximately 70%–80% of neurons are glutamatergic neurons, with the remainder comprising GABAergic interneurons (Hanada, 2020). However, in recent years the assumption that neurotransmitter types (such as glycine) determine uniquely inhibitory or excitatory types of neurotransmission has been questioned, and evidence started to accumulate indicating that this distinction might be outdated (Stroebel and Paoletti, 2021; Stroebel *et al.*, 2021). In the next sections we will briefly introduce the main

inhibitory receptors present in the brain before focusing on the main classes of excitatory receptors of the CNS.

### 1.2.1 Inhibitory transmission: GABA<sub>B</sub>, GABA<sub>A</sub>, Glycine receptors

There are two main classes of inhibitory receptors: metabotropic inhibitory receptors and ionotropic inhibitory receptors. Metabotropic GABA<sub>B</sub> receptors are members of the family 3 (or family C) G-protein-coupled receptors (GPCRs). This is a superfamily of receptors which show 7 transmembrane domains coupled to G-proteins, the C group of GPCR. GABA<sub>B</sub> receptors are one of the most important inhibitory receptors in the mammalian brain. They mediate slower GABA responses by activating G-proteins and influencing second messenger systems (Pinard *et al.*, 2010). These receptors assemble as dimeric heterodimers composed by GABA<sub>B(1)</sub> (two variants GABA<sub>B(1)</sub> and GABA<sub>B(1a)</sub>) and GABA<sub>B(2)</sub> subunits, also referred to as GABA<sub>B</sub>R1 and GABA<sub>B</sub>R2. Each GABA<sub>B</sub> is a seven transmembrane spanning protein (Figure 4 Panels A,B). Each subunit fulfills a distinct role, as GABA<sub>B(1)</sub> has a binding site for the neurotransmitter, while GABA<sub>B(2)</sub> binds the G-protein. Their activation, like other metabotropic receptors, leads to a signaling cascade which among other effects reduces the activity of adenylyl cyclase or enhances the production of cyclic AMP. Other effects of GABA<sub>B</sub> activation are suppression of calcium signaling, resulting in hyperpolarization of the membrane potential by opening of K<sup>+</sup> channels (Bettler *et al.*, 2004; Enna, 2007).

Among the ligand gated inhibitory ion channels there are glycine receptors and GABA<sub>A</sub> receptors (Mody and Pearce, 2004). Both of these classes of receptors are chloride permeable channels that contribute to the summation of IPSPs, often located at inhibitory synapses proximal to GABA- or glycine-releasing nerve terminals. Contrary to GABA<sub>B</sub> receptors, both GABA<sub>A</sub> and glycine receptors are heteropentamers containing four transmembrane domains (Moss and Smart, 2001). Glycine receptors assemble from two subunit classes,  $\alpha$  (four isoforms) and  $\beta$  (one isoform). It is thought that the majority of receptors assemble with a ratio of  $\alpha$ 3: $\beta$ 2 (Betz *et al.*, 1999). Ionotropic GABA receptors can be subdivided into GABA<sub>A</sub> and GABA<sub>C</sub> receptors based on their pharmacological properties. GABA<sub>A</sub> receptors have been an intense focus of drug testing research, as they are targets for the site of action for barbiturates and benzodiazepines (Moss and Smart, 2001). GABA<sub>A</sub> receptor subunits can be divided into seven families with multiple isoforms:  $\alpha$  (six isoforms),  $\beta$  (three isoforms),  $\gamma$  (three isoforms),  $\delta$ ,  $\epsilon$ ,  $\theta$  and  $\pi$  (one isoform each) (Figure 4 Panel C). Many differences are present in terms of receptor stoichiometry depending on developmental phases and spatial location in the CNS. Their modalities of assembly are

complex, and determine which receptors can successfully go at the membrane. It has been hypothesized that most GABA<sub>A</sub> receptor subtypes *in vivo* consist of  $\alpha$ ,  $\beta$  and  $\gamma$  subunits. GABA<sub>C</sub> receptors assemble in pentameric complexes from three  $\rho$  subunits that are thought to form homomeric or heteromeric assemblies (Enna, 2007).

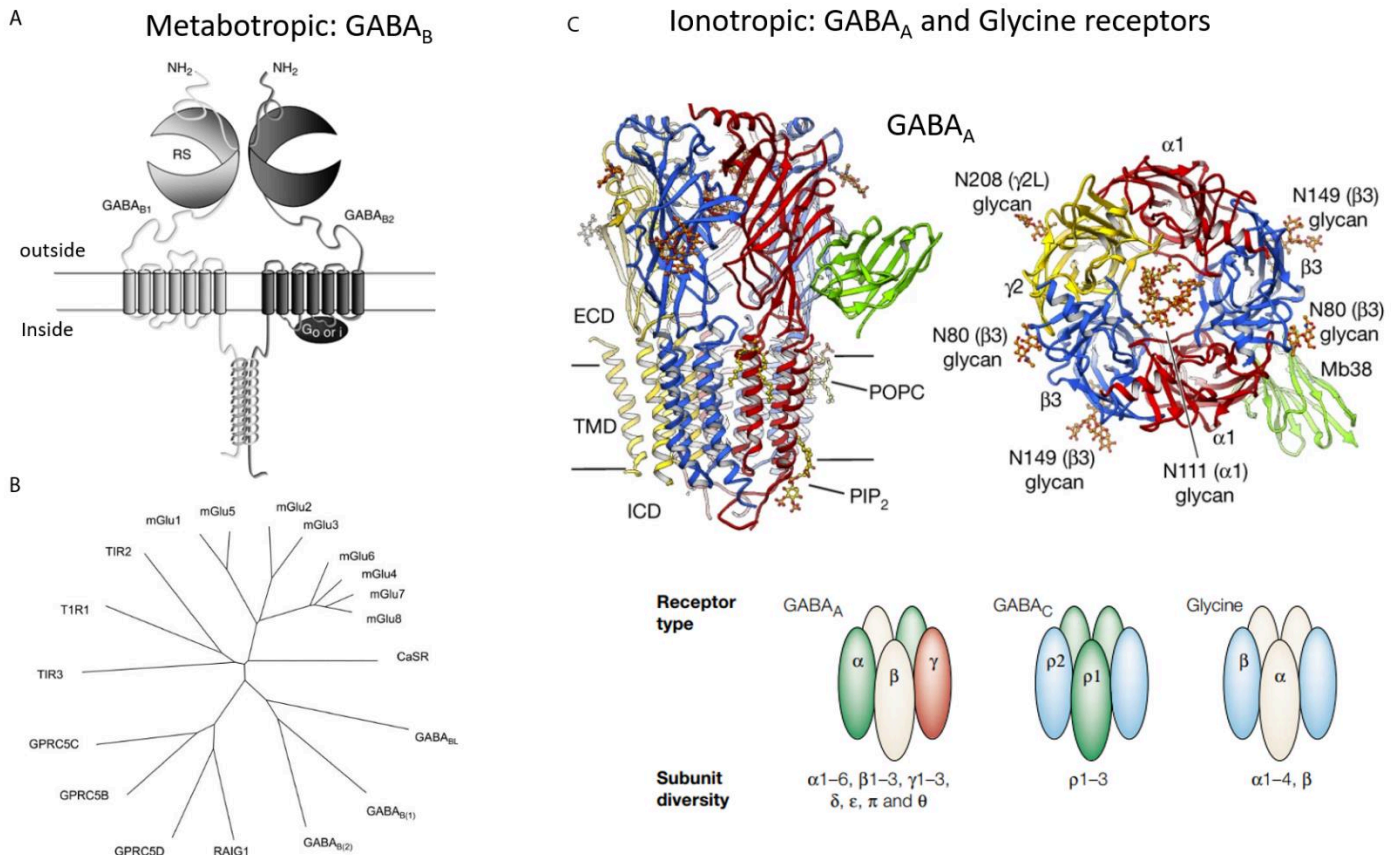


Figure 4 Structure and diversity of inhibitory metabotropic and ligand-gated ion channels.

Panel A, inset taken from (Enna, 2007) showing a schematized structure of the architectural domain of GABA<sub>B</sub> heterodimers containing an extracellular domain, a transmembrane domain and an intracellular C-terminal domain. Panel B, inset taken from (Bettler et al., 2004) showing the phylogenetic tree of human family 3 GPCRs. Within this family we can see both GABA<sub>B</sub> receptors and glutamate sensitive mGluR subunits. Panel C taken from (Moss and Smart, 2001) and (Lavery et al., 2019), showing on top a top and lateral view of the Cryo-EM structure of the GABA<sub>A</sub> receptor  $\alpha 1\beta 3\gamma 2$  receptor-Mb38 complex embedded in a lipid nanodisc in ribbon representation, with glycans and lipids in ball-and-stick representation. On the bottom, schematized structure and existing subunit diversity of pentameric GABA<sub>A</sub> and glycine receptors.

## 1.2.2 Excitatory neurotransmission

In this section we will discuss the main classes of receptors which are activated by glutamate. Excitatory glutamatergic neurotransmission in the mammalian central nervous system (CNS) comprises both metabotropic glutamate receptors (mGluRs) and ionotropic glutamate receptors (iGluRs). We will briefly introduce mGluRs and the various classes of iGluRs before focusing on NMDARs.

### 1.2.2.1 mGluRs

mGluRs (metabotropic glutamate receptors) belong to the family 3 or C group of GPCRs, same as GABA<sub>B</sub> receptors previously discussed (Figure 4 Panel B). Unlike iGluRs, they do not mediate ionic permeation in the cell. When activated by neurotransmitters binding, they trigger biochemical cascades which can cause various modifications of other proteins, including LGICs. They participate in the shaping of synapse excitability, for example by regulating neurotransmitter release (Sladeczek *et al.*, 1993) or modulation of postsynaptic responses (Bonsi *et al.*, 2005) by effectively coupling with G-proteins (Conn and Pin, 1997). mGluRs were discovered later than iGluRs, and at first it was shown how these receptors can stimulate formation of inositol phosphate formation upon glutamate stimulation (Sladeczek *et al.*, 1985; Nicoletti *et al.*, 1986). Cloning of the eight subunits from 7 different genes happened in the 90s (Masu *et al.*, 1991; Conn and Pin, 1997), when it was shown that these receptors assemble and are functional in the CNS. They have been classified in three groups: in Group 1 there are mGlu1 and mGlu5, in Group 2 mGlu2 and mGlu3, while in the last group 3 there are mGlu4, mGlu6, mGlu7 and mGlu8 (Acher *et al.*, 2022) (Table 1).

Group	Receptor/splice variants	CNS expression	Synaptic localization	Signaling pathways of group
Group I	mGluR1 a,b,c,d,e,f Taste mGluR1	Widespread in neurons Taste buds	Predominantly postsynaptic	Phospholipase C stimulation Stimulation of adenylyl cyclase (some systems) MAP kinase phosphorylation
	mGluR5 a,b	Widespread in neurons, astrocytes		
Group II	mGluR2	Widespread in neurons	Presynaptic and postsynaptic	Inhibition of adenylyl cyclase Activation of K <sup>+</sup> channels Inhibition of Ca <sup>++</sup> channels
	mGluR3 GRM3Δ2 GRM3Δ4 GRM3Δ2Δ3	Widespread in neurons, astrocytes		
Group III	mGluR4  Taste mGluR4	Widespread in neurons, High in cerebellum  Taste buds	Predominantly presynaptic	Inhibition of adenylyl cyclase Activation of K <sup>+</sup> channels Inhibition of Ca <sup>++</sup> channels  Stimulation of cGMP phosphodiesterase (mGluR6)
	mGluR6 a,b,c	Retina	Postsynaptic in ON-bipolar retinal cells	
	mGluR7 a,b,c,d,e	Widespread in neurons	Active zone of presynaptic terminals	
	mGluR8 a,b,c	Lower and more restricted expression than mGluR4/7	Predominantly presynaptic	

Table 1. mGluR summary table.

*Inset taken from (Niswender and Conn, 2010) showing the main characteristics of mGluRs, such as their taxonomy, the anatomical expression in the CNS, at the synapse and signaling pathways.*

This grouping refers to several aspects of their function, genetic identity and transduction mechanisms. Group 1 mGluRs are mostly found in postsynaptic dendrites, they are bound by 3,5-DHPG, while activating phospholipase C. This enzyme is important for activating secondary messengers such as inositol-1-4-5-triphosphate which can induce Ca<sup>2+</sup> release when binding endoplasmic reticulum receptors (Watkins and Jane, 2006). Both group 2 and group 3 mGluRs inhibit the activity of adenylyl cyclase. This enzyme is important for production of cyclic AMPc from ATP, which in turn activates the protein kinase A. Hence, this whole process is impaired by the activity of group 2 and group 3 mGluRs. Group 2 is activated by LY354740, while group 3 strongest activator is L-ap. Both groups are mostly located in the presynaptic region. Overall, it is thought that while group 1 increased synaptic activity, while group 2 and 3 modulate negatively synaptic activity. Structurally, mGluRs assemble as dimers. Recently, mGluRs have been shown to co-assemble as both homomeric and heteromeric proteins, increasing the number of potential mGluR dimer combinations (Doumazane *et al.*, 2011). Therefore, the aforementioned classification has to be intended as a schema of mGluR function that does not always

apply. They have a layered domain architecture, similar to GABA<sub>B</sub>Rs (Figure 4 Panel A). The large amino Terminal Domain (NTD) sits on top of the large transmembrane domain (TMD) connected by a cysteine rich domain (Acher *et al.*, 2022). This NTD, like other iGluRs homologues, is comprised of a bi-lobar module connected by a flexible hinge. Upon glutamate binding, the two lobes are thought to undergo large conformation change and close themselves like a venus flytrap (VFT) causing downstream pulling and consequent receptor activation (Koehl *et al.*, 2019). Overall, mGluRs are thought to modulate slow components of synaptic events due to their slow onset of activation (>50 ms) (Attwell and Gibb, 2005). This slow component is most likely a limiting factor in their activatory processes, as mGluRs need to be exposed to prolonged applications of glutamate to be activated (Shen and Johnson, 1997), like a train of pre-synaptic action potentials.

### 1.2.2.2 iGluRs

iGluRs can be defined as a family of transmembrane channels which mediate a common fundamental feature of neurotransmission, the excitatory pathways of neuronal communication. iGluRs are a large family, which comprises numerous classes of channels. These are amino-3-hydroxy-5-methyl-4-isoxazolepropionic acid (AMPA) receptors, kainate receptors, N-methyl-D-aspartate (NMDA) receptors, and GluD (delta) receptors (Hansen *et al.*, 2021; Stroebel and Paoletti, 2021). The division of channels in distinct classes or families was done on the basis of distinct sequence identities and genetic correlations, and how these relate to pharmacological properties (Figure 5 panel A).

If we sum all iGluRs protein types, we have a total of 4 functional classes expressing 18 subunits deriving from 18 functional genes. These are 4 AMPAR subunits (GluA1-4) encoded by GRIA1-4, 5 kainate subunits (GluK1-5) encoded by GRIK1-5, 7 NMDAR subunits (GluN1, GluN2A-D, GluN3A-B) encoded by GRIN1, GRIN2A-D, GRIN3A-B and 2 GluD subunits (GluD1-2) encoded by GRID1-2 (Figure 5 Panel A). All of these functional classes assemble as tetramers, even though each functional class follows its own specific rules of assembly (Figure 5 Panel B). To date, no combinations of iGluR subunits belonging from different functional classes have been found to co-assemble in the rodent brain (Stroebel and Paoletti, 2021). Fundamentally, each iGluR subunit either binds glutamate or glycine, and influence cellular potentials by ion influx (except delta assemblies). Out of the 18 iGluR subunits, five bind glycine (but not glutamate): GluN1, GluN3A-B and GluD1-2 (Stroebel *et al.*, 2021). AMPARs, Kainate receptors and NMDARs all mediate excitatory postsynaptic potentials (EPSPs) with different time courses decays and



kinetics, with the NMDARs being the slowest and AMPARs the fastest (although kainate can display slow kinetics in certain conditions). Together, these channels regulate the excitability of the cell, regulating mechanisms such as synaptic connections, synapse morphology and plasticity. This fine-tuned machinery offers an incredible diversity in terms of synaptic contributions due to the abundance of different temporal and spatial inputs that are provided by the many individual combinations of channel assemblies. Dysfunctions of the iGluR channels are correlated with a large array of pathologies that can arise when the homeostasis between neuronal excitation and inhibition is altered (see 2.3 NMDARs in pathology and drug development). In turn, this fact makes iGluRs an ideal pharmacological target for drug development aimed at curing many of these pathologies, and few drugs targeting iGluRs have been approved by health organization regulators as tools to cure a variety of diseases.

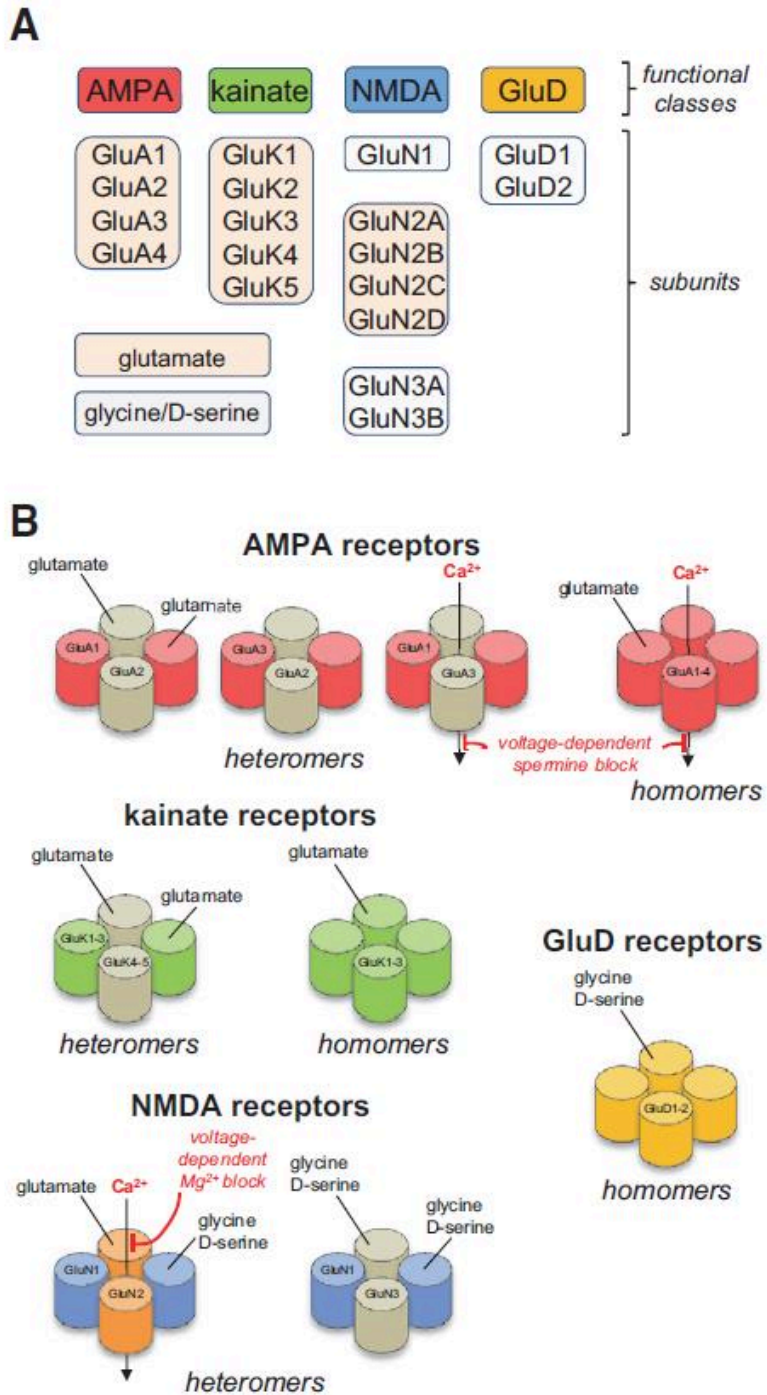


Figure 5 iGluRs functional classes organization.

*Inset taken from (Hansen et al., 2021) showing structural and functional diversity of iGluRs. Panel A, iGluRs can be divided into four functional classes: AMPA, kainate, NMDA, and GluD receptors. Multiple subunits coded by distinct genes have been isolated, each one binding either glutamate or glycine/D-serine. Panel B, subunits from the same functional classes assemble together as functional ion channels, each following specific sets of rules. AMPA receptor subunits can form functional homomers and heteromers, but GluA2-containing heteromers prevail throughout the CNS. Kainate receptor subunits GluK1-3 can assemble as functional homomers and heteromers, but GluK4-5 must coexpress with GluK1-3 to form functional receptors.*

*NMDA receptors are heteromeric receptors with two obligatory GluN1 subunits and two GluN2 subunits (GluN1/2) or two GluN3 subunits (GluN1/3). GluD subunits form homomers, but they do not seem capable of mediating ionotropic signaling.*

#### **1.2.2.2.1 Delta receptors**

Glutamate delta receptors can be distinguished between the two families Delta 1 (GluD1) and Delta 2 (GluD2). These receptors have a much more puzzling function than the other 3 iGluR families, whose roles in synaptic plasticity and development have been extensively dissected by many years of research. This is because delta receptors, although being classified as iGluRs, do not bind glutamate and do not seem to have a functional pore able to carry ions from the extracellular space inside the cell (Andrews and Dravid, 2021). GluD2 receptors are mostly expressed in the cerebellum, while GluD1 receptors can be found in many neuronal populations and synaptic subtypes (Hepp *et al.*, 2015), being especially upregulated in postnatal development (Naur *et al.*, 2007; Andrews and Dravid, 2021). GluD1 seems to be mainly localized at the postsynaptic density of excitatory synapses on pyramidal cells. GluD receptor extracellular domains comprise a distal N-Terminal domain and a Ligand Binding Domain, binding glycine and D-serine. Differently to other iGluRs, GluD receptors do not seem to exhibit “domain-swapping” between NTD and LBD regions (Burada *et al.*, 2020a). These receptors do not show channel opening following ligand binding, but their C-terminal domain seems to be important for synaptic plasticity (Kohda *et al.*, 2013). A naturally occurring mutation in a mouse strain termed “Lurcher”, A654T, causes spontaneous channel openings resulting in membrane constitutive currents in GluD2 (GluD2), indicating that their pore can be functional if key residues are mutated (Hansen *et al.*, 2021). On these constitutive open channels, glycine and D-serine inhibit receptor function, a feature that has been compared to desensitization in the other iGluR families. Interactions between the N-terminal domain of these receptors and perisynaptic proteins such as the cerebellin family are very important in transducing the activation of these receptors to secondary messenger cascades in the cells. Together, delta receptors, neuexin and cerebellin proteins form adhesion complexes forming large transynaptic entities (Cheng *et al.*, 2016).

#### **1.2.2.2.2 Kainate receptors**

Kainate receptors (KARs) are another class of iGluRs which are expressed in the mammalian CNS. They principally affect brain functions such as activity of neural circuits, neuronal excitability and synaptic

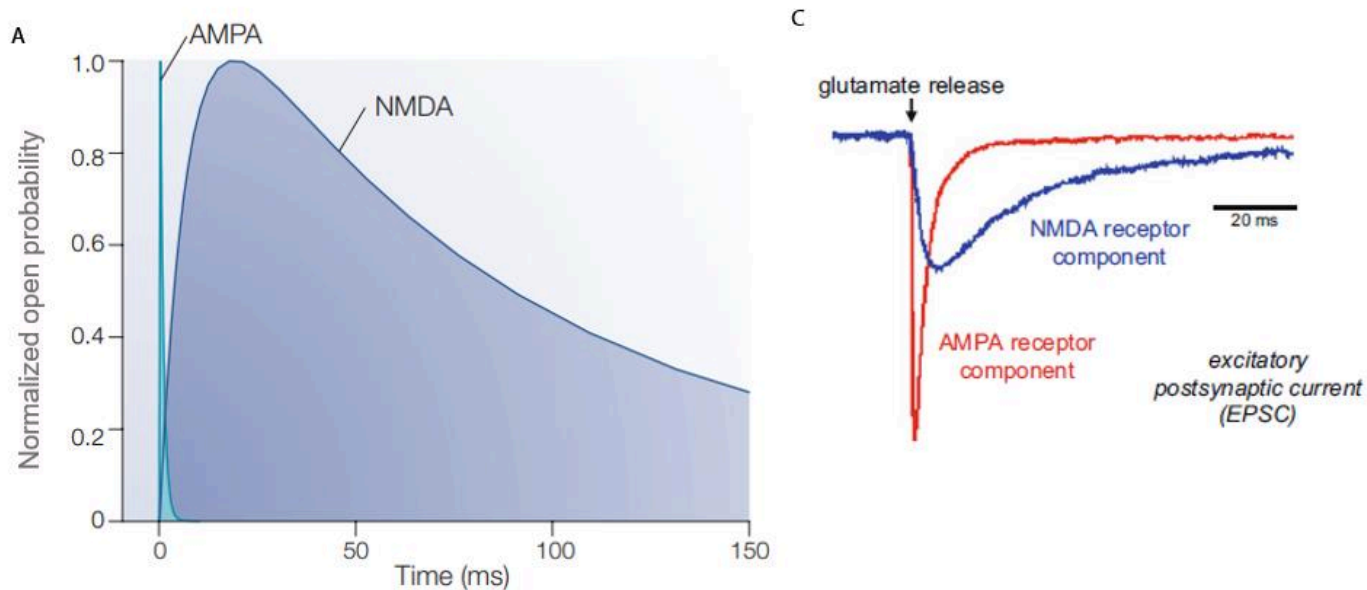
development (Mayer, 2021; Nair *et al.*, 2021). Structurally, they assemble as hetero-tetramers from a pool of 5 genes (GluK1-5) encoded by genes GRIK1-5. GluK1 and GluK3 form functional homomeric or heteromeric receptors, while GluK4 and GluK5 only participate in functional receptors when associating with any of the GluK1–GluK3 subunits (Lerma and Marques, 2013). Further structural diversity is provided by GluK1 and GluK2 RNA editing in the Q/R in the channel pore forming P-loop controls cation permeability (Burnashev *et al.*, 1996). Receptors containing Q/R edited subunits have significantly reduced calcium permeability and lower single channel conductance (Swanson *et al.*, 1996). Functionally, they exhibit low permeability to calcium, and no Mg dependence. They have an intermediate time course in between than AMPARs and NMDARs. Like other iGluRs, functional properties depend on subunit composition, upon assembly in the ER. However, studying of these receptors suffered from a lack of specific agonists that can activate Kainate receptors, as most known agonists also activate other iGluRs like AMPARs. Kainate receptors have been found to have a wide array of interacting proteins like a unique set of PDZ and non-PDZ ligand mediated protein-protein interactions. It is now considered that the function of kainate receptors in physiology has to be considered as an ensemble with their interacting proteins (Lerma and Marques, 2013).

Gating of kainate receptors require both external monovalent cations and anions, as wild-type kainate receptors are entirely unresponsive during recordings performed with solutions lacking external ions (Bowie, 2010). This binding modality also been shown in crystallographic studies (Plested and Mayer, 2007), pointing to a charged ionic binding site in the extracellular domain unique to kainate receptors. The reason for this necessary gating prerequisite remains mysterious, although it has been hypothesized that it may serve as a regulatory brake in situations of intense neuronal activity by stabilizing specific receptor conformations (Plested *et al.*, 2008) (Bowie, 2002; Plested and Mayer, 2007). Desensitization happens extremely fast on the ms scale, but recovery from desensitization after glutamate induced activation in kainate receptors is slower when compared to other iGluRs. This slower conformation transition is due to agonist-stabilized desensitized conformations in the LBD. Kainate receptors have been shown to communicate both via ionotropic signaling and metabotropic signaling (Frerking *et al.*, 2001; Lerma and Marques, 2013). Sustained low-frequency kainate receptor stimulation causes receptor downregulation by endocytosis, while transient stimulation causes a metabotropic biochemical cascade which causes new synthesis of receptors at the membrane (Jane *et al.*, 2009).

### 1.2.2.2.3 AMPARs

AMPA receptors are tetramers composed of four types of subunits (GluA1 to GluA4), and can be either homo- or hetero-tetrameric. The GluA2 subunit seems the most abundantly expressed subunit in the CNS, and the one determining many biophysical properties of these receptors. The expression of the different receptor subunits is developmentally regulated and is brain region specific (Attwell and Gibb, 2005). All individual AMPAR subunits exist in two alternatively spliced versions, flip and flop, which in turn define their biophysical properties. Structurally, the subunits are similar in the extracellular and transmembrane regions, but vary in the CTD (Shepherd and Huganir, 2007). The receptors assemble as dimers of dimers like other iGluRs, but contrary to NMDARs, they are known to associate with several auxiliary proteins like TARPs, which influence receptor properties (Nicoll *et al.*, 2006).

Because of their speed of activation and deactivation, AMPARs can finely tune the synaptic potential of the cells (Huganir and Nicoll, 2013). AMPARs show low permeability to calcium when containing the GluA2 subunit, and no dependence from the magnesium block. They have a lower affinity for glutamate than other iGluRs, also due to the need for their very rapid off-kinetics of glutamate: the  $EC_{50}$  for glutamate ranges from 500 to 2000  $\mu$ M depending on the subunit and the flip/flop editing (Hansen *et al.*, 2021). Few agonists have been identified to be selective for this receptor, as often they also activate kainate receptors. Among those there is the glutamate analog AMPA, which gave the name to the receptor. AMPA receptor turnover at synapses is considered to be a fast and continuous process (Hanada, 2020). Synaptic potentiation and depression are also regulated by alterations in the number of synaptic AMPA receptors. One of the key characteristics is that AMPARs are extremely fast iGluRs, as their activation and deactivation happen on the millisecond timescale (Hanada, 2020) (Figure 6). Another core feature of AMPARs is their extremely quick desensitization. Desensitization occurs in many ion channels, but at different rates (Sun *et al.*, 2002). For AMPARs this process happens on the ms scale (Figure 6). It has been shown that AMPA receptors desensitize from partly and fully liganded closed channel states, as well as from the open state, and by glutamate concentrations much lower than those required for activation (Sun *et al.*, 2002).



B

Table | **Kinetic properties of AMPA and NMDA receptors at room temperature**

Receptor	$k_{on}$	$k_{off}$	$k_{off}/k_{on}$	Steady-state $EC_{50}$	Weighted $\tau_{decay}$
AMPA	$4 \times 10^6 \text{ M}^{-1} \text{ s}^{-1}$	$2,000 \text{ s}^{-1}$	0.5 mM	46 $\mu\text{M}$	0.84 ms
NMDA	$5 \times 10^6 \text{ M}^{-1} \text{ s}^{-1}$	$5 \text{ s}^{-1}$	1 $\mu\text{M}$	0.6 $\mu\text{M}$	150 ms

AMPA,  $\alpha$ -amino-3-hydroxy-5-methyl-4-isoxazole propionic acid; NMDA, *N*-methyl-D-aspartate.  $k_{on}$  and  $k_{off}$  are the rate constants for glutamate binding and unbinding ( $k_1$  and  $k_{-1}$  in the schemes of FIG. 3); steady-state  $EC_{50}$  is the glutamate concentration that activates a half-maximal steady-state current; weighted  $\tau_{decay}$  (the mean of the time constants of each exponential decay component weighted by their amplitudes) was calculated from the kinetic schemes in FIG. 3a and FIG. 3b for a brief pulse of glutamate.

Figure 6 AMPARs and NMDARs compared in their kinetic properties.

Panels A & B, Figures adapted from (Attwell and Gibb, 2005). Time courses of AMPARs and NMDARs gating properties following a brief pulse of agonist application 0.3 ms of 1 mM glutamate application. In Panel B, a table comparing the main parameters of receptor gating in NMDARs and AMPARs. Panel C adapted from (Burnashev and Szepietowski, 2017) comparing EPSCs time courses contributions of NMDARs and AMPARs. The NMDA receptor-mediated component is isolated in the absence of  $Mg^{2+}$  using the AMPA receptor antagonist CNQX, whereas the fast AMPA receptor-mediated component is isolated using the NMDA receptor antagonist AP5. The original figure is adapted from (Traynelis et al., 2010)



## 2 Introduction to NMDARs

NMDARs are ligand-gated ionotropic channels that are central in the functioning of the central nervous system. They exhibit a fundamental role in excitatory glutamatergic neurotransmission, mediating key processes such as synaptic plasticity, memory formation, neural development, learning, and others (Paoletti *et al.*, 2013; Hansen *et al.*, 2021). Structurally NMDARs are tetramers, co-assembling subunits from a pool of 7 genes. The subunit GluN1 is the only one necessary for co-assembly, in combination with four possible different GluN2 subunits (GluN2A-D), or with two GluN3 subunits (GluN3A-B) (Cull-Candy and Leszkiewicz, 2004; Ulbrich and Isacoff, 2008) (Figure 7 Panels A,B). Subunit composition determine unique biophysical and pharmacological properties of NMDARs, and interaction with local regulatory proteins. Furthermore, expression levels for the different subunits vary depending on anatomical localization and developmental stages, providing a rich variety of NMDAR subtypes that finely tune synaptic and circuit adaptability in the CNS (Paoletti *et al.*, 2013; Hansen *et al.*, 2021) (Figure 7 Panel B).

Individual NMDAR subunits are arranged through a modular architecture in which different domains perform different tasks. Modules have been hypothesized to have developed specialized functions, such as ligand binding, transmembrane ion transport, allosteric modulation, interprotein interactions or others. The domain architecture of NMDARs, and in general of all iGluRs, can be divided in two main realms, the extracellular region and the intracellular region. Each individual subunit of NMDARs displays in the extracellular space a N-terminal domain (NTD), a single linker connecting the NTD to the ligand binding domain (LBD), while the LBD further connects to the transmembrane segment of the TMD pore region through another three small linkers (Figure 7, Figure 12). Finally, a flexible C-terminal domain extends intracellularly (see chapter: “3 Receptor architecture: modular design”).

In the LBDs GluN1s and GluN3s bind glycine or D-serine, and GluN2 subunits bind glutamate (Lee *et al.*, 2014). Upon agonist binding, the double clamshell-like extracellular regions undergo structural rearrangements to activate the receptor. The transmembrane domain (TMD) forms a pore blocked by magnesium at resting potential, while the intracellular C-Terminal Domain (CTD) interacts with auxiliary proteins while anchoring the receptor to the membrane (Figure 7 Panel C) (Paoletti, 2011; Stroebel *et al.*, 2014). While our knowledge of “classical” glutamatergic GluN2-containing NMDARs has greatly increased in the last decades, the role of GluN3 subunits in the larger NMDAR picture has been puzzling. In the next sections, I will briefly introduce the key characteristics of NMDARs, focusing on their



physiology, ontogenetic profile, their role in pathology and the main classes of drugs targeting this family of receptors.

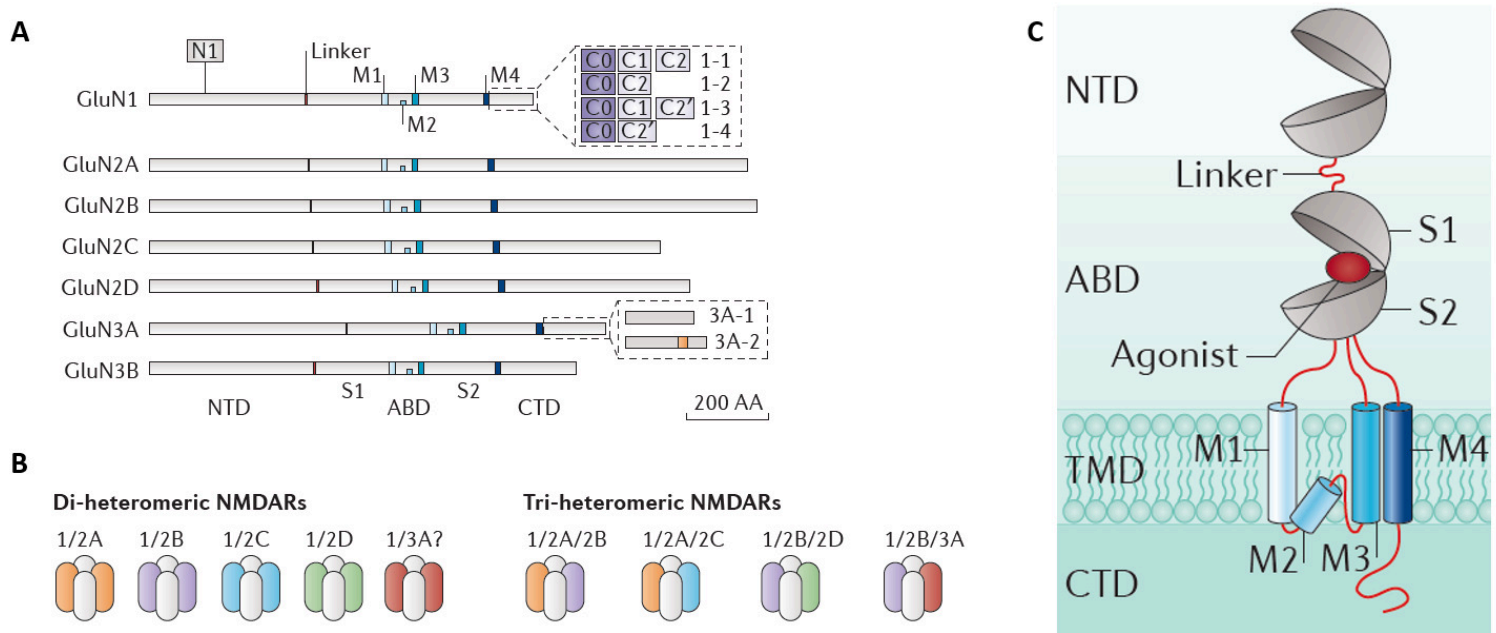


Figure 7 NMDAR subunit diversity and structure.

*Inset taken from (Paoletti et al., 2013). Seven NMDAR subunits coded by 7 different genes are shown: GluN1, GluN2A–GluN2D and GluN3A and GluN3B. Subunits can also be differentiated by alternative splicing of GluN1 and GluN3A subunits via multiple cassettes in the CTD. M1–M4 indicate transmembrane segments. Panel B, different types of populations of co-expressing NMDARs that are thought to exist in the CNS are shown. Both di-heteromeric and tri-heteromeric channels can functionally assemble, always with two GluN1 subunits present. Panel C, Schematized drawing showing that all GluN subunits share a layered modular architecture that is made of four distinct domains the NTD (Amino-Terminal Domain) in the top layer, the LBD (Ligand Binding Domain) layer in the middle, the TMD (Transmembrane Domain) layer below embedded in the phospholipid membrane, and at the bottom the CTD (C-Terminal Domain). Extracellular regions have a clamshell like aspect. The NTD is important for allosteric modulation, influencing open probability of the receptor. The LBD binds the agonist and is necessary for activation of the receptor. NMDARs can undergo different structural re-arrangements following ligand binding or allosteric modulation, which influence many inter-subunit contacts and conductive properties at the pore.*

## 2.1 Developmental and regional expression

Different stoichiometries of NMDAR assemblies can be found in different spatiotemporal profiles depending on developmental phases and brain regions. The subunit GluN1, being the only subunit mandatory for assembly is expressed ubiquitously in the brain and at all developmental stages, from the embryonic stage. However, differences concerning the expression of the many GluN1 splice variants apply both to development and to regional patterns. To give an example, GluN1-1a can be found as the

predominant type in CA1 cells within the hippocampus, while GluN1-1b predominates exclusively in CA3 cells (Laurie and Seeburg, 1994; Paoletti *et al.*, 2013). The GluN2 subunits developmental profile varies with time. In embryonic stages, GluN2A and GluN2C are poorly expressed throughout the whole CNS, while GluN2B and to a lesser extent GluN2D are abundant (Figure 8). Within the normal development of an organism, expression of the subunit GluN2A starts right after birth and takes the place of the subunit GluN2B as the dominant GluN2 subunit in the majority of brain regions. This process is called the developmental switch of GluN2A over GluN2B. In adolescents or adults, the GluN2A subunit is ubiquitously expressed in the CNS, while GluN2C expression is restricted to areas like the cerebellum, the brain stem and the olfactory bulb, or within the astrocytes (Figure 9). Following birth, the expression of GluN2D subunit is downregulated and its expression becomes restricted to regions such as the diencephalon or the mesencephalon, for example in regions such as the thalamus. GluN2B, in turn, is maintained at high levels but sees its expression becoming restricted to the forebrain (including cortex and hippocampus).

It has been hypothesized that GluN1/GluN2B assembly might be found more at extra synaptic locations, while GluN1/GluN2A or GluN1/GluN2A/GluN2B might be found more clustering post-synaptically, colocalizing in proximity of AMPARs (Köhr, 2006). NMDARs are also found pre-synaptically, with the majority in the developing cerebral cortex containing the subunit GluN2B (Mameli *et al.*, 2005; Bouvier *et al.*, 2015). However, this is probably a simplification, as differences exist at anatomical and developmental stages. The expression of the GluN3A and GluN3B subunits is discussed later (see “5.2 GluN3A expression: anatomical and developmental aspects, cell types specificity and subcellular localization” and “5.9 GluN3B”). Cell specificity is another characteristic of NMDAR subunits. For example, GluN2C and GluN2D are respectively are expressed in hippocampal and cortical interneurons but are barely expressed in principal cells (Paoletti *et al.*, 2013) (Figure 9). In addition, these differences can be synapse specific, as in another example GluN2B is present in hippocampal neurons at the CA3 synapse, where it relays neurotransmission from the perforant path and neighboring CA3 cells, but is barely detected at mossy fiber synapses (Fritschy *et al.*, 1998)

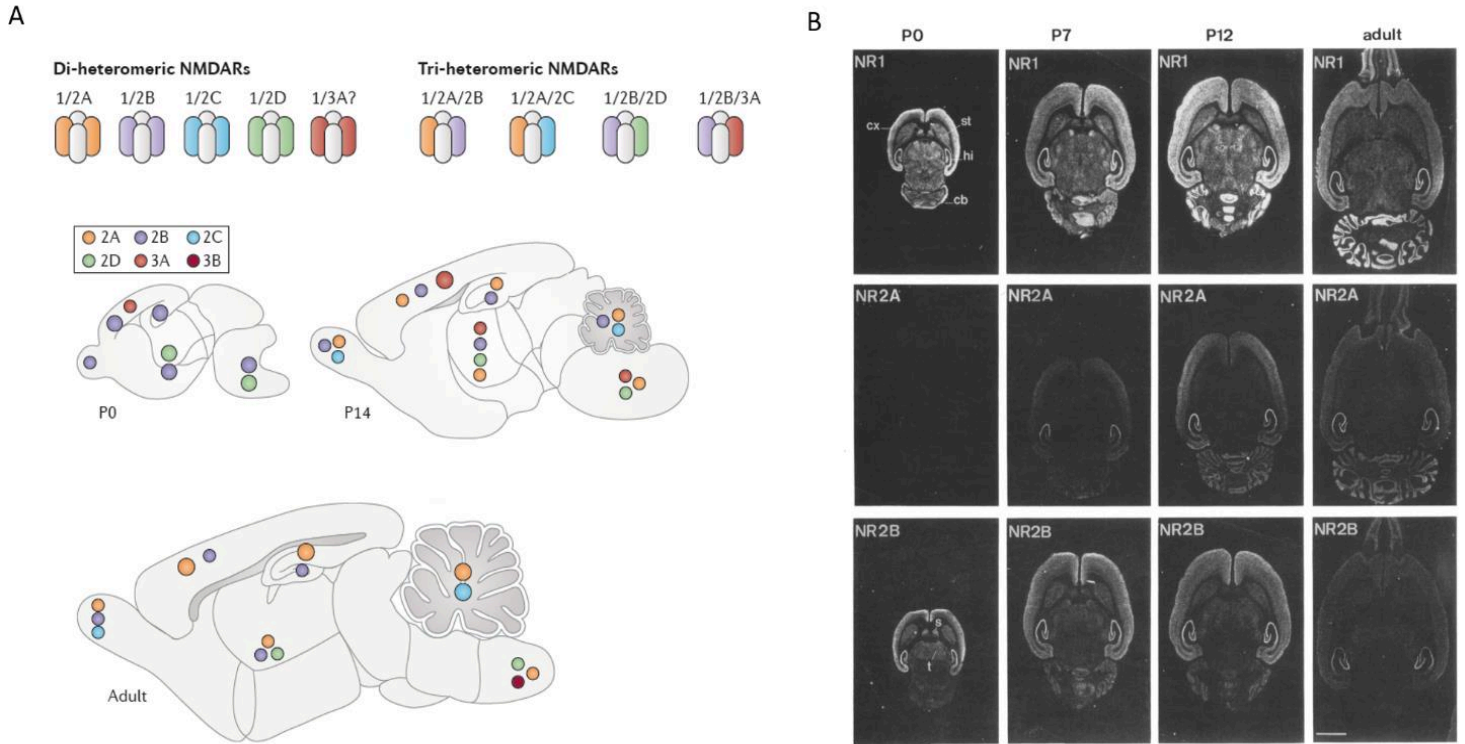


Figure 8 NMDAR developmental and regional expression.

Images obtained and modified from (Monyer et al., 1994; Paoletti et al., 2013). Panel A, representation of the various populations of di-heteromeric (identical GluN1 and GluN2 subunits) and tri-heteromeric (different GluN2 subunits) NMDARs that have been documented to exist in the CNS. Below, expression of GluN1, GluN2A and GluN2B subunits are shown being expressed differently according to their developmental profile in the mouse brain at 3 stages: day of birth (postnatal day 0 (P0)), 2 weeks following birth (P14) and at the adult stage. Panel B, distribution of the GluN1, GluN2A, and GluN2B subunit mRNAs transcripts in horizontal rat brain sections from P0, P7, P12, and adult animals. Abbreviations: cb, cerebellum; cx, cortex; hi, hippocampus; s, septum; st, striatum; t, thalamus.

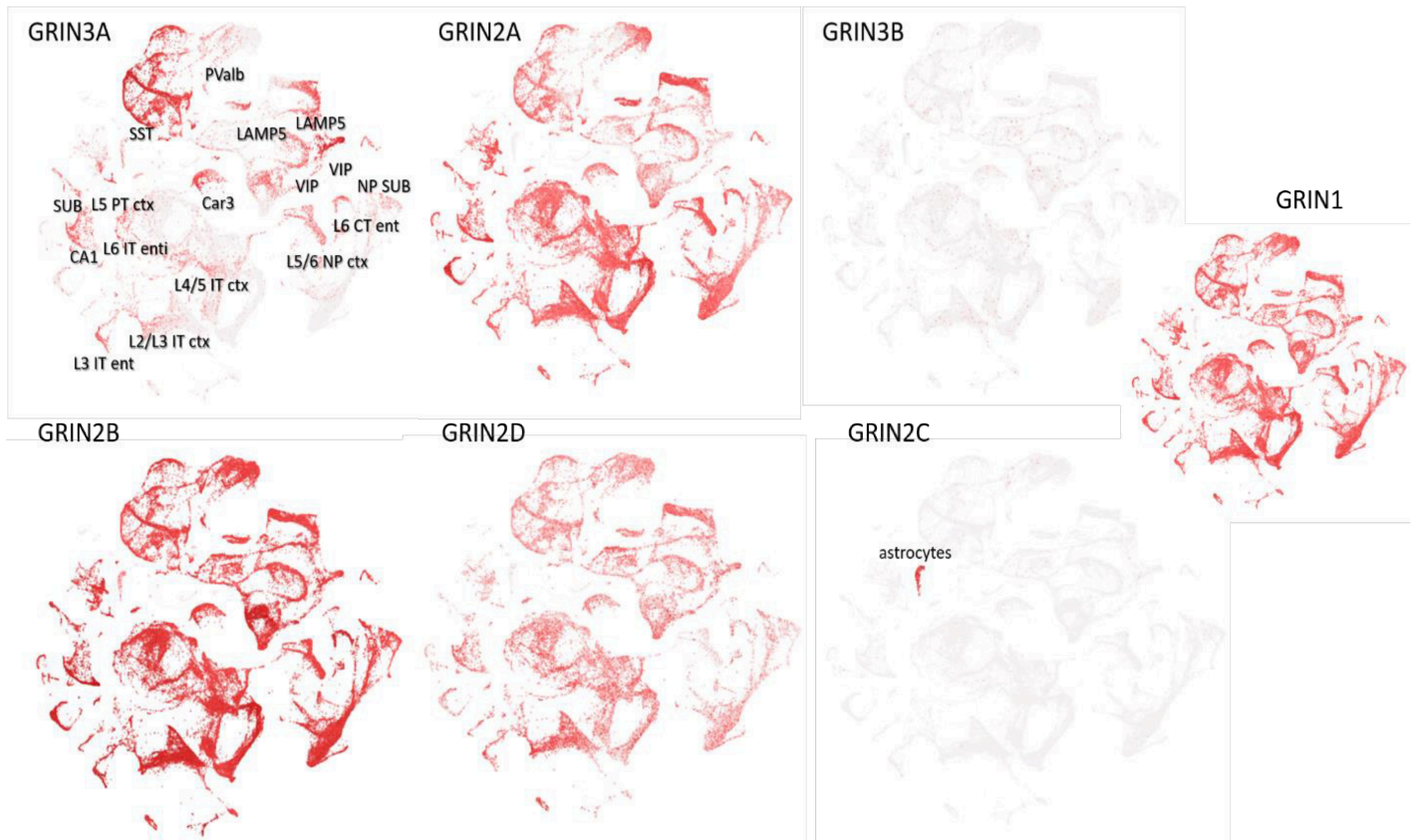


Figure 9 Comparison among GRIN genes expression levels in the rat forebrain.

Single cell (or single nucleus) RNA sequencing (RNA-Seq) in the Allen Brain atlas project "WHOLE CORTEX & HIPPOCAMPUS - SMART-SEQ (2019) WITH 10X-SMART-SEQ TAXONOMY (2021)" with-Smart-Seq Taxonomy. Samples were collected from dissections of brain regions from ~8-week-old male and female mice. Cells were then separated by principal component analysis. Filters were applied to compare side by side GRIN1, GRIN2A, GRIN2B, GRIN2C, GRIN2D, GRIN3A, GRIN3B. For GRIN3A, markers for classification of neurons and interneurons of excitatory and inhibitory cells used in transcriptomic studies to ease identification of cell types in the CNS have been added.

It has been hypothesized that the majority of NMDARs in the adult brain in the excitatory synapses might be triheteromers containing GluN1-GluN2A-GluN2Bs (Al-Hallaq *et al.*, 2007). These triheteromers have been studied in the last decade, as new methodologies in molecular engineering have been developed to express them selectively in heterologous expression systems (Hansen *et al.*, 2014; Stroebel *et al.*, 2014). Remarkably, their biophysical and pharmacological properties resemble more closely that of GluN1/GluN2A receptors than that of the GluN2B counterparts. Their assembly follow the same arrangement of dimer of dimers like it has been observed for diheteromeric receptors (Yi *et al.*, 2019). However, their coupling to intracellular signaling partners might be more mediated by GluN2B.

## 2.2 Function in physiology

NMDARs have been described as coincidence detectors. At cellular resting potentials (around -70 mV), NMDARs are physiologically inhibited by extracellular levels of  $Mg^{2+}$ . For the gate to open and ions to flow through, several conditions need to be satisfied. First, simultaneous binding of glycine or D-serine to GluN1 and glutamate to GluN2. Secondly, relief of the magnesium block. The relief can happen when the neuron is depolarized by either activation of neighboring kainate or AMPA receptors, or if there is back propagation of an action potential (Hansen *et al.*, 2021). Therefore, the coincidence detection property of NMDARs refers to both the presynaptic release of glutamate activating NMDARs and the post synaptic depolarization that relieves the  $Mg^{2+}$  block.

NMDAR currents have a slow time course of deactivation allowing large quantities of  $Ca^{2+}$  inside the cell. NMDARs can thus trigger many intracellular signaling pathways, effectively altering the plasticity and synaptic efficacy of the neurons. Coincidence detection and strong bursts of activity in short periods of time can lead to NMDAR activation and consequent long-term plasticity of the synapses. NMDAR mediated transmission is paramount in regulating key aspects of neuronal circuit function: synaptic plasticity, temporal summation and membrane excitability. The activity of NMDARs causes changes within the synapses that alter the morphology of the cell, shaping its properties with time (Paoletti *et al.*, 2013). NMDAR activated with high frequency stimulation can cause long term synaptic plasticity (LTP) at glutamatergic synapses by causing changes in numbers and subunit compositions of postsynaptic AMPA receptors and by remodeling the synaptic morphology of cells (Nicoll, 2017). Other consequences of NMDAR mediated LTP are changes of NMDAR composition, exocytosis of NMDARs, lateral movement of NMDAR channels and potential changes in AMPAR  $Ca^{2+}$  permeability (Traynelis *et al.*, 2010; Paoletti *et al.*, 2013). One common factor of NMDAR LTP is an increase of intracellular  $Ca^{2+}$ , also associated with the activation of group I mGluRs or adenosine 2A receptors. LTP can be somehow considered an umbrella term, as there are multiple terms of synapse remodeling. Many variables to take into consideration when talking about LTP are the synapse type, the type of stimulation, the age of development and others. One of the most well studied forms of LTP refer to the changes happening at CA3 to CA1 hippocampal synapses, and at mossy fiber to CA3 pyramidal cells (Nicoll and Schmitz, 2005). At the CA3-CA1 synapse, LTP is dependent on NMDAR activity, and typically post-synaptic, while at Mossy fibers-CA3 LTP is mostly pre-synaptic and NMDAR independent (Paoletti *et al.*, 2013).

NMDAR long term depression (LTD) refers changes mediated via NMDARs that trigger a plasticity opposite to LTP, i.e., a reduction in synaptic efficacy. Low frequency stimulation protocols are used *ex vivo* to simulate LTD changes mediated via NMDARs in many regions of the brain. LTD can lead to cell internalization of NMDARs, and it has been observed at Mossy Fibers-CA3 and CA3-CA1 synapses (Montgomery *et al.*, 2005; Jo *et al.*, 2010). Destabilization of the postsynaptic scaffold, concomitant with lateral displacement of GluN2A-containing NMDARs away from synaptic sites has also been described as LTD-related mechanisms (Morishita *et al.*, 2005; Peng *et al.*, 2010).

Since many of the changes in synaptic plasticity depend on the amounts of intracellular  $Ca^{2+}$  that permeate the cell, subunit composition is a key determinant in regulating how NMDARs can influence LTP processes, as different NMDAR subtypes have different deactivation time-course. Therefore, different subtype mediated charge transfer properties cause different postsynaptic  $Ca^{2+}$  increase. There has been a large debate over if the subunit composition of NMDARs dictates whether LTP or LTD is produced. Much evidence points to GluN2A having a direct role in synaptic plasticity, both pharmacologically and genetically. (Paoletti *et al.*, 2013). GluN2A knockout mouse lines have severely impaired LTPs (Sprengel *et al.*, 1998). Contrarily, GluN2B specific antagonists seem to inhibit LTD, and knockout GluN2B mice line have impaired LTDs (but also LTP) (Brigman *et al.*, 2010). This evidence points to a direct role of GluN2B in mediating LTD processes. However, much contradicting evidence exists, with some studies implicating GluN2B for LTP processes, but not for LTD (Berberich *et al.*, 2005; Paoletti *et al.*, 2013), suggesting that the dichotomy GluN2A-LTP and GluN2B-LTD is most likely a large oversimplification. Overall, there seems to be no simple rule relating unique NMDAR subunits to the direction of synaptic plasticity, also because of confounding variables such as differences in induction protocols and anatomical region analyzed in different studies. In triheteromers and mixed populations, it has been hypothesized that GluN2A and GluN2B work together, with the GluN2A subunit being important for maximizing calcium influx, while the GluN2B subunit providing structural functions due to its interactions with signaling proteins such as the CaMKII, essential for memory formation and the induction of synaptic potentiation (Paoletti *et al.*, 2013). A theory reconciling part of the discrepancies of the literature postulates that LTP might be mediated by GluN1/2A/2B tri-heteromers (Hansen *et al.*, 2021).

### 2.3 NMDARs in pathology and drug development

As mentioned previously in the excitation and inhibition section, the correct functioning of ligand-gated ion channels is of paramount importance to maintain the correct homeostasis in the brain between excitation and inhibition. Therefore, it is not surprising that dysfunctions in NMDARs have been linked to a spectrum of neurodevelopmental disorders. Both hypo-activity and hyper-activity of NMDARs have been found to be correlated with pathological states. Interestingly, NMDAR genes in humans are among the most intolerant to variations pointing to their critical importance (Endele *et al.*, 2010; Stroebel and Paoletti, 2021). Modifications have often been linked to a large number of neurodevelopmental disorders (Swanger *et al.*, 2016). Together, malfunctioning mutated receptors may exhibit altered gating, expression or interactions with other proteins. This results in pathologies such as childhood epilepsies and encephalopathies associated with cognitive deficits or pathologies such as schizophrenia and autism spectrum disorder (Traynelis *et al.*, 2010). Furthermore, NMDARs have also been linked more indirectly with depression, stroke, traumatic brain injury, Parkinson's disease. Several reviews have been written on this topic (Lakhan *et al.*, 2013; Zhou and Sheng, 2013; Liu *et al.*, 2019), and for sake of shortness, we will only give few examples of the role and which drugs targeting NMDARS are currently used in medical practice.

Single point mutations in NMDARs can lead to malfunctioning channels which cause excitability problems both in the cell and at the whole network level. Recent genetic wide association studies (GWAS) and linkage analysis in epilepsy-patients, as well as other neurological disorders, have characterized over 300 inherited and de-novo mutations found within different domains of the GRIN genes (Endele *et al.*, 2010; Swanger *et al.*, 2016; Xu and Luo, 2018). Several studies have identified a direct causal role of GRIN2A mutations in young patients diagnosed with a subset of similar epileptic disorders called epilepsy-aphasia spectrum (Carvill *et al.*, 2013; Lemke *et al.*, 2013; Lesca *et al.*, 2013). Mutations within GluN subunits can lead to changes in glutamate or glycine affinity, current density, magnesium sensitivity, zinc sensitivity and/or variations in surface expression levels (Yuan *et al.*, 2014; Serraz *et al.*, 2016; Platzer *et al.*, 2017). Whereas the gain-of-function of GluNs can, intuitively, explain the apparition of seizures (by producing excessive channel-activity and unwarranted depolarization of the neuron), many of the observed mutations in the GluN2A LBD do quite the opposite, explicitly cause a decrease in channel function and expression levels, while still causing an epileptic phenotype (Addis *et al.*, 2017). It has been hypothesized that compensatory changes at the network level might be causing the epileptic phenotype, alongside the effect of NMDARs on inhibitory interneurons.

Another pathological condition caused by aberrant activity of NMDARs is excitotoxicity, and their roles in neurodegeneration within pathologies such as Huntington's, Alzheimer's or Parkinson's disease has been highlighted (Dong *et al.*, 2009). Specifically, the GluN2B subunit has a pro-apoptotic role that has been hypothesized to have a role within each one of these disorders. Hence, drugs that limit excitotoxicity mediated by NMDARs, and that display subunit specificity, have a lot of potential for treatment in humans (Reinert and Bullock, 1999), although with limited success in clinical trials so far. There are only few drugs targeting NMDARs that are currently commercialized or that show potential for drug development. The NMDA receptor open channel blocker memantine has been approved as a therapeutic for Alzheimer's disease in the early 2000s to limit neuronal death (Hansen *et al.*, 2021). Finally, amantadine a low-affinity NMDAR channel blocker which is prescribed against L-DOPA-induced dyskinesia in Parkinson disease (AlShimemeri *et al.*, 2020). Recently, ketamine has received a lot of attention in the scientific community. This drug is an open channel blocker that was approved as an anesthetic in 1970s, and that is showing great potential against severe treatment-resistant depression (Yang *et al.*, 2018), especially for its rapid antidepressant effects.

## **2.4 Pharmacology of NMDARs**

### **2.4.1 Orthosteric agonists**

The majority of iGluRs are activated by glutamate, which is the main excitatory neurotransmitter of the brain. In NMDARs, all four GluN2 subunits bind glutamate, although with different affinities (Figure 23). The GluN2D subunit has the lowest EC<sub>50</sub> (i.e. highest affinity) for glutamate, followed by GluN2C, GluN2B and GluN2A (Erreger *et al.*, 2007). Other endogenous agonists acting on the GluN2 subunits are D- and L-aspartate, homocysteate, and cysteinesulfinate (Paoletti *et al.*, 2013; Hansen *et al.*, 2021). All GluN2 subunits have a highly conserved glutamate binding pocket, and differences in affinities for the agonist are influenced by the NTD and its interdomain interactions with the LBD (Yuan *et al.*, 2009). For a successful gating of NMDAR channels, both GluN1 and GluN2 subunits need to be activated at the same time by glutamate and glycine or D-serine.

A number of iGluR subunits do not bind glutamate but glycine. Glycine is traditionally associated with GABA as mediating core inhibitory neurotransmission in the brain. Among iGluRs, canonical NMDARs require glycine or D-serine binding in addition to glutamate binding as a necessary step for



receptor channel gating receptors. This co-agonism is unique among neurotransmitter receptors. Others iGluRs do not require glutamate at all to activate, this is the case of delta receptors (Kakegawa *et al.*, 2011) GluN1/GluN3 NMDARs (also known as excitatory glycine receptors) (Chatterton *et al.*, 2002). Among all the 18 mammalian iGluR subunits, a total of 5 (GluN1, GluN3A-B, GluD1-D2) are insensitive to glutamate, and bind glycine or D-serine (Stroebel *et al.*, 2021) (Figure 10). The agonist binding pockets of the glycine binding iGluR subunits lack residues located in the D2 lobe to stabilize a distal carboxylate group found in glutamate. However, in the D1 lobe, glycine binds residues similar to those in glutamate binding subunits (Stroebel *et al.*, 2021). Other agonists binding glycine iGluR sites are D- and L- serine, and D- and L- alanine.

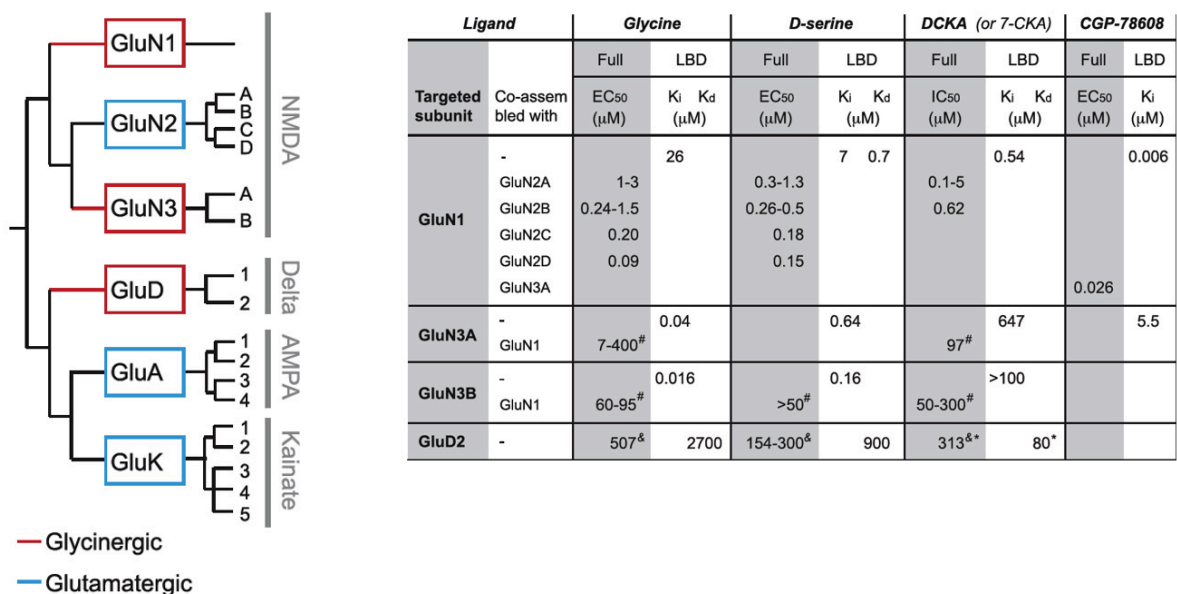


Figure 10 iGluR subunits co-agonism.

Images obtained and adapted from (Stroebel *et al.*, 2021). Evolutionary tree of the iGluR subunits color-coded according to their agonist binding site: blue for subunits binding glutamate and red for subunits binding glycine and D-Serine. On the right, table showing the ligand binding properties of glycinergic iGluRs with sensitivities to glycine, D-serine, DCKA and CGP-78608, divided in isolated LBD or full tetrameric receptors.

### 2.4.2 Orthosteric antagonists

Competitive antagonists to NMDARs are ligands that when bound to the receptor LBD do not cause gating of the receptor and prevent the binding of agonists. Some competitive antagonists at the GluN1 site are CNQX, CGP 78608, DCKA, 7-CKA, L-683,344, L-689,560, L-701,324, ZD 9379, MDL 29951, and MDL 105519 (Hansen *et al.*, 2021). CGP 78608 in particular has an extremely high affinity for GluN1 in the low nM range (Figure 10, Figure 35). A typical GluN2 orthosteric antagonist is D-AP5, used to distinguish NMDARs from other iGluRs. The residues surrounding the agonist binding pockets of GluN2 NMDAR subunits are highly conserved, and drug development for competitive antagonists with high selectivity for one GluN2 versus the other GluN2s have had limited success (Hansen *et al.*, 2021; Stroebel and Paoletti, 2021). The main mechanism of action of orthosteric antagonists is to prevent the receptor to enter the closed clamshell conformation necessary for the rearrangement of the TMD preceding the gating (Hogner *et al.*, 2003). These antagonists interact with both D1 and D2 residues and cause steric hindrance preventing clamshell closure (See 4.3 Kinetic scheme) (Hogner *et al.*, 2003). Some competitive antagonists like CNQX bind to the D1 lobe but permit a lot of conformational freedom to the receptors, as they prevent binding of the agonists but do not force the receptors in specific conformations (Lau and Roux, 2007).

### 2.4.3 Open channel blockers

Many channel blockers targeting NMDAR exist, and have been the only class of drugs which have been approved for drug administration in humans. Some of the most employed channel blockers are ketamine (Yang *et al.*, 2018) and memantine (Pierson *et al.*, 2014) (see 2.3 NMDARs in pathology and drug development), MK-801 (also used to assess receptor open probability), and Mg<sup>2+</sup> blocking NMDARs at resting potentials (see 3.5 The Transmembrane Domain) (Gielen *et al.*, 2009). Channel blockers bind asparagine (N) residues of the Q/R/N site at the top of the vestibule of M2 re-entrant loop (Figure 21). The binding epitope for NMDA channel blockers include residues within the M2 pore loop and residues in other pore-forming elements as well as the pre-M1 region (Song *et al.*, 2018).

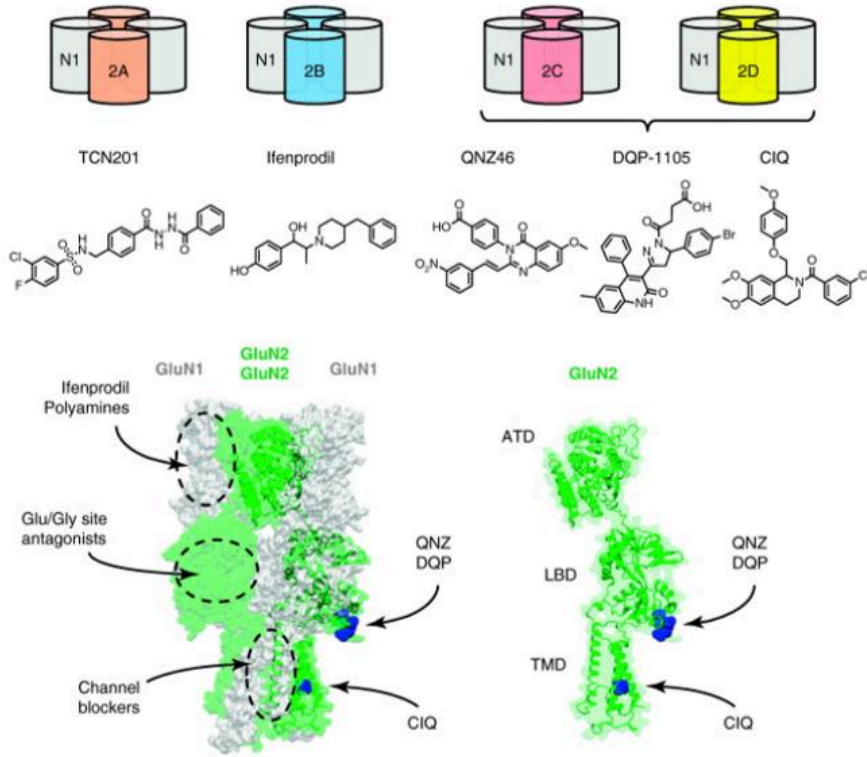
This class of drugs is strongly dependent on membrane voltage, being active only at negative potentials. Channel blockers are usually positively charged at physiological pH and require the channel to be open for binding. Some blockers become trapped inside the pore during deactivation motions (MK-

801, ketamine), and require the channel to re-open to unbind (Sobolevsky and Yelshansky, 2000), and others at lower affinity only partially prevent channel opening (memantine) (Chen and Lipton, 1997).  $Mg^{2+}$  can be found at mM concentrations in the CSF, and therefore it blocks NMDARs at resting potentials (-60mV) (Kuner and Schoepfer, 1996). This is important for the coincidence detection property of NMDARs, which need external postsynaptic depolarization to lift the  $Mg^{2+}$  block. Some key residues in the permeation pathway alter the affinity of  $Mg^{2+}$  for the different GluN2 subunits, with GluN2A and GluN2B being more strongly inhibited than GluN2C and GluN2D (Retchless *et al.*, 2012). At a -100 mV holding potential, the  $IC_{50}$  values for block by external  $Mg^{2+}$  are 2  $\mu$ M, 2  $\mu$ M, 14  $\mu$ M, and 10  $\mu$ M for GluN1/2A, GluN1/ 2B, GluN1/2C, and GluN1/2D, respectively (Kuner and Schoepfer, 1996).

#### **2.4.4 Allosteric modulators**

There is a large variety of both endogenous and exogenous allosteric modulators acting on NMDARs. Allosteric modulators in many cases display some level of subunit selectivity, allowing to isolate the function of specific receptor subtypes in native preparations. We will not give a full overview of all these compounds, as it would exceed the scope of the thesis, but I will mention some of the most important ones. Both positive allosteric modulators (PAMs) and negative allosteric modulators (NAMs) have been identified on NMDARs (Figure 11 Panel B).

A



B

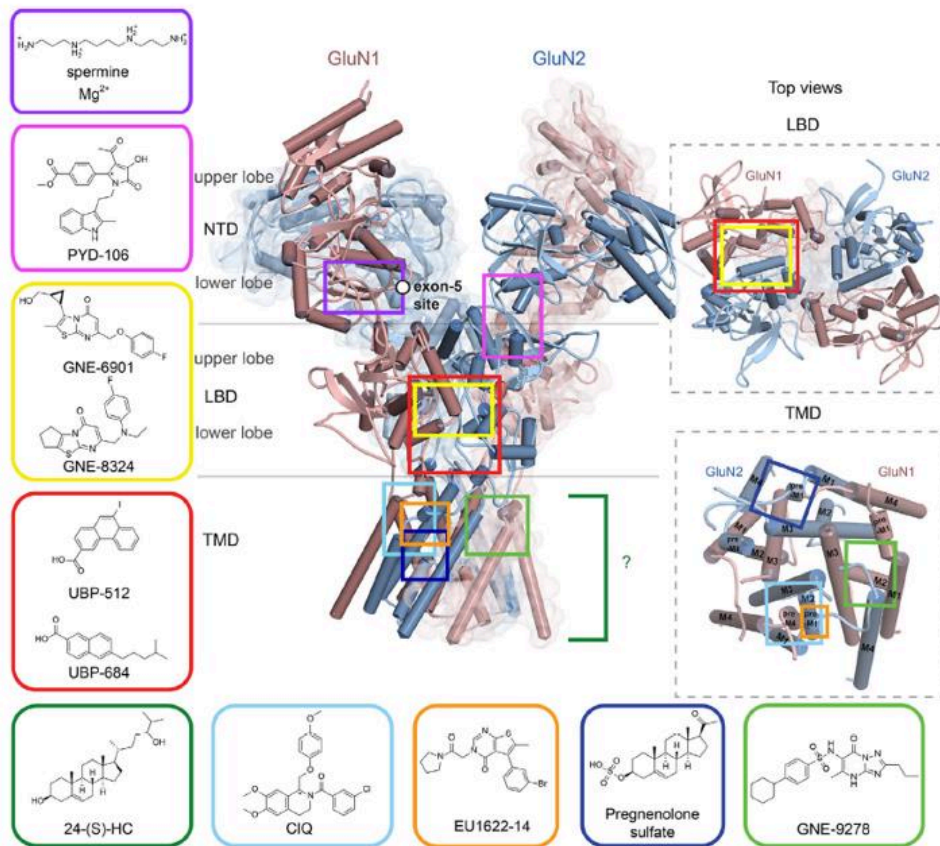


Figure 11 Pharmacology of NMDARs.

Images obtained and adapted from (Ogden and Traynelis, 2011; Geoffroy et al., 2021). Panel A, chemical structure and binding site of several GluN2-specific modulators. Ifenprodil and related GluN2B-selective molecules bind to the ATD as do polyamines. Competitive antagonists of glycine and glutamate bind to the LBD of GluN1 and GluN2, respectively. Channel blockers bind in the TMD. Panel B, chemical structure and binding site of PAMs which bind NMDARs. Binding sites are scattered across the whole receptor structure. Each square represents a class of NMDAR PAMs and contains the chemical structures different PAM classes.

Zinc ( $Zn^{2+}$ ) is a key allosteric modulator of NMDARs. It is a divalent ion whose activity has been studied in both native and recombinant receptors for more than 20 years. Zinc has been shown to be a negative allosteric modulator acting on the NTD of GluN2A and GluN2B NMDAR subunits, although with different affinities (Traynelis et al., 2010; Hansen et al., 2021). Zinc acts at a very high affinity against a binding site in GluN2A NTD ( $IC_{50}$  10–30 nM), with a lower affinity in the NTD of GluN2B receptors (low  $\mu$ M sensitivity), and at much lower affinity ( $IC_{50}$  20–100  $\mu$ M) and with voltage dependency in the TMD (Table 2). Zinc is abundant in the CNS, particularly in the forebrain, where it is packed within synaptic vesicles together with glutamate at many excitatory synapses (Frederickson et al., 2000; Paoletti, A. M. Vergnano, et al., 2009; Sensi et al., 2009). During synaptic activity, zinc is released in the synaptic cleft (together with glutamate) and inhibits postsynaptic NMDARs (Paoletti, A. M. Vergnano, et al., 2009). More information regarding zinc modulation be found at the sections “3.4.1 NTD dimerization and effect of allosteric modulators” and “4.6 Allosteric modulation: focus on zinc, protons and ifenprodil”.

NMDA receptors are fully inhibited by protons with an  $IC_{50}$  of 50–100 nM, roughly corresponding to pH 7.4–7.0 (Traynelis and Cull-Candy, 1990). It follows that in vivo NMDARs are tonically inhibited by protons under physiological conditions. Therefore, NMDARs respond to small changes in pH, something relevant in pathological cases such as ischemic situations, which can modify the pH of the affected area (Lee et al., 2015). The main molecular determinants that confer sensitivity to external pH are the subunit GluN2 subtype, and alternative splicing of exon 5 in GluN1 (Traynelis et al., 1995). The structural determinants of proton inhibition are not fully clarified, probably multiple sites throughout the receptor synergize to sensitize NMDA receptors to the extracellular protons (Gielen et al., 2008).

There is a complex interplay of allosteric modulation between zinc and protons, as zinc activity enhances proton activity at the NTD (Jalali-Yazdi et al., 2018). Activity of zinc and pH determine at which sites the heterodimer interfaces of the NTD interact (1 knuckle conformations vs 2 knuckle conformations, see 4.6 Allosteric modulation: focus on zinc, protons and ifenprodil).

Target	Subtype	Effect	Sensitivity EC <sub>50</sub> or IC <sub>50</sub> (μM)	Comments
NMDARs	NR1/NR2A	Inhibition	0.02	Voltage-independent and non-competitive inhibition. High-affinity NR2A-specific inhibition not total (max. inhibition ~60–80%). For NR2A-containing receptors, measured using tricine-buffered zinc solutions.
	NR1/NR2B		2	
	NR1/NR2C		20	
	NR1/NR2D		10	
AMPA receptors	All subtypes	Inhibition	>20 (At –60 mV)	Voltage-dependent pore block Flip variants more sensitive than flop variants. No zinc buffer used. Inhibition at very high zinc concentrations (low mM).
	Homomeric GluR1	No effect		
	Homomeric GluR3	Potentiation	ND	
Kainate receptors	Heteromeric GluR6/KA2	Inhibition	~7	No zinc buffer used.
Transporters	EAAT1	Inhibition	~10	Non-competitive partial inhibition (max. inhibition ~60%). No zinc buffer used.
	EAAT2	No effect		

Table 2 Zinc properties at Glutamatergic synapses.

Inset taken from (Paoletti, A.M. Vergnano, et al., 2009) showing zinc effect on different iGluR co-assemblies

Polyamines are a class of PAMs selective for GluN1/GluN2B NMDARs. Within this class, one of the most famous polyamines is the molecule spermine which has two binding sites, one unspecific acting through a pore block mechanism (inward rectification), and one in the NTD specific for the GluN2B subunit (Mony *et al.*, 2009). This drug can potentiate steady state currents by reducing the receptor tonic inhibition by protons, [121]. Spermine acting specifically on GluN2B has been proposed to be acting through a binding site located in the lower lobe interface between GluN1 and GluN2B NTD (Mony *et al.*, n.d.). The proposed mechanism is that spermine may help stabilizing the compact form of the clamshell, causing the receptor to have a higher Po (Geoffroy *et al.*, 2021). This same binding site is likely to be used by magnesium, which at low mM concentrations potentiate NMDARs (Paoletti *et al.*, 1995). A GluN2B specific NAM that has been thoroughly investigated and employed in many studies on NMDARs is ifenprodil, a compound binding in the NTD upper lobe GluN1/GluN2B intradimer interface and displaying >200-fold selectivity over other GluN2 receptor subtypes. I will describe this compound more in detail in the section “3.4.1 NTD dimerization and effect of allosteric modulators” and “4.6 Allosteric modulation: focus on zinc, protons and ifenprodil” sections in the manuscript. Several compounds sharing a similar structure to ifenprodil and binding within the same binding site have been developed, including Ro 25-6981 (Fischer *et al.*, 1997).

Many NMDAR allosteric modulators bind the GluN1-GluN2 LBD heterodimer interface, also expressing subunit selectivity towards some GluN2 subunits rather than others. We discuss these compounds in depth in the “3.3.2 Drugs targeting the LBD intradimer interface” section, being relevant for my project. Many other PAMs and NAMs with a specific selectivity for GluN2 subunits exist. For e

comprehensive review on this topic and the mechanisms of action of these compounds, the review (Hansen *et al.*, 2021) is very comprehensive. In the section “5.5 Pharmacology”, I will describe the compounds acting on receptors containing this subunit.

### 3 Receptor architecture: modular design

The architecture of NMDARs, and in general of iGluRs can be divided in different domains or modules based on sequence homology and analogy in domain folding. Some of these modules have been evolutionarily conserved in a large number of membrane proteins (Bork *et al.*, 1996). High resolution electron density maps of NMDARs revealed that the receptors adopt a dimer-of-dimers arrangement, with two dimers of GluN1-GluN2 heterodimers, both at the levels of the NTD and LBD. (Figure 12). While both the LBD and NTD are assembled as heterodimers, the domain layers are arranged in way that the heterodimers are swapped from one layer to the other. If we name the subunits A-B-C-D, the dimers at the NTD interface will be A/B and C/D, while at the LBD will be A/D and B/C (Figure 12), while at the transmembrane level we will observe pseudo a 4-fold symmetry. We can see from the image how this domain swapping organization applies to all iGluR clones, although unswapped structures have been proposed for delta receptors (Burada *et al.*, 2020b). Specifically, for NMDARs the GluN1 subunit always partners in the dimers with a GluN2 subunit.

I will now introduce the advances brought by the field of structural biology on iGluRs, before dissecting the individual modules of NMDARs. I will start with the functional unit of the extracellular domains: the bilobate clamshell-like domain. Afterwards, I will talk about the dimerization of the extracellular domains focusing on each domain individually before talking about the transmembrane domain and the C-terminal domain.



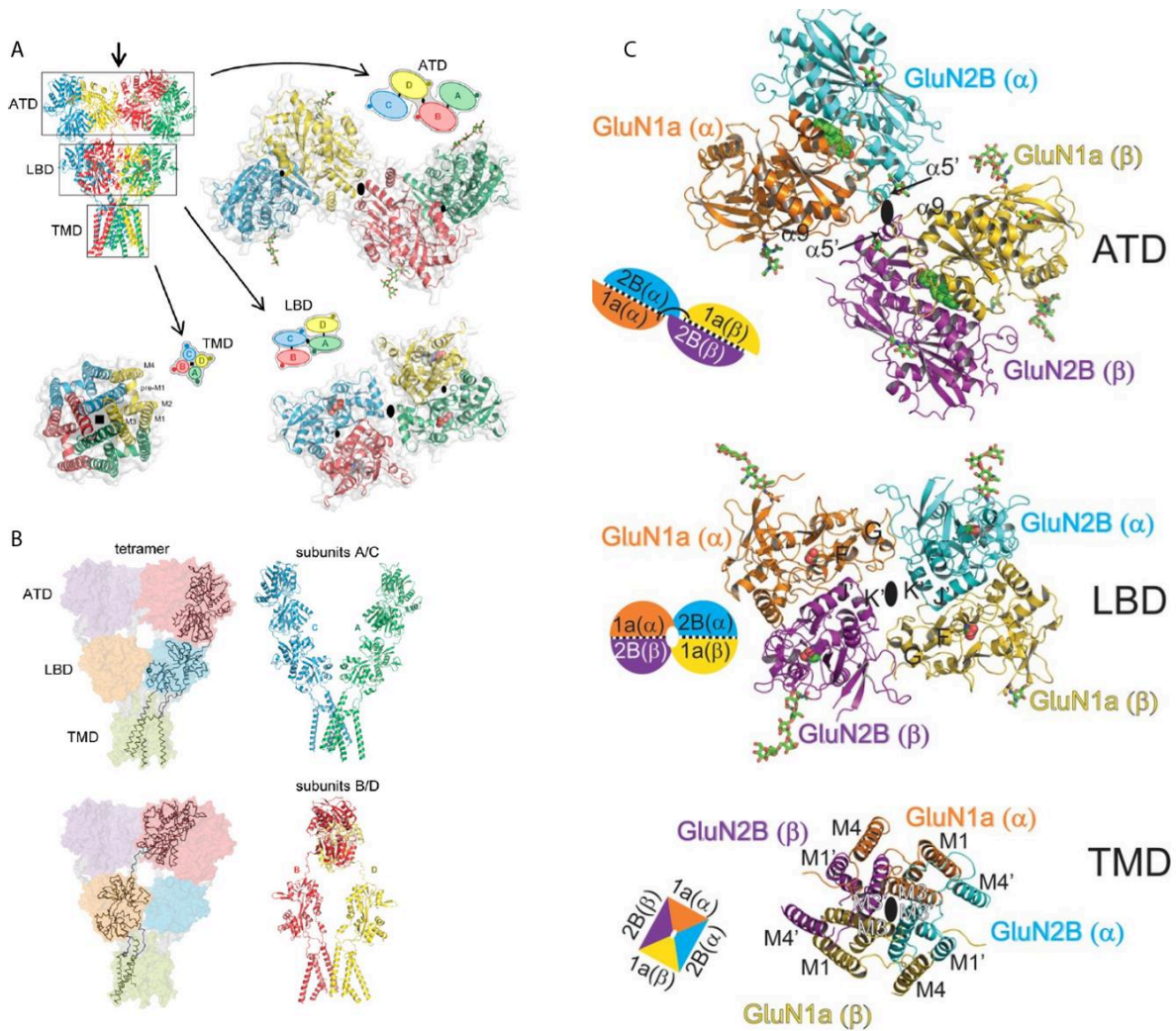


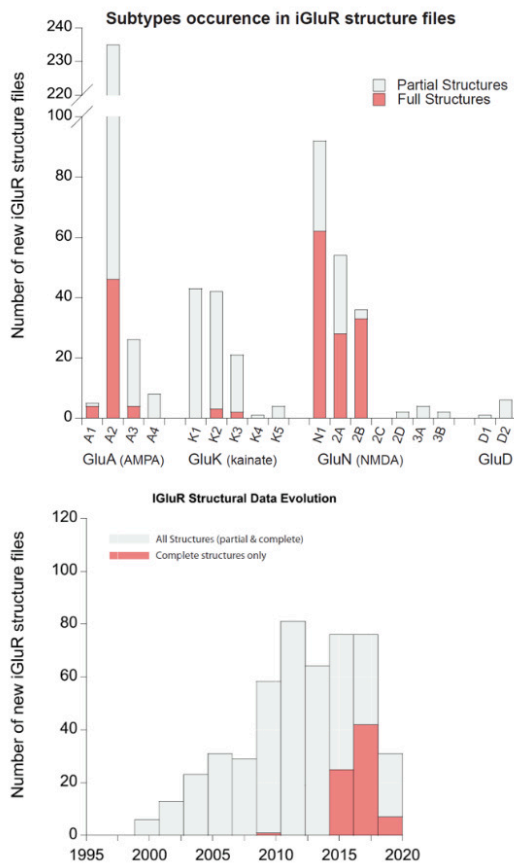
Figure 12 Subunit arrangement in iGluRs.

Figure obtained and adapted from (Traynelis et al., 2010), (Sobolevsky et al., 2009) and (Karakas and Furukawa, 2014). Panel A: subunit interfaces between the NTD, LBD, and TMD of the four subunits in the GluA2 homotetrameric AMPA receptor. The subunits are viewed from top down showing the 2-fold axis of symmetry. The NTDs and LBDs have a 2-fold axis of symmetry, whereas the TMDs have 4-fold axis of symmetry. Panel B, the symmetry mismatch between the TMDs and the extracellular domains (NTDs and LBDs) as well as the subunit crossover (or domain swapping) from the LBD to the NTD give rise to two distinct types of subunit interfaces in the iGluR receptors with two distinct conformations. The subunits are referred to as the A/C and B/D subunits. Panel C, crystal structures of tetrameric GluN1/GluN2B NMDA receptors. viewed from the top of the receptors. All of the domains assemble around the a two-fold axis located at the center of GluN1a-GluN2B (large black oval). The small schematic figures next to the structures represent subunit organization for each modular domain, and subunits on each side of the black dots in between represent pairs of dimers. Molecules such as Ifenprodil, glycine, L-glutamate, and ZK200775 are shown in spheres.

### 3.1 NMDARs crystal and Cryo-EM structures: a major advance in the field

A major step forward in our understanding of the NMDAR architectures came in the early 2000s when X-ray crystallography provided the first structures at high resolution of NMDARs. These were isolated LBDs containing the clamshell of an individual subunit such as GluN1 LBD coupled with different agonists, partial agonists or antagonists (Furukawa and Gouaux, 2003; Inanobe *et al.*, 2005). Within these fundamental works that advanced the field of NMDAR research, the authors managed to isolate different LBD conformations depending on the ligand bound to the subunits. Afterwards, GluN1 LBD was purified in a crystal structure co-assembled with GluN2A LBD at high resolution (Furukawa *et al.*, 2005). The first full NMDAR tetramers were solved in 2014 in which co-assemblies of GluN1 and GluN2B are bound to agonists, while being allosterically inhibited by NAMs (Karakas and Furukawa, 2014; Lee *et al.*, 2014). These studies have lagged behind in comparison to other iGluRs like AMPARs because of the difficulties associated with purifying and co-assembling multiple NMDAR subunits in a solvent different from the endogenous plasma membrane in X-ray crystallography techniques.

Nowadays, we have a much richer diversity in terms of conformations and resolution of full-length NMDAR structures. As of 2020, we counted 41 structures of 'full length' NMDARs (but without CTD), 21 structures of isolated NTD domains (monomer and dimer), and 39 structures of isolated LBD domains (monomer and dimer), but more have already been released since that date (Figure 13) (Data courtesy of David Stroebel). Comparatively, we have many more structures available for AMPARs, with a richer diversity in conformational states, especially for GluA2-containing AMPARs (Mayer, 2016). Furthermore, the first density maps of NMDARs obtained with cryo-EM have started to be available only in recent years (Tajima *et al.*, 2016), allowing for low Å resolution structures in which it is possible to avoid the possible bias of the artificial crystallized conformations. The use of computer programs to model the time-varying behavior of a dynamical system (dynamic simulation modeling) also started to produce a diversity of available structures, with a focus on complex transitions from and to specific states (Iacobucci and Popescu, 2017). Thanks to these advances and structure/function studies that were released during the years, we have been able to greatly enhance our understanding on many structural mechanisms of GluN2- containing NMDARs.



As of beginning of 2020

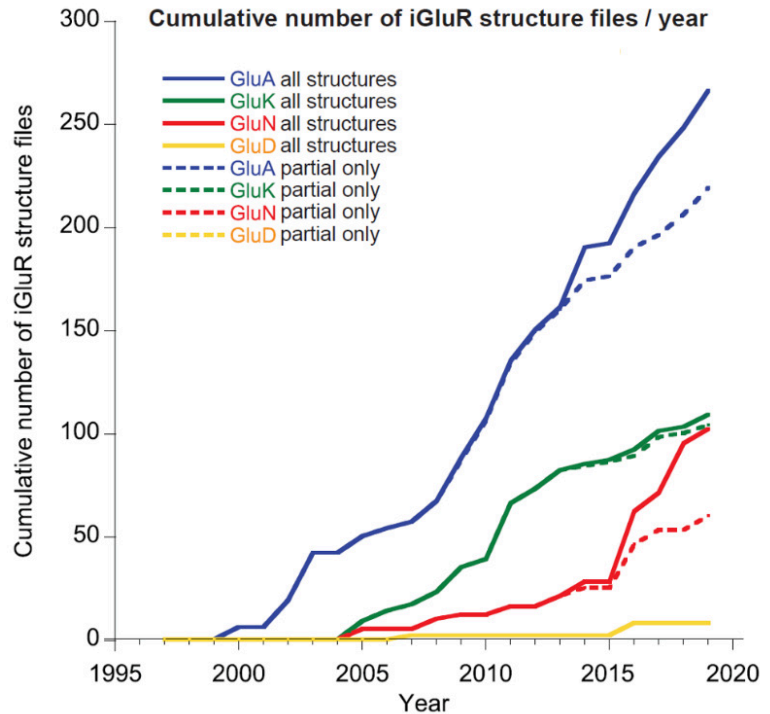


Figure 13 iGluR available structures as a function of time.

Top left, a histogram showing the number of both partial and full structures for each 18 iGluR subunits from the 4 iGluR families that have been solved and became available on the PDB database site for analysis. Bottom right, histogram showing the progressive increase of new iGluR structures being solved with the passing of years from the early 2000s, with full structures appearing from the mid-2010s. On the right, a plot showing the cumulative numbers of new structures being solved (partial and full) for each iGluR family in function of time. The graphs are updated to the beginning of 2020. Images are a courtesy of David Stroebel.

### 3.2 Functional unit of the extracellular region: the bilobate clamshell-like domain

It is thought that the characteristic modular architecture of eukaryotic iGluRs probably arose during evolution through the fusion of separate genes encoding distinct proteins in prokaryotes (Stroebel and Paoletti, 2021). This hypothesis came from protein sequence analysis indicating that many iGluRs individual components share specific motifs that are conserved across species that are far from an evolutionary perspective, but similar in mechanism and structural correlates (O'Hara *et al.*, 1993; Mayer, 2006). Individual domains like the LBD and the NTD show sequence homology with bacterial proteins whose structures are known. Both the NTD and the LBD have a module design of clamshell like domains.

These specific domains, also known as venus flytrap domains (VFT) are widely integrated in the nervous system as building blocks of many ion channels and transmembrane proteins for their mechanistic role in neuronal transmission and communication, especially in iGluRs (Traynelis *et al.*, 2010). Historically, clamshell like domains became focus of studies when bacterial periplasmic binding protein (BPB) structures were firstly identified and crystallized. This was the case for the LIVBP (leucine/Isoleucine/Valine binding protein or PBP type 1) in Gram-negative bacteria (Saper and Quijoch, 1983; Quijoch *et al.*, 1990). While the NTD of NMDARs resemble the LIVBP, the LBD closely resemble the glutamine-binding protein (QBP or PBP type 1) (Stroebel and Paoletti, 2021) (Figure 14). This class of proteins is usually located between the inner and outer membranes of bacteria (i.e. the periplasmic space) and has a role in transport of small molecules across the membrane. Since then, more than 2000 structures of PBPs have been solved, greatly expanding our understanding of their mechanistic aspects.

PBP share common aspects in their structural features regulating protein function. These are made of two globular lobes, (usually one upper and one lower) connected by a flexible hinge, and that contain a large cleft in between the two lobes (Figure 14). The hinge can contain two or more segments connecting the lobes. One of the main differences between prokaryotes and eukaryotes is that in prokaryotes the PBP usually act as monomers, with a single clamshell with two lobes acts a functional unit. In eukaryotes clamshell domains are usually found in multimers. Clamshells are part of back to back dimers like in ANPRs (Atrial Natriuretic Peptide Receptors) (He *et al.*, 2006), or GPCRs like GABA<sub>B</sub> receptors (Geng *et al.*, 2012) or mGluRs (Kunishima *et al.*, 2000). In the case of iGluRs, clamshell domains are found in a tetrameric organization, in which two couples of back-to-back dimers give rise to complex machineries. Furthermore, the clamshell domains can be found both in the NTD and LBD, for a total of 8 clamshells in a single receptor. This abundance of binding sites and intersubunit contacts offers a large variability of mechanisms for regulation of the activity of the receptor.

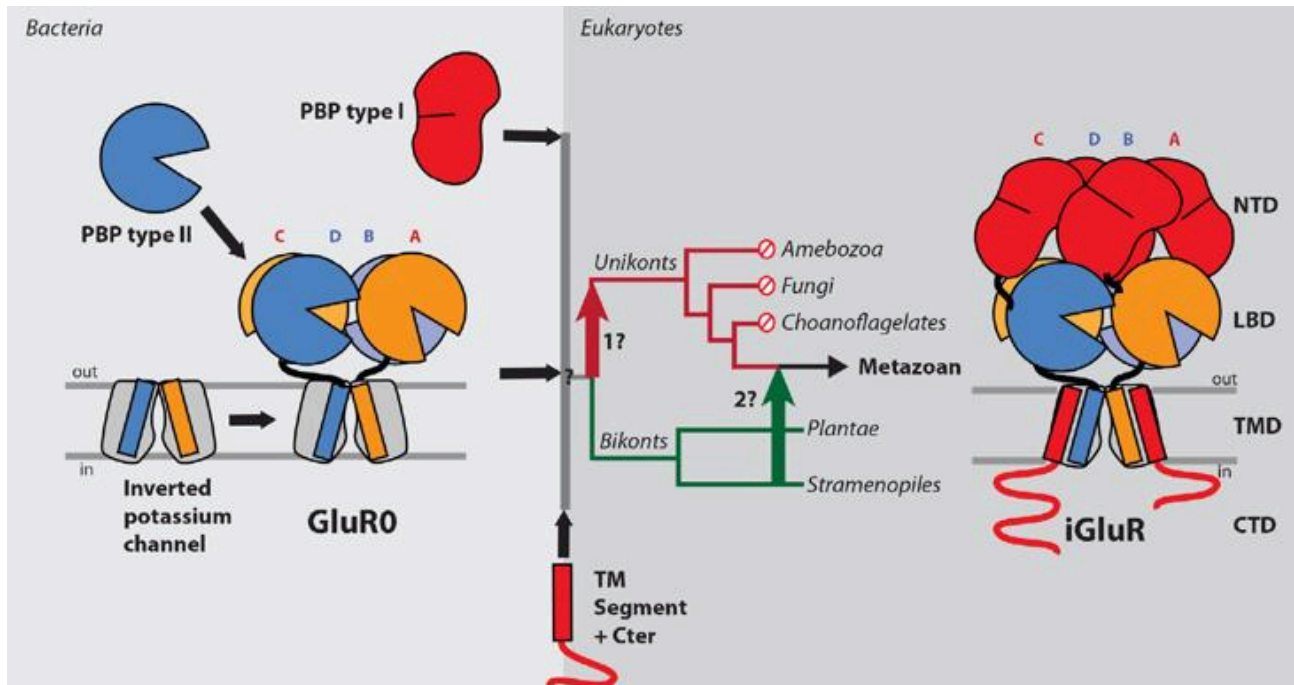


Figure 14 Evolution of NMDAR domains.

Figure taken from (Stroebel and Paoletti, 2021). On the left, one of the simplest architectures for the iGluR GluR0 from the photosynthetic cyanobacterium *Synechocystis PCC6803* only containing the transmembrane pore and the 4 LBD clamshells (bacteria). In eukaryotes such as unikonts and bikonts, a larger diversity is attained when the NTD from PBP type 1 is added (4 clamshells), plus a C-terminal for intracellular interactions and signaling.

One of the fundamental properties of clamshell-like domains is that they change conformation when binding a ligand. Usually, the ligand binds to the cleft region between the two lobes (D1 and D2), and can become buried or trapped inside this space by movement of the two lobes. Furthermore, the clamshells can oscillate between the open cleft conformation and the closed cleft conformation. These changes of conformations are important for regulating gating principles because of their pulling to the downstream regions in more complex proteins such as iGluR (Amin *et al.*, 2021). Agonist binding causes a clamshell closed conformation, while competitive antagonist binding causes the clamshell to take an open conformation (Figure 15), following the same principle of LIVPB mechanism of agonist binding. Partial agonists in NMDARs have been identified to cause the same angle of clamshell closure as full agonists. (Inanobe *et al.*, 2005; Chou *et al.*, 2020). However, full agonists seem to favor more the open conformation than partial agonists, likely because of greater stabilization of the closed-cleft stabilization (Yao *et al.*, 2013; Dolino *et al.*, 2015). Agonist mediated clamshell closure in GluN1 and GluN2A is

rendered stable by the formation of strong interlobe interactions between lobes D1 and D2 (Yu and Lau, 2018).

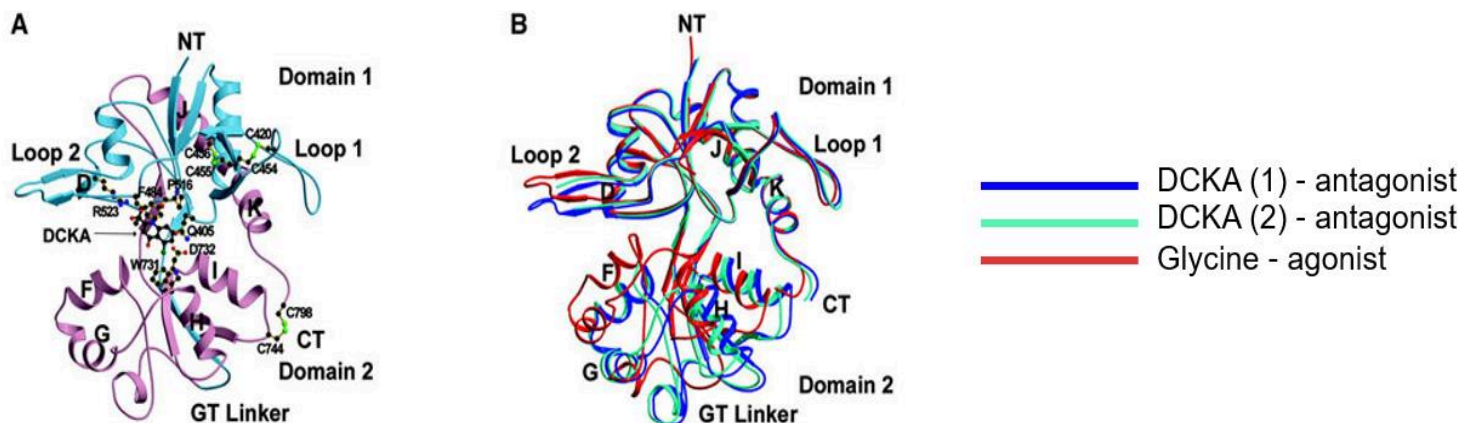


Figure 15 Clamshell conformations change depending on ligand binding.

Image obtained and modified from (Furukawa and Gouaux, 2003). The binding mechanisms of the competitive antagonist DCKA is shown and compared to the agonist glycine. Panel A, a ribbon representation of the DCKA binding site located in the cleft of GluN1 S1 S2 structure (DCKA molecule A) with S1 and S2 segments of the LBD colored in blue and purple respectively. Panel B, superposition of two different asymmetric DCKA molecules bound to GluN1 (DCKA molecules A and B in blue and light blue, respectively) and the glycine bound molecule (red). The root mean square deviation for DCKA molecules A and B is 0.74 Å. The glycine-bound form displays a bilobed structure closed by 23.8° and 18.2° compared with the DCKA molecules A and B, respectively.

### 3.3 The Ligand Binding Domain (LBD)

The extracellular LBD comprises two different segments, S1 and S2, which are separated by the M1, M3 transmembrane helices and the M2 pore loop (Figure 7, Figure 15). The LBD is linked to the NTD through the NTD-S1 polypeptide linker and to the TMD through the S1-M1, M3-S2, and S2-M4 linkers. The linkers are flexible region fundamental to relay conformation changes downstream to the lower modules. The linkers connecting the LBD to the TMD transmit the movement following agonist binding and clamshell closure to the gate itself, while the linkers connecting the NTD to the LBD are important for relaying allosteric modulators effects to the LBD (Traynelis *et al.*, 2010; Paoletti *et al.*, 2013; Hansen *et al.*, 2021). Overall, the tertiary structure of the LBD is highly conserved among many different species, with a shape of a bilobed clamshell domain (Stroebel and Paoletti, 2021). Two main segments compose the LBD, a D1 (upper lobe) and a D2 (lower lobe). The LBD is the NMDARs binding region for orthosteric agonists and



antagonists. Within all iGluRs, the LBDs assemble in dimers of low affinity, which still dimerize during the tetramerization process and contributing to the domain swap observed in functional assemblies (Sun *et al.*, 2002; Furukawa *et al.*, 2005).

### 3.3.1 LBD dimerization

In 2005 the first functional dimer of the LBD comprising GluN1 and GluN2A was solved with a high resolution within a crystal structure (Furukawa *et al.*, 2005). It was shown that at the LBD level, NMDARs form couples of functional GluN1-GluN2 heterodimers which make extensive back-to-back contacts in the upper lobe. This subunit arrangement has also been seen in non-desensitizing conformations of AMPARs (Armstrong and Gouaux, 2000; Sun *et al.*, 2002). The heterodimer assembles with two subunits related by a pseudo two-fold axis located at the center of the interface burying a large solvent-accessible surface area (Figure 16). This LBD heterodimer interface, which we will call the **intradimer interface**, has three main sites of contacts where the two subunits enter in close contact with each other. The authors named those sites as sites I-II-III. Site I (inner side) and Site III (outer side) are related by the pseudo two-fold axis, while site II (central side) is on the pseudo one-fold axis (Figure 16). The authors, and others later on, found that modification in all of these sites can modify the resulting receptor properties, and that addition of disulfide bridges by cysteine mutants can strengthen the individual sites of the interface, favoring dimerization of the interface (Furukawa *et al.*, 2005; Gielen *et al.*, 2009; Bledsoe *et al.*, 2019). By analyzing the biochemical properties of residues located on opposing subunits but at close spatial proximity, it was found that several hydrophobic connections and polar contacts between apolar residues in both the inner side and the outer side of these receptors can keep the interface tightly interconnected and stable when the receptor enter specific conformations (Gielen *et al.*, 2008). Notably, in NMDARs chemical bonds also connect the upper lobe (D1) of one subunit to the lower lobe (D2) of the other subunit LBD, a feature that seems absent in AMPARs (Armstrong and Gouaux, 2000; Sun *et al.*, 2002). Indeed, while the D1 arrangement seems similar between GluN1/GluN2A receptors and GluR2 homodimers, the D2 superimposes poorly when comparing the two iGluRs (Furukawa *et al.*, 2005). Furthermore, within the same subunit agonist mediated closure of the clamshell is stabilized by interactions between D1 and D2 which make the transmembrane channel open conformation stable (Paganelli *et al.*, 2013; Yu and Lau, 2018)

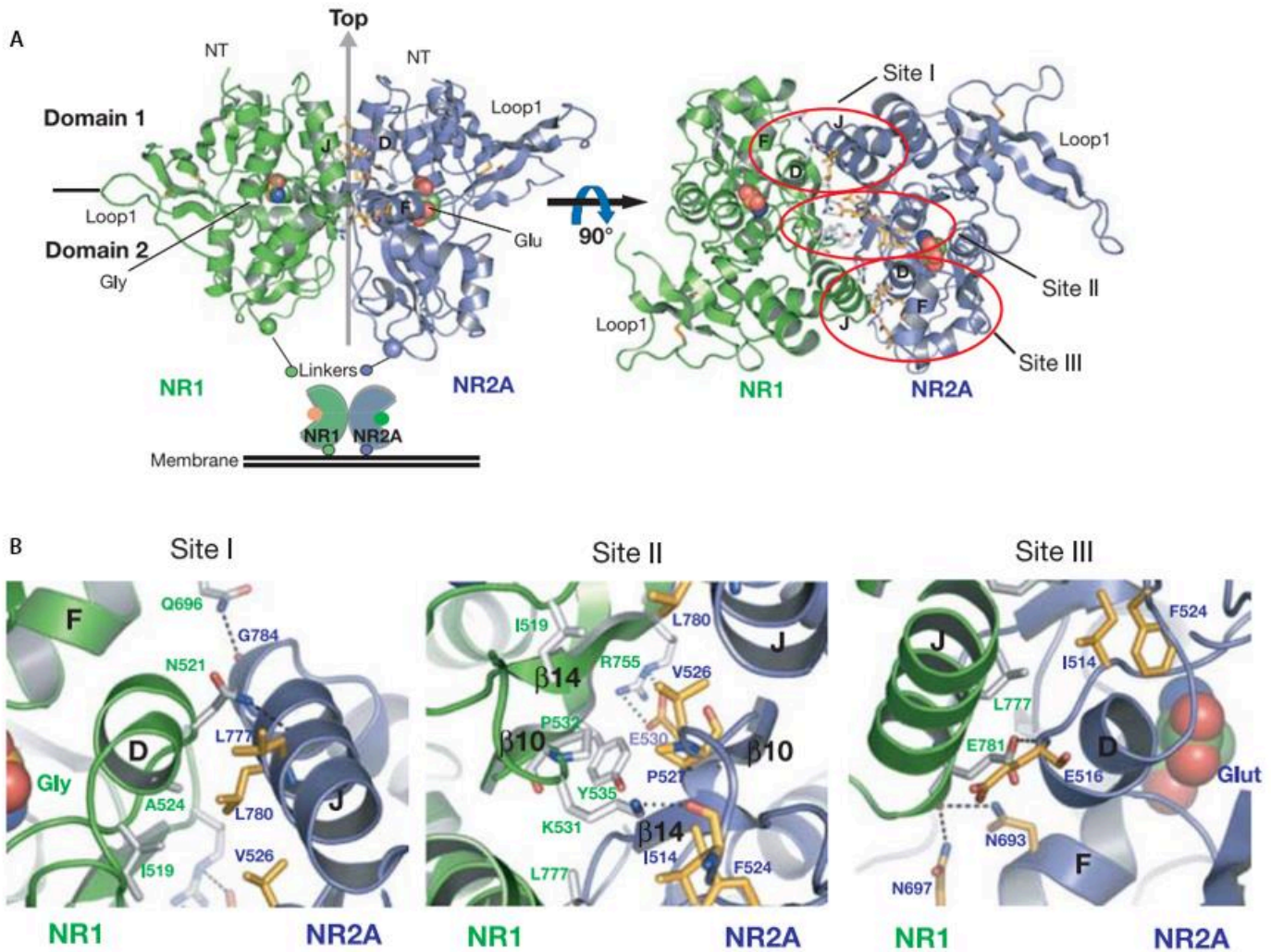


Figure 16 NMDAR LBD dimerization.

Figure taken from (Furukawa et al., 2005). Two different views (side and top) of cartoon representations of the GluN1 (green)–GluN2A (blue) LBD heterodimer bound to glycine and glutamate respectively. The interface between GluN1 and GluN2A is divided into three different sections named sites I–III. Panel B, Zooms on interactions at sites I, II and III respectively. Dashed lines indicate hydrogen bonds or salt bridges. The interacting residues from GluN1 and GluN2A are colored white and orange, respectively.

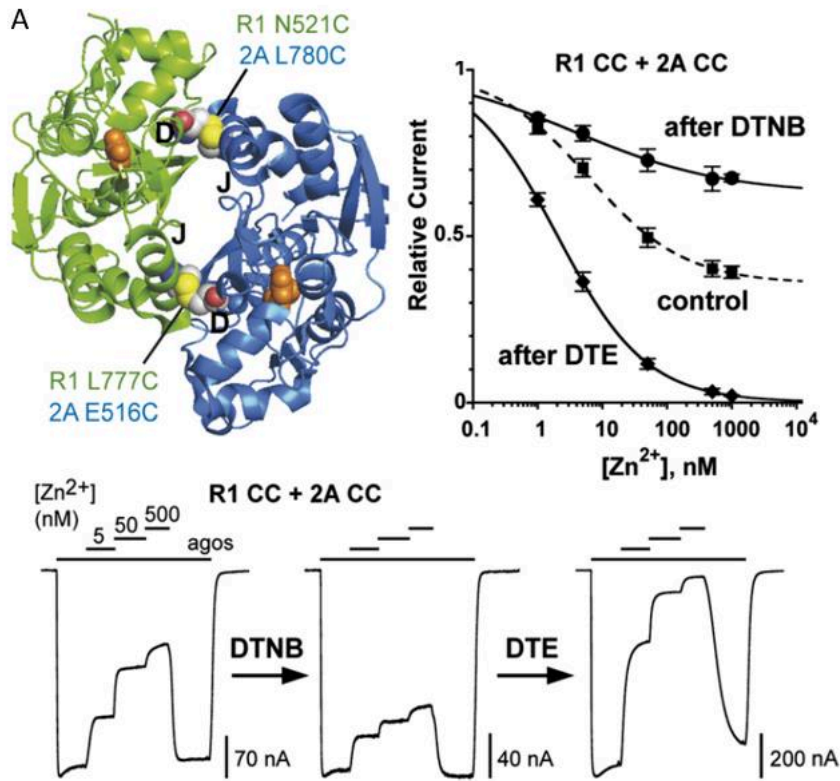
Intradimer LBD interactions are important for the mediation of the allosteric modulation coming from the NTD of GluN2A containing receptors. The strength of this interface determines the functional coupling between NTD modulators such as zinc and protons (Gielen et al., 2008; Esmenjaud et al., 2018; Tian et al., 2021). In GluN1/GluN2A NMDARs, strengthening the intersubunit LBD contacts (e.g. by introducing disulfide bridges) weakens the sensitivity to allosteric inhibitors like zinc acting on the NTD



(Figure 17 Panel A), while weakening it increases the sensitivity to these modulators. Furthermore, strengthening of the interface via disulfide bridge insertion generates current phenotypes that were slightly desensitizing, smaller in size, and with lower  $P_o$  (Borschel *et al.*, 2011). Therefore, it has been hypothesized that in NMDARs the dimer interface needs to retain a certain degree of flexibility to gate efficiently the pore and relay allosteric modulation (Borschel *et al.*, 2011). In GluN2B, the importance of this interface seems reduced compared to GluN2A, as allosteric modulation from the NTD has been shown to be relayed more through interfaces located between (and not within) the dimers (Esmenjaud *et al.*, 2018; Tian *et al.*, 2021) (see 4.7 A unified model of NMDAR gating and the end of this section).

There are some important differences between AMPARs and NMDARs. Weakening or destabilizing this interface in other iGluRs such as kainate or AMPA receptors has been found to increase the speed and the extent of desensitization in these receptors (Sun *et al.*, 2002; Horning and Mayer, 2004; Armstrong *et al.*, 2006; Priel *et al.*, 2006; M. C. Weston *et al.*, 2006; Plested and Mayer, 2007; Plested *et al.*, 2008). Conversely, it has been found that strengthening the interface via mutagenesis that promotes dimerization of the interface in AMPARs reduces the extent and speed of desensitization, showing gain of function phenotypes (Sun *et al.*, 2002) (Figure 17 Panel B). In NMDARs, contacts mediated by site II like the residue GluN1-Y535, were identified as critical for maintaining the characteristically slow NMDA receptor deactivation (Furukawa *et al.*, 2005; Borschel *et al.*, 2015). Mutants in this region favoring stronger intersubunit connections have been found to reduce energy barriers necessary for receptor activation, favoring NMDARs pre-open states and slowing down deactivation by slowing glutamate dissociation rate (Borschel *et al.*, 2015).

## GluN1/GluN2A



## B GluA2/GluA2

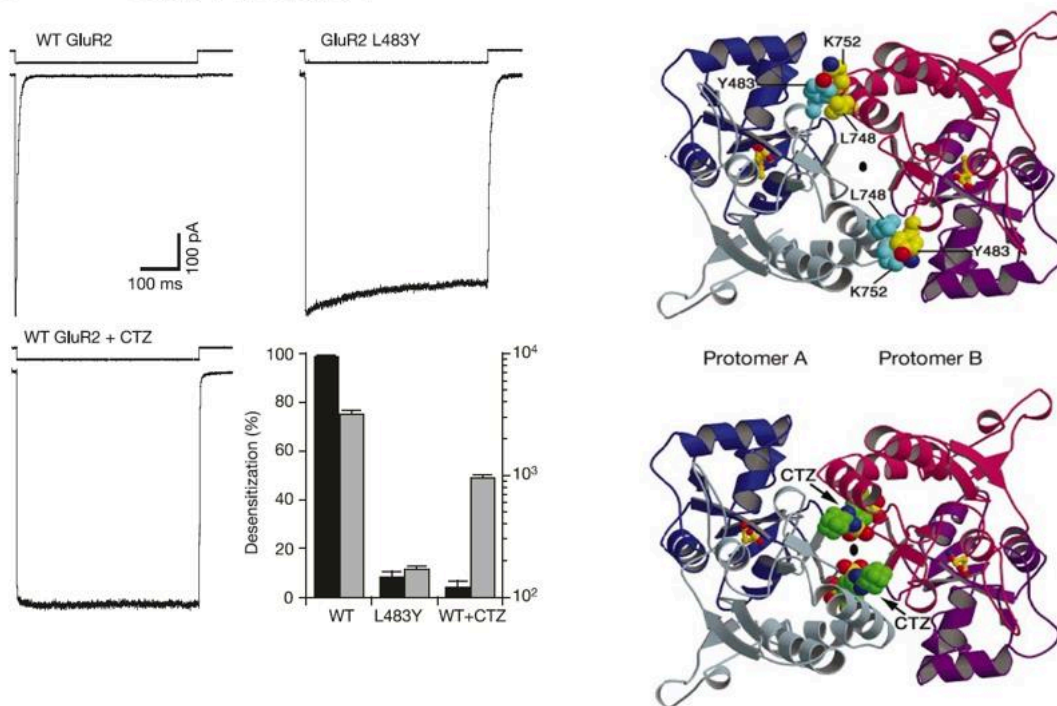


Figure 17 Function of the intradimer interface in NMDAR and AMPARs.

Panel A figure adapted from (Gielen et al., 2008) with structure adapted from (Furukawa et al., 2005). Top view of GluN1/GluN2A LBD dimer highlighting the intersubunit disulphide bridges (CC bonds) introduced on 2 symmetrical sides (inner and outer side) at the dimer interface (sulfurs are shown in yellow). Below, representative traces showing inhibition by increasing zinc concentrations (5, 50, and 500 nM) applications on currents in the mutant GluN1CC/GluN2ACC receptors expressed in xenopus oocytes and treated sequentially with DTNB (oxidizing agent, 0.5 mM, 5 min), DTE (reducing agent, 5 mM, 15 min). On the right, zinc inhibition concentration-response curves for NR1-CC/NR2A-CC in control, DTE and DNTB conditions. Panel B adapted from (Sun et al., 2002), comparing the quick desensitization of the WT GluR2 tetrameric receptor to the non-desensitizing GluR2 L483Y mutation and CTZ treated GluR2 receptors. Within the histogram, the black columns show percentage of desensitization, while the grey columns show deactivation rate. On the right, top view of the crystal structures of 1) LBD dimer of GluR2 AMPARs L483Y and below 2) LBD dimer of GluR2 AMPARs containing the CTZ molecule looking down the 2-fold axis.

Another property mediated by this interface in GluN1/GluN2A receptors is the intersubunit negative allosteric modulation that is reflected in the negative cooperativity between glutamate and glycine binding. The “destabilization” of the closed cleft state at the second site is linked to the lower affinity of the second agonist when the first agonist is present and this negative cooperativity passes through the relay of the interface (Durham et al., 2020).

Recently, it has been shown that the different subunits of the LBD do not only communicate via the back-to-back dimer interface. An **interdimer** interface has been found to be important for the regulation of receptor activity, located between the two constitutive dimers. Indeed, the LBD does not interact only at the dimer level, but also at the tetrameric level in a dynamic assembly (Figure 12). A rolling motion between the two constitutive LBD dimers is a key structural mechanism for the NMDAR activation and NTD-mediated allosteric modulation in GluN1/GluN2B receptors (see “3.4.1 NTD dimerization and effect of allosteric modulators”) (Esmenjaud et al., 2018; Tian et al., 2021; Wang et al., 2021). Structural data indicates that when the GluN1/GluN2B activates, they undergo a large rotational movement when the receptor is passing from a non-active to an active conformation (Tajima et al., 2016). In his work (Esmenjaud et al., 2018), Esmenjaud et al., showed that by crosslinking it is possible to lock GluN1/GluN2B receptors in different states at high and low PO respectively if the receptors are cross-linked in a rolled or unrolled state. Therefore, the interdimer LBD rolling acts as a gating switch that controls the energetics of channel opening. This mechanism is likely not conserved in GluN1/GluN2A receptors.

### 3.3.2 Drugs targeting the LBD intradimer interface

The intradimer interface is a binding site for molecules that are PAMs or NAMs selective for some GluN2 subunits, or for AMPARs (Kane and Costa, 2015) (Volgraf *et al.*, 2016). One of the most famous positive allosteric modulators selective for AMPARs is the molecule cyclothiazide (CTZ), which has been found to promote dimerization of the GluA2 LBD interface when binding residues located within both subunits that are part of the dimer (Figure 17 Panel B). Also the AMPAR PAM molecule aniracetam binds within this region (Borschel *et al.*, 2015). A class of PAMs (thiazolopyrimidinone derivatives) has been found to be selective for the GluN1/GluN2A LBD intradimer interfaces, with much lower affinity for the other GluN2 subunits. Among these PAMs, the molecule GNE-3419 acts on both NMDARs composed of GluN1/GluN2A and on AMPARs containing GluA2 homotetramers (Hackos *et al.*, 2016; Wang *et al.*, 2021) (Figure 18 Panels A,B) (Table 3). The resulting effect on GluN2 NMDARs and GluA2 AMPARs is a potentiation in current size, and for GluA2 there is also a decrease in desensitization kinetics. A single GluN2A residue (V783) has been found to control the compounds selectivity for the GluN2A subunit over others. The large residue F784 in GluN2B has been found to prevent PAM GNE-3419 binding to GluN1/GluN2B NMDARs, while the homologous position V783 in GluN2A allows its binding (Figure 18 Panel A, B). Some of these PAMs, like GNE-8342 potentiate GluN2A containing NMDARs currents by slowing channel deactivation kinetics, while also increasing glutamate potency (Hackos *et al.*, 2016; Volgraf *et al.*, 2016). This is not the case for other PAMs belonging to the same family like GNE-6901 that only affect  $P_o$  (Geoffroy *et al.*, 2021). It has been hypothesized that the enhanced dimerization provided by the PAM molecules prevents channels from entry of the receptor into a desensitized-like, inhibited state.

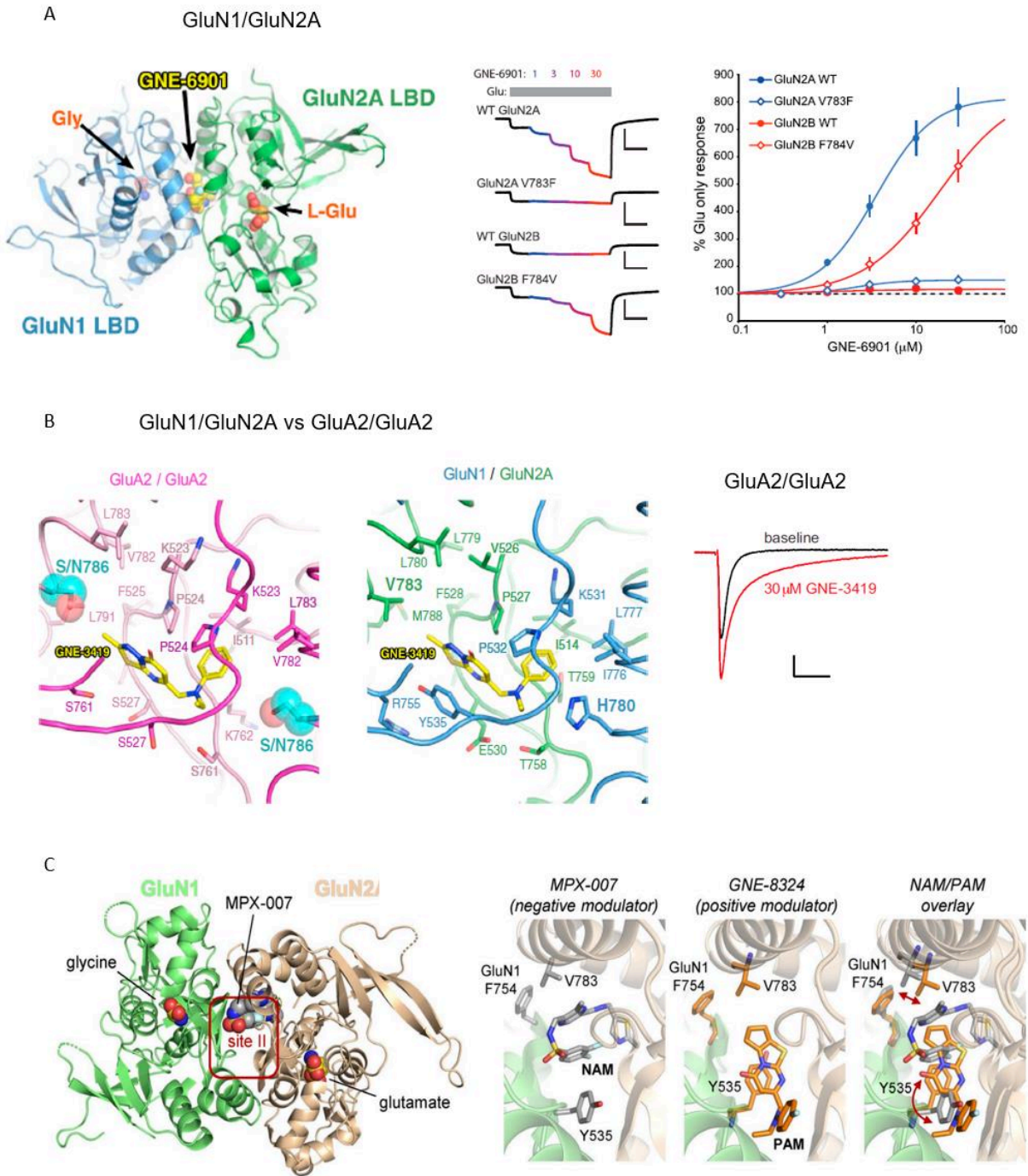


Figure 18 GluN2A-selective PAM binding site located in the intradimer interface.

Image adapted from (Hackos et al., 2016) and (Hansen et al., 2018). Panel A, LBD crystal structure of GluN1/GluN2A in complex with GNE-6901 is shown from a lateral perspective. Glutamate (L-Glu), Glycine (Gly), and GNE-6901 are shown as spheres and binding sites are labeled. Below, example traces from NMDAR currents measured in oocytes expressing mutant or WT GluN2A or GluN2B. Dose responses curves and representative traces with increasing concentrations of GNE-6901 are shown during application of agonist. Panel B, comparison of crystal structures of GNE-3419 in complex with the GluA2 LBD and with the GluN1/GluN2A LBD are shown. Residues that interact with GNE-3419 are shown as stick models. On the right,



representative trace showing evoked AMPA EPSPs recorded from CA1 pyramidal neurons in hippocampal brain slices. Average EPSPs before (black) and after application of 30 mM GNE-3419 (red). Panel C, structure of the agonist-bound GluN1/2A LBD heterodimer with the NAM MPX-007 bound at site II in the subunit interface (PDB 5I59, (Yi et al., 2016)). On the right, magnified views of site II in GluN1/2A LBD heterodimer comparing structures containing NAM MPX-007 (PDB 5I59, (Yi et al., 2016)) or PAM GNE-8324 (PDB 5H8Q, (Hackos et al., 2016)). The overlay illustrates the distinct effects of NAM and PAM binding on Val783 in GluN2A and Tyr535 in GluN1.

The same binding site within the intradimer interface is also used by a different class of modulators that are NAMs like the TCN-201, which is also selective for GluN2A containing NMDARs. This selectivity also depends on the amino acid identity of F784 in GluN2B and V783 in GluN2A (Hansen *et al.*, 2012; Yi *et al.*, 2016). Therefore, the GluN2 derived selectivity of both NAMs and PAMs binding at this modulatory site is non-conserved among GluN subunits (Val in GluN2A, Phe in GluN2B and Leu in GluN2C/GluN2D shaping it) (Hansen *et al.*, 2018). TCN-201 inhibition of GluN2A is insensitive to glutamate concentration, but has a diminished efficacy in high concentrations of glycine. MPX-004 is another GluN2A specific NAM which binds to the same binding site, but with increased potency, performing more complete inhibition at saturating concentrations. Crystallographic studies of these NAMs show that the molecule stabilizes the open conformation of the GluN1 LBD to facilitate glycine unbinding and consequently reduce glycine potency (Figure 18 C) (Table 3) (Yi *et al.*, 2016).

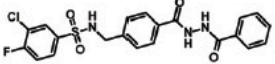
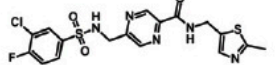
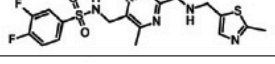
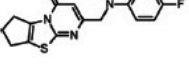
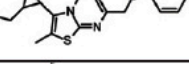
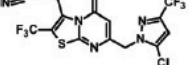
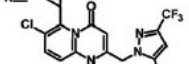
Compound	Mode of Action	Affinity or potency at GluN1/GluN2 ( $\mu\text{M}$ )						
		2A	2B	2C	2D	2A/2B	2A/2C	
 TCN-201	NAM	$K_B^{a,\dagger}$	0.045	NE	NE	NE	-	-
		$K_B^{b,\dagger}$	0.070	NE	NE	NE	-	-
		$K_B^{c,\dagger}$	0.027	NE	NE	NE	-	-
		$IC_{50}^{d,\dagger}$	0.20	-	-	-	1.46	-
		$IC_{50}^{e,\dagger}$	0.52	-	-	-	-	2.3
 MPX-004	NAM	$IC_{50}^{f,\dagger}$	0.079	NE	-	NE	-	-
		$IC_{50}^{g,\dagger}$	0.198	NE	NE	NE	-	-
		$IC_{50}^{d,\dagger}$	0.22	-	-	-	0.84	-
 MPX-007	NAM	$IC_{50}^{f,\dagger}$	0.027	NE	-	NE	-	-
		$IC_{50}^{g,\dagger}$	0.143	ND	NE	NE	-	-
		$IC_{50}^{d,\dagger}$	0.20	-	-	-	0.86	-
 GNE-8324	PAM	$EC_{50}^h$	2.43	NR	NR	NR	-	-
		(% Control)	(500%)	(125%)	(150%)	(150%)	-	-
		$EC_{50}^i$	ND	-	-	-	ND	-
 GNE-6901	PAM	(% Control)	(2500%)	-	-	-	(500%)	-
		$EC_{50}^h$	0.33	NR	NR	NR	-	-
		(% Control)	(400%)	(100%)	(125%)	(250%)	-	-
 GNE-0723	PAM <sup>i</sup>	$EC_{50}^j$	ND	-	-	-	-	-
		(% Control)	(2000%)	-	-	-	-	-
		$EC_{50}^j$	0.021	ND	7.4	6.2	-	-
 GNE-5729	PAM <sup>i</sup>	(% Control)	(252%)	(149%)	(333%)	(260%)	-	-
		$EC_{50}^k$	0.037	ND	4.7	9.5	-	-
		(% Control)	(236%)	(196%)	(343%)	(240%)	-	-

Table 3 Allosteric modulators binding the LBD Intradimer interface of GluN1/GluN2 receptors.

Table obtained from (Hansen et al., 2021). †Maximal inhibition is limited by glycine concentration. - denotes no available data, NE denotes no effect at the highest concentrations evaluated, ND denotes that the compound displayed some activity, but the affinity or potency could not be determined. NR denotes some activity, but that the numerical value was not reported.

Both GluK1 and GluK2 (kainate) subunits possess a single anion binding pocket at the LBD intradimer interface, whereas there are two cation pockets per dimer sitting above at the apex flanking the anion site (Plested and Mayer, 2007; Nayeem et al., 2009). These binding sites were resolved by X-ray crystallography at sites of the LBD dimer interface. Modulation by these molecules regulate the amplitude and time course of kainate responses, also with an effect on desensitization (Bowie, 2002). Within these receptors, there is a formation of hydrogen bonds and salt bridges that make the receptor desensitized conformation more stable than other iGluRs (M. C. Weston et al., 2006). The GluK3 subunit of kainate receptors contains a Zn<sup>2+</sup> binding site in the lower side of the interface, just below the anion binding site in AMPARs. Within this class of receptors, zinc binding potentiates current size by stabilizing dimerization and reducing desensitization (Veran et al., 2012). Occupation of the cation binding pocket by a similar mechanism favors activation by favoring dimerization of the interface. Another way of stabilizing the LBD Intradimer Interface of kainate receptors is by inserting cysteine crosslinking mutants which prevent desensitization, similarly to how it has been shown by AMPARs (Matthew C. Weston et al., 2006).

### 3.4 The N-terminal Domain (NTD)

The first ~370 residues within each individual iGluR subunit form the NTDs, which have a clamshell like shape with two lobes (named R1 and R2) like the previously described LBDs. As for the LBDs, the four subunits composing the NTD assemble as dimers of dimers. The NTD of NMDARs is different from the NTDs of other iGluRs. In NMDARs the NTD are indeed in much closer proximity to the LBDs, being more tightly paired to them. Functional deletion of the NTDs have furthermore much more drastic effects on current phenotypes in comparison to other iGluRs (Figure 19) (Gielen et al., 2009; Yuan et al., 2009). Functional data support this argument, as the NTD has been found to influence key gating properties such as deactivation time course, open probability (Gielen et al., 2009) and ligand potency (Yuan et al., 2009).

NTDs have an important role in the assembly of iGluRs, ensuring that subunits within a family only assemble with other subunits belonging to the same family (Stroebel *et al.*, 2011). Several crystal structures of the NTD domains have been solved, showing a common architecture among all iGluRs with two lobes (R1 and R2) connected by a hinge composed of three segments. The upper lobe is more conserved than the lower lobe (Herguedas *et al.*, 2013). Differently from other iGluRs, there is a lack of a specific loop connecting the upper NTD with the NTD dimer interface, making NMDARs NTDs much more flexible than the other iGluRs (Karakas *et al.*, 2009; Zhu *et al.*, 2013). Another differentiating factor separating NMDARs from other iGluRs is that NMDAR NTDs are very important sites for allosteric modulation, as binding sites have been individuated for zinc, polyamines and many synthetic compounds that can act in a subunit specific manner (Zhu and Paoletti, 2015; Hansen *et al.*, 2018). This is not the case for kainate, AMPA or Delta receptors, where there is no known small ligand binding these regions. In NMDARs, the NTD conformation has been found to be very important for regulation of overall receptor Po (Gielen *et al.*, 2009; Yuan *et al.*, 2009). By oscillating between the open and the closed conformation, and by transducing its conformational changes to the LBD and the TMD, the NTD acts as a regulator of receptor activity in a subunit and dimer dependent manner.

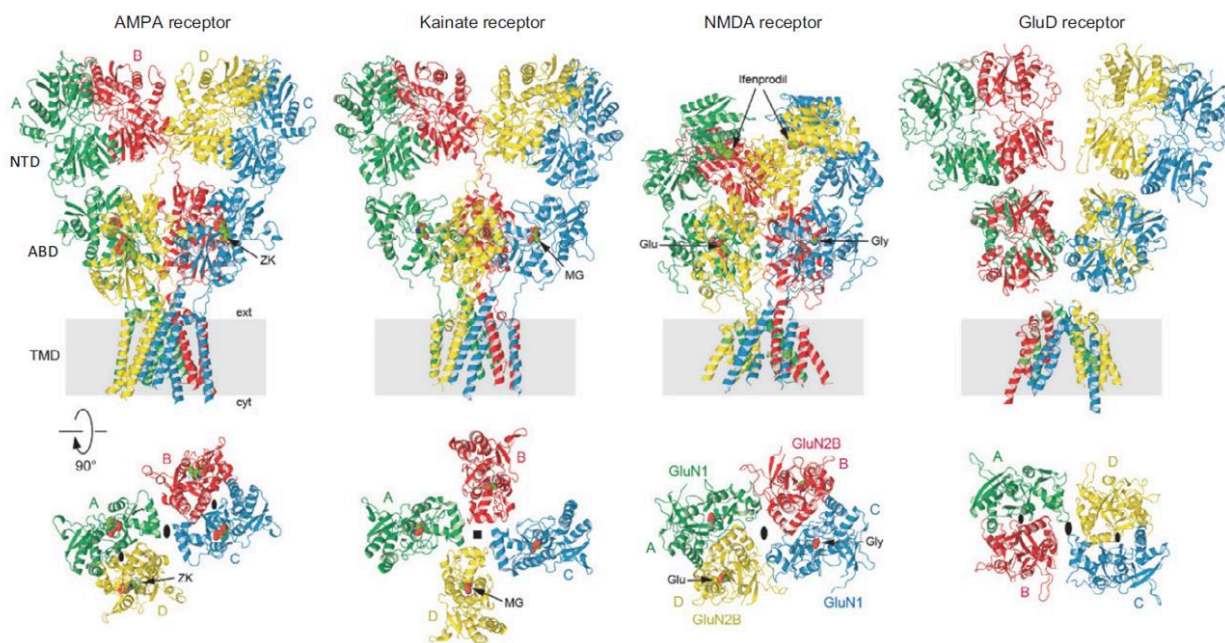


Figure 19 iGluRs NTDs compared within the complete tetrameric structures for all 4 classes of iGluRs.

*Inset obtained by (Hansen et al., 2021). The structures are: 1) Homomeric GluA2 AMPA receptor with competitive antagonist ZK 200775 (PDB: 3KG2). 2) Homomeric GluK2 kainate receptor with agonist SYM2081 (PDB: 5KUF). 3) GluN1/2B NMDA receptor in complex with Glutamate and Glycine and the allosteric inhibitor ifenprodil (PDB: 4PE5). 4) Homomeric GluD1 receptor with Ca<sup>2+</sup> and the competitive antagonist 7-CKA (PDB:*



6KSS). Two different views are shown: The view on top shows iGluRs viewed perpendicular to the membrane, and the view below shows LBD layers viewed from the extracellular POV. Black ovals indicate the receptor overall and NTD and LBD dimers local 2-fold rotational symmetry, while black square indicates the 4-fold symmetry.

### 3.4.1 NTD dimerization and effect of allosteric modulators

Similarly to the LBD, the NTDs arrange as dimers where the two protomers of individual GluN1 and GluN2 subunits are in close contact through an intradimer interface. Depending on the type of GluN2 subunit and the consequent residue identity present, the electrical charges and stability of these interfaces are modified (Tian *et al.*, 2021). This interface is the binding site for NMDAR subunit specific allosteric modulators. Several crystal structures exist showing that a class of NAMs which is GluN2B specific binds this region (Karakas *et al.*, 2011; Burger *et al.*, 2012; Tajima *et al.*, 2016) (Figure 20 Panel A). Among these NAMs, the compound ifenprodil is the best-known pharmacological agent targeting GluN2B subunits specifically. There are some important differences in how the dimerization takes place between GluN2B and GluN2A, as in GluN2A the pocket where ifenprodil binds is absent due a different subunit arrangement with a  $\sim 10^\circ$  inter-protomer rotation compared with GluN1/GluN2B (Romero-Hernandez *et al.*, 2016) (Figure 20 Panel B). When ifenprodil binds at the interface, it causes large-amplitude clamshell closure (by  $20^\circ$ ) of the GluN2B NTD, with the bilobes approaching each other, a typical example of clamshell activation, but much less so in the GluN1 NTD ( $5^\circ$ ) (Sirrieh *et al.*, 2013, 2015). These conformational changes happen first in the NTD, but their effects influence the conformation of the whole receptor (see “4.6 Allosteric modulation: focus on zinc, protons and ifenprodil”) (Burger *et al.*, 2012; Tajima *et al.*, 2016). The distances between the GluN1 and GluN2B upper lobes do not undergo any significant conformational changes. However, measurements from R2 of the GluN2B NTD to the R1 of GluN1 NTD show a decrease in the distance upon ifenprodil binding, indicating a rotating motion in GluN2B NTD.

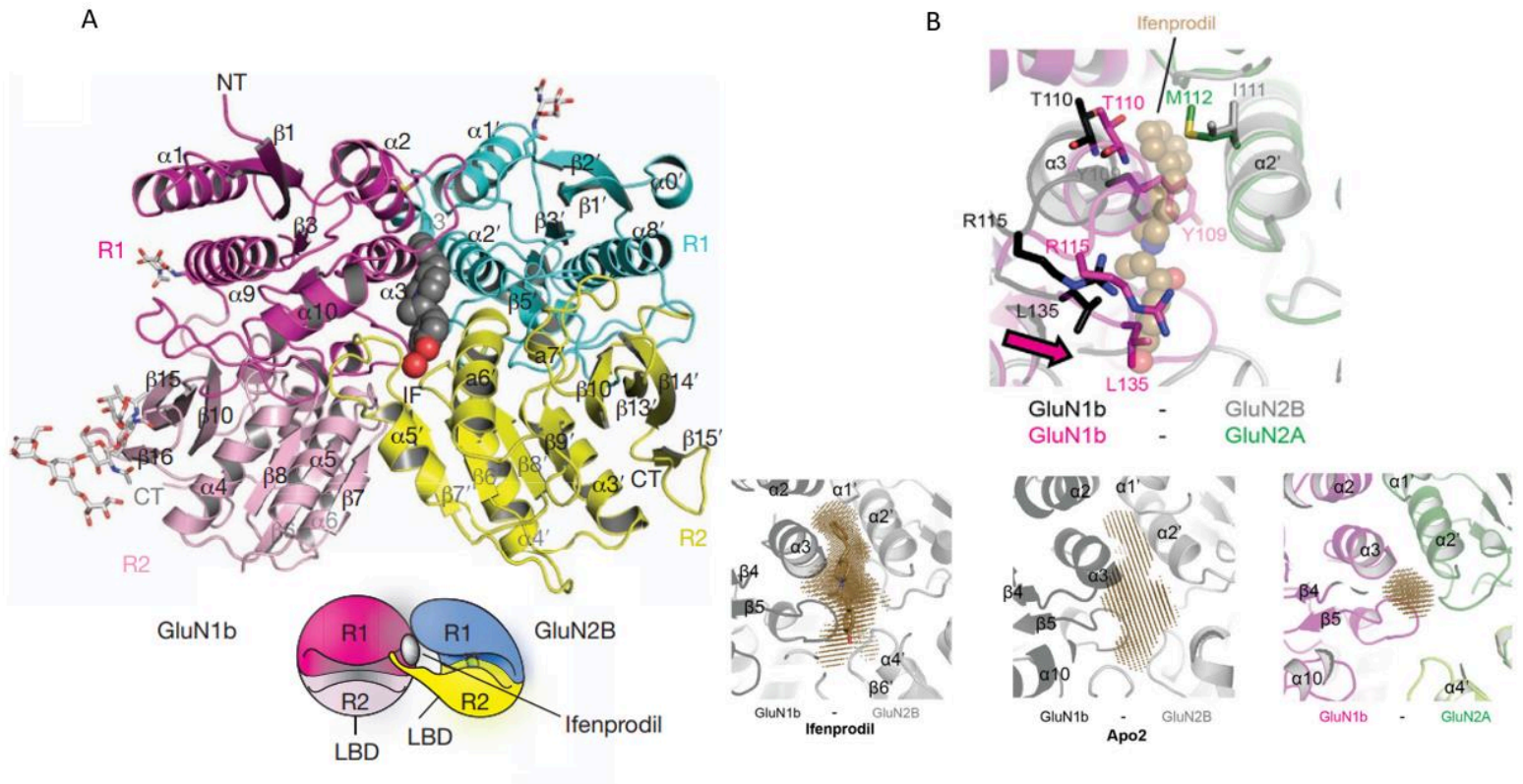


Figure 20 NTD intradimer interface.

Images taken from [108], and [109] Panel A, Side view of the NTD heterodimer. The GluN1 and GluN2B NTDs have a bi-lobed clamshell domain architecture composed of R1 (magenta and cyan) and R2 (light pink and yellow) domains. In grey, Ifenprodil is shown sitting at the intradimer interface. The cartoon below shows a schematization of approximate orientations of the GluN1 and GluN2B NTDs. Panel B, Superimposition of the zinc bound GluN1/GluN2A NTD and the ifenprodil bound GluN1-GluN2B NTD. The ifenprodil binding pocket is occupied by the residues from GluN1 in the GluN1b-GluN2A NTD Intradimer interface (pink color) because of the smaller distance gap between the two subunits (arrow). Below, volume of the gap (in brown dots) at the intrasubunit interface for the ifenprodil bound GluN1/GluN2B NTD (PDB: 3QEL), the Apo GluN1/GluN2B NTD, and the Zinc bound GluN1/GluN2B NTD. The subunit interface gap in the GluN1 GluN2B NTDs is predicted to fit ifenprodil in both cases (volumes 697 and 550 Å<sup>3</sup> respectively), whereas in GluN1/GluN2A NTD it is not (volume ~130 Å<sup>3</sup>).

As mentioned in the section “2.4.4 Allosteric modulators”, zinc is an important endogenous negative modulator of NMDARs. The GluN2A NTD contains a high affinity (nM) zinc binding site located within the cleft and mediated by two histidines and two acidic residues (one aspartate, one glutamate) (Paoletti *et al.*, 1997a; Choi and Lipton, 1999; Serraz *et al.*, 2016; Jalali-Yazdi *et al.*, 2018) (Paoletti *et al.*, 2000). The GluN2B NTD also contains a zinc binding site, although it is hundred fold less sensitive (IC<sub>50</sub> around 2 μM), while GluN2C and GluN2D only have voltage dependent channel block (Rachline *et al.*, 2005; Paoletti, A. M. Vergnano, *et al.*, 2009). In the GluN2B NTD, one of the two key histidines found in

the GluN2A NTD and coordinating the zinc ion (GluN2A-H44) is missing likely accounting for the lower zinc sensitivity of GluN2B vs GluN2A receptors. (Romero-Hernandez *et al.*, 2016). Cryo-EM structures of tetrameric GluN1/GluN2A bound to zinc indicates that zinc facilitates closure of GluN2A NTD clamshell. (Romero-Hernandez *et al.*, 2016; Jalali-Yazdi *et al.*, 2018) However, zinc binding also causes separation of the heterodimer pair, splaying the NTD dimer of dimers apart other than the dimer interfaces as well. The rupture of intersubunit contacts has been suggested to allow the lower lobe of the LBD to move closer, which in turn could relieve tension on the gate after agonist binding and LBD clamshell closure around the agonist, favoring channel closure. This allosteric route is discussed in more detail into the section “4.6 Allosteric modulation: focus on zinc, protons and ifenprodil”. Furthermore, in the NTD of NMDARs a twisted conformation has been shown to occur, adding another further dimension to the possible clamshell movements (Stroebel *et al.*, 2011).

### **3.5 The Transmembrane Domain (TMD)**

In the full tetramer, the four transmembrane domains belonging to the 4 subunits are in close proximity, and together form the ion channel pore where physically the charged ions can cross through the membrane. The individual subunits assemble following a schema in which the subunits GluN1/GluN2/GluN1/GluN2 named 1,2,3,4 assemble in 2 diagonal pairs (Figure 21). Within an individual subunit, the TMD consists of 3 major segments composed of  $\alpha$  helices named M1, M3, and M4. There is also a M2 which is a reentrant pore loop (Hansen *et al.*, 2021). When observed from a top view, it is possible to see that the pore is composed from all 4 NMDARs subunits, arranged with a 4-fold symmetry with the center located within the axis of the pore opening itself (Karakas and Furukawa, 2014; Lee *et al.*, 2014) (Figure 21 Panel A).

The M1-M3 pore region has been described to resemble an inverted KcsA potassium channel (Tikhonov and Zhorov, 2020), among which the pore loop (p-loop) is involved in ion selectivity. This specific architecture is common to a large pore loop family of transmembrane receptors whose characteristic is to present two segments crossing the cellular membrane (M1s and especially M3s) joined by a pore loop (M2) that enters and exits from the same side of the membrane (Figure 21 Panel B). Within iGluRs, the M2 pore loop reenters the membrane from the intracellular side (Wollmuth and Sobolevsky, 2004; Tikhonov and Zhorov, 2020). The M1, M2, M3 helices forming the pore region is a common lineage among all iGluR subunits that have been characterized. The M3s of each subunit line

the pore towards the extracellular side in the permeation pathway, while the M2 is lining the pore in the intracellular side (Hansen *et al.*, 2021). At the top of the M3 helices, towards the extracellular side, M3s form a bundle, which represents functionally an activation gate. This gate physically blocks cation flux when the channel adopts a closed conformation (Karakas and Furukawa, 2014; Lee *et al.*, 2014). Activation of the receptor comports entering into an open conformation, which splays apart this region, letting space for the ions to flow through (Twomey and Sobolevsky, 2018). Just above this bundle there is a highly conserved motif which is called the SYTANLAAF region, found in all iGluR subunits (Figure 21 Panel B). This region is important for the channel gating (Sobolevsky *et al.*, 2009; Twomey *et al.*, 2017a) in all iGluRs, and modifications to it allow to deeply change receptor function. For example, in Delta receptors, it is the site for the Lurcher mutant that makes mutant receptors constitutively open (Zuo *et al.*, 1997). Cysteine mutant substitutions in the SYTANLAAF region allow to evaluate NMDARs receptor Po after MTSEA covalent binding (Yuan *et al.*, 2005; Gielen *et al.*, 2009). Below the channel gate, the M2 loop forms the selectivity filter. This constriction is different for each iGluRs, and is determined by the residue identity at the tip of the M2 helix. Residue identities in a site called the Q/R/N site determine which ions can flow through. The selectivity filter is also important for determining the rate of passage of these ions, as the rate of ions passage can reach a saturating point, determine single-channel conductance, channel block and Ca<sup>2+</sup> permeation (Wollmuth and Sobolevsky, 2004; Traynelis *et al.*, 2010; Hansen *et al.*, 2018). The low affinity channel block for molecules such as zinc or spermine is located at the reentrant M2 pore loop involving residues similar to those important for Mg<sup>2+</sup> block.

The transmembrane helix M4, which is located more peripheral in the pore region, is eukaryote specific (Stroebel and Paoletti, 2021). The M4 of a subunit associates with the transmembrane helices of other subunits (Sobolevsky *et al.*, 2009; Karakas and Furukawa, 2014; Lee *et al.*, 2014; Meyerson *et al.*, 2014). Specifically, the M1-M3 of a subunit cooperate with the M4 of a partner subunit in order to form a functional triad that acts in a concerted manner for the gating of the receptor (Gibb *et al.*, 2018) (Figure 21 Panels C) (for more details, see the section “4.4 Pore motions”). The role of M4 is less clear than other transmembrane helices, but its presence seems a requirement for correct tetramerization of the receptors in AMPARs (Salussolia *et al.*, 2013). In NMDARs, it is a prerequisite for correct gating (Schorge and Colquhoun, 2003). The terminal part of the M4s in each subunit is attached to the intracellular CTD, which in turn affects gating and ion permeability (Murphy *et al.*, 2014).

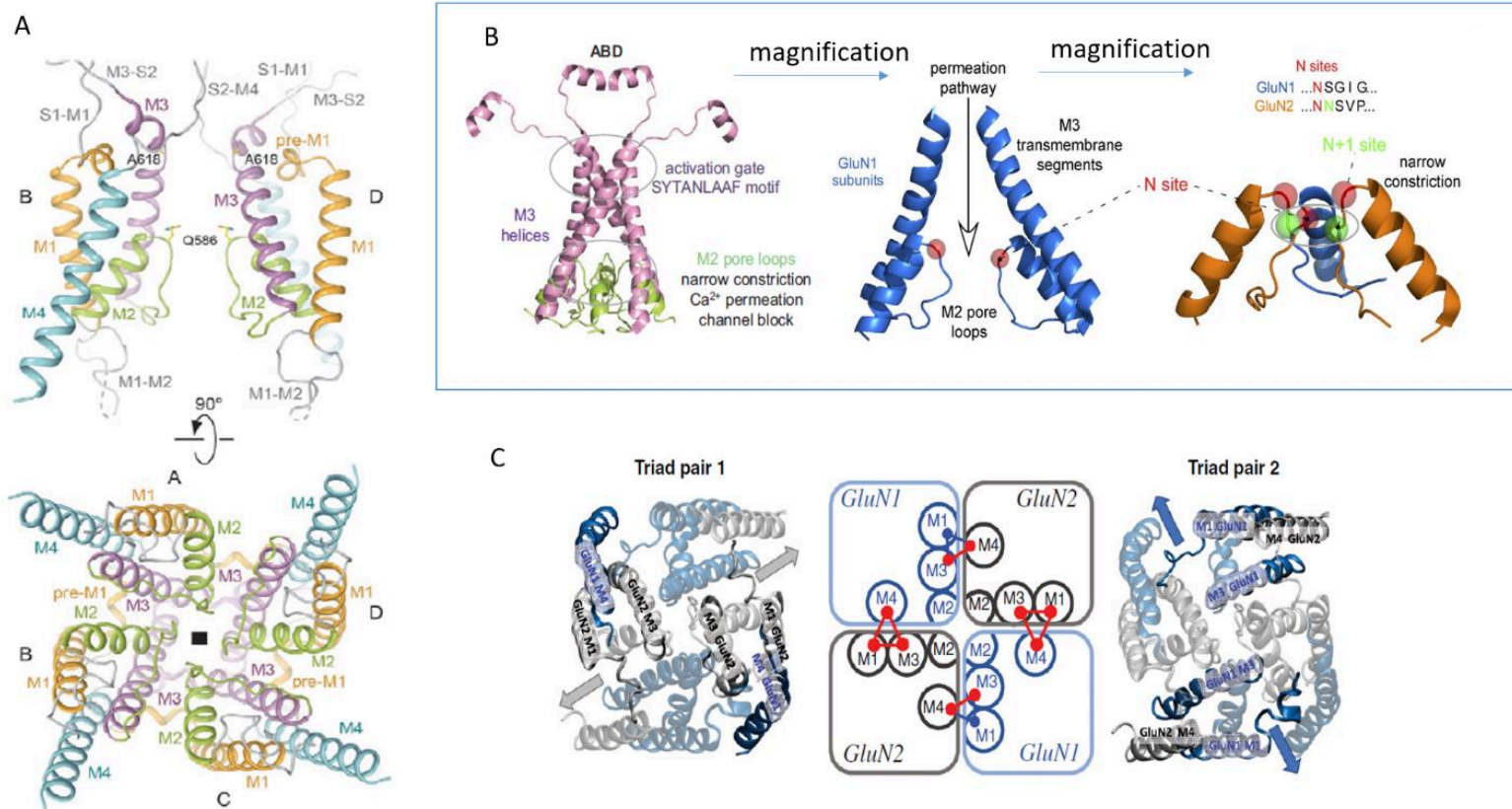


Figure 21 iGluR and NMDAR transmembrane domain.

Images obtained and modified from (Gibb et al., 2018; Hansen et al., 2018, 2021). Panel A, (B) Cartoon side view of TMD of tetrameric GluA2 AMPAR in closed conformation (PDB: 5WEK (Twomey et al., 2017a)). Each subunit is shown with a different color. TMD is shown composed of M1, M3, M4 transmembrane helices and the membrane re-entrant loop M2. Below, top view of the ion channel pore with a black square as a 4-fold center of symmetry. Panel B, simplified representation of the TMD pore to contain some key pore elements. The top part of the M3 segment contains the SYTANLAAF, a highly conserved motif in iGluRs preventing ion flux in the closed state. Below, the M2 pore loop forms the narrow constriction constituting the selectivity filter. Zooming and taking the NMDA perspective (blue PDB: 5UN1; (Song et al., 2018)). The M3 lines the extracellular part of the permeation pathway, whereas the M2 lines the intracellular part. Zooming more, we can see the selectivity filter formed by non-homologous asparagine residues, the GluN1 N site (blue) and the GluN2 N+1 site (orange) at the tip of the M2 loop. Panel C, ribbon structure of the NMDA receptor pore highlighting two symmetrical pre-gating 'triads' composed by the GluN1 subunit pre-M4 region and GluN2 subunit pre-M1 and M3-SYTANLAAF. 2 symmetrical additional triads with reversed subunits are shown on the right. At the center of the panel, a schematic diagram illustrates the four proposed NMDA receptor gating triads.

### 3.6 The C-terminal domain (CTD)

The C-terminal domain of NMDARs and iGluRs in general is the only part of the receptor located purely intracellularly. This region exhibits a high variability on residue identity and length depending on the subunit, making it one of the less conserved regions in iGluRs (Hansen *et al.*, 2021). It is thought that CTDs are flexible regions, lacking proper tertiary structure formation (Choi *et al.*, 2013; Chatterjee *et al.*, 2019). These regions are binding sites for many intracellular molecules and receptor partners, also providing many phosphorylation sites that alter receptor function. Furthermore, this region is important for trafficking the receptors to the plasma membrane, anchoring receptors at synaptic sites and protein degradation [191]. The CTD of some NMDAR subunits contain endoplasmic reticulum retention signals in alternatively spliced exons (Horak and Wenthold, 2009). However, NMDARs artificially lacking the C-terminal can still traffic to the plasma membrane, although they often present modified functional properties (Hansen *et al.*, 2021). This is shown in genetic deletion studies, in which animal models lacking whole or parts of the C-terminals show severe phenotypes of physiological malfunction, in some cases even lethal (Mori *et al.*, 1998; Rossi *et al.*, 2002). One of the most famous partner binding the GluN2B subunit is the Ca<sup>2+</sup>/calmodulin-dependent protein kinase II (CaMKII), which plays a pivotal role in synaptic plasticity processes (Bayer and Schulman, 2019). Furthermore, the CTD is important in synaptic iGluRs for interactions with the postsynaptic density (PSD), the protein interaction network important for synaptic organization (Sheng and Kim, 2011). NMDARs undergo alternative splicing in their CTD, where several isoforms are expressed depending on temporal and regional patterns (Hansen *et al.*, 2021). The GluN1 subunit can be spliced in eight different isoforms from alternative splicing of three exons, modifying the NTD and two regions of the CTD (Figure 22). Alternative splicing also exists in GluN2A and GluN3A, where the CTD has two different splice variants in both cases. In GluN3A, A longer isoform named GluN3A-L contains an insertion of 20 amino acids, but is only found in rodents and not in humans (Sun *et al.*, 1998; Andersson *et al.*, 2001).

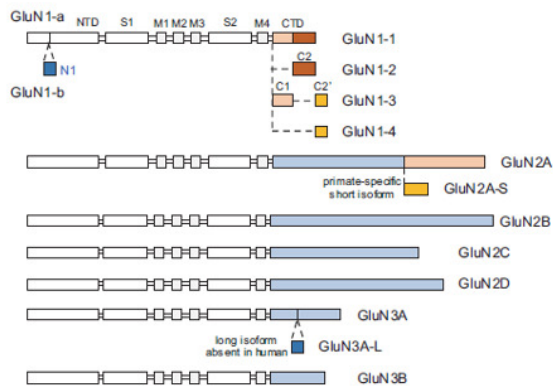


Figure 22 Splice variants in NMDAR subunits.

Image taken and modified from (Hansen et al., 2021). Schematic depictions of the polypeptide chains illustrate sites of modifications resulting from alternative RNA splicing. GluN1 is shown in 8 different isoforms because of alternative splicing of exon 5, exon 21, and exon 22; N1 (21 aa) in the NTD is encoded by exon 5, C1 (37 aa) in the CTD is encoded by exon 21, C2 (38 aa) in the CTD is encoded by exon 22. Deletion of exon 22 creates a shift in the open reading frame, resulting in the alternate exon 220 that encodes C20 (22 amino acids). GluN2A two isoforms are shown with short and long CTDs, the short form is primate-specific. GluN3A two isoforms are shown with GluN3A-L isoform containing a 20-amino acid insertion in the CTD. This longer isoform is not found in human.





## 4 Gating mechanisms

The activation of NMDARs has been evolutionarily designed to respond to high concentrations of agonist for few milliseconds before reuptake of the neurotransmitter. (Hansen *et al.*, 2021) Therefore, there is a need for NMDARs to be able to quickly chain the agonist binding to the opening of the pore, and afterwards shut the pore in the absence of the chemical stimulus. In other words, it is necessary to mechanistically translate changes that happen upstream to a downstream region via multiple necessary steps in just a few milliseconds. Channels become gated, which in the most basic representation usually translates in opening of the pore briefly after a stimulus, followed afterwards by re-entering into a nonconductive state. At the simplest level, there are two possible functional states for iGluRs, a closed channel C and an open channel O. In reality, the non-conductive states are qualitatively different, among which there are various inhibited or desensitized states. If we were to decompose the activation and inactivation process in many chronologically separated steps, we would see that channels can pass transiently in many structurally different conformations, among which the open conformation is one of the more energetically stable conformations among the many transient ones (Gibb, 2004; Alberts, 2010). At the level of the tetramers, different conformations are reflected by different angle orientations between the heterodimers in the LBD, in the NTD, and in the pore. Data that try to explain the gating model of NMDARs usually comes from three different sources: structural data from crystal or cryo-EM structures, functional data from electrophysiological recordings and modeling data carried out by computational analyses. All these sources of information are interrelated to each other, but none of them is free from bias, and sometimes multiple hypothetical explanations may exist for a channel to enter a functional state that is observed with one of these methodologies. Alternatively, a functional state could be reached by multiple pathways, and it can be extremely challenging to unify the various pieces of information that we have coming from many different branches of ion channels investigation. In this section, we will try to detail the major elements of the gating steps, summarizing the major changes underlying conformational receptor re-organization during the activation processes.

### 4.1 Macroscopic processes of activation and deactivation

The gating process of NMDARs starts when the agonist, both in cases of glycine or glutamate, binds to the residues located on the upper lobe of extracellularly located ligand-binding domains (LBDs). It has been estimated that steady state levels of glutamate in the extracellular space range around 80 nM (Moldavski *et al.*, 2020). In physiological conditions of phasic release, glutamate reaches high

concentrations in the low mM range, but it remains in the synaptic cleft for just a few milliseconds before diffusion and reuptake mechanisms reduce its concentration (Clements *et al.*, 1992). These phasic concentrations come from estimates that may differ from the anatomical region taken into consideration in different studies. Regardless, in normal physiological conditions the receptors are usually exposed to the agonist for very brief time, shorter than the time necessary for NMDARs to achieve a full activation and deactivation cycle (Figure 23, Figure 29) (Budisantoso *et al.*, 2013). Therefore, the rate at which glutamate dissociates from synaptic receptors has been hypothesized to be the strongest determinant of the time course and charge transfer of postsynaptic currents (Paoletti *et al.*, 2013). For extrasynaptic receptors, most likely their affinity for glutamate will control their response (Kessler, 2013). Glycine and D-serine have been hypothesized to have tonic extracellular concentrations such as 6  $\mu$ M and 2  $\mu$ M in cerebrospinal fluid (D'Souza *et al.*, 2000; Madeira *et al.*, 2015). From these observations, it follows that the GluN1 site is not saturated in NMDARs (Figure 23), and sudden phasic changes in levels of these ligands may influence receptor activity as they do for glutamate.

In continuous application of glutamate, it has been shown the rates of entry and exit from the non-conductive desensitized state determine the synaptic response time course (Zampini *et al.*, n.d.). It takes several ms (Figure 23) for NMDA receptors to produce a response, much longer than AMPARs and Kainate receptors. The same observation applies to inactivation, which is much slower than other ionotropic glutamate receptors. One of the most important differences in NMDARs vs AMPARs mediated cationic transmission at the synapse is the amount of charge transfer, with AMPARs showing rapid activation and short response time course before the appearance of quick desensitization (Figure 6 Panel B). Among NMDARs, GluN2A deactivates the fastest (35ms), then GluN2B (200ms) and then GluN2C and GluN2D. Deactivation time kinetics and  $P_o$  are correlated in the sense that subunits with lower  $P_o$  take longer to deactivate (Gielen *et al.*, 2009; Hansen *et al.*, 2021). GluN3A containing NMDARs exhibit a current phenotype which is quite different from GluN2 containing NMDARs, and desensitize much faster than the GluN2 counterparts, which is as soon as GluN1 binds glycine right after glycine binds GluN3A (see 5.4 GluN1/GluN3A unusual current phenotype: structural determinants).

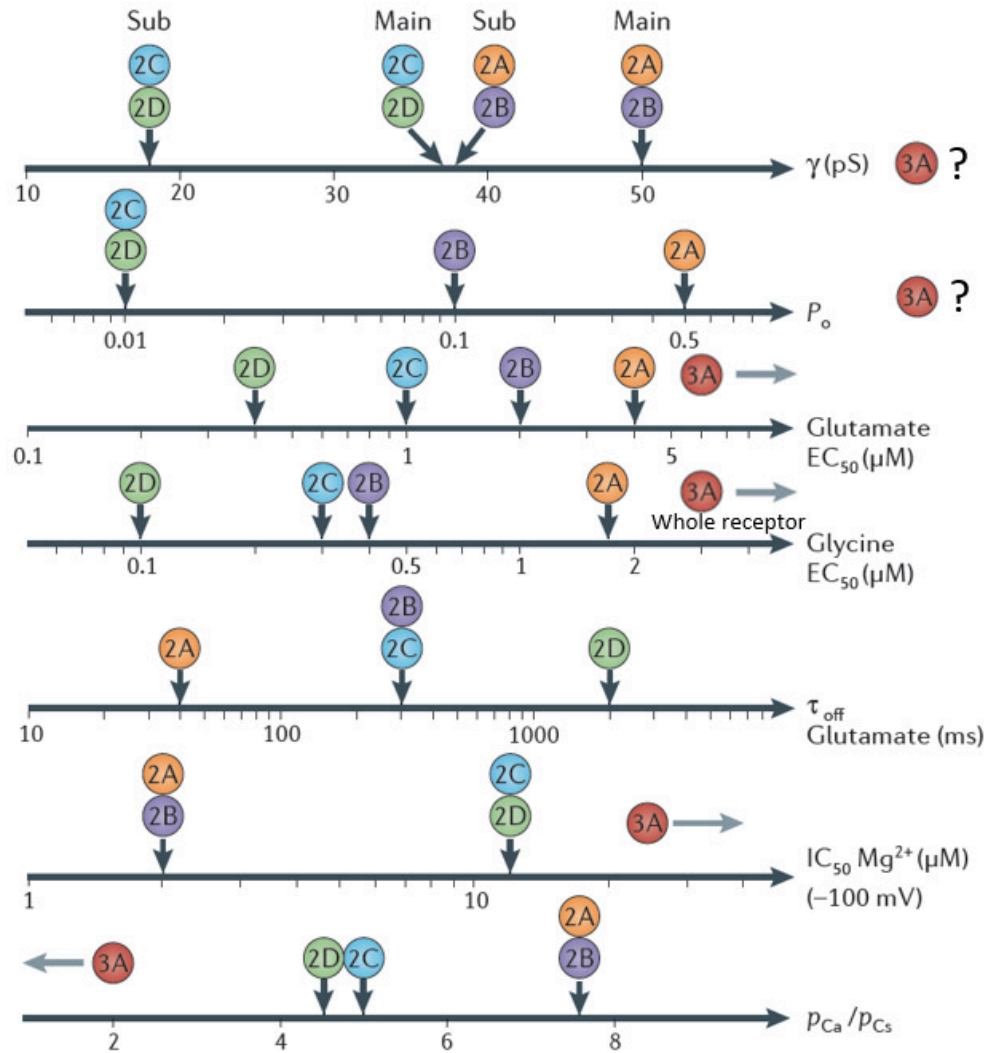


Figure 23 NMDAR subunit composition determines receptor properties.

Picture adapted from (Paoletti et al., 2013). Graphical representation of the various NMDAR subunits displaying distinct gating and permeation properties.  $\gamma$  = single-channel conductance, main and sub-levels.  $P_o$  = channel maximal open probability.  $EC_{50}$  = measure of sensitivity representing concentration eliciting half maximal response to the agonists glutamate and glycine.  $\tau_{off}$  = glutamate deactivation time constant.  $IC_{50} Mg^{2+}$  = measure of sensitivity representing concentration eliciting half maximal inhibition to magnesium at  $-100$  mV.  $Ca^{2+}$  permeation ( $p_{Ca}/p_{Cs}$ ) are shown

## 4.2 Single channel properties and open probability

Single channel recordings of NMDARs have been characterized for a number of different subunit combinations and give us insight about the behavior of channels as unitary conductance units. It has been shown that NMDARs mediate currents with a large conductance 20-50 pS which require co-

activation of both GluN1 and GluN2 sites (Cull-Candy and Usowicz, 1987; Stern *et al.*, 1992). All four subunits must have been activated to produce functional receptor gating (Hansen *et al.*, 2014). Sometimes NMDARs under particular conditions have been described to exist in low activity states, where glutamate pulses fail to trigger receptor responses (Erreger *et al.*, 2005). Another common observation for NMDARs is to show secondary subconductances with lower pS (Stern *et al.*, 1992), which also usually contributes to a smaller number of events compared to the main larger conductance. In triheteromers containing two different GluN2 subunits, biophysical properties are often the result of a complex mix of individual properties of the two GluN2 subunits, rather than a perfect average between the two (Jones and Gibb, 2005; Hansen *et al.*, 2014; Stroebel *et al.*, 2014) (Bhattacharya *et al.*, 2018). This highlights the role of the dimer pair within the full tetrameric receptor, as sometimes the receptor can shift between conductances mediated by the different dimers, like it has been observed between receptors containing GluN1/GluN2A and GluN1/GluN2C dimers coexpressed in the same tetrameric ensemble (Bhattacharya *et al.*, 2018).

Different GluN2 subunits have been shown to have different open probabilities ( $P_o$ ). Different  $P_o$  determine single channels behavior by conferring them unique charge transfer capacities a deriving from the mean time spent in the open state or by the mean time spent in bursting behavior vs closed states.  $P_o$  has been shown to depend on characteristics of proper of each receptor subunits (Gielen *et al.*, 2009; Yuan *et al.*, 2009). GluN2 NMDAR subunits differences in  $P_o$  largely originate away from the channel gating core. It has been shown by multiple methodologies such as single channel analysis, MK-801 inhibition kinetic analysis and MTSEA- induced potentiation that the NTD and the short linker connecting the NTD to the LBD account for a large part of the  $P_o$  differences among the different GluN2 subtypes (Gielen *et al.*, 2009). NTD conformations, dimerization states, spontaneous oscillations, and bound ligands have been shown to determine the  $P_o$  of a subunit. They do so by conferring positive or negative allosteric input that is transduced to lower structure. This modulation can favor or not pre-gating states by lowering or increasing the energetic requirements necessary to undergo the conformational changes that produce the opening of the pore (pre-gating steps).

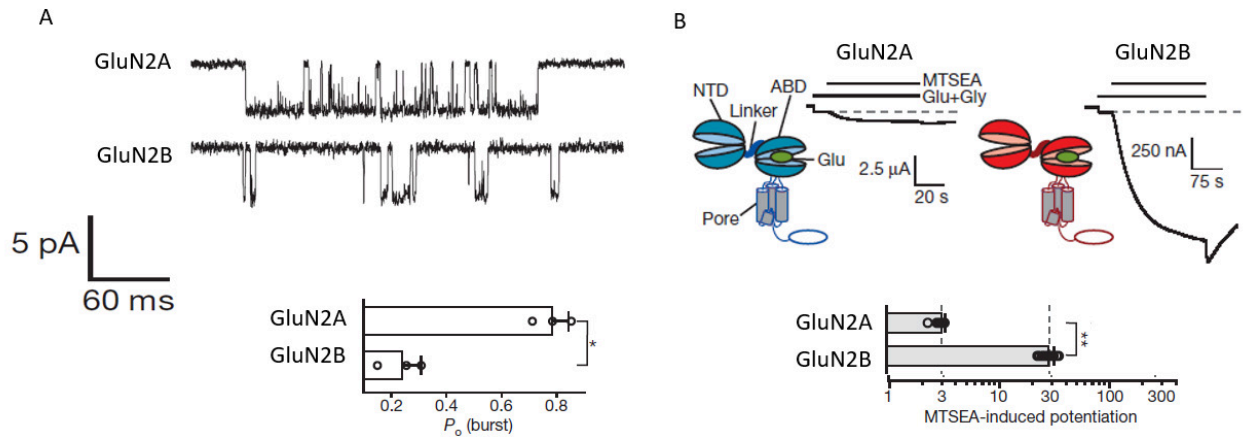


Figure 24 NMDAR GluN2A and GluN2B POs compared.

Image modified from (Gielen et al., 2009) Panel A, representative traces on human embryonic kidney cell (HEK) outside-out patches showing single channel recordings comparing burst activity for GluN1/GluN2A and GluN1/GluN2B. Panel B, Potentiation by MTSEA of receptors coexpressing GluN1-A652C and GluN2A WT or GluN2B WT showing large differences in baseline PO.

For receptors containing the combination of GluN1/GluN3A subunits, the literature is scarce. Only one paper seems to have recorded diheteromeric GluN1/GluN3A co-assemblies in purely glycinergic conditions, but most of the data presented in the paper refers to GluN1/GluN3B subunits, whose two mean conductances are reported to be 37 and 12 pS (Chatterton *et al.*, 2002). Several experiments showed co-injection of the GluN3A subunit with GluN1 and GluN2A in several heterologous expression systems, with the appearance of a subunitary conductance (Das *et al.*, 1998; Pérez-Otaño *et al.*, 2001a; Sasaki *et al.*, 2002; Tong *et al.*, 2008) smaller than the mean unitary conductance usually pertaining GluN2 receptors. However, it is unclear if this subconductance belongs to diheteromeric or triheteromeric assemblies. In the presence of CGP, a weighted mean unitary conductance of 6 pS has been suggested (Zhu *et al.*, 2020).

### 4.3 Kinetic scheme

The steps of agonist binding the receptor and the following activation and inactivation of the receptors can be formally put in a sequential kinetic model of activation. From the analysis of several single channel electrophysiological recordings, scientists have been able to obtain transition rates that allow to isolate the singular components of activation and deactivation of NMDARs depending on the subunits expressed

at the cell membrane (Figure 25 Panel A). For example, it is possible to qualitatively distinguish between several sequential closed states when the clamshells still aren't all yet bound to agonists before triggering the pore opening. Various kinetic models describing NMDARs gating exist, and some are simpler, while others are more complex. In the next section we will discuss the main steps of a simple one, but more comprehensive ones exist (See (Gibb *et al.*, 2018)).

Usually, the activation sequence of diheteromeric NMDARs includes binding steps (two for glutamate and two for glycine), gating steps (C3–C2–C1–O1–O2), and desensitizing steps (D1 and D2) (Figure 25 Panel A). As we mentioned in earlier sections, one of the main actors upstream, both in the receptor structure and gating process, are the clamshells of the LBD. This is because they are being the physical binding site for agonists in NMDARs, triggering the activation process. In x-ray structures of PBP and NMDARs it has been shown agonist binding in the cleft of the clamshell causes closure of the two lobes around the agonist (Furukawa *et al.*, 2005; Trakhanov *et al.*, 2005). Even without agonist, the clamshells can oscillate between open and closed conformations. When the agonist binds the subunit at the cleft of the clamshell, it also makes contact with the residues located in the lower lobe of the LBD, bridging the cleft between the two lobes (Paganelli *et al.*, 2013). This event, as it has been described in the clamshell and LBD dimerization sections, is a major element triggering a large conformational rearrangement involving both the individual clamshell and the dimer back-to-back contacts.

The strength of the intradimer interface has been found to be directly correlated with kinetics involving activation and deactivation (Borschel *et al.*, 2011, 2015) of NMDARs, but not desensitization. This is different from other iGluRs such as AMPARs and kainate receptors, where desensitization kinetics are strongly linked to a disrupted intradimer interface network. Two distinct conformational changes following agonist binding with two different kinetic parameters have been identified to precede channel opening, deriving from patch clamp on single channel experiments and analysis of the individual components of closed time distributions (Banke and Traynelis, 2003; Erreger *et al.*, 2005) (C3-C2 and afterwards C2-C1). These processes also happen in slightly different manner depending on the subunits, (different C2 and all consecutive steps) (Schorge and Colquhoun, 2003; Popescu *et al.*, 2004). These differences in kinetics may reflect many differences in linker conformations, including side chain rotations for key residues or repositioning of the polypeptide chains (Gibb *et al.*, 2018). Hence, since the subunits are co-assembled together, differences also are due to the biochemical makeup of the tetrameric interfaces, for example depending on the strength of the LBD intradimer interfaces and the LBD interlobe contacts that further stabilize or disrupt dimerization and the closed cleft conformations.

Agonist efficacy has been hypothesized to be a direct measure of the degree of agonist-induced cleft-closure and may have a direct relationship with the stability of the closed-cleft conformation (Lester and Jahr, n.d.). Importantly, the conformational changes that gate the channel after agonist binding also prevent the dissociation of the glutamate from the clamshell. Therefore, if the channel enters the open state through a sequence of precise motions, it will first have to undergo the reverse sequence of conformational changes before glutamate can dissociate (Iacobucci and Popescu, 2018).

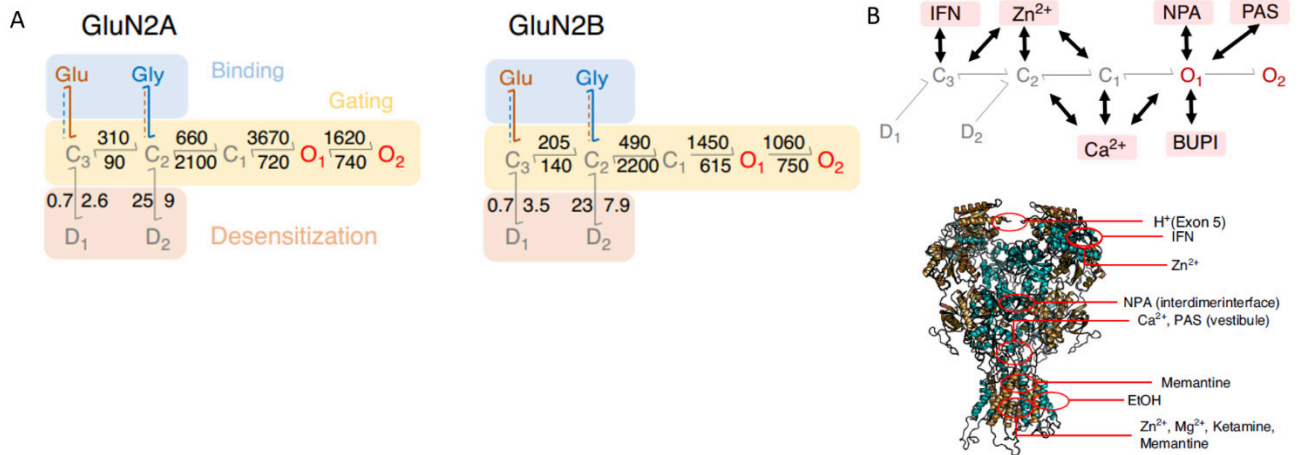


Figure 25 Kinetic scheme of NMDARs.

Images obtained and adapted from (Iacobucci and Popescu, 2018). Panel A, a comparison between two distinct, yet similar kinetic models created from single-channel recordings of GluN1/GluN2A (left) and GluN1-1a/GluN2B receptors (right). Different functional states are described: after binding glutamate (Glu) and glycine (Gly), receptors cycle among five closed states, C1–3 and D1–2, and two open states, O1–2. Rate constants are in S<sup>-1</sup>. Panel B, the same reaction scheme structure described in Panel A, with the addition of few modulator-bound receptors depicted by the pink box, which has modulator-dependent rate constants. Black arrows indicate the preferred transition states influenced by each modulator. The indicated modulators are NTD binding allosteric modulators protons (H<sup>+</sup>), ifenprodil (IFN), Zn<sup>2+</sup>. Modulators Ca<sup>2+</sup>, bupivacaine (BUPI), naphthoic acid (NPA), and pregnanolone sulfate (PAS). Below, full structure of tetrameric receptors (GluN1, gold; GluN2, light blue; PDB ID: 4PE5) with highlighted regions of modulator-binding sites.

Two more closed channel states have been described that are not categorized as resting or pre-gating steps. These are conformations in which the receptors are bound to the agonist, but in a closed state. These are a desensitized state 1 (D1) from C3 (C3–D1) and a desensitized state 2 (D2) from C2 (C2–D2). Usually, these states in NMDARs describe states mainly available for receptors which have been exposed for longer periods of time to the agonist, longer than the usually short period of time in which glutamate is available within the synapse before reuptake. Therefore, desensitized states have a relevant physiological role for extrasynaptic NMDARs (Iacobucci and Popescu, 2017). Finally, the open channel

states exist, these are states in which the receptor pore is open and ion flux is possible. Two different open states have been hypothesized to exist, although with similar conductance. As it was mentioned before, different rates have been theorized for different GluN2 subunits, also depending on subunit Po.

Within this linear scheme of activation, it is possible to hypothesize that specific pharmacological compounds can have an influence on specific rates of transitions. A schematic summary for some of the most famous NMDA modulators can be seen in (Figure 25 Panel B). Some of the modulators, such as zinc or ifenprofil bind preferentially to closed states such as C3 or C2 (Amico-Ruvio *et al.*, 2011, 2012). This is different from open channel blockers such as Magnesium, which is thought to bind preferentially during channel open states. As it is possible to remark for the Panel B of Figure 25, there seems to be a correlation between the structural locations of the binding epitopes of similar drugs and the type of rate that is affected. This had led to the hypothesis that changes within the receptor may happen in a top-down hierarchical fashion, starting extracellularly from the N-terminal domain and going down to the transmembrane and intracellular regions (Iacobucci and Popescu, 2018).

#### **4.4 Pore motions**

The rates describing conformational rearrangements between gating modes are slower than the activation/deactivation transitions. Very important are the concerted motions linking vertically the movements from upstream to downstream domains, such as the linkers connecting the D1 and D2 sections of the LBD to the TMD (C1-O1). After the clamshell closes, the D2 section of the LBD moves away from the plasma membrane. These pre-gating steps of linker movements are separated from closure of clamshell conformations, since clamshell closure is estimated to happen on a faster timescale below the ms, as experiments of very short time agonist application can still elicit a response (Banke and Traynelis, 2003). The conformational changes started at the LBD level cause an all or nothing opening of the ion channel pore (Kazi *et al.*, 2014). In the resting state of the iGluRs, the M3 helices form a bundle in the most upward region towards the linker tightly sealing the permeation pathway (Sobolevsky *et al.*, 2009). However, depending on the subunit position within the receptor, different linkers take on different orientations. Specifically, the M3-S2 linkers in the A/C position (GluN1) are almost perpendicular to the membrane and those in the B/D position (GluN2) are nearly parallel to the membrane (Karakas *et al.*, 2009; Sobolevsky *et al.*, 2009; Lee *et al.*, 2014). Therefore, the two subunit pairs must undergo different movements to displace the bundle. There is a vertical movement of the



GluN1 pre-M3 linker, and the lateral separation of GluN2B pre-M3 linker by 7 Å and 11 Å, respectively (Dai and Zhou, 2013; Tajima *et al.*, 2016) (Figure 26 Panel A). These linker movements in turn pull the M3 transmembrane helices apart in different directions. These differences in pulling directions depending on the subunit identity may reflect the differences of the two components of gating rates observed in NMDARs (Banke and Traynelis, 2003; Auerbach and Zhou, 2005). Much of what we know about the pore displacement refers to AMPARs, but it is hypothesized that the main gate movements of NMDARs resemble AMPARs (Chou *et al.*, 2020; Wang *et al.*, 2021). This transition of the M3 transmembrane helices from a closed to an open conformation physically allows for the cations to be able to cross the pore.

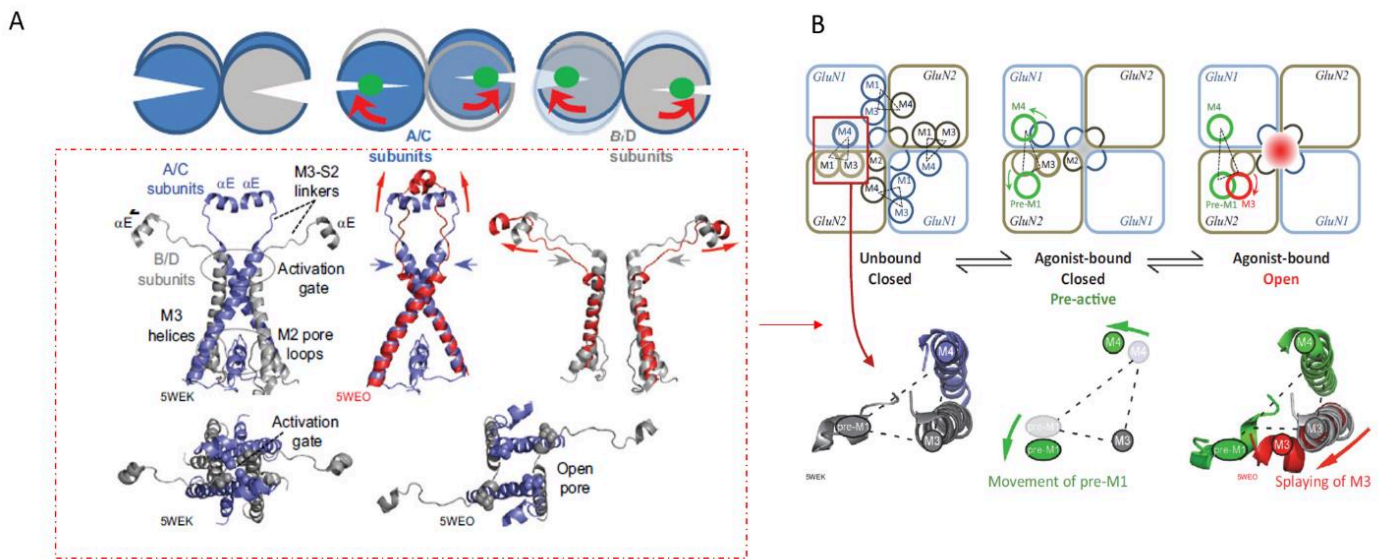


Figure 26: Pore motions in iGluR gating.

Image obtained and adapted from (Hansen *et al.*, 2021). Panel A, clamshell arrangement of a LBD dimer (left) and the two A/C (middle) and B/D (right). The LBDs are bound to agonists, which produces clamshell closure. Below in the dotted red square and on the left, resting conformation of the M3-S2 linkers and the M3/M2 transmembrane helices, forming the ion permeation pathway. M1 and M4 transmembrane helices are omitted for simplicity. Moving to the middle panel, illustration of how LBD clamshell closing motions rearrange the M3 helices of the A/C subunits, with a vertical upward movement (red arrow). Moving to the right, panel illustrating how clamshell closing motion rearranges the B/D subunits, and laterally displaces the M3 helices (red), causing the SYTANLAAF conserved motif to splay apart. At the bottom, view of the extracellular side of the transmembrane domain perpendicular to the axis of the permeation path for AMPAR closed (PDB ID: 5WEK) and open receptors (PDB ID: 5WEO). Panel B, schematization of the gating triad comprising the pre-M1 helix, the M3 helix, and the pre-M4 linker of the adjacent subunit. The cartoon illustrates two steps which are prerequisites for gating of the pore, including pre-M1 helix motion and repositioning of the M4 linker (green, pre-active state). These motions are hypothesized to occur prior to the displacement of the M3 helix to reach the active state and open the channel pore. Below, the GluN2 (B/D position in the tetramer) pre-M1 helix, the GluN2 M3 transmembrane helix, and the GluN1 M4 transmembrane helix from one gating triad are

shown as ribbon structures. As above, motions represent movements from closed gate (left, ID PDB: 5WEK) to the open (right, ID PDB: 5WEO) states.

However, the M3 helices and linkers do not act as an isolated entity in the gating of the receptor. First, these structures are surrounded by the outer M1 and M4 transmembrane helices and the linkers S1-M1 and S2-M4 connecting the transmembrane helices to the LBD. These regions are also important for gating, and contain allosteric binding sites for pharmacological compounds that have been found to influence NMDAR function (Lee *et al.*, 2014; Yelshanskaya *et al.*, 2017; Hansen *et al.*, 2021). Analysis of NMDARs crystal structures has brought forward the hypothesis that a functional gating triad is composed by a M3 of a subunit, the M4 of that same subunit and a M1 of the partner subunit, each with their respective linkers relaying from the LBD (Gibb *et al.*, 2018; Perszyk *et al.*, 2020; Amin *et al.*, 2021). However, our knowledge of pore movement is fragmentary and incomplete. Analysis of shut time in prolonged single channel recordings indicated that multiple movements and rearrangements happen in the pore before the gating effectively takes place (Banke and Traynelis, 2003). It has been hypothesized that there is an outward motion of the pre-M1 helix following agonist binding, which might have an effect in the energetics necessary for reaching the open state (Dolino *et al.*, 2016; Durham *et al.*, 2020) (McDaniel *et al.*, 2020) When decoupling the pre M1 helix of GluN2A from the S1-M1 linker by adding glycine amino acid insertions in the linker itself, mutant NMDA receptors cannot produce rapid synaptic-like channel opening (Amin *et al.*, 2021). Similar results have been obtained when mutating a conserved proline in the Pre-M1 helix of GluN2A in close proximity to the M3 helix (Ogden *et al.*, 2017; Gibb *et al.*, 2018). The M4 helix does not seem to directly contribute to the pore permeation, but seems to be a required structural element stabilizing the pore architecture (Schorge and Colquhoun, 2003). Residues in the M4 have been found to influence deactivation time courses by influencing M3 conformations (Lemke *et al.*, 2016; Platzer *et al.*, 2017).

#### **4.5 Desensitization: AMPARs vs NMDARs**

Desensitization can be described as a reduction of the response while in the continuous presence of a stimulus. Therefore, usually desensitization follows the activation steps, being slower in kinetic than the activator process, and entails a closure of the channel pore following an activator stimulus. Desensitization may serve a protective effect, in order to limit the amount of current that can pass through the pore in the presence of a continuous agonist release. The process of desensitization differs greatly between the different iGluRs. AMPARs and Kainate receptors have been described to have much faster and complete desensitization compared to NMDARs (intended as closer steady state current to

baseline holding potential) (Figure 27 Panel A). Furthermore, these iGluR classes enter the desensitized state also following brief exposures of glutamate. Desensitization in AMPARs and kainate receptors has been studied by combining many different functional approaches. As it was mentioned before in the structure part, it has been found that a key determinant in these receptors for the regulation of desensitization is the back-to-back heterodimer or intradimer interface at the LBD level. Rearrangement of this interface within AMPARs after agonist binding has been found to control this process.

The binding of many positive allosteric modulators such as cyclothiazide, CX614 and aniracetam at this site has been found to favor dimerization and decrease of extent and speed of desensitization in AMPARs (Partin *et al.*, 1995; Sun *et al.*, 1998; Jin *et al.*, 2005). Similarly, crosslinking studies were found to deeply influence desensitization kinetics in both AMPARs and kainate (Armstrong *et al.*, 2006; Daniels *et al.*, 2013). It has shown that the desensitized conformations of these receptors are similar to the open state in terms of clamshell closeness, but the D1 lobes are pulled apart, becoming separated in space, and making the D2 lobes and linkers adopt a closed conformation (Armstrong *et al.*, 2006). Therefore, in the desensitized state the D1-D1 interface is completely disrupted. Similarly, in kainate receptors it has been hypothesized that the desensitized state shows the D1 dimers to be broken into two functional monomers (Schauder *et al.*, 2013). Crystal structures of the desensitized state in AMPARs show a decoupling between the LBD and the TMD and a ruptured interface (Chen *et al.*, 2017; Twomey *et al.*, 2017a) (Figure 27 Panel B). These desensitized conformations have no more a 2-fold symmetry, because the subunits in the positions A and C rotate away from the B and D dimer partners, creating clefts in the sites that were adopted by the dimer interfaces. The D2 lobes of each subunit reproach each other, and the channels lower LBD D2 lobes take a conformation resembling the ones of the closed states, also exerting a pull on the linkers that makes the receptors close the pore. (Chen *et al.*, 2017; Twomey *et al.*, 2017a). While the pore configurations of the desensitized and closed states are very similar, the rest of the receptor structure is quite different. There is an overall increase of the receptor compaction on the axis perpendicular to the membrane by 5 Å compared with the closed state and a large rotation of the entire NTD module. Structures of kainate receptors into desensitized states also show monomerization of the LBD dimer, to an even greater extent than AMPARs (Meyerson *et al.*, 2014; Kumari *et al.*, 2019).

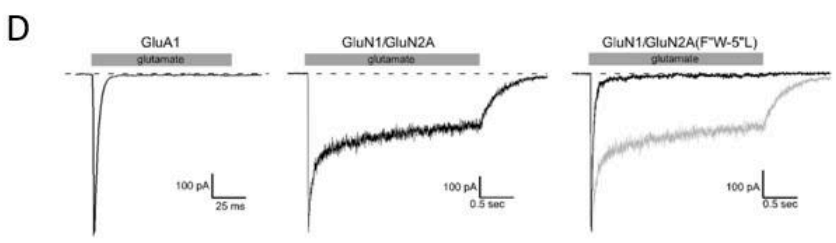
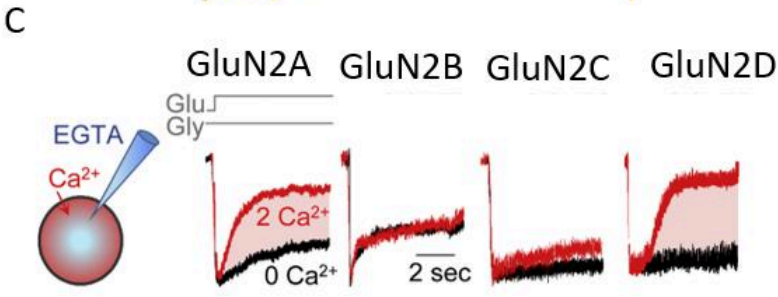
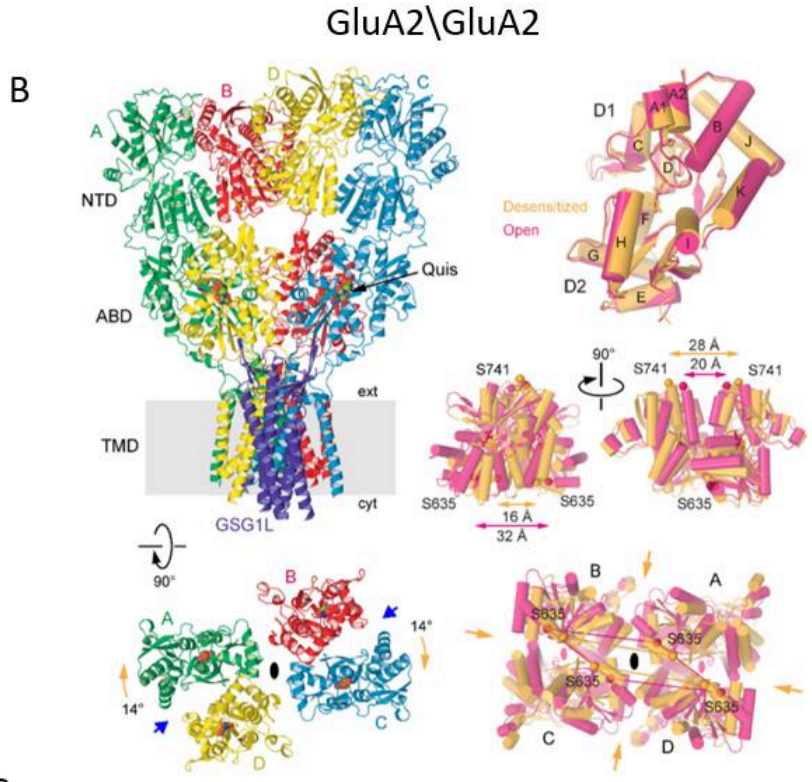
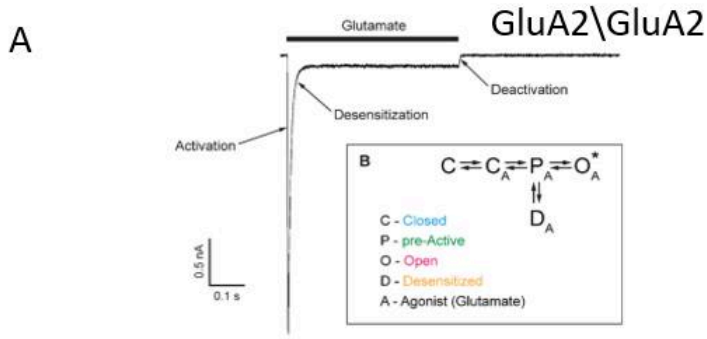


Figure 27 AMPARs vs NMDAR desensitization:

Images obtained and adapted from (Alsaloum et al., 2016; Iacobucci and Popescu, 2020; Hansen et al., 2021). Panel A, example trace from whole cell current from GluA2 homomeric receptors following saturating glutamate application. Below, a theoretical kinetic model describing conformations accessed by AMPA receptors. Panel B, top left cartoon showing full tetrameric structure for the desensitized state of GluA2 (ID pdb: 5VHZ) from the side view. Below, a top view of the LBD from the same structure showing decreased dimerization in the desensitized state. Orange arrows indicate desensitization associated rotation of monomers A/C away from B/D subunits. Blue arrows point to the cleft between the LBD dimers. On the right, comparison of individual LBDs, LBD dimers and LBD layers viewed intracellularly in desensitized (pdb ID: 5VHZ, orange) and open (pdb ID: 5WEO; pink) states. At bottom right, compression of the LBD gating ring for the desensitized state is compared to the open state (orange arrows). Images adapted from (Twomey and Sobolevsky, 2018). Panel C, outside-out patch recording of in HEK 293 cells transfected with GluA1 (left), GluN1/GluN2A (middle) or GluN1/GluN2A (F536L) (right) in cells treated with glutamate, showing how desensitization differences between AMPARs and NMDARs are also due to hydrophobic box located at the extracellular interface of transmembrane helices. Panel D, calcium dependent inactivation of NMDA receptor currents depending on the GluN2 subunit. Superimposed whole-cell traces recorded in no external  $Ca^{2+}$  (black) or with 2 mM  $Ca^{2+}$  (red) from HEK-293 cells expressing GluN1 and the indicated GluN2 subunit, with EGTA.

As reported before, in NMDARs the crosslink of the interface does not have effect on desensitization of the receptor (Borschel et al., 2011). Desensitization is observed in NMDARs when receptors are exposed to agonist application for longer periods of time than the ms synaptic exposure to the agonist. Furthermore, several qualitatively different desensitization processes have been described for NMDARs. There is glycine dependent desensitization, calcium-dependent inactivation, zinc dependent desensitization, and glycine and calcium independent desensitization (Hansen et al., 2021). The molecular mechanisms underpinning this diversity of mechanisms are poorly understood. The intradimer interface may have a role in at least some of them. When glutamate is bound to GluN2A in non-saturating glycine concentrations, this interface mediates negative allosteric modulation between the subunits, and causes a decrease of affinity in the glycine binding site, therefore causing some glycine to unbind from the epitope (Benveniste et al., 1990; Lester et al., 1993; Durham et al., 2020). Likewise, glycine binding triggers an analogous mechanism in the glutamate binding subunit. It has been hypothesized that this desensitization is influenced by a hydrophobic box located at the extracellular interface of transmembrane helices, non-conserved between NMDARs and AMPARs, and mutations within these regions can produce intermediate phenotypes between NMDARs and AMPARs (Figure 27 Panel C) (Alsaloum et al., 2016). Several molecules have been described to cause a desensitization phenotype in NMDARs. Increases in intracellular  $Ca^{2+}$  have been found to reduce PO in GluN2A receptors, but not in GluN2B, because it triggers uncoupling from cell actin (Rosenmund and Westbrook, 1993; Iacobucci and Popescu, 2020), and therefore a change in the steady state current levels (Figure 27 Panel D). Similarly, calmodulin binding to GluN1 CTD has been found to reduce GluN1 receptor PO and mean

open time (Rycroft and Gibb, 2002). Another molecule that causes a desensitization like phenotype is zinc. The reason for this change in current phenotype is the positive allosteric modulation between glutamate binding in the LBD and zinc binding in the NTD. Since Zinc inhibits GluN2A-containing NMDARs currents, receptor currents decay to a more positive steady state current level with higher occupancy of the NTD by ambient zinc after glutamate binding (Hansen *et al.*, 2021). Overall, even though there are several types of desensitization and several molecules cause a desensitization-like phenotype in NMDARs, desensitization plays a less prominent role in GluN2 containing NMDARs than AMPARs. In GluN1/GluN3A receptor desensitization is an extremely quick and prominent process resembling more AMPARs or kainate receptors than GluN2 containing NMDARs. The structural determinants for this behavior are described in the GluN3A chapter of the introduction.

#### **4.6 Allosteric modulation: focus on zinc, protons and ifenprodil**

Some NMDAR allosteric modulators such as zinc, protons or ifenprodil are able to bind the intradimer interface of the NTD, modifying its conformation. We have much structural information on how these compounds can modulate receptor activity through the NTD-mediated allosteric routes. Zinc is able to stabilize closed conformations of the clamshells in the NTD (Karakas *et al.*, 2009; Sirrieh *et al.*, 2013), locking receptors into low  $P_o$  states (Figure 28 Panel A). Zinc also separates the GluN1/GluN2A NTD heterodimer pairs, splaying the dimer of NTD dimers as well as GluN1/GluN2A LBD dimer interfaces. (Romero-Hernandez *et al.*, 2016) Mutagenesis carried out with the aim of disfavoring clamshell closure in the GluN2A subunit both alleviate the zinc inhibition while increasing the overall receptor  $P_o$  (Romero-Hernandez *et al.*, 2016). Proton sensitivity and zinc sensitivity are related, as exon5 splicing regulates both of these properties. There is a strong correlation between pH and zinc modulation because, in the transduction of allosteric inhibition from the NTD to the LBD, proton binding takes place downstream of zinc-induced closure of the NTDs. Zinc bound receptors remain active, but display altered modified  $pK_a$  for proton inhibition. A recently published paper solved many different structural conformations of zinc bound NMDARs. It proposed zinc to shift the proportions of receptors towards conformations with reduced interactions between the two heterodimer NTDs in a proton-dependent manner. With no zinc and at basic pH, there are two contact points between the two NTD heterodimers, a conformation which displays a high  $P_o$  (2 knuckle conformation). The conformations change progressively with the addition of either zinc or acidic pH (Figure 28 Panels A, B), reducing the contact points (extended, 1 knuckle and

then supersplayed), with increasingly lower  $P_o$  and separation of the NTD dimers (Jalali-Yazdi *et al.*, 2018; Zhang *et al.*, 2018). These NTD conformational changes are transduced downstream to the LBD layer to reduce the tension in the linkers connecting the LBDs to the channel pore. It has been found that mutations that weaken the LBD intradimer interface stability increase zinc inhibition (Gielen *et al.*, 2009), whereas crosslinking the intradimer interface through disulfide bridges has an opposite effect, indicating how motions between these two interfaces influence each other. Increased glutamate affinity induced by allosteric zinc inhibition at the NTD level is observed because separation of the agonist-bound LBD relieves the strain exerted by the linkers from the transmembrane segments, thus stabilizing the closed conformation of the LBD (Gielen *et al.*, 2008). In GluN2B, zinc inhibition follows a different route. It binds and closes the GluN2B NTD, which afterwards shifts the NTD dimer in a relaxed configuration, with the GluN1 and GluN2B R2s separating. This promotes downstream a rolling-down of the LBD inter-dimer interface, causing releasing the tension of the LBD-TMD linkers and promoting channel closure (Tian *et al.*, 2021).

For GluN2B selective negative allosteric modulation, ifenprodil mechanism has been dissected in great detail. As we mentioned in the NTD Intradimer interface section, the binding site for ifenprodil resides at the interface between the GluN1 and GluN2B NTD heterodimer (Karakas *et al.*, 2011). Similar to zinc modulation, also ifenprodil influences LBD agonist affinities, displaying a positive allosteric coupling between ifenprodil and glutamate binding (Kew *et al.*, 1996), and having reduced inhibition with increasing glycine concentrations (Williams, 1993). Binding of ifenprodil causes the NTD clamshells to close, with a repositioning of the NTD heterodimers compared to the LBD (Burger *et al.*, 2012; Tajima *et al.*, 2016; Chou *et al.*, 2020). This modification has been hypothesized to resemble an inactive conformation adopted by the receptor, which is also named inactive 1 (Figure 28 Panel C). Within this conformation the lower lobes (R2) lobes of the NTD are separated (17 Å) at the heterodimer interfaces, and both the GluN1-GluN2B LBD dimers pairs are rolled down toward the membrane. This in turn lowers the tension on the linkers connecting to the TMD. In the active conformation, the NTD clamshells are in an open conformation, and this leads the R2 lobes of the GluN1 and GluN2 NTDs to reproach each other (12 Å). This causes an opposite motion in the LBD heterodimer, with the two dimers rolling up away from the membrane, pulling tensions in the linkers necessary for pore motions. It has been suggested that these differences conformational changes leading to a drop in channel  $P_o$ , are similar for all ifenprodil, zinc and protons (Jalali-Yazdi *et al.*, 2018).



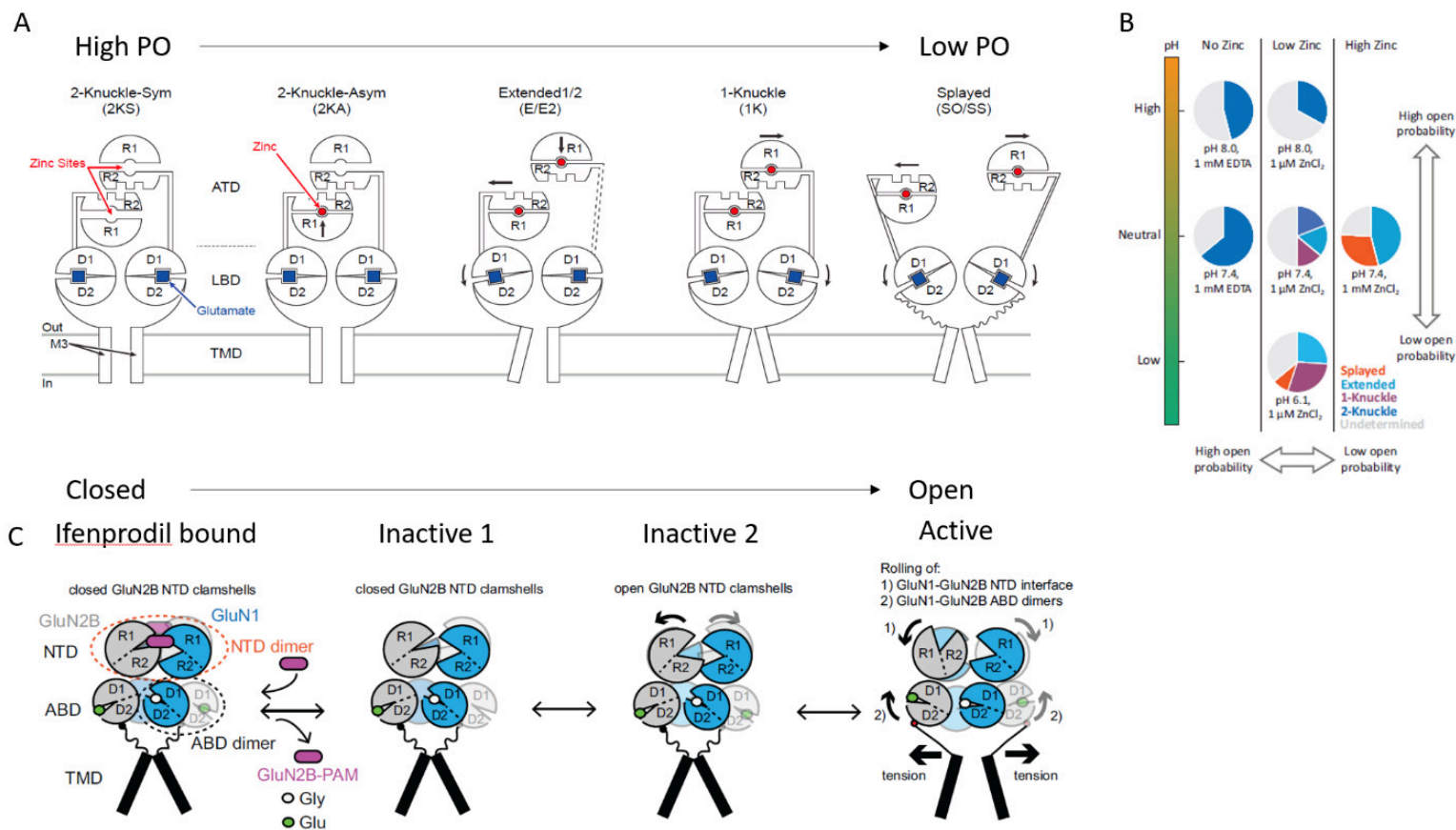


Figure 28 Allosteric modulation in NMDARs: ifenprodil, protons and zinc.

Images obtained and adapted from (Jalali-Yazdi et al., 2018; Hansen et al., 2021). Panel A, schematic of the conformational changes caused by zinc and proton allosteric modulation in GluN1/GluN2A. They are ranging from high PO conformations (2 knuckles), to lower PO states (extended) to states with PO close to zero (supersplayed). Closure of both NTD clamshells caused by binding of either zinc or protons causes downstream motions of the LBD clamshells, LBD D2 lobes come closer, releasing the tension on the gate and closing it. In the extended conformations, where one NTD heterodimer does not interact with the rest of the receptor, zinc and proton inhibitions are not transduced efficiently through the LBD, leading to higher PO as compared to the 1-knuckle state. Panel B, The occurrence of these structural conformations in various conditions of zinc and protons availability. Panel C, schematic illustration of domain and subunit arrangement of GluN1/2B in various conformations. Iifenprodil targets the subunit interfaces of GluN1/2B NTDs stabilizing the closed GluN2B NTD clamshell, stabilizing a conformation similar to inactive 1 and 2. No rolling occurs in NTDs and LBD of conformations inactive 1 and 2, but they differ by whether the GluN2B NTD clamshell is open or closed. The population of inactive 1 increases with lower pH. In the active state, the GluN2B NTD clamshell is open, and the NTD heterodimer interfaces roll, and the LBD heterodimers roll to create tensions in the LBD-TMD linkers, that leads to channel opening.

## 4.7 A unified model of NMDAR gating

Intersubunit and inter-domain rearrangements are critical molecular determinants of functional transitions in NMDARs, accounting for receptor channel gating and its allosteric regulation. In this



picture, the NTD is key in controlling gating properties as mentioned in the NTD dimerization section. Through allosteric relay to lower structures, the NTD influences channel biophysical properties such as PO and speed of deactivation. There are some key differences in how GluN2A and GluN2B regulate receptor gating through allosteric modulation, even though they have somewhat similar macroscopic structures. While both subunits show a functional NTD intradimer interface, crosslinking at this interface follows two different downstream routes of allosteric modulation depending on the subunit. A key experiment showed that real time photo crosslinking the local conformation of individual NTD dimers has major influence on GluN2B receptor activity, but much less on GluN2A receptors (Tian *et al.*, 2021). This indicates that GluN2B requires larger conformational rearrangements of the NTD to produce gating, while GluN2A NTD interfaces are tightly packed, conferring a high Po to the receptors. Furthermore, the two interfaces are also different structurally, as we have shown before there is a binding pocket for molecules in GluN2B interface which is missing in GluN2A (Hansen *et al.*, 2021). However, the positions of the two adjacent NTD dimers, which form an interdimer interface between the two GluN2 NTD lower lobes, affect allosteric in GluN2A receptors, but not in GluN2B receptors, and become very important for zinc modulation (Figure 28). The GluN1 NTD, together with the GluN2 NTD, undergoes large-scale conformational dynamics preceding and during receptor gating, involving motions such as interlobe opening-closure and twist-untwisting motions (Esmenjaud *et al.*, 2018). These features highlight the difference between AMPARs and NMDARs, in which in NMDARs the NTD imposes strong structural constraints on lower lobes, but it does not on AMPARs.

The coupling between the NTD and the LBD regions uses different routes in GluN2A and GluN2B receptors. In GluN2A, NTD conformations are relayed to a great extent by the upper D1 intradimer interface (Gielen *et al.*, 2008; Tian *et al.*, 2021) (explained in the dimerization of the LBD intradimer interface section), while in GluN2B they are largely relayed via the recently discovered interdimer interface (Esmenjaud *et al.*, 2018; Tian *et al.*, 2021) (Figure 29 Panel A). Structural dynamics performed on GluN2A motions indicate that this interface might break temporarily during motions of the LBD, while it does not in GluN2B (Tian *et al.*, 2021). Molecular modeling indicated that in GluN2B the LBD intradimer interface might be more stable overall. This increased stability could explain why in GluN2B the NTD mediated allosteric route is not much influenced by the conformations assumed by the intradimer interface, as more flexibility in this region might be needed to relay upstream conformational rearrangements to the back-to-back dimers. Conformational mobility is a must at several interdomain and intersubunit interfaces, as disulfide bridges formation via cysteine mutants insertion produces

silenced receptors, that are rendered WT-like again upon requiring mobility upon reducing agent treatment (Esmenjaud *et al.*, 2018). In GluN2B close apposition of the NTD lower lobes favors the rolling motion which is an important pre gating step as it largely increases receptor PO (Tajima *et al.*, 2016; Esmenjaud *et al.*, 2018). It has been hypothesized that polyamine molecules such as spermine act stabilizing this rolled conformation in GluN2B receptors (Mony *et al.*, 2011; Esmenjaud *et al.*, 2018). Vice-versa, NAM molecules such as ifenprodil, protons or zinc might stabilize the opposite conformation, which is the unrolled one. This hypothesis is reinforced by the fact that cysteine mutants forming disulfide bridges that stabilize either the rolled or the unrolled state become unresponsive to the NAMs or PAMs respectively (Esmenjaud *et al.*, 2018). In GluN1, rolling of the LBD is followed by a vertical movement that compresses the downstream linkers. in GluN2B, LBD rolling is followed by a lateral separation of the linkers away from the ion channel central axis (Esmenjaud *et al.*, 2018).

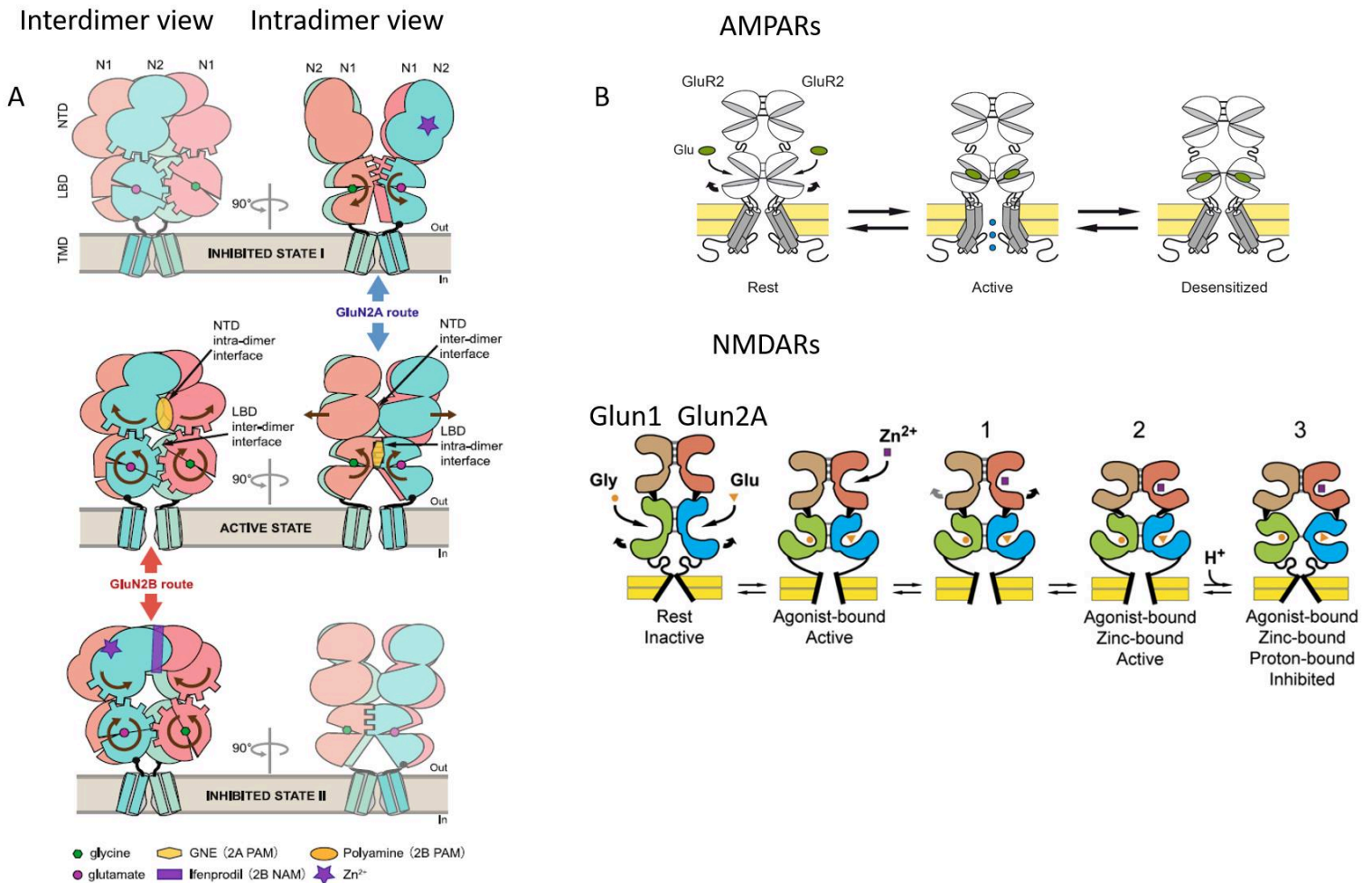


Figure 29 Activation scheme and allosteric routes of different types of iGluRs.

*Panel A, image obtained and adapted from (Tian et al., 2021). Proposed mechanisms for diverging inter-layer allosteric transduction in GluN2A vs GluN2B receptors. Two views rotated of 90 degrees are shown, one for the intradimer and one for the interdimer perspectives. Domain swapping is removed for simplicity. Different allosteric routes with different subunit–subunit interfaces and conformational rearrangements to couple the NTD layer to the LBD and TMD. In the middle and upper rows, GluN2A route. In the middle and lower rows, GluN2B route. Several binding sites for PAMS and NAMs are indicated. Brown arrows indicate rearrangement motions during allosteric transduction. Panel B, image obtained and adapted from (Gielen et al., 2008), and courtesy of David Stroebel. Simplified differential activation schemes for AMPARs and NMDARs. In AMPARs a 3-model activation scheme shows the 3 main receptor conformations: resting, inhibited and desensitized (mostly NTD-independent). In NMDARs, the desensitized state is less prominent, while we have a variety of low PO states catalyzed by different compounds many of which bind the NTD of these receptors.*

It is important to remark that motions of the intradimer and interdimer interfaces are important in regulating the receptor overall Pos and the energy barriers that underlie the pre-gating steps of the channel, but they are not sufficient for the gating itself to take place. For gating to successfully take place, it is still necessary to have the agonist binding followed by the conformational changes described in the section 4.3 kinetic scheme. However, these complex inter and intra interactions between the modules and subunits of NMDARs highlight the differences between the activation scheme of AMPARs and NMDARs (Figure 29 Panel B). In AMPARs desensitization is the mechanism that regulates the receptor mean opening times, a mechanism tightly controlled by the dimerization of the LBD. While in AMPARs the NTDs have a limited role in determining the time course and properties of the receptor, in NMDARs these structures have a fundamental role in determining many biophysical properties that shape the slow response of these receptors and determine subunit unique properties. Therefore, differences in the strength of the Intradimer interface determine different properties in NMDARs versus AMPARs, namely the relay of allosteric modulation in NMDARs GluN2As, and the desensitization kinetics in AMPARs.



## 5 The GluN3 subunits

One of the most puzzling and exciting NMDAR subunits is GluN3A (encoded by the human gene *GRIN3A*, *Grin3a* in rodents), the more widely expressed of the 'non-conventional' GluN3 subfamily comprising both GluN3A and GluN3B. Receptors containing GluN3A are believed to be important regulators of synapse maturation and neuronal circuitry in critical developmental stages right after birth in mammals (Pérez-Otaño *et al.*, 2016; Crawley *et al.*, 2022). For long time it has not been known if GluN1/GluN3A would form functional channels *in vivo* or just exist as artifacts of recombinant expression systems, but this paradigm has radically changed in recent years with the discovery that GluN1/GluN3A receptors are bona fide neuronal receptors present *in vivo* with impact on adult brain function and behavior (Grand *et al.*, 2018; Otsu *et al.*, 2019; Bossi *et al.*, 2022). In this chapter, I will provide an overview of what is currently known about this subunit. Several reviews exist on the topic and can be consulted at (Henson *et al.*, 2010; Low and Wee, 2010; Pachernegg *et al.*, 2012; Pérez-Otaño *et al.*, 2016; Crawley *et al.*, 2022).

### 5.1 Historical introduction

The GluN3A subunit was first described in 1995 in two contiguous articles, reporting the cloning of this subunit from the rodent CNS (Ciabarra and Sevarino, 1995; Sucher *et al.*, 1995). The GluN3B subunit was firstly described even more recently, in 2001 (Andersson *et al.*, 2001). Hydropathy analysis and sequence homology indicated that the structure of these subunits resembles the classical NMDAR subunits. It was also found the presence of a pore with conserved iGluRs motifs (including the SYTANLAAF pore motif) which prompted to hypothesized a possible ionotropic function for this subunit. The striking feature of receptors in recombinant expression systems containing the GluN3A subunit co-expressed with either GluN1 or GluN2s was a complete lack of physiological responses when exposed to glutamate. The first indications of activity were recorded through single channel recordings in mixed populations of GluN1/GluN2a/GluN3A, with the appearance of an unusual smaller conductance additional to the traditional large conductance mediated by GluN1/GluN2A diheteromers (Ciabarra and Sevarino, 1995; Das *et al.*, 1998; Pérez-Otaño *et al.*, 2001a; Sasaki *et al.*, 2002). Initial studies on macroscopic (i.e. whole-cell current) showed that GluN3A acts as a dominant negative subunit, reducing current size when co-injected with GluN1 and GluN2 subunits (Das *et al.*, 1998; Pérez-Otaño *et al.*, 2001a). In addition, GluN3A mediated conductances displayed biophysical properties different from canonical GluN2 containing

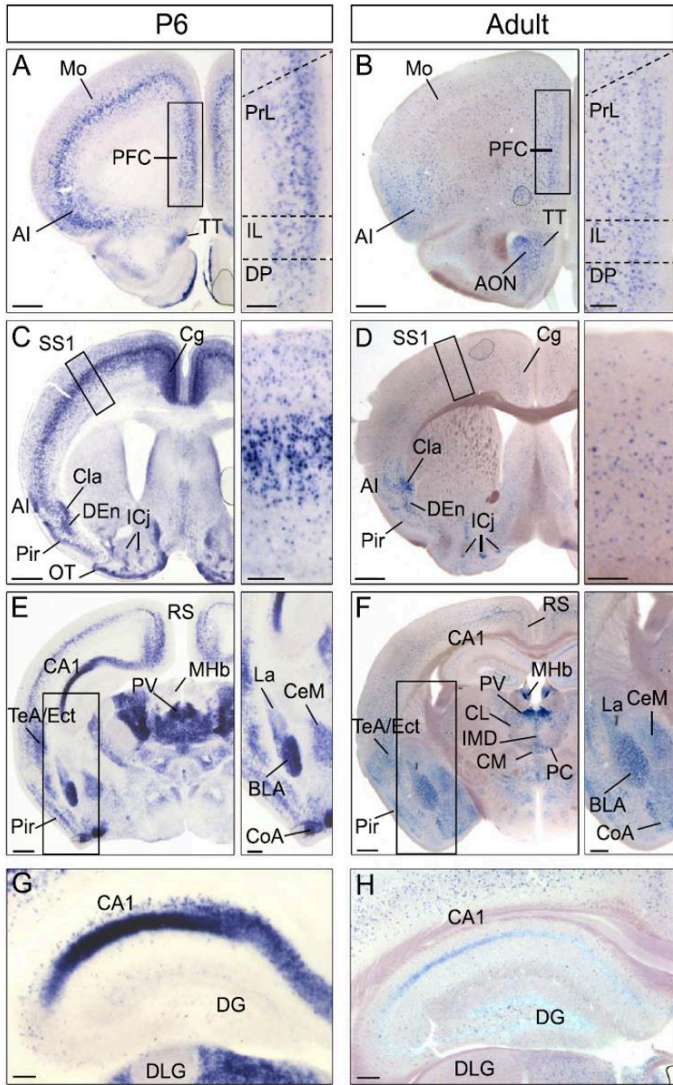
NMDARs, as they were less calcium permeable (Das *et al.*, 1998; Pérez-Otaño *et al.*, 2001a; Sasaki *et al.*, 2002), and insensitive to magnesium block (Sasaki *et al.*, 2002; Tong *et al.*, 2008).

Only in 2002, decades after the first conventional NMDAR electrophysiological characterizations, it was shown that it is possible to trigger ionotropic activity from GluN3A when co-expressing this subunit with GluN1 in heterologous expression systems, and perfusing it with glycine (Chatterton *et al.*, 2002). GluN1/GluN3A receptors mediated small glutamate-insensitive glycinergic inward currents. This finding makes diheteromeric GluN1/GluN3A the first excitatory glycinergic receptors to ever be characterized (they recently been named eGlyRs). It has been found that homomeric GluN3A and di-heteromeric GluN2A/GluN3A complexes are retained in the endoplasmic reticulum and do not reach the cell surface (Pérez-Otaño *et al.*, 2001a).

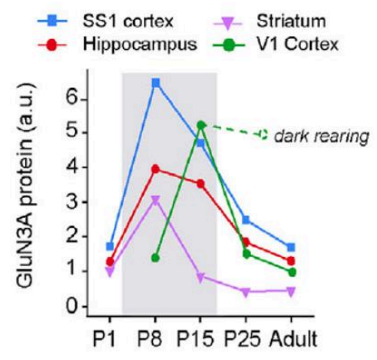
## **5.2 GluN3A expression: anatomical and developmental aspects, cell types specificity and subcellular localization**

GluN3A expression ontological profile varies with age, starting with low levels in the embryonic CNS. Afterwards, there is a peak of expression postnatal in rodents, culminating in the first postnatal week (Henson *et al.*, 2010; Wee *et al.*, 2016a), before decreasing to steady levels in adulthood (Figure 30). It has been shown that throughout the period of time of maximal expression, high levels of GluN3A can be identified in many brain anatomical structures such as the hippocampus CA1, the cortex, amygdala, thalamus, hypothalamus, olfactory nuclei, and others (Wong *et al.*, 2002; Henson *et al.*, 2010; Pachernegg *et al.*, 2012; Murillo *et al.*, 2021; Crawley *et al.*, 2022) (Figure 30 Panel A). Afterwards, expression of the protein steadily decreases in the second and third postnatal weeks, which roughly compare to human childhood and adolescence (Crawley *et al.*, 2022) (Figure 30 Panel B). The emergence and consecutive downregulation of protein expression in the different brain regions is different depending on the anatomical structure taken into consideration, which could reflect differences in the maturation of the circuit, and the development of that particular brain region. The development of expression of GluN3A in the primary sensory cortex region indicates that GluN3A enriches the layers 5, and only afterwards spreads to layers 2-4 (Murillo *et al.*, 2021) (Figure 30 Panel C). This type of layered expression patterns seems to mirror the more general maturation patterns of the cortex. Accordingly, the peak of expression of GluN3A is delayed in the primary visual cortex (compared to other cortical regions), a region that develops later in the rodent life cycle, as the eyes are not functional until after 2 weeks postnatal. Furthermore, it has been shown that visual deprivation even further delays the developmental loss of GluN3A, tightly coupling GluN3A expression with sensory development (Larsen *et al.*, 2014).

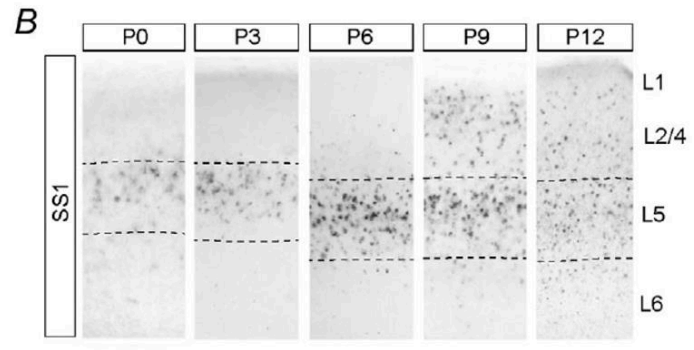
A



B



C



D

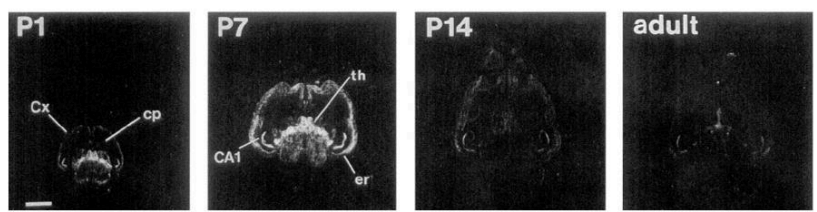


Figure 30 Temporal expression pattern of GluN3A in the brain.

Images obtained and adapted from (Ciabarra and Sevarino, 1995; Murillo et al., 2021; Crawley et al., 2022). Panel A, Comparison of GRIN3A expression in postnatal (P6) vs adult coronal slices at different rostro-caudal levels are displayed. Small sections on the right are magnifications of the black boxes on the left panels. AI, granular insular cortex; AON, anterior olfactory nucleus; BLA, basolateral amygdala; CA1, Cornu Ammonis 1; CeM, central amygdala; Cg, cingulate cortex; CL, centrolateral thalamic nucleus; Cla, claustrum; CM, centromedial thalamic nucleus; CoA, cortical amygdala; DEn, dorsal endopiriform nucleus; DG, dentate gyrus; DLG, dorsal lateral geniculate nucleus; DP, dorsal peduncular cortex; Ect, ectorhinal cortex; ICj, islands of Calleja; IL, infralimbic cortex; IMD, intermediodorsal thalamic nucleus; La, lateral amygdala; MHb, medial habenula nucleus; Mo, motor cortex; OT, olfactory tubercle; PC, paracentral thalamic nucleus, PFC, prefrontal cortex; Pir, piriform cortex; PrL, prelimbic cortex; PV, paraventricular thalamic nucleus; RS, retrosplenial cortex; SS1, somatosensory cortex 1; TeA, temporal association cortex; TT, tenia tecta. Scale bars: 500  $\mu$ m (A-F); 200  $\mu$ m. Panel B, schematization of regional postnatal expression profiles of GluN3A. Panels C, In situ hybridization showing time course of Grin3a mRNA regulation fluctuating across layers in primary somatosensory cortex (SS1). Panel D, GluN3A expression in the brains of P1, P7, P14, and the adult rat as revealed by in situ hybridization in one of the first papers that cloned the GluN3A subunit.

Significant levels of GluN3A are maintained in specific brain regions in adults. Studies employing single cell transcriptomics and RNAscope hybridization techniques investigated the expression levels of GRIN3A in various brain tissues (Pfeffer *et al.*, 2013; Paul *et al.*, 2017; Fulcher *et al.*, 2019; Murillo *et al.*, 2021). mRNA expression patterns highlight high levels of GluN3A expression in the amygdala, medial habenula, thalamic nuclei and association cortices, and to some degree in the hippocampus (Pérez-Otaño *et al.*, 2016; Murillo *et al.*, 2021) (Allen Brain Atlas). Among these regions, specific cell types where expression is retained are cells such as excitatory neurons, cholinergic and inhibitory GABAergic interneurons (Pérez-Otaño *et al.*, 2016). Expression of GluN3A had been documented in a variety of cell types, and seems to be very high in cells expressing specific biomarkers (Figure 31 Panel A). Especially high seems to be the expression within somatostatin interneurons (SST) in the hippocampus and neocortex (Paul *et al.*, 2017; Murillo *et al.*, 2021) (Figure 31 Panels B,C). GluN3A was found to be a secondary marker for SST interneurons among which Martinotti cells (Paul *et al.*, 2017). SST interneurons are important for innervating distal dendrites of pyramidal neurons and other interneurons, regulating dendritic input gating (Crawley *et al.*, 2022). Furthermore, GRIN3A expression has been found through RNAseq methods in other cell types other than neurons such as oligodendrocytes (Spitzer *et al.*, 2019), microglia (Expression of N-methyl D-aspartate receptor subunits in amoeboid microglia mediates production of nitric oxide via NF- $\kappa$ B signaling pathway and oligodendrocyte cell death in hypoxic postnatal rats - Murugan - 2011 - Glia - Wiley Online Library, n.d.), and endothelial brain cells (Mehra *et al.*, 2020).

Classical NMDARs cluster at postsynaptic density (PSD) sites, depending on the subunit type and the anatomical region (Paoletti *et al.*, 2013). GluN3A subcellular localization has been investigated by employing EM and biochemical fractionation, revealing that these receptors can be present at PSDs, but are found predominantly perisynaptically and extrasynaptically (Pérez-Otaño *et al.*, 2016). Even within the PSD, GluN3A seems to concentrate towards the edge. The C-terminal of GluN3As lacks PSD-binding motifs (Pérez-Otaño *et al.*, 2016). A recent study employing 2P (two photon) uncaging of caged glycine to map the subcellular localization of glycine-gated GluN1/GluN3A receptors reported no enrichment to specific site on the neuronal surface (in particular between spines and dendritic shaft) but rather a homogenous distribution on the cell membrane. (Bossi *et al.*, 2022).. Immunogold EM studies have also observed GluN3A at presynaptic locations, although they are hypothesized to be less predominant than their counterparts at other sites (Larsen *et al.*, 2011; Savtchouk *et al.*, 2019).



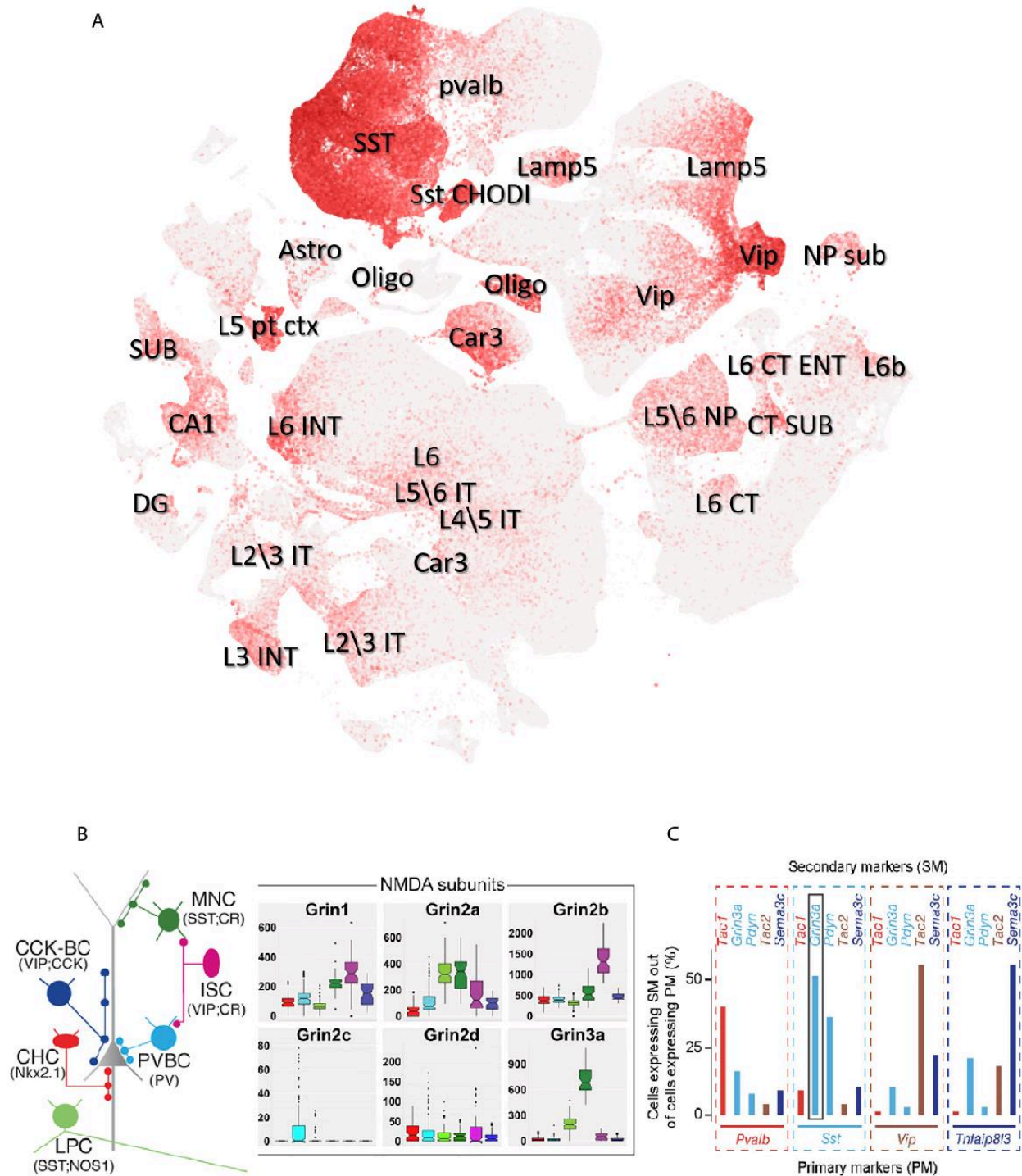


Figure 31 GluN3A expression in the mouse brain.

Images obtained and modified from (Paul et al., 2017; Crawley et al., 2022). Panel A, single cell (or single nucleus) RNA sequencing (RNA-Seq) GRIN3A filter applied on the Allen Brain atlas project "WHOLE CORTEX & HIPPOCAMPUS - 10X GENOMICS (2020) WITH 10X-SMART-SEQ TAXONOMY (2021) on ~8 week-old male and female mice belonging to pan-neuronal transgenic lines from 1.1M total cells. Single cell RNA-Seq is a

*scalable approach to provide genome-wide expression profiles for thousands of cells. Anatomical specificity is achieved by microdissecting tissue from defined brain areas, such as cortical layers or cell groups in LGd. This data set includes single cell and nuclear transcriptomic profiles, assayed from mouse brain regions such as cortex and hippocampus. Cells are then separated by principal component analysis. SST=somatostatin, pvalb=Parvalbumin, INT=Interneuron, DG= dentate gyrus, VIP= Vasoactive intestinal peptide-expressing (VIP) interneurons, Astro= astrocytes. Lamp5, Car3 etc. are all markers for classification of neurons and interneurons of excitatory and inhibitory cells used in transcriptomic studies to ease identification of cell types in the CNS. Panel B, single-cell transcriptomes of 6 genetically labeled and phenotypically well-characterized GABAergic types or subpopulations from microdissected motor and somatosensory cortex of 6-week-old mice. These are (1) Chandelier cells (CHCs) of pyramidal neurons; (2) basket cells (PVBCs) of the perisomatic region (3) the long-projecting GABAergic cells (LPCs), (4) the Martinotti cells (MNCs) in distal dendrites and likely another cell type; (5) the interneuron-selective cells (ISC) and likely other types, and (6) the CCK basket cells (CCKC) and likely other types. Physiological and molecular evidence indicate that these are non-overlapping subpopulations. On the right, GRIN genes transcriptomic levels are compared. GRIN3A is especially highly expressed in LPC and MNC cells, which are both SSH expressing populations. Panel C, molecularly distinct interneuron categories defined by scRT-PCR, with primary and secondary markers. GriN3A is shown having high expression in SST interneurons.*

### **5.3 GluN3A modular architecture**

Currently, only the LBD of GluN3s have been solved by crystallization, both in closed conformations bound to agonists (Yao *et al.*, 2008), and in Apo state (Yao *et al.*, 2013). The GluN3A and GluN3B LBDs, which display the classical bilobate clamshell-like folding, are highly conserved in sequence identity (75%, unpublished data) and structure architecture, in particular in the interlobe agonist binding pockets (same residues). Comparison of these structures to GluN1 and GluN2s has allowed to highlight some structural differences. First of all, GluN3 LBDs have a unique loop 1 structure different from other iGluR LBDs (Figure 50). When comparing GluN3s and GluN1 whole LBD, there is a pronounced similarity between folding, mechanism of ligand binding and extent of domain closure, but a large difference in homology of residue identity (Yao *et al.*, 2008) (Figure 32 Panel A). Some differences can be ascribed to changes in residue identity in the binding pocket itself, which mediate the agonist-induced rearrangements. As a consequence, chemical bonds are modified with neighboring amino-acids and the surrounding network of water molecules, with the effect of increasing the stabilization of the closed conformation in GluN3A over GluN1 (Figure 32 A) (Yao *et al.*, 2008). Furthermore, this higher stability of the closed conformation is also tightly regulated by many protein contacts between lobes 1 and 2. Interestingly, like in GluN1, the closed cleft conformation of the GluN3 subunit LBD can be accessed from the Apo state, without binding of the agonist (Yao *et al.*, 2013), indicating agonist binding follows a conformational selection mechanism (Yao *et al.*, 2008) (Figure 32 Panel A). Integrity of the binding sites for both GluN1 and GluN3A has been

found to be a predictor of the amount of the expression of the protein at the cell membrane (Skrenkova *et al.*, 2019).

At present times, we lack full structural information describing the whole receptor and quaternary information concerning co-assembly modalities with the partner subunit. Therefore, we have limited information concerning dimerization both at the LBD and the NTD level. One paper hypothesized that the LBD intradimer interface, if forming, might be important for the binding site for protons (Cummings and Popescu, 2016), and hypothesized that its instability might contribute to the pH dependent desensitization observed within these receptors. However, no other studies exist to describe subunit interactions at this interface. In fact, the subunit stoichiometry and the dimer formation at this and other module interfaces have never been proven with certainty. Furthermore, no information is currently available if the domain swap described in classical NMDARs and other iGluRs (see section '3 Receptor architecture: modular design') also apply to GluN3A containing NMDARs.

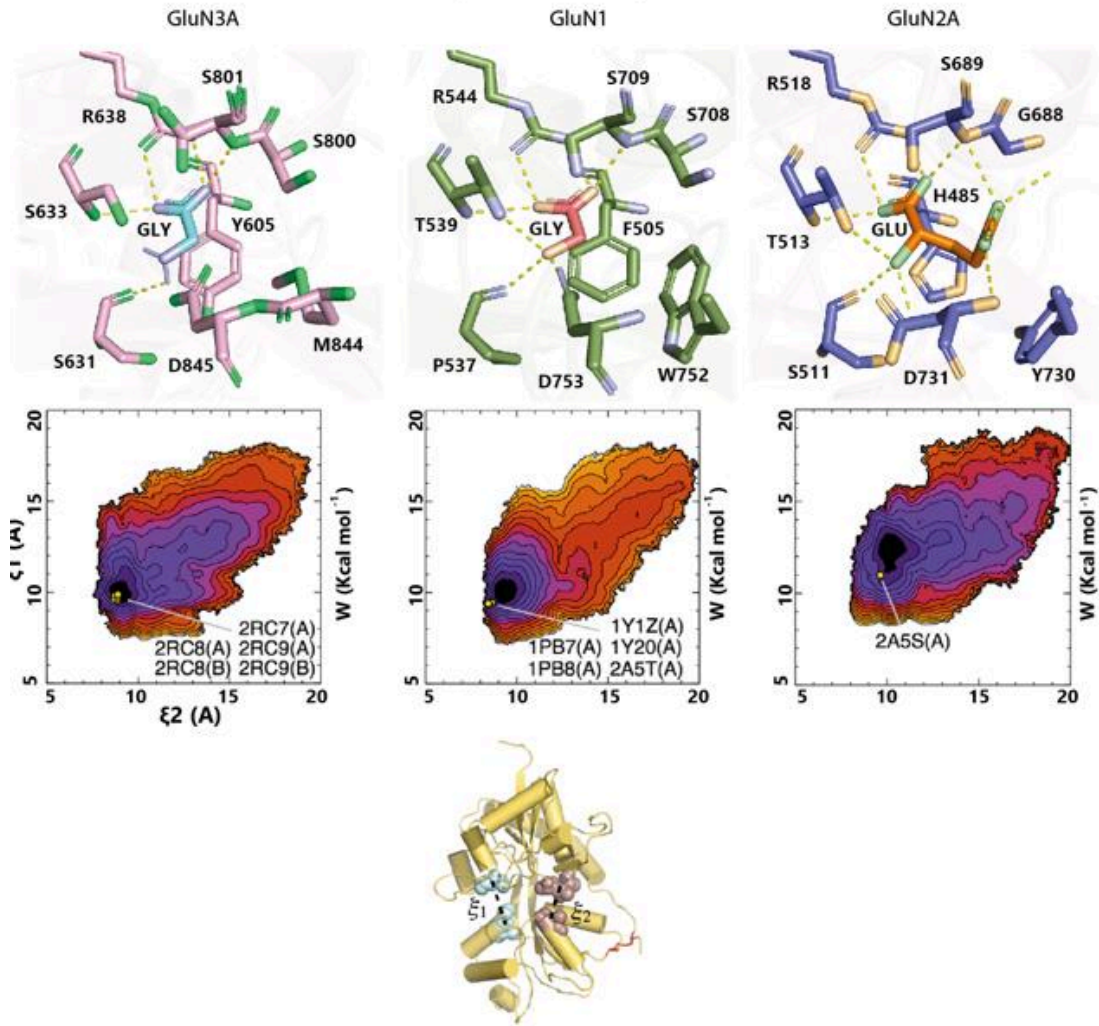
Pore differences apply in comparison to classical NMDARs, due to changes in selectivity and permeability to divalent ions such as  $Mg^{2+}$  and  $Ca^{2+}$  (Chatterton *et al.*, 2002; Wada *et al.*, 2006; Yuan *et al.*, 2013). GluN3A containing diheteromers and triheteromers exhibit a large reduction to endogenous magnesium block, and reduced calcium permeability compared to the GluN2 counterparts (Pérez-Otaño *et al.*, 2001a; Chatterton *et al.*, 2002; Sasaki *et al.*, 2002; Pérez-Otaño *et al.*, 2016). The fact that they are not blocked by endogenous extracellular magnesium and they contribute less to calcium permeation mechanisms points to a differential role than the coincidence detection attributed to canonical GluN2 containing NMDARs. Sequence differences are present at the M3 segment hypothesized to form a non-mobile, rigid structure that participates in a modified formation of the outer vestibule of the channel, as this region does not undergo extensive molecular rearrangement during channel gating (Wada *et al.*, 2006). More sequence differences are present at the Q/R/N site narrow constriction of the M2 pore loop, where the asparagine (N) site of GluN1, but not GluN3A, has been hypothesized to contribute to the selectivity filter of GluN1/GluN3A channels (Wada *et al.*, 2006). Together, these findings could explain differences in ion permeation with canonical NMDARs (Yao *et al.*, 2008) (Figure 32 Panel B) (Wada *et al.*, 2006).

Little is known about the NTD of GluN3A receptors. Currently, it is unknown if the NTDs assume a dimer of dimers conformation like canonical NMDARs or not, although an inter-dimer crosslink has been attempted (Mesic *et al.*, 2016). Sequence analysis of the GluN3A subunit shows one small ( $\approx 15$  aa) and one large stretches of amino acids ( $>60$ aa) that are unique among iGluRs and whose function is not

known (Figure 50). Multiple glycosylation sites mediated by asparagine residues exist alongside the NTDs of both GluN1 and GluN3A, and are required for surface delivery of GluN3A-containing NMDARs (Skrenkova *et al.*, 2018). The CTD of GluN1 has been found to be a key regulator of properties of GluN1/GluN3A receptors, influencing both the expression of the protein at the membrane and the kinetics of desensitization of these receptors (Cummings *et al.*, 2017). Specifically, co-expression of GluN3A with the isoform GluN1-4a results in much larger current densities than with other GluN1 splice variants. For this reason, recent *in vitro* studies have commonly employ this GluN1 isoform for co-expression with GluN3A.

A

Ligand Binding Domain



B

Transmembrane Domain

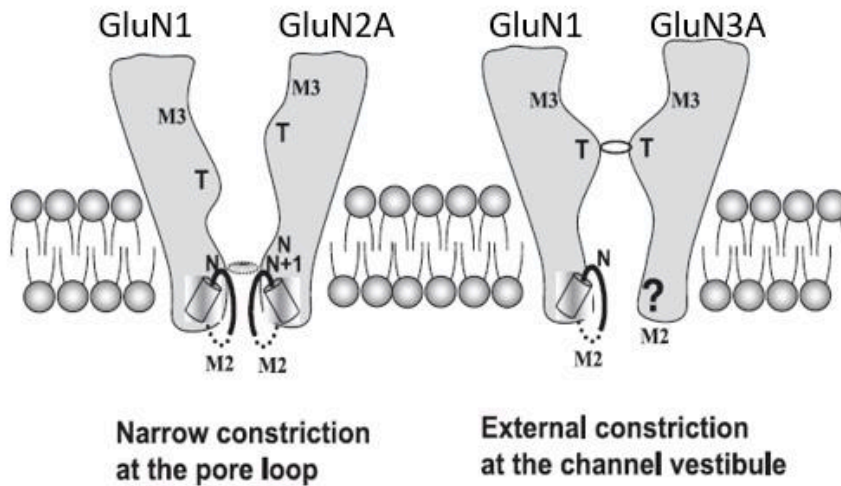


Figure 32 Comparison of LBDs of different NMDAR subunits.

Panel A: Illustrations are adapted from PDBs 1PB7, 2RC7, and 2A5S (Mechanisms of activation, inhibition and specificity: crystal structures of the NMDA receptor NR1 ligand-binding core, 2003; Furukawa et al., 2005; Yao et al., 2008) Overlapping crystal structure representations of GluN3A, GluN1 and GluN2A with highlighted key residues known for interacting with the agonist. Residues are shown as cartoons with visible side-chains, and hydrogen bonds are highlighted with cut-off set at 3 Å. Below, for each subunit is shown a 2-D representation of the free energy landscape of the bound ligand binding domain complexes taken from (Yao et al., 2013). On the x and y-axis potential mean forces are calculated as  $W(\xi_1, \xi_2)$ , two-dimensional order parameters, corresponding to a difference of 1 kcal mol<sup>-1</sup>.  $\xi_1$  and  $\xi_2$  are each center of mass distances from atom selection in lobe 1 and lobe 2. Contour lines are shown with darker colors being lower in free energy. The GluN1 and GluN3A subunits show a double conformational free energy minima in the 1D PMFs, where the minima are separated by a barrier of 1 kcal/mol. On the contrary, GluN2A is better described by a single basin. At the bottom, a representation of the movements for the order parameter  $\xi_1, \xi_2$  used to describe large-scale conformational transitions. Panel B: illustration adapted from (Wada et al., 2006). Model of the permeation pathway proposed for GluN1/GluN2 and GluN1/GluN3A NMDAR channels. The N-site residue in the M2 segment of GluN1 and the N<sub>1</sub> site residue in GluN2A constitute the selectivity filter of the channel. GluN3A forms a more symmetrical channel with GluN2A than GluN1. The M3 segment results in a ring of threonine from residues of both GluN1 and GluN3A forming a constriction in the outer vestibule of the NMDA receptor channel additional to the known selectivity filter in pore loop of the M2 region (labeled as N-site asparagines). This may limit ionic flow, produce less calcium permeability and change render the channel less sensitive to magnesium block. The conformation and role of the M2 segment from NR3A subunits remain to be investigated

#### 5.4 GluN1/GluN3A unusual current phenotype: structural determinants

Co-immunoprecipitation studies have shown that GluN3A can assemble with GluN1 and GluN2, but cannot form homomers. In addition, GluN3A is retained in the endoplasmic reticulum in the absence of the GluN1 (Pérez-Otaño *et al.*, 2001a). I will discuss the assembly of receptors containing GluN1, GluN2 and GluN3A in the section below “5.8 Triheteromers containing GluN1/GluN2/GluN3A: fact or fiction?”. However, co-injection of GluN1 and GluN3A causes tetrameric channels to be present at the membrane (Chatterton *et al.*, 2002; Al-Hallaq *et al.*, n.d.), but in which none of the subunit is a binding target for glutamate. Di-heteromeric GluN1/GluN3A have been shown to conduct purely glycinergic inward currents in heterologous expression systems (Chatterton *et al.*, 2002; Madry *et al.*, 2007; Skrenkova *et al.*, 2019). This makes them the first purely excitatory glycinergic receptor (eGlyRs). Macroscopic currents exhibit a unique waveform phenotype among NMDARs. Receptors perfused with saturating glycine concentrations display a peak current, and then rapidly enter desensitization to a smaller steady state current following a bell-shaped dose-response curves to glycine (schematic current examples next to basic reaction schemes are visible in Figure 33).

The activation mechanism producing these atypical current traces can be explained by mutating key residues inside the GluN1 and GluN3A LBDs to prevent glycine binding. Introducing a binding killer mutation in the GluN1 LBD results in 'square' currents that display little desensitization yielding dose-response curves of 'classical' shape (Figure 33, second example). On the contrary, introducing the homologous mutation in the binding pocket of the GluN3 subunits has dramatic effects by completely preventing receptor activation by glycine (Awobuluyi *et al.*, 2007; Madry *et al.*, 2007; Kvist *et al.*, 2013; Skrenkova *et al.*, 2019).

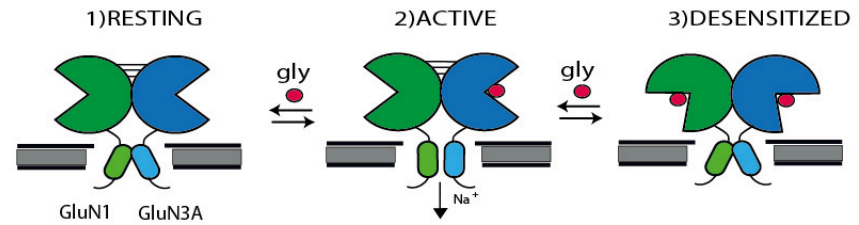
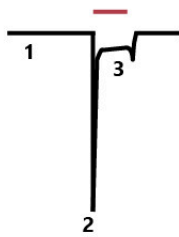
From these findings, an activation mechanism of kinetic competition between the constitute subunits has been proposed. The GluN3A subunit drives pore opening and inward currents conductance upon binding glycine with high affinity. Glycine binds with lower affinity to the GluN1 subunit, which acts as a negative modulator, driving entry into desensitized states and causing pore closure (Figure 33). The structural determinants and correlates for the auto-inhibitory function of GluN1 remain elusive. The mechanism of activation of GluN1/GluN3A NMDARs has some resemblance to other iGluRs, such as heteromeric kainate GluR5/KA2 receptors, in which only GluR5 subunits are necessary for activation, while KA2 promotes entry into desensitized states (Swanson *et al.*, 2002).

In addition, GluN1/GluN3A receptors show a very strong sensitivity to redox modulation (Grand *et al.*, 2018). In the reduced state, two endogenous disulfide bridges in the lower lobe (D2) of both GluN1 and GluN3A LBDs (one on each subunit) are broken. The resulting effect is an enhanced sensitivity for glycine at the GluN3A subunit. Reduced receptors have such a high affinity for glycine that ambient glycine levels (known to be present in external solutions (Ascher, 1990)) are sufficient to produce tonic activation of GluN1/GluN3A receptors. While glycine application produces an inward current followed by a desensitization to a more positive steady-state than baseline (i.e., prior glycine application). Removal of the agonist causes receptors to display large rebound (tail) currents, produced when glycine transiently unbinds from GluN1, while GluN3A subunits are still bound to glycine (Figure 33 third example).



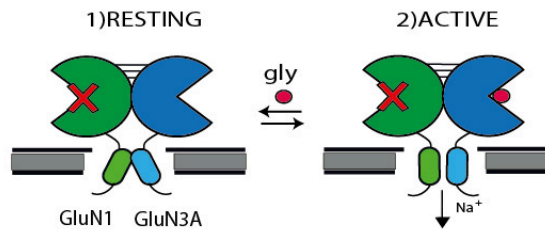
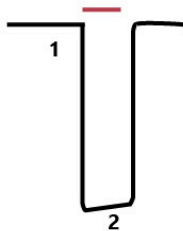
### 1 GluN3A/GluN1 WT

WT activity: small desensitizing currents



### 2 GluN3A/GluN1F484A

No more glycine binding site in GluN1



### 3 GluN3A CS/GluN1 CS

Glycine affinity in GluN3A is shifted, making window of activation larger

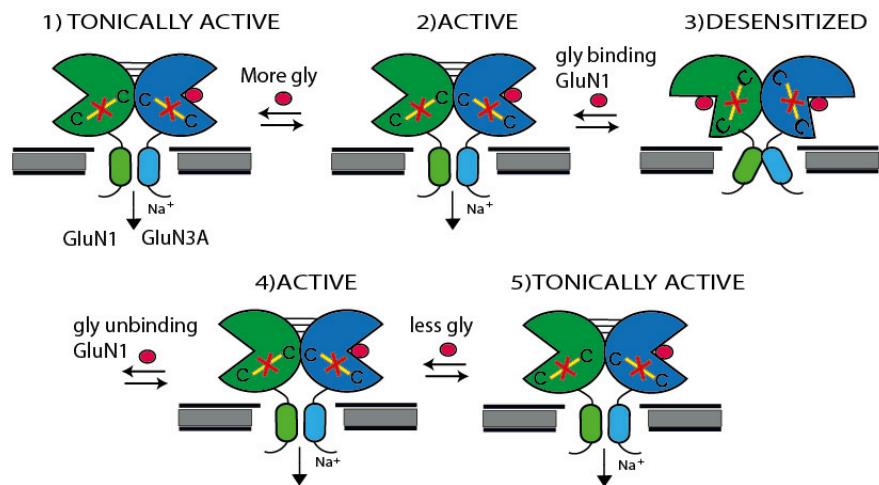
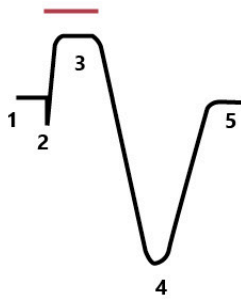


Figure 33 GluN1/GluN3A receptor gating mechanism and current phenotypes.

Current phenotypes are shown for (1) GluN3A\GluN1 WT receptors, (2) GluN3A\GluN1 F484A receptors and (3) GluN3A CS\GluN1 CS receptors, all in the presence of saturating glycine application (100  $\mu$ M). On the side, graphic reaction schemes with numbered states are shown. Numbers next to the waveforms components indicate the corresponding biophysical states of the reaction scheme. The WT trace (1) is explained by a simple 3-states reaction scheme in which fast desensitization mediated by GluN1 binding glycine occurs rapidly after activation mediated by the GluN3A subunit. When a mutation preventing glycine binding in GluN1 (2) is inserted in the receptor, steady state current is mostly unaffected by desensitization. Hence, a 2-states reaction scheme explains mutant currents similar to canonical GluN2 NMDARs. When in reduced



state (3), the affinity of GluN3A for glycine is increased, and recording solutions can tonically activate the GluN3A subunit. Following agonist application, the steady state current becomes more positive than baseline because of desensitization of all receptors, among which also the tonically activated ones. Upon removal of the agonist, a large rebound current appears caused by glycine dissociation from lower affinity inhibitory GluN1.

## 5.5 Pharmacology of GluN1/GluN3A receptors

In this section we will describe the main classes of drugs that have been found to influence GluN1/GluN3A receptor activity. Overall, there are less pharmacological agents that have been characterized as being effective or being specific towards GluN1/GluN3As compared to GluN2 containing receptors. However, thanks to the development of new methodologies to investigate GluN1/GluN3As receptor function, and the renewed interest towards the role of GluN1/GluN3A in the CNS, this field has started to rapidly evolve.

### 5.5.1 Orthosteric agonists

GluN1/GluN3A receptors pharmacology is still in its infancy, as we lack many tools that are available for conventional GluN1/GluN2 NMDARs. The common NMDAR co-agonist D-serine has a complex effect on GluN1/GluN3A receptors. Like glycine, it has a double effect: it activates the GluN3A subunit (albeit with lower affinity, Kd on isolated LBD of ~650nM), and causes desensitization acting on the GluN1 binding site (Kd on the isolated LBD of ~7.0  $\mu$ M) (Chatterton *et al.*, 2002; Yao, 2006; Awobuluyi *et al.*, 2007; Madry *et al.*, 2007). However, the ratio of affinity for GluN3A over GluN1 is only 10, while the affinity for GluN1 is higher than glycine. As a consequence, D-serine acts as a weak partial agonist when administered alone, but becomes an antagonist when administered in the presence of glycine, as it causes more desensitization (Awobuluyi *et al.*, 2007; Smothers and Woodward, 2007). Other common GluN1 agonists such as D-alanine, D-cycloserine and ACPC are able to cause small to no activation of the receptors in the absence of glycine (Chatterton *et al.*, 2002; Madry *et al.*, 2007).

The comparison of individual GluN3A and GluN1 isolated LBD sensitivities to glycine, measured from binding studies on isolated LBDs, reveals 600-fold higher sensitivity for GluN3A (Kd 40.4  $\pm$  3.7nM) versus GluN1 (26.4  $\mu$ M)(Figure 35 Panel B) (Yao, 2006). However, when GluN3A and GluN1 co-assemble in a tetrameric complex in a heterologous expression system, the EC<sub>50</sub> of glycine induced activation of

the GluN3A subunit seems much higher than the proposed sensitivity obtained in the isolated LBD studies (Madry *et al.*, 2007; Grand *et al.*, 2018; Skrenkova *et al.*, 2019), although for unclear reasons (Figure 35 Panel B). It is important to remark that measurement of the EC<sub>50</sub> of glycine at the whole receptor level is a complex task, as it depends on many experimental factors such as the speed of perfusion within an electrophysiological setup, and the interpretation of areas on the bell-shaped curve where one subunit is activating and the other is simultaneously inhibiting.

### 5.5.2 Potentiators

GluN1/GluN3A NMDARs have been shown to be potentiated by acidic pH (Cummings and Popescu, 2016; Cummings *et al.*, 2017), in contrary to classical NMDARs, by a novel site that has been speculated to be located at the LBD intradimer interface (Cummings and Popescu, 2016). Similarly, extracellular zinc has been shown to potentiate GluN1/GluN3 responses without acting on the NTD (Wada *et al.*, 2006; Cummings and Popescu, 2016; Cummings *et al.*, 2017; Madry and Betz, n.d.), and also in the absence of glycine (zinc would then act as an *agonist*). Its binding site has been hypothesized to be located near the GluN1 LBD binding site, as no effect was found in receptors containing the mutant that classically prevents glycine binding on GluN1 (Madry and Betz, n.d.). However, others (McClymont *et al.*, 2012; Otsu *et al.*, 2019) were unable to reproduce these results, while one paper highlighted the inhibitory nature of zinc on GluN3A containing receptors (Wada *et al.*, 2006). In addition, a large number of glycosylation sites on both GluN3A and GluN3B can be modulated by lectins, and some of these have been found to reduce GluN1 subunit mediated desensitization (Hemelikova *et al.*, 2019).

A specific subset of drugs has been found to be an extremely useful tool to study GluN1/GluN3A receptors. These are GluN1 site competitive antagonists which display higher affinity for the GluN1 LBD than the GluN3A LBD, mirroring the effect of the mutants that prevent glycine binding to GluN1. Several of these have been characterized: L68956 (Grand *et al.*, 2018), MDL (Madry *et al.*, 2007; Grand *et al.*, 2018), 7-CKA (Smothers and Woodward, 2009; Grand *et al.*, 2018) and others (Yao, 2006; Smothers and Woodward, 2007). Each drug slows differently the Tau of desensitization depending on its affinity and potency for each subunit, potentiating the peak and steady state current to a different extent. A compound named CGP-78608 stood out among the other GluN1 antagonists for its extremely high affinity for the GluN1 subunit estimated at  $K_d = 6.33 \pm 1.64$  nM range, while showing thousand-fold lower affinity at GluN3A sites [19], [22]. Glycinergic currents following CGP pre-incubation are potentiated more than hundred folds in both their peaks and steady states, greatly facilitating their detection both

in vitro and in vivo (Grand *et al.*, 2018; Otsu *et al.*, 2019; Zhu *et al.*, 2020). In fact, more than twenty-five years after the discovery of glycine-gated GluN1/GluN3A receptors in heterologous expression system (Grand *et al.*, 2018; Otsu *et al.*, 2019), the use of CGP-78608 as an ‘awakener’ of these receptors is what allowed the demonstration that GluN1/GluN3A receptors are not just artefacts of recombinant system but bona fide neuronal receptors functionally expressed in the brain.

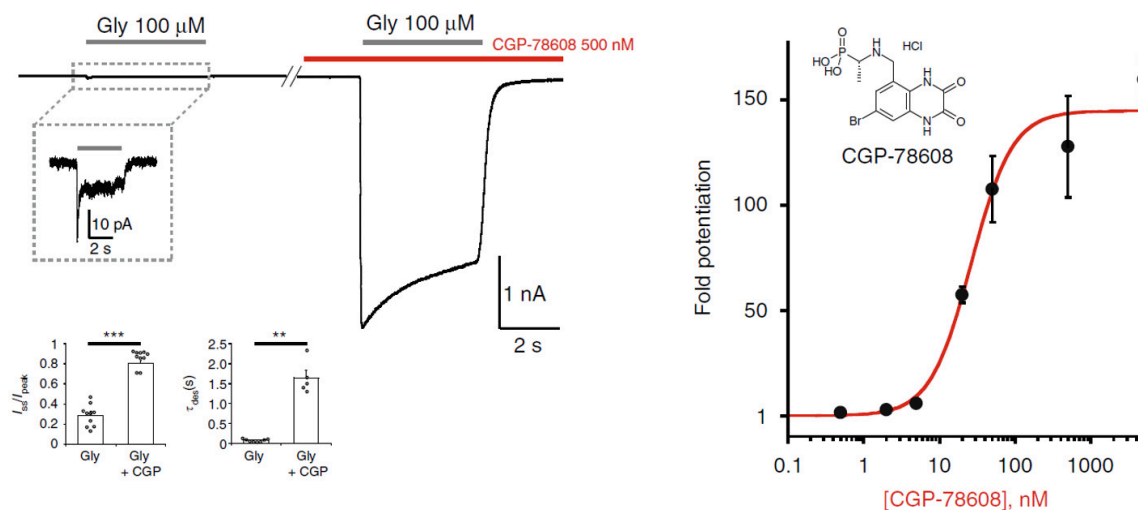


Figure 34 CGP “awakening” on GluN1/GluN3A receptors.

Image adapted from (Grand *et al.*, 2018). Pre-application of CGP-78608 massively potentiates excitatory glycine GluN1/GluN3A receptor peak and steady state currents, also reducing the speed of desensitization. On the right, a dose-response of the potentiation by CGP on these receptors in presence of 100 μM glycine.  $EC_{50} = 26.3 \pm 5$  nM. Current traces in the panel were recorded in HEK cells

### 5.5.3 Open channel blockers and inhibitors

Another unconventional feature of GluN1/GluN3A NMDARs is their unresponsiveness to open channel blocker administration. I/V curves for magnesium are mostly linear, and little to no sensitivity has been shown for drugs such as MK-801, ketamine, memantine and others (Chatterton *et al.*, 2002; Smothers and Woodward, 2007; Tong *et al.*, 2008; McClymont *et al.*, 2012). Differences in channel block selectivity are partially due to amino acid changes at the ‘N and N+1 sites’ (in the selectivity filter region (M2), known to contain a binding site for Mg<sup>2+</sup> in conventional NMDARs (McClymont *et al.*, 2012; Hemelikova *et al.*, 2019). Recently however, a compound, the 7-methoxy derivative of tacrine, was described as a

foot-in-the-door open channel blocker working on both GluN1/GluN2 and GluN1/GluN3A NMDA receptors (Kaniakova *et al.*, 2018).

GluN3A NMDARs show a large reduction in sensitivity to the common GluN2 NMDAR competitive antagonist AP5 (Chatterton *et al.*, 2002), as (Chatterton *et al.*, 2002) showed about 15%-20% inhibition with 100  $\mu$ M application. Moreover, GluN1/GluN3A receptors are also insensitive to the widely-used GluN2B negative allosteric modulator ifenprodil (Smothers and Woodward, 2007). TK80 is a novel competitive antagonist that has been found to selectively inhibit GluN1/GluN3B receptors. Furthermore, two non-competitive antagonists TK13 and TK30 have been found to be effective on both GluN3 receptor subtypes, although only with a modest preference over GluN2 (5 to 10 fold) (Kvist *et al.*, 2013). Antagonists that have been used in the literature to inhibit diheteromeric GluN1/GluN3 responses are CNQX and 5,7-DCKA (Madry *et al.*, 2007; Grand *et al.*, 2018; Otsu *et al.*, 2019). The CNQX affinity for GluN1 is only slightly higher than for GluN3A (3-fold; in the  $\mu$ M range), making it a good inhibitor when applied at high concentrations ( $>50 \mu$ M) (Yao, 2006; Madry *et al.*, 2007). 5,7-DCKA has a 1000 fold higher affinity for GluN1, potentiating responses at low (1-50  $\mu$ M concentrations, but completely abolishing responses at saturating concentrations ( $>100 \mu$ M) (Chatterton *et al.*, 2002; Yao, 2006; Awobuluyi *et al.*, 2007). Recently, a new GluN3A-selective allosteric modulator named EU1180-438 has been described exploiting sequence differences with classical NMDARs in the pre-M1 region (Zhu *et al.*, 2020). This pharmacological tool has been shown to work on recombinant and native GluN1/GluN3A receptors, and therefore seems promising for future experimentations *in vivo* (Zhu *et al.*, 2020). Another promising allosteric modulator acting on GluN3A is the recently characterized WZB117, also binding in the pre-M1 region of the GluN3A subunit in a glycine-, voltage- and pH-independent manner (Zeng *et al.*, 2022).

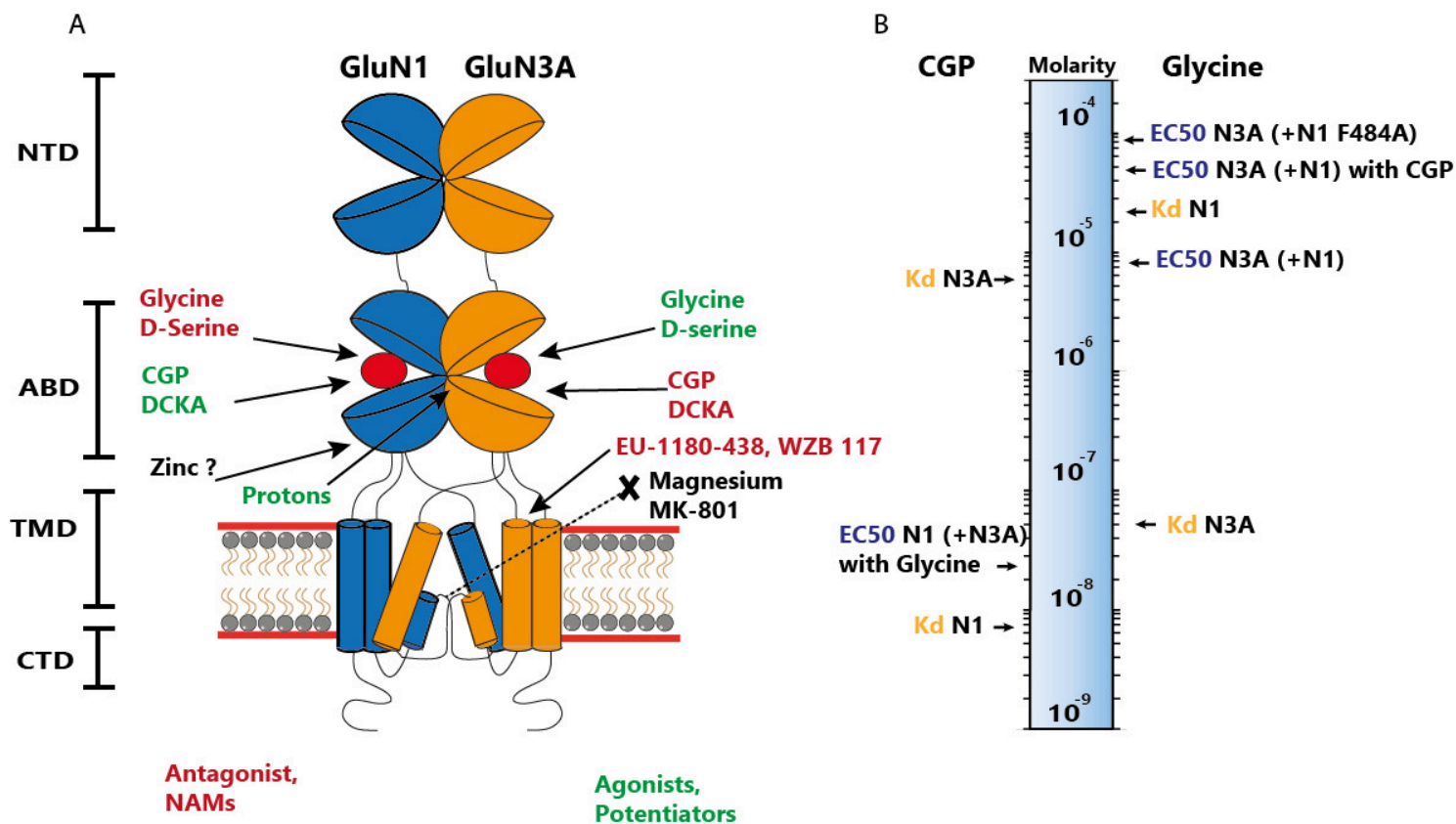


Figure 35: Pharmacology of GluN1/GluN3A NMDARs.

Panel A, schematic representation of a functional dimer composed two distinct NMDARs subunits. Activators and Inhibitors are shown to have opposed effects at different subunits sites. There is reduced to no activity for known open blocker channels, while a novel binding site has been hypothesized for modulators such as protons and zinc. New classes of allosteric inhibitors binding the pre-M1 of GluN3A are shown. Panel B, Graphical representation on a logarithmic scale of the different affinities and efficacies for CGP-78608 and glycine, respectively on the left and on the right of the scale. These compounds are necessary for the reveal of GluN3A activity in the mammal brain. Data in the representation: 1) K<sub>d</sub> glycine GluN3A 40.4 ± 3.7nM, 2) K<sub>d</sub> glycine GluN1 26.4 μM, 3) K<sub>d</sub> CGP GluN3A 5.52 ± 0.13 μM, 4) K<sub>d</sub> CGP GluN1 6.4 nM, 5) EC<sub>50</sub> Glycine GluN1 F484S\GluN3A 82 ± 11 μM, 6) EC<sub>50</sub> Glycine GluN1\GluN3A WT 6.5 ± 1.1 μM, 7) EC<sub>50</sub> CGP GluN1\GluN3A WT in the presence of 100 μM Glycine, 26.3 ± 5 nM, 8) EC<sub>50</sub> Glycine GluN1\GluN3A WT in the presence of 500 nM CGP 38,9. ± 0.8 μM. Data obtained from (Yao, 2006; Madry et al., 2007; Grand et al., 2018)

## 5.6 GluN3A in plasticity, cognition and pathology.

As mentioned in the first chapter of the Introduction, plasticity in the CNS allows for the rewiring of the intercellular connectivity which is a prerequisite for the high-order functions of the organism. Both new connections are necessary in some areas of the brain, while pruning of unnecessary connections is also

a fundamental factor for the homeostasis of the brain. In this context, the GluN3A subunit has been indicated as an important player in the regulation of plasticity at key stages of brain development. GluN3A expression peaks after birth, and then starts to decrease in a critical developmental stage when sensory experience starts to shape brain maturation. (Larsen *et al.*, 2014; Crawley *et al.*, 2022). It has been hypothesized that GluN3A may act as a suppressor of synaptic maturation, until the onset of sensory experience. It would do so by regulating which synapses are maintained or suppressed, also triggering pruning mechanisms (Crawley *et al.*, 2022). Therefore, its gradual decrease in expression levels after the first peak of expression may correlate with an increase in experience dependent plasticity.

Overall, it has been shown that GluN3A expression regulates the morphology of excitatory synapses and GluN3A knock-out (KO) animal models have an increased number of dendritic spines with spine heads appearing enlarged and spine necks elongated (Das *et al.*, 1998). The GluN3A knockout at CA3-CA1 synapses has been found to correlate with a much earlier onset of LTP plasticity, also due to a switch to GluN1/GluN2 receptor expression (Henson *et al.*, 2012; Larsen *et al.*, 2014) (Roberts *et al.*, 2009). At L4–L2/3 visual cortex synapses, there are correlations between the developmental down-regulation of GluN3A and reductions in release of glutamate and ability to induce presynaptic LTD, which are processes linked to the stabilization of sensory maps (Larsen *et al.*, 2011; Feldman, 2012). While genetic deletion of GluN3A accelerates the onset of plasticity, overexpression of these receptors delays it. Another synaptic mechanism that seems regulated by GluN3A-containing receptors is the lack of long term stabilization of certain synapses by plasticity-inducing stimuli (Roberts *et al.*, 2009; Kehoe *et al.*, 2014). It has been hypothesized that GluN3A interacts with structural scaffold proteins like GIT1 and others in the post-synapse to block synapse stabilization (Fiuza *et al.*, 2013). Behaviorally, young GluN3A KO mice show increased pre-pulse inhibition (Brody *et al.*, 2005), while in adults enhanced object recognition and spatial learning have been shown (Mohamad *et al.*, 2013). These cognitive enhancement performances have also been reported in humans with low expression of the GRIN3A gene (Sadat-Shirazi *et al.*, 2019). In adults, there is retention of GluN3A expression in areas implicated in higher cognitive processing with strong requirements for plasticity and input control and also in areas important for emotional circuitry.

Since GluN3A is an important mediator of synaptic plasticity in key moments of brain development, it is no surprise that its role has been implicated in the onset of some pathological diseases, both neurodevelopmental ones and in adults where it can reinstate inappropriate juvenile synaptic alterations (Table 4). Among the most prominent diseases associated with GluN3A there is schizophrenia,

where elevated GRIN3A transcripts have been found in schizophrenic brains, and rare allele variants of the gene are also linked to clinical cases (Mueller and Meador-Woodruff, 2004; Greenwood *et al.*, 2016). In these clinical cases, there could be an aberrant synaptic pruning leading to a variety of clinical symptoms. The same study found reduced transcripts levels in patients diagnosed with bipolar disorder (Mueller and Meador-Woodruff, 2004). Autism is another neurodevelopmental disorder that is thought to be associated with altered synaptic refinement in development and imbalances in excitation and inhibition. GluN3A KO animal models exhibit behaviors that might overlap symptoms of autism (Lee *et al.*, 2018). Rare missense GRIN3A variants have been found in autistic patients, sometimes overlapping with schizophrenic risk factors (Kushima *et al.*, 2018). Single cell transcriptomics in cortex samples from patients with epilepsy also showed major upregulation of GRIN3A (Pfisterer *et al.*, 2020). Furthermore, it was highlighted that upregulation was stronger in L5/6 excitatory neurons and two SST interneuron subtypes, consistent with the cell types expressing GluN3A shown in Figure 31. Another class of disorders that has been linked with the GRIN3A gene is substance addiction. Genome wide association studies found elevated mRNA transcript levels in alcohol and nicotine addiction patients (Chen *et al.*, 2018). Many GluN3A rarer genetic alleles or variants have also been linked with a number of cases of addiction, also involving opioids and heroin (Liu *et al.*, 2021). An experiment showed that cocaine assumption leads to GluN3A being inserted at the membrane in the mammalian brain, modifying the type of channels present at the synapse, among which inserting calcium-permeable GluA2-lacking receptors (Yuan *et al.*, 2013). GluN3A related pathologies have also been linked to neurodegenerative disorders. Reactivation of GluN3A in adults has been linked to Huntington's disease (Mahfooz *et al.*, 2016), where GluN3A accumulates at the cell surface of striatal neurons causing pruning (Marco *et al.*, 2013). Some studies also indicated that GluN3A might have a neuroprotective role in the adult brain in situations of brain trauma like ischemia or hypoxia following stroke where neuronal death occurs due to excitotoxicity by excess glutamate (Wang *et al.*, 2013; Lee *et al.*, 2015). Therefore, GluN3A has been indicated as a target for the development of therapeutic treatment of stroke.

dbSNP ID	dbSNP allele	Amino acid change	Domain	Phenotype	Disease related	Reference
-	G > A	Val132Leu	Extracellular (NTD)	Possibly damaging	Nicotine dependence	(Yang <i>et al.</i> 2015)
rs556419599	C > T	Asp133Asn	Extracellular (NTD)	—	Schizophrenia (SCZ)	Shen <i>et al.</i> (2009)
rs769491656	G > A, C, T	Arg137Ser	Extracellular (NTD)	Disease causing	Autism spectrum disorder (ASD)	Yu <i>et al.</i> (2018)
rs773593066	G > A	Arg337Trp	Extracellular (NTD)	Possibly damaging	ASD, SCZ	Yu <i>et al.</i> (2018)
rs10989591	C > A, T	Val362Met	Extracellular (NTD)	Higher P300 amplitude Better associative and/or recognition memory	Prefrontal cortex-dependent-memory	Gallinat <i>et al.</i> (2007); Papenberg <i>et al.</i> (2014)
-	A > C	Val389Leu	Extracellular (NTD)	Possibly damaging	Nicotine dependence	Yang <i>et al.</i> (2015)
rs200120504	C > T	Val389Ile	Extracellular (NTD)	Disease causing	SCZ	Yu <i>et al.</i> (2018)
rs34755188	C > T	Arg480His	Extracellular (NTD)	Possibly damaging	Nicotine dependence	Yang <i>et al.</i> (2015)
rs149729514	G > A, C	Arg480Gly	Extracellular (NTD)	Probably damaging	SCZ	Shen <i>et al.</i> (2009); Takata <i>et al.</i> (2013)
rs189425146	T > C	Lys488Glu	Extracellular (NTD)	Disease causing	ASD, SCZ	Yu <i>et al.</i> (2018)
-	C > T	Gln508*	Extracellular (NTD)	Patient with catatonic SCZ, inherited from mother in SCZ spectrum	SCZ	Tarabeux <i>et al.</i> (2011)
rs75981117	T > C	Asn549Ser	Extracellular - glycosylation site (LBD S1)	Possibly damaging	Nicotine dependence, Bipolar suicide attempting	Yang <i>et al.</i> (2015); Gaynor <i>et al.</i> (2016)
rs10989563	C > T	Asp835Asn	Extracellular (LBD S2)	Susceptibility for Alzheimer's disease (AD) pathogenesis	AD	Liu <i>et al.</i> (2009)
-	C > A	Gly898Trp	Extracellular (LBD S2)	Possibly damaging	ASD	Yu <i>et al.</i> (2018)
-	C > T	Arg1024*	Intracellular (CTD)	Possibly damaging	SCZ	Shen <i>et al.</i> (2009)
rs3739722	C > T	Arg1041Gln	Intracellular (CTD)	AD susceptibility, increased risk of cerebral palsy and postoperative delirium	AD, dementia, cerebral palsy, non-substance-abuse delirium	Liu <i>et al.</i> (2009); Cacabelos <i>et al.</i> (2012); Costantine <i>et al.</i> (2012); Kazmierski <i>et al.</i> (2014)
-	G > C	Gln1091His	Intracellular (CTD)	Possibly damaging	SCZ	Shen <i>et al.</i> (2009)
rs10121600	C > T	-	Intronic	Possibly damaging	Nicotine dependence	Ma <i>et al.</i> (2010)
rs11788456	G > A	-	Intronic	Possibly damaging	Nicotine dependence	Ma <i>et al.</i> (2010); Yang <i>et al.</i> (2015)
rs1323423	T > A, C, G	-	Intronic	Surrounding DNA region harbours an enhancer element	Nicotine dependence	Chen <i>et al.</i> (2019)
rs17189632	T > A, G	-	Intronic	Possibly damaging	Nicotine dependence, heroin addiction	Ma <i>et al.</i> (2010); Yang <i>et al.</i> (2015); Xie <i>et al.</i> (2016)
rs2067056	T > C	-	5' UTR	Upstream transcript variant	Nicotine dependence	Chen <i>et al.</i> (2019)
rs2485530	C > G, T	-	Intronic	Possibly damaging	Bipolar suicide attempting	Gaynor <i>et al.</i> (2016)
rs45537432	C > G, T	-	Intronic	Possibly damaging	Bipolar suicide attempting	Gaynor <i>et al.</i> (2016)
rs7030238	A > C	-	3' UTR	Possibly damaging	Nicotine dependence	Ma <i>et al.</i> (2010)

dbSNP is a NCBI public database for human single nucleotide polymorphisms. \*Non-sense mutation. NTD; amino terminal domain; LBD, ligand-binding domain; CTD, carboxy-terminal intracellular domain.



Table 4 GluN3A mutations linked to human pathology.

Image obtained and modified from (Crawley et al., 2022). Table illustrating a number of point mutations in different modules of the GluN3A subunit that have been linked to pathological cases in humans.

## 5.7 GluN1/GluN3A diheteromers in the brain

Thanks to the discovery that CGP 78-608 (hereafter named CGP) massively potentiates GluN1/GluN3A receptors (eGlyRs), it has finally become possible to show that these receptors are expressed and functional in native neuronal tissue. In the first paper published in 2018, it was shown that GluN1/GluN3A receptors are functionally expressed in the juvenile hippocampus (P8-12) (Grand *et al.*, 2018). With CGP pre-incubation (which acts as an inhibitor on GluN2-containing NMDARs), it was possible to trigger large excitatory glycinergic currents in CA1 following glycine puffs, and these currents were abolished either by application of DCKA, or by recording from GluN3A KO animal slices (Figure 36 Panel A). Since then, additional papers have been published showing eGlyR-mediated currents in several areas of the brain, allowing to isolate and characterize this receptor function in vivo and strongly renewing the excitement surrounding these puzzling receptors (Otsu *et al.*, 2019; Bossi *et al.*, 2022).

Within these papers, large eGlyR-mediated currents were evoked in diverse areas of the mouse adult brain such as the medial habenula (Otsu *et al.*, 2019), in the SST interneurons of the somatosensory cortex and in pyramidal neurons of the basolateral amygdala (Bossi *et al.*, 2022). In the medial habenula, it was found that thanks to glycine puffs it is possible to increase the firing rate and observe eGlyR-mediated currents, even in the absence of CGP. It was hypothesized that the endogenous source of glycine activating these receptors could be the astrocytes in the circuitry. Furthermore, in behavioral tests, eGlyRs from the medial habenula were shown to be critically involved for the ability to acquire conditioned place-aversion. Both in (Otsu *et al.*, 2019), and in (Bossi *et al.*, 2022), the authors found no evidence of the expression of triheteromeric GluN1/GluN2/GluN3A receptors in any regions of the habenula, amygdala or neocortex in adulthood.

By using 2P glycine uncaging and performing EM microscopy in (Bossi *et al.*, 2022), the authors found that eGlyRs are not enriched in spines, as for conventional GluN1/GluN2 NMDARs, but are rather expressed ubiquitously in the synaptic and extra synaptic compartments. This fact, coupled with the observation that in many regions where these receptors are highly expressed there is no glycine innervation (Zeilhofer *et al.*, 2005), led to the hypothesis that eGlyR act as sensors of endogenous tonic

levels of glycine, rather than being activated phasically by neurotransmitter release. Indeed, in the pyramidal neurons of basolateral amygdala, glycine bath application was found to depolarize receptors, and application of the glycine transporter inhibitor sarcosine was found to also increased tonic inward currents (experiments performed in the absence of CGP) (Espinosa and Bellone, 2022). Contrarily, application of DCKA at high concentration shifted holding currents to more positive values, indicating that some eGlyRs are tonically activated by ambient glycine. However, in the cortex S1, sarcosine did not change the holding currents recorded from somatostatin interneurons. This finding indicates that in different brain regions or within different cell types, different levels of tonic agonist may regulate the occupancy of these receptors. In turn, this has an effect on the excitability of the cells, and their threshold requirements for triggering action potentials. The in vivo effects of a reduction of expression of these channels in the S1 SST-Interneurons were modified calcium transients during locomotion. In vivo effects of decreased expression of these channels in the BLA showed that during fear conditioning the tonic currents levels were increased indicating that the activity of eGlyR is plastic and regulated by the behavioral state of the animal. This translated into a behavioral effect of impaired recall of fearful cued memories. Finally, it was found that the neuromodulator dopamine seems to have an effect on these receptors' activity, perhaps indirectly regulating of extracellular levels of glycine in the CSF.

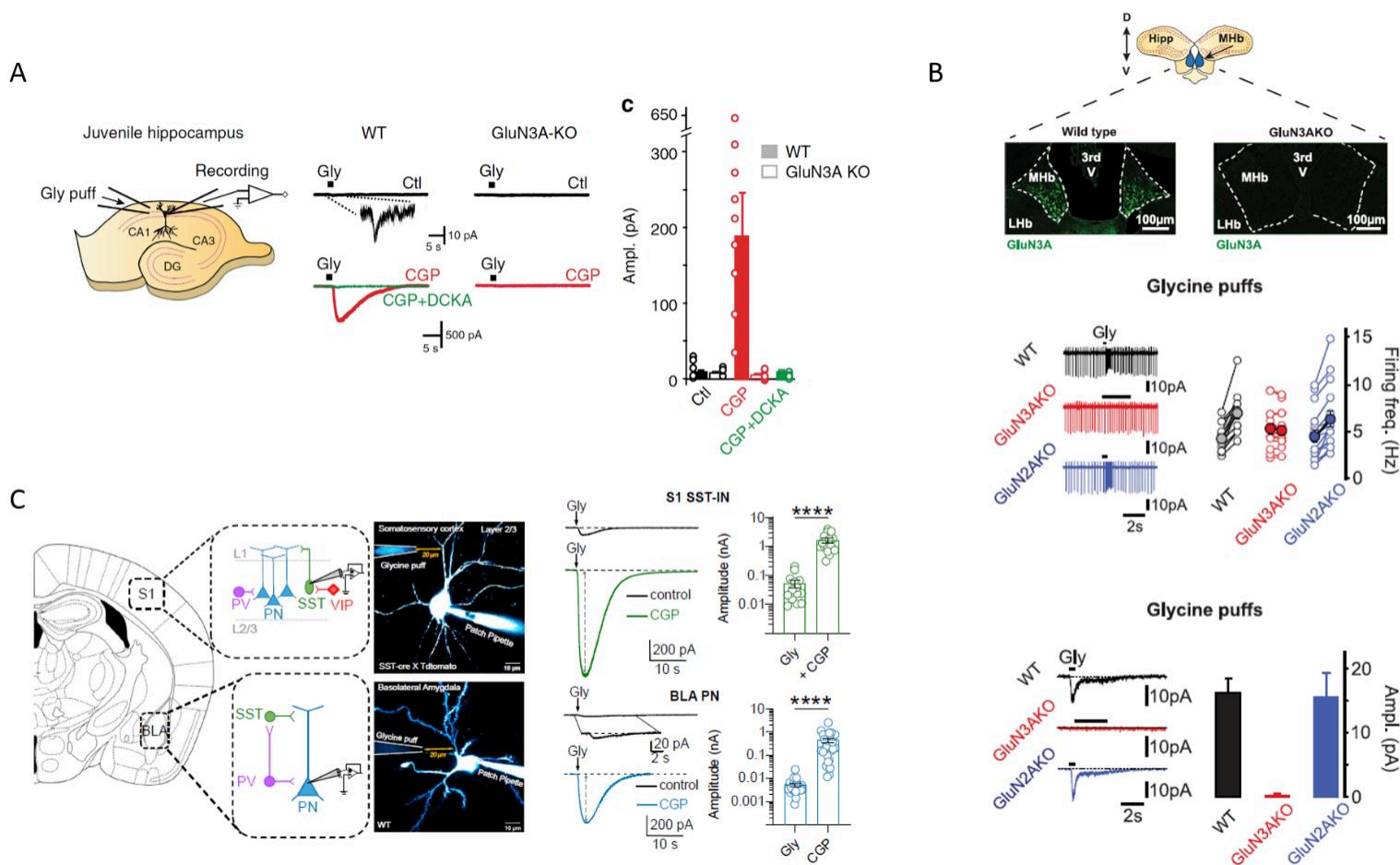


Figure 36 eGlyR currents in the adult mouse brain.

Images obtained and adapted from (Grand et al., 2018; Otsu et al., 2019; Bossi et al., 2022) Panel A, 10 mM glycine is puffed in CA1 hippocampal cells slices from young (P8-12) mice. In control conditions, glycine puffs trigger very small currents in both wild-type (WT) and GluN3A-KO mice. Pre-application of CGP leads to massive potentiation of glycine-elicited currents in WT mice, but has no effect in GluN3A-KO animals. In WT mice, addition of 500  $\mu$ M DCKA eliminates responses, confirming that GluN1/GluN3A eGlyRs mediate the responses to glycine. Panel B, confocal microscopy showing that GluN3A subunits are expressed in the ventral medial habenula. Glycine puffs in these cells increase firing rates in control and GluN2A KO mice, but not in GluN3A KO animals. Glycine puffs elicit small peak currents within the same conditions, but not in GluN2A KO mice. Panel C, schematic representation of the hierarchical cellular organization of S1 and BLA circuitry. Right: two-photon laser scanning microscopy images of a patched cortical somatostatin interneuron in S1 and pyramidal neurons in the basolateral amygdala with the location of the pipette. On the right, representative current traces of glycine (10 mM) puff mediated currents in these two regions with and without pre-application of CGP.

## 5.8 Triheteromers containing GluN1/GluN2/GluN3A: fact or fiction?

The effective existence of triheteromeric NMDA receptors containing all three main families of NMDAR subunits, that is GluN1s, GluN2s, and GluN3s is an important, and still open, question in the field. For a large part of the community working on the physiological aspects of GluN3 containing NMDARs and until recent years, their existence is considered as the standing paradigm used to interpret functional results of GluN3A studies in which it is in fact impossible to precisely determine the stoichiometry of GluN3A-containing NMDARs under study. Many *ex vivo* experiments on brain slices describe properties ascribed to triheteromeric receptors containing GluN3A, but come from a period in which the existence of diheteromeric GluN1/GluN3A receptors *in vivo* was unknown and uncharacterized (Das *et al.*, 1998; Martínez-Turrillas *et al.*, 2012; Pilli and Kumar, 2012; Al-Hallaq *et al.*, n.d.) (and others, >20 publications). In some cases, the results that were observed could be retroactively explained by what we now know about the biophysical properties of diheteromeric GluN1/GluN3A receptors, albeit a posteriori explanation for experiments cannot be proven. In other experiments, the recorded receptors containing the GluN3A subunits show properties that seem hybrid between GluN1/GluN3A diheteromers and what we know about conventional GluN1/GluN2 NMDARs, such as magnesium block and APV sensitivity, pointing towards the hypothesis that triheteromers may form in the brain (Káradóttir *et al.*, 2005; Yuan *et al.*, 2013) (Table 5). However, the more recent physiological studies that studied eGlyRs did not find any evidence for the presence of functional triheteromers in the adult forebrain (Otsu *et al.*, 2019; Bossi *et al.*, 2022).

Another source of data on GluN3A triheteromers comes from *in vitro* experiments, and it involves co-immunoprecipitations, colocalization data, and single channel recordings. Several total membrane co-immunoprecipitation studies from neural tissues show that GluN3A co-assembles with GluN2s (Das *et al.*, 1998; Wong *et al.*, 2002; Nilsson *et al.*, 2007; Roberts *et al.*, 2009; Piña-Crespo *et al.*, 2010; Martínez-Turrillas *et al.*, 2012). Similar studies done on heterologous expression systems such as HEK and COS cells similarly show that co-assemblies of GluN3As are possible with GluN2s and GluN1s (Pérez-Otaño *et al.*, 2001a; Sasaki *et al.*, 2002; Wong *et al.*, 2002; Al-Hallaq *et al.*, 2007; Burzomato *et al.*, 2010). However, none of these studies distinguished between total and plasma membrane-only co-immunoprecipitations, not excluding the option that GluN3A and GluN2s might assemble intracellularly, but be prevented from trafficking to the cell surface. Two colocalization studies have been performed, these involve investigation with FRET methodology the luminescence of GluN3A with partner subunits. One study showed that colocalization of GluN3A with GluN2A is possible in HEK cells (Schüler *et al.*, 2008),

while another one showed that GluN3A and GluN2B do not coassemble in xenopus oocytes (Ulbrich and Isacoff, 2008). A few studies with single-channel recordings from GluN3A expression cells have been performed, albeit suffering from the same interpretational issue as the early studies on physiology, which is that the authors did not know that GluN1/GluN3A diheteromers can be formed (Das *et al.*, 1998; Pérez-Otaño *et al.*, 2001b; Chatterton *et al.*, 2002; Sasaki *et al.*, 2002; Tong *et al.*, 2008). In these studies, co-injection of the three subunits GluN1, GluN2 and GluN3A in heterologous expression systems leads to the appearance of a small GluN3A-related conductance, but the lack of diheteromeric GluN1/GluN3A control experiments did not allow to distinguish if this conductance was mediated by GluN1/GluN3A diheteromers or GluN1/GluN2/GluN3A triheteromers (or both) (note that in all these studies, glycine is systematically added to the extracellular solutions for activation of presumably triheteromers). However, in (Sasaki *et al.*, 2002) it was reported that the small conductance single-channel current was inhibited by APV application, which pointed to triheteromers since GluN1/GluN3A diheteromers are insensitive to APV (Chatterton *et al.*, Nature 2002). It should be noted however that the APV sensitivity was just illustrated within a one trace panel with no indication of % of inhibition or number of repeats.

CO-IP Paper- Neural tissues	Origin tissue	IP	Triheteromers
<i>Das et al Nature 1998</i>	Total membrane extracts: Mouse cortex lysate - membrane	Anti wt GluGluN3A	Yes
<i>Nilsson et al. Brain Res. 2007</i>	Total membrane extracts: Human brain	Anti wt GluGluN3A	Yes
<i>Roberts et al. Neuron. 2009</i>	Total membrane extracts: Mouse hippocampus	IP on anti-GFP modified GluGluN3A	Yes
<i>Pina Crespo et al. J Neurosci. 2010</i>	Total membrane extracts: Mouse Optic nerve	Anti wt GluGluN3A	No
<i>Martínez-Turrillas et al., Neurobiology of disease, 2012</i>	Total membrane extracts: Mouse striatum	IP on anti-GFP modified GluGluN3A	Yes
<i>Wong et al. J Comp. Neuro 2002</i>	Total membrane extract :Rat brain	Anti wt GluGluN3A	Yes

CO-IP Paper- heterologous systems	Cells	IP	GluN1-GluN2-GluN3	GluN2-GluN3	GluN1-GluN3
<i>Perez-Otano et al. J Neurosci. 2001</i>	HEK	Anti wt GluN3A ?	Yes?	Yes	Yes
<i>Wong et al. J Comp. Neuro 2002</i>	HEK	Anti wt GluN3A	tested with no GluN1	Yes?	Yes
<i>Sasaki et al. J Neurophy. 2002</i>	COS	Anti myc-GluN3A	tested with no GluN1	Yes	Yes
<i>Matsuda et al. J Neurosci. 2003</i>	HEK Total & plasma membrane	Anti HA-GluN3B	? Could be diheteromerss	Yes, 3B doesn't go at the membrane	Yes Yes
<i>Burzumata et al. J Phys. 2010</i>	HEK	GluN2C IP on anti-GFP-GluN3A	Yes?	Only tested with GluN1	n.d.
<i>Al-Hallaq et al. Mol Pharm. 2002</i>	HEK	Anti wt GluN3A	Yes?	Only tested with GluN1	n.d.

Single channel recordings papers	Expression system	Pharmacology	Parameters tested
<i>Perez-Otano et al. J Neurosci. 2001</i>	Hek cells	NMDA (0.5–5 $\mu$ M) and glycine (0.5 $\mu$ M)	Conductances, Calcium permeability
<i>Sasaki et al. J Neurophy. 2002</i>	Oocytes GluN1,GluN2A,GluN3A, cortical p8 neurons	10–20 M NMDA plus 10 $\mu$ M glycine	Conductances, Calcium permeability, Mg affinity, Apv inhibition
<i>Das et al Nature 1998</i>	Oocytes GluN1,GluN2A,GluN3A - GluN1,GluN2B,GluN3A	20 $\mu$ M NMDA and 10 $\mu$ M glycine	Conductances, Calcium permeability
<i>Chatterton et al, Nature, (2002)</i>	Oocytes, single channel recordings of GluN1/GluN3B, GluN1/GluN3A diheteromers (not shown)	Gly alone, 10 $\mu$ M	Conductances, Magnesium affinity
<i>Tong et al., Neurophysiology (2008)</i>	Hippocampal cultures of transgenic GluGluN3a overexpressing mice	NMDA (10 M) and glycine (20 M)	Conductances

Table 5 Summary of papers and main findings on triheteromeric GluN1/GluN2/GluN3A receptors.

Protein expression was based on co-immunoprecipitations from various tissues or from single channel analysis. N.D indicated not determined

Another problem surges from the fact that no one has been able to characterize triheteromer properties in isolation without being able to exclude the presence of GluN1/GluN3A diheteromers in the receptor populations analyzed. Therefore, the pharmacological properties and stoichiometry of triheteromers remains unknown and we are currently lacking a pharmacological way (or any other ways)

to distinguish triheteromeric properties from a sum of two different diheteromeric populations (Table 6). More studies containing the appropriate controls such as cell surface vs whole cell distinction for colIPs, proper characterization of APV sensitivities for single-channel recordings and appropriate diheteromeric controls for experiments both in vitro, ex vivo and in vivo seem necessary to answer this question.

Overall, we lack strong evidence for the existence of functional triheteromeric Glu1/Glu2/Glu3A receptors, be it in recombinant systems or native tissues. Some indirect pharmacological clues point to a possible existence of the triheteromers, especially in multicellular systems. However, interpretation of the results obtained in the past suffered from a lack of knowledge that only nowadays we are starting to possess, with the discovery that glycine-gated GluN1/GluN3A receptors can form functional receptors in native tissues. Some other experiments point to the fact that triheteromers may not assemble in some heterologous expression systems such as xenopus oocytes, while co-immunoprecipitation studies are inconclusive since they only focus on total membrane extracts.

		Diheteromer			Triheteromer	
Biochem	IP total	Yes	Yes	Yes	Unclear	
	IP memb	Yes	Yes	No	N.d	
Cellular	Coloc tot	Yes	Yes	Yes	Yes	
	Coloc memb	Yes	Yes	N.d	N.d	
Electrophy	Single chan	Yes	Yes, but n.d	No or N.d.	Not clear	
	TEVC (ooc)	Yes	Yes	No	No	
	Neurons	Yes	Yes	No	Contradictory	
Pharmacology		<i>Sensitivity</i>	<i>Sensitivity</i>	<i>Sensitivity</i>	<i>Sensitivity</i>	<i>Sensitivity</i>
	Mg <sup>2+</sup> block	High	Low	N.d	Low ?	N.d
	Ca <sup>2+</sup> permeation	High	Low	N.d	Low ?	N.d.
	APV block	High	Low	N.d	Intermediate	High ?

Table 6 Interpretation of triheteromeric vs diheteromeric GluN1/GluN2/GluN3A datasets.

*Table recapitulating the main findings that have been observed for the different combinations of both proven and hypothesized assemblies between GluN1, GluN2 and GluN3s. N.D indicated not determined. Some entries required interpretation of the results based on the type of controls employed and the current knowledge we have now on GluN1/GluN3A diheteromers.*

## **5.9 GluN3B**

Of the two subunits composing the GluN3 family, GluN3B has received less attention than the GluN3A subunits, due to its much less abundant expression in the CNS (see Figure 9). Overall, the GRIN3B gene expression is weakly or completely absent in the neonatal brain (Chatterton *et al.*, 2002; Matsuda *et al.*, 2003), and starts to increase in the early postnatal period (P7) and maintain consistent expression levels into adulthood (Wee *et al.*, 2008, 2016b). GluN3B has been found to be expressed in regions such as pons, midbrain, medulla, and spinal cord but at (very) low levels in forebrain and cerebellum. The only region where it is expressed as early as embryonic stage is the somatic motoneurons, where it has been hypothesized to have a protective role and influence dendrite morphogenesis (Prithviraj and Inglis, 2008). Its physiological role is poorly understood, but GluN3B KO mice have been shown to have problems in motor learning behavior (Niemann *et al.*, 2007), consistent with its expression in motoneurons. These mice also exhibited abnormalities in their social interactions, and anxiety like phenotype. Only the crystal structure of the isolated GluN3B LBD in complex with agonists and competitive antagonists is available, solved in the same study that solved the structure of GluN3A (Yao *et al.*, 2008). Overall, the GluN3 subunit has a very high sequence homology with GluN3A, albeit showing a shorter CTD (Figure 22). Co-expression of GluN1 and GluN3B subunits yield functional glycine-gated excitatory ion channels as for GluN1/GluN3A receptors (Chatterton *et al.*, 2002; Awobuluyi *et al.*, 2007). Single channel recordings from this subunit co-expressed in diheteromeric GluN1/GluN3B channels in xenopus oocytes show 2 conductance levels, with 37 and 12 pS recorded (Chatterton *et al.*, 2002). The protein GluN3B is among the 7 NMDAR and all 18 iGluR subunits the one with the most tolerance to variation and genetic drift (Hansen *et al.*, 2021), indicating that its role in the CNS may be less important than the other subunits.



## **Second chapter: Results**

## **Question and objectives**

During my PhD project, we aimed to investigate the structural correlates of the gating mechanism of GluN1/GluN3A diheteromeric receptors. We tried to investigate specific regions of GluN1 individually, GluN3A individually or GluN1/GluN3A interfaces with a mutagenic approach and 2-electrode voltage clamp recordings in xenopus oocytes to determine if we could tie specific functions to structural regions of the receptor. Specifically, key interests were to try to understand the origin of the atypical gating behavior of GluN1/GluN3A receptors, and the structural correlates of GluN1 acting as auto-inhibitory subunit rather than a co-activatory subunit like in GluN1/GluN2 complexes. We undertook many different approaches in order to understand at which interfaces the crosstalk between the two subunits take place, and if it is possible to distinguish and modulate and the different components of gating. Alongside these objectives, we tried to develop new methodological tools that would help us and others in the investigation of GluN3A containing NMDARs.

## Introduction: challenges and molecular perspectives of GluN1/GluN3A receptor study

This chapter describes several aspects of my main project that I developed, and in particular those that were not kept in the attached publication (see 8.3 Article: The LBD Dimer Interface Tunes Activation of Glycine-Gated GluN1/GluN3A Receptors). Hopefully this introduction will allow to explain the challenges we had to face during the 4 years of the PhD, the progress we made, and the directions we took. We think presenting unsuccessful results could be interesting to feed methodological discussions but also for future investigations on these receptors. The study into the molecular mechanisms of GluN1/GluN3A receptors is not a trivial task as we had to overcome several challenges. I tried to schematize them as following:

Challenge 1: When GluN1/GluN3As are exposed to an agonist such as glycine, above the micromolar concentration, the receptors display small and quickly desensitizing currents. This behavior makes the characterization of receptor properties a challenging task in native conditions (without aids such as specific GluN1 antagonists like CGP-78608 (Grand *et al.*, 2018)). This challenge applies both to native and to recombinant expression system conditions. Overall, GluN3As small current phenotypes, which were even considered an artefact of recombinant expression systems when initially discovered, slowed the field of study of these receptors. Practically for me, only xenopus oocytes batches of the highest quality allowed to characterize WT receptors (without CGP), making the number of possible fruitful experiments more limited than the canonical GluN2s-containing NMDARs.

Challenge 2: The structural information describing GluN3A-containing receptors are limited compared to other iGluRs or other NMDAR subunits. Currently, there are no cryo-EM structure of full tetrameric GluN1-GluN3A receptors. The structures available in the PDB database are X-ray diffractions (high quality) of the isolated GluN3A LBD bound to glycine, D-serine or ACPC (Yao *et al.*, 2008), or in Apo state (Yao *et al.*, 2013) without GluN1. However, we do not even have any information about GluN1-GluN3A co-assemblies, and quaternary structure formation. Contrarily, GluN1-GluN2 LBD dimerization was already structurally described in 2005 (Furukawa *et al.*, 2005) (see 3.3.1 LBD dimerization). This lack of structural information is a remarkable limitation when investigating the molecular interplay between two subunits hypothesized to finely interact with each other.

Challenge 3: GluN1/GluN3A receptors have been shown in the literature to be unresponsive or largely less sensitive to many pharmacological compounds that normally act on GluN2 containing subunits. A large pharmacological library allows to target specific GluN2 subunits of NMDARs, often with

a domain specificity. This has allowed to finely-tune the activity of these receptors for different applications, from molecular studies to neuronal circuitry function and even pathology (Memantine, Ketamine etc.). The absence of such variety of drugs targeting GluN3A receptors is in part due to the aforementioned challenges (see points 1 and 2 above), which slowed the drug development of GluN3A for many years, in comparison to other NMDARs. To give an example relevant for us, channel blockers like MK-801 have been shown to be mostly ineffective on GluN3A, and therefore cannot be used to estimate the PO of these receptors (Chatterton *et al.*, 2002). Therefore, less tools are available for the characterization of GluN1/GluN3A receptors in comparison to the “canonical” GluN2 containing NMDARs.

The three challenges discussed above represent an obvious limitation for a structure/function approach to study GluN1/GluN3A receptors, but at the same time they also represent voids of knowledge that we can attempt to fill. Therefore, when trying to determine the molecular mechanisms regulating the gating process of GluN1/GluN3A receptors we undertook several approaches. We schematized them as follows:

- 1) We undertook an effort to develop new methodologies that allow to study GluN1/GluN3A receptors. Specifically, we were interested in trying to determine if there was a way to measure GluN3A receptor PO and if we could find new drugs that can expand the tools available to study GluN3A.
- 2) As a consequence of the lack of structural data, we had to rely on *ab initio* modeling when choosing which sites to target to affect receptor function. This approach forced us to make assumptions about structural conformations adopted by GluN3A receptors (see 7.1 Building a working 3D model of GluN1/GluN3A receptor).
- 3) In our attempts to understand the structural mechanism of aimed at obtaining some modified GluN1/GluN3A receptors that gain-of-function mutants that would allow to study receptor function with more ease. This was done in part to specifically tackle the challenge 1 related to very low steady state current of GluN1/GluN3A WT receptors.

To tackle these objectives, we attempted different strategies based on the previous existing knowledge on NMDAR structure/function. Often, I was working on different approaches at the same time, and there have been moments in which I, alongside my supervisors, had to make decisions on which directions to proceed. Sometimes, choosing to pursue a promising direction meant that we had to abandon other less successful approaches to focus on what seemed to be the most encouraging path for the continuation of the project. Therefore, some sets of experiments, although they showed potential or

novelty, have not been pursued to obtain a full scientific story. A number of negative results are indeed equally important to describe, as they helped delimiting what is theoretically correct or possible and what isn't. The positive results are often the end product of the bricks laid by the negative results, in other words the result of persistence in researching.

There are three chapters in this section. First, I will talk about the efforts we undertook to develop new methodologies and pharmacological compounds to study GluN1/GluN3A receptors. Second, I will talk about the efforts we took trying to stabilize specific GluN3A conformational states by mutagenesis and crosslinking. Third, I will detail our attempts and successes investigating the molecular determinant of GluN3A function at the LBD dimer interface.



## 6: New modulators, methodologies and tests to study GluN1/GluN3A receptor functions

In the following part of the results, I will describe in more detail than in the manuscript how we developed the methodologies to study GluN1/GluN3A, with an initial focus on open channel blockers among which magnesium and pentamidine. Continuing thematically in the pore region, I will describe how we implemented a technic of PO measurement based on MTSEA covalent binding in the M3 TM helices of the receptor. I also worked with an unpublished promising inhibitor of GluN1/GluN3A receptors. I will also talk about some attempts I made to explore the properties of zinc modulation, before concluding on how we looked into D-serine and CGP state dependence.

These TEVC studies of GluN3 containing receptors have been made possible thanks to the usage of two conditions that allow to work with large and stable currents. **1)** The first is based on the application of the molecule CGP 78608, a drug that allow to potentiate enormously GluN1/GluN3A WT receptor currents (see(Grand *et al.*, 2018)), but that has the drawback to be difficult to wash and be very sticky within the perfusion system and recording chambers of TEVC. CGP potentiated GluN1/GluN3A currents are also always slowly desensitizing in TEVC. **2)** The second is based on the usage of the GluN1 constructs F484A and F484A-T518L that also block glycine binding within GluN1 ligand binding pocket (Awobuluyi *et al.*, 2007; Madry *et al.*, 2007). We can see that both mutants display square currents as described in the literature but exhibit a 10-fold increase of glycine EC<sub>50</sub> (Figure 37 – please note that it is currently not understood why these mutants lowers glycine EC<sub>50</sub>). Even though the level of absolute current is much lower with these mutants than with CGP application on the WT, these mutants are useful to get squared and non-desensitizing GluN3A currents without sticky-CGP addition.

### 6.1 Pore block: Magnesium

Endogenous magnesium (Mg<sup>2+</sup>) pore-block effect at resting potential is one of the key functional feature of GluN2-containing NMDARs and for its neural role and function (Hansen *et al.*, 2021) (see 2.2 Function in physiology). In GluN3A containing receptors Mg<sup>2+</sup> has been described as a poor pore-blocker (Chatterton *et al.*, 2002). This difference of Mg<sup>2+</sup> sensitivity thus corresponds to a major functional marker to distinguish GluN3 and GluN2 NMDAR activity in the brain (as well as in heterologous system). To our knowledge, no magnesium I/V curves of diheteromeric GluN1/GluN3A receptors has been measured in heterologous expression system, which is problematic when we want to compare its pore-

block properties with other pore-block compounds. This absence probably originates from the difficulty to record large and stable currents from these fast and deep desensitizing receptors. We thought that the best available construct to record such IV curves was the GluN1 mutant in the glycine binding site which prevents glycine binding below the mM concentration and makes the current squares and easily recordable when coexpressed with GluN3A (Awobuluyi *et al.*, 2007; Madry *et al.*, 2007). Initially we carried out a glycinergic dose response for the constructs GluN1 F484A/GluN3A and GluN1 F484A-T518L/GluN3A to validate that these GluN1 mutants work in our hands in the same way that has been published in the existing literature. We show that both mutants display a  $EC_{50}$  for glycine shifted to the right of about 10X fold (Figure 37), and that they display square currents as described in the literature (Awobuluyi *et al.*, 2007; Madry *et al.*, 2007).



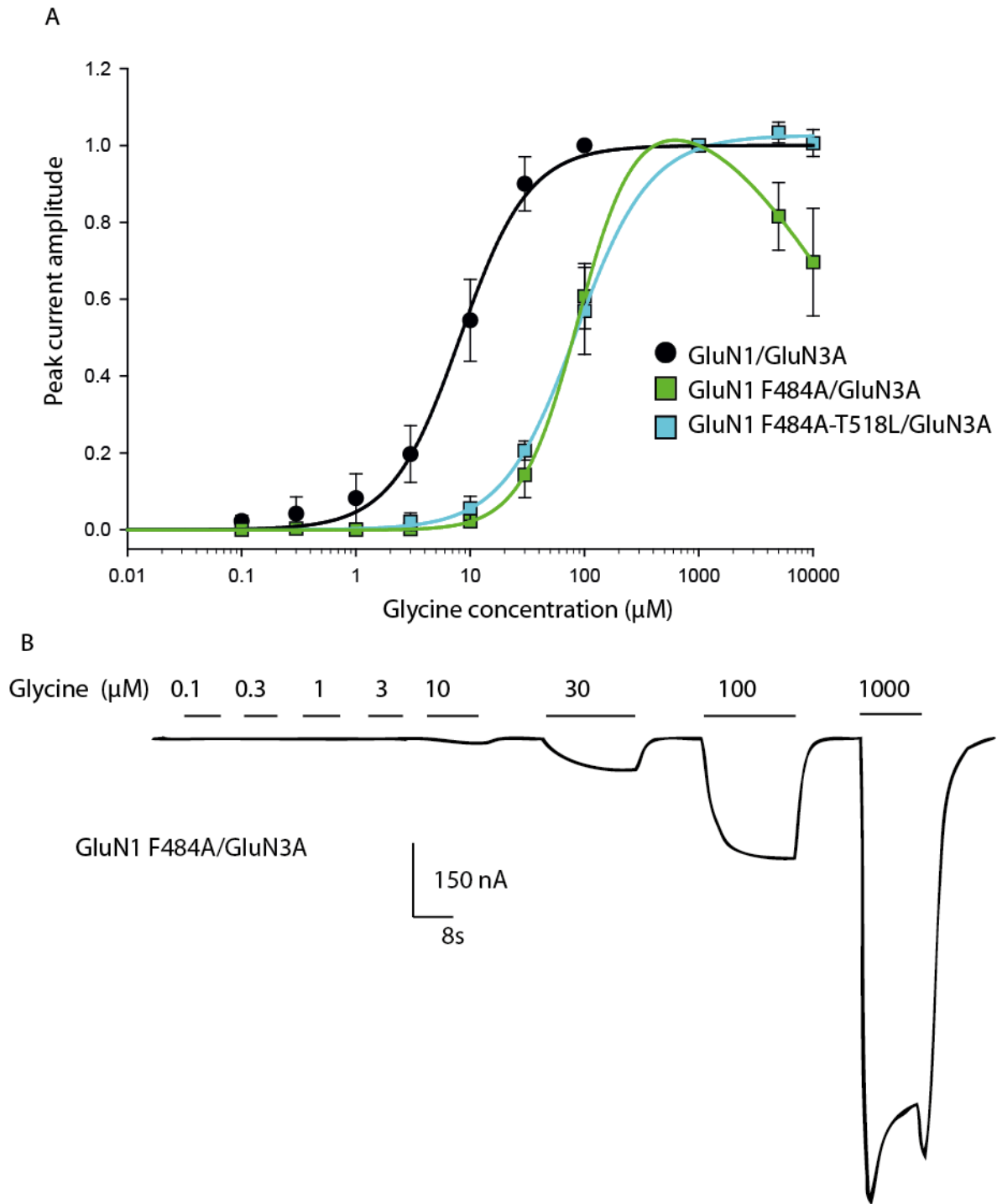


Figure 37 Glycine dose responses of GluN1 binding site mutants.

Panel A, glycine dose response curve of GluN3A/GluN1 WT ( $N=5$ ), GluN1 F484A/GluN3A ( $N=5$  for concentrations  $0.1 \mu\text{M}$ - $1 \text{ mM}$ ,  $N=3$  for concentrations  $100 \mu\text{M}$ - $10 \text{ mM}$ ) and GluN1 F484A-T518L/GluN3A ( $N=5$  for concentrations  $3 \mu\text{M}$ - $1 \text{ mM}$ ,  $N=5$  for concentrations  $100 \mu\text{M}$ - $10 \text{ mM}$ ).  $EC_{50}$ s were estimated to be  $8.1 \pm 0.5$ ,

88.5 ± 0.7, and 80 ± 4.3 μM respectively. GluN1 F484A/GluN3A fit was calculated with a bimodal distribution fit equation. Panel B, Example trace of glycinergic dose response of GluN1 F484A/GluN3A, displaying square currents in the μM range.

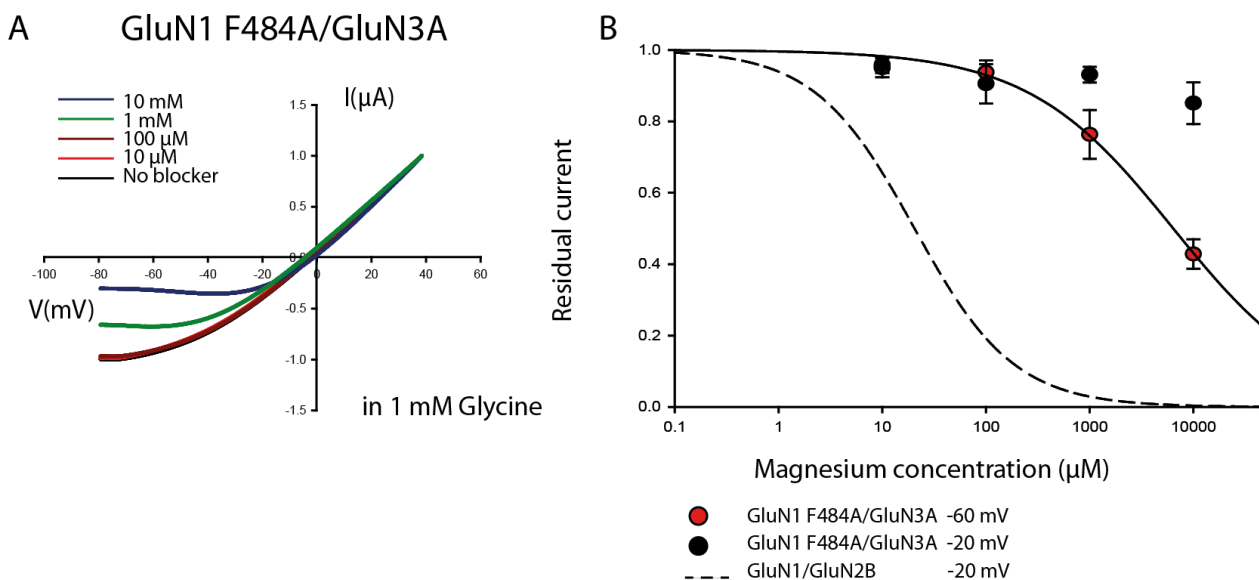


Figure 38 Magnesium sensitivity and IV curve in GluN1 F484A/GluN3A receptors.

Panel A, IV curves normalized to +40 mV with 1 mM glycine in black, and glycine + increasing Mg<sup>2+</sup> concentrations in various colors (N=3 for each condition). Panel B, dose responses of Mg<sup>2+</sup> at -60 (red) and -20 (black) mV of GluN1 F484A/GluN3A derived from the IV curves. Black dashed line shows GluN1/GluN2B Mg<sup>2+</sup> sensitivity -60 mV (data obtained from(Kuner and Schoepfer, 1996)). Dashed line IC<sub>50</sub> for Mg<sup>2+</sup> with the construct GluN1 F484A/GluN3A was estimated to be 6.3 mM ± 0.84 at -60 mV

We tested various magnesium concentrations while performing voltage ramps ranging from -80 to +40 mV (Figure 38). We observed that concentrations below 100 μM magnesium do not cause inhibition in these receptors, and that only concentrations above 1 mM Mg<sup>2+</sup> induce current reduction. The corresponding Mg inhibition is voltage dependent and can be seen only at lower potentials than -20 mV. The resulting IC<sub>50</sub> for Mg<sup>2+</sup> at -60 mV is estimated at about 6.3 mM ± 0.84 for GluN1/GluN3A receptors which is ~ 1000x fold higher than for GluN2 containing NMDARs (Kuner and Schoepfer, 1996). Differences in the QRN-site amino-acid composition and pore structure largely explain this functional difference. More interestingly, the observed Mg IC<sub>50</sub> lies above 1mM, that corresponds to the physiological concentration of Magnesium in the cerebrospinal fluid. Our results indicate that

contrary to GluN2 containing NMDAR, native functional GluN3A receptor in the brain should remain poorly sensitive to ambient magnesium.

## 6.2 Pore block: Pentamidine

Receptor open probability PO is a major and basic characteristic of receptor pore and gating activity, but that remain still poorly known for GluN3A containing receptors. In GluN2 containing receptor, MK-801 pore-blocker has been used (and validated) as a powerful tool to easily estimate the relative open probability (PO) of different variants, chimeras and mutants by TEVC ((Gielen *et al.*, 2009; Zhu *et al.*, 2013; Esmenjaud *et al.*, 2018)). This measurement relies on the observation that the kinetic of dissociation of this inhibitors is directly related to the opening rate of the pore, thus the PO of the receptor. Measurements of absolute PO using the single channel recording methodologies validated this approach (Wada *et al.*, 2006).

PO of GluN1/GluN3A receptors remains poorly known because the single channel recording methodology do not work so well on such deeply desensitizing receptors. Currently, we do not have yet any method available to estimate relative open probability (PO) for GluN3A containing receptors without recurring to single channel recordings. Finding an efficient GluN3A pore blocker to be used as MK801 would be a first important step, however most known GluN2 pore blockers are not efficient on GluN3 receptors.

Among different possible molecules, we tested pentamidine, a drug that is known to inhibit many iGluRs, and is FDA approved for its use in human patients for pneumonia (Reynolds' and Aizenman, n.d.). This drug has been suggested by Laetitia Mony, INSERM CR researcher in the Paoletti Lab. We describe pentamidine effect in the joined article (see 8.3 Article: The LBD Dimer Interface Tunes Activation of Glycine-Gated GluN1/GluN3A Receptors). To summarize the results, we followed the same strategy than with magnesium and find that pentamidine can inhibit GluN1 F484/GluN3A receptors (glycine alone) with an  $IC_{50}$  of  $26 \mu\text{M} \pm 5$  and GluN1/GluN3A WT receptors (glycine+CGP) with an  $IC_{50}$  of  $14.90 \pm 1.72 \mu\text{M}$  (Figure 39). We estimated the maximal inhibition of GluN1/GluN3A WT to be  $92 \pm 2 \%$  at  $500 \mu\text{M}$  pentamidine.

We then performed I/V curves on GluN1 F484A/GluN3A with 1mM glycine and on GluN1/GluN3A WT with 100  $\mu\text{M}$  glycine pre-incubated with 200 nM CGP (Figure 3, Panels A-B). In both cases we

observed that the effect of pentamidine is active only at negative potentials, and that we start to observe inhibitions at about 1  $\mu\text{M}$  compound concentration. Therefore, pentamidine appears among the first open channel blocker inhibiting GluN1/GluN3A receptors at low  $\mu\text{M}$  concentrations (Kaniakova *et al.*, 2018).

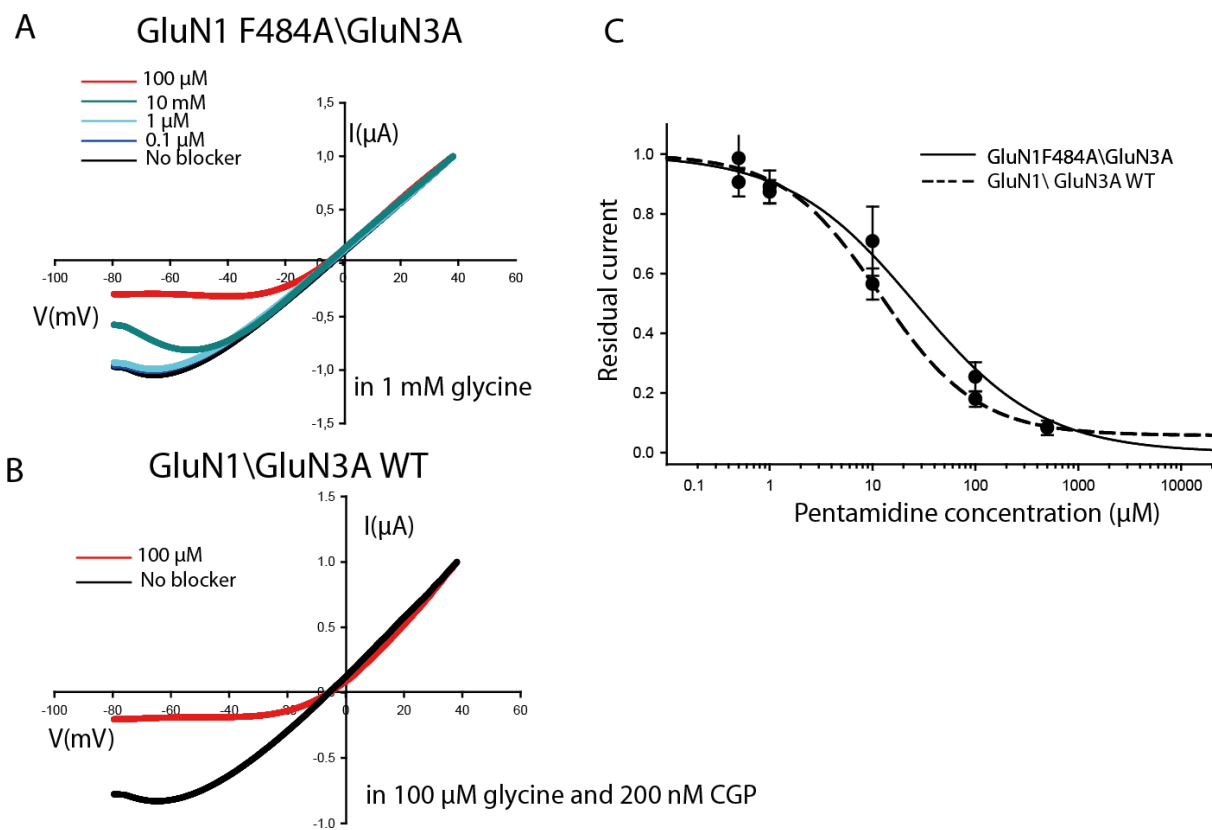


Figure 39 Pentamidine sensitivity and IV curves in GluN1/GluN3A receptors.

Panel A, IV curves normalized to +40 mV for GluN1F484A/ GluN3A WT with 1 mM glycine in black, and increasing  $\text{Mg}^{2+}$  concentrations in various colors (N=5). Panel B, IV curves normalized to +40 mV for GluN1/ GluN3A WT with 1 mM glycine in black, and glycine + increasing  $\text{Mg}^{2+}$  concentrations in various colors (N=4). Panel C, dose response of  $\text{Mg}^{2+}$  for both GluN1/GluN3A WT (dotted line) and for GluN1F484A/ GluN3A WT.  $\text{IC}_{50}$  for Pentamidine was estimated to be of  $14.90 \pm 1.72 \mu\text{M}$  for GluN1/GluN3A WT, and of  $26 \pm 5 \mu\text{M}$  for GluN1F484A/ GluN3A.

Initially, we were interested to find a pore blocker we could use to estimate the receptor PO, in a similar way than MK801 on GluN2 containing NMDARs. However, such a compound could only be used if its k-on of inhibition is slow enough to be accurately observed and distinguished from the perfusion speed of the TEVC. Pentamidine k-on appears way too fast to be used as it. We tried perfusing cells with

a pentamidine concentration below the  $IC_{50}$  ( $3 \mu M$ ) and a non-saturating glycine concentration ( $20 \mu M$ ), but we again observed very rapid on-set and off-set kinetics of inhibition (Figure 40). **Thus pentamidine cannot be used as a PO estimation tool.** Still, we later used in our work high concentration of pentamidine as a tool to fully block GluN1/GluN3A pore activity in case of constitutively activated mutants.

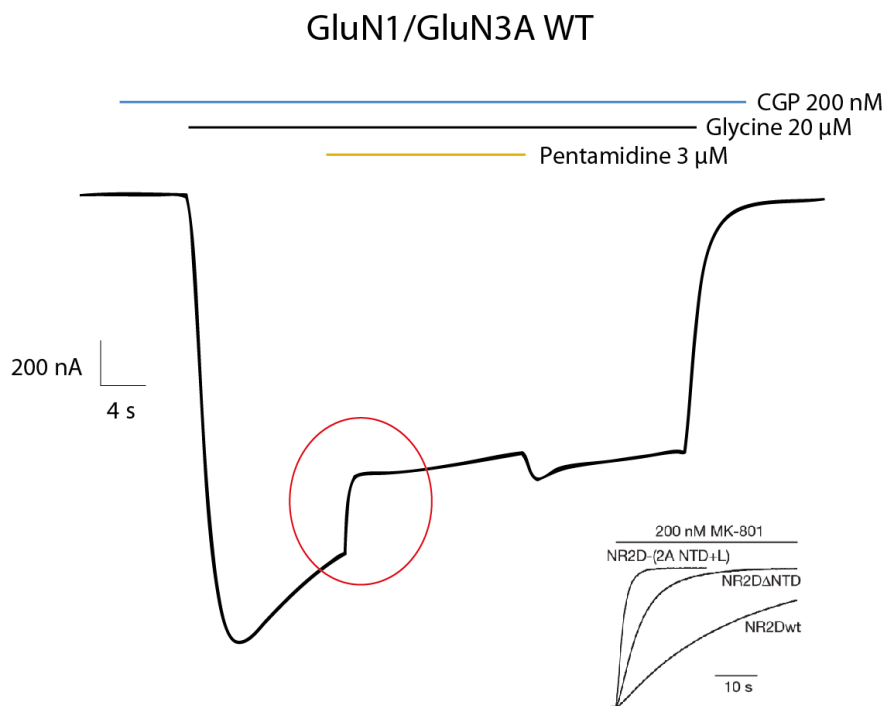


Figure 40 Kinetics of pentamidine inhibition.

Fast inhibition at low glycine and pentamidine concentrations. Small insert from (Gielen et al., 2009) indicating MK 801 activity to measure PO on canonical NMDARs.

### 6.3 Echinatin modulation

We received from a collaborator of the lab, professor Shujia Zhu, group leader at the Institute of Neuroscience (ION), Chinese Academy of Sciences, Shanghai, China a promising compound named echinatin that was hypothesized to display inhibitory activity on GluN1/GluN3A receptors. Echinatin is a licorice extract with anti-inflammatory effects We proceeded to test it on GluN1 F484A/GluN3A WT with 1mM glycine to evaluate its potency and efficacy. The compound display a low  $IC_{50}$  ( $2.78 \pm 0.01 \mu M$ ), and

close to 100% efficacy at 50  $\mu\text{M}$  echinatin (Figure 41). We do not know echinatin site of action. We tested its inhibition at lower glycine concentration (100  $\mu\text{M}$  glycine) but the  $\text{IC}_{50}$  we estimated was virtually identical. This indicates that the compound may not act as a competitive antagonist, but rather through an allosteric route. We also tested echinatin on a the GluN1/GluN3A S892L-K895F mutant (described in the manuscript) that do not target the ligand binding site. With this mutant, tested with 1  $\mu\text{M}$  glycine, which makes currents squares like the GluN1F484A at low  $\mu\text{M}$  concentrations, we recorded similar potency and efficacy, further pointing to the allosteric route hypothesis. 100% efficacy was also recorded within the GluN1/GluN3A WT in presence of 100  $\mu\text{M}$  glycine and 200 nM CGP (not shown). We did not proceed with further tests on this compound because we were informed that a publication describing it is currently in revision as of 2022.

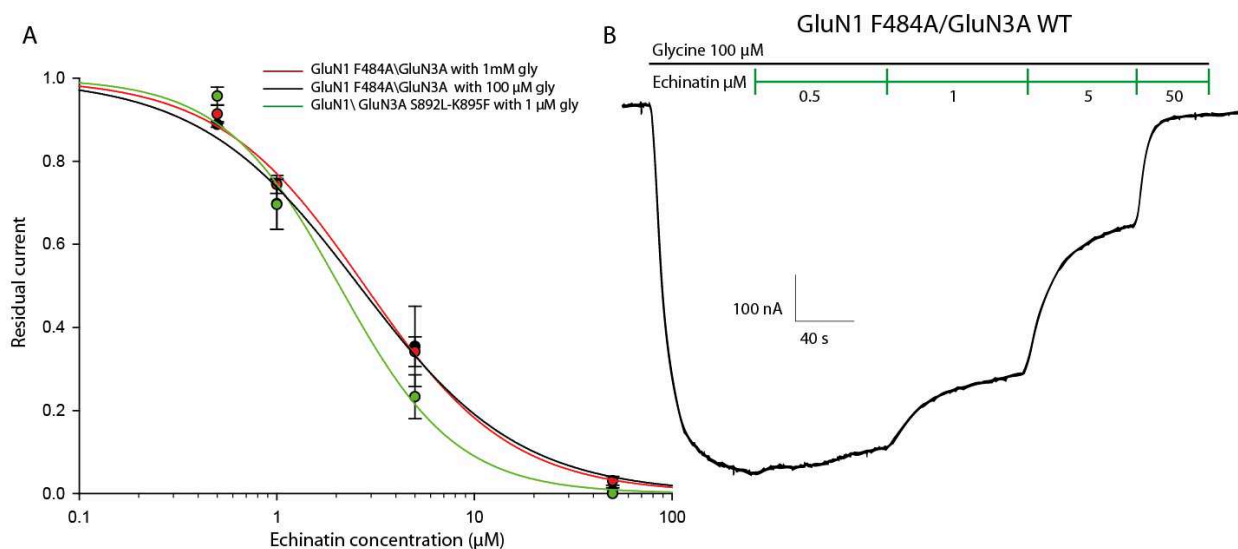


Figure 41 Echinatin inhibition dose responses in GluN1/GluN3A.

Panel A, dose response of echinatin for both GluN1 F484A/GluN3A WT (red and black lines with 1mM and 100  $\mu\text{M}$  glycine respectively) and for GluN1/ GluN3A S892L-K895F with 1  $\mu\text{M}$  glycine.  $\text{IC}_{50}$  for echinatin was estimated to be of  $2.78 \pm 0.01 \mu\text{M}$  ( $N=5$ ) and  $2.61 \pm 0.01$  ( $N=3$ ) for GluN1 F484A/GluN3A WT at 100  $\mu\text{M}$  and 1 mM glycine respectively. For GluN1/GluN3A S892L-K895F  $\text{IC}_{50}$  was estimated to  $2.07 \pm 0.01 \mu\text{M}$  ( $N=4$ ). Panel B, example dose response trace for GluN1 F484A/GluN3A WT in the presence of 100  $\mu\text{M}$  glycine.

## 6.4 Assessing channel open probability of GluN1/GluN3A receptors

When evaluating new ways to estimate GluN1/GluN3A open probability (PO) (see 4.2 Single channel properties and open probability), we decided to try an approach that has already been successful in past publications of the lab on GluN2 containing NMDARs (Gielen *et al.*, 2009) It has been shown to be possible to force open the pore GluN2 containing receptors by the covalent fixation of MTSEA (2-aminoethylmethanethiosulphonatehydrobromide) on an artificially introduced cysteine within the ion channel. The most efficient position to mutate in cysteine is the Alanine at position 7 of the SYTANLAAF motif in the M3 TMD helix. Thus, application of MTSEA on this cysteine pore mutant renders possible to reach the receptor maximal activation. Compared to the current of activation by agonist alone, the extent of MTSEA potentiation on NMDAR currents is then inversely related to the channel Po. The current limitation of this approach is that we add mutant in the pore that could also directly perturb the transduction mechanism of the receptor. However it worked fine for relative comparison of PO between non-pore mutants and chimeras (Gielen *et al.*, 2009).

We decided to evaluate if this approach can be employed on GluN1/GluN3A receptors and we mutated the homologous positions GluN3A A765C and GluN1 A652C and tested them individually (co-injected with the corresponding WT partner subunit). These constructs were expressing well in CGP and were indeed potentiated by MTSEA applications (Figure 42 panels A, B). We could then measure average MTSEA potentiation of  $16.4 \pm 2.9$ -fold for the mutant GluN1 A652C/GluN3A and of  $4.4 \pm 1.4$ -fold for GluN1/GluN3A A765Cs in the presence of 200 nM CGP and 100  $\mu$ M glycine (Figure 42). When tested at sub-saturating CGP concentration (50nM, (Grand *et al.*, 2018)) similar potentiations were measured ( $10.5 \pm 1.8$  and  $3.4 \pm 0.6$  respectively). **These potentiations thus represent a promising way to measure relative open probability of the GluN3A containing receptors in the presence of glycine and CGP.** It is interesting to note that GluN1 mutated pore gives a stronger potentiation than the GluN3A homologous position, pointing to asymmetrical roles of the M3 of the different subunits in receptor channel opening mechanism.

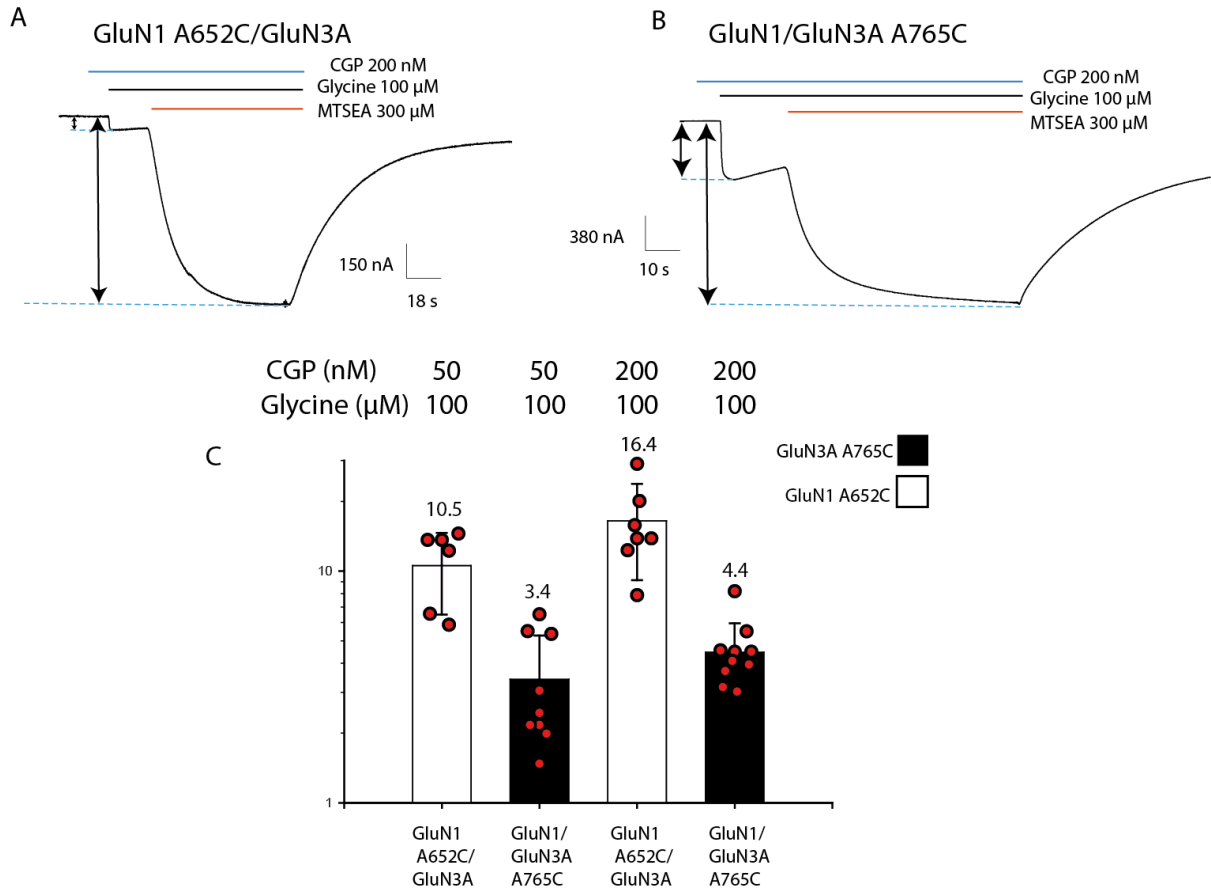


Figure 42 MTSEA activity on GluN1 and GluN3A pore mutants.

Panel A, example trace from GluN1 A652C/GluN3A WT with CGP 200 nM, glycine 100 μM, and MTSEA 300 μM. Panel B, example trace from GluN1 WT/GluN3A A765C with CGP 200 nM, glycine 100 μM, and MTSEA 300 μM. Panel C, histogram summarizing mean values obtained for individual pore mutants at two different CGP concentrations: 50 and 200 nM CGP. GluN1 A652C/GluN3A WT and GluN1 WT/GluN3A A765C are represented in white and black respectively.

#### 6.4.1 Control experiments of MTSEA treatment on GluN1/GluN3A receptors

We tested some controls to exclude non-specific MTSEA effect on GluN1/GluN3A receptors : **1)** We tested if MTSEA alone can open WT GluN1/GluN3A receptors by itself without glycine and CGP but it does not seem to be able to activate all receptors (N=3) (only barely detectable activation, that is observed probably linked to glycine leftovers in the recording solution - Figure 43 Panel B). We obtained the same results when applying glycine + MTSEA without CGP (not shown), indicating MTSEA has no effect by itself on WT receptor activation. **2)** We tested MTSEA activity on WT receptors without the



cysteine substitution in the pore. MTSEA did not display any quantifiable effect on GluN1/GluN3A receptors, indicating that the cysteine mutant is needed for MTSEA to open the pore (N=4) (Figure 43 Panel A).

#### **6.4.2 Behavior of MTSEA cross-linked receptors**

Interestingly we noticed that the activation of GluN1/GluN3A receptors mutant (with one cysteine in the pore) by MTSEA in full activation condition can be well washed after agonist removal (Figure 43 Panel B). This surprising finding differs compared to the non-washable constitutive activation of GluN2 containing NMDARs by MTSEA (Figure 43 Panel C). However, when looking at the new receptor resting potential baseline after MTSEA application, it appears that the MTSEA effect could not be fully washed, as we measured a 15% remaining constitutive current.

This behavior probably reflects several features. First, the pore of GluN1/GluN3A assemblies might assume a different conformation than GluN1/GluN2 assemblies, trapping differently the MTSEA molecule. Possibly, MTSEA bound-GluN2 receptors might be more stable than in GluN3s, locked in a low energy state. Furthermore, the remaining constitutive activation that we observe in GluN1/GluN3A receptors post-MTSEA treatment could be a result of tonic activation, as 100  $\mu$ M pentamidine application on the constitutive steady state current was found to inhibit the receptors baseline (not shown). Tail currents appear following washout of glycine applications post MTSEA treatment (not shown), another indication that GluN3A affinity for glycine has been increased after MTSEA application (Grand *et al.*, 2018). Therefore, receptors may display tonic activation with ambient glycine in the recording chamber. A previous study employed MTSEA to study GluN3A gating properties, but not PO, and in the absence of CGP (Wada *et al.*, 2006). In that study, the authors concluded that cysteine substitutions in the M3 region affect permanently gating kinetics, and pointed to an asymmetrical role of the M3s of GluN1 and GluN3A in the receptor gating.

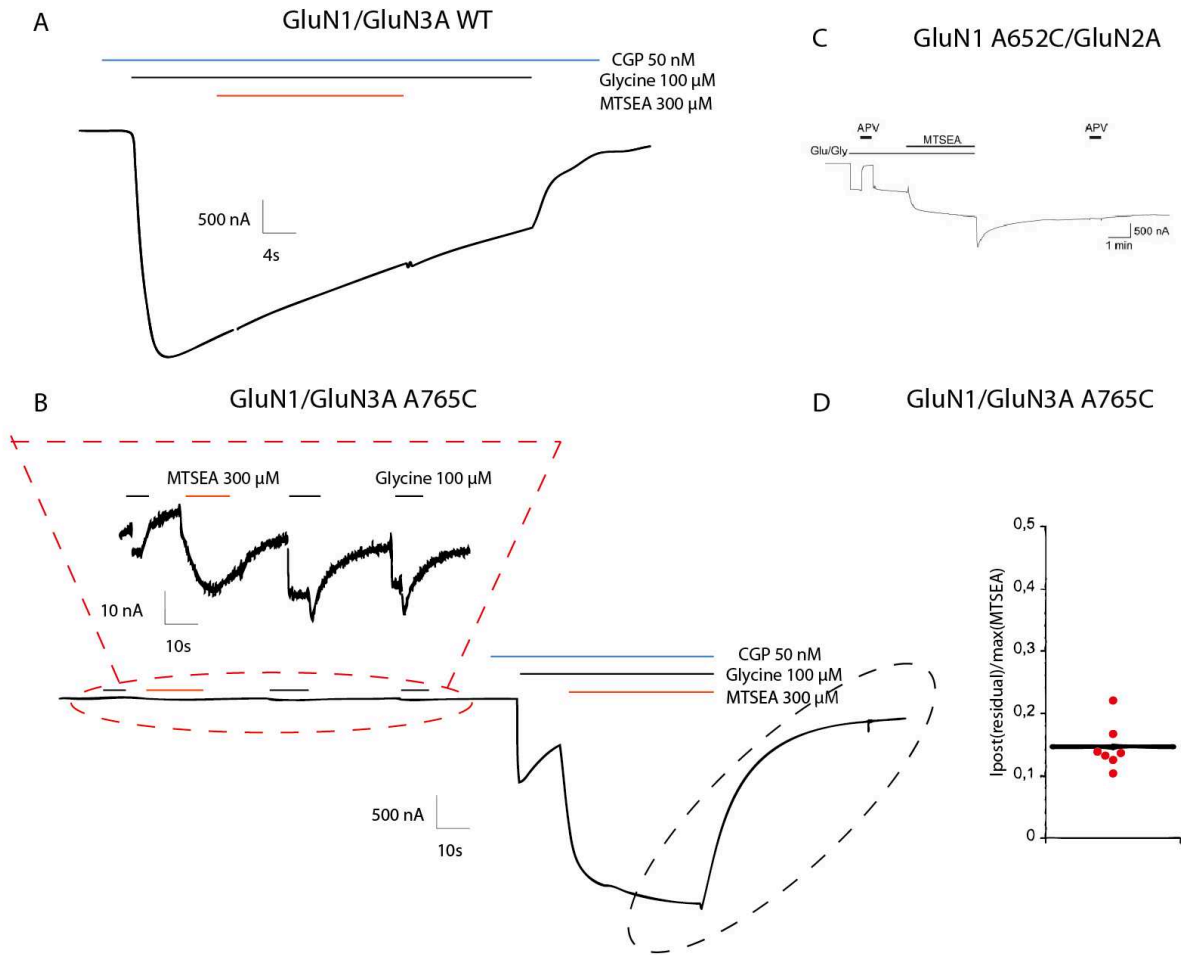


Figure 43 Control experiments for MTSEA treatment.

Panel A, MTSEA displays no effect in GluN1/GluN3A WT receptors in the presence of 100  $\mu$ M glycine +200 nM CGP ( $N=4$ ). Panel B, application of MTSEA alone is not sufficient to shift all receptors into a covalent open state. Red dotted zoomed section, a magnification of the individual applications of MTSEA and glycine in GluN1 WT/GluN3A A765C, before achieving the full protocol of receptors activation with CGP+ glycine and 300  $\mu$ M MTSEA application. The black dotted section highlights how removal of the agonist and MTSEA causes receptors to go back to a steady state close to baseline. Panel C, a trace insert taken from (Yuan et al., 2005) which shows how conventional GluN2 receptors remain constitutively open even after MTSEA and agonist removal. Panel D, a quantification of GluN1/GluN3A A765C constitutive activity after MTSEA and agonist removal, showing about 15% tonic current remaining normalized to the maximal peak current obtained with MTSEA.

We were interested in trying to understand how different availabilities of glycine correlate to changes in overall GluN3A receptors POs, and if these levels influence the receptor gating kinetics. We would expect that with GluN1 bound to CGP, higher concentrations of glycine available for GluN3A would have higher baseline activity in comparison to lower concentrations of glycine, but (Wada *et al.*, 2006)

indicated that the M3 of GluN3A does not undergo extensive molecular rearrangement during gating. We decided to test different glycine concentrations for the cysteine mutant GluN1/GluN3A A765C in presence of CGP 200 nM and MTSEA 300  $\mu$ M to determine if different concentrations of glycine correlate with different MTSEA potentiations (Figure 44 Panel A). We observed that when decreasing concentrations of glycine, the MTSEA-induced potentiations were indeed becoming much larger indicating an inverse correlation. In other words, receptors perfused with non-saturating glycine concentrations display lower POs in comparison to saturating concentrations in presence of CGP. From these observations we could draw a dose response on the receptor PO normalized to the highest POs recorded with the highest glycine concentrations and obtained an estimated  $EC_{50}$  for glycine at  $31 \pm 1.07$   $\mu$ M (Figure 44 Panel B). This  $EC_{50}$  is close from the  $EC_{50}$  for glycine for the GluN1/GluN3A WT in the presence of 200 nM ( $EC_{50}$   $45.98 \pm 1.77$  – in manuscript chapter 3.3). We also calculated with the same methodology an  $EC_{50}$  for glycine for GluN1 A652C/GluN3A (not shown), estimated at  $19.2 \pm 0.17$   $\mu$ M, a value that is close to the value obtained for the GluN3A pore mutant. From the same recordings we could also calculate the Tau on of MTSEA activation for the different glycine concentrations (Figure 44 Panel C). We found that these Taus follow the same trend we observed for the glycine potentiations, with lower glycine concentrations having slower kinetics of activations (higher tau).

Therefore, we observe that lower glycine concentrations correlate with lower POs and slower gating of MTSEA activations are inversely correlated (Figure 8 Panel D), both for the GluN1 pore mutant and the GluN3A pore mutant. The authors of (Wada *et al.*, 2006) pointed to an asymmetrical role of the M3s of GluN1 and GluN3A in gating of the receptor, suggesting that the role of the GluN3A subunit in is to modulate channel properties rather than to gate transduction in response to agonist binding at micromolar concentrations. In our hands, in the presence of CGP we found that agonist levels affect both kinetic of activation and extent of baseline activity of both GluN1 and GluN3A M3 modified receptors.

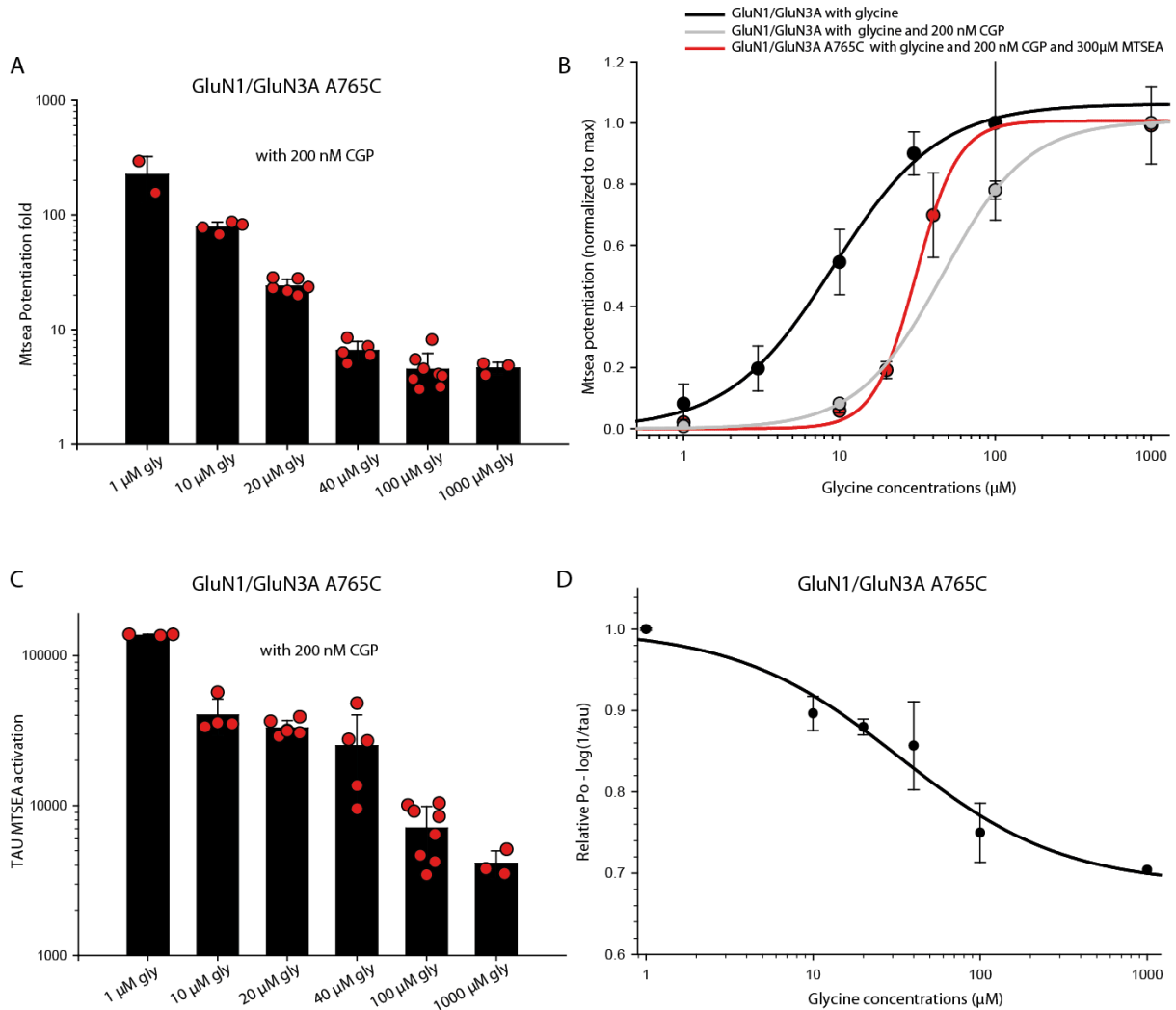


Figure 44 Characterization of GluN1 WT/GluN3A A765C.

Panel A, potentiation fold obtained with different concentrations of glycine in the presence of 200 nM CGP and 300 μM MTSEA. Since each concentration causes a permanent change in receptor properties, each dot represents different individual cells tested at different concentrations. Panel B, Dose response obtained from Panel A and compared to GluN1/GluN3A WT DRs. In red, glycine DR obtained by treating GluN1/GluN3A A765C receptors with glycine 100 μM+ 200 nM CGP+ 300 μM MTSEA and normalized to maximal PO ( $EC_{50}$   $31 \pm 1.07$  μM glycine) In black and in grey, DRs of the GluN1/GluN3A WT with glycine only and glycine +50 nM CGP respectively ( $EC_{50}$ s  $8.14 \pm 0.58$  (N=5) and  $45.98 \pm 1.77$  (N=5)) respectively. Panel C, Tau values of MTSEA induced potentiation calculated with the standard exponential formula of Clampfit 10.7 for different concentrations of glycine with 200 nM CGP and 300 μM MTSEA. Panel D, plotted tau values of MTSEA potentiation as  $\log(1/\tau)$  show how increasing concentrations of glycine increase the speed of receptors gating.

In conclusion, we showed that we can use the MTSEA methodology to measure the relative Po of GluN1/GluN3A receptors. The method appears robust and valid although its requires to use one pore

cysteine mutant either on the GluN1 or the GluN3A subunit. Interestingly, the two mutants differ in the amplitude of MTSEA potentiation: the amplitude being much higher in GluN1 than in GluN3A. This means that we have the choice to use either of them in a project. In general, in our hand the relative Po measurements give the same trend with one or the other. However, we have to keep in mind that a relative PO measured with one of the cysteine mutants cannot be directly compared to the relative Po measured with the cysteine mutant on the other subunit, because they correspond to two different and independent measurements (even if the trend should be similar). For a full project of relative Po measurements, we thus advise to make of the measurement using only one of the cysteine constructs. In principle LOF mutant relative PO may be more accurately measured with the GluN3A mutant (because initial current is higher with this current) while GOF mutant PO will be more accurately measured with GluN1 mutant (because the room for potentiation is larger). But of course, measuring relative Po with one AND the other will make a double check of the relative PO measurement that may be useful. In Figure 45 and Table 7 we summarize all mutants that we tested throughout the project to give a comprehensive overview showing how different mutants in different regions of the receptor can increase or decrease receptor PO. The MTSEA methodology was successfully used to characterize several interesting GLuN1/GluN3A mutants that will be described in the manuscript (3.3) and in the following sections (3.4 and 3.5).

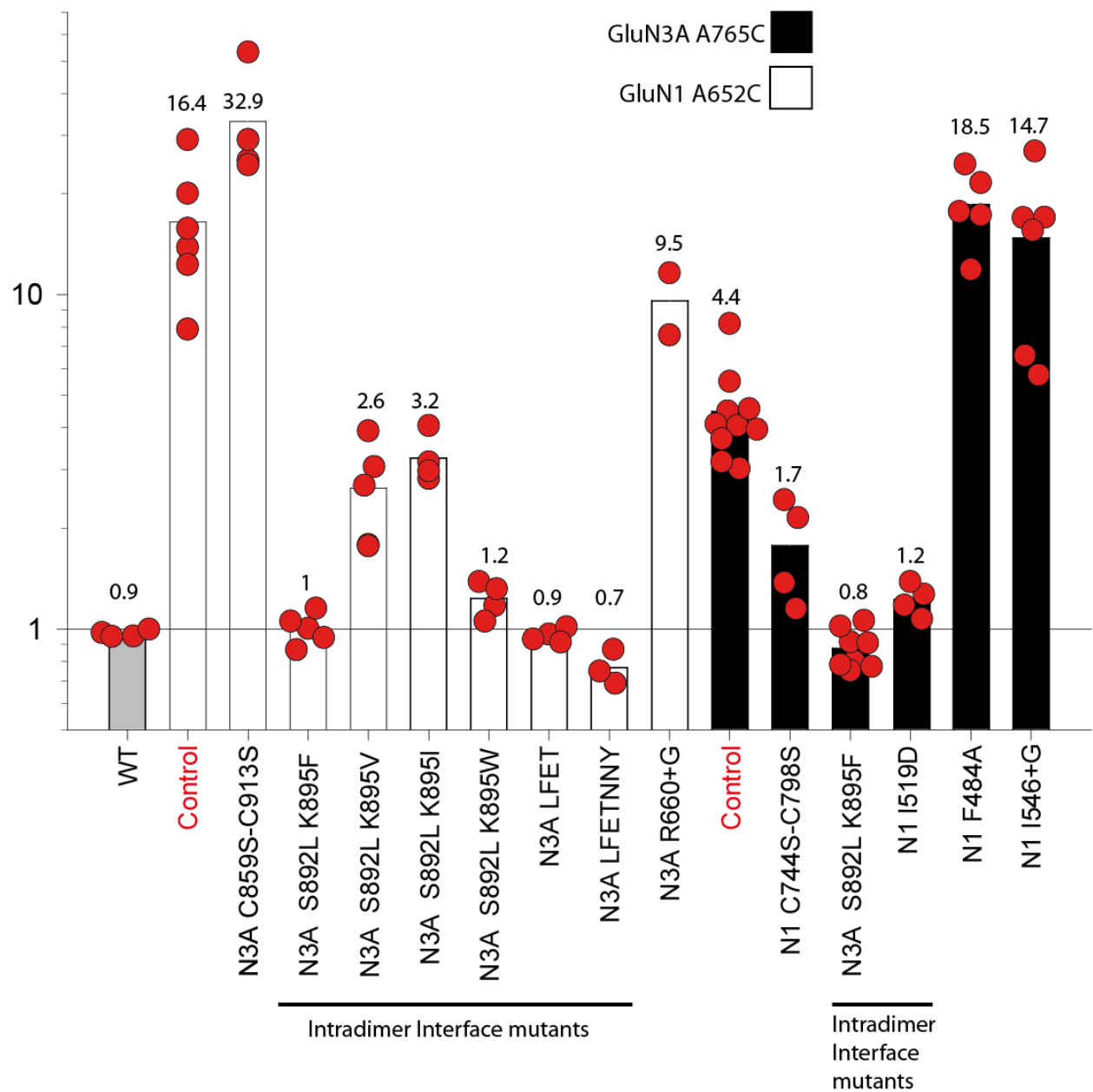


Figure 45 Summary of mutants tested with MTSEA.

Clustered in white are the mutants tested in combination with GluN1 A652C. Clustered in black are the mutants tested in combination with GluN3A A765C. Mutants pertaining to the Intradimer Interface, which is focused within the manuscript, are highlighted. All mutants were tested with 200 nM CGP pre-incubation and 100  $\mu$ M glycine

Column	Size	Mean	Std Dev	Std. Error	C.I. of Mean
WT ( No pore mutant)	4	0.968	0.0232	0.0116	0.037
N1 652C (control)	6	16.478	7.342	2.997	7.705
N3A C859S-C913S	4	32.942	13.62	6.81	21.672
N3A S892L K895F	5	1.004	0.109	0.0487	0.135
N3A S892L K895V	5	2.641	0.902	0.403	1.12
N3A S892L K895I	4	3.248	0.554	0.277	0.882
N3A S892L K895W	4	1.232	0.147	0.0736	0.234
N3A LFET	4	0.956	0.0441	0.022	0.0701
N3A LFETNNY	3	0.768	0.0926	0.0535	0.23
N3A R660+G	2	9.586	2.838	2.007	25.503
N3A A765C (control)	10	4.469	1.485	0.47	1.062
N1 C744S-C798S	4	1.776	0.613	0.307	0.975
N3A 892 895LF	8	0.876	0.119	0.0419	0.0991
N1 484A	5	18.597	4.792	2.143	5.95
N1 519D	4	1.225	0.134	0.067	0.213
N1 I546+G	6	14.789	7.806	3.187	8.192
N1 484A no cgp	8	27.111	8.255	2.919	6.901

Table 7 MTSEA mutants descriptive statistics.

In grey are shown all mutants with the cysteine insertion in GluN1. In blue are shown all mutants with the insertion in GluN3A

## 6.5 State-dependency of D-serine action

Contrary to the full agonist glycine, D-serine has been described as a partial agonist of GluN1/GluN3A receptors (Chatterton *et al.*, 2002; Awobuluyi *et al.*, 2007). Since CGP is now commonly used with glycine to reveal and work with GluN1/GluN3A receptors currents, we realized that no tests have been done on CGP interaction with D-serine. It has previously been observed a state dependency of CGP and glycine actions. Indeed, if GluN1 is already bound to glycine, CGP application activates the receptor extremely slowly. A pre-incubation of CGP is a necessary step for the full activation of the receptor (Grand *et al.*, 2018). We wondered if this was the same behavior for D-serine, since GluN1 affinity for D-serine is lower than the one for glycine and could be more easily displaced by CGP. Therefore, we tested 1) to pre-incubate CGP 200 nM before applying the agonist at 500  $\mu$ M (saturating concentrations), 2) to try the opposite, applying D-serine and only afterwards CGP to see if CGP was able to displace the bound D-serine. Like it was observed for glycine, CGP preincubation proved to be a necessary step to achieve the full receptor activation, with CGP being unable to displace D-Serine (Figure 46). Therefore, the modalities

of action of CGP appears to be similar in the presence of glycine and d-serine. This point is important in the context of physiological conditions of CGP usage since d-serine is present in sub-regions of the CNS and it is currently unclear which endogenous ligand (glycine or d-serine) predominantly activates GluN1/GluN3A in native conditions.

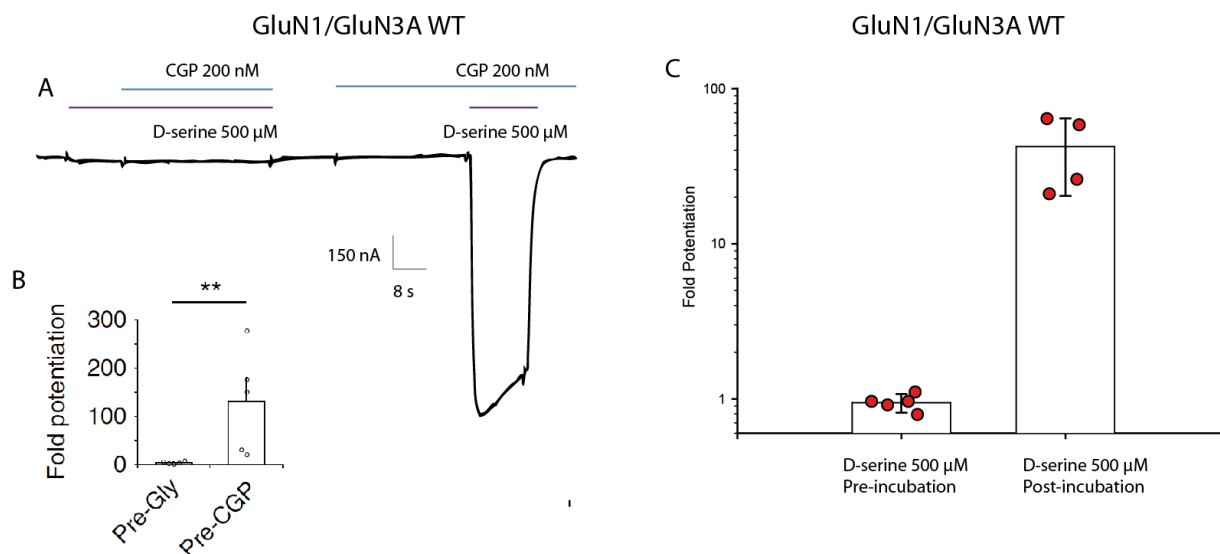


Figure 46 D-serine state dependency.

Panel A example trace from GluN1 /GluN3A WT with different orders of application of D-serine 500 μM, and CGP 200 nM. Panel B inset from (Grand et al., 2018) showing state dependence between glycine and CGP. Panel C histogram showing quantification of differences in fold potentiation between preincubation and non preincubation of CGP on D-serine application.

## 6.6 Zinc modulation

Zinc is a divalent cation that is endogenously packed into some synaptic vesicles in many regions of the CNS (Paoletti, A. M. Vergnano, *et al.*, 2009). It is well established that zinc inhibits both native and recombinant GluN2 containing receptors, albeit with different affinities depending on the subunit (Paoletti *et al.*, 1997a). Three papers (Cummings and Popescu, 2016; Cummings *et al.*, 2017; Madry and Betz, n.d.) surprisingly highlighted a potentiating zinc effect on GluN3A, while one reported an inhibitory effect (Wada *et al.*, 2006). Even more surprisingly, it was reported that the zinc effect is NTD-independent (Madry *et al.*, 2007) but requires a functional GluN1 binding site, since the potentiation had been shown to not be present when the mutant GluN1 F484A was coexpressed with GluN3A. Furthermore, it was hypothesized that zinc could activate GluN3A receptors even in the absence of GluN3A agonists such as



glycine, being an agonist per se. Since all these studies have been made before the discovery of CGP as a major tool to reveal and study GluN1/GluN3A receptor activity, we decided to reinvestigate the effect of zinc on GluN1/GluN3A receptors.

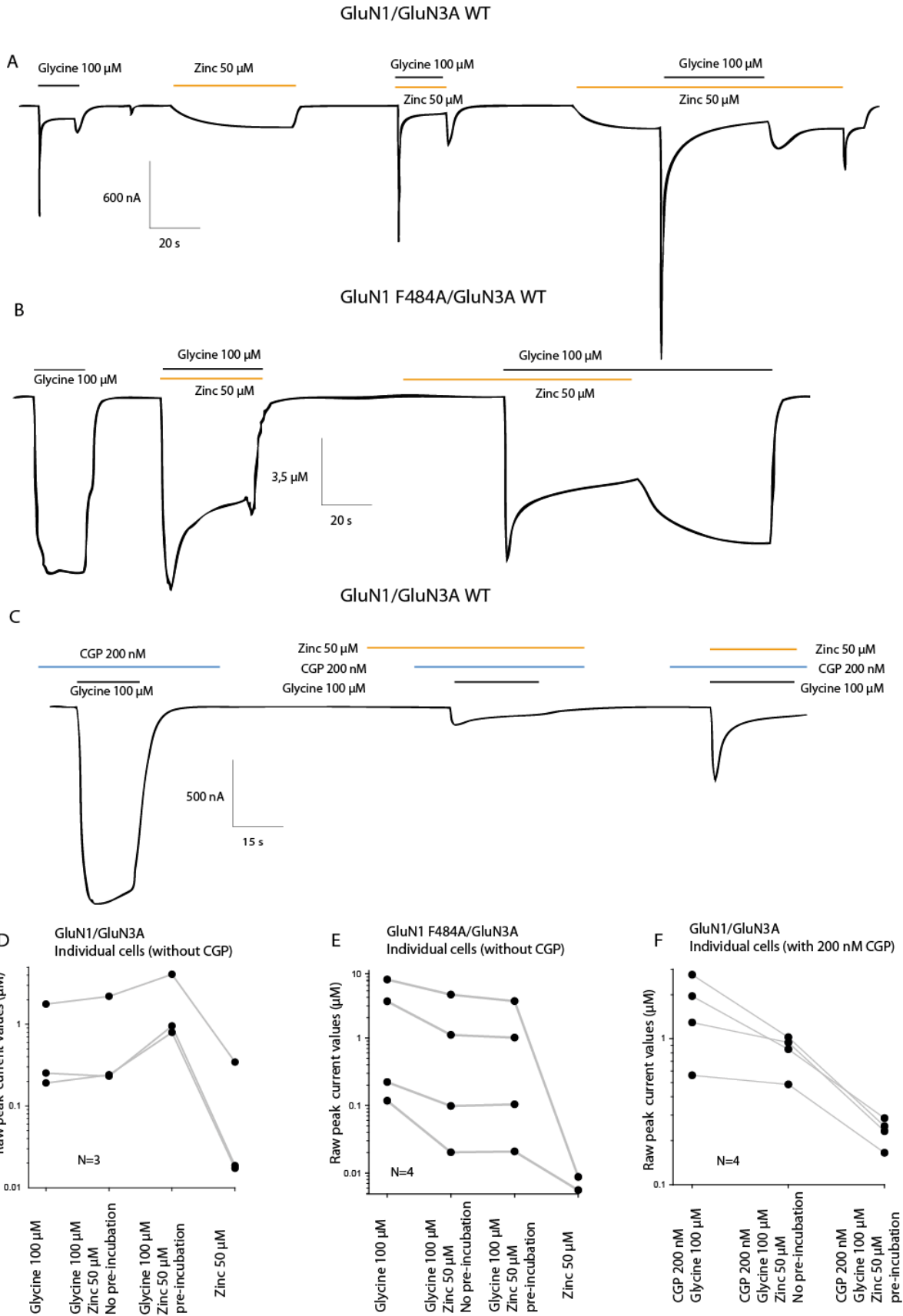


*Figure 47 Zinc effect on GluN1/GluN3A receptors.*

*Panel A, example trace from GluN1 /GluN3A WT with glycine 100  $\mu$ M, and Zinc 50  $\mu$ M. Different orders of drug applications are attempted, and a complex state dependence can be observed where zinc acts mostly as a potentiator. Panel B , example trace for Zinc effect in GluN1 F484A/GluN3A receptors with glycine 100  $\mu$ M, and zinc 50  $\mu$ M. within this mutant, zinc seems to act mostly as an inhibitor. Panel C, example trace from GluN1 /GluN3A WT with glycine 100  $\mu$ M, CGP 200 nM and Zinc 50  $\mu$ M. In the presence of CGP, zinc acts mostly as an inhibitor. Panels D,E and F at bottom of the page summarizing changes in raw current levels for different state dependences of zinc applications. Each line connecting dots represents an individual cell. Each plot refers to a different construct tested in Panels A,B and C.*

We prepared zinc solution at 50  $\mu$ M like it had been done in previous literature (Cummings *et al.*, 2017; Madry and Betz, n.d.) and buffered them to pH 7.3. Initially, we tested zinc on the GluN1/GluN3A WT receptor in the presence of glycine only. We found that, as described in the literature, zinc was able to produce receptor activation by its own, but with a slow kinetic and a modest peak current amplitude. Zinc did not seem to change current amplitude to great extent when perfused at the same time as the agonist, but potentiated currents when pre-incubated before glycine application (Figure 47 Panel A and D). Therefore, although differently in terms of effect sizes, we have been able to reproduce some of the zinc potentiating results that have been published before (Madry and Betz, n.d.).

Afterwards, we tested zinc activity on the constructs GluN1 F484A, which had been described as not showing potentiation by zinc in the literature. We tested the same conditions as we did for the GluN1/GluN3A WT, and we were able to produce a robust zinc-induced inhibition of glycinergic currents both with and without pre-incubation before glycine application. In addition, 50  $\mu$ M zinc alone could only produce minuscule currents (Figure 47 Panels B and E). The inhibition we just described has never been characterized before, as (Madry and Betz, n.d.) did not show tests with glycine and zinc at the same time on GluN1 F484A. Afterwards, we tested GluN1/GluN3A WT receptors in the presence of glycine and CGP. CGP, like the mutant F484A, prevents glycine binding to GluN1, blocking the clamshell from entering the closed conformation. Zinc application produced robust inhibitions of CGP+ glycine elicited currents, that were even smaller when zinc was preincubated before the CGP application (Figure 47 Panels C and F), confirming the inhibitory nature of zinc in GluN1-antagonist bound conformations.

We continued these preliminary tests by testing assaying the zinc effect on some mutants that we had available in the lab. First, we tested it on the cysless mutants GluN1 C744S/GluN3A C913S recently published in (Grand *et al.*, 2018), which have an increased EC<sub>50</sub> for glycine, and display positive steady state currents upon application of saturating agonist concentrations. We attempted 50  $\mu$ M zinc application and we observed a more positive steady state than the baseline, without a peak current

appearing before the steady state was stabilized (Figure 48 Panel A). Furthermore, pre-incubation of 50  $\mu\text{M}$  zinc seemed to block the normal glycine-induced activation, pointing to a possible inhibitory state induced by zinc. Finally, we also attempted testing the mutant GluN1/GluN3A S892L-K895F-H904E-K909T in the intradimer Interface that greatly shifts the GluN3A receptor  $\text{EC}_{50}$  to the left and supposedly modifies interactions between the two subunits at the LBD level (see 8.3 Article: The LBD Dimer Interface Tunes Activation of Glycine-Gated GluN1/GluN3A Receptors) (Figure 57 Panel A). Also within this mutant Zinc acted as an inhibitor, and pre-incubation of it completely inhibited the square 1  $\mu\text{M}$  glycine induced currents.

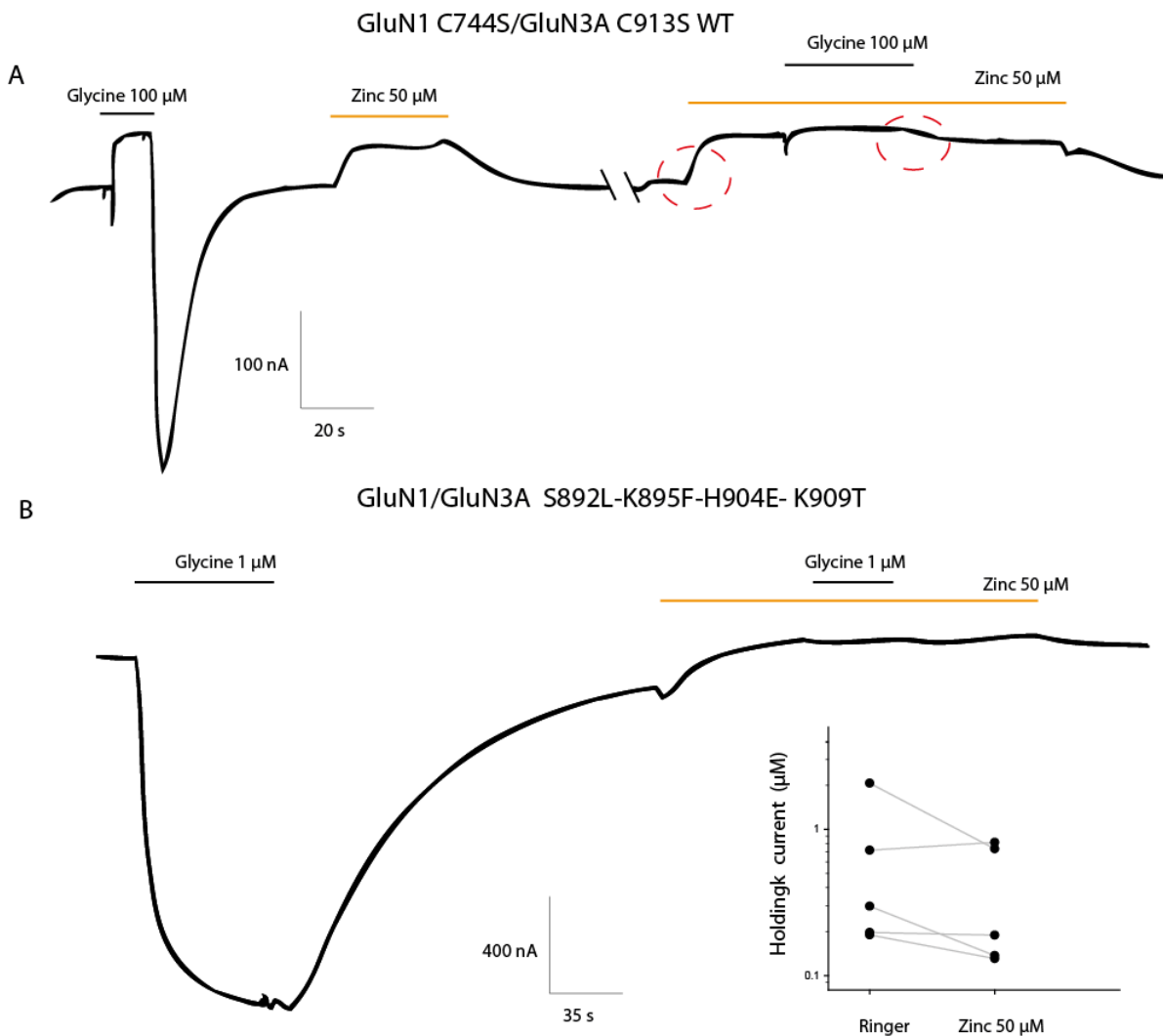


Figure 48 Zinc effect in mutants.

*Panel A, example trace from GluN1 C744S/GluN3A C913S with glycine 100  $\mu$ M, and Zinc 50  $\mu$ M. Different orders of drug applications are attempted to test state dependencies. It can be observed that zinc depolarizes the holding potential to a positive steady state. Panel B, example trace for zinc effect in GluN1/GluN3A S892L-K895F-H904E- K909T receptors with glycine 100  $\mu$ M, and zinc 50  $\mu$ M. Within this mutant, zinc acts mostly as an inhibitor blocking glycine-induced receptor gating. The inset in Panel B shows how raw current levels in  $\mu$ M, where zinc application has an inhibitory effect on these recombinant receptors.*

Therefore, it seems that zinc is able to produce a triple effect 1) A potentiation of glycinergic currents on WT GluN1/GluN3A receptors when pre-incubated before agonist application. 2) A modest receptor activation with slow kinetics on WT GluN1/GluN3A receptors. 3) A strong receptor inhibition (or desensitization?) when the GluN1 LBD site is mutated or bound to CGP. Inhibition was also observed in mutants with an enhanced glycine sensitivity. So far, a comprehensive mechanism describing the zinc binding site and modalities of action in GluN1/GluN3A receptors is missing. In these preliminary results we show that zinc can act both as an activator and inhibitor depending on the constructs tested, and depending on the conformation of the receptor at the time of zinc application. Further tests will need to test lower concentrations of zinc with a metal chelator like tricine to perform a DR of this compound, and to evaluate the affinities if more binding sites are present. Further studies will also need to employ mutated constructs to try to identify the zinc binding sites.



## **7: Investigating GluN1/GluN3A receptor molecular mechanisms: stabilizing conformational states**

The core of my PhD project aims at investigating the molecular mechanisms and ideally finding the structural correlates of the gating steps of GluN1/GluN3A NMDARs function. Previously our lab and others demonstrated that the extracellular domain of GluN2 containing NMDARs (composed by 8 closely packed domains) governs the gating properties of the receptor through a combination of open-closure of the individual domains and coordinated motion between those domains, involving different inter-domain interfaces and linkers (Tajima *et al.*, 2016; Esmenjaud *et al.*, 2018; Jalali-Yazdi *et al.*, 2018; Tian *et al.*, 2021). In GluN3A, the role and function of individual subunit domains and intersubunit interfaces remains unclear or completely unknown ((Cummings and Popescu, 2016; Mesic *et al.*, 2016; Crawley *et al.*, 2022)). We decided to investigate in this direction with several different approaches already used in many structure/function studies of ion channels. Specifically, we attempted to 1) genetically delete some parts of the receptors to test their importance and role, to 2) trap specific conformations by crosslink through disulphide bridge formation, 3) to perform targeted mutagenesis on selected residues with the aim of changing the biochemical properties of certain receptor regions, and finally 4) by attempting to photocrosslink the receptors with UV light by employing unnatural amino acids (UAAs). Among these approaches the two last (3 & 4) are described in chapter 3, while the two first are described here.

### **7.1 Building a working 3D model of GluN1/GluN3A receptor**

Our work is based on a 3D model of full-length GluN1/GluN3A NMDAR in an inhibited state conformation that was based upon the ifenprodil allosterically inhibited GluN1/GluN2B receptor (PDB 4PE5) (Karakas and Furukawa, 2014) that was produced by homology using Modeller by Davis Stroebel (Eswar *et al.*, 2006), combined with the existing GluN3A LBD crystal structure bound to glycine(Yao *et al.*, 2008).

Since we do not have access of the full GluN3A protein structure, the modelization approach underlies making assumptions about the GluN1-GluN3A subunit arrangement and folding based on alignments made on protein sequence analogies that are predicted by the software. This represents a limitation on the precision we can employ when targeting interfaces, since we have to assume that the interface will form in GluN1/GluN3A complexes with the same stoichiometry as how they form in the GluN1/GluN2 counterparts. GluN2A and GluN2B entire protein sequence shares about 54% of residue

identity and 65% of residue homology (common evolutionary ancestry). Contrarily, GluN2A and GluN2B both share only 22% of residue identity with GluN3A whole subunits. When looking at the whole LBD and only at the residues present at the intradimer interface, the residue identity percentages are 82-94 % for GluN2A vs GluN2B respectively, and 37-51 % for GluN2A vs GluN3A respectively (unpublished data). Therefore, to some extent the identity of the dimerization interface is conserved between GluN2s and GluN3A. As a template structure, we decided to pick an inhibited conformation of GluN2B because it is thought that GluN3A might be in a conformation with low energetics in the closed channel state, as the receptor desensitizes very quickly and deeply. Therefore, we decided to pick a closed channel structure, with the ifenprodil inhibition possibly mimicking the desensitized state of GluN3A. Some interfaces required adapting, like the NTD-LBD interface, as there is a GluN3A specific LBD loop making steric clashes with the NTD. This region has been highlighted as very important for the gating of the receptor, as cross-linking the two modular domains makes the whole receptors almost silent (Esmenjaud *et al.*, 2018). Still, we think our model corresponds to the most reasonable approximation of what we know about the intradimer interface in NMDARs, and works as the best available tool at our disposal before a high-resolution structure will be available in the future.

## 7.2 Investigating the role of domains and loops

Our team and others have characterized many properties of GluN2-containing NMDARs and found many chimeras and mutants with interesting phenotypes in GluN2 containing NMDARs. We were first interested in defining the macroscopic role of the GluN3A domains NTD, LBD, CTD and specific loops of the receptors. The NTD is important in determining the PO of GluN2 containing NMDARs, and it has been found to deeply influence the deactivation kinetics, entry into high or low PO pre-gating energetic states, and allosteric modulation over the LBD and TMD among others (see 4.6 Allosteric modulation: focus on zinc, protons and ifenprodil, 4.7 A unified model of NMDAR gating)(Esmenjaud *et al.*, 2018; Hansen *et al.*, 2021; Tian *et al.*, 2021). For GluN3A, there is minimal information existing concerning the NTD role in gating of the receptor, except that deletion of it potentiates current sizes and reduces the potentiating effect of GluN1 specific antagonists on receptor activity (Mesic *et al.*, 2016). The LBD is physical binding site for the agonists, and its conformational rearrangements following clamshell closure upon agonist binding are the molecular trigger for the pore opening in NMDARs (see 3.3.1 LBD dimerization , 4.3 Kinetic scheme). When assembled with GluN3A, glycine binding GluN1 LBD has been indicated at the force causing auto-inhibition of the receptor. The CTD is also key in regulating receptor properties, its



interactions with regulatory proteins in the membrane and trafficking of the receptor. When assembled with GluN3A, the GluN1 CTD has been shown to affect expression and desensitization kinetics of the receptors (see 3.6 The C-terminal domain) (Cummings *et al.*, 2017). We thus attempted large scale deletions or engineering of chimeras of those domains to modify receptor function. A summary and mapping of the modifications attempted can be found in Figure 49.

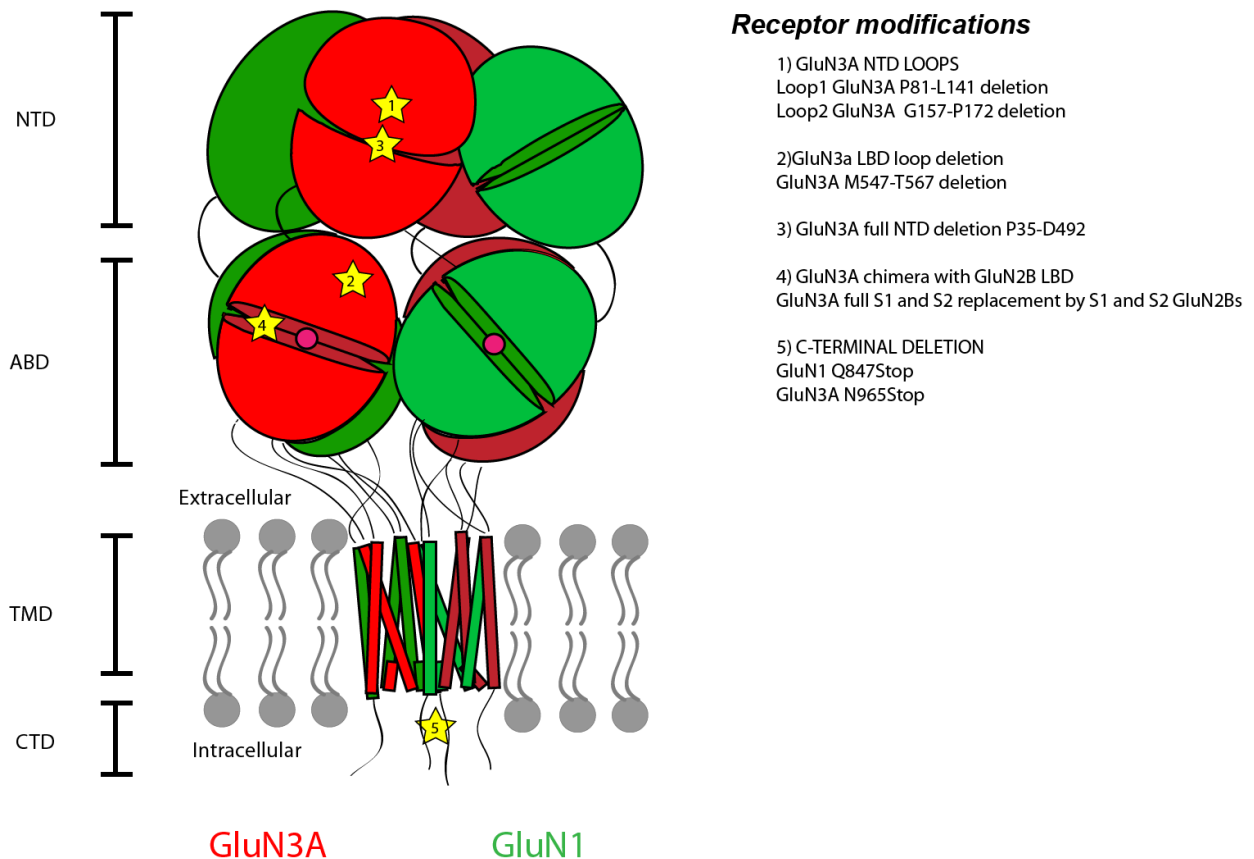


Figure 49 Major receptor deletions and modifications.

GluN1/GluN3A NMDAR cartoon with stars indicating regions where large modifications or deletions were attempted and grouped in 5 major groups: NTD loop deletions, , LBD loop deletions, full NTD deletions, GluN3A LBD replacement by GluN2B, and C-terminal deletions.

GluN3A receptors have 3 unique loops that are specific to this subunit and absent in other NMDAR: 2 on the NTD and 1 on the LBD. The function of these loops of the extracellular domain is yet unknown. In the NTD, the loop 1 (P81-L147) is a very large region sitting on top of the NTD, while the loop 2 is much smaller (G157-P172), while the loop in the LBD is about 20 residues long (M547-T567) (Figure 50 Panel A). Deletion of the loop 1 in the NTD and deletion of the LBD loop dramatically decreased

the raw current levels in CGP + glycine, probably because of a large drop in expression due to protein misfolding or default of assembly. Deletion of Loop 2 of the NTD did not seem to affect receptor expression or current levels, and we were even able to record glycinergic currents in the absence of CGP (not shown) (Figure 50 Panel B). However, we this mutant didn't change the current phenotype compared to GluN1/GluN3A WT.

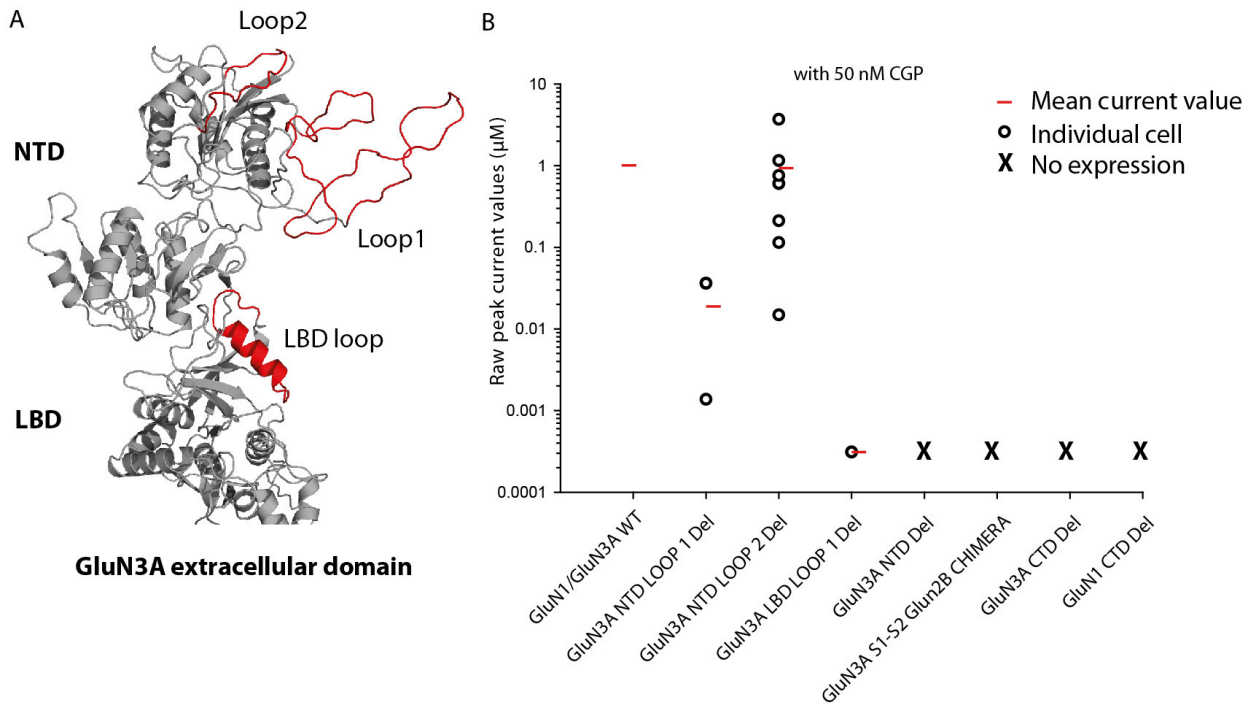


Figure 50 GluN3A deletions and reorganizations.

Panel A, structure of the upper extracellular region of GluN3A subunit obtained with Pymol. The cartoon is colored in grey, and in red are highlighted the positions of the GluN3A-specific loops, 2 in the NTD and one in the LBD. Panel B, a quantification of the individual sizes of currents recorded in the presence of 50 nM CGP from constructs with large deletions or modifications described in this section. For GluN1/GluN3A WT an average value of 1  $\mu\text{A}$  has been shown as mean current size to give a reference to compare to other mutants. X represent constructs that did not display electrical activity upon agonist application.

We then created a construct lacking the whole NTD of GluN3A, knowing this domain is critical for other NMDAR gating and pharmacology. We deleted the whole NTD of GluN3A basing ourselves on published  $\Delta\text{NTD}$  GluN3A construct (Skrenkova *et al.*, 2019; Madry and Betz, n.d.). In those papers, the authors successfully managed to create constructs that lacked the NTD and had modified properties than WT receptors, on one case affecting receptor expression levels at the membrane, and in the other case influencing current phenotype. However, in our hand, GluN3A  $\Delta\text{NTD}$  did not give any electrical activity,

neither when co-expressed with GluN1 WT or with a GluN1  $\Delta$ NTD. Although we sequenced again the whole construct, we could not determine why the construct was functionally silent.

We also attempted to produce a chimeric GluN3A-GluN2B receptor containing all the backbone of GRIN3A gene, but with a GluN2B LBD. To create this construct, we designed the S1 and S2 LBD fragments that we amplified by PCR, and hybridized them sequentially with a Gibson PCR kit to the GluN3A backbone. We validated the correct insertion of the GluN2B S1 and S2 fragments by sequencing and tried to test them with a combination of pharmacological approaches. Again, the construct was electrically silent and we could not draw any conclusions from it.

Finally, we tried to record currents from GluN1 and GluN3A constructs with the truncated C-terminal to investigate the role of these region. Recently, a paper produced a constructs that showed  $\Delta$  GluN3A CTD, but could successfully go to the membrane in HEK cells (Skrenkova *et al.*, 2019). Both constructs seemed to be silent and we could not record electrical activity from them. We also attempted to perform western blots on these constructs and would not see a band corresponding to GluN3A monomer (Not shown). However, since we were forced to pick random transformed oocytes (for which usually more than half do not express the protein of interest) for the immunoblots. We may thus have made WB on oocytes having no protein expression despite the truncated C-terminal may still expressed in some other cells. We reasoned on why many of these constructs could be not functional at the end of section 3.2

### **7.3 Cysteine scanning of interfaces**

Previously in the lab a successful strategy to study specific functional states of iGluRs has been to trap receptors into specific conformations (Gielen *et al.*, 2008; Esmenjaud *et al.*, 2018; Tian *et al.*, 2021). In particular, we showed it was possible to strengthen functionally important interfaces by introducing pairs of cysteine mutants in partner subunits so that they form stable crosslink. Indeed, if the cysteines are close enough in space and at the right angle ( $C\alpha$ - $C\alpha$  distance  $< 7 \text{ \AA}$ ) (Careaga and Falke, 1992), they can form a disulphure covalent bond restraining the conformational mobility of the targeted interface. Some recent published examples from the host laboratory of a successful implementation of this technique on NMDAR interfaces concerns the GluN1-GluN2B LBD Interdimer Interface regulating rolling motion and PO (Esmenjaud *et al.*, 2018) or the GluN1-GluN2A LBD Intradimer Interface mediating NTD allosteric

modulation and gating. In the GluN1/GluN3A context we tested crosslink at 6 different interfaces already described (Gielen *et al.*, 2008) and (Esmenjaud *et al.*, 2018) to be involved in GluN2 function : 1) LBD Intradimer Interface, 2) LBD Interdimer Interface 3) GluN1 NTD-LBD interface 4) LBD GluN1-NTD GluN3A interface, 5) AMPAR-like lower LBD interface, 6) Intradimer NTD Interface (Figure 51).

1) The Intradimer Interface has been described long time ago to be a critical structural element whose formation and rupture controls the gating cycle of AMPA receptors and most probably for all iGluRs (See 3.3.1 LBD dimerization , 4.5 Desensitization: AMPARs vs NMDARs and (Furukawa *et al.*, 2005)). In addition, it has been later identified in NMDARs (Esmenjaud *et al.*, 2018) as a major structural element which permits the coupling between the NTD and the LBD in GluN1/GluN2s. However, the dimer interface takes different functions in different iGluRs. 2) The Interdimer Interface is an interface located between the two dimers in the LBD which mediates the rolling motion in GluN1/GluN2Bs, a necessary step for the gating switch regulating channel opening depending on the conformation of the NTD layer. This Interface has been trapped in two distinct states, a superactive state (high PO) and an inhibited state (low PO), depending if the LBD has rolled or not. There is currently no information describing if this interface may exist in GluN1/GluN3A or not. We created homology mutants in GluN3A to the ones that were designed in (Esmenjaud *et al.*, 2018) to test if we could trap specific conformations also in GluN1/GluN3A. Two other interfaces that have been described in (Esmenjaud *et al.*, 2018) are the 3) GluN1 intrasubunit NTD-LBD interface and the 4) GluN1 LBD - GluN2B NTD interfaces. When constricted by disulfide bridges, each of these interfaces greatly reduces receptor electrical activity, while WT activity can be restored by applying reducing agents aimed at breaking these contacts. We decided to test both of these interfaces in GluN1/GluN3A too by mutating the homologous residues of GluN2B in GluN3A. Another interface that has been described in iGluRs, specifically in AMPARs, is the 5) lower lobe (domain 2) Intradimer Interface, which has been crosslinked (Armstrong *et al.*, 2006) to stabilize a low conductance desensitized state. We decided to test the homologous position in GluN1/GluN3A receptors. Finally, 6) crosslink of NTD Intrasubunit Interface has been described in GluN1/GluN3A receptors by introducing a cysteine mutant in the position GluN1/GluN3A R319C with effects such as decrease in the glycine induced maximal current with a marked increase in GluN1 antagonist-mediated current potentiation. We wanted to test this mutant in our hands to deepen our understanding of the NTD in the GluN1/GluN3A receptors. For all these couple of cysteine mutants, all the mutagenesis on GluN1 was redone anew to have the mutants on the splice variant GluN1-4A, since it has been shown to

co-assemble better with GluN3A with more protein levels at the cell membrane (Smothers and Woodward, 2009).

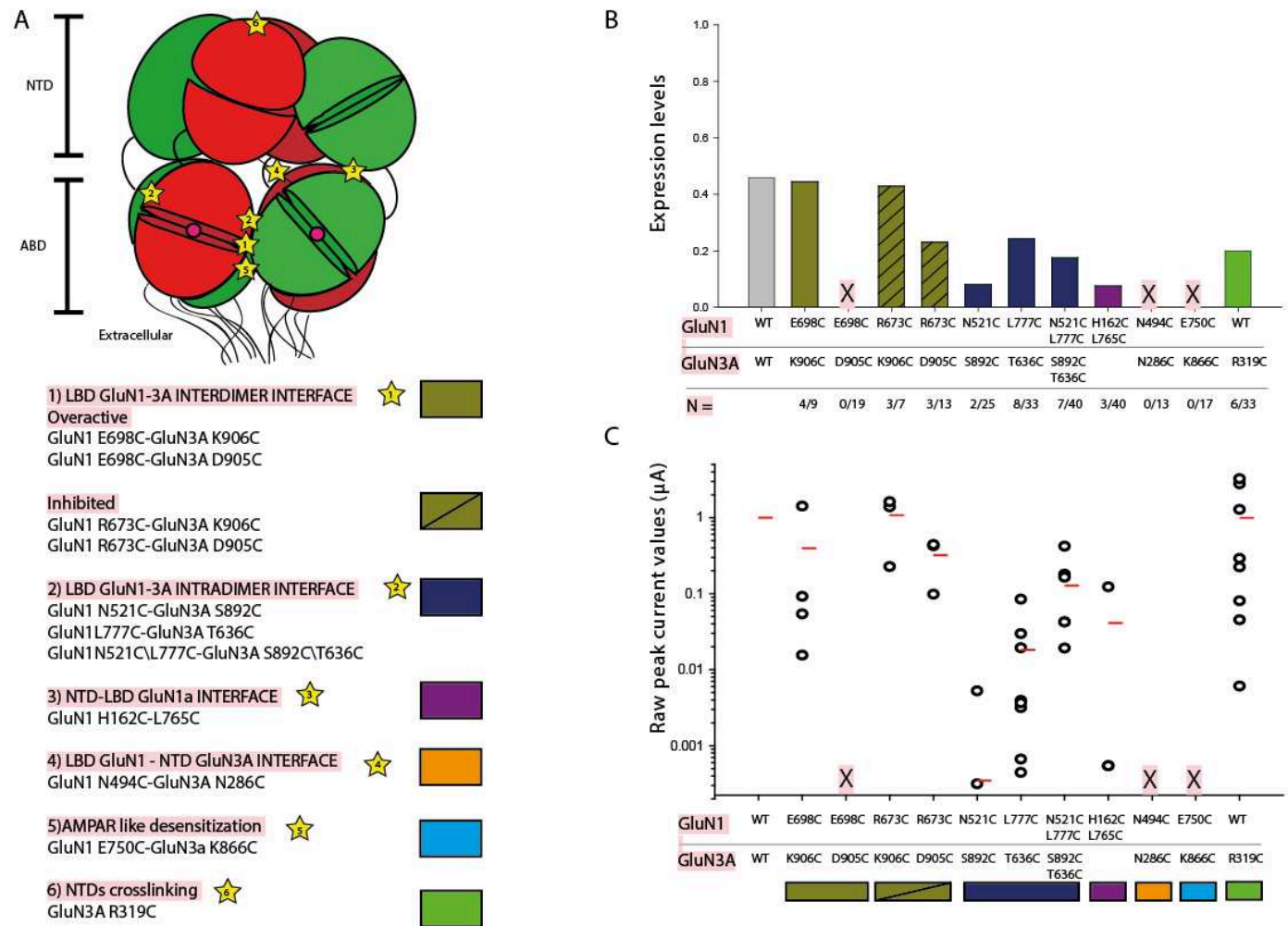


Figure 51 Cysteine bridges interfaces.

Panel A, GluN1/GluN3A NMDAR cartoon with stars indicating regions where Interface trapping was attempted and grouped in in 6 thematic regions: 1) Interdimer Interface, 2) Intradimer Interface 3) GluN1 NTD-LBD interface 4) GluN1 LBD-GluN3A NTD interface, 5) AMPAR-like lower LBD interface, 6) GluN3A Intrsubunit NTD Interface. Each Interface has been color coded and indicated in the structure above with a star and a number. Panel B, histogram indicating averaged expression levels indicated as cells displaying electrical activity when receiving co-application of glycine 100  $\mu$ M and CGP 200 nM. Mutant constructs not showing any currents in presence of CGP have been indicated with an X. Panel C, a quantification of the individual sizes of currents recorded in the presence of 50 nM CGP for the different mutants. For GluN1/GluN3A WT an average value of 1  $\mu$ A has been shown as mean current size to give a reference to compare to other mutants. X represent constructs that did not display electrical activity upon agonist application.

We first screened all our cysteine mutants on TEVC with glycine application alone in case we would obtain a gain of function phenotype (GOF). Then we screened with glycine + CGP, since this strategy allows to reveal activity of receptors blocked in non-active conformations. We found that the majority of mutants exhibit reduced expression levels in comparison to the GluN1/GluN3A WT even with CGP (Figure 51 Panel B). However, some mutants from the interdimer interface were similar to WT in expression levels (GluN1-E698C/GluN3A-K906C and GluN1 R673C/GluN3A-K906C). Other cysteine mutants from the LBD GluN1-NTD GluN3A interface or AMPAR-like lower LBD interface didn't give any current both with and without CGP.

When looking at the phenotype of the currents we recorded for these interface mutants, we found that cysteine mutants from Interfaces like the LBD intradimer Interface or GluN1 NTD-LBD interface showed currents that were smaller in size than the WT, as we were not able to record currents larger than few 100s of nA even with CGP pre-incubation, with most currents being so small to be easily confounded with artifacts of the perfusion system. With CGP, we were able to record currents with the same size of the WT from the Interdimer Interface, both from the "overactive" and "inhibiting" mutants, and from NTD crosslinking mutant GluN1/GluN3A-R319C (Figure 51 Panel C). The only mutants from which we could record glycinergic currents were 1) interdimer Interface "overactive" GluN1 E698C /GluN3A-K906C and 6) "NTD-crosslinked GluN1/GluN3A R319C". GluN1/GluN3A-R319C seemed to display a shifted glycine sensitivity (Figure 52 Panels B and C) due to larger steady state current levels compared to the GluN3A WT, and the appearance of a small tail current. Overall, the remaining cysteine mutants either completely silenced or greatly reduced the current sizes of the receptor, making recordings of these constructs very complicated. This lack of usable current on these mutants could be link to expression or plasma membrane addressing defaults, or greatly reduced activity of correctly expressed receptors, in particular if the putatively formed disulfide bonds maintain the receptor in a inactive state.

### **7.3.1 Reducing agent treatment on cysteine mutants**

If a disulfide bond maintains a receptor in a inactive state at the plasma membrane rendering it electrically silent, we should be able to reveal their presence with TEVC if we manage to break the bond. As shown previously for GluN2 containing receptors (Zhu *et al.*, 2013; Esmenjaud *et al.*, 2018; Tian *et al.*,

2021), reducing treatments can break artificially introduced disulphide bridge and release the constraint introduced by the crosslink. Activity awakenings of completely silent GluN2 receptor that has been reported with this approach (Esmenjaud *et al.*, 2018) may also occur in GluN3A receptors.

However, redox treatment has the drawback to putatively reduce all other native disulfide bonds within the receptor, thus modifying some of its functional properties. GluN1/GluN3A NMDARs reaction to reducing agent application has been described in (Grand *et al.*, 2018). We replicated those findings by screening oocytes with the agonists, then incubated the individual oocytes in either 5 mM DTE or 5 mM TCEP in Barth solution for 15 minutes before screening it again in the same agonist conditions. As already described, the breaking of GluN1/GluN3A endogenous cysteine bridges (in particular those in the lower lobe of the LBD) induced an increased GluN3A affinity for the agonist, with tonic activation, large tail currents and increased current sizes (Figure 52 Panel A).

We then performed the same protocol of redox treatment on the mutants displaying glycinergic currents. The mutant GluN1\GluN3A-R319C produced a phenotype similar to the GluN3A WT, with positive steady state currents, large tail currents and increased current sizes. (Figure 52, Panel B). Interestingly, we were not able to revert to a WT-like redox sensitive phenotype with the mutant GluN1 E698C /GluN3A K906C, whose current sizes just became slightly larger after reducing agent treatment (N=3), but do not show any major changes in current shape (Figure 52, Panel C). We do not know if this lack of effect might be due to an inability of the reducing agent to break the endogenous cysteine bridge in the GluN3A lower lobe (the one responsible for the shift in GluN3A affinity) or if our mutant had specific properties due to the cysteine we inserted.

We also applied the reducing treatment on the other mutants that gave current only with CGP. However, the test in presence of CGP led to large variability of current changes between oocytes after DTE treatment, even for the control GluN1/GluN3A WT receptors (Figure 52 Panel E-F). Thus, this condition wasn't good enough to accurately measure anything for the planned functional-screen of GluN3A mutants. Altogether, we were not able to reveal any hidden phenotype by breaking the hypothesized disulfide bridges that that we had tried to introduce. In few interesting cases, the small current size impaired the precise quantification of the biophysical properties of the mutants. Only the mutant GluN1-H162C-L765C/GluN3A gave an impressive potentiation of >30X fold upon DTE treatment (Figure 52 Panel G). Unfortunately, we haven't been able to reproduce this phenotype even after several attempts.

**Insert**

Measuring  $P_o$  of DTE treated GluN3A receptors. (Figure 52 Panel H) We attempted to see if we could calculate the  $P_o$  of broken endogenous cyteine-bridge receptors applying MTSEA to GluN1/GluN3A receptors previously treated with DTE. In this condition we observed that MTSEA application induces substantial current reduction (current reduction  $\sim 37\%$ , N=6) and not a augmentation as expected if DTE-treated GluN1/GluN3A were not 100% active. An hypothesis explaining this result could be that DTE treatment frees cysteines in the receptor that becomes a new target for MTSEA. This confounding variable represents an obvious limitation for utilizing MTSEA after DTE treatment.



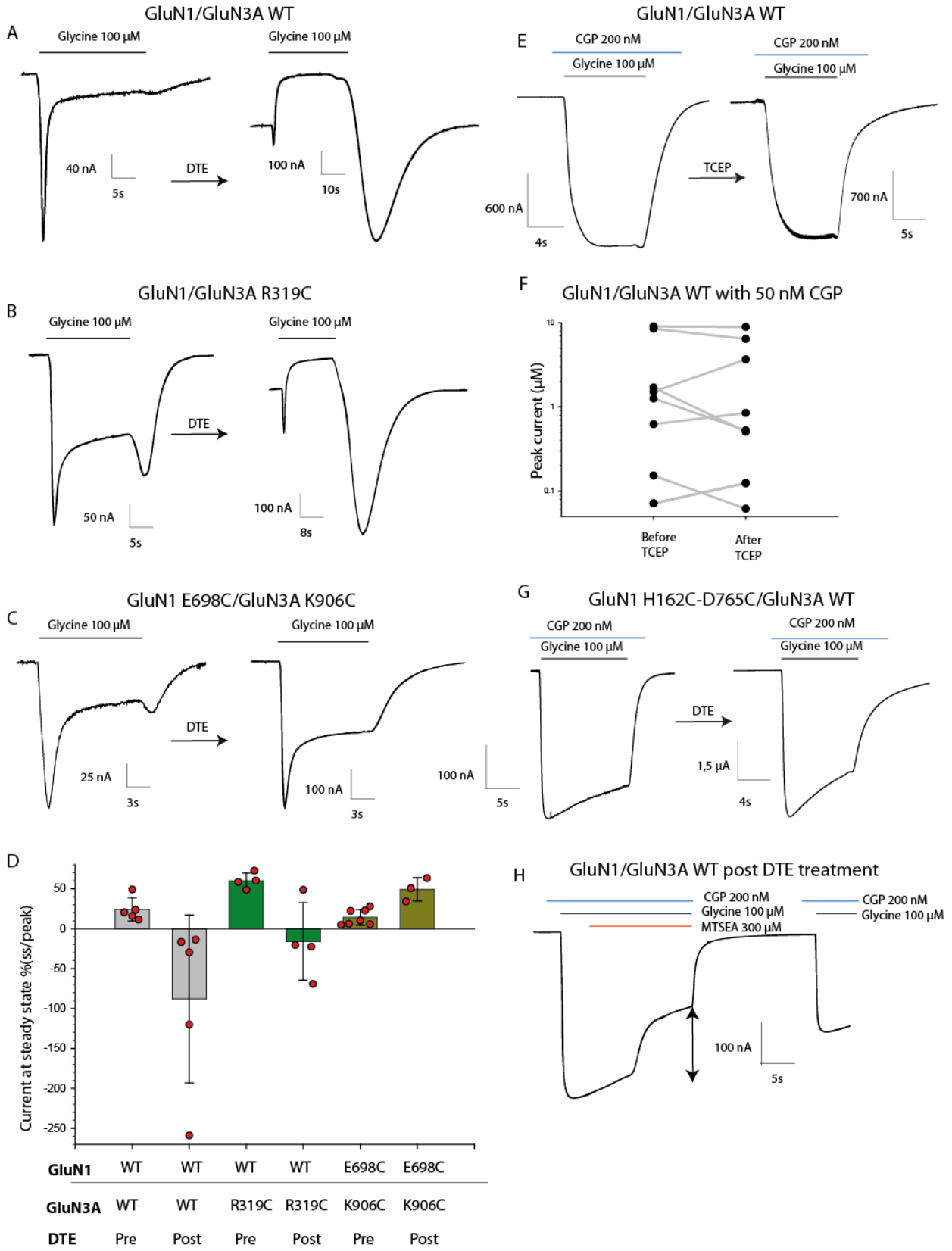


Figure 52 Reducing agent treatment on WT GluN1/GluN3A receptors and cysteine mutants.

Panels A-C example traces from GluN1 /GluN3A WT, GluN1/GluN3A R319C and GluN1 E698C/GluN3A K906C respectively with application of saturating glycine at 100  $\mu$ M. Each panel shows 2 representative traces of the same cell with the comparison pre and post 15 minutes incubation with the reducing agent. Panel D, histogram showing steady state current levels quantified as % SS current/peak with cells before and after DTE treatment. Negative values indicate positive steady state currents. The color coding for the Interfaces represented is the same as Figure 18. Panel E, example trace from GluN1 /GluN3A WT, with glycine 100  $\mu$ M and CGP 200 nM before and after DTE treatment. Panel F, histogram showing raw peak current levels pre and post reducing agent treatment in the GluN1/GluN3A receptors. Each line represents an individual cell. Panel G, example trace showing large potentiation ( $N=1$ ) from GluN1 H162C-L765C/GluN3A, with glycine 100  $\mu$ M and CGP 200 nM before and after DTE treatment. Panel H, example trace showing current reduction upon application of 300  $\mu$ M MTSEA in a previously DTE treated cell expressing GluN1/GluN3A WT, with glycine 100  $\mu$ M and CGP 200 nM.

### 7.3.2 Western blots on cysteine mutants

We then wondered if the cysteine mutants, even if electrophysiologically silent, indeed generated crosslinked dimers. To answer this question we performed western blot experiments (WB) of homogenized xenopus oocytes injected with the corresponding GluN1/GluN3A mutants. As a control, we tested WB on cystein cross-linked dimers already published in the lab : GluN1/GluN2B WT (2BWT) and GluN1 R673C/GluN2B L795C ("2BCC" in GluN2B) or uninjected (UN) samples (Figure 53 Panel A). The monomer band (M1) appears clearly with both the antibodies against GluN1 and against GluN2B for the constructs GluN1/GluN2B WT and GluN1 R673C/GluN2B L795C conditions, but not in the uninjected condition (UN). As expected, the GluN1 R673C/GluN2B L795C showed a band corresponding to the heterodimer (~290 kDa). Still, the dimer band was more clearly noticeable with the GluN2B antibody compared to the GluN1 antibody showing a fainter band. This is linked to a well-known problem of variability of dimer detection by WB in the lab (Riou *et al.*, 2012)

We then tested the WB profile the most promising mutants : GluN1 R673C/GluN3A K906C (Interdimer), GluN1 E698C/GluN3A K906C (Interdimer), and GluN1/GluN3A R319C (NTD crosslink) with UN, GluN1/GluN3A WT and GluN1 WT/GluN2B L795C as controls (Figure 53 Panel B). As expected the GluN1 antibody blot revealed the presence of monomer on the blot for all conditions (except the UN one). Interestingly, two faint bands seemed to appear at about the height expected for a GluN1/GluN3A heterodimer ~250 kDa for both the constructs GluN1 R673C/GluN3A K906C, GluN1 E698C/GluN3A K906C. These bands may suggest a possible dimer formation by cystein crosslink but they can also be seen in the UN and the GluN1/GluN3A WT conditions. However, in our hand and conditions, WB with anti-GluN3A

antibody  $\alpha$  GluN3A rabbit 07-356 (Sigma-Aldrich) gave rise to several non-specific bands complicating the interpretation of the blot. Thus our western blot tests remained inconclusive despite several attempts. Employing a different (better for WB) antibody against GluN3A may allow to solve this issue.

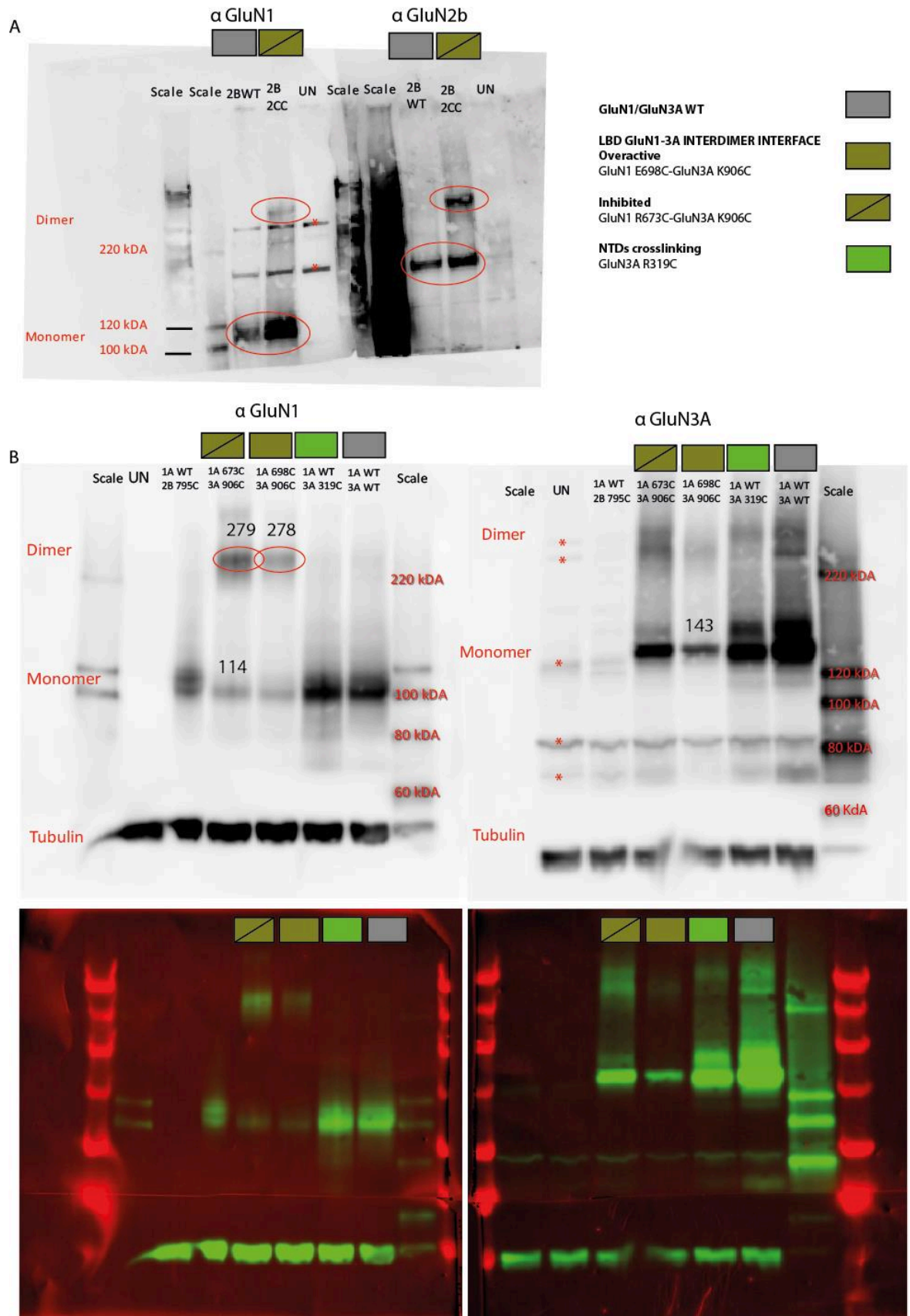


Figure 53 Western blots on cysteine mutants.

Panel A, control immunoblots from *Xenopus* oocytes expressing GluN1 /GluN2B WT (2BWT) or GluN1 R673C/GluN2B L795C (2BCC) or uninjected (UN) samples. Samples were analyzed using anti-GluN1 or anti-GluN2B antibodies. GluN1 monomer (M1) runs at ~110 kDa (red circle), and GluN2B monomer at ~180 kDa (M2), and GluN1-GluN2 heterodimer at ~290 kDa (D2/2). \* Indicates non-specific background bands. A legend showing the color coding of interfaces corresponding to the cysteine location is shown. Panel B middle and bottom: immunoblots from *Xenopus* oocytes expressing uninjected (UN) samples, GluN1 R673C/GluN2B L795C (control), GluN1 R673C/GluN3A K906C, GluN1 E698C/GluN3A K906C, GluN1/GluN3A R319C and GluN1/GluN3A WT (control). Samples were analyzed using anti-GluN1 or anti-GluN3A antibodies. GluN1 monomer (M1) runs at ~110 kDa, and GluN3A monomer at ~140 kDa (M2), and GluN1-GluN3A heterodimer at ~250 kDa (D2/2). \* Indicates non-specific background bands. Below a different fluorescent contrast of the same blot is showing, where bands are more clearly visible than the black and white contrast.

Despite having worked very well in GluN2 containing receptors, this cysteine cross-linking approach on GluN1/GluN3A receptors did not appear successful enough in terms of mutant expression, redox awakenings and Western Blots to teach us anything about the receptor functional mechanism. It was thus put aside to focus on more promising approaches.



## 8: The LBD dimer interface controls GluN1/GluN3A receptor activity.

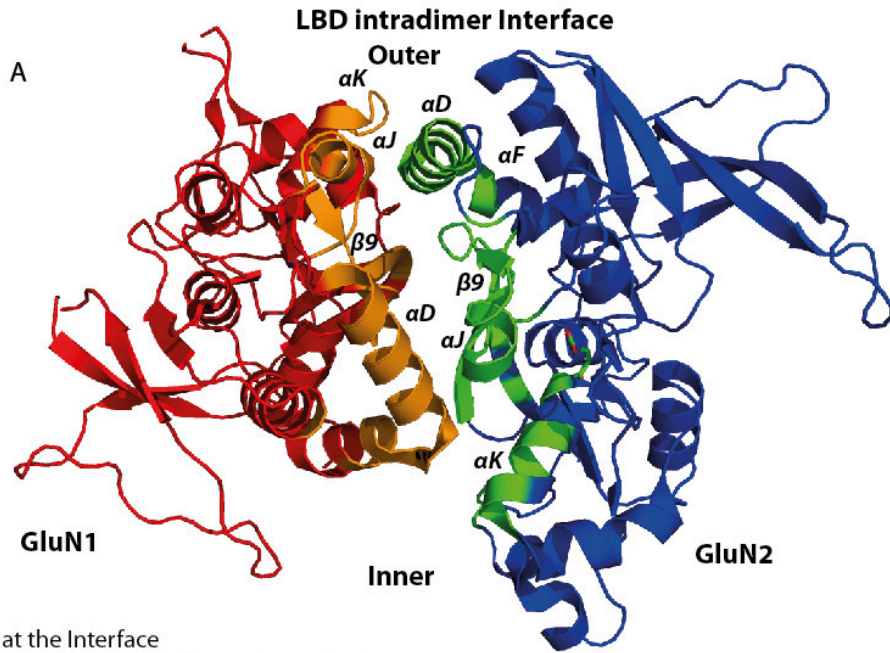
The LBD intradimer interface appears as a common critical element in all vertebrates iGluRs for the control of gating and particularly for the process of desensitization in AMPARs, or inhibition in GluN2 containing receptors (See 3.3.1 LBD dimerization , 4.5 Desensitization: AMPARs vs NMDARs). In our quest to understand GluN1/GluN3A receptors desensitization, we thus naturally focused our attention on this interface. According to what is known in other iGluRs, one obvious and simple explanation of the strong desensitization observed in GluN3A receptors could be that the upper lobe-upper lobe LBD intradimer contact at this interface is particularly unstable and dissociate easily. However as previously described ((Awobuluyi *et al.*, 2007; Grand *et al.*, 2018)) desensitization of these receptors appear also controlled by Glycine binding. In this chapter we decrypt the functional importance of this interface.

### 8.1 Contact Maps of the LBD intradimer interface

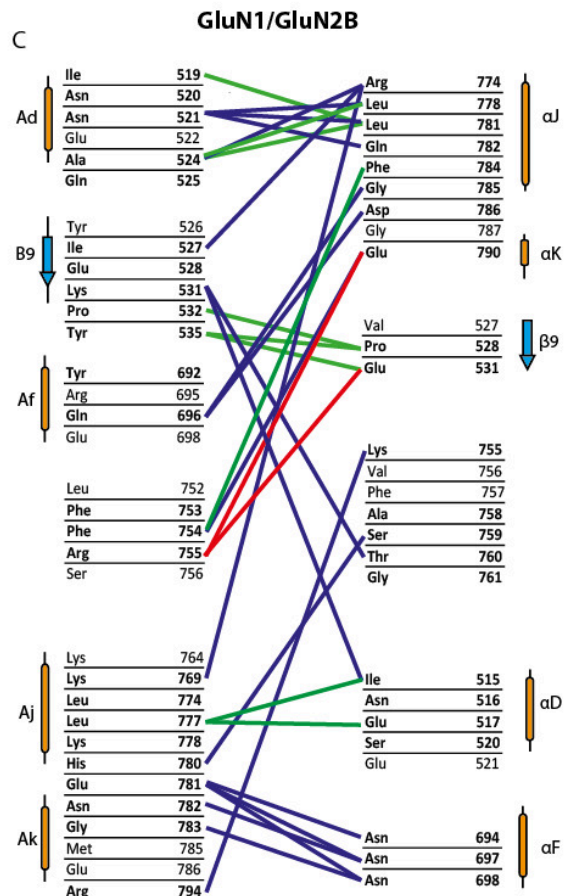
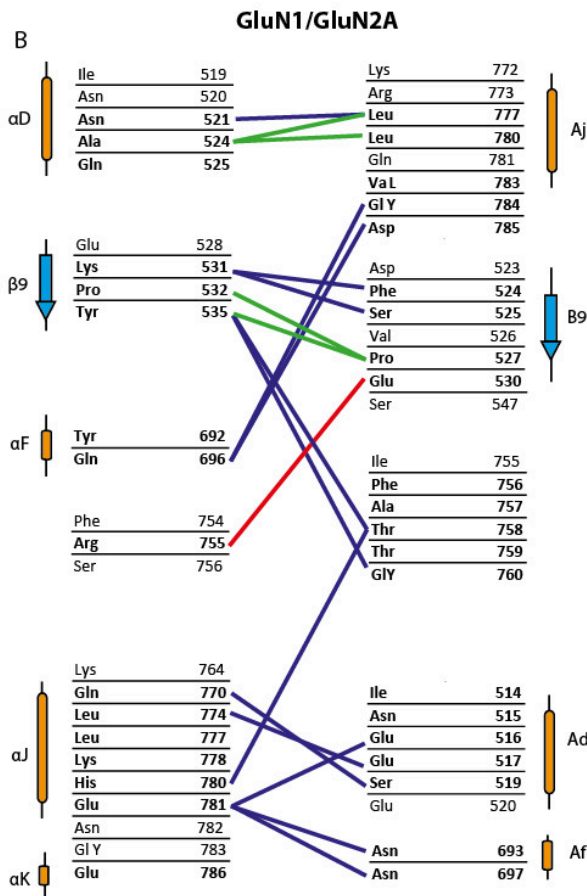
The strength of any interface depends on the amino-acid composition and distribution of the two partners at this interface and the network of individual interaction they are forming. Since no full-length structure of GluN1/GluN3A receptors are available, we have to rely on our GluN2-based model with a canonical stable LBD dimer interaction (see 7.1 Building a working 3D model of GluN1/GluN3A receptor) to look at the putative interaction network of amino-acids. To facilitate our understanding of the interactions between GluN3A and GluN1 we drew a contact map using the online tool 'Cocomaps' (<https://www.molnac.unisa.it/BioTools/cocomaps/>). This web tool predicts and analyses interfaces in biological complexes such as protein-protein and produces intermolecular contact maps, highlighting the atoms within the individual residues that can form the interactions (Vangone *et al.*, 2011). We used it to compare the PDB files of several iGluRs of interest focusing on the LBD dimer. We highlighted residues selected to be at <4 Armstrong distance from the partner subunit, and therefore capable of making hydrophobic contacts, electrostatic interactions and H-bonds with the partner subunit (Bissantz *et al.*, 2010). We thus chose to analyze the interface of the following iGluRs structures 1) GluN1/GluN3A WT, based on modeler predictions from the structure GluN1/GluN2B 4pe5, 2) GluN1/GluN2B 4pe5, Ifenprodil inhibited full tetramer, 3) GluN1/GluN2A PDB 2a5t (2Å) resolution, LBD isolated with glycine and glutamate 4) GluN1/GluN2B model built on molecular dynamics modeling active state transition published in (Esmenjaud *et al.*, 2018). 5) GluN1/GluN2A model built on molecular dynamics, modeling an inhibited state with disrupted interface. 6) AMPA GluA2 in complex with competitive antagonist ZK

7) AMPA subtype ionotropic glutamate receptor GluA2 in the Apo state (Sobolevsky *et al.*, 2009; Dürr *et al.*, 2014) (5 and 6 not shown). We chose these structures for precise reasons. The GluN1/GluN3A structure is self-explanatory as it is the focus of the project. GluN1/GluN2B (4pe5) inhibited was the original published structure on which the GluN3A model is based upon, and serves for a comparison of a strong interface in the inhibited state. GluN1/GluN2A PDB (2a5t) is a high resolution structure that should represent a less solid, more mobile interface than GluN2B. Structures 4, and 5 were used to model the same GluN2 subunits in different conformations to see how would the contact map differ after rearrangement in a different step of the gating process. Structure 6 and 7 expanded the analysis to other iGluRs.





Arg: residue at the Interface  
**Arg**: residue at <4 Å distance from other subunit



**Residues at interface**  
 GluN1: 24 GluN2A: 27  
 GluN1: 33 GluN2B: 27

**H bonds**  
 GluN2A: 13  
 GluN2B: 18

**Hydrophobic**  
 GluN2A: 4  
 GluN2B: 9

**Electrostatic**  
 GluN2A: 1  
 GluN2B: 2

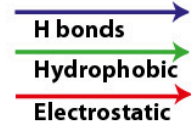


Figure 54 Contact Maps of LBD Interdimer Interface of GluN2s containing NMDARs.

Panel A, graphical representation obtained with Pymol of the intradimer Interface where GluN1 (red) and GluN2B (blue) partner subunit are shown, and residues at the interface predicted to be at less than 4 Å are displayed with different colors (orange and green respectively for GluN1 and partner). Panels B and C: contact maps of GluN1/GluN2B (PDB 4pe5) and GluN1/GluN2A (PDB 2at5) side by side. The residues shown are predicted to become buried by interface formation, and they are in bold if bond formation has been predicted by the software and by our criteria. The type of possible bonds formed are depicted in different colors: Purple for H bonds, green for hydrophobic interactions and red for electrostatic interactions.

For each structure, we generated a list describing which atoms are at <4 atoms from each individual residue. We then categorized the type of possible bonds into 3 types: Hydrophobic, H-bonds and electrostatic interactions. We restricted hydrophobic interactions to specific cases such as between these atoms: any Carbon (excluding C and C $\alpha$ ) with all hydrophobic and aromatic residues (alanine, valine, leucine, isoleucine, proline, phenylalanine, tryptophan, tyrosine, methionine) or with C $\alpha$  of Glycine or with Carbohydrate parts of other amino-acids: lysine C $\beta$ , C $\gamma$ , C $\Delta$ , arginine C $\beta$ , C $\gamma$ , histidine C $\beta$ , threonine C $\gamma$ , glutamic acid C $\beta$ , glutamine C $\beta$ . Finally, we considered O-O, O-N or N-N contacts to be either H-bonds or electrostatic interactions, depending on the residue identity. If the residues have opposite charges, such as positive ones like arginine, lysine or histidine making contact with a negative one such as glutamic acid or aspartic acid they were considered electrostatic, otherwise all the rest were set to H bonds. One important limitation of this analysis is that the program does not take into consideration the presence of buried water molecules within the interface, so we had to leave possible water-bridge out of the analysis. Still our analysis should be able to map well possible direct ionic and hydrophobic interactions.

To validate this approach, we first compared GluN2A and GluN2B Intradimer interfaces (PDB codes 4pe5 and 2at5) since both of these structures have been solved by X-ray crystallography at a good resolution and in a state with a canonical stable LBD dimer configuration (Figure 54). GluN2A buries a large surface of ~ 1900 Å with 51 residues at the interface making 18 bonds, while GluN2B buries about ~ 2200 Å with 60 residues at the interface making 29 bonds (Table 8, Figure 54) Overall, both interfaces were predicted to be similar in terms of general architecture and majority of intersubunit contacts. Major points of contact are the inner side of the interface (chain  $\alpha$ D of GluN1 and  $\alpha$ J of GluN2s), the center/inner side of the Interface ( $\beta$  sheets 9) and the outer side of the interface (chain  $\alpha$ J of GluN1 and  $\alpha$ D of GluN2s). In both inner sides of the interface of GluN2A and GluN2B there are hydrophobic contacts

present. GluN2B appears to form bit more interaction with GluN1 than GluN2A, as it is expected from the literature (Hackos *et al.*, 2016; Tian *et al.*, 2021).

We then tested how the transition to other functional states of receptor (that involve the LBD intradimer interface) do affect the distribution of interactions in GluN2. We based ourselves on a model of active state of GluN2B (Esmenjaud *et al.*, 2018) and on a model of inhibited (desensitized) state of GluN2A (Tian *et al.*, 2021). (Figure 55). The transition to the active conformation of GluN1/GluN2B to we can see how the LBD interface is much less densely interconnected than the previous inhibited state of 4pe5 we used (2300 Å buried with 69 residues at the interface, but only 17 bonds predicted, compared to the 29 of the inhibited one). There are less connections in each side of the interface, and the predicted hydrophobic bonds drop from 9 to 3. This finding may indicate that there are probably differences of stability in these two conformations, but it is difficult to draw certain conclusions. Concerning the GluN2A inhibited state with LBD broken interface (Figure 55 Panel B), it is striking how asymmetrical this conformation becomes compared to the other states. Indeed, the inner side of the interface appears to be completely splayed apart with no more residues predicted to be at the interface making contact with each other. On the outer side no more hydrophobic connections is present and only 2 H-contacts predicted for the whole LBD dimer (not shown). This conformation with an asymmetrical broken interface is thought to be representative of a fully desensitized receptor.

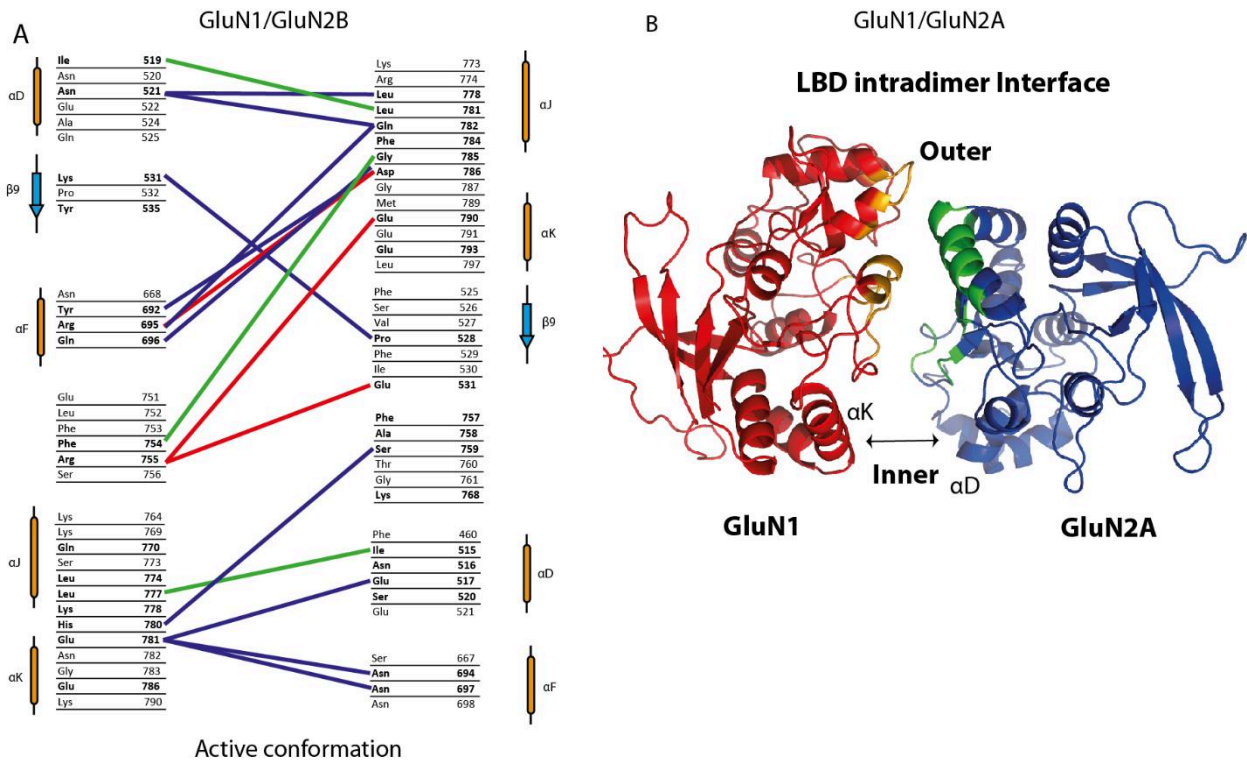
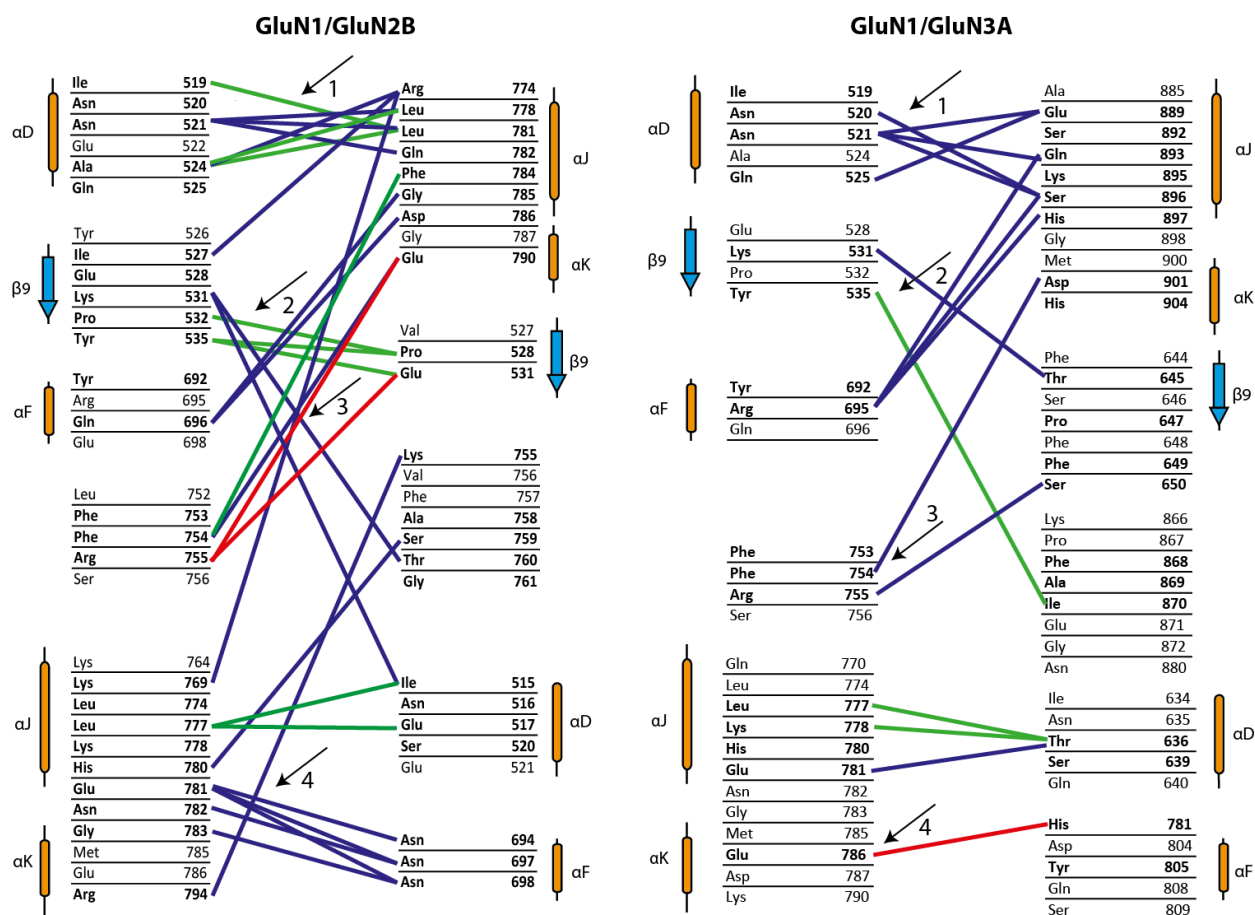


Figure 55 Active conformations of GluN1/GluN2s Intradimer Interface.

Panel A, contact maps of GluN1/GluN2B in the active conformation derived from molecular dynamic simulation of the LBD rolling motion. The residues shown are predicted to become buried by interface formation, and they are in bold if bond formation has been predicted. The type of possible bonds formed are depicted in different colors: Purple for H bonds, green for hydrophobic interactions and red for electrostatic interactions. Panel B, graphical representation obtained with Pymol of the GluN1/GluN2A Intradimer Interface in the active conformation obtained from molecular dynamics simulations. GluN1 (red) and the GluN2A partner subunit (blue) are shown and residues at the interface predicted to be at less than 4 Å are displayed with different colors (orange and green respectively for GluN1 and GluN2A).



Res at interface		H bonds	Hydrophobic	Electrostatic
GluN1: 33	GluN1: 28	GluN2B: 18	GluN2B: 9	GluN2B: 2
GluN2B: 27	GluN3A: 36	GluN3A: 12	GluN3A: 3	GluN3A: 1

Figure 56 Intradimer Interfaces of GluN1/GluN2B vs GluN1/GluN3A.

Side by side contact maps of GluN1/GluN2B in the inhibited conformation derived from 4pe5 and GluN1/GluN3A model derived from the GluN1/GluN2B 4pe5. The residues shown are predicted to become buried by interface formation, and they are in bold if bond formation has been predicted. The type of possible bonds formed are depicted in different colors: Purple for H bonds, green for hydrophobic interactions and red for electrostatic interaction. The arrows indicate 4 positions where interface bonding is predicted to be different.

We then applied this analysis to our GluN3A model based on the former stable inhibited state of GluN2B (Figure 56). GluN1/3A interface appears less densely interconnected than GluN1/GluN2B, even though the number of residues predicted to be at the interface are similar to the one predicted to be in the interface of GluN2B (2000 vs 2020 Å with 64 vs 60 residues at the interface making 16 vs 29 bonds for GluN3A vs GluN2B respectively (Table 8). We could infer some specific observations about which regions of the interface are predicted to assemble differently and how. 1) Loss of hydrophobic

connections between GluN1  $\alpha$ D and GluN3A  $\alpha$ J indicating that the inner side of the intradimer interface may be less hydrophobic and less interconnected. 2) Loss of hydrophobic connections between GluN1  $\beta$ 9 and GluN3A  $\beta$ 9 3) Loss of electrostatic interactions from GluN1 R755 to GluN3A 4) Loss of H-bonds between GluN1  $\alpha$ J-K and GluN3A  $\alpha$ F. Interestingly, the core hydrophobic connections between GluN1  $\alpha$ J and GluN2B  $\alpha$ D are maintained in GluN3A. It also suggests an asymmetrical model in which the central and inner side of the interfaces are modified and may lose important hydrophobic residues stabilizing hydrophobic bonding, while the outer side of the interface resembles GluN2s-like interfaces. Overall, these findings point to a less stable LBD dimer interface in GluN3A than in GluN2B, in agreement this the observed desensitizing behavior of GluN1/GluN3A receptors.

Category	GluN2A	GluN2B inhib	GluN3A inhib	GluN2B active
Buried area upon the complex formation (A)	1889.2	2268.8	2031.2	2343.1
Buried area upon the complex formation (%)	7.28	8.01	6.85	7.63
Interface area (A)	944.6	1134.4	1015.6	1171.55
Interface area MOL1 (%)	7.49	8.07	6.56	7.72
Interface area MOL2 (%)	7.08	7.95	7.17	7.53
POLAR Buried area upon the complex formation (A)	1192.5	1336.2	1110.3	1376.4
POLAR Buried area upon the complex formation (%)	63.12	58.89	54.66	58.74
POLAR Interface area (A)	596.25	668.1	555.15	688.2
NO POLAR Buried area upon the complex formation (A <sup>2</sup> )	696.8	932.6	921	966.7
NO POLAR Buried area upon the complex formation (%)	36.88	41.11	45.34	41.26
NO POLAR Interface area (A)	348.4	466.3	460.5	483.35
Residues at the interface_TOT (n)	51	60	64	69
Residues at the interface_Mol1 (n)	24	33	28	32
Residues at the interface_Mol2 (n)	27	27	36	37

Table 8 Summary of NMDAR contact maps.

Table representing a summary of Cocomaps predictions for LBD Intradimer Interface formation for the different NMDARs combinations tested.

## 8.2 Scanning approach to build a GluN3A LBD intradimer interface GluN2B-like chimera

Individual positions → Mutant construct ↓	T636E	Q640E	S646V	S650E	Y805 N	S809N	F810Y	D850N	K865SGK P867V	I870S E871T	P879K N880D	T884K S885R S888D E889L	S892L	K895F	K895V	H904E K909T	Results	Description	Expression	Phenotype change	
T636E	█																X				
Q640E		█																gly	=	No	
T636E Q640E	█	█															X				
S646V S650E			█	█														cgp+gly	↓	Minuscule currents	
Y805N S809N F810Y					█	█	█											cgp+gly	=	No	
D851N								█										cgp+gly	↓	Small currents, Gly affinity change	
K865SGK P867V I870S E871T									█	█								X			
I870S E871T											█							X			
P879K N880D												█						X			
T884K S885R S888D E889L												█						X			
I870S E871T T884K S885R S888D E889L										█		█						X			
S892L													█						gly	=	Gly affinity change
K895F														█	█			cgp + gly	↓	Small currents, Gly affinity change	
S892L K895F														█	█			gly	↑↑	Gain of function	
S892L K895V														█		█		gly	↑↑	Gain of function	
H904E K909T																█		cgp+gly	=	Gly affinity change	
<b>FULL CHIMERAS</b>																					
SH51																		gly	↑↑	Gain of function	
SHSDY2				█														gly	↑	Gain of function	
SHSDY3				█														cgp+gly	↓	Minuscule currents	
CHIMERA A			█	█	█	█	█	█										X			
CHIMERA B			█	█	█	█	█	█										X			
CHIMERA C	█		█	█	█	█	█	█			█							X			
CHIMERA D	█	█	█	█	█	█	█	█			█							X			
CHIMERA E	█	█	█	█	█	█	█	█			█							X			
CHIMERA F	█	█	█	█	█	█	█	█		█								X			
CHIMERA G	█	█	█	█	█	█	█	█		█								X			
CHIMERA FINAL	█	█	█	█	█	█	█	█		█								X			
<b>FULL REVERSION</b>																					
NR2B LBD on NR3A																		X			
<b>PARTIAL CHIMERAS</b>																					
Y805N S809N F810Y S892L K895F					█	█	█												gly	↑	Gain of function
Y805N S809N F810Y S892L K895F H904E K909T					█	█	█									█			gly	↑	Gain of function
S892L K895F D850N								█											gly	↓	Gain of function but small currents
S892L K895F Q640E		█																	gly	↑	Same as double mutant
S892L K895F Q640E D850N		█						█													
CHIMERA Z					█														X		
CHIMERA Y						█	█														
CHIMERA X						█	█														
CHIMERA W						█	█	█									█		cgp + gly	↓	Small Currents
CHIMERA V						█	█												X		
CHIMERA U						█	█												X		

Table 9 GluN3A chimeric approach in LBD Intradimer Interface to recreate full GluN2B-like charges properties.

Three sets of mutants are represented: in green individual cohorts of mutants with mutated charges, in orange a progressive recreation of the full chimera containing all mutated charges, in blue partial chimeras containing stackings of individual cohort mutants that were shown to be individually functionally active. On the right of the table, a color coding red/blue binary output if the currents had any phenotype change in comparison to the GluN1/GluN3A WT, the type of currents recorded, a qualitative quantification of expression levels and phenotype changes observed.

The observation of GluN3A LBD surface specificities compared to other known GluN2 indicates that the functional properties of GluN1/GluN3A receptors (in particular their desensitization) could well originate from a difference in amino-acid composition at this interface. We then decided to make a chimera to



replace the whole LBD of GluN2B at the place of the one of GluN3A within the GluN3A receptor sequence. But this chimeric construct didn't give current.

Since the core of the LBD appear unchanged between GluN3A and GluN2B it raises the possibility to mutate only the surface to try to recreate the GluN2B like interface profile within the GluN3A LBD intradimer interface (Table 9 green constructs). We did so by making point mutations or by doing cohorts of mutants that were in close proximity to each other with similar charge or hydrophobic properties (e.g., a hydrophobic residue next to a hydrophobic residue). Using this strategy, we discovered mutants with interesting GOF phenotypes that are now in the core of the following manuscript (See 8.3 Article: The LBD Dimer Interface Tunes Activation of Glycine-Gated GluN1/GluN3A Receptors). However, many mutants did not display any electrical activity and we could not analyze their properties. Since the LBD intradimer Interface is a large interface with three main sites (inner, central and outer), we reasoned that perhaps an incomplete shift of all the residues biochemical properties to GluN2B-like identity might have been the cause for some of the mutants to not be functional. This could come from the perturbations in the folding process or assembly problems linked to disturbed interface properties. One possibility to solve this issue would be to introduce more surrounding GluN2B residues to reach an GluN2B environment that we know is properly folded, assembled and functional.

Later, we were hoping that by progressively recreating the full GluN2B interface we would have been able to further shift the phenotype we observed with our GOF mutants. We thus created a series of chimeras where we progressively added mutants on top of the important double mutant GluN1/GluN3A S892L-K895F (Table 9, Table 7 orange constructs). **It allowed to obtain even larger gain of function phenotype** with the mutant GluN1/GluN3A S892L-K895F-H904E-K909T (shs1) that was drastically shifting the glycine affinity even further to the left in comparison to the GluN1/GluN3A WT. ( $EC_{50}$  SS glycine  $0.11 \pm 0.001 \mu\text{M}$ , N=5) (Figure 57 Panels A, B). However, further additions of individual cohorts of mutants to the chimera gave nonfunctional constructs. Finally, even the full chimera, where all LBD interface residues of GluN3A mutated in their GluN2B counterpart, didn't give any current.

We therefore attempted another approach putting together all the mutants that individually gave some current (Table 9 blue constructs). With this approach, we created a GluN3A mutant containing 7 GluN2B-like mutants at the interface GluN1/GluN3A Y805N-S809N-F810Y-S892L-K895F-H904E-K909T. This mutant gave large tonic activation with saturating glycine applications giving rise to large positive steady state currents, and absence of tail currents upon removal of glycine (Figure 57 Panels C, D).



Overall, with the stacking of GluN2B-like mutants at the intradimer interface, we managed to further increase the GluN3A affinity for glycine, showing phenotypes with very large tonic activity.

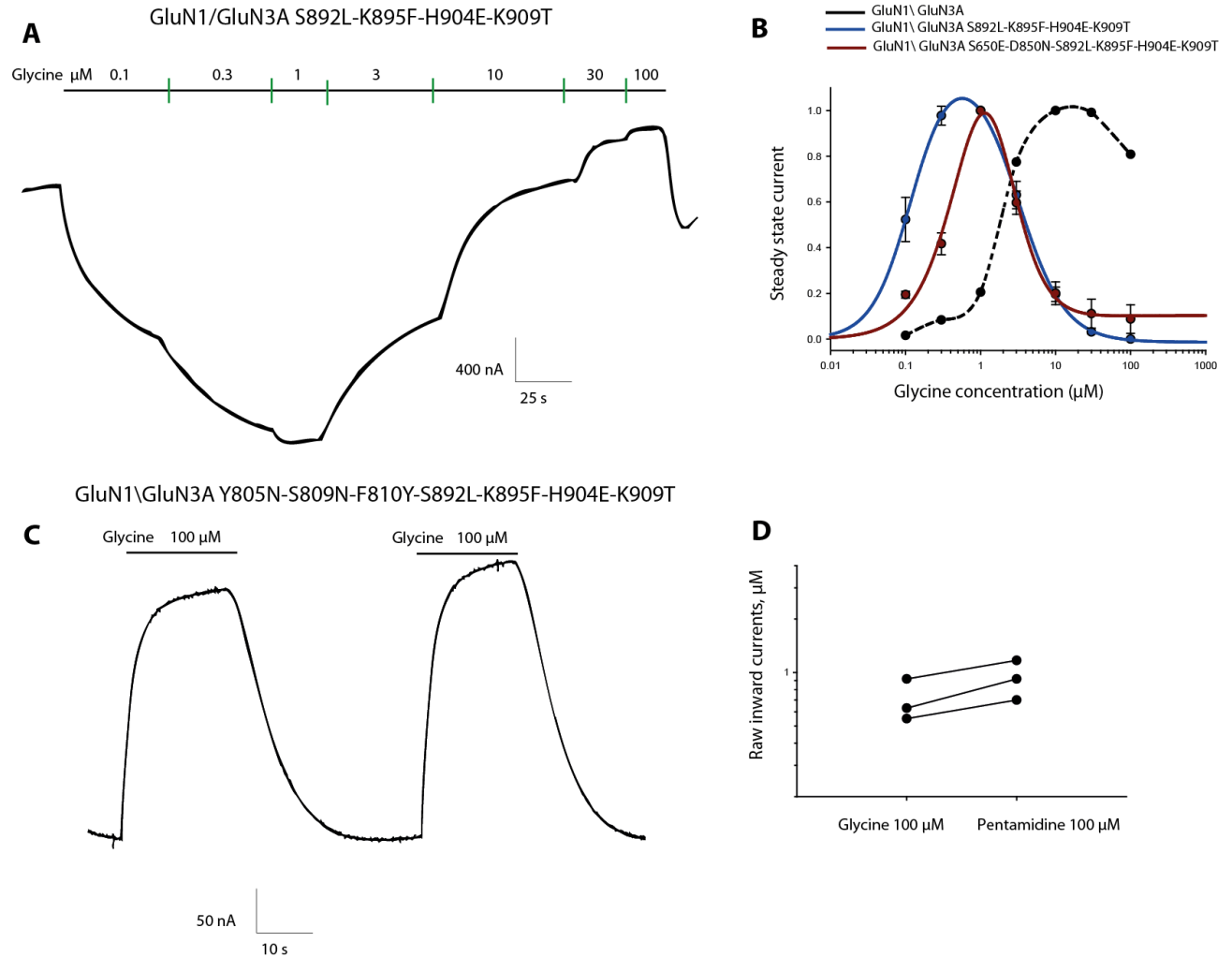


Figure 57 Chimeric mutants in the intradimer interface.

Panel A, representative trace displaying glycinergergic dose responses of GluN1/GluN3A S892L-K895F-H904E-K909T (*Shs1*). Panel B, dose response of chimeric constructs GluN1/GluN3A S892L-K895F-H904E-K909T and GluN1/GluN3A S650E-D850N-S892L-K895F-H904E-K909T (*shsdy2*). The  $EC_{50}$  for glycine steady state for *shs1* and *shsdy2* are estimated at  $0.11 \pm 0.01 \mu\text{M}$ , ( $N=5$ ) and  $0.33 \pm 0.07 \mu\text{M}$  ( $N=4$ ). The steady state for GluN1/GluN3A WT is  $N=1$ , with only one representative trace selected and shown due to the minuscule size of these currents. Panel C, representative trace showing the mutant GluN1/GluN3A Y805N-S809N-F810Y-S892L-K895F-H904E-K909T positive steady state currents upon glycine application. Panel D, a comparison showing that 100  $\mu\text{M}$  glycine and 100  $\mu\text{M}$  pentamidine application cause similar positive inward currents pointing to the mutant being in a state of tonic activation with ambient glycine in the recording solutions.

The successful expression of this construct with mutants scattered within the interface is somehow surprising when thinking about the general low success rate of mutagenesis of GluN3A receptors. Indeed, most other mutant combinations (in the LBD and other) failed to give functional receptors. Thinking of this low success rate, it really pushes the idea that if some mutations are well tolerated in GluN3A, most are very deleterious for some folding or assembly process of the receptor. This could somehow make sense from an evolutionary perspective, with some observations from the lab (data not shown) about the much lower selective pressure applying on GluN3A (and 3B) than on other NMDAR subunits. Following this idea this receptor may have accumulated a lot of functionally neutral but structurally weakening mutants. This hypothesis could help explaining why the cysteine scanning produced so many low-expression or low current mutants. Furthermore, some constructs with major module deletion we created in the section 2.2 were not functional, although they have been validated in the literature. For these constructs, it is unclear why we could not achieve a current phenotype, perhaps due to some unexpected issues in the construct. The constructs remain at disposal for further tests in the laboratory. Altogether, we found no simple solution to this problem of sensitivity to mutagenesis. Experimentally it thus means that only intensive mutation scanning can help to find expressing mutant in GluN3A. This is precisely how we ended up with an interesting series of observations detailed in the following manuscript.

## **8.3 Article: The LBD Dimer Interface Tunes Activation of Glycine-Gated GluN1/GluN3A Receptors**

---

# The LBD Dimer Interface Tunes Activation of Glycine-Gated GluN1/GluN3A Receptors

Marco De Battista, Laetitia Mony, Noémie Lacour, Pierre Paoletti<sup>#</sup> and David Stroebel<sup>#</sup>

*Institut de Biologie de l'Ecole Normale Supérieure (IBENS), Ecole Normale Supérieure, Université PSL, CNRS, INSERM, F-75005 Paris, France. <sup>#</sup> These authors jointly supervised this work.*

---

## ABSTRACT

GluN1/GluN3A receptors were recently shown to define a novel signaling modality in the brain by which extracellular glycine tonically tunes neuronal excitability, a role that strikingly departs from that of conventional GluN1/GluN2 NMDARs. While phylogenetically and structurally related to the NMDA receptor family of ionotropic glutamate receptors (iGluRs), GluN1/GluN3A receptors exhibit several distinctive properties that shape their function: 1) activation by glycine alone but insensitivity to glutamate; 2) bell-shaped curve of activation; 3) profound desensitization through GluN1-mediated auto-inactivation; 4) poor sensitivity to known NMDAR pore blockers. The molecular origin of GluN1/GluN3A receptors atypical functional properties remains poorly understood in the absence of full structural description of these receptors. We thus implemented specific tools to modulate their activity and study their function. This led us to identify and characterize strong gain-of-function mutants with marked increase in channel open probability and glycine sensitivity. All these GoF mutants target the ligand-binding domain (LBD) dimer interface, a region known to be critical for the gating and desensitization in other iGluRs. A double-mutant in particular exhibited the strongest high-affinity and high-efficacy phenotype, allowing to fully separate activation and inactivation mediated by the GluN3A and GluN1 subunits, respectively. Our work brings novel insights into the molecular mechanisms underpinning the atypical gating behavior of GluN1/GluN3A receptors.

---

## Introduction

NMDA Receptors are glutamate gated ionotropic receptors (iGluRs) that fulfill critical roles in the CNS (central nervous system), from neural development to synaptic communication and plasticity (Traynelis *et al.*, 2010; Paoletti *et al.*, 2013; Hansen *et al.*, 2021). The 7 Vertebrates paralogs of NMDAR form heterotetrameric assemblies composed of two obligatory GluN1 subunits (that are glycine sensitive), and two other subunits among the 4 GluN2 subunits (GluN2A-D - that are glutamate sensitive) or the 2 GluN3 subunits (GluN3A-B that are glycine sensitive) (Stroebel *et al.*, 2021). GluN1 and GluN2s subunits associate to form canonical diheteromeric NMDARs, widely expressed in the brain and coactivated both by glutamate and glycine. More than 40 years of extensive studies revealed the crucial importance of these GluN1/GluN2s receptors

*This work was supported by the French government ("Investissements d'Avenir" ANR-10-LABX-54 MEMOLIFE, ANR-11-IDEX-0001-02 PSL Research University, ANR-11-LABX-0011-01, ANR-GluBrain3A, and ANR-EXCIGLY) and the European Research Council (ERC Advanced Grant #693021 toPP). This work was supported by the Fondation pour la Recherche Médicale (FRM), grant number FDT202106013195.*

*The authors declare no competing interests.*

for brain functions in general and synaptic plasticity in particular (Citri and Malenka, 2008; Hansen *et al.*, 2021; Paoletti *et al.*, 2013).

The GluN3A subunit was cloned in 1995 (Ciabarra and Sevarino, 1995). It was long thought to act exclusively during brain development as a negative regulatory subunit of GluN2 containing receptors through the formation of triheteromeric complexes (GluN1/GluN2/GluN3) (Chatterton *et al.*, 2002; Ulbrich and Isacoff, 2008; Yuan *et al.*, 2013; Crawley *et al.*, 2022). We now know that GluN1/GluN3A diheteromeric receptors are present (Murillo *et al.*, 2021) and functionally active in the different regions of the CNS : juvenile hippocampus (Grand *et al.*, 2018), adult medial habenula (Otsu *et al.*, 2019) and adult neocortex and amygdala (Bossi *et al.*, 2022). In these structures GluN1/GluN3A receptors appear to control neuronal excitability of specific cell types through the sensing of endogenous glycine levels and thus contribute to the regulation of specific behaviors, like aversion (Otsu *et al.*, 2019) and fear (Bossi *et al.*, 2022). These recent discoveries stimulated a renewed interest about the function and roles of those atypical iGluRs.

GluN1/GluN3A NMDARs display unique functional properties compared to GluN2 containing NMDAR subunits. 1) They form atypical excitatory receptors that are purely glycine-sensitive (eGlyRs) – and not glutamate sensitive (Chatterton *et al.*, 2002;

Awobuluyi *et al.*, 2007; Madry *et al.*, 2007). 2) GluN1/GluN3A receptors exhibit a bell-shape glycine activation curve. Low micromolar concentrations of glycine activate the receptors through binding to the high-affinity GluN3A subunit, while dozen of micromolar concentrations lead to rapid desensitization induced by glycine binding to the lower affinity GluN1 binding site, (Yao, 2006; Awobuluyi *et al.*, 2007; Madry *et al.*, 2007). The resulting activation of WT GluN1/GluN3A receptors thus displays small and rapid desensitizing inward currents, which complicates their detection and studies. 3) They display low  $\text{Ca}^{2+}$  permeation and  $\text{Mg}^{2+}$  block (Das *et al.*, 1998; Chatterton *et al.*, 2002; Sasaki *et al.*, 2002; Wada *et al.*, 2006; Tong *et al.*, 2008) and appear to be insensitive to most classical GluN2 containing NMDAR antagonists like APV and MK-801 (Chatterton *et al.*, 2002; Madry *et al.*, 2007). However, a high affinity (nM) GluN1 competitive antagonist CGP-78608 (mentioned as CGP below), was found to massively potentiate GluN1/GluN3A currents by preventing GluN1-induced desensitization (Yao, 2006; Grand *et al.*, 2018). Its use has been a game-changer to reveal the existence and functionality of di-heteromeric eGlyRs in the CNS (Grand *et al.*, 2018; Otsu *et al.*, 2019; Zhu *et al.*, 2020; Bossi *et al.*, 2022).

Still, the molecular mechanisms and structural correlates of GluN1/GluN3A properties remain poorly understood compared to other iGluRs. Despite only sharing a maximum of 23% identity with their NMDA orthologs, the GluN3 subunits share the typical modular architecture of an iGluR gene: an extracellular domain (ECD) composed of two clamshell domains: a large N-terminal Domain (NTD), a Ligand Binding Domain (LBD); followed by a Transmembrane Domain (TMD) carrying the channel pore and a short cytoplasmic C-terminal Domain (CTD). Yet, since no full-length structures of these receptors has been solved so far, we don't know how GluN1 and GluN3 subunits coassemble within a full GluN1/GluN3A tetrameric receptor. The assumptions about GluN1/GluN3A receptor molecular mechanisms thus rely on experimental functional read-outs (mostly TEVC) and on our extensive knowledge about the function and structure of other iGluRs.

The canonical iGluR gating mechanism is described by a model of equilibrium between three main states: 1) a unliganded resting state; 2) an active state in which ligand-binding in the LBDs induces its closure, promoting the opening of the TMD channel pore through increased tension on the LBD-TMD linker; 3) an inactive state in which the ligand-bound LBDs reorganize between each other to release the LBD-TMD linker tension leading to pore closure (Furukawa and Gouaux, 2003). The desensitization process of AMPA and Kainate receptors, and inhibition in GluN2 NMDARs do correspond to two different modalities of receptor inactivation that were both shown to critically involve conformational changes at the LBD-dimer interfaces (Sun *et al.*, 2002; Furukawa *et al.*, 2005; Weston *et al.*, 2006; Tajima *et al.*, 2016; Tian *et al.*, 2021). Overall, the typical 3-steps iGluR gating

mechanism should apply to GluN1/GluN3A receptors, but many key molecular details are still missing to explain their peculiar functional properties. In particular, we have to explain how glycine binding on GluN1 LBD can lead to the desensitization of GluN1/GluN3A receptors, while it acts as a co-agonist required for GluN1/GluN2 receptors activation.

Looking for the molecular determinants of the GluN1/GluN3A activation and desensitization mechanism, we implemented new methods to measure, inhibit or potentiate these receptors. In particular, we found strong gain-of-function (GoF) mutants, that allow the receptors to reach full active state. Overall, our data show that the intra-dimer LBD interface plays a key role in the gating properties of GluN1/GluN3A receptors. The functional analysis of these receptors allowed us to pinpoint a possible molecular origin for their atypical behavior, supporting their tonic activity in the central nervous system.

## Materials and Methods

**Molecular Biology.** The GluN1 splice variant 4A (named GluN1 herein) construct in pcDNA3 (Cummings *et al.*, 2017), the rat GluN3A in pcl\_NEO and site directed mutagenesis procedure were already described (Mony *et al.*, 2011).

**Oocyte treatment and microinjection.** *Xenopus laevis* eggs were used for heterologous expression of recombinant NMDA receptors. Oocytes were harvested and maintained as previously described (Hatton and Paoletti, 2005). Expression of recombinant NMDA receptors was obtained by oocyte nuclear co-injection of 46 nL of a mixture of cDNA (50 ng/ $\mu\text{l}$  at 1:1 ratio). Oocytes were kept at 18°C in 96-well plates containing standard Barth solution (in mM 88 NaCl, 1 KCl, 0.33  $\text{Ca}(\text{NO}_3)_2$ , 0.41  $\text{CaCl}_2$ , 0.84  $\text{MgSO}_4$ , 2.5  $\text{NaHCO}_3$ , and 7.5 HEPES, pH adjusted to 7.3 with KOH). The incubation solution was supplemented with Gentamycin (100  $\mu\text{g}/\mu\text{l}$ ) and CNQX (50  $\mu\text{g}/\mu\text{l}$ ), a NMDAR receptor antagonist.

**Two-electrode voltage-clamp recordings.** TEVC recordings were performed 48-72 hours after injection. TEVC recordings were performed using an oocyte Clamp Amplifier OC-725 (Warner Instruments). The recording system was controlled by employing the computer software pClamp 10.5 (Axon, Molecular devices) and a 1440A Digidata acquisition system (Molecular Devices). During the recording, cells were perfused with an external Ringer recording solution (in mM: 100 NaCl, 0.3  $\text{BaCl}_2$ , 5 HEPES, 2.5 KOH, pH adjusted to 7.3 with NaOH). A control solution (Ringer) was used for washout of drugs and test solutions. All recordings were performed at -60 mV holding potential and at room temperature. I/V curves were performed by doing voltage ramps ranging from -80 to +40 mV at different concentrations of open channel blockers. Values in the graphs have been normalized to +40 mV.

**Pharmacology.** CGP-78608 (Tocris) was prepared as a stock solution of 25 mM in 2.2 eq. NaOH solution and applied at 50 nM (slightly above  $\text{EC}_{50}$ ) or at 200 nM (saturation) before agonist perfusion (Grand *et al.*, 2018). CNQX (Alomone) was prepared in DMSO at stock concentrations of 50 mM or in water at a stock concentration of 20 mM. DCKA (Tocris) stocks (50 mM) were prepared in a 1 eq. NaOH solution. Aminoethyl-methanethiosulfonate (MTSEA; Biotium, Toronto Research Chemicals Inc.,) was prepared at 100 mM in DMSO. Pentamidine isethionate salt (Pentamidine, Sigma) was prepared at a stock concentration of 10 mM in water.

**Modeling.** 3D atomic model of the GluN1/GluN3A NMDAR (rat sequence) was produced using Modeller (Eswar *et al.*, 2006) with, as a template, the X-ray structure of

GluN1/GluN2B ifenprodil allosterically inhibited receptor : ID PDB: 4PE5 (Karakas and Furukawa, 2014) combined to the existing GluN3A LBD crystal structure 2RC7 (Yao *et al.*, 2008), but without the flexible C-terminal domain. We performed additional *ab-initio* loop-model reconstruction of missing loops. Analysis of residues contact at the LBD intradimer interface was performed with Cocomaps (Vangone *et al.*, 2011) with a cut-off contact distance <4 Å (<https://www.molnac.unisa.it/BioTools/cocomaps/>). AlphaFold 2 prediction of the LBD dimer structure of GluN1/GluN3A corresponds to the best model obtained using the multimer mode with 0.9 confidence score (Jumper *et al.*, 2021). The hydrophobic contribution of the substituted residues were estimated using the standard hydrophobicity scale free energy of transfer DG from water to POPC (White and Wimley, 1999). Structural illustrations were prepared with PyMOL (<http://pymol.org>).

**Data analysis.** Dose responses were fitted using different equations. Inhibitory dose response curves (DRC) of open channel blockers were fitted with the following Hill equation  $I_{\text{antago}}/I_{\text{control}} = 1 - (1 - \text{max}) / (1 + ([B]/IC_{50})^{nH})$ . In the equation :  $I_{\text{antago}}/I_{\text{control}}$  is the mean relative current, [B] is the concentration of the blocker, nH is the Hill coefficient (>0) and  $IC_{50}$  is the antagonist concentration that gives the half-maximal current inhibition max, the maximal inhibition, was fixed to 1 unless if stated otherwise. All parameters were set as free parameters.

Glycine DRC in CGP were fitted with the following Hill equation :  $I_{\text{rel}} = 1 / (1 + (EC_{50} / [Gly])^{nH})$ . In the equation  $I_{\text{rel}}$  is the relative mean current (Measured current / maximal current), [Gly] is the drug concentration, a is the maximal potentiation, nH is the Hill coefficient (>1) and  $EC_{50}$  is the concentration that gives the half-maximal current potentiation. The parameters were set as free parameter. Individual values for each glycine concentration were adjusted for tonic activation revealed by 100  $\mu$ M pentamidine application.

For the DRC of CGP potentiation in saturating glycine concentration (100  $\mu$ M), the following Hill equation was used:  $I_{\text{rel}} = 1 + 1 / (1 + (EC_{50} / [CGP])^{nH})$ . In the equation  $I_{\text{rel}}$  is the relative mean current, [CGP] is the drug concentration, nH is the Hill coefficient (>1) and  $EC_{50}$  is the concentration that gives the half-maximal current potentiation. The parameters were set as free parameters.

For the biphasic glycine-alone DRC, fitting was performed with the following Hill equation :  $I_{\text{rel}} = \text{max} / (1 + (EC_{50} / [Gly])^{nH1}) - \text{min} / (1 + (IC_{50} / [Gly])^{nH2})$ . In the equation  $I_{\text{rel}}$  is the relative mean current, nH1 is the hill slope of the activation component, nH2 is the hill slope of the inactivation component, [Gly] is the glycine concentration, max is the maximal potentiation, min is the maximal inhibition,  $EC_{50}$  is the  $EC_{50}$  of the excitatory component of GluN3A and  $IC_{50}$  is the  $IC_{50}$  of the inhibitory component of GluN1. The constraints were  $a > 0$ , [Gly] > 1,  $nH1 > 0$ ,  $nH2 > 0$ ,  $EC_{50} > 0$ ,  $IC_{50} > 0$ . Since we could test simultaneously a maximum 7 different ligand concentrations and the number of equation parameters is 6, the fit could not always converge satisfactorily without fixing an extra parameter to a constraint. When so, we fixed nH1 to a value rounded to the 0.1 precision by screening different values to produce the best possible  $R^2$  for the fit of the whole equation.  $EC_{50}$  and  $IC_{50}$  values reported for all bimodal glycinergic DRCs were calculated individually for each cell and then averaged to a mean for better accuracy

Remaining currents related to tonic activation were measured as:  $I_{\text{rel-tonic}} = |I_{\text{pent}}| / (|I_{\text{pent}}| + |I_{\text{max}}|)$ , where  $I_{\text{rel-tonic}}$  corresponds to the relative contribution of tonic ambient activation,  $|I_{\text{pent}}|$  is the inhibition of the baseline obtained with 100  $\mu$ M pentamidine,  $|I_{\text{max}}|$  is the maximal current recorded with glycine alone or glycine + CGP. For the DRC (see above), the obtained values of tonic current ( $I_{\text{tonic}} = I_{\text{max}} \times I_{\text{rel-}}$

tonic) for each conditions were added at each glycine concentration point..

CGP potentiation values were computed by calculating the ratio of peak current size for individual cells:  $I_{\text{Gly+CGP}} / I_{\text{Gly}}$ , with glycine at 100  $\mu$ M and CGP at 200 nM. The speed of glycine + CGP current relaxation was estimated by fitting the 10 seconds of slope using the straight line equation  $I = (a \times t) + b$ , with I the current, t time and a corresponding to the slope of relaxation in mA / second. MTSEA potentiation was calculated by computing the ratio  $I_m / I_a$  where  $I_a$  is the peak current obtained with the agonist after CGP pre-incubation and  $I_m$  is the current plateau obtained when adding MTSEA on top of the Glycine + CGP. Relative  $P_o$  values for the different constructs were obtained by calculating  $1 / \text{MTSEA-potentiation}$ .

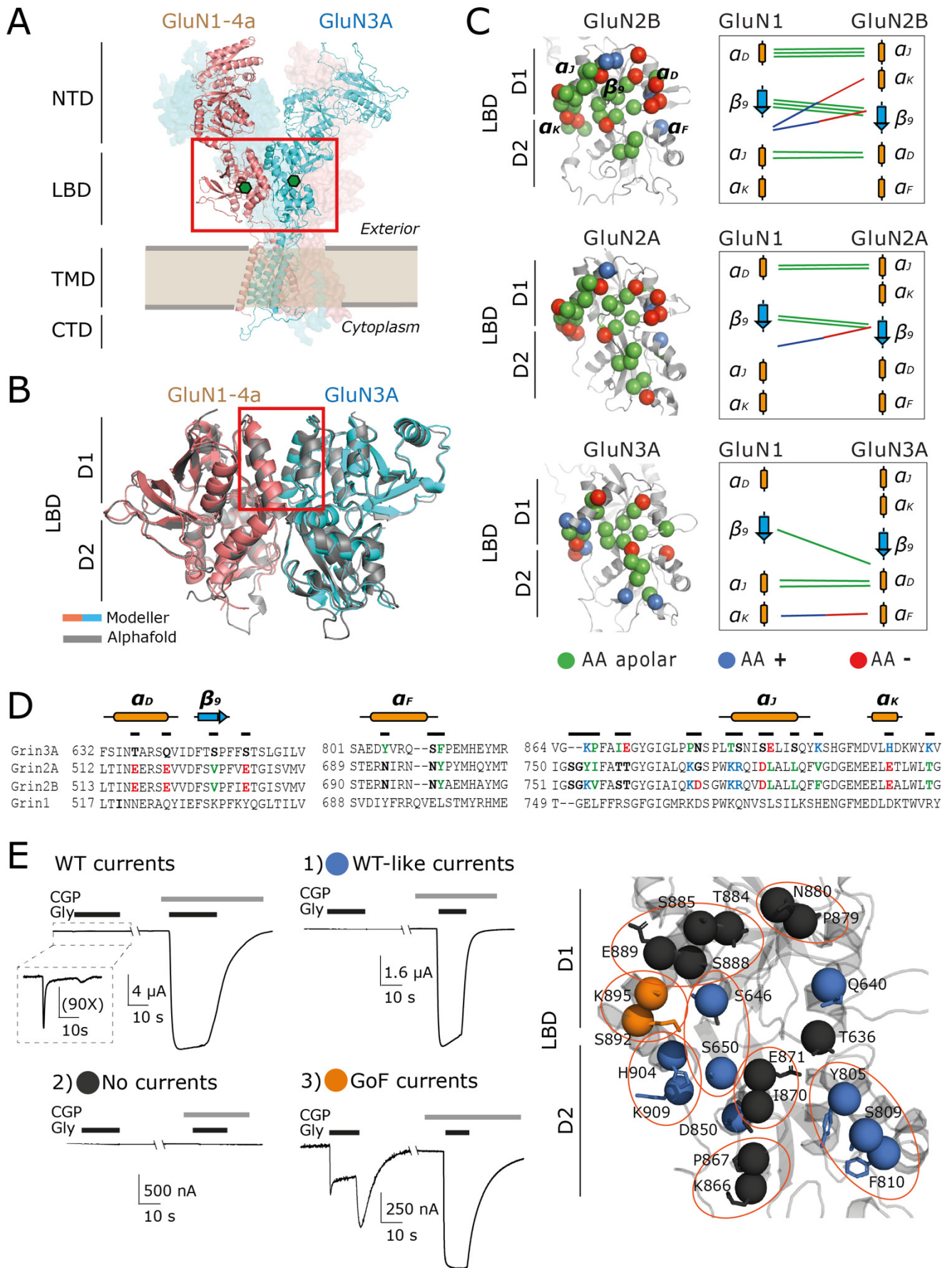
**Statistical analysis.** Data are presented as mean  $\pm$  standard deviation of the mean (SEM). Non-parametric tests were used to assess statistical significance. When comparing two conditions, the non-parametric Mann Whitney test was employed, while for more than two groups the non-parametric Kruskal-Wallis test was employed, with Dunn's multiple comparisons post hoc test. Statistical significances are indicated with \*, \*\*, \*\*\* when p- values are below 0.05, 0.01 and 0.001 respectively. n.s. indicates non-significant.

## Results

**Investigating the molecular specificities of GluN1/GluN3A receptors.** Our knowledge of iGluR molecular mechanism has greatly benefited from the combination of structural information and functional validations using pharmacological modulators and *ad-hoc* mutants (Hansen *et al.*, 2021; Tian *et al.*, 2021; Wang *et al.*, 2021; Yelshanskaya *et al.*, 2022). We implemented a similar approach to the study GluN1/GluN3A receptors functional mechanism by investigating in two directions:

1) The structure. Since only 4 isolated LBD structures of GluN3A are available in the Protein Data Bank (PDB IDs: RC7, 2RC8, 2RC9, 4KCD, (Yao *et al.*, 2008, 2013)), we built several homology models of almost complete tetrameric GluN1/GluN3A receptors. We used as templates the tetrameric structures of the closest NMDAR paralogs available: GluN2B (with 22% sequence identity). In our final model all GluN2B subunits were replaced by GluN3A subunits within an agonist-bound inhibited state of GluN1/GluN2B/GluN1/GluN2B tetrameric structure (Figure 1A). The model thus contains all the functionally important inter-subunit and inter-domain interfaces assembled, in particular the LBDs that form symmetrical dimers through a contact of their upperlobes (ID PDB: 4PE5 (Karakas and Furukawa, 2014), Figure 1A-B). In the absence of experimental full-length structure, the formation of this LBD-dimer remains to be proven for GluN1/GluN3A receptors. It appears as a reasonable hypothesis since such LBD dimers have been structurally observed in all vertebrate iGluR paralogs: AMPAR (Sun *et al.*, 2002; Sobolevsky *et al.*, 2009), GluK (Meyerson *et al.*, 2016), GluD (Burada *et al.*, 2020) and GluN2A or





methods). D1 states for the LBD upper lobe and D2 for the lower lobe. The red square highlights the predicted LBD intradimer interface between the two upper-lobes. **C**: Structural mapping of surface properties and contact-map at the LBD intradimer interface of GluN1/GluN2B, GluN1/GluN2A and GluN1/GluN3A. On the left, the surface distribution of the residues involved in the interface for GluN2B, GluN2A and GluN3A (at <7 Å distance from the partner subunit GluN1). Ca spheres of the corresponding residues are colored according to the properties of their lateral chains such as positively charged (blue), negatively charged (red) and hydrophobic (green). The LBD structure is shown in grey cartoon. In the upper GluN2B representation the location of the involved  $\alpha$  helices and  $\beta$  sheets is indicated. On the right, we mapped the corresponding predicted inter-subunit contacts (see methods), with the involved secondary elements shown as orange rods for  $\alpha$ -helices and arrows for  $\beta$ -sheets. The predicted electrostatic interactions are shown as red and blue lines and hydrophobic contacts as green lines. **D**: Amino acid (AA) sequence alignment of the region involved in the LBD dimer interface in selected GluNMDA receptor subunits. On top are indicated the corresponding secondary structure assignment (see panel C). Bolded AA do correspond to residues located at the interface. They are colored according to their biochemical properties using the same color code than panel C, unless the hydrophilic residues that are in black. The GluN3A residues that were mutated in the present study are indicated by a black line on top. **E**: Mutation scanning at the GluN3A LBD dimer interface. On the right are shown illustrative current traces of the WT phenotype and three different mutant phenotypes that we obtained in standard TEVC recording conditions (See Methods). The protocol involves a first application of saturating glycine (100  $\mu$ M – thick black lines) alone then co-application of CGP (200 nM - thick grey lines) and glycine (100  $\mu$ M). The panel on the left side shows a front view of the GluN3A LBD interface area (same as panel C), where interface residues (as sphere and sticks) are colored according the corresponding mutant phenotypes: in orange gain of function (GoF), in blue WT-like current phenotypes, and in black mutants that were functionally silent. Red circles identify some pairs or cohorts of residues we mutated together.

GluN2B containing NMDAR (Furukawa *et al.*, 2005; Karakas and Furukawa, 2014; Lee *et al.*, 2014; Tajima *et al.*, 2016; Zhu *et al.*, 2016; Jalali-Yazdi *et al.*, 2018) and even in distant plant iGluR paralogs (Gangwar *et al.*, 2021; Green *et al.*, 2021). Independently, we used the latest version of the IA-based *ab-initio* protein folding: alphafold 2, to predict the structure of the GluN1/GluN3A LBD dimer (Jumper and Hassabis, 2022). Supporting the likeliness of our model, the *ab-initio* prediction and our educated-guessed model appear almost fully identical with a rmsd of 1.03 Å (Figure 1B).

2) The modulators. We first revisited the potency of non-orthosteric inhibitors using the mutation GluN1-F484A (Awobuluyi *et al.*, 2007; Madry *et al.*, 2007) that allows to work with non-desensitizing GluN1/GluN3A receptors. GluN2 pore blockers in particular are known to be poorly inhibiting GluN3A containing receptor (Chatterton *et al.*, 2002). At a resting potential of -60mV,  $Mg^{2+}$  blocks GluN2 containing receptors in the  $\mu$ M range conferring to these receptors a coincidence-detector capability that is critical for their role in the CNS (Nowak *et al.*, 1984; Kuner and Schoepfer, 1996). In the same conditions,  $Mg^{2+}$  appear far less efficient against GluN1/GluN3A receptors with an  $IC_{50}$  of  $6.3 \text{ mM} \pm 0.83$  ( $n=3$  – Figure S1A), which is above the physiological concentration of this ion ( $\approx 1 \text{ mM}$ ) in the cerebro-spinal-fluid (CSF) (Kapaki *et al.*, 1989). Looking for potent pore blocker of GluN3A containing receptor, we tested other known NMDAR inhibitors. We found pentamidine (Reynolds and Aizenman, 1992) to be a potent one with an  $IC_{50}$  of  $26 \mu\text{M} \pm 5$  ( $n=6$  – Figure S1B-C) and a maximum inhibition of  $92 \pm 2\%$  at 500  $\mu$ M (Figure S1C). Despite a weaker potency than on GluN2 containing NMDARs ( $IC_{50}$   $2.59 \mu\text{M} \pm 0.19$ ) (Reynolds and Aizenman, 1992), pentamidine is so far the GluN3A pore blocker with the highest  $IC_{50}$  (Kaniakova *et al.* 2018).

**Molecular specificities of GluN1/GluN3A receptors at the LBD dimer interface.** Following a strategy successfully used for GluN2 receptors

(Gielen *et al.*, 2008; Riou *et al.*, 2012; Zhu *et al.*, 2013; Esmenjaud *et al.*, 2019; Tian *et al.*, 2021) we investigated the functional importance of several different interfaces by targeted double-cysteine mutagenesis of GluN1/GluN3A receptors extracellular domain (ECD). However, none of the 11 cysteine mutant pairs we tested gave usable or reliable currents in the absence or presence of CGP and in oxidant or reducing condition (data not shown). Since the cysteine mutant approach appears somehow deleterious for the receptor expression or folding, we looked at another mutagenesis strategy that could modulate GluN3A gating without affecting the agonist binding pocket.

The LBD dimer interface is of critical importance for iGluR gating and desensitization mechanism (Sun *et al.*, 2002; Armstrong *et al.*, 2006; Weston *et al.*, 2006; Gielen *et al.*, 2008). In its 'canonical' active and resting state the LBD dimer interface is formed by the contact between the upper-lobes (D1 – as in Figure 1B) of the two LBDs, behaving as a fulcrum for agonist binding to pull open the pore. The amino-acid composition of this interface determines its stability, thereby controlling its transition to a desensitized state where the interface is broken impairing activation by the agonist (Sun *et al.*, 2002). In NMDAR, hydrophobic contacts were shown to be important for LBD dimer interface stability (Furukawa *et al.*, 2005; Gielen *et al.*, 2008; Hackos *et al.*, 2016). By analyzing available solved structures we can show that the GluN1/GluN2B LBD interface involves three main hydrophobic cluster contacts and two inter-subunit ionic bonds (Figure 1C), while GluN1/GluN2A is stabilized by two of the GluN1/GluN2B hydrophobic clusters and one of its ionic-bonds. This small qualitative difference illustrates the putative weaker stability of this interface in GluN2A compared with that of GluN2B (Tian *et al.*, 2021). The same analysis of our structural template of GluN1/GluN3A LBD dimer interface reveals a completely different inter-subunit points of contacts both in terms of number and localization of hydrophobic contacts and ionic bond



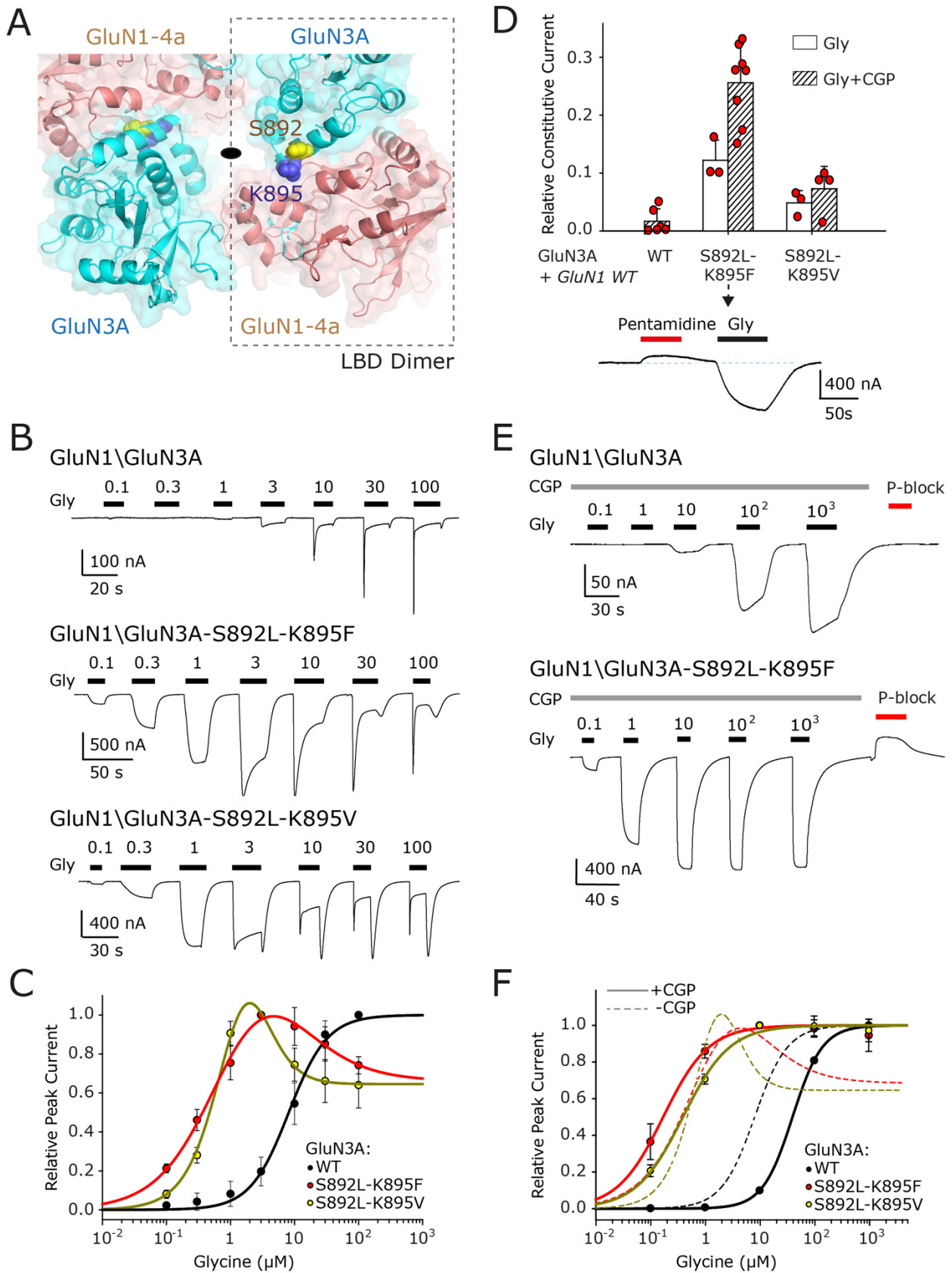


**Figure 2. GluN3A LBD interface mutants with increased glycine sensitivity.** **A:** Structural localization of the GoF double mutant within the LBD tetramer, viewed from the top (same colors than Fig1A). The LBD dimer couple is shown with a black rectangle. The center of the 2-fold symmetry is shown with a black ellipse to highlight the inner region of the tetramer. The GluN3A GoF residues 892 and 895 are shown in spheres with respective colors yellow and blue. **B:** Glycine current traces of GluN1/GluN3A-WT and mutant GluN1/GluN3A-S892L-K895F (GluN2B-like) and GluN1/GluN3A-S892L-K895V (GluN2A-like) obtained with standard TEVC procedure. Glycine concentrations are in  $\mu\text{M}$ . **C:** Glycine dose-response curves (DRC) of peak current are shown in black for GluN1/GluN3A-WT, in red for GluN1/GluN3A-S892L-K895F and in yellow for GluN1/GluN3A-S892L-K895V. Mutant DR had to be fitted with a double-exponential equation to account for the presence of both an activatory and an inhibitory component. For the values of  $\text{EC}_{50}$ ,  $\text{IC}_{50}$ , Hill slope (nH) and statistics, refer to Table 1. **D:** Quantification of tonic currents in GoF mutants. In the inset below, the current trace of the GluN1/GluN3A-S892L-K895F mutant reveals the presence of

tonic current. The application of the open channel blocker pentamidine at 100  $\mu\text{M}$  (thick red lines) induces positive steady state current above the baseline. On the top is represented the relative contribution of tonic current compared to the max current. The max current was recorded either in saturating Glycine alone (white bars) or in Glycine plus CGP (striped bars). **E**: Glycine current traces under CGP application at 50 nM for GluN1/GluN3A-WT and GluN1/GluN3A-S892L-K895F. Glycine concentrations are in  $\mu\text{M}$ . After removal of the agonists, application of 100  $\mu\text{M}$  of the pore-blocker pentamidine allows to quantify tonic current contribution (see panel D). **F**: DRC of glycine peak current in presence of 50 nM CGP (same color code than panel C). Dotted lines correspond to the glycine DRCs of panel 2C. For the values of  $\text{EC}_{50}$  and nH and statistics, refer to Table 1.

(Figure 1C) interrogating the stability of this interface in GluN1/GluN3A receptors.

**Chimeric scanning of the LBD dimer interface of GluN1/GluN3A receptors.** We first attempted to test the functional effect of stabilizing the LBD interface in GluN1/GluN3A by reverting the whole LBD of GluN3A in the GluN2B LBD. This LBD swapping chimeric strategy worked for other iGluRs (Schmid *et al.*, 2009). However, the TEVC test of the corresponding GluN1/GluN3-LBD2B chimera didn't show any current, even with CGP and glycine applications. We then reasoned that we could try to impair desensitization while limiting stability issue, by reverting the GluN3A residues facing the LBD dimer interface to the corresponding ones of GluN2B. We identify 23 residues of the GluN3A side of the interface that are pointing directly toward the GluN1 interface in our models and whose corresponding homologs strongly differ in GluN2B (among which 6 charged to apolar residue conversions) (Figure 1D).

We mutated one by one (mostly by neighboring pairs or clusters) the 23 residues of the putative interface area of GluN3A in order to form a chimera with fully mutated GluN2B-like surface on the GluN3A subunit. This surface chimera showed no current with TEVC (– not shown). However, the functional test of the intermediate partially reverted mutants allowed us to map which region of the GluN3A interface tolerates the reversion into the residue composition of GluN2B (Figure 1E). Applying either glycine alone or glycine plus the potentiator CGP, we were able to distinguish 3 phenotypes: 1) Wild-type-like phenotype with very little or no current in glycine alone but large currents with CGP, 2) Loss of function (LoF) mutants with no detectable currents in both conditions, 3) Gain of function (GoF) mutants with large currents in both conditions.

In particular, a GoF (3) phenotype is observed with GluN1/GluN3A-S892L-K895F, a double mutant located in the inner side of the LBD GluN3A dimer interface (Figure 1E). Its expression success rate, as recorded with glycine induced current, appears almost 5 times superior to GluN1/GluN3A (Figure S2A). Interestingly, the two individual mutants GluN1/GluN3A-S892L and GluN1/GluN3A-K895F exhibit much lower expression (Table 2) pointing towards a synergetic effect of the double mutation. Indeed, the residues S892 and K895 in GluN3A do correspond to L781 and F784 of GluN2B that lie at the core of a hydrophobic cluster at the GluN1-GluN2B interface (Figures 1C-D & 2A). The F784 in GluN2B do correspond to V783 of GluN2A (Figure

1D), and it has been shown that mutation F784V in GluN2B is sufficient to confer the sensitivity to GluN2A-specific positive allosteric modulator at this interface (Hansen *et al.*, 2012; Hackos *et al.*, 2016). While presenting a slightly weaker phenotype than the GluN3A-S892L-K895F mutant, GluN3A S892L-K895V also presents a GoF phenotype (3), with large size glycine-alone induced currents (Figure S2A) and high expression rate (Table 2).

**GluN3A LBD-interface mutants exhibit increased glycine sensitivity.** Both double-mutants exhibit strongly modified glycine dose response (Figures 2B, 2C & S2B) with large non-desensitizing currents at 1  $\mu\text{M}$  glycine. The glycine dose-response (DR) is biphasic with an activation part showing peak-current  $\text{EC}_{50}$ , respectively at  $0.68 \mu\text{M} \pm 0.24$  ( $n=5$ ) and  $0.50 \mu\text{M} \pm 0.11$  ( $n=5$ ) for GluN1/GluN3A-S892L-K895F and GluN1/GluN3A-S892L-K895V, and a steady-state of  $0.59 \mu\text{M} \pm 0.28$  ( $n=5$ ) and  $0.62 \mu\text{M} \pm 0.13$  ( $n=4$ ) respectively (Figure 2B & S2B, Table 1). The inhibition part of the biphasic DR peak presents an  $\text{IC}_{50}$  of  $5.49 \mu\text{M} \pm 1.41$  and  $3.21 \mu\text{M} \pm 1.43$  respectively (Figure S2B). Above 3  $\mu\text{M}$  of glycine application, the mutant receptors faced increasing desensitization linked to glycine binding on GluN1 subunit, like already observed in GluN1/GluN3A WT receptors (Chatterton *et al.*, 2002; Awobuluyi *et al.*, 2007; Grand *et al.*, 2018). The glycine  $\text{EC}_{50}$  of the mutants, that is associated to glycine binding on the GluN3A subunit, thus shows one order of magnitude decrease (on average) compared to GluN1/GluN3A WT. Moreover, the addition of the pore blocker pentamidine (Figure 2D, S1A-B & S2C) on the current baseline of the mutants revealed the inhibition of small constitutive currents. We estimated that the GluN1/GluN3A-S892L-K895F mutant is already  $12\% \pm 3.5$  ( $n=3$ ) activated in our ringer before glycine application, but  $25\% \pm 6.6$  ( $n=8$ ) in the presence of CGP-78608 and glycine (Figure 2D). Indeed, the decrease of glycine  $\text{EC}_{50}$  of the double mutants is even more marked in the presence of CGP (Figure 2E-F). The observed tonic current likely corresponds to residual activation by ambient glycine contamination (around dozen of nM (Ascher, 1990)). Altogether, these observations underline the strong increase of glycine sensitivity in GluN1/GluN3A-S892L-K895F and GluN1/GluN3A-S892L-K895V mutants.

**GluN3A S892L-K895F: a strong gain-of-function mutant.** As already illustrated in the dose-response, the double-mutants didn't prevent the typical GluN1/GluN3 receptor desensitization at high glycine-alone applications. In the presence of CGP-78608,

**Table 1: Effects of LBD intradimer interface mutations on agonist affinity for GluN1/GluN3A receptors**

Construct	Glycine EC <sub>50</sub>				Glycine EC <sub>50</sub> with CGP				Tonic current		
	Peak current (μM)	n <sub>H</sub>	# cells	Steady state (μM)	n <sub>H</sub>	# cells	Peak current (μM)	n <sub>H</sub>	# cells	Ratio tonic current / max current	# cells
GluN3A WT	8.1 ± 0.5	1.28	5	3.9	2.46	1 <sup>c</sup>	45.98 ± 1.77	1.59	5	0.01 ± 0.02 <sup>e</sup>	6 <sup>e</sup>
GluN3A mutant											
GluN3A S650E-D850N-S892L-K895F-H904E-K909T (6x)	N.D.	N.D.	N.D.	0.49 ± 0.03 <sup>a</sup>	1.40 <sup>b</sup>	4	N.D.	N.D.	N.D.	0.08 ± 0.04 <sup>d</sup>	3 <sup>d</sup>
GluN3A S892L-K895F (2x)	0.68 ± 0.24 <sup>a</sup>	0.90 <sup>b</sup>	5	0.59 ± 0.28 <sup>a</sup>	1.07	5	0.16 ± 0.02	1.11	8	0.12 ± 0.03 <sup>e</sup> , 0.23 ± 0.06 <sup>e</sup>	3 <sup>d</sup> , 8 <sup>e</sup>
GluN3A S892L-K895V	0.50 ± 0.11 <sup>a</sup>	1.40 <sup>b</sup>	5	0.62 ± 0.13 <sup>a</sup>	1.40 <sup>b</sup>	4	0.39 ± 0.05	1.01	4	0.04 ± 0.02 <sup>d</sup> , 0.07 ± 0.03 <sup>e</sup>	3 <sup>d</sup> , 4 <sup>e</sup>
GluN3A S892L-K895I	1.13 ± 0.62 <sup>a</sup>	1.38	5	0.63 ± 0.07 <sup>a</sup>	1.50 <sup>b</sup>	5	N.D.	N.D.	N.D.	0.01 ± 0.01 <sup>d</sup> , 0.23 ± 0.3 <sup>e</sup>	3 <sup>d</sup> , 3 <sup>e</sup>
GluN3A S892L-K895W	N.D.	N.D.	N.D.	N.D.	N.D.	N.D.	0.9 ± 0.22	1.11	4	0.17 ± 0.18 <sup>e</sup>	4 <sup>e</sup>
GluN3A S892L-K895F-H904E-K909T (4x)	N.D.	N.D.	N.D.	0.13 ± 0.04 <sup>a</sup>	1.65	5	N.D.	N.D.	N.D.	0.10 ± 0.02 <sup>d</sup>	4 <sup>d</sup>
GluN1 mutant											
GluN1 I519D	N.D.	N.D.	N.D.	N.D.	N.D.	N.D.	1.02 ± 0.18	2.41	2	0.04 ± 0.01 <sup>e</sup>	2 <sup>e</sup>
GluN1 mutant/GluN3A mutant											
GluN3A S892L-K895F/GluN1 I519D	N.D.	N.D.	N.D.	N.D.	N.D.	N.D.	0.16 ± 0.08	1.16	4	0.24 ± 0.09 <sup>e</sup>	4 <sup>e</sup>

A= EC50s were calculated for each individual cells glycine DRs, and then averaged. B= fixed nH to a value rounded to the 0.1 precision by screening different nH values to produce the best possible rsqr for the fit of the equation (see methods). C= due to small sizes of the WT steady state currents, we picked a representative trace with the largest SS current, to avoid bias due to the imprecision of the recordings. D= ((100 μM pentamidine inhibition + maximal peak current values given by glycine) \ 100 μM pentamidine inhibition - baseline resting state). E= (100 μM pentamidine inhibition + maximal peak current value recorded with CGP and glycine) \ 100 μM pentamidine inhibition - baseline resting state). N.D., not determined; Data are presented as mean ± standard deviation of the mean (SEM)

**Table 2: Effects of LBD intradimer interface mutations on biophysical properties for GluN1/GluN3A receptors**

Construct	Expression efficiency of injected cells			GluN1 antagonist Potentiation		MTSEA potentiation (Po)		Desensitization kinetics		Current relaxation	
	Expression % with glycine	Number of oocytes tested	Expression % with glycine + CGP	Ratio [GluN1 antagonist] / [GluN1]	# cells	Ratio [MTSEA] / [GluN1]	# cells	Tau glycine (ms)	# cells	Slope with CGP (mA/s)	SD # cells
GluN3A WT	10.2	136	38.4	164.8 ± 85.8	5	16.4 ± 7.3 <sup>a</sup> , 4.4 ± 1.4 <sup>b</sup>	6 <sup>a</sup> , 10 <sup>b</sup>	367.9 ± 171	9	4.93E-05	3.82E-05
GluN3A mutant											
GluN3A S650E-D850N-S892L-K895F-H904E-K909T (6x)	38.6	44	57.1	57.9 ± 25.18	5	N.D.	N.D.	1032.3 ± 503	4	N.D.	N.D.
GluN3A Y805N-S809N-F810Y-S892L-K895F-H904E-K909T (7x)	35.2	17	N.D.	N.D.	N.D.	0.7 ± 0.1 <sup>a</sup>	3 <sup>a</sup>	N.D.	N.D.	N.D.	N.D.
GluN3A S892L	6.4	31	6.6	62.6 ± 30.6	2	N.D.	N.D.	180.4 ± 10	2	9.65E-06	8.73E-06
GluN3A S892L-K895F (2x)	48	204	66.2	2.4 ± 0.8	12	1 ± 0.1 <sup>a</sup> , 0.8 ± 0.1 <sup>b</sup>	5 <sup>a</sup> , 8 <sup>b</sup>	1846.7 ± 827	13	7.73E-07	6.06E-07
GluN3A S892L-K895V	27.6	71	65.3	8.0 ± 4.4	6	2.6 ± 0.9 <sup>a</sup>	5 <sup>a</sup>	551.4 ± 135.7	4	3.74E-06	3.15E-06
GluN3A S892L-K895I	26.6	69	66.6	8.6 ± 5.8	4	3.2 ± 0.5 <sup>a</sup>	4 <sup>a</sup>	997.8 ± 277	7	6.43E-06	1.11E-05
GluN3A S892L-K895W	26	23	66.6	4.9 ± 1.4	5	1.2 ± 0.1 <sup>a</sup>	4 <sup>a</sup>	908.3 ± 478	5	1.29E-06	4.37E-06
GluN3A S892L-K895F-H904E-K909T (4x)	43.2	81	75	14.4 ± 2.3	4	0.9 ± 0.1 <sup>a</sup>	4 <sup>a</sup>	1196.6 ± 656	4	4.19E-08	4.08E-06
GluN3A K895F	0	24	7.4	N.D.	N.D.	N.D.	N.D.	N.D.	N.D.	3.96E-07	3.67E-07
GluN1 mutant											
GluN1 I519D	0	5	18.5	N.D.	N.D.	1.2 ± 0.1 <sup>b</sup>	4 <sup>b</sup>	N.D.	N.D.	2.24E-05	3.21E-05
GluN1 mutant/GluN3A mutant											
GluN3A S892L-K895F/GluN1 I519D	10.8	37	34.4	28 ± 21.8	4	N.D.	N.D.	611.9 ± 287	5	6.27E-07	5.10E-06

Expression efficiency of injected cells shows the percentage of cells we could obtain electrical activity from, alongside a raw number of cells tested. This quantification shows how some mutants increase or decrease the proportions of cells showing functional activity. For this categorization, 10 nA of current was considered as the minimum threshold to distinguish a current from electrical noise. a : GluN3A WT coexpressed with cysteine pore mutant GluN1 A652C. b : GluN1 WT coexpressed with cysteine pore mutant GluN3A A765C. The tau of desensitization were obtained by fitting currents with a single-exponential component to a time window corresponding to 10–90% of maximum desensitization values. N.D., not determined.

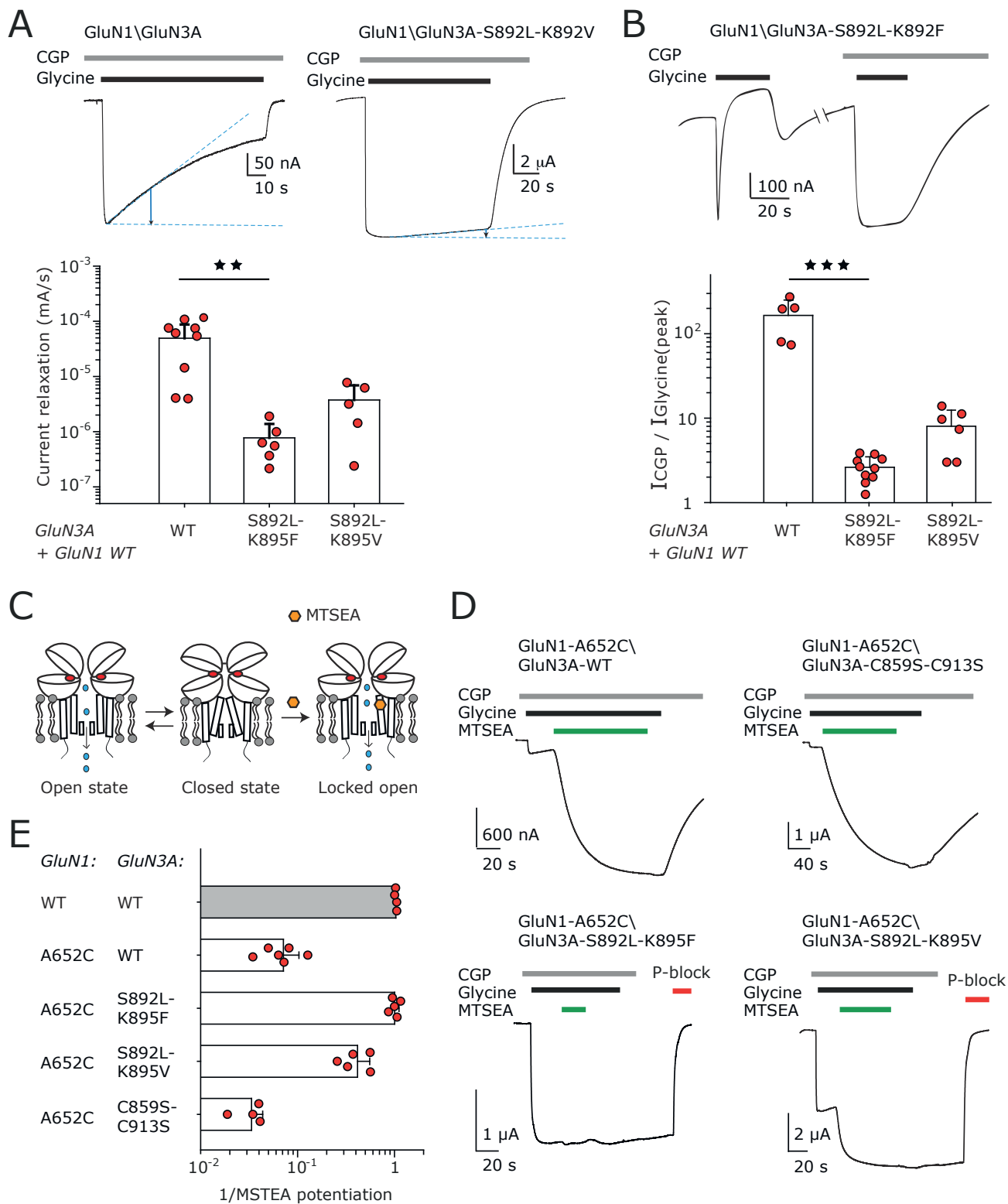


**Figure 3. Gain-of-function mutants phenotype at GluN3A LBD interface.** **A:** The mutants slow the current relaxation kinetics in saturating glycine (100  $\mu$ M) and CGP (200 nM). On the top the current traces show the large kinetic difference between GluN1/GluN3A-WT and GluN1/GluN3A-S892L-K895F, as illustrated by the different angles of the virtual dotted blue lines and the arrows. The histogram at the bottom shows quantification of the linearized slope of the current relaxation for WT and mutants. See Table 2 for the values. **B:** The mutants reduce CGP potentiation. The top trace shows a first activation by 100  $\mu$ M glycine, then the coactivation by CGP (200 nM) and glycine (100  $\mu$ M) for the mutant GluN1/GluN3A-S892L-K895F. The histogram at the bottom shows the quantification of the CGP-induced potentiation compared to the glycine peak current size. Please note the 100-fold difference of CGP potentiation between the WT and the GluN3A-S892L-K895F mutant. **C:** MTSEA molecule mode of action on NMDAR activation mechanism. The agonist (red ellipse) bound receptor on the left schematizes the activation equilibrium between the closed and the open state. The cysteine point mutant (hexagonal orange) in the pore allows MTSEA (green molecule) binding, which locks the receptors into a constitutive open state (on the right). **D:** Current traces showing MTSEA induced potentiation of GluN3A-WT, and GluN3A-C859S-C913S and the interface mutants GluN3A-S892L-K895F, GluN3A-S892L-K895V, all co-expressed with GluN1 A652C for MTSEA attachment. All conditions require pre-incubation with 200 nM CGP, followed by 100  $\mu$ M glycine, before application of 300  $\mu$ M MTSEA. The MTSEA potentiation is abolished in the mutants GluN3A-

S892L-K895F while it is increased in the mutant C859S-C913S compared to the WT. Please note that MTSEA-bound GluN3A WT behaves differently from GluN2 containing NMDARs (Yuan *et al.*, 2005; Gielen *et al.*, 2009) since it does not result in a permanent constitutive activation. However, the GluN3A interface GoF mutants appear trapped in a constitutive active conformation, that can be inhibited by pentamidine (100  $\mu$ M). **E**: Quantification of the relative  $P_o$  of the different GluN3A constructs tested in panel 3D. The relative  $P_o$  is estimated by the ratio between the glycine+CGP max current and the maximal current after MSTEA application (1/MTSEA potentiation). See table 2 and figure S3 for the values and additional informations.

this fast desensitization of GluN1/GluN3A-WT receptor is almost abolished (Grand *et al.*, 2018). Still, the resulting steady state current is slowly reducing with time, likely because of slow CGP washout by glycine within the GluN1 binding site (Grand *et al.*, 2018). Interestingly, our double mutants greatly reduce this current drop in the presence of CGP, allowing to record GluN3A receptors with large stable currents (Figure 3A, table 2).

Glycine-induced current of GluN1/GluN3A-WT can be potentiated more than 100 fold by CGP, highlighting the overall poor gating efficiency of the receptor (Grand *et al.*, 2018). GluN3A S892L-K895F and GluN3A S892L-K895V mutants are respectively  $2.61 \pm 0.86$  fold ( $n=10$ ) and  $8.01 \pm 4.41$  ( $n=4$ ) fold potentiated by CGP (Figure 3B, 1E). This phenotype can't be explained by a lower efficiency of CGP on the mutants since the CGP DR of GluN3A S892L-K895F ( $EC_{50}$  33.1 nM  $\pm 1.2$ ,  $n=5$ , figure S4A) lies in the same range than in the WT ( $EC_{50}$  26.3 nM  $\pm 5$  - Grand *et al.*, 2018). Such a strong reduction of CGP potentiation rather indicate that the mutant receptors are already close to their maximal activation in glycine alone conditions, and thus that the double-mutant is potentiating the GluN1/GluN3A receptor open probability ( $P_o$ ).

Since no simple tool was available to estimate the open probability of GluN1/GluN3A receptors, we implemented an MTSEA cross-linking approach that has already been validated to estimate the relative  $P_o$  of GluN1/GluN2 receptors mutants and chimeras (Yuan *et al.*, 2005; Gielen *et al.*, 2009). The application of the cysteine reactive crosslinker MTSEA on a GluN1/GluN2 receptor with a cysteine point mutation in the SYTANLAAF motif at the M3 TM helix of the gate allows to permanently lock open the ion channel in a constitutive open state (Figure 3C). As in GluN2 receptors, the corresponding mutant GluN1-A652C/GluN3A-WT was potentiated 16.4 fold  $\pm 7.3$  ( $n=6$ ) upon application of MTSEA on top of CGP and glycine (Figure 3D-E), while the control GluN1-WT/GluN3A-WT is not potentiated by MTSEA (not shown). The approach also works with the cysteine mutant A765C on the GluN3A subunit (co-expressed with GluN1 WT) but displays smaller amplitudes of MTSEA potentiation (Figure S3). We also tried MTSEA application on glycine-alone (without CGP) evoked currents but it was too slow to be used experimentally (not shown). The MTSEA methodology thus requires the use of CGP to allow  $P_o$  estimation of GluN1/GluN3A constructs.

If MTSEA potentiated receptors correspond to fully active receptors, then the receptor relative  $P_o$  should

be inversely correlated to the ratio between the agonist induced-current level (before MTSEA application) and the plateau in presence of MTSEA (Yuan *et al.*, 2005; Gielen *et al.*, 2009). We observed that, contrary to GluN1-A652C/GluN3A-WT receptors, the LBD interface double-mutants did show no (or minimal) current increase upon MTSEA application (Figure 3D-E, Table 2). This indicates that the mutant GluN3A-S892L-K895F is already at maximal relative  $P_o$  ( $1.0 \pm 0.1$  fold MTSEA potentiation,  $n=5$ ) in presence of glycine and CGP while the mutant GluN3A-S892L-K895V displays a bit lower relative  $P_o$  ( $2.6 \pm 0.9$  fold MTSEA potentiation,  $n=5$ ).

The MTSEA methodology also allows to determine the activity of other known GluN1/GluN3A mutants. As an alternative to CGP application on WT receptors, GluN1-F484A/GluN3A-WT mutant has been shown to abolish GluN1-dependant desensitization through the impairment of glycine binding to its GluN1 binding site (Awobuluyi *et al.*, 2007; Madry *et al.*, 2007). This mutant thus allows to record large stable currents with GluN1/GluN3A receptors, however it is no more sensitive to CGP (Grand *et al.*, 2018). The MTSEA potentiation of the GluN1-F484A/GluN3A-A765C in the absence of CGP shows a four fold decrease of relative  $P_o$  compared to WT in CGP (Figure S3). Interestingly, the GluN1-F484A mutant appears thus less efficient than CGP to potentiate the receptor likely because of a lower efficiency to reduce the GluN1-dependant desensitization component.

Looking for the gating link between the LBD to the pore, we also analyzed the activity of GluN3A C859S-C913S mutant that partially uncouples the LBD to the TMD, and has been previously been shown to enhance GluN3A glycine sensitivity (Grand *et al.*, 2018). MTSEA-induced current potentiation phenotype of this mutant indicates a two fold decrease of the relative  $P_o$  compared to WT receptors (Figure S3). This loss of  $P_o$  shows that the mutant may have directly uncoupled the transduction mechanism from the GluN3A-LBD to the pore, that would also have released the high glycine affinity potential of GluN3A LBDs (Yao, 2006).

Compared to these latter mutants with increased activity (reduced desensitization for GluN1-F484A/GluN3A and decreased glycine  $EC_{50}$  for GluN3A C859S-C913S) but reduced  $P_o$ , the large  $P_o$  increase of our GoF LBD-interface mutants thus appears specific. The possibility to reach a relative  $P_o$  of 1 (GluN3A S892L-K895F – Figure 3D-E) further highlights the importance of the LBD-dimer interface in regulating GluN1/GluN3A receptor gating activity.



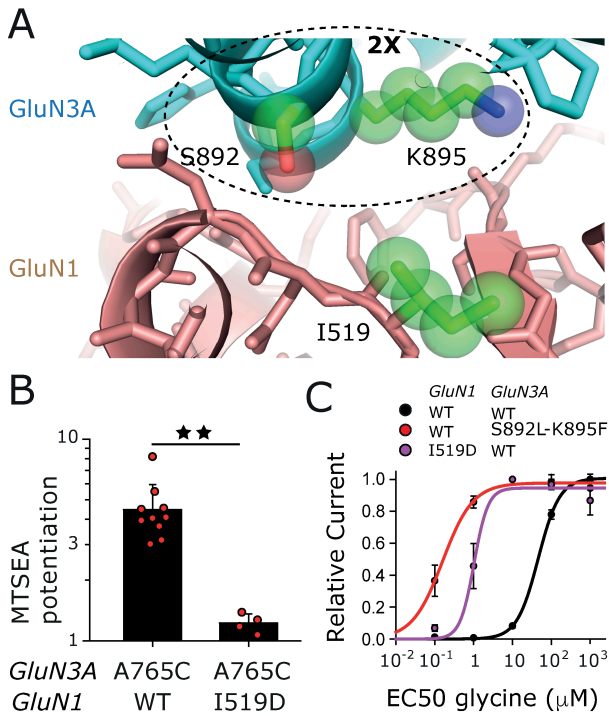


**Figure 4. Validating the GluN1 - GluN3A contact at their LBD intra-dimer interface.**

**A:** Zoom on the dimer interface of the GluN1/GluN3A LBD model. The local environment of the double mutant region (region 2X: circled with dotted line) is shown with the same global color code and top view than Figure 2A, with sticks representation. The lateral chains of the mutated residues are in sphere, and color coding: green, blue and red for C, N, O atoms respectively. **B:** The GluN1-I519D mutant exhibits similar relative Po gain-of-function phenotype than the 2X mutants. The MTSEA potentiation ( $1/Po$ ) of the GluN1 mutant and WT were measured using the MTSEA cross-linking approach (see methods) but on the GluN3A-A765C background. Refer to Table 2 for values. **C:** The GluN1-I519D/GluN3A-WT mutant exhibits similar glycine sensitivity gain-of-function phenotype than the 2X GluN3A mutants. The DRC of glycine peak current in presence of 50 nM CGP is shown for GluN1/GluN3A-WT (black), GluN1/GluN3A-S892L-K895F (red) and GluN1-I519D/GluN3A-WT (purple). Refer to Table 1 for the  $EC_{50}$  and nH and statistics.

**Linking interface properties and gating.** In both our GluN1/GluN3A receptor structural models, the residues of the double-mutant are predicted to contact a corresponding hydrophobic area on GluN1 (Figure 4A). We reasoned that if our mutants gained their GoF phenotype by reforming the hydrophobic LBD contact, disturbing the corresponding hydrophobic patch on the GluN1 side should also disturb their phenotype. In GluN1/GluN2A receptors, the mutant GluN1-I519D has been shown to destabilize the LBD dimer interface through the disruption of the same hydrophobic cluster with minimal effect on GluN1 glycine binding sensitivity (Gielen *et al.*, 2008) (M. Gielen personal communication). In our GluN1/GluN3A model, GluN1-I519D is facing the residues Ser-892 and Lys-895 mutated in our GoF double mutant (Figure 4A). When co-injected with GluN3A-WT receptors, GluN1-I519D leads to a strong increased of glycine  $EC_{50}$  in the presence of CGP ( $1.02 \mu M \pm 0.18$ ,  $n=2$  - Figure 4B) but

also of  $Po$  ( $1.2 \pm 0.1$ ,  $n=4$  - Figure 4C), thus exhibiting a similar GoF phenotype than the double-mutants. Unfortunately, the GluN1-I519D-A652C/GluN3A-S892L-K895F mutant never gave currents, impairing  $Po$  estimation. However, the mutant GluN1-I519D/GluN3A-S892L-K895F exhibits a ten-fold increase of CGP potentiation compared to the double mutant alone (Figure S4C). The absence of additive positive phenotypic effect in the GluN1-I519D/GluN3A-S892L-K895F mutant but rather a LoF phenotype indicates that the single and the double mutants can disrupt each other phenotype, likely through a direct interaction as predicted in our model.

We then questioned which properties of the LBD dimer interface (Figure 4A & 5A) can allow the emergence of such massive GoF mutant phenotype. Since we observed significant phenotypic differences of  $Po$  and CGP potentiation between GluN3A-S892L-K895F and GluN3A-S892L-K895V, we examined the effect of the introduction of other amino-acids at the K895 site on the activity of the receptors. The K895 site (Figure 4A & 5A) seemingly tolerates the introduction of different hydrophobic residues that all present a much higher  $Po$  than the WT. Moreover, a clear tendency can be observed with large hydrophobic residues (Phe or Trp) getting  $Po$  close to 1 and smaller residues (Val, Ile) showing intermediate  $Po$  phenotypes (Figure 5C-D, Table 2 - Figure S3). We noted however that the large Trp exhibit smaller  $Po$  effect than Phe, which may represent some steric limitations linked to the size and/or shape within the hydrophobic contact area with GluN1. These observations underline the critical importance of the distribution of hydrophobic patches on the GluN3A inner-side of the LBD dimer interface.

We then wondered if stronger GoF phenotypes can be obtained by other mutations at the LBD dimer interface. Our initial strategy of chimeric reversion at the GluN3A LBD dimer interface identified other mutants displaying WT-like currents (phenotype 1 - Figure 1E). We attempted to introduce some of these mutants on top of the GluN3A-S892L-K895F mutant. Several mutants gave glycine-alone current with TEVC. Among these, we focused on GluN1/GluN3A-S892L-K895F-H904E-K909T (or GluN3A-4x) and GluN1/GluN3A-Y805N-S809N-F810Y-S892L-K895F-H904E-K909T (GluN3A-7x) that exhibited the largest currents (Figure 5D, S5A-B). When attempting to estimate their  $Po$ , we realized that MTSEA application inhibits rather than potentiates their currents:  $0.9 \pm 0.01$  ( $n=4$ ) fold MTSEA potentiation for GluN3A-4x and  $0.7 \pm 0.01$  ( $n=3$ ) fold MTSEA potentiation for GluN3A-7x (Figure 5B,D). Likely, for these mutants MTSEA binding is unable to increase the  $Po$  of the channel gate that is already at its maximal open state, but the MTSEA molecule itself probably adds some negative conformational constraints to the gate. Thus, GluN3A-4x and GluN3A-7x both present a higher relative  $Po$  than the GluN3A-S892L-K895F mutant, and closer to the maximal  $Po$  of the receptor ( $Po \sim 1$ ).

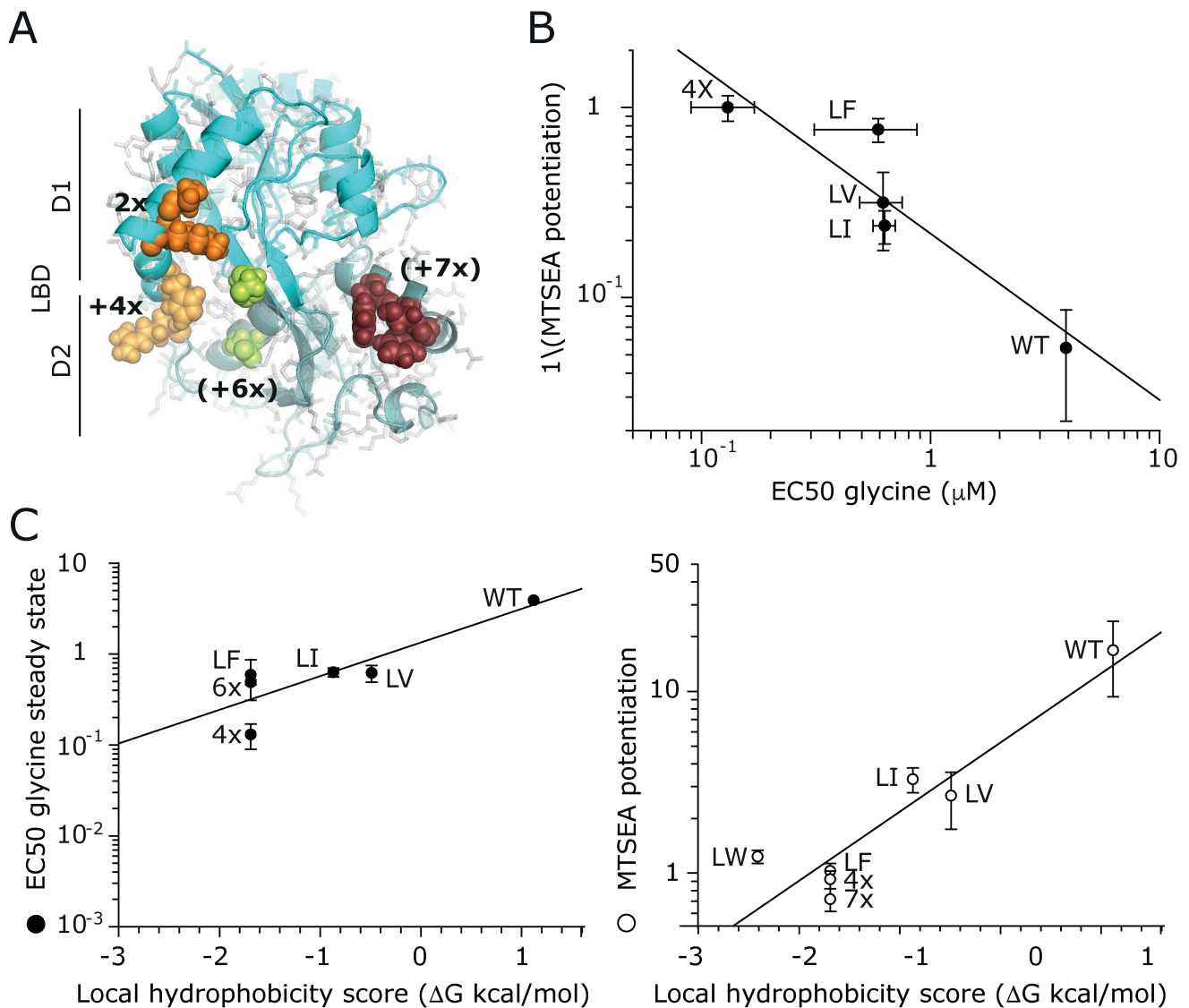


**Figure 5. Improving gain-of-function phenotypes at LBD intra-dimer interface.** **A:** Localization of additional mutations at the GluN3A LBD dimer interface on top of the GluN3A-S892-K895 (2X) GoF mutants (in orange). View of the LBD interface as in Figure 1C, with upper lobe D1 colored in cyan and lower lobe D2 in light-teal. '+4X' states for the two additional mutated residues on top of the 2X (4X: GluN3A-S892L-K895F-H904E-K909T). (+6X) and (+7X) state for two different mutant series (+2 and +3 mutated residues respectively) added on top of the 4X mutant (6X: GluN3A-S650E-D850N-S892L-K895F-H904E-K909T and 7X: GluN3A-Y805N-S809N-F810Y-S892L-K895F-H904E-K909T). **B:** GoF Mutations at the LBD dimer interface induce a correlated increase in glycine sensitivity and relative Po ( $1 / \text{MSTEA}$  potentiation). Data are taken from Table 1 and 2. **C:** Increasing hydrophobic contribution of the residue at 2X position correlates with increased glycine sensitivity (left) and relative Po (right). On the left, the Y-axis correspond to Glycine EC<sub>50</sub> measurements (plain dots) while on the right it corresponds to the MTSEA potentiation measurements (empty dots). All the data are taken from Table 1 and 2. At the X-axis, the local hydrophobicity score ( $\Delta G$  kcal/mol) measures the change in hydrophobicity linked to AA modification at the 892 and 895 (2X) positions only. Each data point within the graph relates to specific mutants either presented in panel A or corresponding to the 2X mutants: GluN3A-S892L-K895F (LF), GluN3A-S892L-K895V (LV), GluN3A-S892L-K895I (LI) and GluN3A-S892L-K895W (LW). The lines represent a linear regression fit of the data points.

Interestingly, the chimeric mutants (Figure 5A) showed further increase in glycine sensitivity compared to the GoF GluN3A-S892L-K895F (Figure 5B-C, S5) with 5-fold steady-state glycine EC<sub>50</sub> with the GluN3A-4x but also the GluN3A-6x (GluN3A S650E-D850N-S892L-K895F-H904E-K909T) (Table 2). Indeed, the glycine sensitivity is so high that the constitutive current linked to ambient glycine activation hides the low glycine concentration part of the dose-response (Figure S5C-D). Thus, the

stabilization of the LBD dimer interface of GluN1/GluN3A receptors through the reinforcement of the hydrophobic contacts and/or the mimicking of GluN2 interface led to receptors with massive increase in both Po and glycine EC<sub>50</sub>. This also shows that the GoF phenotype can be spatially extended in several part of the LBD dimer interface (Figure 5A), although the hinge inner-side region appears particularly prone to produce GoF mutants. Altogether, the striking phenotypes of our GoF mutants strongly support the idea that the amino-acid

composition of the LBD-dimer interface plays a critical role in GluN1/GluN3A receptor gating properties.

## Discussion

GluN1/GluN3A appear as atypical NMDARs both at the physiological and molecular level, but this impression of divergence is most probably linked to our present inability to make complete sense of their peculiar functional properties. Still GluN1/GluN3A receptors belong phylogenetically to the NMDA receptor family and as such have faced some specific architectural constraints of the group (Stroebel and Paoletti, 2021; Stroebel *et al.*, 2021). Understanding and controlling the atypical functional specificities of GluN1/GluN3A should definitely benefit from the large framework of knowledge and methods developed for other iGluRs and more especially for their GluN2 paralogs.

GluN1/GluN3A receptors appears as a unique case within the iGluR field because they appear both activated by one subunit (GluN3A) and inactivated by the other one (GluN1) when binding the same agonist (glycine) (Chatterton *et al.*, 2002; Awobuluyi *et al.*, 2007; Madry *et al.*, 2007). They also appear unique in the NMDAR field because of their fast glycine-dependent desensitization, that greatly contributed to hide their presence in the CNS until recently (Grand *et al.*, 2018; Otsu *et al.*, 2019; Bossi *et al.*, 2022). Their quick desensitization is reminiscent of AMPAR and kainate receptors currents behavior (Nayeem *et al.*, 2009; Twomey *et al.*, 2017; Hansen *et al.*, 2021). In AMPA and kainate receptors, the transition from the active agonist-bound state to the agonist-bound desensitized state is directly linked to the spontaneous breaking of the intra-LBD dimer interface (Sun *et al.*, 2002; Weston *et al.*, 2006). This reorganization of the LBDs induces a release of tension of the TMD-LBD linkers that leads to pore closure (Yuan *et al.*, 2005; Chen *et al.*, 2014; Dürr *et al.*, 2014). In GluN2 containing NMDARs, such desensitization is not usually observed, however the reorganization of agonist-bound LBDs also led to the inactivation of these receptors (Gielen *et al.*, 2009; Tajima *et al.*, 2016). The transition to these 'inhibited states' is under the control of NTD-dependent allosteric modulations that reorganize the LBD layer using different mechanisms depending of the involved GluN2 subunit (Tian *et al.*, 2021). Thus, despite apparent different mechanisms, the control by the LBDs of the transition between activated and inactivated states appears as a shared property between iGluRs. Overall, 30 years of targeted mutagenesis and pharmacology, together with structural approaches, highlighted the critical importance of the LBD intra-dimer interface in the functional transitions of iGluRs (Sun *et al.*, 2002; Gielen *et al.*, 2008; Hansen *et al.*, 2021).

By mutation scanning at the LBD dimer interface of GluN3A we aimed at dissecting the functional

mechanism of GluN1/GluN3A receptors function. Contrary to other iGluRs, this strategy has proven to be difficult because most GluN3A mutants didn't show any (or sufficient) current. In this context, GluN1/GluN3A receptors appeared to be particularly sensitive to mutagenic changes. Using a subtler mutagenic strategy, we tried to confer GluN2 functional properties (like limited desensitization or higher  $P_o$ ) to GluN1/GluN3A receptors, by substituting residues at the GluN3A LBD interface with their corresponding ones in GluN2 (Figure 1). This chimeric approach led us to the discovery of strong gain of function double-mutants GluN3A-S892L-K895F (or S892L-K895V), that are located in inner side of the LBD interface, close to the LBD hinge region. The obtained gain-of-function phenotype is both striking and atypical with a large increase both in  $P_o$  (~15-fold compared to WT) and agonist sensitivity (~10-fold fold glycine  $EC_{50}$  compared to WT).

These completely new gain-of function mutants of GluN3A appear as important tools to dissect the functional mechanism of GluN1/GluN3A receptors, by highlighting unexpected functional and structural similarity with other iGluRs, and narrowing the hypothesis about the molecular origin of their functional specificities.

**LBD dimer interface plays an important role in GluN1/GluN3A receptor function.** At first, our work underlines some architectural homologies of GluN1/GluN3A receptors with other NMDARs and iGluRs, despite marked functional differences. The success of the chimera approach, that aimed at conferring some GluN2 properties to GluN3A receptor, indeed suggests that the subunit cross-talk between GluN1 and GluN3A happen somehow as expected in the established framework of iGluR function. Indeed, stabilizing this interface tends to increase receptor activity as already proposed (Cummings *et al.*, 2016). One key question is if the LBD dimer interface could assemble in the active state of GluN1/GluN3A as it does in other iGluRs? At least two indications point in that direction: 1) The GluN1/GluN3A LBD dimer is predicted by alpha-fold 2 to assemble as in the homology model of GluN1/GluN3A receptors (Figure 1B) we used to design the GoF mutants. 2) In GluN1/GluN2, the LBD dimer interface is stabilized by large hydrophobic patches (Furukawa *et al.*, 2005; Gielen *et al.*, 2008; Jalali-Yazdi *et al.*, 2018; Esmenjaud *et al.*, 2019; Tian *et al.*, 2021) (Figure 1C). In our GluN1/GluN3A model, GoF apolar mutants would be placed at the right position to stabilize the dimer LBD interface by reintroducing an important hydrophobic contact (Figure 1C & 4B). Altogether, it seems likely that the GluN1/GluN3A LBD dimers assemble and interact during the activation mechanism. The existence of this LBD dimer interface of GluN1/GluN3A is then raising new questions, since it seems in contradiction with the peculiar functional properties of the receptor.



It is well documented in AMPAR that desensitization can be abolished by stabilizing the LBD intradimer interface by mutation (like the L483Y mutant) or by pharmacology (like with the cyclothiazide CTZ molecule) (Stern-Bach *et al.*, 1998; Sun *et al.*, 2002). Still, our stabilizing GoF mutants at LBD dimer interface of GluN1/GluN3A receptor do not eliminate the GluN1-dependant desensitization (as seen in the DR Figure 2B). Even the IC<sub>50</sub> of glycine binding on GluN1, that controls the onset of GluN1/GluN3A desensitization process, appears not affected by the GoF mutants (Figure S4B). Only the co-application of CGP on the strongest GoF mutants were able to stabilize the receptor in the active state more efficiently than in WT receptors (Figure 3A). Thus, in GluN1/GluN3A receptors, the stability of the LBD dimer interface in the 2X region (Figure 4A & 5A) appears not to be critical for receptor desensitization but rather to activation efficiency.

Stabilizing the upper-lobe LBD dimer interface has been reported to impair desensitization in AMPAR and to be associated with decrease agonist sensitivity (EC<sub>50</sub>) (Sun *et al.*, 2002). In GluN2A NMDARs, the covalent stabilization of the LBD dimer interface with a disulfide bridge also leads to reduced agonist sensitivity (EC<sub>50</sub>) (Gielen *et al.*, 2008). However, our LBD dimer interface GoF mutants in GluN1/GluN3A receptors exhibit a greatly improved Po and glycine sensitivity (1 order of magnitude EC<sub>50</sub> decrease, See Table 1). This increased glycine sensitivity of the GoF mutant constitutes an additional indication of the limited involvement of the LBD dimer interface in GluN1/GluN3A receptor desensitization. Our GluN1/GluN3A GoF phenotypes resemble more to the effect of Aniracetam on AMPA receptor (Partin *et al.*, 1996; Jin *et al.*, 2005) and GNE-8324 on GluN1/GluN2A receptors (Hackos *et al.*, 2016). These two PAM molecules, that both increase receptor agonist sensitivity and stabilize the LBD dimer interface, mediate their effect through subtle conformational changes. These effects are likely being communicated to the neighboring LBD hinges, affecting LBD open-closure equilibrium and thus agonist sensitivity. Such mechanism probably applies to our GluN1/GluN3A GoF mutants since almost all of them appear to be localized in the LBD hinge region (Figure 5A).

**Toward a global mechanism of GluN1/GluN3A function.** Altogether, our work indicates that the LBD dimer interface is an important determinant of GluN1/GluN3A receptor activity, but how can we integrate this information in our global understanding of the receptor functional mechanism? In particular, the striking phenotype of our GoF LBD interface mutants (Capacity of >100-fold potency for receptor activation (Figure 3B), <10 fold increase of glycine sensitivity (Figure 2) and absence of impairment of GluN1-depend desensitization (Figure 2)), reveals the existence of an inactivation mechanism that is tuned by the LBD-dimer interface properties, but that appears independent from the desensitization

controlled by glycine binding on GluN1. We were thus able to distinguish two distinct mechanisms of GluN1/GluN3A receptors inactivation.

There is obviously much left to be learned about the structure–function relationships underlying the complex behavior of GluN1/GluN3A receptors. In particular, GluN1-dependant desensitization mechanism remains unexplained. We showed in this work that this desensitization may not involve the canonical iGluR pathway involving LBD intradimer interface stability. Thus, at least in this context, GluN1/GluN3A receptors intradimer LBD does not seem to function as in AMPA & kainate receptors, but rather to behave like GluN2 containing NMDARs. This GluN1/GluN3A desensitization mechanism may possibly involve GluN1 specific LBD-TMD communication (Sobolevsky *et al.*, 2009) or GluN1-dependant reorganization of the LBD layer (Tajima *et al.*, 2016; Esmenjaud *et al.*, 2019; Chou *et al.*, 2020; Tian *et al.*, 2021; Wang *et al.*, 2021). In GluK2/GluK5 heterotetrameric receptors, the ligand binding to either GluK2 or GluK5 can activate the receptors, but desensitization requires ligand binding to both subunit types (Reiner and Isacoff, 2014). However, contrary to GluK receptors whose desensitized state appear structurally symmetrical in the gating core (Meyerson *et al.*, 2016), NMDAR heterotetramers exhibit stable architectural asymmetry (Sobolevsky *et al.*, 2009; Karakas and Furukawa, 2014; Lee *et al.*, 2014; Tajima *et al.*, 2016; Zhu *et al.*, 2016; Jalali-Yazdi *et al.*, 2018; Chou *et al.*, 2020; Wang *et al.*, 2021) and a strong functional specialization of each subunits (Stroebe and Paoletti, 2021) (Figure 1A). It is thus tempting to speculate that the heterotetrameric GluN1/GluN3A receptors have integrated a typical NMDAR subunit-specialized function with activation by the two GluN3A subunits (like observed in kainate receptor) and subsequent desensitization by the two GluN1 (resembling that of kainate receptors). Still, such a global mechanism of GluN1/GluN3A receptor function would also have to explain how GluN1 glycine binding doesn't lead to desensitization in the GluN2 context but rather to co-activation.

Finally, we can wonder why GluN1/GluN3A receptors are so poorly active. Compared to the very high glycine affinity of GluN3A isolated LBD : Kd of 40 nM (Yao, 2006; Stroebe *et al.*, 2021), the GluN1/GluN3A-WT receptors appear poorly efficient, with a GluN3A-dependant glycine EC<sub>50</sub> of 46 μM in CGP or 8 μM just with glycine (see Table 1) or 89 μM as previously reported with faster perfusion system (Skrenkova *et al.*, 2019). The 100 fold increases of glycine sensitivity in our interface GoF mutants (Figure 2F, Table 1) further highlights the hidden potential for high glycine sensitivity in GluN3A receptors. Moreover, it suggests that the LBD-dimer interface largely contributes to the conformational constraints lowering GluN3A agonist sensitivity. Our GoF mutants with a Po close to 1 also show that wild-type GluN1/GluN3A receptors (Po of 0.06 in CGP -

Table 1) are far from being fully effective (Estimated absolute  $P_o$  : 0.03) (Sasaki *et al.*, 2002). The GluN1/GluN3A-WT LBD dimer interface composition thus appears at the core of the limited efficiency of the receptor, both in terms of glycine sensitivity and gating activity. Beyond the specific sites we mutated (Figure 5A), the overall LBD dimer interface area of N2B and N3A share 51% sequence identity. In comparison, their whole LBDs share 37%, and the LBD interdimer interface area only 17%, suggesting a strong selective pressure was specifically maintained at the dimerization interface (Stroebele and Paoletti, 2021). Since GluN1/GluN3A-WT receptors have been shown to be involved in the regulation of neural excitability under the control of ambient glycine, our GoF mutants reveal the fingerprint of evolution at the LBD dimer interface, where selection shaped the amino-acid composition of the interface to avoid inadequate or excessive neural activation.

## Conclusion

GluN1/GluN3A receptors are new players in brain signaling with still underestimated physiological roles. The underlying difficulty of studying these receptors relates in part to their sparse pharmacology and unclear molecular function. In the present work we demonstrated the functional importance of GluN3A LBD intra-dimer interface assembly for the gating of the receptor, highlighting its functional similarities with that of other iGluRs. This finding thus reorients the search for the origin of GluN1/GluN3A receptors functional specificities (such as glycine-dependent desensitization) at other regions and interfaces. We believe the large GoF mutants we characterized offer unique opportunities to further elucidate GluN1/GluN3A receptors gating mechanism and structure, similarly than the GoF mutants of GluN2 receptor recently used to solve structures of NMDARs pre-active state (Esmenjaud *et al.*, 2019; Chou *et al.*, 2020; Wang *et al.*, 2021). Advances in this field are critical to tackle new questions about the pathological roles of these receptors (Lee *et al.*, 2015; Mahfooz *et al.*, 2016; Liu *et al.*, 2021; Crawley *et al.*, 2022). The molecular tools we validated should be of great help for functional and pharmacological tests in the framework of these future therapeutic developments.

## Acknowledgments

We thank Dr Marc Gielen for sharing unpublished data on GluN1/GluN2A glycine DR.

## Authorship Contributions

M.D.B performed all the experiments and analyzed the data. N.L. and L.M. provided help with molecular biology and pharmacology. D.S and M.D.B analyzed the data. D.S. performed the structural analysis. P.P. and D.S. designed the study and supervised the project. D.S. and M.D.B wrote the manuscript.

## References

- Armstrong N, Jasti J, Beich-Frandsen M, and Gouaux E (2006) Measurement of Conformational Changes accompanying Desensitization in an Ionotropic Glutamate Receptor. *Cell* **127**:85–97.
- Ascher P (1990) Measuring and Controlling the Extracellular Glycine Concentration at the NMDA Receptor Level, in *Excitatory Amino Acids and Neuronal Plasticity* (Ben-Ari Y ed) pp 13–16, Springer US, Boston, MA.
- Awobuluyi M, Yang J, Ye Y, Chatterton JE, Godzik A, Lipton SA, and Zhang D (2007) Subunit-Specific Roles of Glycine-Binding Domains in Activation of NR1/NR3 N-Methyl-d-aspartate Receptors. *Mol Pharmacol* **71**:112–122.
- Bossi S, Dhanasobhon D, Ellis-Davies GCR, Frontera J, de Brito Van Velze M, Lourenço J, Murillo A, Luján R, Casado M, Perez-Otaño I, Bacci A, Popa D, Paoletti P, and Rebola N (2022) GluN3A excitatory glycine receptors control adult cortical and amygdalar circuits. *Neuron* **110**:2438–2454.e8.
- Burada AP, Vinnakota R, and Kumar J (2020) The architecture of GluD2 ionotropic delta glutamate receptor elucidated by cryo-EM. *Journal of Structural Biology* **211**:107546.
- Chatterton JE, Awobuluyi M, Premkumar LS, Takahashi H, Talantova M, Shin Y, Cui J, Tu S, Sevarino KA, Nakanishi N, Tong G, Lipton SA, and Zhang D (2002) Excitatory glycine receptors containing the NR3 family of NMDA receptor subunits. *Nature* **415**:793–798.
- Chen L, Dürr KL, and Gouaux E (2014) X-ray structures of AMPA receptor–cone snail toxin complexes illuminate activation mechanism. *Science* **345**:1021–1026, American Association for the Advancement of Science.
- Chou T-H, Tajima N, Romero-Hernandez A, and Furukawa H (2020) Structural Basis of Functional Transitions in Mammalian NMDA Receptors. *Cell* **182**:357–371.e13.
- Ciabarra M, and Sevarino A (1995) Cloning and Characterization of  $\alpha$ -1: A Developmentally Regulated Member of a Novel Class of the Ionotropic Glutamate Receptor Family. 11.
- Citri A, and Malenka RC (2008) Synaptic Plasticity: Multiple Forms, Functions, and Mechanisms. *Neuropsychopharmacol* **33**:18–41, Nature Publishing Group.
- Crawley O, Conde-Dusman MJ, and Pérez-Otaño I (2022) GluN3A NMDA receptor subunits: more enigmatic than ever? *The Journal of Physiology* **600**:261–276.
- Cummings KA and Popescu GK (2016) Protons potentiate GluN1/GluN3A currents by attenuating their desensitisation. *Scientific Reports* **6**:23344.
- Cummings KA, Belin S, and Popescu GK (2017) Residues in the GluN1 C-terminal domain control kinetics and pharmacology of GluN1/GluN3A N-methyl- d -aspartate receptors. *Neuropharmacology* **119**:40–47.
- Das S, Sasaki YF, Rothe T, Premkumar LS, Takasu M, Crandall JE, Dikkes P, Conner DA, Rayudu PV, Cheung W, Chen H-SV, Lipton SA, and Nakanishi N (1998) Increased NMDA current and spine density in mice lacking the NMDA receptor subunit NR3A. *Nature* **393**:377–381.
- Dürr KL, Chen L, Stein RA, De Zorzi R, Folea IM, Walz T, Mchaurab HS, and Gouaux E (2014) Structure and Dynamics of AMPA Receptor GluA2 in Resting, Pre-Open, and Desensitized States. *Cell* **158**:778–792.
- Esmenjaud J, Stroebel D, Chan K, Grand T, David M, Wollmuth LP, Taly A, and Paoletti P (2019) An inter-dimer allosteric switch controls NMDA receptor activity. *EMBO J* **38**.
- Eswari N, Webb B, Marti-Renom MA, Madhusudhan M s., Eramian D, Shen M, Pieper U, and Sali A (2006) Comparative Protein Structure Modeling Using Modeller. *Current Protocols in Bioinformatics* **15**:5.6.1-5.6.30.
- Furukawa H, and Gouaux E (2003) Mechanisms of activation, inhibition and specificity: crystal structures of the NMDA receptor NR1 ligand-binding core. *The EMBO Journal* **22**:2873–2885, John Wiley & Sons, Ltd.
- Furukawa H, Singh SK, Mancusso R, and Gouaux E (2005) Subunit arrangement and function in NMDA receptors. *Nature* **438**:185–192.
- Gangwar SP, Green MN, Michard E, Simon AA, Feijó JA, and Sobolevsky AI (2021) Structure of the Arabidopsis Glutamate Receptor-like Channel GLR3.2 Ligand-Binding Domain. *Structure* **29**:161-169.e4.
- Gielen M, Le Goff A, Stroebel D, Johnson JW, Neyton J, and Paoletti P (2008) Structural Rearrangements of NR1/NR2A NMDA Receptors during Allosteric Inhibition. *Neuron* **57**:80–93.
- Gielen M, Retchless BS, Mony L, Johnson JW, and Paoletti P (2009) Mechanism of differential control of NMDA receptor activity by NR2 subunits. *Nature* **459**:703–707.
- Grand T, Abi Gerges S, David M, Diana MA, and Paoletti P (2018) Unmasking GluN1/GluN3A excitatory glycine NMDA receptors. *Nat Commun* **9**:4769.
- Green MN, Gangwar SP, Michard E, Simon AA, Portes MT, Barbosa-Caro J, Wudick MM, Lizzio MA, Klykov O, Yelshanskaya MV, Feijó JA, and Sobolevsky AI (2021) Structure of the Arabidopsis thaliana glutamate receptor-like channel GLR3.4. *Molecular Cell* **81**:3216-3226.e8.
- Hackos DH, Lupardus PJ, Grand T, Chen Y, Wang T-M, Reynen P, Gustafson A, Wallweber HJA, Volgraf M, Sellers BD, Schwarz JB, Paoletti P, Sheng M, Zhou Q, and Hanson JE (2016) Positive Allosteric Modulators of

- GluN2A-Containing NMDARs with Distinct Modes of Action and Impacts on Circuit Function. *Neuron* **89**:983–999.
- Hansen KB, Ogden KK, and Traynelis SF (2012) Subunit-Selective Allosteric Inhibition of Glycine Binding to NMDA Receptors. *Journal of Neuroscience* **32**:6197–6208.
- Hansen KB, Wollmuth LP, Bowie D, Furukawa H, Menniti FS, Sobolevsky AI, Swanson GT, Swanger SA, Greger IH, Nakagawa T, McBain CJ, Jayaraman V, Low C-M, Dell'Acqua ML, Diamond JS, Camp CR, Perszyk RE, Yuan H, and Traynelis SF (2021) Structure, Function, and Pharmacology of Glutamate Receptor Ion Channels. *Pharmacol Rev* **73**:1469–1658.
- Hatton CJ, and Paoletti P (2005) Modulation of Triheteromeric NMDA Receptors by N-Terminal Domain Ligands. *Neuron* **46**:261–274.
- Jalali-Yazdi F, Chowdhury S, Yoshioka C, and Gouaux E (2018) Mechanisms for Zinc and Proton Inhibition of the GluN1/GluN2A NMDA Receptor. *Cell* **175**:1520–1532.e15.
- Jin R, Clark S, Weeks AM, Dudman JT, Gouaux E, and Partin KM (2005) Mechanism of Positive Allosteric Modulators Acting on AMPA Receptors. *J Neurosci* **25**:9027–9036, Society for Neuroscience.
- Jumper J, Evans R, Pritzel A, Green T, Figurnov M, Ronneberger O, Tunyasuvunakool K, Bates R, Židek A, Potapenko A, Bridgland A, Meyer C, Kohl SAA, Ballard AJ, Cowie A, Romera-Paredes B, Nikolov S, Jain R, Adler J, Back T, Petersen S, Reiman D, Clancy E, Zielinski M, Steinegger M, Pacholska M, Berghammer T, Bodenstein S, Silver D, Vinyals O, Senior AW, Kavukcuoglu K, Kohli P, and Hassabis D (2021) Highly accurate protein structure prediction with AlphaFold. *Nature* **596**:583–589, Nature Publishing Group.
- Jumper J, and Hassabis D (2022) Protein structure predictions to atomic accuracy with AlphaFold. *Nat Methods* **19**:11–12, Nature Publishing Group.
- Kaniakova M, Kleteckova L, Lichnerova K, Holubova K, Skrenkova K, Korinek M, Krusek J, Smejkalova T, Korabecny J, Vales K, Soukup O, Horak M (2018) 7-Methoxyderivative of tacrine is a 'foot-in-the-door' open-channel blocker of GluN1/GluN2 and GluN1/GluN3 NMDA receptors with neuroprotective activity in vivo. *Neuropharmacology* **140**:217–232.
- Kapaki E, Segditsa J, and Papageorgiou C (1989) Zinc, copper and magnesium concentration in serum and CSF of patients with neurological disorders. *Acta Neurol Scand* **79**:373–378, Wiley-Blackwell, Denmark.
- Karakas E, and Furukawa H (2014) Crystal structure of a heterotetrameric NMDA receptor ion channel. *Science* **344**:992–997.
- Kuner T, and Schoepfer R (1996) Multiple Structural Elements Determine Subunit Specificity of Mg<sup>2+</sup> Block in NMDA Receptor Channels. *J Neurosci* **16**:3549–3558, Society for Neuroscience.
- Lee C-H, Lü W, Michel JC, Goehring A, Du J, Song X, and Gouaux E (2014) NMDA receptor structures reveal subunit arrangement and pore architecture. *Nature* **511**:191–197.
- Lee JH, Wei ZZ, Chen D, Gu X, Wei L, and Yu SP (2015) A neuroprotective role of the NMDA receptor subunit GluN3A (NR3A) in ischemic stroke of the adult mouse. *American Journal of Physiology-Cell Physiology* **308**:C570–C577, American Physiological Society.
- Liu SX, Gades MS, Swain Y, Ramakrishnan A, Harris AC, Tran PV, and Gewirtz JC (2021) Repeated morphine exposure activates synaptogenesis and other neuroplasticity-related gene networks in the dorsomedial prefrontal cortex of male and female rats. *Drug and Alcohol Dependence* **221**:108598.
- Madry C, Mesic I, Bartholomäus I, Nicke A, Betz H, and Laube B (2007) Principal role of NR3 subunits in NR1/NR3 excitatory glycine receptor function. *Biochemical and Biophysical Research Communications* **354**:102–108.
- Mahfooz K, Marco S, Martínez-Turrillas R, Raja MK, Pérez-Otaño I, and Wesseling JF (2016) GluN3A promotes NMDA spiking by enhancing synaptic transmission in Huntington's disease models. *Neurobiology of Disease* **93**:47–56.
- Meyerson JR, Chittori S, Merk A, Rao P, Han TH, Serpe M, Mayer ML, and Subramaniam S (2016) Structural basis of kainate subtype glutamate receptor desensitization. *Nature* **537**:567–571.
- Mony L, Zhu S, Carvalho S, and Paoletti P (2011) Molecular basis of positive allosteric modulation of GluN2B NMDA receptors by polyamines. *The EMBO Journal* **30**:3134–3146, John Wiley & Sons, Ltd.
- Murillo A, Navarro AI, Puellas E, Zhang Y, Petros TJ, and Pérez-Otaño I (2021) Temporal Dynamics and Neuronal Specificity of Grin3a Expression in the Mouse Forebrain. *Cerebral Cortex* **31**:1914–1926.
- Nayeem N, Zhang Y, Schweppe DK, Madden DR, and Green T (2009) A Nondesensitizing Kainate Receptor Point Mutant. *Mol Pharmacol* **76**:534–542.
- Nowak L, Bregestovski P, Ascher P, Herbet A, and Prochiantz A (1984) Magnesium gates glutamate-activated channels in mouse central neurones. *Nature* **307**:462–465, Nature Publishing Group.
- Otsu Y, Darceq E, Pietrajtis K, Mátyás F, Schwartz E, Bessaih T, Abi Gerges S, Rousseau CV, Grand T, Dieudonné S, Paoletti P, Acsády L, Agulhon C, Kieffer BL, and Diana MA (2019) Control of aversion by glycine-gated GluN1/GluN3A NMDA receptors in the adult medial habenula. *Science* **366**:250–254.
- Paoletti P, Bellone C, and Zhou Q (2013) NMDA receptor subunit diversity: impact on receptor properties, synaptic plasticity and disease. *Nat Rev Neurosci* **14**:383–400.
- Partin KM, Fleck MW, and Mayer ML (1996) AMPA Receptor Flip/Flop Mutants Affecting Deactivation, Desensitization, and Modulation by Cyclothiazide, Aniracetam, and Thiocyanate. *J Neurosci* **16**:6634–6647, Society for Neuroscience.
- Reiner A, and Isacoff EY (2014) Tethered ligands reveal glutamate receptor desensitization depends on subunit occupancy. *Nat Chem Biol* **10**:273–280, Nature Publishing Group.
- Reynolds IJ, and Aizenman E (1992) Pentamidine is an N-methyl-D-aspartate receptor antagonist and is neuroprotective in vitro. *J Neurosci* **12**:970–975, Society for Neuroscience.
- Riou M, Stroebel D, Edwardson JM, and Paoletti P (2012) An Alternating GluN1-2-1-2 Subunit Arrangement in Mature NMDA Receptors. *PLOS ONE* **7**:e35134, Public Library of Science.
- Sasaki YF, Rothe T, Premkumar LS, Das S, Cui J, Talantova MV, Wong H-K, Gong X, Chan SF, Zhang D, Nakanishi N, Sucher NJ, and Lipton SA (2002) Characterization and Comparison of the NR3A Subunit of the NMDA Receptor in Recombinant Systems and Primary Cortical Neurons. *Journal of Neurophysiology* **87**:2052–2063.
- Schmid SM, Kott S, Sager C, Huelsken T, and Hollmann M (2009) The glutamate receptor subunit delta2 is capable of gating its intrinsic ion channel as revealed by ligand binding domain transplantation. *Proceedings of the National Academy of Sciences* **106**:10320–10325, Proceedings of the National Academy of Sciences.
- Skrenkova K, Hemelikova K, Kolcheva M, Kortus S, Kaniakova M, Krausova B, Horak M. (2019) Structural features in the glycine-binding sites of the GluN1 and GluN3A subunits regulate the surface delivery of NMDA receptors. *Sci Rep* **9**(1):12303.
- Sobolevsky AI, Rosconi MP, and Gouaux E (2009) X-ray structure, symmetry and mechanism of an AMPA-subtype glutamate receptor. *Nature* **462**:745–756, Nature Publishing Group.
- Stern-Bach Y, Russo S, Neuman M, and Rosenmund C (1998) A Point Mutation in the Glutamate Binding Site Blocks Desensitization of AMPA Receptors. *Neuron* **21**:907–918.
- Stroebel D, Mony L, and Paoletti P (2021) Glycine agonism in ionotropic glutamate receptors. *Neuropharmacology* **193**:108631.
- Stroebel D, and Paoletti P (2021) Architecture and function of NMDA receptors: an evolutionary perspective. *J Physiol* **599**:2615–2638.
- Sun Y, Olson R, Horning M, Armstrong N, Mayer M, and Gouaux E (2002) Mechanism of glutamate receptor desensitization. *Nature* **417**:245–253.
- Tajima N, Karakas E, Grant T, Simorowski N, Diaz-Avalos R, Grigorieff N, and Furukawa H (2016) Activation of NMDA receptors and the mechanism of inhibition by ifenprodil. *Nature* **534**:63–68.
- Tian M, Stroebel D, Piot L, David M, Ye S, and Paoletti P (2021) GluN2A and GluN2B NMDA receptors use distinct allosteric routes. *Nat Commun* **12**:4709.
- Tong G, Takahashi H, Tu S, Shin Y, Talantova M, Zago W, Xia P, Nie Z, Goetz T, Zhang D, Lipton SA, and Nakanishi N (2008) Modulation of NMDA Receptor Properties and Synaptic Transmission by the NR3A Subunit in Mouse Hippocampal and Cerebrocortical Neurons. *Journal of Neurophysiology* **99**:122–132.
- Traynelis SF, Wollmuth LP, McBain CJ, Menniti FS, Vance KM, Ogden KK, Hansen KB, Yuan H, Myers SJ, and Dingledine R (2010) Glutamate Receptor Ion Channels: Structure, Regulation, and Function. *Pharmacol Rev* **62**:405–496, American Society for Pharmacology and Experimental Therapeutics.
- Twomey EC, Yelshanskaya MV, Grassucci RA, Frank J, and Sobolevsky AI (2017) Structural Bases of Desensitization in AMPA Receptor-Auxiliary Subunit Complexes. *Neuron* **94**:569–580.e5.
- Ulbrich MH, and Isacoff EY (2008) Rules of engagement for NMDA receptor subunits. *Proceedings of the National Academy of Sciences* **105**:14163–14168.
- Vangone A, Spinelli R, Scarano V, Cavallo L, and Oliva R (2011) COCOMAPS: a web application to analyze and visualize contacts at the interface of biomolecular complexes. *Bioinformatics* **27**:2915–2916.
- Wada A, Takahashi H, Lipton SA, and Chen H-SV (2006) NR3A Modulates the Outer Vestibule of the “NMDA” Receptor Channel. *Journal of Neuroscience* **26**:13156–13166.
- Wang H, Lv S, Stroebel D, Zhang J, Pan Y, Huang X, Zhang X, Paoletti P, and Zhu S (2021) Gating mechanism and a modulatory niche of human GluN1-GluN2A NMDA receptors. *Neuron* **109**:2443–2456.e5.
- Weston MC, Schuck P, Ghosal A, Rosenmund C, and Mayer ML (2006) Conformational restriction blocks glutamate receptor desensitization. *Nat Struct Mol Biol* **13**:1120–1127, Nature Publishing Group.
- White SH, and Wimley WC (1999) MEMBRANE PROTEIN FOLDING AND STABILITY: Physical Principles. *Annu Rev Biophys Biomol Struct* **28**:319–365.
- Yao Y (2006) Characterization of a Soluble Ligand Binding Domain of the NMDA Receptor Regulatory Subunit NR3A. *Journal of Neuroscience* **26**:4559–4566.

- Yao Y, Belcher J, Berger AJ, Mayer ML, and Lau AY (2013) Conformational Analysis of NMDA Receptor GluN1, GluN2, and GluN3 Ligand-Binding Domains Reveals Subtype-Specific Characteristics. *Structure* **21**:1788–1799.
- Yao Y, Harrison CB, Freddolino PL, Schulten K, and Mayer ML (2008) Molecular mechanism of ligand recognition by NR3 subtype glutamate receptors. *EMBO J* **27**:2158–2170.
- Yelshanskaya MV, Patel DS, Kottke CM, Kurnikova MG, and Sobolevsky AI (2022) Opening of glutamate receptor channel to subconductance levels. *Nature* **605**:172–178, Nature Publishing Group.
- Yuan H, Erreger K, Dravid SM, and Traynelis SF (2005) Conserved Structural and Functional Control of N-Methyl-d-aspartate Receptor Gating by Transmembrane Domain M3. *Journal of Biological Chemistry* **280**:29708–29716.
- Yuan T, Mameli M, O'Connor EC, Dey PN, Verpelli C, Sala C, Perez-Otano I, Lüscher C, and Bellone C (2013) Expression of Cocaine-Evoked Synaptic Plasticity by GluN3A-Containing NMDA Receptors. *Neuron* **80**:1025–1038.
- Zhu S, Stein RA, Yoshioka C, Lee C-H, Goehring A, Mchaourab HS, and Gouaux E (2016) Mechanism of NMDA Receptor Inhibition and Activation. *Cell* **165**:704–714.
- Zhu S, Stroebel D, Yao CA, Taly A, and Paoletti P (2013) Allosteric signaling and dynamics of the clamshell-like NMDA receptor GluN1 N-terminal domain. *Nat Struct Mol Biol* **20**:477–485, Nature Publishing Group.
- Zhu Z, Yi F, Epplin MP, Liu D, Summer SL, Mizu R, Shaulsky G, XiangWei W, Tang W, Burger PB, Menaldino DS, Myers SJ, Liotta DC, Hansen KB, Yuan H, and Traynelis SF (2020) Negative allosteric modulation of GluN1/GluN3 NMDA receptors. *Neuropharmacology* **176**:108117.

**List of Supplementary Figures:**

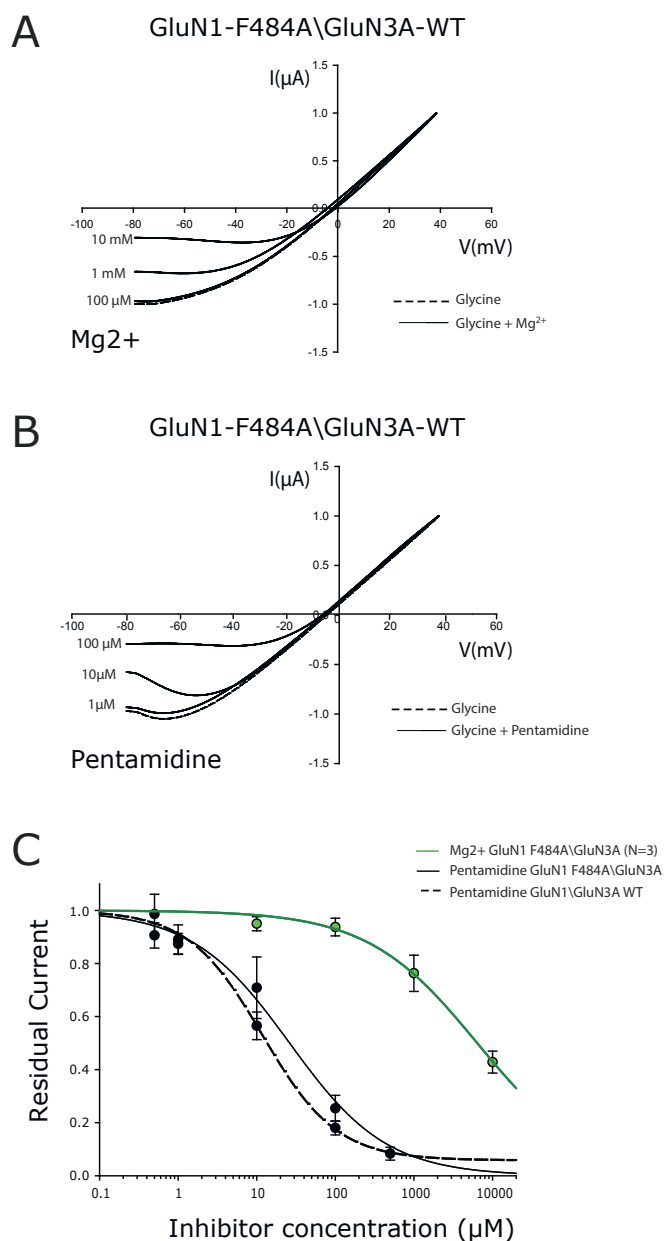
Figure S1: GluN1/GluN3A receptors pore blockers: pentamidine & magnesium sensitivity.

Figure S2: Double-mutants properties: raw currents, SS glycine DR & pentamidine response.

Figure S3: MTSEA method result summary.

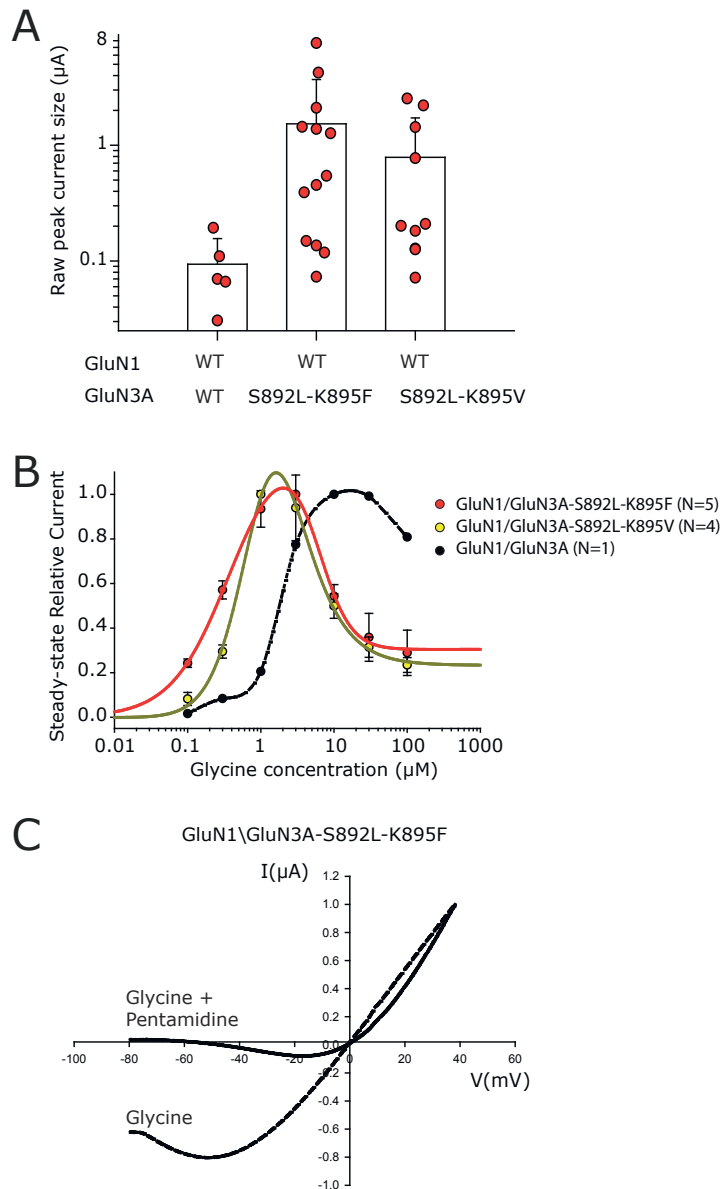
Figure S4: Mutagenesis and pharmacology reveal the influence of inter-LBD communication.

Figure S5: Glycine sensitivity of chimeric mutants of the LBD dimer interface.



**Figure S1. GluN1/GluN3A receptors pore blockers: Pentamidine & Magnesium sensitivity.**

**A: Magnesium I/V curves** normalized to +40 mV for GluN1-F484A/GluN3A-WT with 1 mM glycine in black dotted line, and 1 mM glycine + increasing Mg<sup>2+</sup> concentrations in continuous line (n=3). **B: Pentamidine I/V curves** normalized to +40 mV for GluN1-F484A/GluN3A-WT with 1 mM glycine in black dotted line, and 1 mM glycine + increasing pentamidine concentrations in continuous line (n=5). **C: Pentamidine and magnesium inhibitory dose responses** for both GluN1/GluN3A-WT (dotted black line, n=4) with 100 μM glycine pre-incubated with 200 nM CGP and for GluN1-F484A/GluN3A-WT (straight black line, n=5) with 1 mM glycine, both at -60 mV. The green straight line represents the inhibitory dose response of Mg<sup>2+</sup> for GluN1-F484A/ GluN3A-WT in the presence of 1 mM glycine (n=3), obtained from the IV curves shown in Panel B. IC<sub>50</sub> for Pentamidine was : 14.90 μM ± 1.72 for GluN1/GluN3A-WT, and of 26 μM ± 5 for GluN1-F484A/GluN3A-WT. IC<sub>50</sub> for Mg<sup>2+</sup> for GluN1-F484A/GluN3A-WT was measured at 6.3 ± 0.83 mM.



**Figure S2. Double mutants properties : Raw currents, SS glycine DR & pentamidine response.**

**A: Raw peak current size of the two double mutants** GluN1/GluN3A-S892L-K895F and GluN1/GluN3A-S892L-K895V, compared to GluN1/GluN3A-WT. Each dot corresponds to the recording of individual oocyte - oocytes with no current were not included (See Table 2). **B: Steady-state glycine dose-responses** for GluN1/GluN3A-WT (n=1), GluN1/GluN3A-S892L-K895F (n=5) and GluN1/GluN3A-S892L-K895V (n=4) following application of different glycine concentrations. EC50s were calculated as 3.9,  $0.59 \pm 0.2$ , and  $0.62 \pm 0.13$   $\mu\text{M}$  for GluN1/GluN3A-WT, GluN1/GluN3A-S892L-K895F and GluN1/GluN3A-S892L-K895V respectively. EC50s were calculated for each individual cell, and then averaged. Due to the small sizes of the desensitized GluN1/GluN3A-WT steady state currents after glycine application, we picked a representative trace with the largest current size we could record. **C : Pentamidine I/V curves of the mutant GluN1/GluN3A-S892L-K895F** normalized to +40 mV with 1  $\mu\text{M}$  glycine in black dotted line, and 1  $\mu\text{M}$  glycine + 100  $\mu\text{M}$  pentamidine in black straight line (n=4). The positive current at hyperpolarized potentials reveals small tonic activity at resting potential.

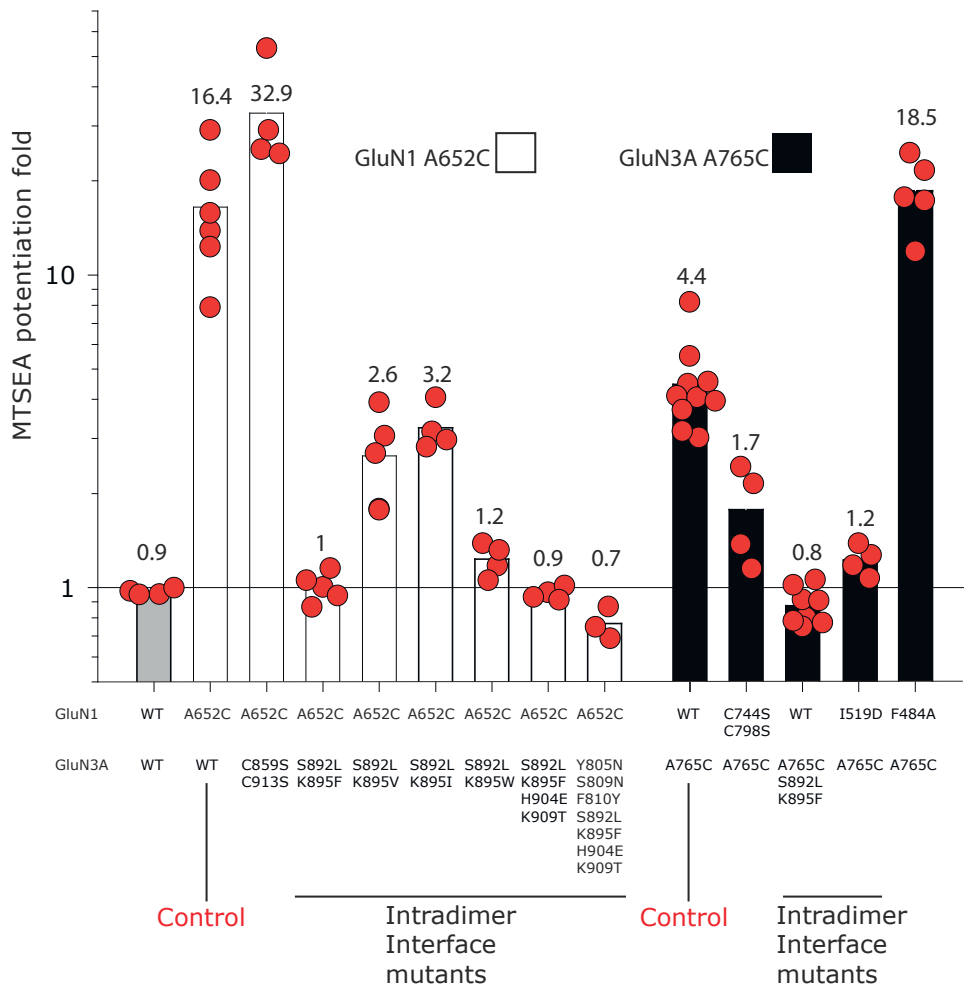


**Figure S3. MTSEA method result summary.**

Clustered in white are the GluN3A mutants tested by coinjecting the GluN1-A652C pore mutant. In black are the conditions recorded with pore mutant GluN3A-A765C. All mutants were tested with 200 nM CGP pre-incubation and 100  $\mu$ M glycine application followed by 300  $\mu$ M MTSEA application. The MTSEA induced potentiation on the Y axis corresponds to the ratios between the peak currents following agonist application and the steady state current obtained with MTSEA application on top of the glycine+CGP.



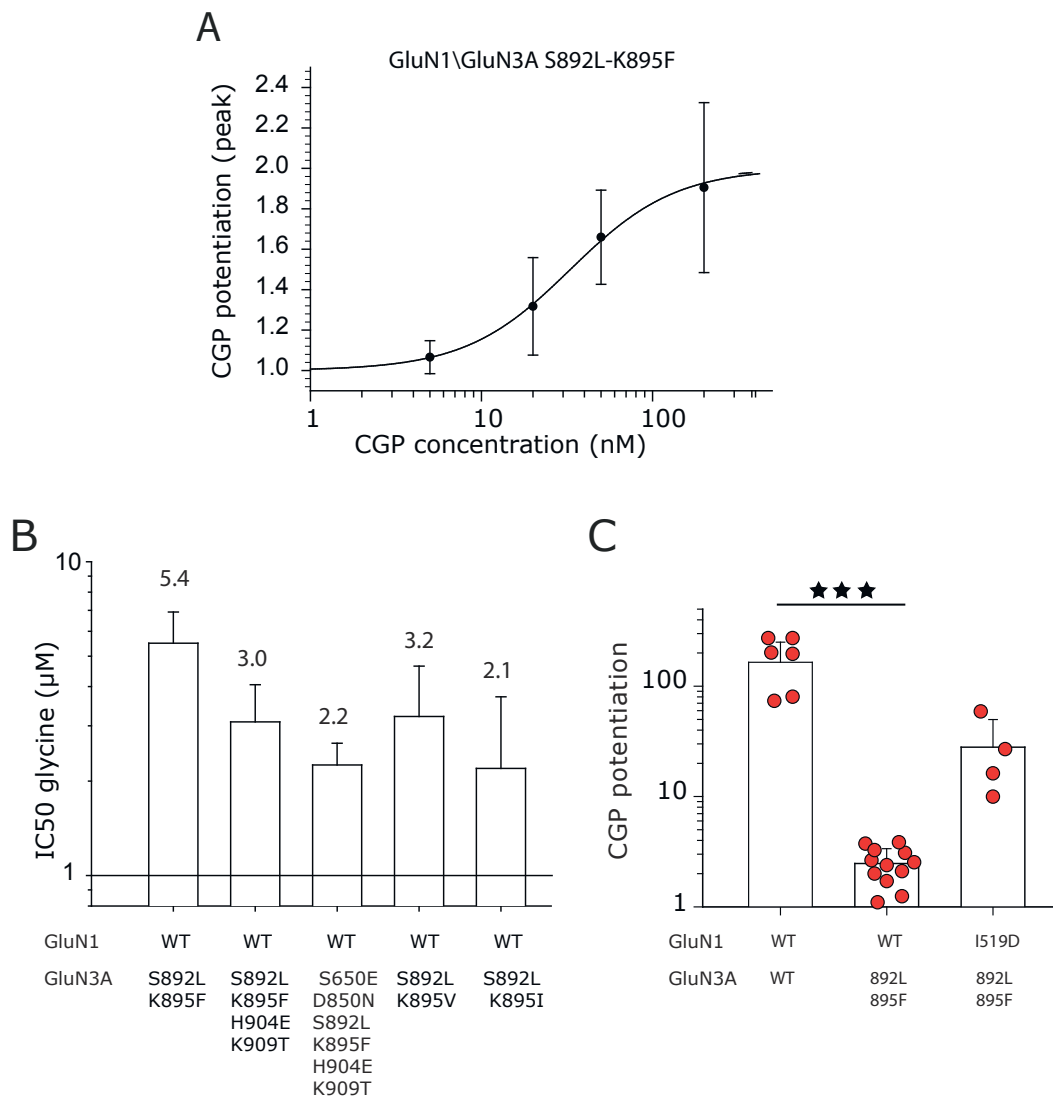


**Figure S4. Mutagenesis and pharmacology reveal the influence of inter-LBD communication.**

**A: Dose-responses of CGP-induced potentiation for GluN1/GluN3A-S892L-K895F** in the presence of 100  $\mu\text{M}$  glycine,  $\text{EC}_{50} = 33.1 \pm 1.25$  nM,  $n\text{H} = 1.41$ , ( $n=5$ ). For the GluN1/GluN3A-WT, Grand et al., 2018 reported a value of CGP-induced potentiation of the peak current of  $\text{EC}_{50} = 26.3 \pm 5$  nM. **B: GluN1 glycine  $\text{IC}_{50}$  components of the biphasic dose-responses** (Figure 2B) calculated with the steady state currents for different GoF mutants of the intradimer interface. For each condition,  $\text{IC}_{50}$  was calculated per each cell, then all the values were averaged to be plotted. **C: CGP potentiation values for the reverting interface mutants** GluN1-I519D with the GoF mutant GluN3A-S892L-K895F (see also Figure 4).

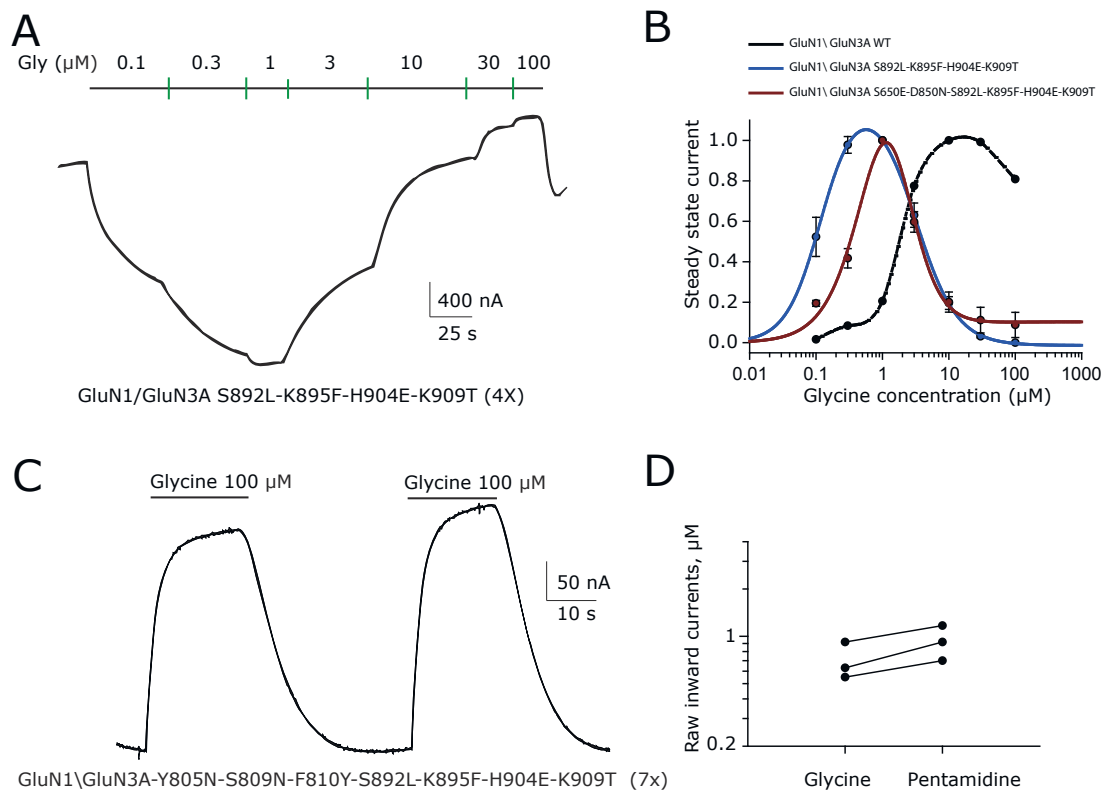


**Figure S5. Glycine sensitivity of chimeric mutants of the LBD dimer interface.**

**A. Current trace of glycine dose-response for the mutant GluN3A-4X** (GluN1/GluN3A-S892L-K895F-H904E-K909T). **B. Glycine dose response of chimeric constructs** GluN1/GluN3A S892L-K895F-H904E-K909T (GluN3A-4X) and GluN1/GluN3A-S650E-D850N-S892L-K895F-H904E-K909T (GluN3A-6X). The resulting EC50 for glycine steady state for GluN3A-4X and GluN3A-6X are  $0.13 \pm 0.04 \mu\text{M}$ , ( $n=5$ ) and  $0.49 \pm 0.03 \mu\text{M}$  ( $n=4$ ) respectively. As in figure S2, due to the small sizes of the desensitized GluN1/GluN3A-WT steady state currents after glycine application, we picked a representative trace with the largest current size we could record. **C. Current trace of the GluN3A-7X mutant** (GluN1/GluN3A-Y805N-S809N-F810Y-S892L-K895F-H904E-K909T) showing positive steady state currents upon saturating glycine application and thus revealing the extent of the tonic current activation in recording solution for this mutant. **D. Extent of tonic current in GluN3A-7X mutant.** Comparison of saturating 100  $\mu\text{M}$  glycine and 100  $\mu\text{M}$  pentamidine applications on the mutant inward currents ( $n=3$ ).

**Continuation of the second chapter: results**

#### 8.4 Unnatural-Amino-Acid (UAA) crosslinking attempts at the LBD dimer interface

In the manuscript we demonstrated that the intra-LBD-dimer interface is a key element regulating GluN3A function. The identification of such promising site to modulate receptor function pushes us to investigate if it can be used for optomodulation. Optogenetic approaches have never been tested for GluN3A, but were successfully developed for GluN2A and GluN2B receptors in the lab (Zhu *et al.*, 2014; Tian *et al.*, 2021) (and were even used at the same LBD intradimer interface). It can be achieved by inserting photocrosslinking photosensitive unnatural amino acids (UAAs) such as AzF (Azido-phenylalanine) or BzF (Benzoyl-phenylalanine) at the receptor interfaces in iGluRs. These photosensitive amino acids can be inserted at any place in the polypeptide chain by genetic code expansion by mutating the target residues in an amber stop codon (Figure 58 Panel A). If placed in an interface and exposed to UV, the inserted AzF or BzF can react with residues from the neighboring subunit and form a covalent crosslink, thereby interfering with putative conformational changes of this interface. Based on our contact map and mutagenesis success on GluN3A receptors, we made educated guesses and tried to introduce UAAs into the key spots we identified at the intradimer interface. The objective was both to validate the GluN1-GluN3A LBD dimer contact by an independent cross-linking approach and to build the first GluN3A photosensitive receptor.

We proceeded to select a number of targets mainly sitting in either sides of the LBD intradimer Interface (inner, medium, outer), or picking residues that have already been previously employed in the literature as successful site for crosslinking in NMDARs (Zhu *et al.*, 2014; Tian *et al.*, 2021). A comprehensive list of our targets can be seen at Table 10. Overall, we tested 13 amber-stop point mutant, among which 11 in the LBD intradimer Interface and two in the NTD. Their positions within the Interface can be seen in (Figure 59 Panel A)

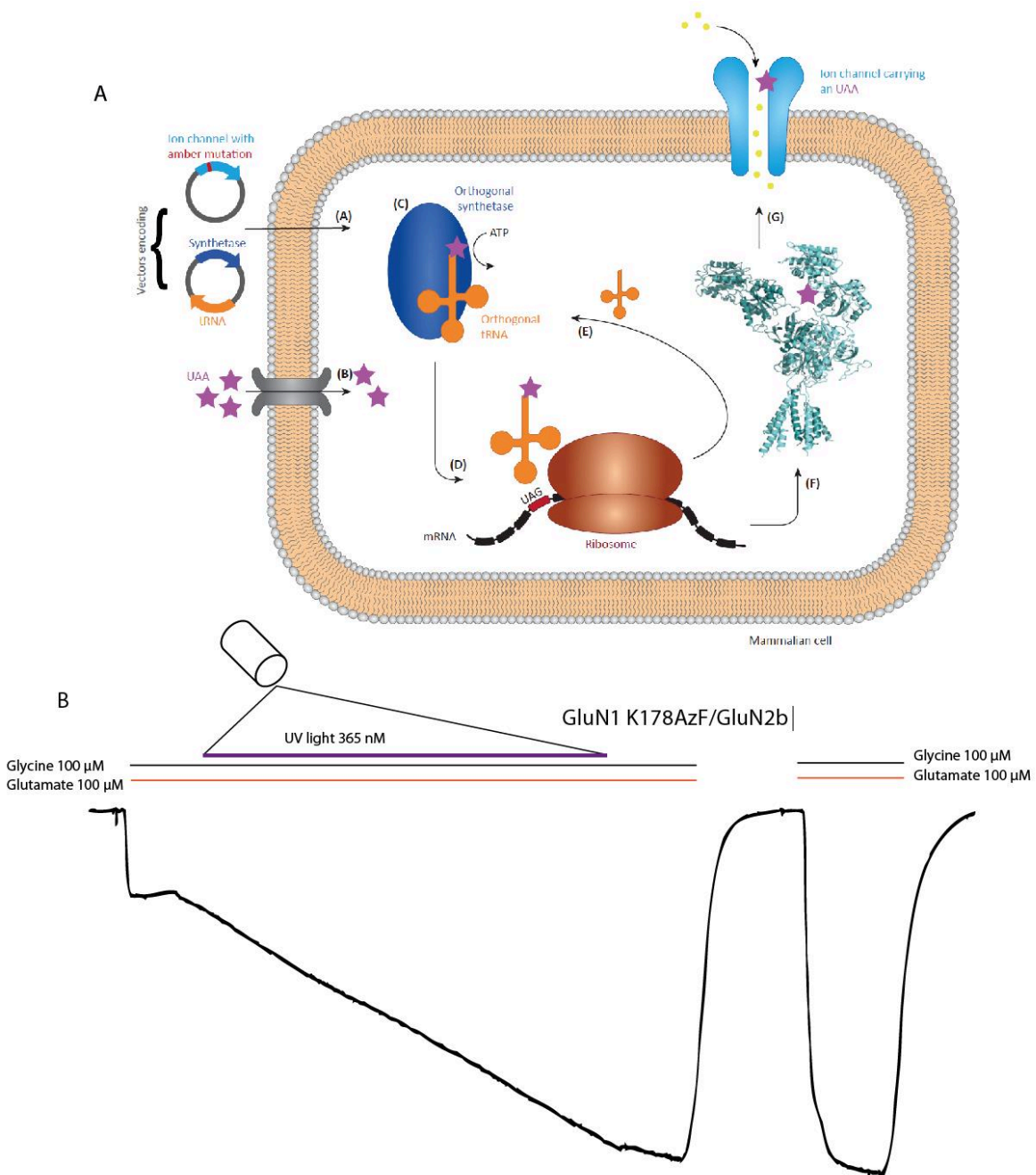


Figure 58 Unnatural amino acid crosslink in NMDARs.

Panel A, Inset and figure legend taken from (Klippenstein et al., 2014) here reported. The UAA genetic encoding methodology, as performed for mammalian cell lines, is represented schematically. (A) Vectors carrying genes for an ion channel of interest (light blue) and an orthogonal suppressor tRNA (orange)/aminoacyl synthetase (dark blue) pair are introduced into the cell by means of transient transfection. The amber stop codon (TAG, red) replaces a native codon at a permissive site within the sequence of the ion channel gene. (B) The light-sensitive UAA (purple asterisks) is added to the cellular growth medium and spontaneously enters the cell through amino acid transporters (gray). (C) Within the cell, the orthogonal

synthetase specifically aminoacylates the suppressor tRNA with the UAA, a catalytic reaction driven by ATP. (D) The UAA-carrying tRNA, which contains a CUA anticodon, enters the ribosomal machinery to incorporate the UAA in response to the complementary amber codon on the ion channel mRNA (black). (E) Once relieved from the charge at the ribosome, the tRNA can be reused for further UAA aminoacylation by the cognate synthetase. (F) The full-length polypeptide chain [shown here for two NMDA receptor (NMDAR) subunits, Protein Data Bank 4PE5(Karakas and Furukawa, 2014); light blue], site specifically carrying the UAA, undergoes folding and assembly into a functioning ion channel. (G) The newly formed membrane protein migrates to its assigned location (e.g., the cell surface) to selectively conduct ions (yellow), thus contributing to cellular functions. Panel B, example trace from GluN1 K178AzF/GluN2B with simultaneous applications of glycine 100  $\mu$ M and glutamate 100  $\mu$ M. UV application is shown to potentiate current sizes due to covalent NTD crosslinking, which increases receptor PO (Tian et al., 2021).

Position	Location	Reasoning	Current	Effect pre UV	Type of current	UV change
GluN1 K178 (control) with GluN2B	NTD Intradimer interface	Tested, UV validation			large	
GluN3A S892	Inner side, $\alpha$ J	Functional effect on GluN3A, previously published			large	
GluN3A K895	Inner side, $\alpha$ J	Functional effect on GluN3A, at minimum distance from GluN1				
GluN3A H904	Inner side, $\alpha$ K	Functional effect on GluN3A, at minimum distance from GluN1			large	
GluN3A Y805	Outer side, $\alpha$ F	Functional effect on GluN3A, at minimum distance from GluN1, tyrosine			large	
GluN1 N521	Inner side, $\alpha$ D	at minimum distance from GluN3A with H bonds , previously published			large	
GluN1 Y692	Inner side, $\alpha$ F	At minimum distance from GluN3A $\alpha$ J, tyrosine			large	
GluN1 R755	Inner\ central side, $\alpha$ F	At minimum distance, making H bonds with ser 650, electrostatic interaction in GluN2A and GluN2B			small	
GluN1 L777	Outer side, $\alpha$ F	Gielen residue, making hydrophobic contact with GluN3A $\alpha$ D			large	
GluN1 S530	Central side, $\beta$ 9	previously published with PSAA			minuscule	
GluN1 P532	Central side, $\beta$ 9	previously published with PSAA			large	
GluN1 I519	Inner side, $\alpha$ D	At minimum distance from GluN3A , Functional effect on GluN3A			large, only glycine	
GluN1 K178 with GluN3A	NTD	Functional effect when coupled with GluN2B			large	
GluN1 Y109	NTD	Functional effect when coupled with GluN2B			medium	

Table 10 Summary of UAA tests in GluN1\GluN3A.

Table showing individual mutant constructs described in each line of the table. For each mutant the location and chain name in the LBD intradimer interface is specified, the selection criteria for including it in this study,

*a bicolor green/red output if we could record functional currents from it, a bicolor green/red output if the current phenotype was different than GluN1/GluN3A WT pre UV modulation, a qualitative analysis on current sizes with 50 nM CGP and 100 μM glycine, and a bicolor green/red output if we could achieve a change in current phenotype when applying the UV light protocol.*

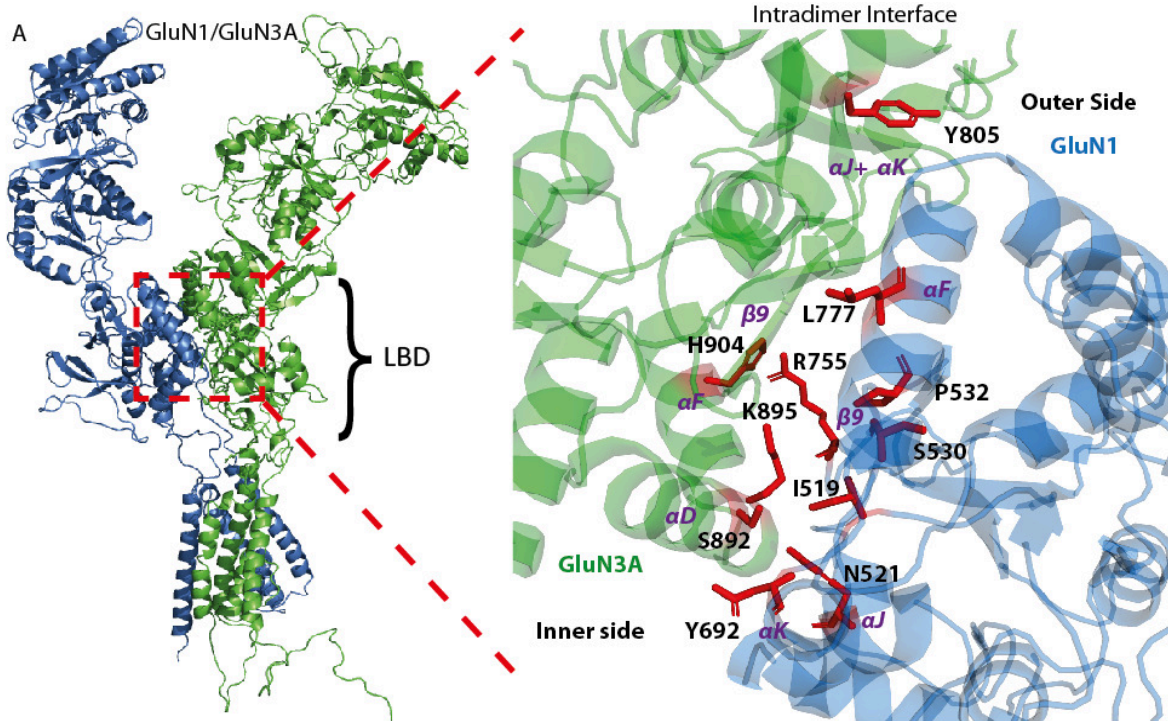
As a control of the UAA approach and conditions we tested UV-mediated AzF potentiation at 365nM in the published mutant GluN1 K178AzF/GluN2B construct (Tian *et al.*, 2021). We managed to obtain current potentiations with this recombinant construct (although potentiations were slightly inferior in size compared to the size previously published in the literature – Figure 58 Panel B). Similarly to what we did with the control, we tested the current and UV sensitivity of the AzF-mutated GluN3A receptors. The main idea in our case is to catch putative modifications of their desensitization properties upon UV application.

We started screening our AzF mutants activity (without UV light) both with glycine 100 μM or with glycine 100 μM and 50 nM CGP. We managed to record currents with CGP (but not with glycine alone) for all mutants (except 2) (Table 10), with the majority of mutants producing robust currents. Interestingly, two mutants -GluN1/GluN3A Y805AzF and GluN1 P532AzF/GluN3A desensitized faster than the GluN1/GluN3A WT in the absence of UV light. While the GluN1/GluN3A WT desensitizes of only about ~ 10% after 10 seconds of continuous agonist application, the mutants GluN3A Y805AzF and GluN1 P532AzF showed 25% and 53% respectively (Figure 59 panels D-E, Figure 60 panel B). We noted that the mutant GluN1 P532 is located in the hinge of the GluN1 LBD (β9). Therefore, it might influence affinities of glycine and CGP binding to the ligand-binding-pocket (LBD), or the mutant might influence the synergy of the intradimer interface. The other mutants present current phenotypes similar to the GluN1/GluN3A WT, and we could record glycinergic currents from the mutants GluN1 N521AzF/GluN3A and the mutant GluN1 I519AzF when paired with GOF mutant GluN3A S892L-K895F (Figure 59 Panels F, G)

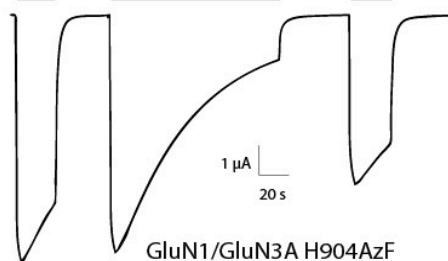
**The application of UV light on the activated GluN3A AzF mutants led to a noticeable but small (10%) reduction of peak current, however this effect is also observed in GluN1/GluN3A WT receptors.** Therefore, we hypothesized that either there is 1) an incomplete recovery from desensitization caused by the long time spent in desensitized state during the protocol of UV application or 2) the UV light might cause an unspecific reduction in activity on GluN1/GluN3A receptors (Figure 59 Panel B, Figure 60 Panel A). Looking closer at the different mutants we can notice different sizes of reductions in peak current. Some mutants located in the Inner side of the Intradimer Interface like GluN1/GluN3A H904AzF or GluN1 Y694AzF/GluN3A had the peak currents become half in size when comparing pre and post UV treatment

(Figure 59 Panel C, Figure 60 Panel A). On the contrary, the NTD mutants had the same reduction of peak current size pre/post UV as the WT, ~ 10% (Figure 60 Panel A). Still the effects are small and lie at the limit of significance. We also checked if the kinetic properties of the mutant were affected (Figure 61) but none of the mutants had any significant change in the speed of desensitization after the UV protocol.

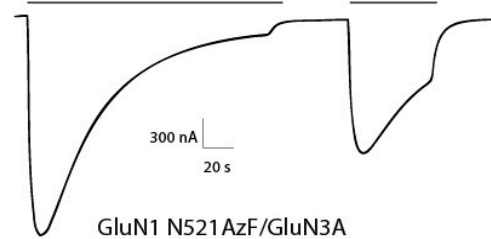




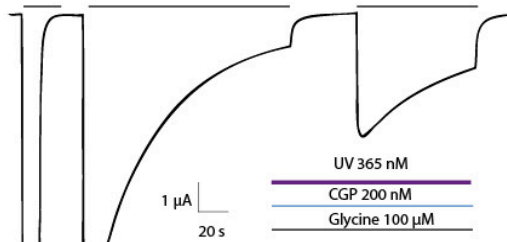
**B** GluN1/GluN3A WT



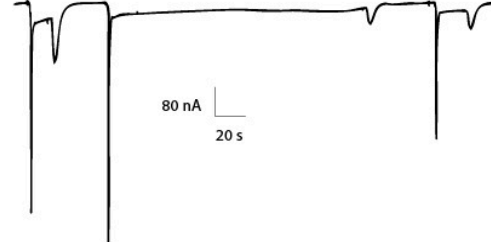
**E** GluN1/GluN3A Y805AzF



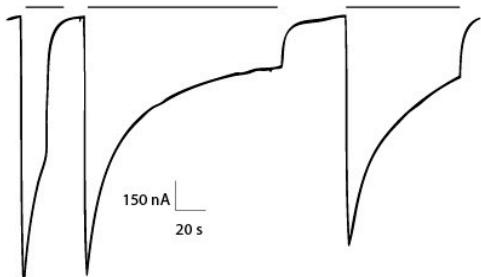
**C** GluN1/GluN3A H904AzF



**F** GluN1 N521AzF/GluN3A



**D** GluN1/GluN3A P532AzF



**G** GluN1 I519AzF/GluN3A S892L-K895F

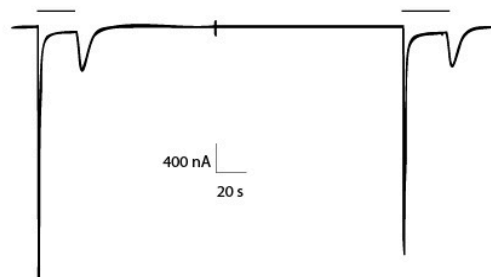


*Figure 59 UAA mutants in GluN1/GluN3A Intradimer Interface.*

*Panel A, graphical representations obtained with Pymol of the whole GluN1/GluN3A dimer on the left, and of the magnified LBD intradimer Interface represented as a cartoon on the right. Residues that were chosen within this interface and modified into AzF are highlighted with their numbering and the side chains visible in red. Chain numbering and positions are noted in purple. Panels B-G, example traces for GluN1-GluN3A receptors containing AzF mutants and treated with UV application during agonist application for ~100 seconds. Conditions shown are GluN1/GluN3A WT, GluN1/GluN3A H904AzF, GluN1/GluN3A P532AzF, GluN1/GluN3A Y805AzF, GluN1 N521AzF/GluN3A and GluN1 I519D/GluN3A S892L-K895F respectively for panels B-G. Constructs GluN1 N521AzF/GluN3A and GluN1 I519D/GluN3A S892L-K895 are shown in the absence of CGP. Each subunit was injected at 120 ng/L for with the aminoacyl synthetase at 5 ng/L and an orthogonal suppressor tRNA at 10 ng/L in the Barth incubation media containing the UAA and incubated in the dark for 72 hours before testing.*

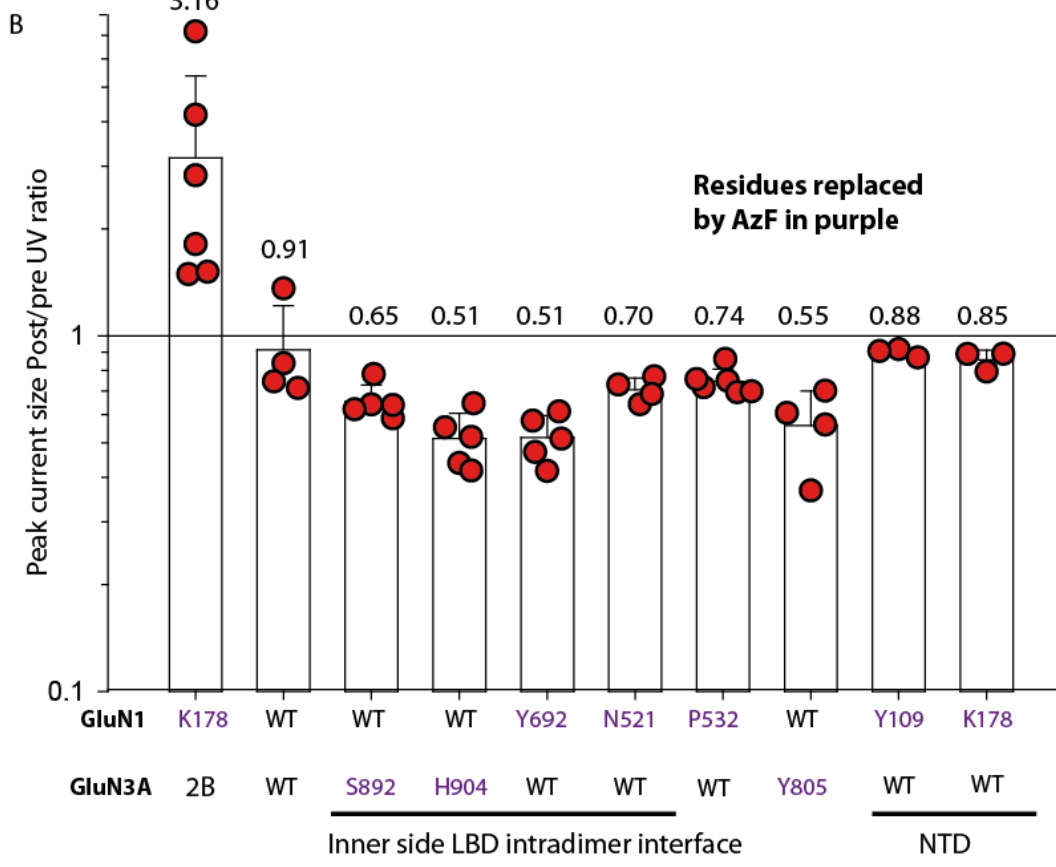
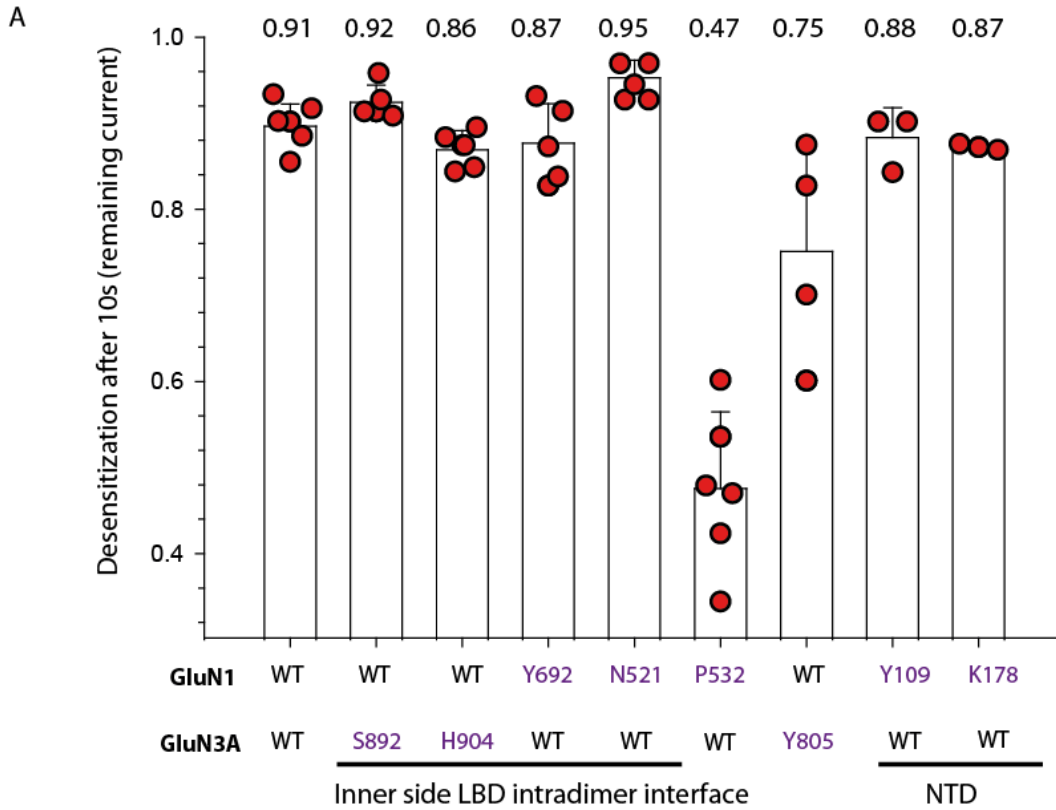


Figure 60 UAA peak currents and desensitization.

Panel A, a quantification of the speed of desensitization in the presence of 50 nM CGP and 100  $\mu$ M glycine for the different mutants in the absence of UV light. The histogram shows on the Y axis the steady state current size/peak current after 10 seconds of continuous agonist application. The mutants displayed are GluN1/GluN3A WT, GluN1 Y109AzF/ GluN3A, GluN1 K178AzF/GluN3A, GluN1/GluN3A Y805AzF GluN1 P532AzF /GluN3A GluN1 N521AzF/GluN3A, GluN1Y692AzF/GluN3A GluN1/GluN3A H904AzF GluN1/GluN3AS892AzF. Panel B, ratio of peak current size in the presence of 50 nM CGP and 100  $\mu$ M glycine for the different mutants before and after UV application for 100s. The mutants displayed are the same displayed in Panel A, with the addition of the control GluN1 K178AzF/GluN2B tested with 100  $\mu$ M glutamate and 100  $\mu$ M glycine.

We tried to quantify the speed of desensitization of the mutants in comparison to the WT after the UV treatment to see if light application had modified the properties of the receptors or not. The majority of the mutants were within the standard deviation of the desensitization of the WT before the UV application (~ 10%), and the UV application protocol did not significantly change this value for any of the mutants (Figure 61 Panel A). Concerning the mutants that displayed a difference in the speed of desensitization than the GluN3A WT before the UV protocol, they also were unchanged after the UV protocol. This is also the case for the mutant GluN1 I519D/GluN3A S892L-K895F, which was tested in the absence of CGP, but only in presence of 100  $\mu$ M glycine (Figure 61 Panel B).

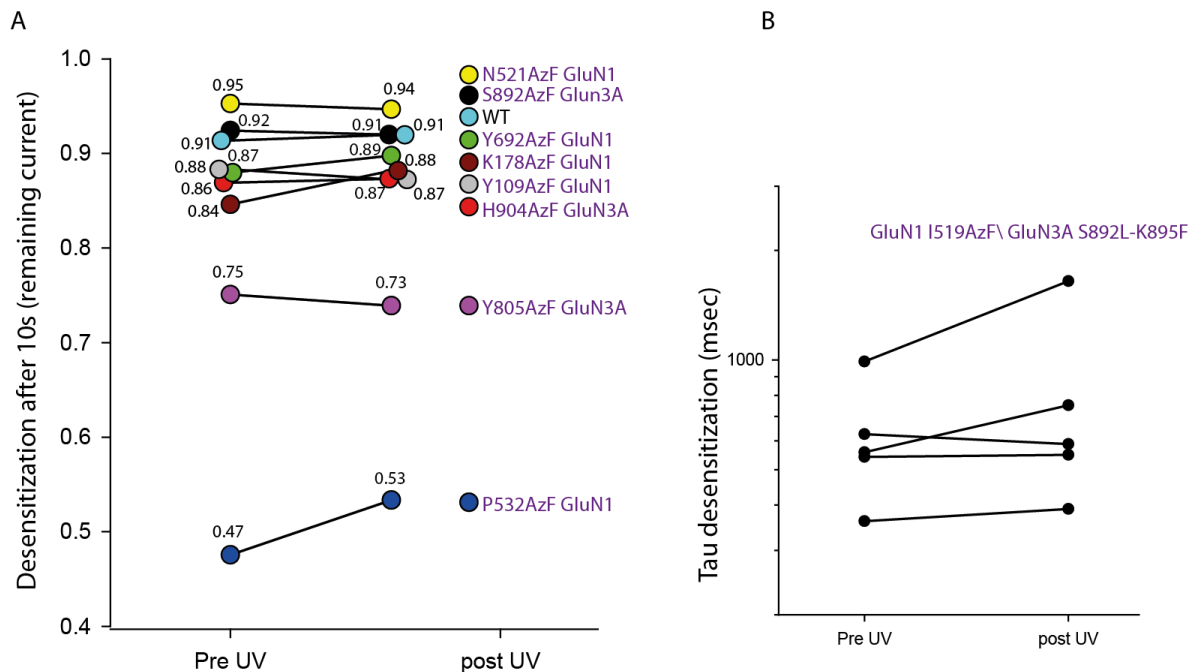


Figure 61 UV effect on desensitization in UAA mutants.

Panel A, averaged mean 10 seconds desensitization of steady state current compared before and after UV application. The histogram shows on the Y axis the steady state current size/peak current after 10 seconds of continuous agonist application (100  $\mu$ M glycine after 50 nM CGP pre-incubation). Each dot represents a different mutant. The mutants displayed are GluN1/GluN3A WT, GluN1 Y109AzF/ GluN3A, GluN1 K178AzF/GluN3A, GluN1/GluN3AY805AzF GluN1P532AzF/GluN3A GluN1N521AzF/GluN3A, GluN1Y692AzF/GluN3A, GluN1/GluN3A H904AzF, GluN1/GluN3AS892AzF. Panel B, plot showing tau of desensitization (msec) fitted with a single exponential equation for individual cells of the mutant GluN1 I519D/GluN3A S892L-K895F in the presence of 100  $\mu$ M glycine .

It was a disappointing result that we could not produce a clear example of real-time current modification of the AzF GluN1/GluN3A mutant receptors upon light illumination. The change in current sizes in GluN1/GluN3A WT receptors was a confounding variable when trying to infer potential effects caused by the UV light protocol. Since we observed the reduction on the GluN1/GluN3A WT, the results point to the artefactual hypothesis, but the different sizes of current reduction in different mutants' point to a possible effect mediated by the crosslink of the mutants. Overall, it is unclear if we were able to have a successful LBD dimer crosslinking or not.

To further test if we could modulate the receptor function in real time with optocontrol methodologies, we tried to test the positions GluN1 S530 and GluN1 P532 with single photoswitchable amino acids (PSAAs) modifications to attempt real time photoswitchable isomerization like in (Klippenstein *et al.*, 2017), but we could not detect any electrical activity with these constructs. At this point, we decided to not push the experiments further since the absence of UV induced current-change phenotype indicated we didn't obtain the opto-tool we had intended to achieve.

Still, our screening allowed to identify the position GluN1 P532 as an interesting target to mutate (even outside of the context of opto-tool development). Since this position appears to change the speed of desensitization of GluN1/GluN3A receptors, we decided to further modify the residue into a much shorter one: Alanine but also in Tyrosine: a hydrophobic aromatic amino acid reassembling the most to AzF. Interestingly, we saw that the mutant in Tyr had a much faster desensitization kinetic like with AzF, while the mutant in A desensitized at the same speed as the GluN1/GluN3A WT (Figure 62). Therefore, this position appears seemingly to be involved in the desensitization properties of GluN1/GluN3A receptors, although it is unclear if this effect comes from the modification of the GluN1 affinities to the agonists, the modification of the clamshell closure through the hinge, or the influence of the contacts with GluN3A LBD.

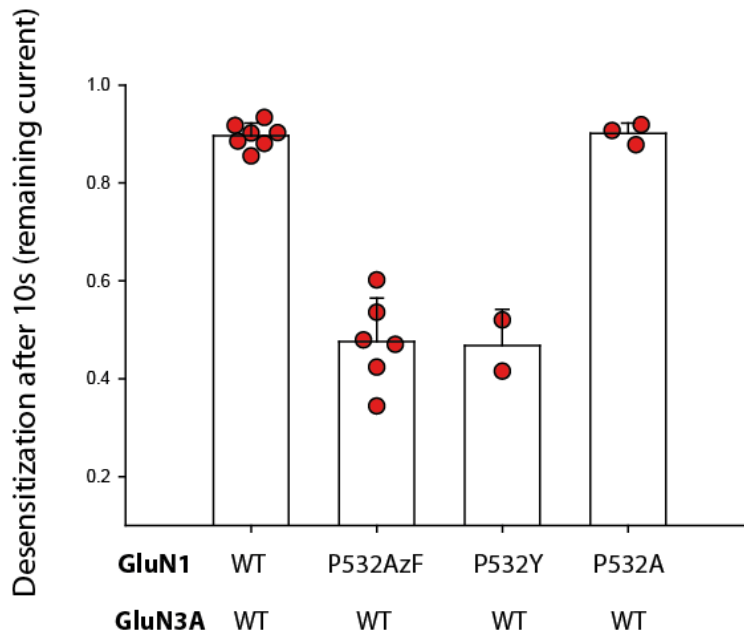


Figure 62 GluN1 P532 mutants.

Quantification of the speed of desensitization in the presence of 50 nM CGP and 100  $\mu$ M glycine for the different GluN1 P532 mutants. The histogram shows on the Y axis the steady state current size/peak current after 10 seconds of continuous agonist application. The mutants displayed are GluN1/GluN3A WT, GluN1 P532AzF/GluN3A, GluN1 P532Y/GluN3A, GluN1 P532A/GluN3A.

### 8.5 GluN1 agonist binding sites function in the GluN1/GluN3A context

Because of its strong potentiating effect on GluN1/GluN3A receptor, the mutant GluN1-F484A, has had a paramount role in clarifying the activation mechanisms of GluN1/GluN3A receptors in the literature. Since it prevents or greatly reduces the binding of glycine to GluN1, it almost abolishes the activation of the GluN1 desensitization component thus allowing to activate GluN3A component of the receptor with glycine alone (No CGP). **However, the PO of this mutant has never been measured.** We thus coexpressed GluN1-F484A with GluN3A-A765C in xenopus oocytes (Figure 63 Panel A) for relative PO estimation with the MTSEA approach. MTSEA application on this co-assembly produced very large and slow potentiations (average  $27.1 \pm 2.9$ ), which were much larger ( $4.4 \pm 0.4$ ) than with GluN1-WT/GluN3A-A765C. This result clearly indicates that GluN1-F484A mutant has a much lower PO than the WT. We also attempted to record the relative PO from the same mutant, but in presence of glycine and 200 nM CGP, albeit the receptor should be virtually insensitive to CGP (Figure 63 Panel B). We were able to confirm the same tendency, with the GluN1-F484A mutant receptors displaying a much lower PO ( $18.5 \pm 2.1$ ), albeit a little

higher than what we had measured without CGP. **This test thus unexpectedly show that the reference mutant GluN1-F484A has a reduced PO.** We can hypothesize that the mutant GluN1-F484A favors a mean conformation of GluN1 LBD that is less opened than with CGP. The mutant will thus be less potent than CGP to reduce the desensitizing effect of GluN1 within GluN1/GluN3A receptors.

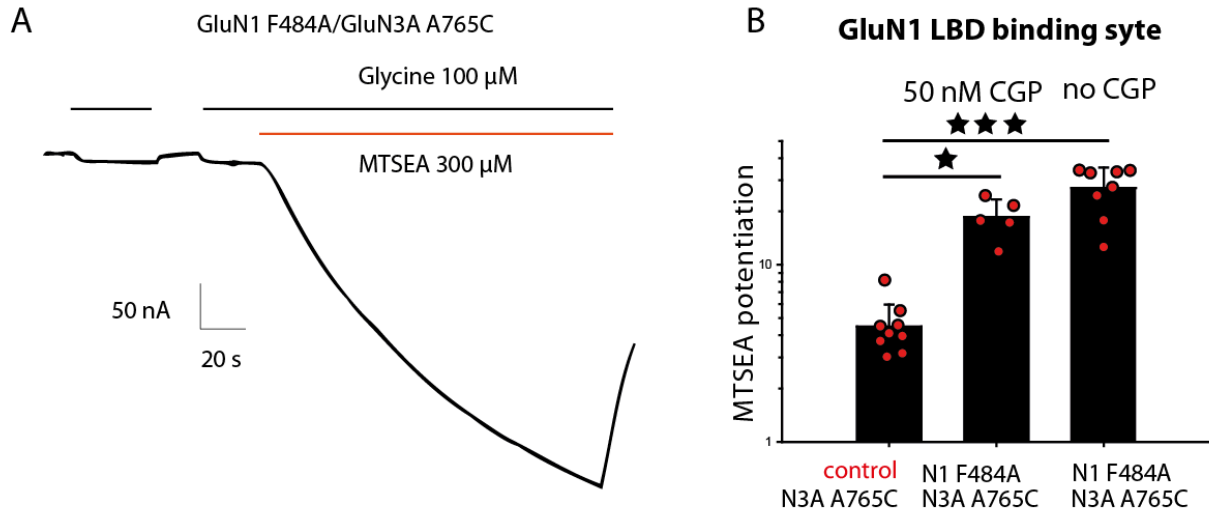


Figure 63 Glycine binding site mutant PO.

Panel A, example trace from GluN1 F484A/GluN3A A765C with glycine 100 μM, and MTSEA 300 μM. Panel B, histogram showing significant differences between the control pore mutant in GluN3A and the mutants F484A both in presence and absence of CGP (potentiations of  $4.4 \pm 0.4$ ,  $18.5 \pm 2.1$  and  $27.1 \pm 2.9$  respectively)

## 8.6 Attempts to study the LBD-TMD transduction mechanism

LBD-TMD linkers are key elements in the gating process of iGluRs function that communicate the LBDs agonist sensing states to the pore (Amin *et al.*, 2021; Hansen *et al.*, 2021). In GluN2 containing NMDAR, we don't know yet precisely how the transduction signal occurs through the linkers. It is a complex phenomenon since it involves 12 (3x4) LBD-TMD linkers per NMDARs, but it is genuinely thought that increases in linker tension leads to pore opening while relaxation of linker tension allows to reach resting and desensitized states. In GluN3A containing receptors this process should also take place somehow but its importance in the function of this receptor has not been tested. We decided to test the effect of mutants in the linker that could perturb the coupling the LBD to the TMD in GluN1/GluN3A receptors. Using the strategy employed in (Amin *et al.*, 2021) on GluN2-containing NMDARs, we made insertion mutagenesis to add glycine residues in the linker. We created 3 individual mutant constructs for each

subunit: GluN1 I546+G S802+G, G666+G, and the homologous positions in GluN3A R660+G, S917+G, G779+G and. It corresponds to one glycine addition for each linker for each subunit, the D2-M1, D1-M4 and D2-M3 (Figure 64 Panel A). I presented here some preliminary results obtained with these mutants.

None of the GluN1/GluN3A linker mutants gave currents with glycine application alone, but some were functional in the presence of 200 nM CGP. The mutants GluN1 I546+G and GluN3A R660+G gave us the highest level of expression and do correspond to the homologous positions located in the D2-M1 linker (Figure 64 Panel A). The glycine dose response of GluN1/GluN3A R660+G (in 50 nM CGP) gave an  $EC_{50}$  of  $10.1 \pm 1.4$ , compared to the GluN1/GluN3A WT ( $45.9 \pm 1.7$ ) (Figure 64 Panel B). Interestingly, the mutation of the cysteine GluN3A C859S-C913S (Grand *et al.*, 2018) sitting just above the linker region (D1-M4) were also found to greatly increase affinity for GluN3A ( $EC_{50} = 3.0 \pm 0.3 \mu\text{M}$ ). These results seem to point in the same direction. Releasing the tension between the LBD and the TMD lead to increase of glycine affinity in the GluN3A subunit.

Using the MTSEA approach, we measured the PO of the GluN3A R660+G and of the original GluN3A C859S-C913S but also the corresponding GluN1 C744S-C798S mutant (Grand *et al.*, 2018). The GluN1 C744S-C798S exhibit increased PO ( $1.76 \pm 0.6$ ) vs the control ( $4.4 \pm 0.4$ ), while both the mutant GluN3A C859S-C913S (potentiation =  $32.9 \pm 6.8$ ) and the GluN1 I546+G ( $14.7 \pm 3.1$ ) mutants lowers the PO (Figure 64 Panel C). We did not have sufficient data for the mutant GluN3A R660+G, but the data points to a possible lower PO than the control (Figure 64 Panel D). The high PO mutant GluN1 C744S-C798S is compatible with the findings of (Grand *et al.*, 2018), where it was proposed that removing this cysteine bridge potentiates current sizes. The reduced PO of GluN1 I546+G appears compatible with (Amin *et al.*, 2021) that also found insertions in the linker connecting the LBD to M1 in GluN1 to reduce NMDARs gating when coupled to GluN2s. It is highly possible that GluN1 linkers also play a different role in transducing the gating mechanism from the LBD to the TMD in a GluN3A context. Contrarily, the mutant GluN3A C859S-C913S seems to release tension in this region thus lowering the PO, even if it is associated to a gain of function in terms of left shift of glycine sensitivity. Altogether, these preliminary data appear promising but more data and a systematic scanning of these residues would be necessary to reach conclusions about the complex interplay of linker tensions, LBD states, receptor gating properties and POs.



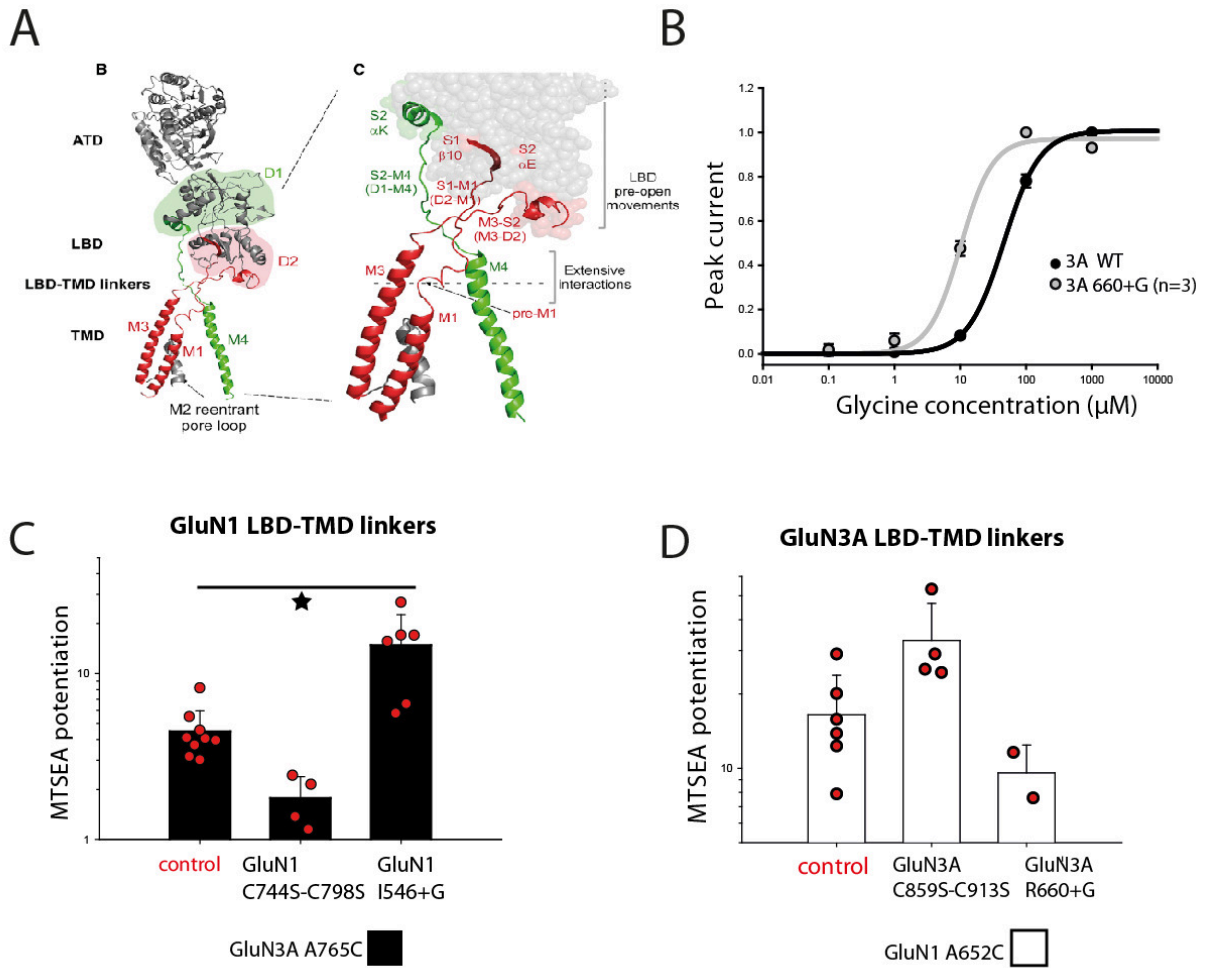


Figure 64 LBD-TMD linker mutants.

Panel A, inset taken from (Amin et al., 2021) showing dimer LBD-TMD linker architecture with an highlight on connections between D1,S2, and M1,M3,M4. Panel B, glycine dose responses for GluN1/GluN3A WT in black and for GluN1/GluN3A R660+G in grey, both in the presence of 50 nM CGP.  $EC_{50}$ s for glycine in  $\mu M$  were estimated to be  $45.98 \pm 1.77$  ( $N=5$ ) and  $10.1 \pm 1.4$  ( $N=3$ ) for GluN3A WT and GluN3A R660+G respectively. Panels C and D, histogram summarizing mean values obtained for MTSEA-induced potentiations on GluN1 linker mutants (C) and GluN3A linker mutants (D) with 200 nM CGP and 300  $\mu M$  MTSEA.

## 8.7 Attempts to reveal triheteromeric GluN1/GluN2B/GluN3A receptor activity

In our manuscript we showed how by employing the recombinant construct GluN1/GluN3A S892L-K895F we can obtain square non-desensitizing currents when applying 1  $\mu M$  of glycine alone. We reasoned that by employing our mutant, we could perhaps for the first time isolate the electrophysiological response of GluN1/GluN2B/GluN3A triheteromeric receptors. In the GluN1/GluN2B/GluN3A receptors are considered as one of the main form of active GluN3 in the brain, but the literature is contrasting on the

topic, and no one recorded isolated triheteromeric currents in recombinant expression systems (Chatterton *et al.*, 2002; Ulbrich and Isacoff, 2008; Crawley *et al.*, 2022). Still, the difficulty of isolating triheteromer currents comes from the difficulty to separate the contributions of the different co-injected subunits that would also spontaneously form standard GluN1/GluN3A and GluN1/GluN2B receptors at the plasma membrane, but also because the GluN1/GluN3A and triheteromer component may desensitize together so quickly and deeply that they will barely be distinguished. The GluN3A non-desensitized mutant (that could be activated by Glycine alone and therefore avoid the usage CGP that would interfere with all GluN1 subunit present) may thus offer the possibility to overcome on this important initial difficulty and help to pharmacologically isolate the triheteromer component. Indeed, according to the literature, the triheteromer is expected to be  $Mg^{2+}$  insensitive (because it contains GluN3A) but inhibited by APV (because it contains GluN2B), while GluN1/GluN2B should be inhibited by  $Mg^{2+}$  and GluN1/GluN3A is APV insensitive.

We co-injected the construct GluN3A S892L-K895F with GluN1 and GluN2B in the proportions (0.6:1:0.4) in xenopus oocytes and incubated for 48 hours. The GluN3A mutant activation component is first revealed with 1  $\mu$ M glycine application, then the one of GluN2B by adding 100  $\mu$ M glutamate on top of the glycine (Figure 65), confirming that the three subunits are well expressed at the plasma membrane – at least as diheteromers. As a test we added 1mM  $Mg^{2+}$ , inhibiting all GluN1/GluN2B diheteromers and about only 20% of GluN1/GluN3A diheteromers (Figure 38). We then added on top of it 100  $\mu$ M APV, a concentration supposed to inhibit triheteromers (and about 10-15% of GluN1/GluN3A diheteromeric currents (Chatterton *et al.*, 2002)). The observed APV inhibition should thus correspond to the triheteromer contribution (Figure 29). When we normalized this inhibition to the GluN3A+GluN2B full activation (L1 parameter) versus the same protocol done on the control condition GluN1/GluN2B diheteromers, we obtained a value of inhibition of about 4.1 %  $\pm$  0.9 vs 0.8 %  $\pm$  0.3 respectively. When normalizing the inhibition to the size of the activation of the GluN2B component only (L2 parameter) we obtained values of 11.1%  $\pm$  5.6 vs 0.8%  $\pm$  0.3 respectively. However the observed APV inhibition appear almost identical (if not smaller) with the values predicted by (Chatterton *et al.*, 2002) for APV inhibition on the diheteromeric GluN1/GluN3A component alone (about 10-15% of GluN1/GluN3A diheteromeric currents predicted by Chatterton et al, (Chatterton *et al.*, 2002)). If we hypothesize that GluN1/GluN2B/GluN3A triheteromers have an intermediate APV sensitivity between GluN1/GluN2B and GluN1/GluN3A, we should have observed a larger APV-mediated inhibition. Although these experiments are preliminary and indirect, the small APV inhibition

we observed corresponds well to the sum of properties of GluN1/GluN2B diheteromers and GluN1/GluN3A diheteromers with no involvement of a triheteromeric component. This result points in the direction of (Ulbrich and Isacoff, 2008), who suggested that GluN1/GluN2B/GluN3A may not assemble at the membrane of xenopus oocytes.

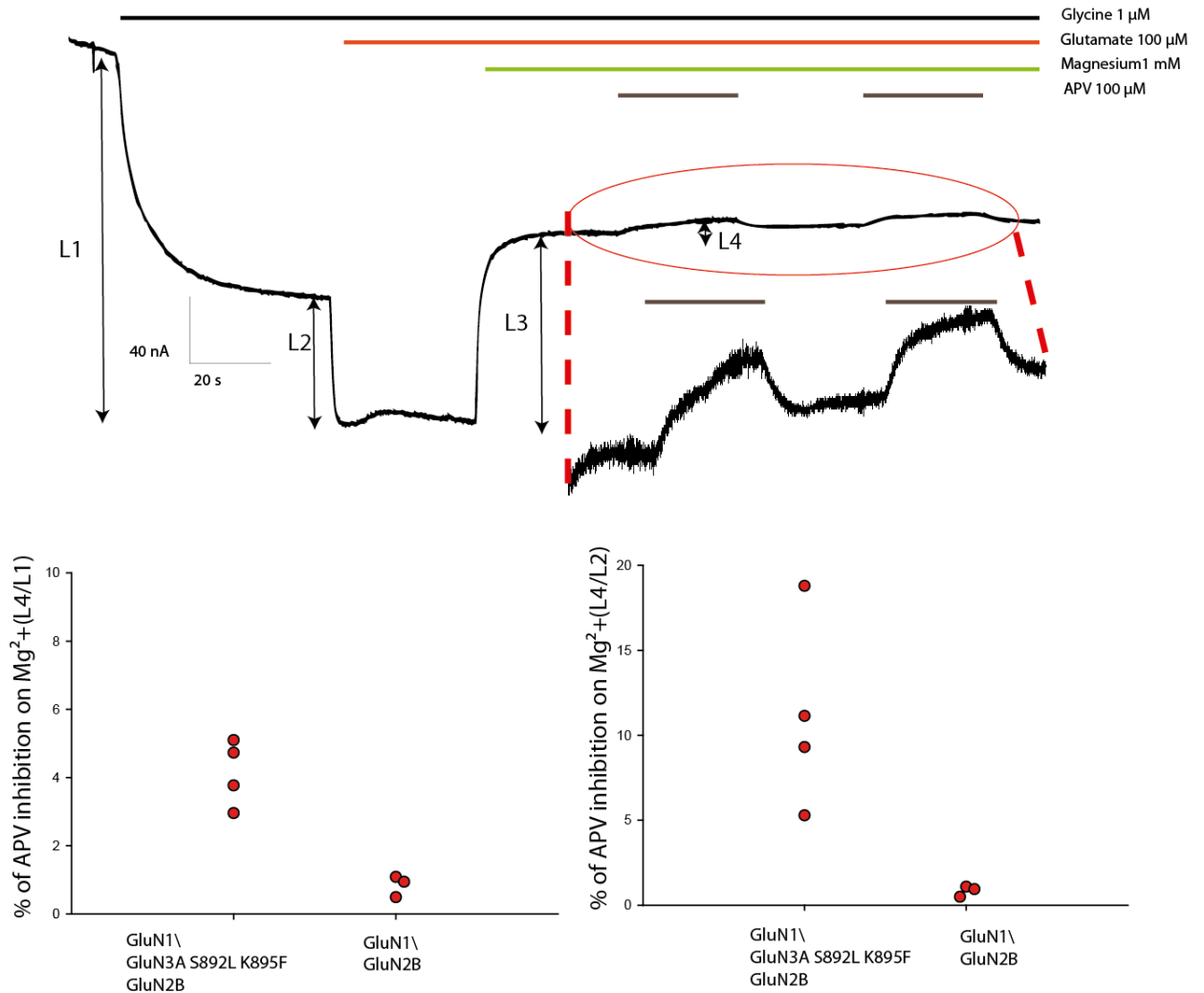


Figure 65 Triheteromer GluN1/GluN2B/GluN3A experiments.

Representative trace displaying pharmacological properties of receptor populations containing coinjections of GluN1 (1), GluN3A S892L-K895F (0.6), GluN2B (0.4). Agonists are glycine 1 μM and glutamate 100 μM. Inhibitors are magnesium 1 mM and APV 100 μM. Components of receptor activation and inhibitions are quantified as following: GluN3A+GluN2B activation (L1), GluN2B activation(L2), Magnesium inhibition(L3), Apv inhibition (L4). On the bottom, Panels quantifying APV inhibition in GluN1/GluN2B/GluN3A coinjection populations versus GluN1/GluN2B coinjection populations.



## **Third chapter: Discussion**

## 9 General discussion

In the span of about 70 years the scientific understanding of the physiological correlates of brain function has increased at an astounding rate. We have progressed from formulating the hypothesis of the existence of electrical stimuli propagating through living tissues in the 1950s to performing the characterization with atomic precision of the receptors structures responsible for those same electrical currents. We have discussed the complexity of the chemical and electrical organization of the synapse in the introduction, and how ion channels regulate its function and allow for a correct homeostasis in the brain and for cellular communication. For several decades now it is known that GluN2 containing NMDA receptors are fundamental for the shaping of the synaptic properties in the CNS through key mechanisms such as synaptic plasticity, learning and cell excitability. It is thus astounding that it is only in the last 5 years we have been able to finally prove that GluN3A, one of the 7 subunits that compose this family of receptors, is directly contributing to ionotropic activity in the brain(Grand *et al.*, 2018; Otsu *et al.*, 2019; Bossi *et al.*, 2022) For more than twenty years these receptors were considered as a regulatory subunit. This recent discovery indicates that we still lack fundamental knowledge on some aspects of the ionotropic activity in the CNS.

Often key advancements in the field, either methodological, pharmacological or conceptual, allow to quickly open new possibilities for the investigation of subjects that were previously considered unexplained and unapproachable. In some regards, the pharmacological discovery of the selectivity of CGP for GluN1 over the GluN3A subunit has had this precise effect in the field of GluN3A research (Yao, 2006; Grand *et al.*, 2018). It has allowed to discover that these receptors are expressed and functional in the CNS, and this finding has generated a renewed interest in a subunit whose effective importance had been questioned historically. These functional data, alongside new generation single cell transcriptomics and RNAscope hybridization techniques analysis are showing that GluN3A expression levels are retained in specific cell types in adulthood (Paul *et al.*, 2017; Murillo *et al.*, 2021), which is highlighting how our knowledge of GluN3As role in the CNS may have been at times misinterpreted. For many years it was believed that GluN3A was mainly co-expressing together with GluN2s and GluN1s being a dominant negative regulatory subunit that would decrease the synaptic contribution of these channels (Das *et al.*, 1998; Pérez-Otaño *et al.*, 2001b; Pachernegg *et al.*, 2012), as no currents seemed to be detectable with the diheteromers alone. Even after the discovery that GluN1/GluN3A diheteromers are functional in heterologous expression systems (Chatterton *et al.*, 2002; Awobuluyi *et al.*, 2007; Madry *et al.*, 2007),

the idea of GluN3A being mostly expressed in a triheteromeric fashion *in vivo* had become the standing paradigm in the interpretation of the data concerning GluN3As. Hence, only recently we have started to challenge this idea, as the latest results point to diheteromeric GluN1/GluN3As being expressed and functional in some anatomical regions of the adult mammalian brain (Grand *et al.*, 2018; Otsu *et al.*, 2019; Bossi *et al.*, 2022).

However, while some aspects of the GluN3A containing NMDARs begin to be better understood, especially in the physiological and developmental fields, others have been lacking behind. These are the aspects, among others, that describe the relationships between the structural correlates of the protein and its function. Especially, its puzzling gating mechanism has been explored only in a handful of key studies, but many questions remain concerning its structural correlates. For example, one of the main questions that remains unanswered is why (in the context of GluN1/GluN3A receptors) the GluN1 subunit acts as an auto-inhibitory subunit in a unique fashion among NMDARs, and what is the molecular support of this behavior within the receptor. In my research, we have tried to tackle some of those key questions, alongside trying to develop new methodological tools to ease the study of GluN3As. Some attempts have been quite successful, while others did not. In the following section I will try to summarize and conclude what we found within my PhD project, and I will give some perspectives to continue the research on GluN3A containing receptors.

## 9.1 Methodological developments

We have successfully developed some methodologies to study GluN1/GluN3A receptors, namely thanks to the discovery of a potent open channel blocker and by implementing the MTSEA methodology to estimate the  $P_o$  of GluN3A receptors. Concerning pentamidine, this compound can be used to inhibit GluN3A WT and mutant receptors, is already approved for its use in humans, and we are the first group to characterize its efficiency on GluN3A. Future studies will have to investigate more precisely its binding site, in order to understand why this open channel blocker is able to inhibit GluN3A at low  $\mu\text{M}$ , while other standard NMDA receptor open channel blockers only work in the mM against this receptor (Chatterton *et al.*, 2002; McClymont *et al.*, 2012). Concerning the MTSEA methodology, it provides a readout to compare mutants to a baseline WT activity, allowing us to deepen our understanding of how different mutations at key spots in the receptor can influence the activity of GluN3A. We have employed this methodology to investigate key mutants that have been used in the literature to characterize the

activity of GluN3A receptors like the mutant GluN1 F484A (Awobuluyi *et al.*, 2007; Madry *et al.*, 2007), or to investigate new mutants like the double mutant at the LBD intradimer interface S892L-K895F to highlight its gain of function properties. The results we obtained with MTSEA have been surprising, like when we tested GluN1 F484A or the double endogenous cystless mutant C744S-C798S. We revealed that these mutants decrease overall receptors PO, although they were previously shown to facilitate the recordings of glycinergic currents, the former by preventing glycine binding at GluN1, and the latter by shifting the GluN3A subunit glycine EC<sub>50</sub> to the left. In addition, MTSEA helps dissecting complex mutant mechanisms. This was the case for S892L-K895F, which both shifts the glycine EC<sub>50</sub> to the left, and also increases receptor PO, therefore having a complex interplay effect on receptor biophysical properties. Therefore, with MTSEA we provide a new tool to the field that can be used in future studies to help characterize new mutants without recurring to single channel recordings.

Continuing with the methodological developments, we have shown that zinc modulation on receptor function seem more nuanced than what had been hypothesized on the papers that have described it before. Interestingly, some papers found zinc to be a GluN3A potentiator, while others did not, adding uncertainty on the topic (Cummings and Popescu, 2016; Otsu *et al.*, 2019; Madry and Betz, n.d.). Specifically, three papers used zinc to show that its pre-incubation potentiates glycinergic currents, while also being able to activate receptors on their own, also in receptors lacking the NTD (Cummings and Popescu, 2016; Cummings *et al.*, 2017; Madry and Betz, n.d.), which is the binding site for zinc in the GluN2 subunits (Paoletti *et al.*, 1997b; Jalali-Yazdi *et al.*, 2018). The only case where zinc was not having functional effects was in receptors containing the mutation F484A which prevents glycine binding. One papers found zinc to be an inhibitor of glycinergic currents (Wada *et al.*, 2006), while another paper found zinc to not have an effect on GluN3A mediate currents *ex vivo* (Otsu *et al.*, 2019). In our hands, zinc appeared to be both a potentiator and an inhibitor of GluN3A mediated currents, depending on the conformational state of the receptor, and on the molecules already bound to it. We found zinc to be potentiating or generating currents when applied to the WT receptor in the presence of glycine. Inversely, zinc was inhibiting currents when the mutant F484A was present in GluN1, or when receptors were pre-incubated with CGP. Similar results were observed with mutants located at the intradimer interface. One hypothesis that could explain this complex relationship is the existence of multiple binding sites for this molecule, some of which could be accessible only in specific conformations, or competing with other molecules. We are the first to reveal this complex state dependence of zinc and GluN3A, and future studies will have to try to determine where the binding sites are located in the molecule, and



which recording conditions can favor which effect. In addition, a dose response to verify its  $EC_{50}$  and  $IC_{50}$  in different functional states also seem a key prerequisite to draw conclusions about zinc modulation on GluN3A. If it is revealed to be efficient at low concentrations, the modulation of zinc might be especially important considering that GluN3A is often found in brain regions without afferent glycinergic terminals, leaving open the question of what are the endogenous neurotransmitters that modulate this receptor (Paoletti, A.M. Vergnano, *et al.*, 2009; Bossi *et al.*, 2022).

## 9.2 GOF mutants

Another aim of my research was to try to create GOF mutants, and for this aim we have had successful results. However, the mutants we isolated are different from what we had originally hoped to characterize. We started the research hoping to be able to create a mutant that is able to eliminate the desensitization during glycinergic stimulation, like the mutants that do so for glutamate transmission in AMPARs (Sun *et al.*, 2002; Armstrong *et al.*, 2006). We have not been able to isolate a mutant with those characteristics, and desensitization of the tetrameric complex by the GluN1 auto-inhibition still remains a fundamental, yet unexplained, determinant of the shape of GluN3A receptors. However, we have been able to isolate not one, but many mutants within an interface that exhibits GOF mutant phenotypes. These mutants have differences in their current phenotype, and biophysical properties, but share the general core properties of increased PO and left shift of glycine affinity in the GluN3A subunit. These properties allow to have a much ampler window of GluN3A mediated activation in the presence of glycine, before the GluN1 mediated autoinhibition kicks in, allowing to produce qualitatively square GluN2-like currents at concentrations  $< 3 \mu\text{M}$ . Quicker perfusion systems will have to be used to evaluate the speed of desensitization in the presence of only glycine, to determine if the GluN1 auto-inhibition is slower than the WT. In the presence of CGP, the currents of these mutants present a squared shape, indicating a more stable, less-desensitizing open conformation than the WT. It is unclear if the decreased desensitization kinetics in the presence of CGP might be due to changes in affinity for glycine or to a decrease of the desensitization strength in itself. Perhaps our mutants can also be used to sense the levels of glycine, since they display tonic activation with ambient glycine, therefore being active only when the glycine concentrations reach a certain threshold. We hope that these mutants will be used in the future to help characterizing the activity of GluN3A receptors, as they allow to ease a lot the electrophysiological recordings on these receptors, without employing CGP.

Although CGP potentiates GluN3A receptors, its employment has limitations in studies of structure/function, since it forces the GluN1 subunit in an artificial conformation preventing desensitization by preventing the agonist binding-derived conformational changes following clamshell closure. By preventing these changes to occur, CGP renders complicated to infer at which point a mechanism associated with gate opening in GluN1/GluN2 complexes becomes a mechanism of inhibition in GluN1/GluN3A receptors.

We attempted to use one of these mutants, the GluN3A S892L-K895F, in a preliminary experiment to see if we could reveal the co-assembly of triheteromers containing the GluN1\GluN2B\GluN3A subunits when coinjected in xenopus oocytes. Although we could not draw definitive conclusions from this experiment, for the first time we have been able to separate the component of GluN3A activation with glycine from the GluN2 component of activation with glutamate + glycine, showing that it is possible to separate properties of diheteromers from triheteromers. New studies will have to better characterize the sensitivity of the GluN3A subunit to APV, in order to understand if it can be used to pharmacologically distinguish the existence of GluN3A containing diheteromers from the triheteromers. Only studies employing rigorous diheteromeric WT controls GluN1/GluN2B and GluN1/GluN3A, also distinguishing between receptors that are retained in the ER and receptors successfully trafficked at the membrane, will be able to indicate if triheteromeric receptors are active and contributing to the synaptic properties of GluN3A receptors in vivo and in vitro.

### **9.3 Molecular mechanisms of GluN3A containing receptors**

Concerning the main aspect of the project, which is trying to determine the molecular determinants of the mechanisms regulating the gating of GluN3A receptors, we successfully found a key structural determinant regulating receptor activity. The LBD intradimer interface is established as a key structural determinant for gating and allosteric modulation in NMDARs, and for gating and desensitization both in AMPARs and kainate receptors. In the latter receptors, a decreased strength of the interface causes a decreased dimerization at the LBD level, which is in turn responsible for the quick desensitization observed within these channels. This fact has also been shown in experimental structures of putative desensitized states where the dimers are highly separated, in some cases even separating in individual protomers turning towards a 4-fold symmetry(Schauder *et al.*, 2013; Twomey *et al.*, 2017b). Since GluN3A current phenotype shows quick desensitizing phenotype reminiscent of these classes of channels

more than currents mediated by the GluN1/GluN2 channels, we investigated the GluN3A LBD intradimer interface to determine how it was structurally organized, and to determine if it was important for receptor function. The lack of existing structural data concerning the interface obliged us to proceed by performing educated guesses based on sequences homology between GluN3A and GluN2B for the modeling of the interface. This modelling required making assumptions about the stoichiometry of the subunit co-assembly, since the effective dimerization of GluN1 and GluN3As at the LBD and other domain levels has never been proven. Hence, it is of the utmost importance for structural biologists to manage to provide high resolution structures of diheteromeric GluN1\GluN3A receptors, perhaps thanks to the advances in cryo-EM visualization and purification techniques, a field which is booming and rapidly advancing in terms of methodology. A solved tetrameric structure will finally prove which structural arrangement is undertaken by the protein at the different levels of the modular architecture. Since it seems highly problematic for structuralist biologists to purify GluN3As due its general conformational instability, perhaps our mutants could be useful as they seem to stabilize the open state, similarly to how GluN2 receptor mutants with higher PO in the rolled state were used recently used to solve structures of pre-active GluN2A containing NMDARs (Esmenjaud *et al.*, 2019; Wang *et al.*, 2021). In this context, a collaborating team is attempting to solve the structure of GluN1/GluN3A receptors, also with our mutants.

By creating the contact maps of the intradimer interfaces of GluN3A vs GluN2s we have highlighted how a loss of hydrophobic connections in the inner side of the interface could pinpoint a fragile or ruptured interface due to hydrophobic side chains in GluN1 facing non-hydrophobic residues on GluN3A. By showing that re-introducing hydrophobicity in the area by targeted mutagenesis we are able to modify the receptor properties, our results point towards the hypothesis that dimerization of the LBD may happen for GluN1/GluN3A diheteromers as it does for other NMDARs subunits, but with an incoherent biochemical make-up. There are two other proofs pointing towards the dimerization to take place. First, we tried to introduce the mutation GluN1 I519D, predicted to be in close proximity of the double mutant GluN3A S892L-K895F. This mutant is located on the partner subunit of the interface, and the mutation is designed to substitute a hydrophobic (I) residue with a negative charge residue. This substitution would theoretically weaken the GluN3A recreated hydrophobic network in the presence of the double mutant. With the introduction of this mutant, we are able to partially revert the GOF phenotypes to an intermediate effect between the double mutant and the WT (intermediate CGP potentiation and desensitization kinetics) indicating that we can modulate similar biophysical properties

while acting on both sides of the interface. Independently, the double mutant GluN3A S892L-K895F modifies GluN1- mediated properties such as the CGP-induced potentiation on peak and steady state current, and desensitization kinetics, indicating that the crosstalk between the two subunits must somehow have changed. Albeit these are all indirect proofs for the formation of the interface, they still represent important indications that the dimer interface may be forming for GluN1/GluN3A receptors. All these clues point to a dimerization of the LBD interface to take place in GluN1/GluN3A receptors.

During my project we failed to produce a successful crosslinking phenotype for the LBD intradimer interface. Although we attempted mutating several sites that seemed promising based on past experiments on canonical NMDARs or AMPARs and on our newly created contact map, both with conventional cysteine scanning mutagenesis and with UAA UV-mediated crosslinking techniques, we were not able to modify receptor properties in a way that could be uniquely be due to the crosslink effect. With conventional mutagenesis, we were able to produce constructs exhibiting functional phenotypes that were different than the WT, but we deemed the phenotypes we observed as not sufficiently interesting to produce a full characterization of the mutants, since with reducing agent application we could not reveal large hidden phenotypes. With the UAAs, we tried several insertion sites, but none was able to change receptor biophysical properties. This inability to make a crosslink with either methodology may constitute a contradictory indication that this interface might be quite different from how it appears in AMPARs of classical NMDARs, or even not forming at all. A Structures of the protein may help explaining why the crosslink was not successful, perhaps due to methodological or conceptual issues that might have impacted the successful implementation of these techniques. However, being able to produce a cross-link of the interface could help stabilize specific conformations that might help in a second time structural biologists to achieve high resolution structures of GluN3As, and should continue to be pursued. Perhaps just broadening the number of cysteine insertions by doing a systematic scanning of the positions most likely predicted to be at the interface could produce successful results. It is still remarkable how a subunit that is supposed to display some tolerance to genetic variation and genetic drift (unpublished data from the lab) showed to be intolerant (e.g. reduced expression or reduced current sizes) to many of the mutations we inserted. However, a different interpretation for this finding is possible if the genetic drift might have caused the GluN3A subunit to have accumulated mutations on its background that might have made the rigid core of the protein fragile. In this situation, adding further mutations that further destabilize the folding process may cause mutated receptors to not be assembled correctly.

One of the biggest questions that still remains unanswered is why so many residues located on the GluN3A LBD interface are able to modify the affinity of this subunit for glycine. It seems that residues located in both the D1 and D2 of GluN3A LBD are able to achieve this feature, as we shift the glycine EC<sub>50</sub> with several of our LBD mutants, similarly to how it was published for the D2 GluN3A endogenous cystless mutant published in (Grand *et al.*, 2018). Cross-linking the dimerization interface in GluN1/GluN2A by insertion of cysteine mutants was shown to also modulate agonist affinity, decreasing both glycine and glutamate affinity and shifting the EC<sub>50</sub>s to the right when cross-linked, thus in the opposite direction than GluN1/GluN3A receptors. However, the reasons for this shift were unclear. One possible explanation for this finding stems from the observation that affinities for glycine in the isolated LBD of the GluN3A subunit versus the affinities of the GluN3A subunit in the context of the whole tetramer differ by few orders of magnitude (Yao, 2006) (Figure 35). This observation indicates that some unknown constraints (for example some negative allosteric modulation mechanisms) might be in place to prevent the GluN3A subunit to display the theoretical K<sub>D</sub> for glycine, decreasing it by a large factor when co-assembled as a functional tetramer. However, we do not currently know why these two values differ by several orders of magnitude. Perhaps our mutations modify the receptor properties and are able to free the GluN3A subunit from some of these hypothetical constraints, partially approaching the EC<sub>50</sub> to the subunit theoretical K<sub>D</sub>. It is well established how the desensitized states in iGluRs display enhanced affinity for the agonist, which allows trapping of the ligand in the binding pocket without having a conductive state in the pore region. Our mutations seem to disfavor the desensitized state by showing slower desensitization kinetics, but at the same time increase the affinity for the agonist, going against the aforementioned paradigm of increased agonist affinity with the desensitized state. This observation is mostly unexplained at present time, perhaps indicating that several forms of desensitization are at play at the same time in GluN3A receptors. Finally, another mechanism that is important for agonist affinity is the negative allosteric modulation or negative cooperativity between the two binding sites within a dimer, which is influenced by the intradimer interface in GluN2 containing NMDARs (Durham *et al.*, 2020). We observed that our mutants do not cause major modification in the GluN1 binding site affinity for glycine, with the GluN1-mediated desensitization processes still appearing with more than > 1 μM glycine for both the WT and the mutants. Furthermore, the GluN1/GluN3A S892L-K895F dose response for the CGP affinity in the presence of glycine did not seem to significantly change from GluN3A WT. Therefore, it is currently unclear if in GluN3A the agonist intradimer interface is relying the cooperativity mechanisms between the subunits or not. Future studies will have to investigate the interplay between

intradimer interface and agonist affinities, as a description on how this cooperativity is regulated in GluN3A receptors does not yet exist.

#### **9.4 Concluding remarks and future perspectives**

Overall, many key molecular questions concerning GluN3A still exist. Future studies will have to try to determine why GluN1 acts as inhibitory subunit. It is possible that this unique gating behavior may be the sum of many effects arising from a complex interplay of several structural determinants influencing receptor activity. Other than the aforementioned differences present at the intradimer interface that we discussed throughout the manuscript, differences at the NTD and TMD levels could also play a role in determining the shape of the GluN3A responses. It is well established how the NTD is a key structural determinants of NMDARs Pos and allosteric modulation, contributing to subunit selective mechanisms. Few studies already exist that point at the GluN3A NTD role as a determinant shaper of its activation profile (Mesic *et al.*, 2016). Preliminary low-resolution data from a collaborating group indicates that the NTD conformation of GluN3A might be quite different from classical NMDARs, perhaps contributing to the unique gating behavior of GluN3A. More studies will be necessary to address the role of these domains in GluN3As.

Concerning the more general role of GluN3A in the brain, further research is necessary to determine if this receptor mainly exist in its diheteromeric form, or if cellular or temporal patterns can determine if the triheteromeric form may be expressed at different points. Preliminary evidence indicates that this receptor may act as a glycine sensor for levels of tonic glycine, but further work is necessary to determine which endogenous ligand act on this receptor in the different brain areas where it is highly expressed. There is a growing interest in trying to determine how GluN3A may be active pre-synaptically (Crawley *et al.*, 2022), and elucidating its role within these cellular compartments will help to better clarify its physiological role. Finally, several key questions remain about the role of this receptor in pathology, and how it may be used as a target for developing therapeutics. Existing studies have shown that GluN3A shows promising potential to be targeted in diseases such as the Huntington's disease (Marco *et al.*, 2013), for brain injuries like ischemia (Wang *et al.*, 2013) or for rare caused by the GRIN3A gene containing rare variants or point mutations (Crawley *et al.*, 2022). In vitro characterization of the gating mechanisms differentiating WT receptors from these latter GluN3A mutants could help to clarify how malfunctioning GluN3As contribute to neural circuitries in a way that leads to the onset of pathological conditions.

# Résumé Français de la thèse

## Introduction et discussion générale

Au cours d'environ 70 ans, la compréhension scientifique des corrélats physiologiques de la fonction cérébrale a augmenté à un rythme étonnant. Nous sommes passés de la formulation de l'hypothèse de l'existence de stimuli électriques se propageant à travers les tissus vivants dans les années 1950 à la caractérisation avec précision atomique des structures des récepteurs responsables de ces mêmes courants électriques. Nous avons discuté de la complexité de l'organisation chimique et électrique de la synapse dans l'introduction, et de comment les canaux ioniques régulent sa fonction et permettent une homéostasie correcte dans le cerveau, et finalement de la communication cellulaire. Depuis plusieurs décennies, il est connu que les récepteurs NMDA contenant GluN2 sont fondamentaux pour la formation des propriétés synaptiques dans le SNC à travers des mécanismes clés tels que la plasticité synaptique, l'apprentissage et l'excitabilité cellulaire. Il est donc étonnant qu'il n'ait été prouvé que ces 5 dernières années que GluN3A, l'une des 7 sous-unités qui composent cette famille de récepteurs, contribue directement à l'activité ionotropique dans le cerveau. Pendant plus de vingt ans, ces récepteurs ont été considérés comme une sous-unité régulatrice. Cette découverte récente indique que nous manquons encore de connaissances fondamentales sur certains aspects de l'activité ionotropique dans le SNC.

Souvent, les avancées clés dans le domaine, soit méthodologiques, pharmacologiques ou conceptuelles, permettent d'ouvrir rapidement de nouvelles possibilités pour l'investigation de sujets qui étaient auparavant considérés comme inexplicables et inabornables. En quelque sorte, la découverte pharmacologique de la sélectivité de CGP pour la sous-unité GluN1 plutôt que pour GluN3A a eu un effet précis dans le domaine de la recherche sur GluN3A (Yao, 2006 ; Grand et al., 2018). Cela a permis de découvrir que ces récepteurs sont exprimés et fonctionnels dans le SNC, et cette découverte a généré un nouvel intérêt pour une sous-unité dont l'importance effective avait été questionnée historiquement. Ces données fonctionnelles, ainsi que les nouvelles techniques d'analyse de transcriptomique à une seule cellule et d'hybridation RNAscope, montrent que les niveaux d'expression de GluN3A sont conservés dans des types cellulaires spécifiques à l'âge adulte (Paul et al., 2017 ; Murillo et al., 2021), ce qui met en évidence la manière dont notre connaissance du rôle de GluN3A dans le SNC peut avoir été parfois mal interprétée. Pendant de nombreuses années, on a cru que GluN3A était principalement coexprimé avec GluN2 et GluN1 en tant que sous-unité négative régulatrice dominante qui réduirait la contribution synaptique de ces canaux (Das et al., 1998 ; Pérez-Otaño et al., 2001b ; Pachernegg et al., 2012), car aucun courant n'était détectable avec les dihéromères seuls. Même après la découverte que les dihéromères GluN1/GluN3A sont fonctionnels dans des systèmes d'expression hétérologues



(Chatterton et al., 2002 ; Awobuluyi et al., 2007 ; Madry et al., 2007), l'idée que GluN3A soit principalement exprimé de manière trihétéromérique in vivo était devenue le paradigme dans l'interprétation des données concernant GluN3A. C'est donc seulement récemment que nous avons commencé à remettre en question cette idée, car les derniers résultats indiquent que les dihétéromères GluN1/GluN3A sont exprimés et fonctionnels dans certaines régions anatomiques du cerveau adulte de mammifères (Grand et al., 2018; Otsu et al., 2019; Bossi et al., 2022).

Cependant, alors que certains aspects des récepteurs NMDAR contenant GluN3A commencent à être mieux compris, en particulier dans les domaines physiologiques et de développement, d'autres ont été laissés en arrière. Ce sont ces aspects, entre autres, qui décrivent les relations entre les corrélats structurels de la protéine et sa fonction. En particulier, son mécanisme de verrouillage énigmatique a été exploré dans seulement quelques études clés, mais de nombreuses questions restent concernant ses corrélats structurels. Par exemple, l'une des principales questions qui reste sans réponse est pourquoi (dans le contexte des récepteurs GluN1 / GluN3A) la sous-unité GluN1 agit en tant que sous-unité auto-inhibitrice de manière unique parmi les récepteurs NMDAR, et quelle est la base moléculaire de ce comportement à l'intérieur du récepteur. Dans ma recherche, nous avons essayé de résoudre certaines de ces questions clés, tout en cherchant à développer de nouveaux outils méthodologiques pour faciliter l'étude des GluN3As. Certaines tentatives ont été assez réussies, tandis que d'autres n'ont pas. Dans la section suivante, je vais essayer de résumer et de conclure ce que nous avons trouvé dans mon projet de doctorat, et je donnerai quelques perspectives pour poursuivre la recherche sur les récepteurs contenant GluN3A.

## **Développements méthodologiques**

Nous avons réussi à développer des méthodologies pour étudier les récepteurs GluN1 / GluN3A, notamment grâce à la découverte d'un bloqueur de canal ouvert puissant et en implémentant la méthodologie MTSEA pour estimer le  $P_o$  des récepteurs GluN3A. En ce qui concerne la pentamidine, ce composé peut être utilisé pour inhiber les récepteurs GluN3A WT et mutants, est déjà approuvé pour son utilisation chez l'homme et nous sommes le premier groupe à caractériser son efficacité sur GluN3A. Les études futures devront enquêter plus précisément sur son site de liaison, afin de comprendre pourquoi ce bloqueur de canal ouvert peut inhiber GluN3A à des concentrations basses de  $\mu\text{M}$ , tandis que d'autres bloqueurs de canal standard de NMDA ne fonctionnent que dans les mM contre ce

récepteur (Chatterton et al., 2002; McClymont et al., 2012). En ce qui concerne la méthodologie MTSEA, elle fournit une lecture pour comparer les mutants à une activité de référence WT, ce qui nous permet de mieux comprendre comment différentes mutations à des endroits clés dans le récepteur peuvent influencer l'activité de GluN3A. Nous avons utilisé cette méthodologie pour enquêter sur des mutants clés qui ont été utilisés dans la littérature pour caractériser l'activité des récepteurs GluN3A comme le mutant GluN1 F484A (Awobuluyi et al., 2007; Madry et al., 2007), ou pour enquêter sur de nouveaux mutants comme le double mutant à l'interface intradimère LBD S892L-K895F pour souligner ses propriétés de gain de fonction. Les résultats que nous avons obtenus avec MTSEA ont été surprenants, comme lorsque nous avons testé GluN1 F484A ou le double mutant cysless endogène C744S-C798S. Nous avons révélé que ces mutants réduisent le PO global des récepteurs, bien qu'ils aient été montrés auparavant pour faciliter l'enregistrement de courants glycinergiques, le premier en empêchant la liaison de la glycine à GluN1, et le second en décalant l'EC50 de la glycine de la sous-unité GluN3A vers la gauche. De plus, MTSEA aide à disséquer des mécanismes complexes de mutants C'était le cas pour S892L-K895F, qui déplace à la fois la EC50 de la glycine vers la gauche et augmente également le PO du récepteur, ce qui a un effet d'interaction complexe sur les propriétés biophysiques du récepteur. Par conséquent, avec MTSEA, nous fournissons un nouvel outil au domaine qui peut être utilisé dans les études futures pour aider à caractériser de nouveaux mutants sans recourir aux enregistrements de canal unique.

Continuant avec les développements méthodologiques, nous avons montré que la modulation par le zinc sur la fonction des récepteurs semble plus nuancée que ce qui avait été hypothétisé dans les articles qui l'ont décrite auparavant. De façon intéressante, certains articles ont trouvé que le zinc était un potentiateur de GluN3A, tandis que d'autres non, ajoutant de l'incertitude sur le sujet (Cummings et Popescu, 2016; Otsu et al., 2019; Madry et Betz, n.d.). Spécifiquement, trois articles ont utilisé le zinc pour montrer qu'une préincubation potentialise les courants glycinergiques, tout en étant capable d'activer les récepteurs seuls, également dans les récepteurs manquants de NTD (Cummings et Popescu, 2016; Cummings et al., 2017; Madry et Betz, n.d.), qui est le site de liaison pour le zinc dans les sous-unités GluN2 (Paoletti et al., 1997b; Jalali-Yazdi et al., 2018). Le seul cas où le zinc n'avait pas d'effets fonctionnels était dans les récepteurs contenant la mutation F484A qui empêche la liaison de la glycine. Un article a trouvé que le zinc était un inhibiteur des courants glycinergiques (Wada et al., 2006), tandis qu'un autre article n'a pas trouvé d'effet sur les courants médiés par GluN3A ex vivo (Otsu et al., 2019). De notre point de vue, le zinc apparaît à la fois comme un potentiateur et un inhibiteur des courants

médiés par GluN3A, en fonction de l'état de conformité du récepteur et des molécules déjà liées à celui-ci. Nous avons trouvé que le zinc potentialise ou génère des courants lorsqu'il est appliqué au récepteur WT en présence de glycine. Inversement, le zinc inhibe les courants lorsque le mutant F484A est présent dans GluN1 ou lorsque les récepteurs sont pré-incubés avec CGP. Des résultats similaires ont été observés avec des mutants situés à l'interface intradimère. Une hypothèse qui pourrait expliquer cette relation complexe est l'existence de plusieurs sites de liaison pour cette molécule, certains d'entre eux pouvant être accessibles uniquement dans des conformations spécifiques ou en compétition avec d'autres molécules. Nous sommes les premiers à révéler cette dépendance complexe de l'état du zinc et de GluN3A, et les futures études devront tenter de déterminer où se situent les sites de liaison dans la molécule et quelles conditions d'enregistrement peuvent favoriser tel ou tel effet. De plus, une réponse en fonction de la dose pour vérifier son EC50 et son IC50 dans différents états fonctionnels semble également être une condition préalable essentielle pour tirer des conclusions sur la modulation du zinc sur GluN3A. Si cela se révèle être efficace à faible concentration, la modulation du zinc pourrait être particulièrement importante étant donné que GluN3A se trouve souvent dans des régions cérébrales sans terminaux glycinergiques afférents, laissant ouverte la question de quels sont les neurotransmetteurs endogènes qui modulent ce récepteur (Paoletti, A.M. Vergnano, et al., 2009; Bossi et al., 2022).

## **Mutants GOF**

Un autre objectif de ma recherche était de tenter de créer des mutants GOF, et nous avons obtenu des résultats positifs à ce niveau. Cependant, les mutants que nous avons isolés diffèrent de ce que nous espérions caractériser. Au départ, nous espérions pouvoir créer un mutant capable d'éliminer la désensibilisation pendant la stimulation glycinergique, comme les mutants qui le font pour la transmission de glutamate dans les AMPARs (Sun et al., 2002; Armstrong et al., 2006). Nous n'avons pas réussi à isoler un mutant avec ces caractéristiques, et la désensibilisation du complexe tétramérique par l'auto-inhibition GluN1 reste un déterminant fondamental, pourtant inexpliqué, de la forme des récepteurs GluN3A. Cependant, nous avons réussi à isoler plusieurs mutants dans une interface qui présente des phénotypes de mutants GOF. Ces mutants ont des différences dans leur phénotype courant et leurs propriétés biophysiques, mais partagent les propriétés principales d'augmentation de PO et de décalage à gauche de l'affinité pour la glycine dans la sous-unité GluN3A. Ces propriétés permettent

d'avoir une fenêtre beaucoup plus large d'activation GluN3A en présence de glycine avant que l'auto-inhibition GluN1 ne se produise, permettant de produire des courants de type GluN2 qualitatifs et carrés à des concentrations  $< 3 \mu\text{M}$ . Des systèmes de perfusion plus rapides devront être utilisés pour évaluer la vitesse de désensibilisation en présence de glycine uniquement, afin de déterminer si l'auto-inhibition GluN1 est plus lente que le WT. En présence de CGP, les courants de ces mutants présentent une forme carrée, indiquant une conformation ouverte plus stable et moins désensibilisante que le WT. Il n'est pas clair si la réduction de la cinétique de désensibilisation en présence de CGP peut être due à des changements d'affinité pour la glycine ou à une réduction de la force de la désensibilisation elle-même. Peut-être que nos mutants peuvent également être utilisés pour détecter les niveaux de glycine, car ils présentent une activation tonique avec la glycine ambiante, étant donc actifs uniquement lorsque les concentrations de glycine atteignent un certain seuil. Nous espérons que ces mutants seront utilisés à l'avenir pour aider à caractériser l'activité des récepteurs GluN3A, car ils permettent de faciliter beaucoup les enregistrements électrophysiologiques sur ces récepteurs, sans utiliser de CGP. Bien que CGP puisse potentialiser les récepteurs GluN3A, son utilisation présente des limitations dans les études de structure / fonction, car il oblige la sous-unité GluN1 à adopter une conformation artificielle en empêchant la désensibilisation en empêchant les changements de conformation découlant de la fermeture du clapet. En empêchant ces changements de se produire, le CGP rend compliqué de déduire à quel moment un mécanisme associé à l'ouverture de la porte dans les complexes GluN1 / GluN2 devient un mécanisme d'inhibition dans les récepteurs GluN1 / GluN3A.

Nous avons essayé d'utiliser l'un de ces mutants, le GluN3A S892L-K895F, dans une expérience préliminaire pour voir si nous pouvions révéler la co-assemblée de trihétéromères contenant les sous-unités GluN1, GluN2B et GluN3A lorsqu'ils sont co-injectés dans des oocytes de *Xenopus*. Bien que nous n'ayons pas pu tirer de conclusions définitives de cette expérience, pour la première fois, nous avons pu séparer la composante d'activation de GluN3A avec la glycine de la composante d'activation de GluN2 avec le glutamate + la glycine, montrant qu'il est possible de séparer les propriétés des dihétéromères des trihétéromères. De nouvelles études devront mieux caractériser la sensibilité de la sous-unité GluN3A à l'APV, afin de comprendre si elle peut être utilisée pour distinguer pharmacologiquement l'existence de dihétéromères contenant GluN3A des trihétéromères. Seules les études employant des témoins de dihétéromères de la souche WT GluN1/GluN2B et GluN1/GluN3A, en distinguant également les récepteurs qui sont retenus dans l'ER et les récepteurs qui sont trafiqués avec succès à la membrane,

seront en mesure d'indiquer si les récepteurs trihétéromères sont actifs et contribuent aux propriétés synaptiques des récepteurs GluN3A in vivo et in vitro.

### **Mécanismes moléculaires des récepteurs contenant GluN3A**

En ce qui concerne l'aspect principal du projet, qui consiste à déterminer les déterminants moléculaires des mécanismes de contrôle de l'activation des récepteurs GluN3A, nous avons réussi à trouver un déterminant structural clé régulant l'activité du récepteur. L'interface intradimère LBD est établie comme un déterminant structural clé pour la génération et la modulation allostérique dans les NMDARs, et pour la génération et la désensibilisation à la fois dans les AMPARs et les récepteurs kainates. Dans ces derniers récepteurs, une faible force de l'interface entraîne une diminution de la dimérisation au niveau LBD, ce qui est à son tour responsable de la désensibilisation rapide observée dans ces canaux. Ce fait a également été montré dans des structures expérimentales d'états supposés désensibilisés où les dimères sont fortement séparés, dans certains cas même séparés en protomères individuels se tournant vers une symétrie 4-fold (Schauder et al., 2013; Twomey et al., 2017b). Étant donné que le phénotype courant de GluN3A montre un phénotype de désensibilisation rapide rappelant plus ces classes de canaux que les courants médiés par les canaux GluN1/GluN2, nous avons examiné l'interface intradimère LBD de GluN3A pour déterminer comment elle était structurée et pour déterminer si elle était importante pour la fonction du récepteur. Le manque de données structurales existantes concernant l'interface nous a obligé à procéder en effectuant des hypothèses éduquées basées sur l'homologie des séquences entre GluN3A et GluN2B pour la modélisation de l'interface. Ce modèle a nécessité de faire des hypothèses sur la stœchiométrie de la co-assemblée des sous-unités, car la dimérisation efficace de GluN1 et de GluN3A au niveau LBD et d'autres domaines n'a jamais été prouvée. Il est donc d'une importance cruciale pour les biologistes structuraux de parvenir à purifier les récepteurs GluN1/GluN3A à haute résolution, peut-être grâce aux avancées en matière de visualisation et de purification par cryo-EM, un domaine qui est en plein essor et qui avance rapidement en termes de méthodologie. Une structure tétramérique résolue permettra finalement de prouver quelle disposition structurale est adoptée par la protéine à différents niveaux de l'architecture modulaire. Compte tenu de l'instabilité générale de la conformation de GluN3A, il semble très problématique pour les biologistes structuraux de purifier GluN3A. Cependant, nos mutants pourraient être utiles car ils semblent stabiliser l'état ouvert, de la même manière que les mutants des récepteurs GluN2 avec un PO plus élevé dans l'état roulé ont récemment été utilisés pour résoudre les structures des NMDAR contenant GluN2A pré-

actifs (Esmenjaud et al., 2019 ; Wang et al., 2021). Dans ce contexte, une équipe de collaboration essaie de résoudre la structure des récepteurs GluN1/GluN3A, également avec nos mutants.

En créant les cartes de contact des interfaces intradimères de GluN3A par rapport à GluN2s, nous avons mis en évidence comment une perte de connexions hydrophobes sur le côté interne de l'interface peut indiquer une interface fragile ou rompue en raison de chaînes latérales hydrophobes de GluN1 qui se confrontent à des résidus non hydrophobes sur GluN3A. En montrant que nous pouvons modifier les propriétés du récepteur en réintroduisant l'hydrophobicité dans cette zone par mutagenèse ciblée, nos résultats tendent à prouver l'hypothèse selon laquelle la dimérisation du LBD peut se produire pour les dihéromères GluN1/GluN3A, tout comme cela se produit pour d'autres sous-unités de NMDAR, mais avec une composition biochimique incohérente. Il y a deux autres preuves indiquant que la dimérisation doit se produire. Tout d'abord, nous avons essayé d'introduire la mutation GluN1 I519D, prédite pour être à proximité immédiate du double mutant GluN3A S892L-K895F. Ce mutant se trouve sur la sous-unité partenaire de l'interface et la mutation est conçue pour remplacer un résidu hydrophobe (I) par un résidu à charge négative. Cette substitution affaiblirait théoriquement le réseau hydrophobe recréé de GluN3A en présence du double mutant. Avec l'introduction de ce mutant, nous pouvons inverser partiellement les phénotypes GOF pour un effet intermédiaire entre le double mutant et le WT (potentialisation et cinétique de désensibilisation intermédiaires de CGP), ce qui montre que nous pouvons moduler des propriétés biophysiques similaires en agissant sur les deux côtés de l'interface. Indépendamment, le double mutant GluN3A S892L-K895F modifie les propriétés médiées par GluN1 telles que la potentialisation induite par CGP sur le courant de crête et de saturation, et la cinétique de désensibilisation, ce qui indique que la communication entre les deux sous-unités doit avoir changé de quelque manière. Bien que ce soient toutes des preuves indirectes de la formation de l'interface, elles représentent toujours des indications importantes que l'interface de dimérisation peut se former pour les récepteurs GluN1/GluN3A. Tous ces indices indiquent une dimérisation de l'interface LBD à se produire dans les récepteurs GluN1/GluN3A.

Au cours de mon projet, nous n'avons pas réussi à produire un phénotype de crosslinking réussi pour l'interface intradimère LBD. Bien que nous ayons tenté de muter plusieurs sites qui semblaient prometteurs en fonction d'expériences antérieures sur des NMDARs canoniques ou des AMPARs et sur notre nouvelle carte de contact, aussi bien avec la mutagenèse par balayage cystéine classique qu'avec des techniques de crosslinking par UV-UAs, nous n'avons pas été en mesure de modifier les propriétés du récepteur de manière qui puisse être uniquement due à l'effet de crosslinking. Avec la mutagenèse

classique, nous avons été en mesure de produire des constructions exhibant des phénotypes fonctionnels différents du WT, mais nous avons considéré que les phénotypes que nous avons observés n'étaient pas suffisamment intéressants pour produire une caractérisation complète des mutants, car avec l'application d'un réducteur, nous ne pouvions pas révéler de grands phénotypes cachés. Avec les UAAs, nous avons essayé plusieurs sites d'insertion, mais aucun n'a été en mesure de changer les propriétés biophysiques du récepteur. Cette incapacité à faire un crosslink avec une de ces deux méthodologies peut constituer une indication contraire que cette interface pourrait être très différente de ce qu'elle apparaît dans les AMPARs ou les NMDARs classiques, ou même ne se formant pas du tout. Des structures de la protéine peuvent aider à expliquer pourquoi le crosslink n'a pas été réussi, peut-être en raison de problèmes méthodologiques ou conceptuels qui pourraient avoir impacté la mise en œuvre réussie de ces techniques. Cependant, étant capable de produire un crosslink de l'interface pourrait aider à stabiliser des conformations spécifiques qui pourraient aider, à un second moment, les biologistes structuraux à obtenir des structures de haute résolution de GluN3As et devraient continuer d'être poursuivis. Peut-être que l'élargissement du nombre d'insertions cystéine en effectuant un balayage systématique des positions les plus susceptibles d'être à l'interface pourrait produire des résultats réussis. C'est toujours surprenant comment une sous-unité qui devrait présenter une certaine tolérance à la variation génétique et à la dérive génétique (données non publiées du laboratoire) s'est avérée être intolérante (par exemple, expression réduite ou tailles de courant réduites) aux nombreuses mutations que nous avons insérées. Cependant, une autre interprétation de ce résultat est possible si la dérive génétique a causé la sous-unité GluN3A à accumuler des mutations sur son arrière-plan qui ont pu rendre le noyau rigide de la protéine fragile. Dans cette situation, l'ajout de mutations supplémentaires qui déséquilibrent encore plus le processus de pliage peut empêcher les récepteurs mutés d'être correctement assemblés.

L'une des plus grandes questions qui reste sans réponse est pourquoi de nombreux résidus situés sur l'interface LBD de GluN3A peuvent modifier l'affinité de cette sous-unité pour la glycine. Il semble que les résidus situés à la fois dans le D1 et le D2 du LBD de GluN3A soient capables d'obtenir cette fonctionnalité, car nous déplaçons l'EC50 de la glycine avec plusieurs de nos mutants LBD, de la même manière que cela a été publié pour le mutant cysless endogène de D2 GluN3A publié dans (Grand et al., 2018). La cross-linking de l'interface de dimérisation dans GluN1/GluN2A par insertion de mutants cystéine a également été montrée pour moduler l'affinité pour l'agoniste, diminuant à la fois l'affinité pour la glycine et le glutamate et déplaçant les EC50 vers la droite lorsqu'ils sont croisés, dans la direction

opposée à celle des récepteurs GluN1/GluN3A. Cependant, les raisons de ce décalage restent incertaines. Une explication possible de cette observation découle de l'observation que les affinités pour la glycine dans le LBD isolé de la sous-unité GluN3A par rapport aux affinités de la sous-unité GluN3A dans le contexte du tétramère entier diffèrent de quelques ordres de grandeur (Yao, 2006) (Figure 35). Cette observation indique que certaines contraintes inconnues (par exemple, certains mécanismes de modulation négative allostérique) pourraient être en place pour empêcher la sous-unité GluN3A d'afficher la  $K_d$  théorique pour la glycine, la diminuant considérablement lorsqu'elle est co-assemblée en tant que tétramère fonctionnel. Cependant, nous ne savons pas actuellement pourquoi ces deux valeurs diffèrent de plusieurs ordres de grandeur. Peut-être que nos mutations modifient les propriétés du récepteur et sont capables de libérer la sous-unité GluN3A de certaines de ces hypothétiques contraintes, approchant partiellement l' $EC_{50}$  à la  $K_d$  théorique de la sous-unité. Il est bien établi comment les états désensibilisés dans les récepteurs iGluRs présentent une affinité accrue pour l'agoniste, ce qui permet de piéger le ligand dans la poche de liaison sans avoir un état conducteur dans la région du pore. Nos mutations semblent défavoriser l'état désensibilisé en montrant des cinétiques de désensibilisation plus lentes, mais en même temps, elles augmentent l'affinité pour l'agoniste, allant à l'encontre du paradigme susmentionné d'une affinité accrue pour l'agoniste avec l'état désensibilisé. Cette observation est principalement inexplicée à ce jour, indiquant peut-être que plusieurs formes de désensibilisation sont en jeu en même temps dans les récepteurs GluN3A. Enfin, un autre mécanisme important pour l'affinité pour l'agoniste est la modulation allostérique négative ou la coopérativité négative entre les deux sites de liaison à l'intérieur d'un dimère, qui est influencé par l'interface intradimère dans les NMDAR GluN2 (Durham et al., 2020). Nous avons observé que nos mutants ne causent pas de modification majeure de l'affinité du site de liaison GluN1 pour la glycine, avec les processus de désensibilisation médiés par GluN1 apparaissant toujours avec plus de 1  $\mu$ M de glycine pour le WT et les mutants. De plus, la réponse dose-réponse GluN1/GluN3A S892L-K895F pour l'affinité CGP en présence de glycine ne semble pas avoir significativement changé par rapport à GluN3A WT. Par conséquent, il n'est actuellement pas clair si dans GluN3A, l'interface intradimère pour l'agoniste fait appel aux mécanismes de coopérativité entre les sous-unités ou non. Des études futures devront investiguer l'interaction entre l'interface intradimère et les affinités pour l'agoniste, car une description de la façon dont cette coopérativité est régulée dans les récepteurs GluN3A n'existe pas encore.

## **Conclusions et perspectives futures**



Dans l'ensemble, de nombreuses questions clés sur le GluN3A sont encore en attente de réponse. Les futurs travaux devront tenter de déterminer pourquoi le GluN1 agit comme sous-unité inhibitrice. Il est possible que ce comportement de gating unique soit la somme de nombreux effets résultant d'un jeu complexe de plusieurs déterminants structurels influençant l'activité du récepteur. En plus des différences mentionnées à l'interface intradimère que nous avons abordées tout au long du manuscrit, des différences au niveau des NTD et TMD pourraient également jouer un rôle dans la forme des réponses GluN3A. Il est bien établi que l'NTD est un déterminant clé des Pos de NMDARs et de la modulation allostérique, contribuant à des mécanismes sélectifs de sous-unité. Quelques études existent déjà qui montrent le rôle de l'NTD de GluN3A en tant que formateur du profil d'activation (Mesic et al., 2016). Des données préliminaires de faible résolution d'un groupe collaborateur indiquent que la conformation de l'NTD de GluN3A pourrait être très différente des NMDAR classiques, ce qui pourrait contribuer au comportement de gating unique de GluN3A. De plus amples études seront nécessaires pour aborder le rôle de ces domaines dans les GluN3As.

Concernant le rôle plus général de GluN3A dans le cerveau, des recherches supplémentaires sont nécessaires pour déterminer si ce récepteur existe principalement sous forme de dihéromère, ou si des patrons cellulaires ou temporels peuvent déterminer si la forme trihéromérique peut être exprimée en des points différents. Des preuves préliminaires indiquent que ce récepteur peut agir en tant que capteur de glycine pour les niveaux de glycine tonique, mais des travaux supplémentaires sont nécessaires pour déterminer quel ligand endogène agit sur ce récepteur dans les différentes régions cérébrales où il est hautement exprimé. Il existe un intérêt croissant à déterminer comment le GluN3A peut être actif présynaptiquement (Crawley et al., 2022), et élucider son rôle dans ces compartiments cellulaires aidera à mieux clarifier son rôle physiologique. Enfin, plusieurs questions clés restent sans réponse quant au rôle de ce récepteur dans les pathologies et à son utilisation en tant que cible pour le développement de thérapeutiques. Des études existantes ont montré que GluN3A présente un potentiel prometteur pour être ciblé dans des maladies telles que la maladie de Huntington (Marco et al., 2013), pour des lésions cérébrales telles que l'ischémie (Wang et al., 2013) ou pour des rares causées par le gène GRIN3A contenant des variants rares ou des mutations ponctuelles (Crawley et al., 2022). La caractérisation *in vitro* des mécanismes de modulation différenciant les récepteurs WT de ces derniers mutants de GluN3A pourrait aider à clarifier la façon dont les GluN3A en défaut contribuent aux circuits nerveux d'une manière qui entraîne l'apparition de conditions pathologiques.



# Bibliography

## Bibliography

- Acher FC, Cabayé A, Eshak F, Goupil-Lamy A, and Pin J-P (2022) Metabotropic glutamate receptor orthosteric ligands and their binding sites. *Neuropharmacology* **204**:108886.
- Addis L, Virdee JK, Vidler LR, Collier DA, Pal DK, and Ursu D (2017) Epilepsy-associated GRIN2A mutations reduce NMDA receptor trafficking and agonist potency – molecular profiling and functional rescue. *Sci Rep* **7**:66, Nature Publishing Group.
- Alberts B (ed) (2010) *Essential cell biology*, 3. ed, Garland Science, New York London.
- Al-Hallaq RA, Conrads TP, Veenstra TD, and Wenthold RJ (2007) NMDA Di-Heteromeric Receptor Populations and Associated Proteins in Rat Hippocampus. *J Neurosci* **27**:8334–8343, Society for Neuroscience.
- Al-Hallaq RA, Jarabek BR, Fu Z, Vicini S, Wolfe BB, and Yasuda RP (n.d.) Association of NR3A with the N-Methyl-D-aspartate Receptor NR1 and NR2 Subunits. 10.
- Alsaloum M, Kazi R, Gan Q, Amin J, and Wollmuth LP (2016) A Molecular Determinant of Subtype-Specific Desensitization in Ionotropic Glutamate Receptors. *J Neurosci* **36**:2617–2622, Society for Neuroscience.
- AlShimemeri S, Fox SH, and Visanji NP (2020) Emerging drugs for the treatment of L-DOPA-induced dyskinesia: an update. *Expert Opin Emerg Drugs* **25**:131–144, Taylor & Francis.
- Amico-Ruvio SA, Murthy SE, Smith TP, and Popescu GK (2011) Zinc Effects on NMDA Receptor Gating Kinetics. *Biophys J* **100**:1910–1918.
- Amico-Ruvio SA, Paganelli MA, Myers JM, and Popescu GK (2012) Ifenprodil Effects on GluN2B-Containing Glutamate Receptors. *Mol Pharmacol* **82**:1074–1081, American Society for Pharmacology and Experimental Therapeutics.
- Amin JB, Gochman A, He M, Certain N, and Wollmuth LP (2021) NMDA Receptors Require Multiple Pre-opening Gating Steps for Efficient Synaptic Activity. *Neuron* **109**:488-501.e4.
- Andersson O, Stenqvist A, Attersand A, and von Euler G (2001) Nucleotide Sequence, Genomic Organization, and Chromosomal Localization of Genes Encoding the Human NMDA Receptor Subunits NR3A and NR3B. *Genomics* **78**:178–184.
- Andrews PC, and Dravid SM (2021) An emerging map of glutamate delta 1 receptors in the forebrain. *Neuropharmacology* **192**:108587.
- Armstrong N, and Gouaux E (2000) Mechanisms for Activation and Antagonism of an AMPA-Sensitive Glutamate Receptor: Crystal Structures of the GluR2 Ligand Binding Core. *Neuron* **28**:165–181.

- Armstrong N, Jasti J, Beich-Frandsen M, and Gouaux E (2006) Measurement of Conformational Changes accompanying Desensitization in an Ionotropic Glutamate Receptor. *Cell* **127**:85–97.
- Ascher P (1990) Measuring and Controlling the Extracellular Glycine Concentration at the NMDA Receptor Level, in *Excitatory Amino Acids and Neuronal Plasticity* (Ben-Ari Y ed) pp 13–16, Springer US, Boston, MA.
- Attwell D, and Gibb A (2005) Neuroenergetics and the kinetic design of excitatory synapses. *Nat Rev Neurosci* **6**:841–849.
- Auerbach A, and Zhou Y (2005) Gating Reaction Mechanisms for NMDA Receptor Channels. *J Neurosci* **25**:7914–7923, Society for Neuroscience.
- Awobuluyi M, Yang J, Ye Y, Chatterton JE, Godzik A, Lipton SA, and Zhang D (2007) Subunit-Specific Roles of Glycine-Binding Domains in Activation of NR1/NR3 N -Methyl-d-aspartate Receptors. *Mol Pharmacol* **71**:112–122.
- Banke TG, and Traynelis SF (2003) Activation of NR1/NR2B NMDA receptors. *Nat Neurosci* **6**:144–152.
- Bayer KU, and Schulman H (2019) CaM Kinase: Still Inspiring at 40. *Neuron* **103**:380–394.
- Benveniste M, Clements J, Vyklický L, and Mayer ML (1990) A kinetic analysis of the modulation of N-methyl-D-aspartic acid receptors by glycine in mouse cultured hippocampal neurones. *J Physiol* **428**:333–357.
- Berberich S, Punnakkal P, Jensen V, Pawlak V, Seeburg PH, Hvalby Ø, and Köhr G (2005) Lack of NMDA Receptor Subtype Selectivity for Hippocampal Long-Term Potentiation. *J Neurosci* **25**:6907–6910, Society for Neuroscience.
- Bettler B, Kaupmann K, Mosbacher J, and Gassmann M (2004) Molecular Structure and Physiological Functions of GABAB Receptors. *Physiol Rev* **84**:835–867, American Physiological Society.
- Betz H, Kuhse J, Schmieden V, Laube B, Kirsch J, and Harvey RJ (1999) Structure and Functions of Inhibitory and Excitatory Glycine Receptors. *Ann N Y Acad Sci* **868**:667–676.
- Bhattacharya S, Khatri A, Swanger SA, DiRaddo JO, Yi F, Hansen KB, Yuan H, and Traynelis SF (2018) Triheteromeric GluN1/GluN2A/GluN2C NMDARs with Unique Single-Channel Properties Are the Dominant Receptor Population in Cerebellar Granule Cells. *Neuron* **99**:315–328.e5.
- Bissantz C, Kuhn B, and Stahl M (2010) A Medicinal Chemist's Guide to Molecular Interactions. *J Med Chem* **53**:5061–5084, American Chemical Society.
- Bledsoe D, Vacca B, Laube B, Klein BG, and Costa B (2019) Ligand binding domain interface: A tipping point for pharmacological agents binding with GluN1/2A subunit containing NMDA receptors. *Eur J Pharmacol* **844**:216–224.
- Bonsi P, Cuomo D, De Persis C, Centonze D, Bernardi G, Calabresi P, and Pisani A (2005) Modulatory action of metabotropic glutamate receptor (mGluR) 5 on mGluR1 function in striatal cholinergic interneurons. *Neuropharmacology* **49**:104–113.

- Bork P, Downing AK, Kieffer B, and Campbell ID (1996) Structure and distribution of modules in extracellular proteins. *Q Rev Biophys* **29**:119–167, Cambridge University Press.
- Borschel WF, Cummings KA, Tindell LK, and Popescu GK (2015) Kinetic Contributions to Gating by Interactions Unique to N-methyl-d-aspartate (NMDA) Receptors\*. *J Biol Chem* **290**:26846–26855.
- Borschel WF, Murthy SE, Kasperek EM, and Popescu GK (2011) NMDA receptor activation requires remodelling of intersubunit contacts within ligand-binding heterodimers. *Nat Commun* **2**:498.
- Bossi S, Dhanasobhon D, Ellis-Davies GCR, Frontera J, de Brito Van Velze M, Lourenço J, Murillo A, Luján R, Casado M, Perez-Otaño I, Bacci A, Popa D, Paoletti P, and Rebola N (2022) GluN3A excitatory glycine receptors control adult cortical and amygdalar circuits. *Neuron* **110**:2438-2454.e8.
- Bouvier G, Bidoret C, Casado M, and Paoletti P (2015) Presynaptic NMDA receptors: Roles and rules. *Neuroscience* **311**:322–340.
- Bowie D (2002) External anions and cations distinguish between AMPA and kainate receptor gating mechanisms. *J Physiol* **539**:725–733.
- Bowie D (2010) Ion-dependent gating of kainate receptors. *J Physiol* **588**:67–81.
- Brigman JL, Wright T, Talani G, Prasad-Mulcare S, Jinde S, Seabold GK, Mathur P, Davis MI, Bock R, Gustin RM, Colbran RJ, Alvarez VA, Nakazawa K, Delpire E, Lovinger DM, and Holmes A (2010) Loss of GluN2B-Containing NMDA Receptors in CA1 Hippocampus and Cortex Impairs Long-Term Depression, Reduces Dendritic Spine Density, and Disrupts Learning. *J Neurosci* **30**:4590–4600, Society for Neuroscience.
- Brody SA, Nakanishi N, Tu S, Lipton SA, and Geyer MA (2005) A Developmental Influence of the N-Methyl-D-Aspartate Receptor NR3A Subunit on Prepulse Inhibition of Startle. *Biol Psychiatry* **57**:1147–1152.
- Budisantoso T, Harada H, Kamasawa N, Fukazawa Y, Shigemoto R, and Matsui K (2013) Evaluation of glutamate concentration transient in the synaptic cleft of the rat calyx of Held. *J Physiol* **591**:219–239.
- Burada AP, Vinnakota R, and Kumar J (2020a) Cryo-EM structures of the ionotropic glutamate receptor GluD1 reveal a non-swapped architecture. *Nat Struct Mol Biol* **27**:84–91, Nature Publishing Group.
- Burada AP, Vinnakota R, and Kumar J (2020b) The architecture of GluD2 ionotropic delta glutamate receptor elucidated by cryo-EM. *J Struct Biol* **211**:107546.
- Burger PB, Yuan H, Karakas E, Geballe M, Furukawa H, Liotta DC, Snyder JP, and Traynelis SF (2012) Mapping the Binding of GluN2B-Selective N-Methyl-d-aspartate Receptor Negative Allosteric Modulators. *Mol Pharmacol* **82**:344–359, American Society for Pharmacology and Experimental Therapeutics.

- Burnashev N, and Szepetowski P (eds) (2017) *NMDA Receptors: Methods and Protocols*, Springer New York, New York, NY.
- Burnashev N, Villarroel A, and Sakmann B (1996) Dimensions and ion selectivity of recombinant AMPA and kainate receptor channels and their dependence on Q/R site residues. *J Physiol* **496**:165–173.
- Burzomato V, Frugier G, Pérez-Otaño I, Kittler JT, and Attwell D (2010) The receptor subunits generating NMDA receptor mediated currents in oligodendrocytes. *J Physiol* **588**:3403–3414.
- Careaga CL, and Falke JJ (1992) Thermal motions of surface  $\alpha$ -helices in the d-galactose chemosensory receptor: Detection by disulfide trapping. *J Mol Biol* **226**:1219–1235.
- Carvill GL, Regan BM, Yendle SC, O’Roak BJ, Lozovaya N, Bruneau N, Burnashev N, Khan A, Cook J, Geraghty E, Sadleir LG, Turner SJ, Tsai M-H, Webster R, Ouvrier R, Damiano JA, Berkovic SF, Shendure J, Hildebrand MS, Szepetowski P, Scheffer IE, and Mefford HC (2013) GRIN2A mutations cause epilepsy-aphasia spectrum disorders. *Nat Genet* **45**:1073–1076.
- Chatterjee S, Ade C, Nurik CE, Carrejo NC, Dutta C, Jayaraman V, and Landes CF (2019) Phosphorylation Induces Conformational Rigidity at the C-Terminal Domain of AMPA Receptors. *J Phys Chem B* **123**:130–137, American Chemical Society.
- Chatterton JE, Awobuluyi M, Premkumar LS, Takahashi H, Talantova M, Shin Y, Cui J, Tu S, Sevarino KA, Nakanishi N, Tong G, Lipton SA, and Zhang D (2002) Excitatory glycine receptors containing the NR3 family of NMDA receptor subunits. *Nature* **415**:793–798.
- Chen HS, and Lipton SA (1997) Mechanism of memantine block of NMDA-activated channels in rat retinal ganglion cells: uncompetitive antagonism. *J Physiol* **499**:27–46.
- Chen J, Ma Y, Fan R, Yang Z, and Li MD (2018) Implication of Genes for the N-Methyl-d-Aspartate (NMDA) Receptor in Substance Addictions. *Mol Neurobiol* **55**:7567–7578.
- Chen S, Zhao Y, Wang Y, Shekhar M, Tajkhorshid E, and Gouaux E (2017) Activation and Desensitization Mechanism of AMPA Receptor-TARP Complex by Cryo-EM. *Cell* **170**:1234-1246.e14.
- Cheng S, Seven AB, Wang J, Skiniotis G, and Özkan E (2016) Conformational Plasticity in the Transsynaptic Neurexin-Cerebellin-Glutamate Receptor Adhesion Complex. *Structure* **24**:2163–2173.
- Choi UB, Kazi R, Stenzoski N, Wollmuth LP, Uversky VN, and Bowen ME (2013) Modulating the Intrinsic Disorder in the Cytoplasmic Domain Alters the Biological Activity of the N-Methyl-d-aspartate-sensitive Glutamate Receptor \*. *J Biol Chem* **288**:22506–22515, Elsevier.
- Choi Y-B, and Lipton SA (1999) Identification and Mechanism of Action of Two Histidine Residues Underlying High-Affinity Zn<sup>2+</sup> Inhibition of the NMDA Receptor. *Neuron* **23**:171–180.
- Chou T-H, Tajima N, Romero-Hernandez A, and Furukawa H (2020) Structural Basis of Functional Transitions in Mammalian NMDA Receptors. *Cell* **182**:357-371.e13.

- Ciabarra M, and Sevarino A (1995) Cloning and Characterization of  $\alpha$ -1 : A Developmentally Regulated Member of a Novel Class of the Ionotropic Glutamate Receptor Family. *11*.
- Clements JD, Lester RAJ, Tong G, Jahr CE, and Westbrook GL (1992) The Time Course of Glutamate in the Synaptic Cleft. *Science* **258**:1498–1501, American Association for the Advancement of Science.
- Conn PJ, and Pin J-P (1997) Pharmacology and Functions of Metabotropic Glutamate Receptors. *Annu Rev Pharmacol Toxicol* **37**:205–237.
- Crawley O, Conde-Dusman MJ, and Pérez-Otaño I (2022) GluN3A NMDA receptor subunits: more enigmatic than ever? *J Physiol* **600**:261–276.
- Cull-Candy SG, and Leszkiewicz DN (2004) Role of Distinct NMDA Receptor Subtypes at Central Synapses. *Sci STKE* **2004**.
- Cull-Candy SG, and Usowicz MM (1987) Multiple-conductance channels activated by excitatory amino acids in cerebellar neurons. *Nature* **325**:525–528, Nature Publishing Group.
- Cummings KA, Belin S, and Popescu GK (2017) Residues in the GluN1 C-terminal domain control kinetics and pharmacology of GluN1/GluN3A N-methyl-d-aspartate receptors. *Neuropharmacology* **119**:40–47.
- Cummings KA, and Popescu GK (2016) Protons Potentiate GluN1/GluN3A Currents by Attenuating Their Desensitisation. *Sci Rep* **6**:23344.
- Dai J, and Zhou H-X (2013) An NMDA Receptor Gating Mechanism Developed from MD Simulations Reveals Molecular Details Underlying Subunit-Specific Contributions. *Biophys J* **104**:2170–2181.
- Daniels BA, Andrews ED, Aurousseau MRP, Accardi MV, and Bowie D (2013) Crosslinking the ligand-binding domain dimer interface locks kainate receptors out of the main open state. *J Physiol* **591**:3873–3885.
- Das S, Sasaki YF, Rothe T, Premkumar LS, Takasu M, Crandall JE, Dikkes P, Conner DA, Rayudu PV, Cheung W, Chen H-SV, Lipton SA, and Nakanishi N (1998) Increased NMDA current and spine density in mice lacking the NMDA receptor subunit NR3A. *Nature* **393**:377–381.
- Dolino DM, Adariani SR, Shaikh SA, Jayaraman V, and Sanabria H (2016) Conformational Selection and Submillisecond Dynamics of the Ligand-binding Domain of the N-Methyl-d-aspartate Receptor \*. *J Biol Chem* **291**:16175–16185, Elsevier.
- Dolino DM, Cooper D, Ramaswamy S, Jaurich H, Landes CF, and Jayaraman V (2015) Structural Dynamics of the Glycine-binding Domain of the N-Methyl-d-Aspartate Receptor \*. *J Biol Chem* **290**:797–804, Elsevier.
- Dong X, Wang Y, and Qin Z (2009) Molecular mechanisms of excitotoxicity and their relevance to pathogenesis of neurodegenerative diseases. *Acta Pharmacol Sin* **30**:379–387, Nature Publishing Group.

- Doumazane E, Scholler P, Zwier JM, Trinquet E, Rondard P, and Pin J-P (2011) A new approach to analyze cell surface protein complexes reveals specific heterodimeric metabotropic glutamate receptors. *FASEB J* **25**:66–77.
- Doyle DA, Cabral JM, Pfuetzner RA, Kuo A, Gulbis JM, Cohen SL, Chait BT, and MacKinnon R (1998) The Structure of the Potassium Channel: Molecular Basis of K<sup>+</sup> Conduction and Selectivity. *Science*, doi: 10.1126/science.280.5360.69, American Association for the Advancement of Science.
- D'Souza DC, Gil R, Cassello K, Morrissey K, Abi-Saab D, White J, Sturwold R, Bennett A, Karper LP, Zuzarte E, Charney DS, and Krystal JH (2000) IV glycine and oral d-cycloserine effects on plasma and CSF amino acids in healthy humans. *Biol Psychiatry* **47**:450–462.
- Durham RJ, Paudyal N, Carrillo E, Bhatia NK, Maclean DM, Berka V, Dolino DM, Gorfe AA, and Jayaraman V (2020) Conformational spread and dynamics in allostery of NMDA receptors. *Proc Natl Acad Sci* **117**:3839–3847.
- Dürr KL, Chen L, Stein RA, De Zorzi R, Folea IM, Walz T, Mchaourab HS, and Gouaux E (2014) Structure and Dynamics of AMPA Receptor GluA2 in Resting, Pre-Open, and Desensitized States. *Cell* **158**:778–792.
- Endele S, Rosenberger G, Geider K, Popp B, Tamer C, Stefanova I, Milh M, Kortüm F, Fritsch A, Pientka FK, Hellenbroich Y, Kalscheuer VM, Kohlhase J, Moog U, Rappold G, Rauch A, Ropers H-H, von Spiczak S, Tönnies H, Villeneuve N, Villard L, Zabel B, Zenker M, Laube B, Reis A, Wieczorek D, Van Maldergem L, and Kutsche K (2010) Mutations in GRIN2A and GRIN2B encoding regulatory subunits of NMDA receptors cause variable neurodevelopmental phenotypes. *Nat Genet* **42**:1021–1026.
- Enna SJ (2007) *The GABA Receptors*, SJ Enna and H. Mohler, Eds, Humana Press, Totowa, NJ, USA.
- Erreger K, Dravid SM, Banke TG, Wyllie DJA, and Traynelis SF (2005) Subunit-specific gating controls rat NR1/NR2A and NR1/NR2B NMDA channel kinetics and synaptic signalling profiles: NMDA receptor gating. *J Physiol* **563**:345–358.
- Erreger K, Geballe MT, Kristensen A, Chen PE, Hansen KB, Lee CJ, Yuan H, Le P, Lyuboslavsky PN, Micale N, Jørgensen L, Clausen RP, Wyllie DJA, Snyder JP, and Traynelis SF (2007) Subunit-Specific Agonist Activity at NR2A-, NR2B-, NR2C-, and NR2D-Containing N-Methyl-d-aspartate Glutamate Receptors. *Mol Pharmacol* **72**:907–920, American Society for Pharmacology and Experimental Therapeutics.
- Esmenjaud J, Stroebel D, Chan K, Grand T, David M, Wollmuth LP, Taly A, and Paoletti P (2019) An inter-dimer allosteric switch controls NMDA receptor activity. *EMBO J* **38**.
- Esmenjaud J-B, Stroebel D, Chan K, Grand T, David M, Taly A, and Paoletti P (2018) An inter-dimer allosteric switch controls NMDA receptor activity. *EMBO J* **36**.
- Espinosa P, and Bellone C (2022) The exciting side of unconventional glycine receptors. *Neuron* **110**:2359–2361.



- Eswar N, Webb B, Marti-Renom MA, Madhusudhan M s., Eramian D, Shen M, Pieper U, and Sali A (2006) Comparative Protein Structure Modeling Using Modeller. *Curr Protoc Bioinforma* **15**:5.6.1-5.6.30.
- Expression of N-methyl D-aspartate receptor subunits in amoeboid microglia mediates production of nitric oxide via NF- $\kappa$ B signaling pathway and oligodendrocyte cell death in hypoxic postnatal rats - Murugan - 2011 - *Glia* - Wiley Online Library (n.d.).
- Feldman DE (2012) The Spike-Timing Dependence of Plasticity. *Neuron* **75**:556–571.
- Fischer G, Mutel V, Trube G, Malherbe P, Kew JNC, Mohacsi E, Heitz MP, and Kemp JA (1997) Ro 25–6981, a Highly Potent and Selective Blocker of N-Methyl-d-aspartate Receptors Containing the NR2B Subunit. Characterization in Vitro. *J Pharmacol Exp Ther* **283**:1285–1292, American Society for Pharmacology and Experimental Therapeutics.
- Fiuza M, González-González I, and Pérez-Otaño I (2013) GluN3A expression restricts spine maturation via inhibition of GIT1/Rac1 signaling. *Proc Natl Acad Sci* **110**:20807–20812.
- Frederickson Christopher J., Suh SW, Silva D, Frederickson Cathy J., and Thompson RB (2000) Importance of Zinc in the Central Nervous System: The Zinc-Containing Neuron. *J Nutr* **130**:1471S-1483S.
- Frerking M, Schmitz D, Zhou Q, Johansen J, and Nicoll RA (2001) Kainate Receptors Depress Excitatory Synaptic Transmission at CA3→CA1 Synapses in the Hippocampus via a Direct Presynaptic Action. *J Neurosci* **21**:2958–2966, Society for Neuroscience.
- Fritschy J-M, Weinmann O, Wenzel A, and Benke D (1998) Synapse-specific localization of NMDA and GABAA receptor subunits revealed by antigen-retrieval immunohistochemistry. *J Comp Neurol* **390**:194–210.
- Fulcher B d., Murray John, Zerbi Valerio, and Wang Xiao-Jing (2019) Multimodal gradients across mouse cortex.
- Furukawa H, and Gouaux E (2003) Mechanisms of activation, inhibition and specificity: crystal structures of the NMDA receptor NR1 ligand-binding core. *EMBO J* **22**:2873–2885, John Wiley & Sons, Ltd.
- Furukawa H, Singh SK, Mancusso R, and Gouaux E (2005) Subunit arrangement and function in NMDA receptors. *Nature* **438**:185–192.
- Geng Y, Xiong D, Mosyak L, Malito DL, Kniazeff J, Chen Y, Burmakina S, Quick M, Bush M, Javitch JA, Pin J-P, and Fan QR (2012) Structure and functional interaction of the extracellular domain of human GABAB receptor GBR2. *Nat Neurosci* **15**:970–978, Nature Publishing Group.
- Geoffroy C, Paoletti P, and Mony L (2021) Positive allosteric modulation of NMDA receptors: mechanisms, physiological impact and therapeutic potential. *J Physiol* JP280875.

- Ghatak S, Talantova M, McKercher SR, and Lipton SA (2021) Novel Therapeutic Approach for Excitatory/Inhibitory Imbalance in Neurodevelopmental and Neurodegenerative Diseases. *Annu Rev Pharmacol Toxicol* **61**:701–721.
- Gibb AJ (2004) NMDA receptor subunit gating – uncovered. *Trends Neurosci* **27**:7–10.
- Gibb AJ, Ogden KK, McDaniel MJ, Vance KM, Kell SA, Butch C, Burger P, Liotta DC, and Traynelis SF (2018) A structurally derived model of subunit-dependent NMDA receptor function: Subunit-dependent modelling of NMDA receptor kinetics. *J Physiol* **596**:4057–4089.
- Gielen M, Le Goff A, Stroebel D, Johnson JW, Neyton J, and Paoletti P (2008) Structural Rearrangements of NR1/NR2A NMDA Receptors during Allosteric Inhibition. *Neuron* **57**:80–93.
- Gielen M, Retchless BS, Mony L, Johnson JW, and Paoletti P (2009) Mechanism of differential control of NMDA receptor activity by NR2 subunits. *Nature* **459**:703–707.
- Grand T, Abi Gerges S, David M, Diana MA, and Paoletti P (2018) Unmasking GluN1/GluN3A excitatory glycine NMDA receptors. *Nat Commun* **9**:4769.
- Greenwood TA, Lazzeroni LC, Calkins ME, Freedman R, Green MF, Gur RE, Gur RC, Light GA, Nuechterlein KH, Olincy A, Radant AD, Seidman LJ, Siever LJ, Silverman JM, Stone WS, Sugar CA, Swerdlow NR, Tsuang DW, Tsuang MT, Turetsky BI, and Braff DL (2016) Genetic assessment of additional endophenotypes from the Consortium on the Genetics of Schizophrenia Family Study. *Schizophr Res* **170**:30–40.
- Hackos DH, Lupardus PJ, Grand T, Chen Y, Wang T-M, Reynen P, Gustafson A, Wallweber HJA, Volgraf M, Sellers BD, Schwarz JB, Paoletti P, Sheng M, Zhou Q, and Hanson JE (2016) Positive Allosteric Modulators of GluN2A-Containing NMDARs with Distinct Modes of Action and Impacts on Circuit Function. *Neuron* **89**:983–999.
- Hamill OP, Marty A, Neher E, Sakmann B, and Sigworth FJ (1981) Improved patch-clamp techniques for high-resolution current recording from cells and cell-free membrane patches. *Pflüg Arch* **391**:85–100.
- Hanada T (2020) Ionotropic Glutamate Receptors in Epilepsy: A Review Focusing on AMPA and NMDA Receptors. *Biomolecules* **10**:464, Multidisciplinary Digital Publishing Institute.
- Hansen KB, Ogden KK, and Traynelis SF (2012) Subunit-Selective Allosteric Inhibition of Glycine Binding to NMDA Receptors. *J Neurosci* **32**:6197–6208.
- Hansen KB, Ogden KK, Yuan H, and Traynelis SF (2014) Distinct Functional and Pharmacological Properties of Triheteromeric GluN1/GluN2A/GluN2B NMDA Receptors. *Neuron* **81**:1084–1096.
- Hansen KB, Wollmuth LP, Bowie D, Furukawa H, Menniti FS, Sobolevsky AI, Swanson GT, Swanger SA, Greger IH, Nakagawa T, McBain CJ, Jayaraman V, Low C-M, Dell'Acqua ML, Diamond JS, Camp CR, Perszyk RE, Yuan H, and Traynelis SF (2021) Structure, Function, and Pharmacology of Glutamate Receptor Ion Channels. *Pharmacol Rev* **73**:1469–1658.

- Hansen KB, Yi F, Perszyk RE, Furukawa H, Wollmuth LP, Gibb AJ, and Traynelis SF (2018) Structure, function, and allosteric modulation of NMDA receptors. *J Gen Physiol* **150**:1081–1105.
- He X, Dukkipati A, and Garcia KC (2006) Structural Determinants of Natriuretic Peptide Receptor Specificity and Degeneracy. *J Mol Biol* **361**:698–714.
- Hemelikova K, Kolcheva M, Skrenkova K, Kaniakova M, and Horak M (2019) Lectins modulate the functional properties of GluN1/GluN3-containing NMDA receptors. *Neuropharmacology* **157**:107671.
- Henson MA, Larsen RS, Lawson SN, Pérez-Otaño I, Nakanishi N, Lipton SA, and Philpot BD (2012) Genetic Deletion of NR3A Accelerates Glutamatergic Synapse Maturation. *PLOS ONE* **7**:e42327, Public Library of Science.
- Henson MA, Roberts AC, Pérez-Otaño I, and Philpot BD (2010) Influence of the NR3A subunit on NMDA receptor functions. *Prog Neurobiol* **91**:23–37.
- Hepp R, Hay YA, Aguado C, Lujan R, Dauphinot L, Potier MC, Nomura S, Poirel O, El Mestikawy S, Lambolez B, and Tricoire L (2015) Glutamate receptors of the delta family are widely expressed in the adult brain. *Brain Struct Funct* **220**:2797–2815, Springer Berlin Heidelberg, Berlin/Heidelberg.
- Herguedas B, Krieger J, and Greger IH (2013) Chapter Thirteen - Receptor Heteromeric Assembly—How It Works and Why It Matters: The Case of Ionotropic Glutamate Receptors, in *Progress in Molecular Biology and Translational Science* (Giraldo J, and Ciruela F eds) pp 361–386, Academic Press.
- Hille B (1978) Ionic channels in excitable membranes. Current problems and biophysical approaches. *Biophys J* **22**:283–294.
- Hille B (1970) Ionic channels in nerve membranes. *Prog Biophys Mol Biol* **21**:1–32.
- Hille B (2021) Ionic channels in nerve membranes, 50 years on. *Prog Biophys Mol Biol*, doi: 10.1016/j.pbiomolbio.2021.11.003.
- Hille B, Armstrong CM, and MacKinnon R (1999) Ion channels: From idea to reality. *Nat Med* **5**:1105–1109.
- Hodgkin AL, and Huxley AF (1952) A quantitative description of membrane current and its application to conduction and excitation in nerve. *J Physiol* **117**:500–544.
- Hogner A, Greenwood JR, Liljefors T, Lunn M-L, Egebjerg J, Larsen IK, Gouaux E, and Kastrup JS (2003) Competitive Antagonism of AMPA Receptors by Ligands of Different Classes: Crystal Structure of ATPO Bound to the GluR2 Ligand-Binding Core, in Comparison with DNQX. *J Med Chem* **46**:214–221, American Chemical Society.
- Horak M, and Wenthold RJ (2009) Different Roles of C-terminal Cassettes in the Trafficking of Full-length NR1 Subunits to the Cell Surface \*. *J Biol Chem* **284**:9683–9691, Elsevier.

- Horning MS, and Mayer ML (2004) Regulation of AMPA Receptor Gating by Ligand Binding Core Dimers. *Neuron* **41**:379–388.
- Huganir RL, and Nicoll RA (2013) AMPARs and Synaptic Plasticity: The Last 25 Years. *Neuron* **80**:704–717.
- Iacobucci GJ, and Popescu GK (2020) Ca<sup>2+</sup>-Dependent Inactivation of GluN2A and GluN2B NMDA Receptors Occurs by a Common Kinetic Mechanism. *Biophys J* **118**:798–812.
- Iacobucci GJ, and Popescu GK (2018) Kinetic models for activation and modulation of NMDA receptor subtypes. *Curr Opin Physiol* **2**:114–122.
- Iacobucci GJ, and Popescu GK (2017) NMDA receptors: linking physiological output to biophysical operation. *Nat Rev Neurosci* **18**:236–249, Nature Publishing Group.
- Inanobe A, Furukawa H, and Gouaux E (2005) Mechanism of Partial Agonist Action at the NR1 Subunit of NMDA Receptors. *Neuron* **47**:71–84.
- Jalali-Yazdi F, Chowdhury S, Yoshioka C, and Gouaux E (2018) Mechanisms for Zinc and Proton Inhibition of the GluN1/GluN2A NMDA Receptor. *Cell* **175**:1520-1532.e15.
- Jane DE, Lodge D, and Collingridge GL (2009) Kainate receptors: Pharmacology, function and therapeutic potential. *Neuropharmacology* **56**:90–113.
- Jin R, Clark S, Weeks AM, Dudman JT, Gouaux E, and Partin KM (2005) Mechanism of Positive Allosteric Modulators Acting on AMPA Receptors. *J Neurosci* **25**:9027–9036, Society for Neuroscience.
- Jo J, Son GH, Winters BL, Kim MJ, Whitcomb DJ, Dickinson BA, Lee Y-B, Futai K, Amici M, Sheng M, Collingridge GL, and Cho K (2010) Muscarinic receptors induce LTD of NMDAR EPSCs via a mechanism involving hippocalcin, AP2 and PSD-95. *Nat Neurosci* **13**:1216–1224, Nature Publishing Group.
- Jones S, and Gibb AJ (2005) Functional NR2B- and NR2D-containing NMDA receptor channels in rat substantia nigra dopaminergic neurones. *J Physiol* **569**:209–221.
- Takegawa W, Miyoshi Y, Hamase K, Matsuda S, Matsuda K, Kohda K, Emi K, Motohashi J, Konno R, Zaitsev K, and Yuzaki M (2011) D-Serine regulates cerebellar LTD and motor coordination through the  $\delta 2$  glutamate receptor. *Nat Neurosci* **14**:603–611, Nature Publishing Group.
- Kandel E (n.d.) Principles of Neural Science. 1230.
- Kandel ER (2001) The Molecular Biology of Memory Storage: A Dialogue Between Genes and Synapses. *Science* **294**:1030–1038.
- Kane LT, and Costa BM (2015) Identification of novel allosteric modulator binding sites in NMDA receptors: A molecular modeling study. *J Mol Graph Model* **61**:204–213.
- Kaniakova M, Kleteckova L, Lichnerova K, Holubova K, Skrenkova K, Korinek M, Krusek J, Smejkalova T, Korabecny J, Vales K, Soukup O, and Horak M (2018) 7-Methoxyderivative of tacrine is a “foot-

in-the-door” open-channel blocker of GluN1/GluN2 and GluN1/GluN3 NMDA receptors with neuroprotective activity in vivo. *Neuropharmacology* **140**:217–232.

- Káradóttir R, Cavalier P, Bergersen LH, and Attwell D (2005) NMDA receptors are expressed in oligodendrocytes and activated in ischaemia. *Nature* **438**:1162–1166, Nature Publishing Group.
- Karakas E, and Furukawa H (2014) Crystal structure of a heterotetrameric NMDA receptor ion channel. *Science* **344**:992–997.
- Karakas E, noriko Simonorowski, and Furukawa H (2009) Structure of the zinc-bound amino-terminal domain of the NMDA receptor NR2B subunit. *EMBO J* **28**:3910–3920, John Wiley & Sons, Ltd.
- Karakas E, Simorowski N, and Furukawa H (2011) Subunit arrangement and phenylethanolamine binding in GluN1/GluN2B NMDA receptors. *Nature* **475**:249–253, Nature Publishing Group.
- Kazi R, Dai J, Sweeney C, Zhou H-X, and Wollmuth LP (2014) Mechanical coupling maintains the fidelity of NMDA receptor-mediated currents. *Nat Neurosci* **17**:914–922, Nature Publishing Group.
- Kehoe LA, Bellone C, Roo MD, Zanduetta A, Dey PN, Pérez-Otaño I, and Muller D (2014) GluN3A Promotes Dendritic Spine Pruning and Destabilization during Postnatal Development. *J Neurosci* **34**:9213–9221, Society for Neuroscience.
- Kessler J-P (2013) Control of Cleft Glutamate Concentration and Glutamate Spill-Out by Perisynaptic Glia: Uptake and Diffusion Barriers. *PLOS ONE* **8**:e70791, Public Library of Science.
- Kew JN, Trube G, and Kemp JA (1996) A novel mechanism of activity-dependent NMDA receptor antagonism describes the effect of ifenprodil in rat cultured cortical neurones. *J Physiol* **497**:761–772.
- Kirischuk S (2022) Keeping Excitation–Inhibition Ratio in Balance. *Int J Mol Sci* **23**:5746, Multidisciplinary Digital Publishing Institute.
- Klippenstein V, Ghisi V, Wietstruk M, and Plested AJR (2014) Photoinactivation of Glutamate Receptors by Genetically Encoded Unnatural Amino Acids. *J Neurosci* **34**:980–991.
- Klippenstein V, Hoppmann C, Ye S, Wang L, and Paoletti P (2017) Optocontrol of glutamate receptor activity by single side-chain photoisomerization. *eLife* **6**:e25808.
- Koehl A, Hu H, Feng D, Sun B, Zhang Y, Robertson MJ, Chu M, Kobilka TS, Laeremans T, Steyaert J, Tarrasch J, Dutta S, Fonseca R, Weis WI, Mathiesen JM, Skiniotis G, and Kobilka BK (2019) Structural insights into the activation of metabotropic glutamate receptors. *Nature* **566**:79–84, Nature Publishing Group.
- Kohda K, Kakegawa W, Matsuda S, Yamamoto T, Hirano H, and Yuzaki M (2013) The  $\delta 2$  glutamate receptor gates long-term depression by coordinating interactions between two AMPA receptor phosphorylation sites. *Proc Natl Acad Sci U S A* **110**:E948–E957, National Academy of Sciences, United States.

- Köhr G (2006) NMDA receptor function: subunit composition versus spatial distribution. *Cell Tissue Res* **326**:439–446.
- Kumari J, Vinnakota R, and Kumar J (2019) Structural and Functional Insights into GluK3-kainate Receptor Desensitization and Recovery. *Sci Rep* **9**:10254, Nature Publishing Group.
- Kuner T, and Schoepfer R (1996) Multiple Structural Elements Determine Subunit Specificity of Mg<sup>2+</sup> Block in NMDA Receptor Channels. *J Neurosci* **16**:3549–3558, Society for Neuroscience.
- Kunishima N, Shimada Y, Tsuji Y, Sato T, Yamamoto M, Kumasaka T, Nakanishi S, Jingami H, and Morikawa K (2000) Structural basis of glutamate recognition by a dimeric metabotropic glutamate receptor. *Nature* **407**:971–977, Nature Publishing Group.
- Kushima I, Aleksic B, Nakatochi M, Shimamura T, Okada T, Uno Y, Morikawa M, Ishizuka K, Shiino T, Kimura H, Arioka Y, Yoshimi A, Takasaki Y, Yu Y, Nakamura Y, Yamamoto M, Iidaka T, Iritani S, Inada T, Ogawa N, Shishido E, Torii Y, Kawano N, Omura Y, Yoshikawa Toru, Uchiyama T, Yamamoto T, Ikeda M, Hashimoto R, Yamamori H, Yasuda Y, Someya T, Watanabe Y, Egawa J, Nunokawa A, Itokawa M, Arai M, Miyashita M, Kobori A, Suzuki M, Takahashi T, Usami M, Kodaira M, Watanabe K, Sasaki T, Kuwabara H, Tochigi M, Nishimura F, Yamasue H, Eriguchi Y, Benner S, Kojima M, Yassin W, Munesue T, Yokoyama S, Kimura R, Funabiki Y, Kosaka H, Ishitobi M, Ohmori T, Numata S, Yoshikawa Takeo, Toyota T, Yamakawa K, Suzuki T, Inoue Y, Nakaoka K, Goto Y, Inagaki M, Hashimoto N, Kusumi I, Son S, Murai T, Ikegame T, Okada N, Kasai K, Kunimoto S, Mori D, Iwata N, and Ozaki N (2018) Comparative Analyses of Copy-Number Variation in Autism Spectrum Disorder and Schizophrenia Reveal Etiological Overlap and Biological Insights. *Cell Rep* **24**:2838–2856.
- Kvist T, Greenwood JR, Hansen KB, Traynelis SF, and Bräuner-Osborne H (2013) Structure-based discovery of antagonists for GluN3-containing N-methyl-d-aspartate receptors. *Neuropharmacology* **75**:324–336.
- Lakhan S, Caro M, and Hadzimechalis N (2013) NMDA Receptor Activity in Neuropsychiatric Disorders. *Front Psychiatry* **4**.
- Larsen RS, Corlew RJ, Henson MA, Roberts AC, Mishina M, Watanabe M, Lipton SA, Nakanishi N, Pérez-Otaño I, Weinberg RJ, and Philpot BD (2011) NR3A-containing NMDARs promote neurotransmitter release and spike timing-dependent plasticity. *Nat Neurosci* **14**:338–344, Nature Publishing Group.
- Larsen RS, Smith IT, Miriyala J, Han JE, Corlew RJ, Smith SL, and Philpot BD (2014) Synapse-Specific Control of Experience-Dependent Plasticity by Presynaptic NMDA Receptors. *Neuron* **83**:879–893.
- Lau AY, and Roux B (2007) The Free Energy Landscapes Governing Conformational Changes in a Glutamate Receptor Ligand-Binding Domain. *Structure* **15**:1203–1214.
- Laurie DJ, and Seeburg PH (1994) Regional and developmental heterogeneity in splicing of the rat brain NMDAR1 mRNA. *J Neurosci* **14**:3180–3194, Society for Neuroscience.

- Laverty D, Desai R, Uchański T, Masiulis S, Stec WJ, Malinauskas T, Zivanov J, Pardon E, Steyaert J, Miller KW, and Aricescu AR (2019) Cryo-EM structure of the human  $\alpha 1\beta 3\gamma 2$  GABAA receptor in a lipid bilayer. *Nature* **565**:516–520, Nature Publishing Group.
- Lee C-H, Lü W, Michel JC, Goehring A, Du J, Song X, and Gouaux E (2014) NMDA receptor structures reveal subunit arrangement and pore architecture. *Nature* **511**:191–197.
- Lee JH, Wei ZZ, Chen D, Gu X, Wei L, and Yu SP (2015) A neuroprotective role of the NMDA receptor subunit GluN3A (NR3A) in ischemic stroke of the adult mouse. *Am J Physiol-Cell Physiol* **308**:C570–C577, American Physiological Society.
- Lee JH, Zhang JY, Wei ZZ, and Yu SP (2018) Impaired social behaviors and minimized oxytocin signaling of the adult mice deficient in the N-methyl-d-aspartate receptor GluN3A subunit. *Exp Neurol* **305**:1–12.
- Lemke JR, Geider K, Helbig KL, Heyne HO, Schütz H, Hentschel J, Courage C, Depienne C, Nava C, Heron D, Møller RS, Hjalgrim H, Lal D, Neubauer BA, Nürnberg P, Thiele H, Kurlemann G, Arnold GL, Bhambhani V, Bartholdi D, Pedurupillay CRJ, Miscio D, Frengen E, Strømme P, Dlugos DJ, Doherty ES, Bijlsma EK, Ruivenkamp CA, Hoffer MJV, Goldstein A, Rajan DS, Narayanan V, Ramsey K, Belnap N, Schrauwen I, Richholt R, Koeleman BPC, Sá J, Mendonça C, Kovel CGF de, Weckhuysen S, Hardies K, Jonghe PD, Meirleir LD, Milh M, Badens C, Lebrun M, Busa T, Francannet C, Piton A, Riesch E, Biskup S, Vogt H, Dorn T, Helbig I, Michaud JL, Laube B, and Syrbe S (2016) Delineating the GRIN1 phenotypic spectrum: A distinct genetic NMDA receptor encephalopathy. *Neurology* **86**:2171–2178, Wolters Kluwer Health, Inc. on behalf of the American Academy of Neurology.
- Lemke JR, Lal D, Reinthaler EM, Steiner I, Nothnagel M, Alber M, Geider K, Laube B, Schwake M, Finsterwalder K, Franke A, Schilhabel M, Jähn JA, Muhle H, Boor R, Van Paesschen W, Caraballo R, Fejerman N, Weckhuysen S, De Jonghe P, Larsen J, Møller RS, Hjalgrim H, Addis L, Tang S, Hughes E, Pal DK, Veri K, Vaher U, Talvik T, Dimova P, Guerrero López R, Serratosa JM, Linnankivi T, Lehesjoki A-E, Ruf S, Wolff M, Buerki S, Wohlrab G, Kroell J, Datta AN, Fiedler B, Kurlemann G, Kluger G, Hahn A, Haberlandt DE, Kutzer C, Sperner J, Becker F, Weber YG, Feucht M, Steinböck H, Neophythou B, Ronen GM, Gruber-Sedlmayr U, Geldner J, Harvey RJ, Hoffmann P, Herms S, Altmüller J, Toliat MR, Thiele H, Nürnberg P, Wilhelm C, Stephani U, Helbig I, Lerche H, Zimprich F, Neubauer BA, Biskup S, and von Spiczak S (2013) Mutations in GRIN2A cause idiopathic focal epilepsy with rolandic spikes. *Nat Genet* **45**:1067–1072.
- Lerma J, and Marques JM (2013) Kainate Receptors in Health and Disease. *Neuron* **80**:292–311.
- Lesca G, Rudolf G, Bruneau N, Lozovaya N, Labalme A, Boutry-Kryza N, Salmi M, Tsintsadze T, Addis L, Motte J, Wright S, Tsintsadze V, Michel A, Doummar D, Lascelles K, Strug L, Waters P, de Bellescize J, Vrielynck P, de Saint Martin A, Ville D, Ryvlin P, Arzimanoglou A, Hirsch E, Vincent A, Pal D, Burnashev N, Sanlaville D, and Szepetowski P (2013) GRIN2A mutations in acquired epileptic aphasia and related childhood focal epilepsies and encephalopathies with speech and language dysfunction. *Nat Genet* **45**:1061–1066.
- Lester RA, Tong G, and Jahr CE (1993) Interactions between the glycine and glutamate binding sites of the NMDA receptor. *J Neurosci* **13**:1088–1096, Society for Neuroscience.

- Lester RAJ, and Jahr CE (n.d.) NMDA Channel Behavior Depends on Agonist Affinity. *J Neurosci* **9**.
- Liu J, Chang L, Song Y, Li H, and Wu Y (2019) The Role of NMDA Receptors in Alzheimer's Disease. *Front Neurosci* **13**.
- Liu SX, Gades MS, Swain Y, Ramakrishnan A, Harris AC, Tran PV, and Gewirtz JC (2021) Repeated morphine exposure activates synaptogenesis and other neuroplasticity-related gene networks in the dorsomedial prefrontal cortex of male and female rats. *Drug Alcohol Depend* **221**:108598.
- Low C-M, and Wee KS-L (2010) New Insights into the Not-So-New NR3 Subunits of N-Methyl-d-aspartate Receptor: Localization, Structure, and Function. *Mol Pharmacol* **78**:1–11, American Society for Pharmacology and Experimental Therapeutics.
- Madeira C, Lourenco MV, Vargas-Lopes C, Suemoto CK, Brandão CO, Reis T, Leite REP, Laks J, Jacob-Filho W, Pasqualucci CA, Grinberg LT, Ferreira ST, and Panizzutti R (2015) d-serine levels in Alzheimer's disease: implications for novel biomarker development. *Transl Psychiatry* **5**:e561–e561.
- Madry C, and Betz H (n.d.) Supralinear potentiation of NR1/NR3A excitatory glycine receptors by Zn<sup>2+</sup> and NR1 antagonist. **6**.
- Madry C, Mesic I, Bartholomäus I, Nicke A, Betz H, and Laube B (2007) Principal role of NR3 subunits in NR1/NR3 excitatory glycine receptor function. *Biochem Biophys Res Commun* **354**:102–108.
- Mahfooz K, Marco S, Martínez-Turrillas R, Raja MK, Pérez-Otaño I, and Wesseling JF (2016) GluN3A promotes NMDA spiking by enhancing synaptic transmission in Huntington's disease models. *Neurobiol Dis* **93**:47–56.
- Mameli M, Carta M, Partridge LD, and Valenzuela CF (2005) Neurosteroid-Induced Plasticity of Immature Synapses via Retrograde Modulation of Presynaptic NMDA Receptors. *J Neurosci* **25**:2285–2294, Society for Neuroscience.
- Marco S, Giralt A, Petrovic MM, Pouladi MA, Martínez-Turrillas R, Martínez-Hernández J, Kaltenbach LS, Torres-Peraza J, Graham RK, Watanabe M, Luján R, Nakanishi N, Lipton SA, Lo DC, Hayden MR, Alberch J, Wesseling JF, and Pérez-Otaño I (2013) Suppressing aberrant GluN3A expression rescues synaptic and behavioral impairments in Huntington's disease models. *Nat Med* **19**:1030–1038, Nature Publishing Group.
- Martínez-Turrillas R, Puerta E, Chowdhury D, Marco S, Watanabe M, Aguirre N, and Pérez-Otaño I (2012) The NMDA receptor subunit GluN3A protects against 3-nitropropionic-induced striatal lesions via inhibition of calpain activation. *Neurobiol Dis* **48**:290–298.
- Masu M, Tanabe Y, Tsuchida K, Shigemoto R, and Nakanishi S (1991) Sequence and expression of a metabotropic glutamate receptor. *Nature* **349**:760–765.
- Matsuda K, Fletcher M, Kamiya Y, and Yuzaki M (2003) Specific Assembly with the NMDA Receptor 3B Subunit Controls Surface Expression and Calcium Permeability of NMDA Receptors. *J Neurosci* **23**:10064–10073, Society for Neuroscience.



- Mayer ML (2006) Glutamate receptors at atomic resolution. *Nature* **440**:456–462, Nature Publishing Group.
- Mayer ML (2016) Structural biology of glutamate receptor ion channel complexes. *Curr Opin Struct Biol* **41**:119–127.
- Mayer ML (2021) Structural biology of kainate receptors. *Neuropharmacology* **190**:108511.
- McClymont DW, Harris J, and Mellor IR (2012) Open-channel blockade is less effective on GluN3B than GluN3A subunit-containing NMDA receptors. *Eur J Pharmacol* **686**:22–31.
- McDaniel MJ, Ogden KK, Kell SA, Burger PB, Liotta DC, and Traynelis SF (2020) NMDA receptor channel gating control by the pre-M1 helix. *J Gen Physiol* **152**:e201912362.
- Mechanisms of activation, inhibition and specificity: crystal structures of the NMDA receptor NR1 ligand-binding core (2003) . *EMBO J* **22**:2873–2885, John Wiley & Sons, Ltd.
- Mehra A, Guérit S, Macrez R, Gosselet F, Sevin E, Lebas H, Maubert E, Vries HED, Bardou I, Vivien D, and Docagne F (2020) Nonionotropic Action of Endothelial NMDA Receptors on Blood–Brain Barrier Permeability via Rho/ROCK-Mediated Phosphorylation of Myosin. *J Neurosci* **40**:1778–1787, Society for Neuroscience.
- Mesic I, Madry C, Geider K, Bernhard M, Betz H, and Laube B (2016) The N-terminal domain of the GluN3A subunit determines the efficacy of glycine-activated NMDA receptors. *Neuropharmacology* **105**:133–141.
- Meyerson JR, Kumar J, Chittori S, Rao P, Pierson J, Bartesaghi A, Mayer ML, and Subramaniam S (2014) Structural mechanism of glutamate receptor activation and desensitization. *Nature* **514**:328–334.
- Mody I, and Pearce RA (2004) Diversity of inhibitory neurotransmission through GABAA receptors. *Trends Neurosci* **27**:569–575.
- Mohamad O, Song M, Wei L, and Yu SP (2013) Regulatory roles of the NMDA receptor GluN3A subunit in locomotion, pain perception and cognitive functions in adult mice. *J Physiol* **591**:149–168.
- Moldavski A, Behr J, Bading H, and Bengtson CP (2020) A novel method using ambient glutamate for the electrophysiological quantification of extrasynaptic NMDA receptor function in acute brain slices. *J Physiol* **598**:633–650.
- Montgomery JM, Selcher JC, Hanson JE, and Madison DV (2005) Dynamin-dependent NMDAR endocytosis during LTD and its dependence on synaptic state. *BMC Neurosci* **6**:48.
- Mony L, Kew JN, Gunthorpe MJ, and Paoletti P (2009) Allosteric modulators of NR2B-containing NMDA receptors: molecular mechanisms and therapeutic potential. *Br J Pharmacol* **157**:1301–1317.
- Mony L, Zhu S, Carvalho S, and Paoletti P (2011) Molecular basis of positive allosteric modulation of GluN2B NMDA receptors by polyamines. *EMBO J* **30**:3134–3146, John Wiley & Sons, Ltd.

- Mony L, Zhu S, Carvalho S, and Paoletti P (n.d.) Molecular basis of positive allosteric modulation of GluN2B NMDA receptors by polyamines | The EMBO Journal.
- Monyer H, Burnashev N, Laurie DJ, Sakmann B, and Seeburg PH (1994) Developmental and regional expression in the rat brain and functional properties of four NMDA receptors. *Neuron* **12**:529–540.
- Mori H, Manabe T, Watanabe M, Satoh Y, Suzuki N, Toki S, Nakamura K, Yagi T, Kushiya E, Takahashi T, Inoue Y, Sakimura K, and Mishina M (1998) Role of the Carboxy-Terminal Region of the GluR2 Subunit in Synaptic Localization of the NMDA Receptor Channel. *Neuron* **21**:571–580.
- Morishita W, Marie H, and Malenka RC (2005) Distinct triggering and expression mechanisms underlie LTD of AMPA and NMDA synaptic responses. *Nat Neurosci* **8**:1043–1050, Nature Publishing Group.
- Moss SJ, and Smart TG (2001) Constructing inhibitory synapses. *Nat Rev Neurosci* **2**:240–250, Nature Publishing Group.
- Mueller HT, and Meador-Woodruff JH (2004) NR3A NMDA receptor subunit mRNA expression in schizophrenia, depression and bipolar disorder. *Schizophr Res* **71**:361–370.
- Murillo A, Navarro AI, Puelles E, Zhang Y, Petros TJ, and Pérez-Otaño I (2021) Temporal Dynamics and Neuronal Specificity of Grin3a Expression in the Mouse Forebrain. *Cereb Cortex* **31**:1914–1926.
- Murphy JA, Stein IS, Lau CG, Peixoto RT, Aman TK, Kaneko N, Aromolaran K, Saulnier JL, Popescu GK, Sabatini BL, Hell JW, and Zukin RS (2014) Phosphorylation of Ser1166 on GluN2B by PKA Is Critical to Synaptic NMDA Receptor Function and Ca<sup>2+</sup> Signaling in Spines. *J Neurosci* **34**:869–879, Society for Neuroscience.
- Nair JD, Wilkinson KA, Henley JM, and Mellor JR (2021) Kainate receptors and synaptic plasticity. *Neuropharmacology* **196**:108540.
- Naur P, Hansen KB, Kristensen AS, Dravid SM, Pickering DS, Olsen L, Vestergaard B, Egebjerg J, Gajhede M, Traynelis SF, and Kastrup JS (2007) Ionotropic glutamate-like receptor  $\delta$ 2 binds D-serine and glycine. *Proc Natl Acad Sci U S A* **104**:14116–14121.
- Nayeem N, Zhang Y, Schweppe DK, Madden DR, and Green T (2009) A Nondesensitizing Kainate Receptor Point Mutant. *Mol Pharmacol* **76**:534–542.
- Nicoletti F, Meek JL, Iadarola MJ, Chuang DM, Roth BL, and Costa E (1986) Coupling of Inositol Phospholipid Metabolism with Excitatory Amino Acid Recognition Sites in Rat Hippocampus. *J Neurochem* **46**:40–46.
- Nicoll RA (2017) A Brief History of Long-Term Potentiation. *Neuron* **93**:281–290.
- Nicoll RA, and Schmitz D (2005) Synaptic plasticity at hippocampal mossy fibre synapses. *Nat Rev Neurosci* **6**:863–876, Nature Publishing Group.

- Nicoll RA, Tomita S, and Brecht DS (2006) Auxiliary Subunits Assist AMPA-Type Glutamate Receptors. *Science* **311**:1253–1256, American Association for the Advancement of Science.
- Niemann S, Kanki H, Fukui Y, Takao K, Fukaya M, Hynynen MN, Churchill MJ, Shefner JM, Bronson RT, Brown Jr. RH, Watanabe M, Miyakawa T, Itohara S, and Hayashi Y (2007) Genetic ablation of NMDA receptor subunit NR3B in mouse reveals motoneuronal and nonmotoneuronal phenotypes. *Eur J Neurosci* **26**:1407–1420.
- Nilsson A, Eriksson M, Muly EC, Åkesson E, Samuelsson E-B, Bogdanovic N, Benedikz E, and Sundström E (2007) Analysis of NR3A receptor subunits in human native NMDA receptors. *Brain Res* **1186**:102–112.
- Niswender CM, and Conn PJ (2010) Metabotropic glutamate receptors: physiology, pharmacology, and disease. *Annu Rev Pharmacol Toxicol* **50**:295–322, Annual Reviews, United States.
- Ogden KK, Chen W, Swanger SA, McDaniel MJ, Fan LZ, Hu C, Tankovic A, Kusumoto H, Kosobucki GJ, Schulien AJ, Su Z, Pecha J, Bhattacharya S, Petrovski S, Cohen AE, Aizenman E, Traynelis SF, and Yuan H (2017) Molecular Mechanism of Disease-Associated Mutations in the Pre-M1 Helix of NMDA Receptors and Potential Rescue Pharmacology. *PLOS Genet* **13**:e1006536.
- Ogden KK, and Traynelis SF (2011) New advances in NMDA receptor pharmacology. *Trends Pharmacol Sci* **32**:726–733.
- O’Hara PJ, Sheppard PO, Thøgersen H, Venezia D, Haldeman BA, McGrane V, Houamed KM, Thomsen C, Gilbert TL, and Mulvihill ER (1993) The ligand-binding domain in metabotropic glutamate receptors is related to bacterial periplasmic binding proteins. *Neuron* **11**:41–52.
- Otsu Y, Darcq E, Pietrajtis K, Mátyás F, Schwartz E, Bessaih T, Abi Gerges S, Rousseau CV, Grand T, Dieudonné S, Paoletti P, Acsády L, Agulhon C, Kieffer BL, and Diana MA (2019) Control of aversion by glycine-gated GluN1/GluN3A NMDA receptors in the adult medial habenula. *Science* **366**:250–254.
- Pachernegg S, Strutz-Seebohm N, and Hollmann M (2012) GluN3 subunit-containing NMDA receptors: not just one-trick ponies. *Trends Neurosci* **35**:240–249.
- Paganelli MA, Kussius CL, and Popescu GK (2013) Role of Cross-Cleft Contacts in NMDA Receptor Gating. *PLOS ONE* **8**:e80953, Public Library of Science.
- Paoletti P (2011) Molecular basis of NMDA receptor functional diversity: NMDA receptor functional diversity. *Eur J Neurosci* **33**:1351–1365.
- Paoletti P, Ascher P, and Neyton J (1997a) High-Affinity Zinc Inhibition of NMDA NR1–NR2A Receptors. *J Neurosci* **17**:5711–5725.
- Paoletti P, Ascher P, and Neyton J (1997b) High-Affinity Zinc Inhibition of NMDA NR1–NR2A Receptors. *J Neurosci* **17**:5711–5725, Society for Neuroscience.
- Paoletti P, Bellone C, and Zhou Q (2013) NMDA receptor subunit diversity: impact on receptor properties, synaptic plasticity and disease. *Nat Rev Neurosci* **14**:383–400.

- Paoletti P, Neyton J, and Ascher P (1995) Glycine-independent and subunit-specific potentiation of NMDA responses by extracellular Mg<sup>2+</sup>. *Neuron* **15**:1109–1120.
- Paoletti P, Perin-Dureau F, Fayyazuddin A, Le Goff A, Callebaut I, and Neyton J (2000) Molecular Organization of a Zinc Binding N-Terminal Modulatory Domain in a NMDA Receptor Subunit. *Neuron* **28**:911–925.
- Paoletti P, Vergnano A. M., Barbour B, and Casado M (2009) Zinc at glutamatergic synapses. *Neuroscience* **158**:126–136.
- Paoletti P, Vergnano A.M., Barbour B, and Casado M (2009) Zinc at glutamatergic synapses. *Neuroscience* **158**:126–136.
- Partin KM, Bowie D, and Mayer ML (1995) Structural determinants of allosteric regulation in alternatively spliced AMPA receptors. *Neuron* **14**:833–843.
- Paul A, Crow M, Raudales R, He M, Gillis J, and Huang ZJ (2017) Transcriptional Architecture of Synaptic Communication Delineates GABAergic Neuron Identity. *Cell* **171**:522-539.e20.
- Peng Y, Zhao J, Gu Q-H, Chen R-Q, Xu Z, Yan J-Z, Wang S-H, Liu S-Y, Chen Z, and Lu W (2010) Distinct trafficking and expression mechanisms underlie LTP and LTD of NMDA receptor-mediated synaptic responses. *Hippocampus* **20**:646–658.
- Pérez-Otaño I, Larsen RS, and Wesseling JF (2016) Emerging roles of GluN3-containing NMDA receptors in the CNS. *Nat Rev Neurosci* **17**:623–635.
- Pérez-Otaño I, Schulteis CT, Contractor A, Lipton SA, Trimmer JS, Sucher NJ, and Heinemann SF (2001a) Assembly with the NR1 Subunit Is Required for Surface Expression of NR3A-Containing NMDA Receptors. *J Neurosci* **21**:1228–1237.
- Pérez-Otaño I, Schulteis CT, Contractor A, Lipton SA, Trimmer JS, Sucher NJ, and Heinemann SF (2001b) Assembly with the NR1 Subunit Is Required for Surface Expression of NR3A-Containing NMDA Receptors. *J Neurosci* **21**:1228–1237.
- Perszyk RE, Swanger SA, Shelley C, Khatri A, Fernandez-Cuervo G, Epplin MP, Zhang J, Le P, Bülow P, Garnier-Amblard E, Gangireddy PKR, Bassell GJ, Yuan H, Menaldino DS, Liotta DC, Liebeskind LS, and Traynelis SF (2020) Biased modulators of NMDA receptors control channel opening and ion selectivity. *Nat Chem Biol* **16**:188–196.
- Pfeffer CK, Xue M, He M, Huang ZJ, and Scanziani M (2013) Inhibition of inhibition in visual cortex: the logic of connections between molecularly distinct interneurons. *Nat Neurosci* **16**:1068–1076, Nature Publishing Group.
- Pfisterer U, Petukhov V, Demharter S, Meichsner J, Thompson JJ, Batiuk MY, Asenjo-Martinez A, Vasistha NA, Thakur A, Mikkelsen J, Adorjan I, Pinborg LH, Pers TH, von Engelhardt J, Kharchenko PV, and Khodosevich K (2020) Identification of epilepsy-associated neuronal subtypes and gene expression underlying epileptogenesis. *Nat Commun* **11**:5038, Nature Publishing Group.

- Pierson TM, Yuan H, Marsh ED, Fuentes-Fajardo K, Adams DR, Markello T, Golas G, Simeonov DR, Holloman C, Tankovic A, Karamchandani MM, Schreiber JM, Mullikin JC, Tifft CJ, Toro C, Boerkoel CF, Traynelis SF, and Gahl WA (2014) *GRIN2A* mutation and early-onset epileptic encephalopathy: personalized therapy with memantine. *Ann Clin Transl Neurol* **1**:190–198.
- Pilli J, and Kumar SS (2012) Triheteromeric N-methyl-d-aspartate receptors differentiate synaptic inputs onto pyramidal neurons in somatosensory cortex: Involvement of the GluN3A subunit. *Neuroscience* **222**:75–88.
- Piña-Crespo JC, Talantova M, Micu I, States B, Chen H-SV, Tu S, Nakanishi N, Tong G, Zhang D, Heinemann SF, Zamponi GW, Stys PK, and Lipton SA (2010) Excitatory Glycine Responses of CNS Myelin Mediated by NR1/NR3 “NMDA” Receptor Subunits. *J Neurosci* **30**:11501–11505, Society for Neuroscience.
- Pinard A, Seddik R, and Bettler B (2010) GABAB Receptors: Physiological Functions and Mechanisms of Diversity, in *Advances in Pharmacology* (Blackburn TP ed) pp 231–255, Academic Press.
- Platzer K, Yuan H, Schütz H, Winschel A, Chen W, Hu C, Kusumoto H, Heyne HO, Helbig KL, Tang S, Willing MC, Tinkle BT, Adams DJ, Depienne C, Keren B, Mignot C, Frengen E, Strømme P, Biskup S, Döcker D, Strom TM, Mefford HC, Myers CT, Muir AM, LaCroix A, Sadleir L, Scheffer IE, Brilstra E, van Haelst MM, van der Smagt JJ, Bok LA, Møller RS, Jensen UB, Millichap JJ, Berg AT, Goldberg EM, De Bie I, Fox S, Major P, Jones JR, Zackai EH, Abou Jamra R, Rolfs A, Leventer RJ, Lawson JA, Roscioli T, Jansen FE, Ranza E, Korff CM, Lehesjoki A-E, Courage C, Linnankivi T, Smith DR, Stanley C, Mintz M, McKnight D, Decker A, Tan W-H, Tarnopolsky MA, Brady LI, Wolff M, Dondit L, Pedro HF, Parisotto SE, Jones KL, Patel AD, Franz DN, Vanzo R, Marco E, Ranells JD, Di Donato N, Dobyns WB, Laube B, Traynelis SF, and Lemke JR (2017) *GRIN2B* encephalopathy: novel findings on phenotype, variant clustering, functional consequences and treatment aspects. *J Med Genet* **54**:460–470.
- Plested AJR, and Mayer ML (2007) Structure and Mechanism of Kainate Receptor Modulation by Anions. *Neuron* **53**:829–841.
- Plested AJR, Vijayan R, Biggin PC, and Mayer ML (2008) Molecular Basis of Kainate Receptor Modulation by Sodium. *Neuron* **58**:720–735.
- Popescu G, Robert A, Howe JR, and Auerbach A (2004) Reaction mechanism determines NMDA receptor response to repetitive stimulation. *Nature* **430**:790–793, Nature Publishing Group.
- Priel A, Selak S, Lerma J, and Stern-Bach Y (2006) Block of Kainate Receptor Desensitization Uncovers a Key Trafficking Checkpoint. *Neuron* **52**:1037–1046.
- Prithviraj R, and Inglis FM (2008) Expression of the N-methyl-d-aspartate receptor subunit NR3B regulates dendrite morphogenesis in spinal motor neurons. *Neuroscience* **155**:145–153.
- Quiococho FA, Higgins CF, Kornberg HL, and Henderson PJF (1990) Atomic structures of periplasmic binding proteins and the high-affinity active transport systems in bacteria. *Philos Trans R Soc Lond B Biol Sci* **326**:341–352, Royal Society.

- Rachline J, Perin-Dureau F, Goff AL, Neyton J, and Paoletti P (2005) The Micromolar Zinc-Binding Domain on the NMDA Receptor Subunit NR2B. *J Neurosci* **25**:308–317, Society for Neuroscience.
- Reinert MM, and Bullock R (1999) Clinical trials in head injury. *Neurol Res* **21**:330–338, Taylor & Francis.
- Reingruber J, and Holcman D (2011) The Narrow Escape Problem in a Flat Cylindrical Microdomain with Application to Diffusion in the Synaptic Cleft. *Multiscale Model Simul*, doi: 10.1137/100807612, Society for Industrial and Applied Mathematics.
- Retchless BS, Gao W, and Johnson JW (2012) A single GluN2 subunit residue controls NMDA receptor channel properties via intersubunit interaction. *Nat Neurosci* **15**:406–413, Nature Publishing Group.
- Reynolds' IJ, and Aizenman E (n.d.) Receptor Antagonist and Is. *J Neurosci* **6**.
- Riou M, Stroebel D, Edwardson JM, and Paoletti P (2012) An Alternating GluN1-2-1-2 Subunit Arrangement in Mature NMDA Receptors. *PLOS ONE* **7**:e35134, Public Library of Science.
- Roberts AC, Díez-García J, Rodriguiz RM, López IP, Luján R, Martínez-Turrillas R, Picó E, Henson MA, Bernardo DR, Jarrett TM, Clendeninn DJ, López-Mascaraque L, Feng G, Lo DC, Wesseling JF, Wetsel WC, Philpot BD, and Pérez-Otaño I (2009) Downregulation of NR3A-Containing NMDARs Is Required for Synapse Maturation and Memory Consolidation. *Neuron* **63**:342–356.
- Romero-Hernandez A, Simorowski N, Karakas E, and Furukawa H (2016) Molecular Basis for Subtype Specificity and High-Affinity Zinc Inhibition in the GluN1-GluN2A NMDA Receptor Amino-Terminal Domain. *Neuron* **92**:1324–1336.
- Rosenmund C, and Westbrook GL (1993) Calcium-induced actin depolymerization reduces NMDA channel activity. *Neuron* **10**:805–814.
- Rossi P, Sola E, Taglietti V, Borchardt T, Steigerwald F, Utvik JK, Ottersen OP, Köhr G, and D'Angelo E (2002) NMDA Receptor 2 (NR2) C-Terminal Control of NR Open Probability Regulates Synaptic Transmission and Plasticity at a Cerebellar Synapse. *J Neurosci* **22**:9687–9697, Society for Neuroscience.
- Rycroft BK, and Gibb AJ (2002) Direct Effects of Calmodulin on NMDA Receptor Single-Channel Gating in Rat Hippocampal Granule Cells. *J Neurosci* **22**:8860–8868, Society for Neuroscience.
- Sadat-Shirazi M-S, Ashabi G, Hessari MB, Khalifeh S, Neirizi NM, Matloub M, Safarzadeh M, Vousooghi N, and Zarrindast M-R (2019) NMDA receptors of blood lymphocytes anticipate cognitive performance variations in healthy volunteers. *Physiol Behav* **201**:53–58.
- Salussolia CL, Gan Q, Kazi R, Singh P, Allopenna J, Furukawa H, and Wollmuth LP (2013) A Eukaryotic Specific Transmembrane Segment is Required for Tetramerization in AMPA Receptors. *J Neurosci* **33**:9840–9845, Society for Neuroscience.
- Saper MA, and Quiocho FA (1983) Leucine, isoleucine, valine-binding protein from *Escherichia coli*. Structure at 3.0-Å resolution and location of the binding site. *J Biol Chem* **258**:11057–11062.

- Sasaki YF, Rothe T, Premkumar LS, Das S, Cui J, Talantova MV, Wong H-K, Gong X, Chan SF, Zhang D, Nakanishi N, Sucher NJ, and Lipton SA (2002) Characterization and Comparison of the NR3A Subunit of the NMDA Receptor in Recombinant Systems and Primary Cortical Neurons. *J Neurophysiol* **87**:2052–2063.
- Savtchouk I, Di Castro MA, Ali R, Stubbe H, Luján R, and Volterra A (2019) Circuit-specific control of the medial entorhinal inputs to the dentate gyrus by atypical presynaptic NMDARs activated by astrocytes. *Proc Natl Acad Sci* **116**:13602–13610, Proceedings of the National Academy of Sciences.
- Schauder DM, Kuybeda O, Zhang J, Klymko K, Bartesaghi A, Borgnia MJ, Mayer ML, and Subramaniam S (2013) Glutamate receptor desensitization is mediated by changes in quaternary structure of the ligand binding domain. *Proc Natl Acad Sci* **110**:5921–5926.
- Schorge S, and Colquhoun D (2003) Studies of NMDA Receptor Function and Stoichiometry with Truncated and Tandem Subunits. *J Neurosci* **23**:1151–1158, Society for Neuroscience.
- Schüler T, Mesic I, Madry C, Bartholomäus I, and Laube B (2008) Formation of NR1/NR2 and NR1/NR3 Heterodimers Constitutes the Initial Step in N-Methyl-D-aspartate Receptor Assembly \*. *J Biol Chem* **283**:37–46, Elsevier.
- Sensi SL, Paoletti P, Bush AI, and Sekler I (2009) Zinc in the physiology and pathology of the CNS. *Nat Rev Neurosci* **10**:780–791, Nature Publishing Group.
- Serraz B, Grand T, and Paoletti P (2016) Altered zinc sensitivity of NMDA receptors harboring clinically-relevant mutations. *Neuropharmacology* **109**:196–204.
- Shen K-Z, and Johnson SW (1997) A Slow Excitatory Postsynaptic Current Mediated by G-protein-coupled Metabotropic Glutamate Receptors in Rat Ventral Tegmental Dopamine Neurons. *Eur J Neurosci* **9**:48–54.
- Sheng M, and Kim E (2011) The Postsynaptic Organization of Synapses. *Cold Spring Harb Perspect Biol* **3**:a005678.
- Shepherd JD, and Huganir RL (2007) The Cell Biology of Synaptic Plasticity: AMPA Receptor Trafficking. *Annu Rev Cell Dev Biol* **23**:613–643.
- Sirrieh RE, MacLean DM, and Jayaraman V (2015) A conserved structural mechanism of NMDA receptor inhibition: A comparison of ifenprodil and zinc. *J Gen Physiol* **146**:173–181.
- Sirrieh RE, MacLean DM, and Jayaraman V (2013) Amino-terminal Domain Tetramer Organization and Structural Effects of Zinc Binding in the N-Methyl-d-aspartate (NMDA) Receptor. *J Biol Chem* **288**:22555–22564, Elsevier.
- Skrenkova K, Hemelikova K, Kolcheva M, Kortus S, Kaniakova M, Krausova B, and Horak M (2019) Structural features in the glycine-binding sites of the GluN1 and GluN3A subunits regulate the surface delivery of NMDA receptors. *Sci Rep* **9**:12303.

- Skrenkova K, Lee S, Lichnerova K, Kaniakova M, Hansikova H, Zapotocky M, Suh YH, and Horak M (2018) N-Glycosylation Regulates the Trafficking and Surface Mobility of GluN3A-Containing NMDA Receptors. *Front Mol Neurosci* **11**.
- Sladeczek F, Momiyama A, and Takahashi T (1993) Presynaptic inhibitory action of a metabotropic glutamate receptor agonist on excitatory transmission in visual cortical neurons. *Proc R Soc Lond B Biol Sci* **253**:297–303, Royal Society.
- Sladeczek F, Pin J-P, Récasens M, Bockaert J, and Weiss S (1985) Glutamate stimulates inositol phosphate formation in striatal neurones. *Nature* **317**:717–719, Nature Publishing Group.
- Smothers CT, and Woodward JJ (2009) Expression of Glycine-Activated Diheteromeric NR1/NR3 Receptors in Human Embryonic Kidney 293 Cells Is NR1 Splice Variant-Dependent. *J Pharmacol Exp Ther* **331**:975–984.
- Smothers CT, and Woodward JJ (2007) Pharmacological Characterization of Glycine-Activated Currents in HEK 293 Cells Expressing N -Methyl-D-aspartate NR1 and NR3 Subunits. *J Pharmacol Exp Ther* **322**:739–748.
- Sobolevsky AI, Rosconi MP, and Gouaux E (2009) X-ray structure, symmetry and mechanism of an AMPA-subtype glutamate receptor. *Nature* **462**:745–756.
- Sobolevsky AI, and Yelshansky MV (2000) The trapping block of NMDA receptor channels in acutely isolated rat hippocampal neurones. *J Physiol* **526**:493–506.
- Song X, Jensen MØ, Jogini V, Stein RA, Lee C-H, Mchaourab HS, Shaw DE, and Gouaux E (2018) Mechanism of NMDA receptor channel block by MK-801 and memantine. *Nature* **556**:515–519, Nature Publishing Group.
- Spitzer SO, Sitnikov S, Kamen Y, Evans KA, Kronenberg-Versteeg D, Dietmann S, de Faria O, Agathou S, and Káradóttir RT (2019) Oligodendrocyte Progenitor Cells Become Regionally Diverse and Heterogeneous with Age. *Neuron* **101**:459-471.e5.
- Sprengel R, Suchanek B, Amico C, Brusa R, Burnashev N, Rozov A, Hvalby Ø, Jensen V, Paulsen O, Andersen P, Kim JJ, Thompson RF, Sun W, Webster LC, Grant SGN, Eilers J, Konnerth A, Li J, McNamara JO, and Seeburg PH (1998) Importance of the Intracellular Domain of NR2 Subunits for NMDA Receptor Function In Vivo. *Cell* **92**:279–289.
- Stern P, Béhé P, Schoepfer R, and Colquhoun D (1992) Single-channel conductances of NMDA receptors expressed from cloned cDNAs: comparison with native receptors. *Proc R Soc Lond B Biol Sci* **250**:271–277, Royal Society.
- Stroebe D, Carvalho S, Grand T, Zhu S, and Paoletti P (2014) Controlling NMDA Receptor Subunit Composition Using Ectopic Retention Signals. *J Neurosci* **34**:16630–16636.
- Stroebe D, Carvalho S, and Paoletti P (2011) Functional evidence for a twisted conformation of the NMDA receptor GluN2A subunit N-terminal domain. *Neuropharmacology* **60**:151–158.



- Stroebe D, Mony L, and Paoletti P (2021) Glycine agonism in ionotropic glutamate receptors. *Neuropharmacology* **193**:108631.
- Stroebe D, and Paoletti P (2021) Architecture and function of NMDA receptors: an evolutionary perspective. *J Physiol* **599**:2615–2638.
- Sucher N, Akbarian S, Chi C, Leclerc C, Awobuluyi M, Deitcher D, Wu M, Yuan J, Jones E, and Lipton S (1995) Developmental and regional expression pattern of a novel NMDA receptor- like subunit (NMDAR-L) in the rodent brain. *J Neurosci* **15**:6509–6520.
- Sun L, Margolis FL, Shipley MT, and Lidow MS (1998) Identification of a long variant of mRNA encoding the NR3 subunit of the NMDA receptor: its regional distribution and developmental expression in the rat brain. *FEBS Lett* **441**:392–396.
- Sun Y, Olson R, Horning M, Armstrong N, Mayer M, and Gouaux E (2002) Mechanism of glutamate receptor desensitization. *Nature* **417**:245–253.
- Swanger SA, Chen W, Wells G, Burger PB, Tankovic A, Bhattacharya S, Strong KL, Hu C, Kusumoto H, Zhang J, Adams DR, Millichap JJ, Petrovski S, Traynelis SF, and Yuan H (2016) Mechanistic Insight into NMDA Receptor Dysregulation by Rare Variants in the GluN2A and GluN2B Agonist Binding Domains. *Am J Hum Genet* **99**:1261–1280.
- Swanson GT, Feldmeyer D, Kaneda M, and Cull-Candy SG (1996) Effect of RNA editing and subunit co-assembly single-channel properties of recombinant kainate receptors. *J Physiol* **492**:129–142.
- Swanson GT, Green T, Sakai R, Contractor A, Che W, Kamiya H, and Heinemann SF (2002) Differential Activation of Individual Subunits in Heteromeric Kainate Receptors. *Neuron* **34**:589–598.
- Tajima N, Karakas E, Grant T, Simorowski N, Diaz-Avalos R, Grigorieff N, and Furukawa H (2016) Activation of NMDA receptors and the mechanism of inhibition by ifenprodil. *Nature* **534**:63–68.
- Tian M, Stroebe D, Piot L, David M, Ye S, and Paoletti P (2021) GluN2A and GluN2B NMDA receptors use distinct allosteric routes. *Nat Commun* **12**:4709.
- Tikhonov DB, and Zhorov BS (2020) The pore domain in glutamate-gated ion channels: Structure, drug binding and similarity with potassium channels. *Biochim Biophys Acta BBA - Biomembr* **1862**:183401.
- Tong G, Takahashi H, Tu S, Shin Y, Talantova M, Zago W, Xia P, Nie Z, Goetz T, Zhang D, Lipton SA, and Nakanishi N (2008) Modulation of NMDA Receptor Properties and Synaptic Transmission by the NR3A Subunit in Mouse Hippocampal and Cerebrocortical Neurons. *J Neurophysiol* **99**:122–132.
- Trakhanov S, Vyas NK, Luecke H, Kristensen DM, Ma J, and Quirocho FA (2005) Ligand-Free and -Bound Structures of the Binding Protein (LivJ) of the Escherichia coli ABC Leucine/Isoleucine/Valine Transport System: Trajectory and Dynamics of the Interdomain Rotation and Ligand Specificity. *Biochemistry* **44**:6597–6608, American Chemical Society.

- Traynelis SF, and Cull-Candy SG (1990) Proton inhibition of N-methyl-D-aspartate receptors in cerebellar neurons. *Nature* **345**:347–350, Nature Publishing Group.
- Traynelis SF, Hartley M, and Heinemann SF (1995) Control of Proton Sensitivity of the NMDA Receptor by RNA Splicing and Polyamines. *Science* **268**:873–876, American Association for the Advancement of Science.
- Traynelis SF, Wollmuth LP, McBain CJ, Menniti FS, Vance KM, Ogden KK, Hansen KB, Yuan H, Myers SJ, and Dingledine R (2010) Glutamate Receptor Ion Channels: Structure, Regulation, and Function. *Pharmacol Rev* **62**:405–496, American Society for Pharmacology and Experimental Therapeutics.
- Twomey EC, and Sobolevsky AI (2018) Structural Mechanisms of Gating in Ionotropic Glutamate Receptors. *Biochemistry* **57**:267–276, American Chemical Society.
- Twomey EC, Yelshanskaya MV, Grassucci RA, Frank J, and Sobolevsky AI (2017a) Channel opening and gating mechanism in AMPA-subtype glutamate receptors, in *Single-Particle Cryo-Electron Microscopy* pp 542–558, World Scientific.
- Twomey EC, Yelshanskaya MV, Grassucci RA, Frank J, and Sobolevsky AI (2017b) Channel opening and gating mechanism in AMPA-subtype glutamate receptors. *Nature* **549**:60–65.
- Ulbrich MH, and Isacoff EY (2008) Rules of engagement for NMDA receptor subunits. *Proc Natl Acad Sci* **105**:14163–14168.
- Vangone A, Spinelli R, Scarano V, Cavallo L, and Oliva R (2011) COCOMAPS: a web application to analyze and visualize contacts at the interface of biomolecular complexes. *Bioinformatics* **27**:2915–2916.
- Veran J, Kumar J, Pinheiro PS, Athané A, Mayer ML, Perrais D, and Mulle C (2012) Zinc Potentiates GluK3 Glutamate Receptor Function by Stabilizing the Ligand Binding Domain Dimer Interface. *Neuron* **76**:565–578.
- Volgraf M, Sellers BD, Jiang Y, Wu G, Ly CQ, Villemure E, Pastor RM, Yuen P, Lu A, Luo X, Liu M, Zhang S, Sun L, Fu Y, Lupardus PJ, Wallweber HJA, Liederer BM, Deshmukh G, Plise E, Tay S, Reynen P, Herrington J, Gustafson A, Liu Yichin, Dirksen A, Dietz MGA, Liu Yanzhou, Wang T-M, Hanson JE, Hackos D, Scearce-Levie K, and Schwarz JB (2016) Discovery of GluN2A-Selective NMDA Receptor Positive Allosteric Modulators (PAMs): Tuning Deactivation Kinetics via Structure-Based Design. *J Med Chem* **59**:2760–2779, American Chemical Society.
- Wada A, Takahashi H, Lipton SA, and Chen H-SV (2006) NR3A Modulates the Outer Vestibule of the “NMDA” Receptor Channel. *J Neurosci* **26**:13156–13166.
- Wang H, Lv S, Stroebel D, Zhang J, Pan Y, Huang X, Zhang X, Paoletti P, and Zhu S (2021) Gating mechanism and a modulatory niche of human GluN1-GluN2A NMDA receptors. *Neuron* **109**:2443-2456.e5.

- Wang H, Yan H, Zhang S, Wei X, Zheng J, and Li J (2013) The GluN3A Subunit Exerts a Neuroprotective Effect in Brain Ischemia and the Hypoxia Process. *ASN Neuro* **5**:AN20130009, SAGE Publications Inc.
- Warnet XL, Bakke Krog H, Sevillano-Quispe OG, Poulsen H, and Kjaergaard M (2021) The C-terminal domains of the NMDA receptor: How intrinsically disordered tails affect signalling, plasticity and disease. *Eur J Neurosci* **54**:6713–6739.
- Watkins JC, and Evans RH (1981) Excitatory Amino Acid Transmitters. *Annu Rev Pharmacol Toxicol* **21**:165–204.
- Watkins JC, and Jane DE (2006) The glutamate story. *Br J Pharmacol* **147**:S100–S108.
- Wee KS-L, Tan FCK, Cheong Y-P, Khanna S, and Low C-M (2016a) Ontogenic Profile and Synaptic Distribution of GluN3 Proteins in the Rat Brain and Hippocampal Neurons. *Neurochem Res* **41**:290–297.
- Wee KS-L, Tan FCK, Cheong Y-P, Khanna S, and Low C-M (2016b) Ontogenic Profile and Synaptic Distribution of GluN3 Proteins in the Rat Brain and Hippocampal Neurons. *Neurochem Res* **41**:290–297.
- Wee KS-L, Zhang Y, Khanna S, and Low C-M (2008) Immunolocalization of NMDA receptor subunit NR3B in selected structures in the rat forebrain, cerebellum, and lumbar spinal cord. *J Comp Neurol* **509**:118–135.
- Weston M. C., Gertler C, Mayer ML, and Rosenmund C (2006) Interdomain Interactions in AMPA and Kainate Receptors Regulate Affinity for Glutamate. *J Neurosci* **26**:7650–7658.
- Weston Matthew C., Schuck P, Ghosal A, Rosenmund C, and Mayer ML (2006) Conformational restriction blocks glutamate receptor desensitization. *Nat Struct Mol Biol* **13**:1120–1127, Nature Publishing Group.
- Williams K (1993) Ifenprodil discriminates subtypes of the N-methyl-D-aspartate receptor: selectivity and mechanisms at recombinant heteromeric receptors. *Mol Pharmacol* **44**:851–859, American Society for Pharmacology and Experimental Therapeutics.
- Wollmuth LP, and Sobolevsky AI (2004) Structure and gating of the glutamate receptor ion channel. *Trends Neurosci* **27**:321–328.
- Wong H-K, Liu X-B, Matos MF, Chan SF, Pérez-Otaño I, Boysen M, Cui J, Nakanishi N, Trimmer JS, Jones EG, Lipton SA, and Sucher NJ (2002) Temporal and regional expression of NMDA receptor subunit NR3A in the mammalian brain. *J Comp Neurol* **450**:303–317.
- Xu X-X, and Luo J-H (2018) Mutations of N-Methyl-D-Aspartate Receptor Subunits in Epilepsy. *Neurosci Bull* **34**:549–565.
- Yang Y, Cui Y, Sang K, Dong Y, Ni Z, Ma S, and Hu H (2018) Ketamine blocks bursting in the lateral habenula to rapidly relieve depression. *Nature* **554**:317–322.

- Yao Y (2006) Characterization of a Soluble Ligand Binding Domain of the NMDA Receptor Regulatory Subunit NR3A. *J Neurosci* **26**:4559–4566.
- Yao Y, Belcher J, Berger AJ, Mayer ML, and Lau AY (2013) Conformational Analysis of NMDA Receptor GluN1, GluN2, and GluN3 Ligand-Binding Domains Reveals Subtype-Specific Characteristics. *Structure* **21**:1788–1799.
- Yao Y, Harrison CB, Freddolino PL, Schulten K, and Mayer ML (2008) Molecular mechanism of ligand recognition by NR3 subtype glutamate receptors. *EMBO J* **27**:2158–2170.
- Yelshanskaya MV, Mesbahi-Vasey S, Kurnikova MG, and Sobolevsky AI (2017) Role of the Ion Channel Extracellular Collar in AMPA Receptor Gating. *Sci Rep* **7**:1050, Nature Publishing Group.
- Yi F, Bhattacharya S, Thompson CM, Traynelis SF, and Hansen KB (2019) Functional and pharmacological properties of triheteromeric GluN1/2B/2D NMDA receptors. *J Physiol* **597**:5495–5514.
- Yi F, Mou T-C, Dorsett KN, Volkmann RA, Menniti FS, Sprang SR, and Hansen KB (2016) Structural Basis for Negative Allosteric Modulation of GluN2A-Containing NMDA Receptors. *Neuron* **91**:1316–1329.
- Yu A, and Lau AY (2018) Glutamate and Glycine Binding to the NMDA Receptor. *Structure* **26**:1035-1043.e2.
- Yuan H, Erreger K, Dravid SM, and Traynelis SF (2005) Conserved Structural and Functional Control of N-Methyl-d-aspartate Receptor Gating by Transmembrane Domain M3. *J Biol Chem* **280**:29708–29716.
- Yuan H, Hansen KB, Vance KM, Ogden KK, and Traynelis SF (2009) Control of NMDA Receptor Function by the NR2 Subunit Amino-Terminal Domain. *J Neurosci* **29**:12045–12058, Society for Neuroscience.
- Yuan H, Hansen KB, Zhang J, Mark Pierson T, Markello TC, Fajardo KVF, Holloman CM, Golas G, Adams DR, Boerkoel CF, Gahl WA, and Traynelis SF (2014) Functional analysis of a de novo GRIN2A missense mutation associated with early-onset epileptic encephalopathy. *Nat Commun* **5**:3251.
- Yuan T, Mameli M, O'Connor EC, Dey PN, Verpelli C, Sala C, Perez-Otano I, Lüscher C, and Bellone C (2013) Expression of Cocaine-Evoked Synaptic Plasticity by GluN3A-Containing NMDA Receptors. *Neuron* **80**:1025–1038.
- Zampini V, Liu JK, Diana MA, Maldonado PP, Brunel N, and Dieudonné S (n.d.) Mechanisms and functional roles of glutamatergic synapse diversity in a cerebellar circuit. *eLife* **5**:e15872.
- Zeilhofer HU, Studler B, Arabadzisz D, Schweizer C, Ahmadi S, Layh B, Bösl MR, and Fritschy J-M (2005) Glycinergic neurons expressing enhanced green fluorescent protein in bacterial artificial chromosome transgenic mice. *J Comp Neurol* **482**:123–141.
- Zeng Y, Zheng Y, Zhang T, Ye F, Zhan L, Kou Z, Zhu S, and Gao Z (2022) Identification of a Subtype-Selective Allosteric Inhibitor of GluN1/GluN3 NMDA Receptors. *Front Pharmacol* **13**:888308.

- Zhang J-B, Chang S, Xu P, Miao M, Wu H, Zhang Y, Zhang T, Wang H, Zhang J, Xie C, Song N, Luo C, Zhang X, and Zhu S (2018) Structural Basis of the Proton Sensitivity of Human GluN1-GluN2A NMDA Receptors. *Cell Rep* **25**:3582-3590.e4.
- Zhou Q, and Sheng M (2013) NMDA receptors in nervous system diseases. *Neuropharmacology* **74**:69–75.
- Zhu S, and Paoletti P (2015) Allosteric modulators of NMDA receptors: multiple sites and mechanisms. *Curr Opin Pharmacol* **20**:14–23.
- Zhu S, Riou M, Yao CA, Carvalho S, Rodriguez PC, Bensaude O, Paoletti P, and Ye S (2014) Genetically encoding a light switch in an ionotropic glutamate receptor reveals subunit-specific interfaces. *Proc Natl Acad Sci* **111**:6081–6086, Proceedings of the National Academy of Sciences.
- Zhu S, Stroebel D, Yao CA, Taly A, and Paoletti P (2013) Allosteric signaling and dynamics of the clamshell-like NMDA receptor GluN1 N-terminal domain. *Nat Struct Mol Biol* **20**:477–485, Nature Publishing Group.
- Zhu Z, Yi F, Epplin MP, Liu D, Summer SL, Mizu R, Shaulsky G, XiangWei W, Tang W, Burger PB, Menaldino DS, Myers SJ, Liotta DC, Hansen KB, Yuan H, and Traynelis SF (2020) Negative allosteric modulation of GluN1/GluN3 NMDA receptors. *Neuropharmacology* **176**:108117.
- Zuo J, De Jager PL, Takahashi KA, Jiang W, Linden DJ, and Heintz N (1997) Neurodegeneration in Lurcher mice caused by mutation in  $\delta 2$  glutamate receptor gene. *Nature* **388**:769–773, Nature Publishing Group.



# RÉSUMÉ

---

Les récepteurs NMDA (NMDAR) appartiennent à la famille des récepteurs ionotropiques du glutamate (iGluR). Ils jouent un rôle fondamental dans la neurotransmission glutamatergique excitatrice et dans les processus clés de plasticité synaptique, eux-mêmes critiques pour la formation de la mémoire. Au cours de mon projet de doctorat, nous avons étudié les corrélats structuraux du mécanisme de déclenchement du NMDAR non conventionnel contenant la sous-unité GluN3A. Cette sous-unité s'assemble avec GluN1 formant ainsi des récepteurs excitateurs dépendants de la glycine (eGlyR) et insensibles au glutamate. Des données récentes de notre laboratoire et d'autres ont révélé que les eGlyRs sont répandus dans le cerveau antérieur adulte où ils forment une nouvelle forme de signalisation par laquelle la glycine ambiante contrôle l'excitabilité neuronale et certains comportements. Les connaissances actuelles sur les déterminants structuraux des récepteurs GluN1/GluN3A restent cependant très limitées. En présence de glycine ces récepteurs génèrent des courants de faible amplitude et rapidement désensibilisants, ce qui a compliqué leur caractérisation. Les récepteurs GluN1/GluN3A présentent une courbe d'activation biphasique puisque la liaison de la glycine aux sous-unités GluN3A active le récepteur, tandis que la liaison de la glycine aux sous-unités GluN1 les inhibe. En adoptant une approche méthodologique structure-fonction (mutagenèse dirigée et TEVC dans les ovocytes de xénope), nous avons étudié le rôle fonctionnel de régions spécifiques des récepteurs GluN1/GluN3A dans le contrôle de leur mécanisme d'activation. Nous avons ainsi :

1) développé une méthodologie pour évaluer la probabilité d'ouverture ( $P_o$ ) des récepteurs GluN1/GluN3A-WT et mutants. Nous avons également caractérisé l'effet de plusieurs composés : pentamidine, zinc, magnésium, échinatine et D-sérine sur l'activité des récepteurs GluN1/GluN3A.

2) L'analyse de modèles structuraux des récepteurs GluN1/GluN3A a permis de déterminer d'identifier des sites potentiels pour stabiliser des états conformationnels spécifiques. Nous avons tenté de ponter plusieurs interfaces par ponts disulfures et utilisation d'acides aminés non naturels (UAA) photo-réactifs. Nous avons aussi tenté de retirer génétiquement des domaines et boucles du récepteur afin d'en étudier le rôle. Cependant, ces approches ont eu un succès limité.

3) Nous avons ensuite ciblé l'interface de dimérisation du domaine de liaison au ligand (LBD), région d'une importance critique pour l'activation de tous les iGluRs, mais de fonction inconnue chez les récepteurs GluN1/GluN3A. Grâce à la découverte d'un mutant Gain-de-Fonction (GoF), nous démontrons que les résidus situés à l'interface intra-dimère LBD sont des déterminants clés du comportement d'activation, en particulier de la faible  $P_o$  des récepteurs GluN1/GluN3A. Les mutants qui restaurent le profil d'hydrophobicité de type GluN1/GluN2 présentent une  $P_o$  et une affinité glycine considérablement accrue (>10 fois). Dans l'ensemble, nos données suggèrent que l'interface de dimérisation des LBD chez GluN1/GluN3A joue un rôle clé dans les processus d'activation du récepteur.

Les récepteurs GluN1/GluN3A dépendants de la glycine suscitent un vif intérêt pour leur rôle physiologique dans la signalisation cérébrale qui a été récemment découvert. Dans ce présent travail, nous avons démontré l'importance fonctionnelle de l'assemblage de l'interface intra-dimère GluN1-GluN3A LBD pour l'activation du récepteur, en mettant en évidence des similitudes et des différences avec d'autres iGluRs. Nous pensons que les mutants GoF que nous avons caractérisés offrent des opportunités uniques pour élucider les mécanismes fonctionnels des récepteurs GluN1/GluN3A et leurs rôles physiologiques et pathologiques dans le cerveau. Les outils moléculaires que nous avons validés devraient présenter un intérêt pour de futurs développements pharmacologiques.

## MOTS CLÉS

---

Récepteurs NMDA, neurotransmission, mécanismes moléculaires, GluN3A, structure-fonction

## ABSTRACT

---

NMDA receptors (NMDARs) belong to the tetrameric ionotropic glutamate receptor (iGluRs) family. They exhibit a fundamental role in the excitatory glutamatergic neurotransmission, mediating key processes such as synaptic plasticity by long term potentiation (LTP) and depression (LTD), memory formation, and others. During my PhD project, we investigated the structural correlates of the gating mechanism of unconventional NMDAR containing the GluN3A subunit. This subunit assembles with GluN1 as functional excitatory glycine-gated receptors (eGlyRs) that are insensitive to glutamate. Recent data from our lab and others revealed that eGlyRs are widespread in the adult forebrain where they form a novel signaling modality whereby endogenous glycine controls neuronal excitability, circuit function and behavior. Our current knowledge of the structural determinants for GluN1/GluN3A receptors remain very limited however. When exposed to glycine, these receptors mediate small and quickly desensitizing currents, contributing to hinder their characterization for many years. Glycine binding these receptors causes a biphasic activation curve since glycine binding the GluN3A subunits activates the receptor, while glycine binding the GluN1 subunits inhibits it. By taking a structure-function methodological approach (site-directed mutagenesis and 2-electrode voltage clamp recordings in *xenopus* oocytes), we investigated the role of specific regions of GluN1/GluN3A receptors in the control of their gating mechanism. The results of our work can be divided in three main axes:

1) We developed a methodology to assess GluN1/GluN3A receptors open probability ( $P_o$ ) allowing evaluation of the effect of mutations on the receptor activity. We also characterized the effect of the open channel blocker pentamidine on GluN1/GluN3A receptor activity, alongside several other agents such as zinc, magnesium, echinatin, and D-serine.

2) We created a structural model of GluN1/GluN3A receptors and computed several subunit-subunit contact maps, to determine which sites to target to investigate GluN1/GluN3A function. We aimed at stabilizing specific conformational states by employing several different strategies. We thus attempted to crosslink several interfaces by disulfide bridge formation through cysteine scanning, by employing unnatural amino acids (UAAs) that crosslink upon UV light illumination, or by investigating the role of several domains and loops by performing genetic deletions of large functional portions of the receptors. Unfortunately, we obtained limited success with these approaches.

3) We investigated the role of the putative ligand binding domain (LBD) dimerization interface, that is of critical importance for the gating of all iGluRs but of unknown contribution to GluN1/GluN3A. Thanks to the discovery of large Gain-of-Function (GoF) mutants, we reveal that residues located at the LBD intra-dimer interface are key determinants of the gating behavior, in particular of the low  $P_o$  of GluN1/GluN3A receptors. Mutants that restore the GluN1/GluN2-like hydrophobicity profile, show greatly increased  $P_o$  and glycine affinity. Overall, our data suggest that the GluN3A LBD likely contact GluN1 LBD similarly to other NMDARs, albeit weaker.

Glycine-gated GluN1/GluN3A receptors are generating strong interest for their physiological role in brain signaling recently unveiled. Our understanding of their molecular mechanisms remained sparse however. In the present work, we demonstrated the functional importance of the GluN1-GluN3A LBD intra-dimer interface assembly for the gating of the receptor, highlighting similarities and differences with other iGluRs. We believe that the GoF mutants we characterized offer unique opportunities to further elucidate GluN1/GluN3A receptor gating mechanisms. The molecular tools we validated should be of interest for functional and pharmacological tests in the framework of the physiological and pathological roles of these receptors.

## KEYWORDS

---

NMDA receptors, neurotransmission, molecular mechanisms, GluN3A, structure-fonction